# PLACE IN RETURN BOX to remove this checkout from your record. TO AVOID FINES return on or before date due. MAY BE RECALLED with earlier due date if requested.

DATE DUE	DATE DUE	DATE DUE

6/01 c:/CIRC/DateDue.p65-p.15

## THE USE OF GASEOUS OZONE TO REMEDIATE PYRENE CONTAMINATED SOILS: A STUDY OF BYPRODUCT PRODUCTION, ENVIRONMENTAL EFFECTS ON REMEDIATION EFFORTS, AND SCALE-UP

VOLUME I

By

Stephanie Luster-Teasley

#### A DISSERTATION

Submitted to
Michigan State University
in partial fulfillment of the requirements
for the degree of

**DOCTOR OF PHILOSOPHY** 

Department of Civil and Environmental Engineering

2003

#### **ABSTRACT**

THE USE OF GASEOUS OZONE TO REMEDIATE PYRENE CONTAMINATED SOILS: A STUDY OF BYPRODUCT PRODUCTION, ENVIRONMENTAL EFFECTS ON REMEDIATION EFFORTS, AND SCALE-UP

By

#### Stephanie Luster-Teasley

Ozonation studies were performed in 15 cm soil columns to determine the affect various soil conditions would have on pyrene oxidation and the subsequent byproduct formation. The conditions evaluated included 0, 5%, and 10% soil moisture contents and the pH levels of 2, 6, and 8. Ozonation experiments were conducted in soils at 13°C and 25°C. A comparison of ozonation in freshly contaminated soils and soils contaminated with pyrene for 6 months were conducted to determine the effect soil age has on the ability to remediate soils with ozone. An ozonation system using a 3.5 foot column was also designed to evaluate the ozone transport model proposed by Hsu and Masten (1997).

Dry soil with high pH (pH 6, pH 8) resulted in the highest level of contaminant removal. In the presence of soil moisture, the reduction of pyrene concentrations in soil required longer treatment times compared to the dry soils. Temperature was determined to affect pyrene oxidation in the moisturized soils at pH 6 and pH 8. Pyrene removal in the moisturized soils improved when ozonated at 13°C. The colder temperature, however, appeared to harden the packed soil and inhibited gas flow through the soil. In the ozonation experiments for the aged soils, the percentage of pyrene reduction was found to be 3 - 4 times less in the aged soils compared to the freshly contaminated soils.

The pyrene ozonation byproducts produced in soil were consistent with the compounds produced from aqueous pyrene ozonation. The byproducts detected were

phenanthrene-like and biphenyl-like with hydroxyl, aldehyde, and carboxylic acid functional groups.

Two synthesized ozonation byproducts, 2,2',6,6'-biphenyl tetraaldehyde and 2,2',6,6'-biphenyl tetra carboxylic acid, were evaluated using two toxicology assays. The first assay measured the potential for the compounds to block gap junctional intercellular communication (GJIC) using the scrape loading/dye transfer (SL/DT) assay. The second assay evaluated the ability for the compounds to affect neutrophil function by measuring the production of superoxide in a human cell line (HL60). 2,2',6,6'-biphenyl tetraaldehyde was determined to show adverse effects in both toxicity analyses. 2,2',6,6'-biphenyl tetra carboxylic acid did not exhibit any significant effect in either assays.

Copyright by Stephanie Luster-Teasley 2003

## DEDICATION

This work is dedicated to my grandmother, Ruthie Perry Benyard.

#### **ACKNOWLEDGEMENTS**

I would like to take this opportunity to thank the people who were instrumental in helping me during my graduate program. My advisor, Dr. Susan Masten, provided immeasurable knowledge, faith, and support to me throughout this process. I wish to extend a special thank you to Dr. Bruce Dale from the Department of Chemical Engineering. Dr. Dale foresaw the potential in me and provided unwavering support for both my M.S. in Chemical Engineering and the Ph.D. in Environmental Engineering. Thank you to Dr. Aurles Wiggins and the College of Engineering Diversity Programs Office (DPO) for being a foundation for me and many students who use the services provided by the office. I would like to thank my funding sources for research and for completing the dissertation: NIEH Superfund Grant, GAANN Fellowship, and Dr. Percy Pierre and Dr. Barbara O'Kelly from the SLOAN Program.

I extend thanks to all of my family and friends for their prayers and support. I would especially like to acknowledge my husband, Edward Teasley I, and my sons Edward II and William. Thank you for your patience and love. To my parents, Lorenza, Helen, and Mama-T, thank you for all of things that you have done because without each of you I know I would not have completed this degree.

## TABLE OF CONTENTS

LIST OF TABLES
LIST OF FIGURES x
CHAPTER 1: INTRODUCTION AND ENVIRONMENTAL SIGNIFICANCE
1.1 Introduction: Background and Environmental Significance
1.2 Objective and Order of Thesis
1.3 List of References
CHAPTER 2: OZONATION STUDIES
2.1 Introduction
2.2 Background9
(a) Ozonation reactions
(b) Ozone reactions with Polycyclic Aromatic Hydrocarbons (PAHs) 11
2.3 Soil remediation using Ozonation processes
(a) Ozone reaction with organic matter
(b) The influence of water and soil saturation on ozonation
(c) Surface adsorption and bond-localization strength
(d) Temperature in soil
2.4 Experimental Basis
2.4.1 Materials
2.4.2 Methods
2.5 Results and Discussion

2.5.1 Dry soil ozonation	32
(a) Non-contaminated, dry soil studies	32
(b) Pyrene remediation in dry soils	33
2.5.2 Moisturized soil	38
(a) Non-contaminated, 5% moisturized soil	38
(b) Pyrene remediation in 5% moisture content soils	40
(c) Non-contaminated, 10% moisturized soil	42
(d) Pyrene remediation in 10% moisture content soils	45
2.5.3 Ozonation at Colder Temperature	48
2.5.4 Ozonation of aged soil	54
2.6 Conclusions	59
2.7 References	61
CHAPTER 3: HPLC AND GC/MS IDENTIFICATION OF PYRENE OZONATION BYPRODUCTS	
3.1 Introduction	64
(a) Pyrene ozonation byproducts in aqueous systems	64
(b) Pyrene ozonation byproducts formed in solid media	67
3.2 Significance of ozonation byproduct studies	70
3.3 Research Focus	73
3.3.1 Materials	74
3.3.2 Methods	74
3.4 Results and Discussion	76
3.4.1 Pyrene and control HPLC chromatograms	76

3.4.2 HPLC Chromatograms	78
3.4.3 GC/MS Analysis	88
3.5 Conclusion	106
3.6 References	108
CHAPTER 4: AN EVALUATION OF PYRENE OZONATION BYPRO 2,2',6,6'-BIPHENYL TETRAALDEHYDE AND 2,2',6,6'-BIPHENYL TETRACARBOXYLIC ACID	DUCTS:
4.1 Introduction	112
4.2 Experimental Section	116
4.2.1 Materials	116
4.2.2 Methods: Toxicology Assays	118
4.2.2.1 GJIC assay	118
4.2.2.2 HL-60 Neutrophil Assay, Superoxide Anion Assay, and L	DH Assay 120
4.3 Results and Discussion.	123
4.3.1 GJIC Evaluation	123
4.3.2 HL-60NEtrophil Assay	129
4.4 Conclusion	135
CHAPTER 5: REACTION KINETICS AND MODELING	
5.1 Introduction	144
5.2 Section 1: Reaction kinetics	144
5.2.1 Reaction Kinetics for Experiments	146
5.2.1.1 Non-contaminated Dry soil	147

5.2.1.2 Non-contaminated Moisturized Soils	150	
5.2.2 Reaction kinetics for pyrene contaminated soils at 25°C	151	
5.2.3 Reaction kinetics for ozonation at 13°C in pyrene contaminated soils	158	
5.2.4 Reaction kinetics for ozonation in Aged soil	163	
5.3 Discussion of Reaction Kinetics and Introduction of the Model	165	
5.3.1 Modeling	167	
5.3.2 Materials and Methods	171	
5.4 Results	175	
5.4.1 The 3.5 foot column ozonation experiments	175	
5.4.2 Model Application	179	
5.4.2.1 Experiments in the 15 cm column	180	
5.4.2.2 Model application in the 3.5 foot column	182	
5.5 Modeling Discussion and Conclusions	184	
5.6 References		
CHAPTER 6: SUMMARY AND RECOMMENDATIONS		
6.1 Summary	188	
6.2 Recommendations	191	
APPENDIX A	193	
APPENDIX B	260	
APPENDIX C	304	
A PPENDIX D	327	

## LIST OF TABLES

## **TABLE**

2.1	The bond/atom localization energies and the type of ozone reaction that occurs for representative PAH compound	. 15
2.2	Physical and Chemical Characteristics of the Metea Soil	21
2.3	Summary of Ozonation Experiments	31
2.4	Percentage of pyrene removed from air-dried Metea soil at 25°C	37
2.5	Percentage of pyrene removed from Metea soil at 5% moisture content and 25°C	. 40
2.6	Percentage of pyrene removed from Metea soil at 10% moisture content and 25°C	. 45
2.7	Percentage of pyrene removed from soils at 13°C	. 49
2.8	A comparison of pyrene removal in the soils at 13°C and 25°C	. 50
2.9	Percentage of pyrene removed from air-dried Metea soil contaminated for 6 months at 25°C	54
3.1	Byproducts Identified following Pyrene Ozonation in Silica	68
3.2	Byproducts produced in the ozonated column effluent	71
3.3	Intermediates and products in ozonated effluent after various degrees of biotreatment	. 72
3.4	Temperature profile for GC/MS method	. 76
3.5	GC/MS ion peaks for the soil ozonation byproducts	91
5.1	Rate constants for dry, non-contaminated Metea soil	149
5.2	The first order reaction rate constants for 5% and 10% moisture, non-contaminated Metea soil at 25°C	150
5.3	The second order reaction rate constants for 5% and 10% moisture,	16.
5.4	non-contaminated Metea soil at 25°C	

5.5	Second order ozone decomposition rates for pyrene contaminated soils at 25°C
5.6	First order reaction rate constants for 13°C temperature experiments
5.7	Second order reaction rate constants for 13°C temperature experiments 159
5.8	Comparison of first order and second order rate constants For ozonation in Metea soil aged for 6 months
<b>A</b> 1	Summary of Ozonation Experiments
<b>A2</b>	Example of spreadsheet generated for raw data
31	Spreadsheet for Pyrene calibration

## LIST OF FIGURES

## **FIGURE**

1.1	Representative PAH compounds	2
2.1	Mechanism of Aqueous Ozonolysis Reaction with a target solute	10
2.2	Structures for Category II PAH compounds	. 13
2.3	Structures for Category III PAH compounds	. 14
2.4	Seasonal temperature profile for soil 1-3 meters below the soil surface	18
2.5	Pyrene	19
2.6	Schematic of the ozonation system	. 23
2.7	(a) Experimental set-up for 13°C ozonation system	
2.8	Representative ozone breakthrough curve for clean soil	32
2.9	Ozone breakthrough curve for air-dried soil	34
2.10	Breakthrough curve for clean Metea soil at pH 6	39
2.11	Ozone breakthrough curve for 5% moisture, pyrene soil at 25°C	. 41
2.12	Ozone breakthrough curve for non-contaminated Metea at pH 2 and 25°C	. 42
2.13	Ozone breakthrough curve for non-contaminated Metea at pH 6 and 25°C	. 44
2.14	Ozone breakthrough curve for non-contaminated Metea at pH 8 and 25°C	. 44
2.15	Ozone breakthrough curve for 10% moisturized, pyrene soil at 25°C	. 46
2.16	Ozone breakthrough curve for air-dried, pyrene soil at 13°C	51
2.17	Ozone breakthrough for 5% moisture, pyrene soil at 13°C	52
2.18	Ozone breakthrough for 10% moisture, pyrene soil at 13°C	. 53
2.19	Ozone breakthrough curve for short-term and long term contaminated soil at pH 2	. 56

2.20	Ozone breakthrough curve for short-term and long term contaminated soil at pH 6
2.21	Ozone breakthrough curve for short-term and long term contaminated soil at pH 8
3.1	Pyrene ozonation pathways
3.2	Byproducts from pyrene ozonation in 90% acetonitrile/10% water
3.3	Proposed pyrene ozonation Pathway 1 and Pathway 2
3.4	HPLC chromatograms for 2,2',6,6'-biphenyl tetra carboxylic acid, 2,2',6,6'-biphenyl tetra aldehyde, and pyrene
3.5	Acetonitrile extracts from 24 hour oxygen and air sparged pyrene contaminated soil
3.6	Deionized water extracts from 24 hour oxygen and air sparged pyrene contaminated soil
3.7	Deionized extract chromatogram for 5% moisture (pH 6) pyrene contaminated soil
3.8	Deionized extract chromatogram for dry (pH 6) pyrene contaminated soil 83
3.9	Deionized extract chromatogram for 10% moisture (pH 6) pyrene contaminated soil
3.10	Acetonitrile extract chromatogram for 5% moisture (pH 6) pyrene contaminated soil
3.11	Acetonitrile extract chromatogram for dry (pH 6) pyrene contaminated soil 86
3.12	Acetonitrile extract chromatogram for 10% moisture (pH 6) pyrene contaminated soil
3.13	HPLC fractions collected for GC/MS analysis
3.14	Byproducts from ozonation in pyrene contaminated Metea soil
3.15	GC/MS spectra proposed for Compound VII(A) or Compound VIII (B) 94
3.16	GC/MS spectra proposed for Compound XI

3.17	GC/MS spectra proposed for Compound VI	. 98
3.18	GC/MS spectra proposed for Compound III(A) or Compound III(B)	102
3.19	GC/MS spectra proposed for Compound VIII	104
3.20	ACN extract for 10% moisture (pH 2) pyrene soil	105
4.1	Structures for pyrene, 2,2',6,6'-biphenyl tetraaldehyde and 2,2;,6,6;-biphenyl tetra carboxylic acid	114
4.2	Cytotoxicity profile for pyrene and 2,2',6,6'-biphenyl tetraaldehyde	124
4.3	Cytotoxicity profile for 2,2',6,6' -biphenyl tetra carboxylic acid	126
4.4	Dose response curve for cells exposed to pyrene, 2,2',6,6'-biphenyl tetraaldehyde and 2,2',6,6'-biphenyl tetra carboxylic acid	127
4.5	Time response for cells exposed to 5 µM concentration of 2,2',6,6'-biphenyl tetraaldehyde	128
4.6	Time response 2,2',6,6'-biphenyl tetra carboxylic acid at 500 μM concentration	130
4.7	Time recovery for cells exposed to 5 µM concentration of 2,2',6,6' -biphenyl tetraaldehyde	131
4.8	Effect of pyrene and its metabolites on PMS-stimulated superoxide anion (O <sub>2</sub> ) generation by HL-60 cells	132
4.9	Cytotoxicity in HL-60 cells exposed to pyrene or its metabolites	134
5.1	First order plot for dry, non-contaminated Metea soil pH 6 at 25°C	148
5.2	Second order plot for dry, non-contaminated Metea soil pH 6 at 25°C	148
5.3	(a) First order plot of 5% moisturized soil at pH 2 (25°C)	154
5.3	(b) Second order plot of 5% moisturized soil at pH 2 (25°C)	154
5.4	(a) First order plot of 10% moisturized soil at pH 2 (25°C)	155
5.4	(b) Second order plot of 10% moisturized soil at pH 2 (25°C)	155
5.5	The first order rate constants listed in increasing order for Metea	156

5.6	The second order rate constants listed in increasing order for Metea soil ozonated at 25°C
5.7	(a) First order plot for 10% moisture soil, pH 8 at 13°C
5.7	(b) Second order plot for 10% moisture soil, pH 8 at 13°C
5.8	The first order rate constants listed in increasing order for Metea soil ozonated at 13°C
5.9	The second order rate constants listed in increasing order for Metea soil ozonated at 13°C
5.10	Comparison of the first order rate constants for aged soils and short-term contaminated soils at 25°C
5.11	Comparison of the second order rate constants for aged soils and short-term contaminated soils at 25°C
5.12	Schematic of the ozonation system for the 3.5 foot column
5.13	Ozone Breakthrough curve obtained in the empty 3.5 foot column
5.14	Ozone BTC for 3.5 foot column with gas wash bottle
5.15	Ozone BTC in the 3.5 foot column without the gas wash bottle
5.16	Ozone breakthrough curves for Experiments 1, 2, and 3 in the foot column without the gas wash bottle and containing 10 cm of Metea soil
5.17	Finite-difference prediction for the dry, non-contaminated pH 6 soil 181
5.18	Runge-Kutta prediction for the dry, non-contaminated soil at pH 6
5.19	Model prediction for the 3.5 foot column empty and with 42 inches of Ottawa sand
5.20	Model prediction for the BTC in the 3.5 foot column containing 10 cm of Metea soil
A1	Breakthrough curve, first order and second order plots for dry, clean Metea soil (pH 2) at 25°C
A2	Breakthrough curve, first order and second order plots for dry, clean

	Metea soil (pH 6) at 25°C	202
A3	Breakthrough curve, first order and second order plots for dry, clean Metea soil (pH 8) at 25°C	204
A4	Breakthrough curve, first order and second order plots for 5% moisture, clean Metea soil (pH 2) at 25°C	206
A5	Breakthrough curve, first order and second order plots for 5% moisture, clean Metea soil (pH 6) at 25°C	208
<b>A</b> 6	Breakthrough curve, first order and second order plots for 5% moisture, clean Metea soil (pH 8) at 25°C	210
A7	Breakthrough curve, first order and second order plots for 10% moisture, clean Metea soil (pH 2) at 25°C	212
A8	Breakthrough curve, first order and second order plots for 10% moisture, clean Metea soil (pH 6) at 25°C	214
A9	Breakthrough curve, first order and second order plots for 10% moisture, clean Metea soil (pH 8) at 25°C	216
A10	Breakthrough curve, first order and second order plots for dry, pyrene contaminated Metea soil (pH 2) at 25°C	218
A11	Breakthrough curve, first order and second order plots for dry, pyrene contaminated Metea soil (pH 6) at 25°C	220
A12	Breakthrough curve, first order and second order plots for dry, pyrene contaminated Metea soil (pH 8) at 25°C	222
A13	Breakthrough curve, first order and second order plots for 5% moisture, pyrene contaminated Metea soil (pH 2) at 25°C	224
A14	Breakthrough curve, first order and second order plots for 5% moisture, pyrene contaminated Metea soil (pH 6) at 25°C	226
A15	Breakthrough curve, first order and second order plots for 5% moisture, pyrene contaminated Metea soil (pH 8) at 25°C	228
A16	Breakthrough curve, first order and second order plots for 10% moisture, pyrene contaminated Metea soil (pH 2) at 25°C	230
A17	Breakthrough curve, first order and second order plots for 10% moisture, pyrene contaminated Metea soil (pH 6) at 25°C	232

A18	Breakthrough curve, first order and second order plots for 10% moisture, pyrene contaminated Metea soil (pH 8) at 25°C	234
A19	Breakthrough curve, first order and second order plots for dry, pyrene contaminated Metea soil (pH 2) at 13°C	23 <i>6</i>
A20	Breakthrough curve, first order and second order plots for dry, pyrene contaminated Metea soil (pH 6) at 13°C	238
A21	Breakthrough curve, first order and second order plots for dry, pyrene contaminated Metea soil (pH 8) at 13°C	240
A22	Breakthrough curve, first order and second order plots for 5% moisture, pyrene contaminated Metea soil (pH 2) at 13°C	242
A23	Breakthrough curve, first order and second order plots for 5% moisture, pyrene contaminated Metea soil (pH 6) at 13°C	244
A24	Breakthrough curve, first order and second order plots for 5% moisture, pyrene contaminated Metea soil (pH 8) at 13°C	246
A25	Breakthrough curve, first order and second order plots for 10% moisture, pyrene contaminated Metea soil (pH 2) at 13°C	248
A26	Breakthrough curve, first order and second order plots for 10% moisture, pyrene contaminated Metea soil (pH 6) at 13°C	250
A27	Breakthrough curve, first order and second order plots for 10% moisture, pyrene contaminated Metea soil (pH 8) at 13°C	252
A28	Breakthrough curve, first order and second order plots for aged, pyrene contaminated Metea soil (pH 2) at 25°C	254
A29	Breakthrough curve, first order and second order plots for aged, pyrene contaminated Metea soil (pH 6) at 25°C	256
A30	Breakthrough curve, first order and second order plots for aged dry, pyrene contaminated Metea soil (pH 8) at 25°C	258
B1	HPLC chromatograms of acetonitrile extracts. (a) Pyrene soil (control), (b) air-sparged through pyrene soil for 24 hours, (c) oxygen-sparged through pyrene soil for 24 hours.	262
B2	HPLC chromatograms of deionized water extracts. (a) Pyrene soil (control), (b) air-sparged through pyrene soil for 24 hours, (c) oxygen-sparged	

	through pyrene soil for 24 hours	. 263
В3	Examples of the two chromatograms for acetonitrile extracts from pyrene soil	. 264
B4	Acetonitrile extract chromatogram for dry, 25°C (pH 2) pyrene contaminated soil. (a) 2.2 mg O <sub>3</sub> /ppm pyr, (b) 3.85 mg O <sub>3</sub> /ppm pyr, (c) 16 mg O <sub>3</sub> /ppm pyr	. 265
B5	Deionized water extract chromatogram for dry, 25°C (pH 2) pyrene contaminated soil. (a) 2.2 mg O <sub>3</sub> /ppm pyr, (b) 3.85 mg O <sub>3</sub> /ppm pyr, (c) 16 mg O <sub>3</sub> /ppm pyr	. 266
В6	Acetonitrile extract chromatogram for 5% moisture, 25°C (pH 2) pyrene contaminated soil. (a) 2.2 mg O <sub>3</sub> /ppm pyr, (b) 3.85 mg O <sub>3</sub> /ppm pyr, (c) 16 mg O <sub>3</sub> /ppm pyr	. 267
В7	Deionized water extract chromatogram for 5% moisture, 25°C (pH 2) pyrene contaminated soil. (a) 2.2 mg O <sub>3</sub> /ppm pyr, (b) 3.85 mg O <sub>3</sub> /ppm pyr, (c) 16 mg O <sub>3</sub> /ppm pyr	. 268
В8	Acetonitrile extract chromatogram for 10% moisture, 25°C (pH 2) pyrene contaminated soil. (a) 2.2 mg O <sub>3</sub> /ppm pyr, (b) 3.85 mg O <sub>3</sub> /ppm pyr, (c) 16 mg O <sub>3</sub> /ppm pyr	269
В9	Deionized water extract chromatogram for 10% moisture, 25°C (pH 2) pyrene contaminated soil. (a) 2.2 mg O <sub>3</sub> /ppm pyr, (b) 3.85 mg O <sub>3</sub> /ppm pyr, (c) 16 mg O <sub>3</sub> /ppm pyr	. 270
B10	Acetonitrile extract chromatogram for dry, 25°C (pH 6) pyrene contaminated soil. (a) 2.2 mg O <sub>3</sub> /ppm pyr, (b) 3.85 mg O <sub>3</sub> /ppm pyr, (c) 16 mg O <sub>3</sub> /ppm pyr	. 271
B11	Deionized water extract chromatogram for dry, 25 °C (pH 6) pyrene contaminated soil. (a) 2.2 mg O <sub>3</sub> /ppm pyr, (b) 3.85 mg O <sub>3</sub> /ppm pyr, (c) 16 mg O <sub>3</sub> /ppm pyr	. 272
B12	Acetonitrile extract chromatogram for 5% moisture, 25°C (pH 6) pyrene contaminated soil. (a) 2.2 mg O <sub>3</sub> /ppm pyr, (b) 3.85 mg O <sub>3</sub> /ppm pyr, (c) 16 mg O <sub>3</sub> /ppm pyr	. 273
B13	Deionized water extract chromatogram for 5% moisture, 25°C (pH 6) pyrene contaminated soil. (a) 2.2 mg O <sub>3</sub> /ppm pyr, (b) 3.85 mg O <sub>3</sub> /ppm pyr, (c) 16 mg O <sub>3</sub> /ppm pyr	. 274
B14	Acetonitrile extract chromatogram for 10% moisture, 25°C (pH 6)	

	pyrene contaminated soil. (a) 2.2 mg O <sub>3</sub> /ppm pyr, (b) 3.85 mg O <sub>3</sub> /ppm pyr, (c) 16 mg O <sub>3</sub> /ppm pyr	. 275
B15	Deionized water extract chromatogram for 10% moisture, 25°C (pH 6) pyrene contaminated soil. (a) 2.2 mg O <sub>3</sub> /ppm pyr, (b) 3.85 mg O <sub>3</sub> /ppm pyr, (c) 16 mg O <sub>3</sub> /ppm pyr	27 <del>6</del>
B16	Acetonitrile extract chromatogram for dry, 25°C (pH 8) pyrene contaminated soil. (a) 2.2 mg O <sub>3</sub> /ppm pyr, (b) 3.85 mg O <sub>3</sub> /ppm pyr, (c) 16 mg O <sub>3</sub> /ppm pyr	277
B17	Deionized water extract chromatogram for dry, 25°C (pH 8) pyrene contaminated soil. (a) 2.2 mg O <sub>3</sub> /ppm pyr, (b) 3.85 mg O <sub>3</sub> /ppm pyr, (c) 16 mg O <sub>3</sub> /ppm pyr	278
B18	Acetonitrile extract chromatogram for 5% moisture, 25°C (pH 8) pyrene contaminated soil. (a) 2.2 mg O <sub>3</sub> /ppm pyr, (b) 3.85 mg O <sub>3</sub> /ppm pyr, (c) 16 mg O <sub>3</sub> /ppm pyr	. 279
B19	Deionized water extract chromatogram for 5% moisture, 25°C (pH 8) pyrene contaminated soil. (a) 2.2 mg O <sub>3</sub> /ppm pyr, (b) 3.85 mg O <sub>3</sub> /ppm pyr, (c) 16 mg O <sub>3</sub> /ppm pyr	280
B20	Acetonitrile extract chromatogram for 10% moisture, 25°C (pH 8) pyrene contaminated soil. (a) 2.2 mg O <sub>3</sub> /ppm pyr, (b) 3.85 mg O <sub>3</sub> /ppm pyr, (c) 16 mg O <sub>3</sub> /ppm pyr	. 281
B21	Deionized water extract chromatogram for 10% moisture, 25°C (pH 8) pyrene contaminated soil. (a) 2.2 mg O <sub>3</sub> /ppm pyr, (b) 3.85 mg O <sub>3</sub> /ppm pyr, (c) 16 mg O <sub>3</sub> /ppm pyr	. 282
B22	Acetonitrile extract chromatogram for dry, 13°C (pH 2) pyrene contaminated soil. (a) 2.2 mg O <sub>3</sub> /ppm pyr, (b) 3.85 mg O <sub>3</sub> /ppm pyr, (c) 16 mg O <sub>3</sub> /ppm pyr	. 283
B23	Deionized water extract chromatogram for dry, 13°C (pH 2) pyrene contaminated soil. (a) 2.2 mg O <sub>3</sub> /ppm pyr, (b) 3.85 mg O <sub>3</sub> /ppm pyr, (c) 16 mg O <sub>3</sub> /ppm pyr	284
B24	Acetonitrile extract chromatogram for 5% moisture, 13°C (pH 2) pyrene contaminated soil. (a) 2.2 mg O <sub>3</sub> /ppm pyr, (b) 3.85 mg O <sub>3</sub> /ppm pyr, (c) 16 mg O <sub>3</sub> /ppm pyr	. 285
B25	Deionized water extract chromatogram for 5% moisture, 13°C (pH 2) pyrene contaminated soil. (a) 2.2 mg O <sub>3</sub> /ppm pyr, (b) 3.85 mg O <sub>3</sub> /ppm pyr, (c) 16 mg O <sub>3</sub> /ppm pyr	. 286

B26	Acetonitrile extract chromatogram for 10% moisture, 13°C (pH 2) pyrene contaminated soil. (a) 2.2 mg O <sub>3</sub> /ppm pyr, (b) 3.85 mg O <sub>3</sub> /ppm pyr, (c) 16 mg O <sub>3</sub> /ppm pyr	287
B27	Deionized water extract chromatogram for 10% moisture, 13°C (pH 2) pyrene contaminated soil. (a) 2.2 mg O <sub>3</sub> /ppm pyr, (b) 3.85 mg O <sub>3</sub> /ppm pyr, (c) 16 mg O <sub>3</sub> /ppm pyr	288
B28	Acetonitrile extract chromatogram for dry, 13°C (pH 6) pyrene contaminated soil. (a) 2.2 mg O <sub>3</sub> /ppm pyr, (b) 3.85 mg O <sub>3</sub> /ppm pyr, (c) 16 mg O <sub>3</sub> /ppm pyr	289
B29	Deionized water extract chromatogram for dry, 13 °C (pH 6) pyrene contaminated soil. (a) 2.2 mg O <sub>3</sub> /ppm pyr, (b) 3.85 mg O <sub>3</sub> /ppm pyr, (c) 16 mg O <sub>3</sub> /ppm pyr	290
B30	Acetonitrile extract chromatogram for 5% moisture, 13°C (pH 6) pyrene contaminated soil. (a) 2.2 mg O <sub>3</sub> /ppm pyr, (b) 3.85 mg O <sub>3</sub> /ppm pyr, (c) 16 mg O <sub>3</sub> /ppm pyr	291
B31	Deionized water extract chromatogram for 5% moisture, 13°C (pH 6) pyrene contaminated soil. (a) 2.2 mg O <sub>3</sub> /ppm pyr, (b) 3.85 mg O <sub>3</sub> /ppm pyr, (c) 16 mg O <sub>3</sub> /ppm pyr	292
B32	Acetonitrile extract chromatogram for 10% moisture, 13°C (pH 6) pyrene contaminated soil. (a) 2.2 mg O <sub>3</sub> /ppm pyr, (b) 3.85 mg O <sub>3</sub> /ppm pyr, (c) 16 mg O <sub>3</sub> /ppm pyr	293
B33	Deionized water extract chromatogram for 10% moisture, 13°C (pH 6) pyrene contaminated soil. (a) 2.2 mg O <sub>3</sub> /ppm pyr, (b) 3.85 mg O <sub>3</sub> /ppm pyr, (c) 16 mg O <sub>3</sub> /ppm pyr	294
B34	Acetonitrile extract chromatogram for dry, 13°C (pH 8) pyrene contaminated soil. (a) 2.2 mg O <sub>3</sub> /ppm pyr, (b) 3.85 mg O <sub>3</sub> /ppm pyr, (c) 16 mg O <sub>3</sub> /ppm pyr	295
B35	Deionized water extract chromatogram for dry, 13°C (pH 8) pyrene contaminated soil. (a) 2.2 mg O <sub>3</sub> /ppm pyr, (b) 3.85 mg O <sub>3</sub> /ppm pyr, (c) 16 mg O <sub>3</sub> /ppm pyr	296
B36	Acetonitrile extract chromatogram for 5% moisture, 13°C (pH 8) pyrene contaminated soil. (a) 2.2 mg O <sub>3</sub> /ppm pyr, (b) 3.85 mg O <sub>3</sub> /ppm pyr, (c) 16 mg O <sub>3</sub> /ppm pyr	297
<b>B</b> 37	Deionized water extract chromatogram for 5% moisture, 13°C (pH 8) pyrene contaminated soil. (a) 2.2 mg O <sub>3</sub> /ppm pyr,	

		(b) 3.85 mg O <sub>3</sub> /ppm pyr, (c) 16 mg O <sub>3</sub> /ppm pyr	
1	B38	Acetonitrile extract chromatogram for 10% moisture, 13°C (pH 8) pyrene contaminated soil. (a) 2.2 mg O <sub>3</sub> /ppm pyr, (b) 3.85 mg O <sub>3</sub> /ppm pyr, (c) 16 mg O <sub>3</sub> /ppm pyr	
1	B39	Deionized water extract chromatogram for 10% moisture, 13°C (pH 8) pyrene contaminated soil. (a) 2.2 mg O <sub>3</sub> /ppm pyr, (b) 3.85 mg O <sub>3</sub> /ppm pyr, (c) 16 mg O <sub>3</sub> /ppm pyr	
]	B40	Acetonitrile extract chromatogram for aged, dry, 25°C (pH 2) pyrene contaminated soil. (a) 2.2 mg O <sub>3</sub> /ppm pyr, (b) 3.85 mg O <sub>3</sub> /ppm pyr, (c) 16 mg O <sub>3</sub> /ppm pyr	
]	B41	Acetonitrile extract chromatogram for aged, dry, 25°C (pH 6) pyrene contaminated soil. (a) 2.2 mg O <sub>3</sub> /ppm pyr, (b) 3.85 mg O <sub>3</sub> /ppm pyr, (c) 16 mg O <sub>3</sub> /ppm pyr	
Ì	B42	Acetonitrile extract chromatogram for age, dry, 25°C (pH 8) pyrene contaminated soil. (a) 2.2 mg O <sub>3</sub> /ppm pyr, (b) 3.85 mg O <sub>3</sub> /ppm pyr, (c) 16 mg O <sub>3</sub> /ppm pyr	
(	C1	GC/MS spectra for pyrene standard (Compound I)	
(	C2	GC/MS spectra proposed for Compound I	
(	C3	GC/MS spectra proposed for Compound II A/B	
(	C4	GC/MS spectra proposed for Compound III(A)	
	C5	GC/MS spectra proposed for Compound III(B)	
(	C6	GC/MS spectra proposed for Compound IV A/B	
(	C7	GC/MS spectra proposed for Compound V	
(	C8	GC/MS spectra for Compound VI	
(	C9	GC/MS spectra for 2,2',6,6'-biphenyl tetraaldehyde standard (Compound VII)	
(	C10	(a) GC/MS spectra #1 proposed for Compound VII	
		(b) GC/MS spectra #2 proposed for Compound VII	

C11	(a) GC/MS spectra #1 proposed for Compound VIII A/B	316
	(b) GC/MS spectra #2 proposed for Compound VIII A/B	317
C12	(a) GC/MS spectra #1 proposed for Compound IX A/B	318
	(b) GC/MS spectra #2 proposed for Compound IX A/B	319
C13	(a) GC/MS spectra #1 proposed for Compound X	320
	(b) GC/MS spectra #2 for Compound X	32
C14	GC/MS spectra for 2,2',6,6'-biphenyl tetracarboxylic acid standard	
C15	GC/MS spectra proposed for Compound XI	
C16.	GC/MS spectra for unknown compound #1 (m/z 309)	
C17	(a) GC/MS spectra #1 for unknown compound #2 (m/z 340)	
D1	(b) GC/MS spectra #2 for unknown compound #2 (m/z 341)  Example of the ozone breakthrough curve for soil in 15 cm column	
	acting as an ozone destruct unit	344

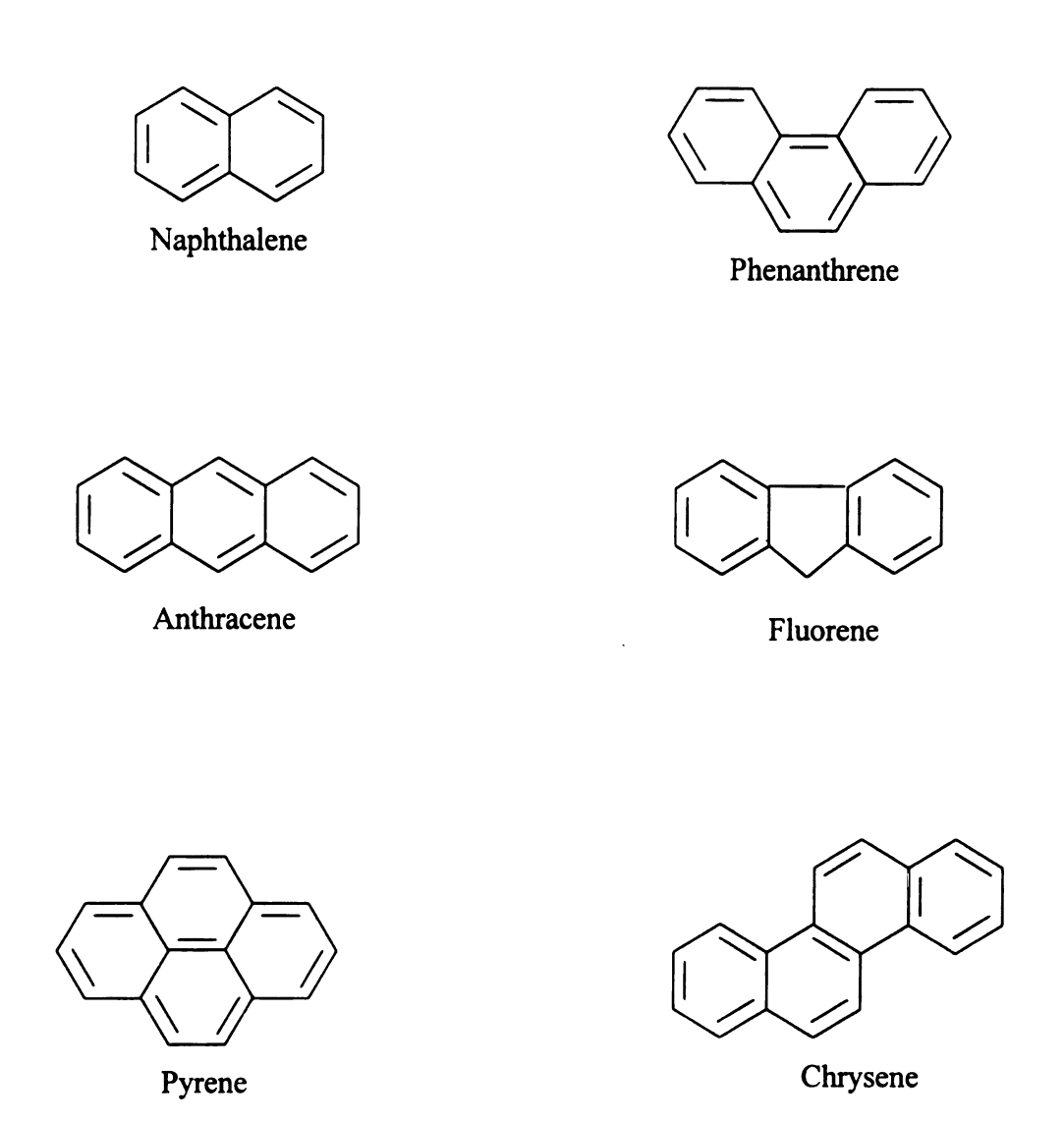
#### Chapter 1

#### 1.1 Introduction

### Background and Environmental Significance

Polycyclic aromatic hydrocarbons (PAHs) are compounds produced during the burning of coal, oil, gasoline, and organic matter and are present in coal tars, diesel fuel, oil and gasoline (Figure 1). In the atmosphere, PAHs are associated with soot, smog, and particulate matter. At petroleum hazardous waste sites, PAHs are components of nonaqueous phase liquids (NAPLs) such as coal tars, creosotes, and petroleum distillates contaminating soil and groundwater [1]. The U.S. Environmental Protection Agency (EPA) lists 16 PAHs as priority pollutants and eight as carcinogens or potential carcinogens causing skin, liver, and/or lung cancer in humans. These compounds present a remediation challenge because they are highly recalcitrant, insoluble in water, and tend to accumulate on solid surfaces [2].

US Superfund Sites with extensive PAH contamination include a number of locations where gas, petroleum, and paper manufacturing facilities operate or once operated. The concentrations seen at these sites depend on the PAH source (i.e., industrial waste, leaking petroleum storage tanks, accidental spills), the properties of the individual chemical (i.e., solubility, structure), and soil properties (i.e. organic matter content, porosity, and degree of water saturation). For Superfund sites contaminated by PAHs, the US Records of Decisions (US ROD) will document the methods considered for the remediation of a site and the rational for the final method chosen for implementation [3-5]. Many of the RODs report excavation of PAH contaminated soil as the primary remediation technique chosen for sites. Following excavation, the soil was either



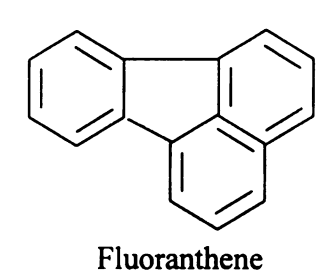


Figure 1. Representative PAH compounds

incinerated or stored at an approved storage facility. For sites where the PAH concentrations were low, sealing and capping of the contaminated area was also a method implemented. Excavating, incinerating, and properly disposing of PAH contaminated soil can be an expensive undertaking and might not be a feasible remediation choice based upon the extent of site contamination. For this reason, *in-situ* processes are of interest to reduce remediation costs.

A novel approach for *in-situ* treatment of PAHs is the use of ozone. Ozonation processes are increasingly being investigated because process application can be both technically efficient and cost effective for PAH removal [6-10]. Ozonation processes are advantageous because they employ the use of highly reactive gaseous ozone (O<sub>3</sub>) molecules or solutions with dissolved O<sub>3</sub> to oxidize contaminants. Ozonation processes are currently being implemented in water treatment to improve color, odor, and to control bacteria growth [11]. Additional applications have shown effective implementation of ozonation in soil [7, 12-13]. The system is versatile because it is a chemical process that can be used in gaseous form or in ozone saturated aqueous form and it is not limited by PAH toxicity like bioremediation.

The disadvantages in implementing ozonation processes are: (1) numerous oxidation byproducts are produced, (2) little research has been performed identifying chemical structures of the byproducts, and (3) few toxicology evaluations of ozonation byproducts are available. Ozonation byproducts in aqueous systems have been identified in numerous studies [14-16]. Ozonation byproducts in soil systems, however, have not been evaluated as extensively [17, 18]. Therefore, more research on the use of PAH ozonation for in-situ remediation is needed.

#### 1.2 Objective and Order of Thesis

The overall objective of this research was to evaluate the efficacy of using gaseous ozone to remediate PAH contaminated soil. The target PAH compound, pyrene, was selected because the literature available provides a good foundation for understanding the ozonolysis of pyrene in aqueous and soil systems [14, 15, 17-19].

The first phase of this study (Chapter 2) was designed to investigate the affect various soil conditions such as soil pH, temperature, soil moisture, and soil contaminant age would have on pyrene oxidation. These variables were selected to represent environmental conditions that could impact *in-situ* ozonation in unsaturated soil. The selected soil was a sandy, loam Metea soil that has been used in previous PAH ozonation studies [7, 9, 20]. Using soil columns, gaseous ozone was supplied to the pyrene contaminated soil for the desired experimental time. The ozone concentration in the inlet and outlet gas stream was monitored to develop ozone breakthrough curves (BTC) and to calculate the ozone dose delivered to the soil. The effect soil conditions had on ozonation efficiency was evaluated by measuring the reduction of pyrene concentrations in the soil.

In the second phase of the study (Chapter 3,) polar and non-polar solutions were used to extract the pyrene ozone byproducts from the soil. The two solvents were used to extract the oxidized compounds that would readily dissolve in groundwater (polar compounds) and the compounds that would remain bound to the soil (non-polar compounds) after treatment. For each experiment, three ozone doses were used to determine the effect ozone dose has on byproduct formation. The byproducts were fractionated and structurally identified using GC/MS. The results were then compared to

the byproducts published in literature for pyrene ozonation byproducts in aqueous systems.

The third phase of the research (Chapter 4) evaluated the toxicity of two pyrene ozonation byproducts. Two synthesized byproducts were used in the analysis because pyrene ozonation byproducts are not commercially available. A previous study by Herner [16] also addressed the difficulty in isolating and purifying pyrene ozonation byproducts from ozonated mixtures. The Scrape Load/Dye transfer assay was used to measure the ability of a compound to interfere with normal Gap Junctional Intercellular Communication (GJIC).

Chapter 5 of the study discusses reaction kinetics for the experimental data collected in the short soil column (15 cm) ozonation studies. This chapter also addresses the ozone transport model developed by Hsu et al. [20]. The goal for this phase of the research was to apply the model to data collected from a 3.5-foot soil column. The model was also applied to experimental data from the 15 cm soil column.

#### 1.3 References

- Ghoshal, S.; Weber, W.; Rummel, A.; Trosko, J.; Upham, B.; "Epigenetic Toxicity of a mixture of Polycyclic Aromatic Hydrocarbons on Gap Junctional Intercellular Communication before and after biogradation". Environ. Sci. Technol. 1999, 33(7), 1044 – 1050.
- 2. Sontag, J. In <u>Carcinogen in Industry and Environment</u>. New York: Marcel Dekher, Inc., 1981, 169.
- 3. United States Record of Decision. EPA/ROD/R-06-89/053, 1989.
- 4. United States Record of Decision. EPA/ROD/R-06091/066, 1991.
- 5. United States Record of Decision. EPA 541-R99-111, 1999.
- 6. Masten, S. and Davies, S.; "The Use of Ozonation to Degrade Organic Contaminants in Wastewaters". *Enviro. Sci. Technol.* 1994, 28(4), 181A 185A.
- 7. Yao, J.; "Ozonation of Soils Contaminated with Polycyclic Aromatic Hydrocarbons (PAHs)", M.S. Thesis, Department of Civil and Environmental Engineering, Michigan State University, 1991.
- 8. Neff, J.; "Polynuclear Aromatic Hydrocarbons in Aqueous Environment: Sources, Fates and Biological Effects", Applied Science, London. 1979, 227.
- 9. Day, J.; "The Effect of Soil Moisture on the Ozonation of Pyrene in Soils", M.S. Thesis, Department of Civil and Environmental Engineering, Michigan State University, 1994.
- 10. Zeng, Y.; Hong, P.; Wavrek, D. "Chemical-Biological Treatment of Pyrene". Water Res. 2000, 34(4), 1157-1172.
- 11. Langlais, B; Reckhow, D; Brink, D. Editors. Ozone in Water Treatment: Application and Engineering. Lewis Publihers, Inc., 1991. 11 43.
- 12. Masten, S.; "Ozonation of VOC's in the presence of Humic Acid". Ozone. Sci. Eng. 1991, 13(3), 287-312.
- 13. Nimmer, M.; Wayner, B.; Morr, A.; "In-situ Ozonation of Contaminated Groundwater". *Environmental Progress.* 19(3). **2000**. 183 196.
- 14. Bailey, P.; Ozonation in Organic Chemistry, Volume II. Non-Olefinic Compounds. Academic Press: New York, 1982. 43 109.

- 15. Yao, J.J; Huang, Z.; Masten, S.; "The Ozonation of Pyrene: Pathway and Product Identification". Water. Res. 1998, 32(10), 3001-3012.
- 16. Herner, H.; "The Reaction of Ozone with Pyrene: The Byproducts and Their Toxicological Implications". Ph.D. Dissertation, Department of Civil and Environmental Engineering, Michigan State University, 1999.
- 17. Eberius, M; Berns, A; Schuphan, I.; "Ozonation of pyrene and benzo[a]pyrene in silica and soil- C<sup>14</sup> balances and chemical analysis of oxidation products as a first step to ecotoxicological evaluation". Fresnius Z. Anal., 1997, 359, 274-279.
- 18. Zeng, Y.; Hong, P.; Wavrek, D. "Chemical-Biological Treatment of Pyrene". Water Res. 2000, 34(4), 1157-1172.
- 19. Copeland, P.; Dean, R.; McNeil, D.; "The Ozonolysis of Polycyclic Hydrocarbons: Part II". J. Chem. Soc. 1961, 1232 1236.
- 20. Hsu, I.; The Use of Gaseous Ozone to Remediation the Organic Contaminants in the Unsaturated Soils, Ph.D. Thesis, Department of Civil and Environmental Engineering, Michigan State University, 1995.

#### **CHAPTER 2**

#### **Ozonation Studies**

#### 2.1 Introduction

In-situ ozonation is increasingly becoming acceptable for groundwater and soil treatment [1]. Ozonation offers a novel approach to remediate a broad range of compounds in aqueous and soil systems [2]. Laboratory studies and field studies in soil show effective reduction of various types of PAHs [4-8]. A recent study of in-situ ozonation showed significant reduction of target petroleum waste in groundwater at contaminated sites in Wisconsin. The studies demonstrated successful reduction of total PAH concentrations to environmentally acceptable levels at three different sites [9]. In 2001, in-situ ozonation was approved by the US EPA and Michigan Department of Environmental Quality (MDEQ) to treat a ground water plume at the Rasmussen Dump in Brighton, MI [10]. The Rasmussen Dump is reported to contain 13 volatile organic compounds (VOCs), 3 semi-VOCs, and 2 metals.

Ozone (O<sub>3</sub>) is known to be effective in oxidizing, or reducing the concentration of, many types of compounds. Many factors can affect the amount and total cost of ozone needed to remediate a site. The feasibility of using ozone for soil remediation is largely determined by the ability to reduce contamination to acceptable levels in a cost effective manner. This issue often becomes the factor which prevents the selection of ozonation processes for field remediation [11]. This chapter focuses on evaluating the effect pH, temperature, and soil moisture will have on ozonation efficiency and pyrene removal.

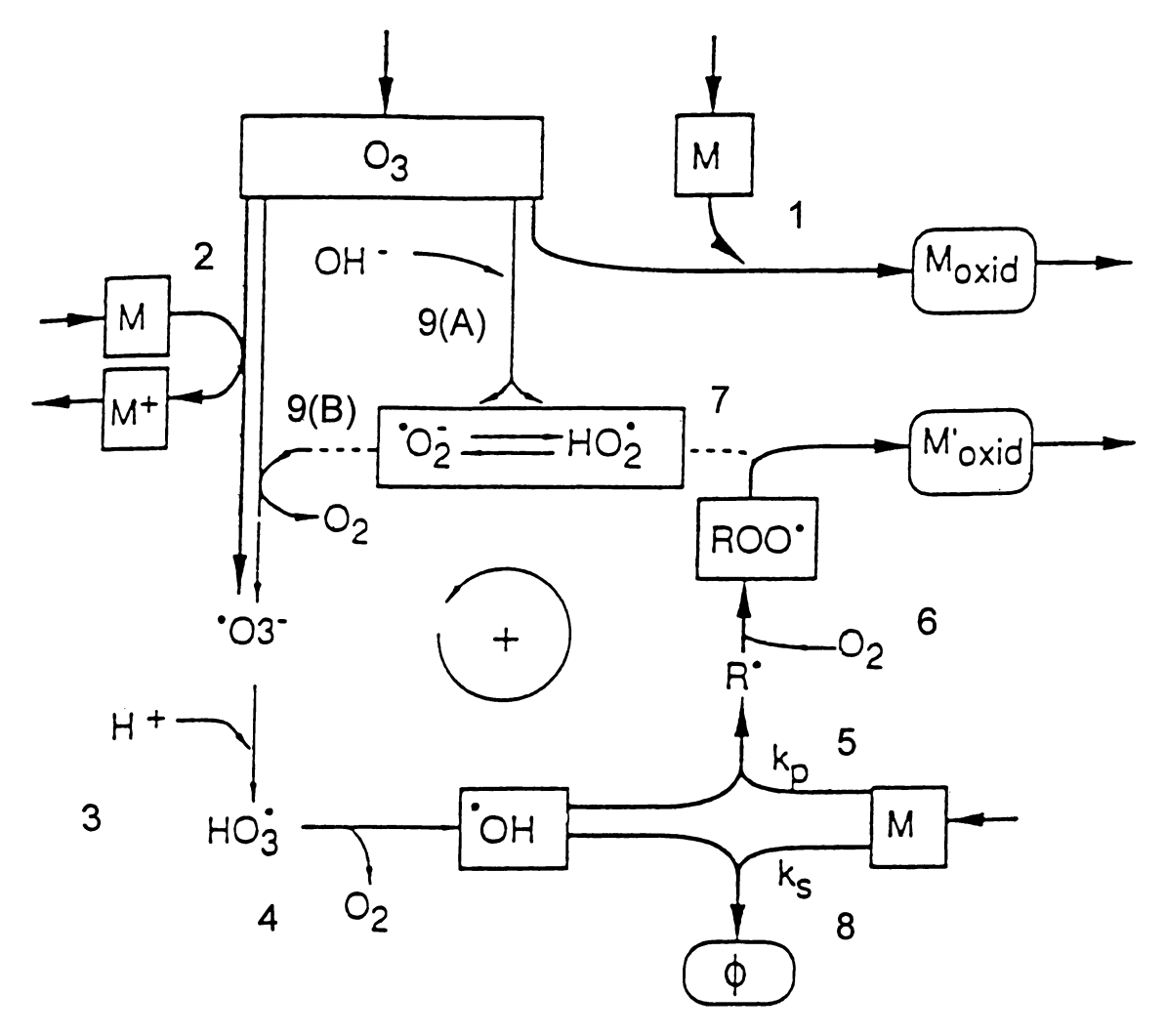
#### 2.2 Background

#### a. Ozone Reactions

Ozone is a very strong oxidant (E<sub>o</sub>= 2.06 V) that can effectively degrade many compounds [12, 13]. Ozone has primarily been implemented in water treatment for disinfection and algae control, oxidation of inorganic and organic pollutants, taste and odor control, and color removal [14]. Staëhelin and Hoigné [15] showed that in aqueous systems with organic components, two mechanisms are involved in the oxidation of constituents within the system. The first mechanism involves the direct reaction of compounds with molecular ozone. The second mechanism involves the indirect reaction of compounds with radical species that are formed when ozone decomposes. This model is also believed to be applicable in soil [6]. If this is true, then like aqueous systems, the extent of compound oxidation by ozone will be affected by direct reactions with ozone and ozone decomposition caused by indirect reactions.

The mechanism by which ozone reacts with organic compounds is complex (see Figure 2.1). Mechanism 1 represents direct ozone attack of target solute M. Solute M, when present in the system, may directly react with ozone to form a new compound  $(M_{oxid})$  (Step 1). Solute M may react with  $O_3$  by electron transfer to produce a protonated reactive compound  $(M^+)$  and an ozonide ion radical  $(^{\bullet}O_3^-)$  (Step 2).

The indirect reaction (mechanism 2) involves the reaction of Solute M with radical species, primarily hydroxyl ions (OH'), created from ozone decomposition. In solution, ozone can react with OH' ions to form one superoxide anion ( $\cdot$ O<sub>2</sub>') and one hydroperoxyl radical (HO<sub>2</sub>°). Both the superoxide anion and the hydroperoxyl radical are



(adapted from Staehelin and Hoigné, 1985)

Figure 2.1. Mechanism of Aqueous Ozonolysis Reaction with a target solute

in acid-base equilibrium and become the driving force for the cyclic reaction. Ozone reacts with  ${}^{\circ}O_2^{-}$  anions, resulting in the production of ozonide ( ${}^{\circ}O_3^{-}$ ) (Step 9b). A two-step reaction using the ozonide and hydrogen ions produces  ${}^{\circ}OH$  radicals (Step 3 – 4). These  ${}^{\circ}OH$  radicals react with Solute M to produce the M oxid and HO2 radicals (Step 7). The cycle continues with HO2 radicals regenerating superoxides (Step 8). The rate of ozone decomposition is readily affected by pH; therefore, OH ion concentrations will determine the initiation rate for this mechanistic pathway.

Direct reactions predominate at low pH. Indirect reactions will also occur at low pH, but to a limited extent [14]. As the pH (i.e., OH ion concentrations) increases, direct ozonation will continue and the occurrence of indirect reactions will increase.

#### b. Ozone reactions with Polycyclic Aromatic Hydrocarbons

PAH oxidation by ozone might involve either the aromatic ring or one of the sidechain constituents [12 - 14]. Fused-ring aromatics are classified into three categories for ozone attack. The three categories are: (I) 1, 3-dipolar cyclo addition (Criegee mechanism) which occurs at across the double bond, (II) ozone attack, which occurs where the bond of lowest bond localization is the same as the atom of lowest atom localization, or (III) ozone attack, which might occur either at the bond of lowest bondlocalization energy or the atom of lowest atom-localization energy [12, 14].

Many aromatic compounds exhibit what is called high para-localization energies, where the atom of lowest atom-localization energy is included in the bond of lowest bond-localization energy (Category II) (See Figure 2.2). These compounds include naphthalene, phenanthrene, benzo[c]phenanthrene, chrysene, triphenylene,

dibenzo[c,g]phenanthrene, perylene, dibenzo[g,p]chrysene, and coronene. Other polycyclic aromatics exhibit competition between bond attack and atom attack for ozone (Category III) (See Figure 2.3). In these compounds, the atom with the lowest localization energy is not included in the bond with the lowest-localization energy. These compounds include pyrene, benzo[a]pyrene, benz[a]anthracene, benzo[r,s,t]pentaphene, anthracene, naphthacene, benzo[c]phenanthrene, dibenz[a,h]anthracene, dibenz[a,j]-anthracene, and pentaphene.

Table 2.1 lists the localization energies and the type of ozone reaction that occurs for selected PAH compounds. Naphthalene exhibits Category II type reactions where ozone attack occurs at the 1, 2 bond with the lowest bond localization energy. The 1, 2 bond also includes the atom of lowest atom-localization. Anthracene (Category III) exhibits ozone attack at the sites with the lowest atom-localization energy. Pyrene (Category III) undergoes ozone attack at the 4, 5 bond exhibiting the lowest bond-localization energy.

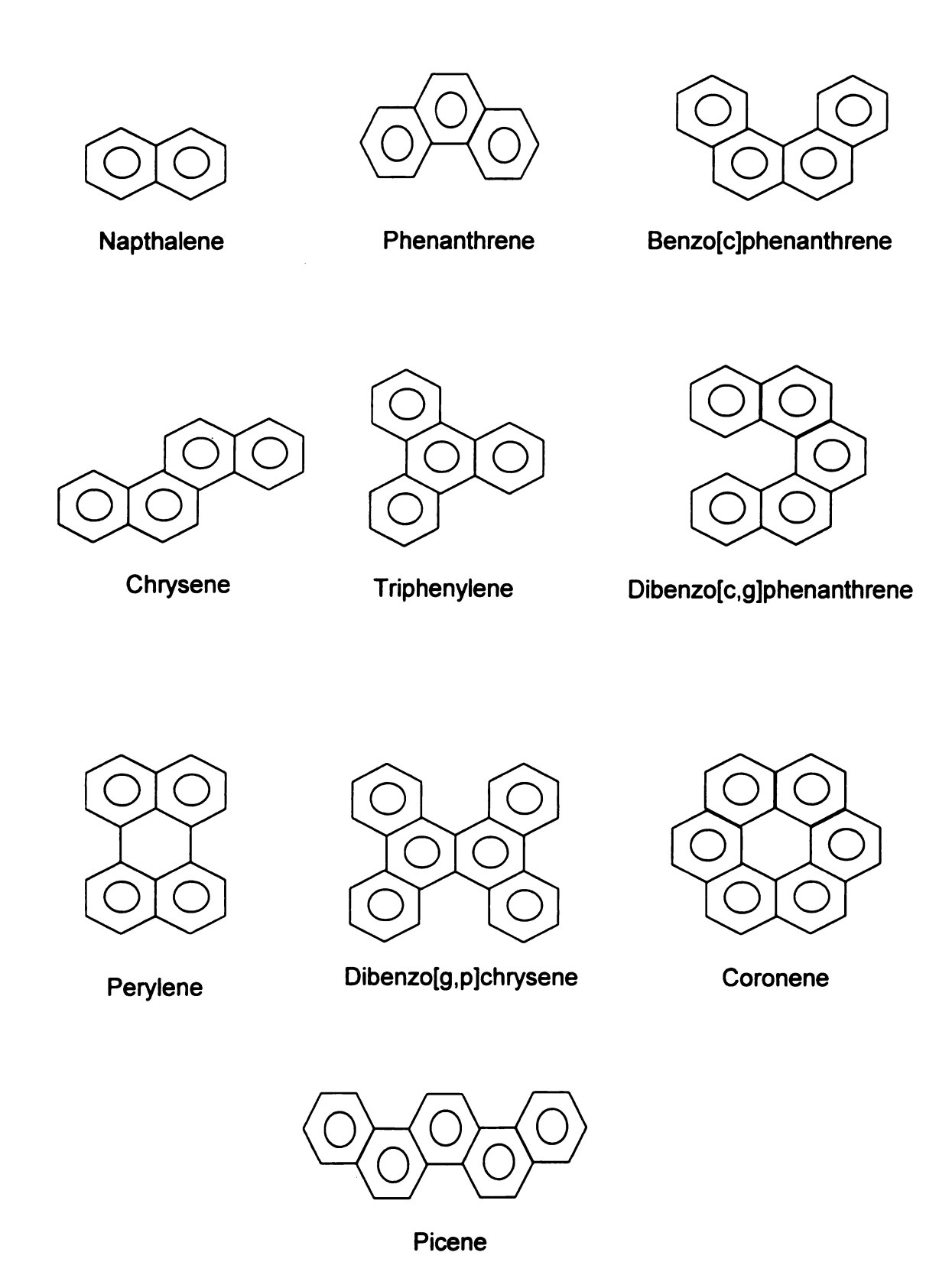


Figure 2.2. Structures for Category II PAH compounds

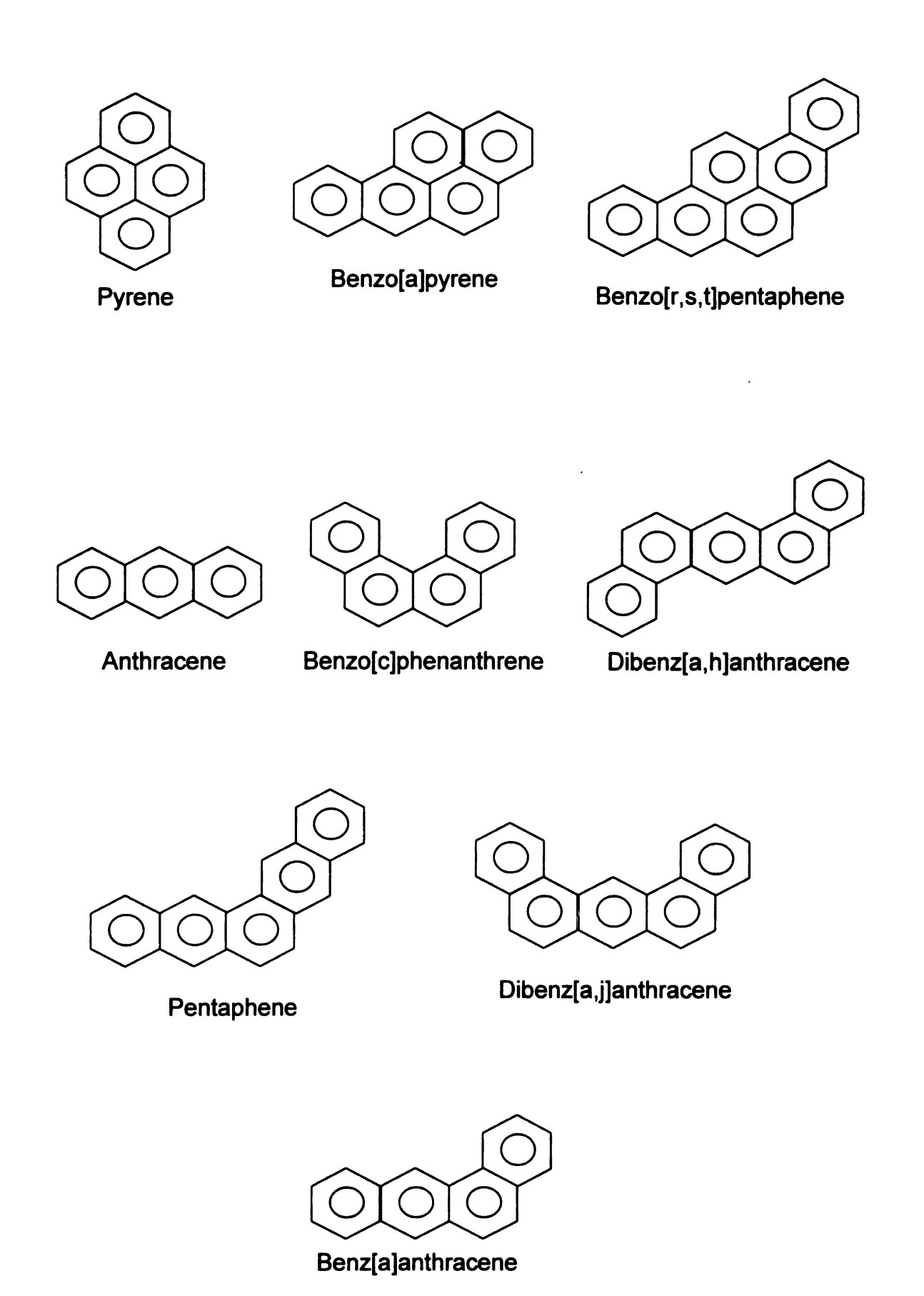


Figure 2.3. Structures for Category III PAH compounds

Table 2.1. The bond/atom localization energies and the type of ozone reaction that occurs for representative PAH compounds.

Hydrocarbon	Most	Bond-	Most	Atom-	Ozone
-	reactive	localization	reactive	localization	reaction Type
	bond	energy <sup>a</sup>	atom	energy <sup>b</sup>	
Phenanthrene	9, 10	1.07	9	1.79	II
Picene	5, 6	1.11	5	1.67	II
Chrysene	5, 6	1.12	6	1.67	II
Naphthalene	1, 2	1.26	1	1.81	II
Pyrene	4, 5	1.06	3	1.51	III
,					Bond Attack
Benzo [a] pyrene	4, 5	1.02	6	1.15	III
					Atom Attack
Anthracene	1, 2	1.20	9	1.26	III
					Atom Attack
Benz[a]anthracene	5, 6	1.03	7	1.35	III
					Bond Attack

- a. Brown (1950) as cited in Bailey [12].
- b. Dewar (1952) as cited in Bailey [12].

# 2.3 Soil remediation using Ozonation processes

Direct ozone reactions and ozone decomposition in soil are affected by soil properties (i.e., organic matter, degree of water saturation, pH, temperature) and by the properties of PAH compounds (i.e., solubility, adsorption strength). Therefore, the amount of ozone required and the efficiency of PAH removal will vary based on these combined environmental factors.

## a. Ozone Reaction with Organic Matter

The consumption of ozone by a number of the constituents in soil organic matter is a concern when assessing the feasibility of *in-situ* ozonation. Soil organic matter is largely comprised of humic acid and fulvic acid that form stable complexes with iron and

manganese [16]. Ozone decomposition occurs as a result of reactions with these components [7]. Xiong and Legube [17] determined that organic matter played both initiation and promotion roles in ozone decomposition. Fulvic acid did not participate in the radical type decomposition of ozone at high pH; although increasing the pH did facilitate the decomposition of ozone in water [17]. Lindsay et al. [16] observed that in the presence of dissolved natural organic matter, fulvic acid, and humic acid increased ozone decomposition by producing hydroxyl radicals. In this study, the indirect reaction of ozone with the radical species inhibited the degradation of pyrene. The rate of pyrene degradation changed from first order to second order [16].

### b. The influence of water and soil saturation on Ozonation

Ozone decomposes in water to form radical species which promote mechanism 2 in ozonolysis. As discussed earlier, OH ions will react with ozone to produce ozonide and hydroxyl peroxide. The OH radicals will increase ozone decomposition and decrease PAH degradation rates [18, 19]. In unsaturated soils, pore water will most likely be present and able to react with molecular ozone. Therefore, if soil ozonation resembles aqueous ozonation, at low pH, direct ozonation will predominate. At higher pH levels, indirect reactions will impact these reactions. Studies researching the behavior of ozone in the presence of organic matter and the various contaminants in soil suggest that the formation of hydroxyl (·OH) radicals may help facilitate the oxidation of PAHs [3, 15, 6-8].

### c. Surface Adsorption and Bond-Localization Strength

Many organic chemicals, including PAHs, bind to organic macromolecules in soil and become relatively immobile. The more hydrophobic compounds are readily adsorbed to lipophilic organic matter in soils. Water can interfere with PAH adsorption onto soil by coating soil surfaces, thereby decreasing the sites available for chemical adsorption [7]. Studies have also suggested that during cycles of wetting and re-wetting of soil surfaces, the polar parts of organic molecule become oriented towards the soil surface and coalesce upon drying [7].

For all soil bound contaminants, the ability to oxidize target compounds is influenced by hydrophobic bonding and the bond-localization energy. The amount of ozone required for removal will vary depending on the PAH mixture present in the soil and the strength by which these compounds are sorbed to the soil. Compounds in soil for long periods of time are theorized to be more strongly sorbed to the soil matrix than those compounds that are the result of recent contamination events. Sorption strength and contaminant age therefore are important factors that might determine ozone efficiency and PAH removal.

PAHs with high partition coefficients (log  $K_{oc}$ ) have strong bond-localization energies and a high affinity for soil organic matter. Thus, the more strongly adsorbed contaminants require higher ozone dosages for removal. PAHs with low  $K_{oc}$  (e.g. phenanthrene, anthracene) values are more easily degraded by ozone than PAHs with high  $K_{oc}$  (e.g. pyrene and chrysene) [3]. In dry Metea soil studies, Yao [3] reported that 95% of phenanthrene ( $K_{oc} = 6.12$ ) was removed using 582 mg O<sub>3</sub>. Pyrene ( $K_{oc} = 6.51$ ) contaminated soil ozonated using 581 mg O<sub>3</sub> resulted in 83% removal. Chrysene ( $K_{oc} = 6.51$ )

6.27), however, was only removed by 40% using 582 mg O<sub>3</sub>. The lower efficiency in pyrene and chrysene removal was attributed to the higher partition coefficients and a higher affinity for the soil.

### d. Temperature in soil

Ozone decomposition increases with increasing temperature [20, 21]. Figure 2.4 shows a soil-temperature profile representing temperature variance from season-to-season in a frost-free region [22]. At winter temperatures, ozone decomposition will decrease and direct ozonation would be more important in the reaction. Summer conditions should increase the rate of ozone decomposition. Sotelo et al. [21] showed that [OH] reactions were negligible at pH below 3 and temperatures from 10 - 40 °C. This result might indicate that the direct reactions occurring at low pH are not influenced by temperature, but at higher pH, the temperature will affect ozone efficiency.

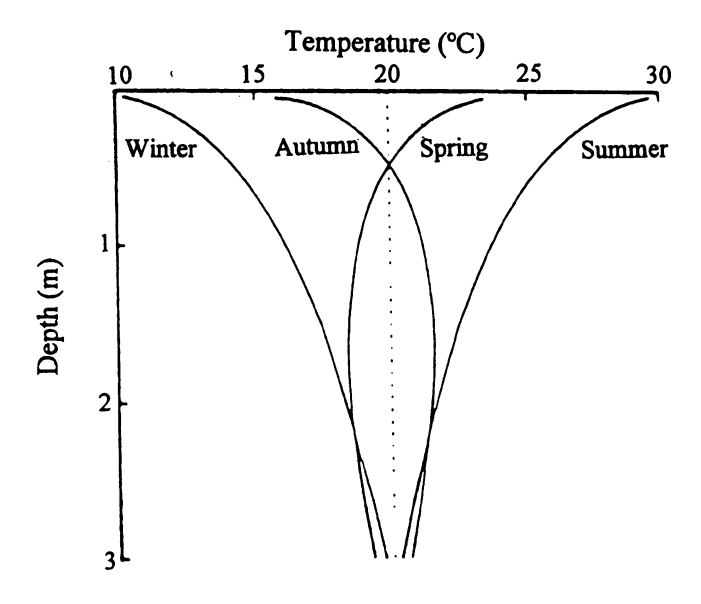


Figure 2.4. Seasonal temperature profile for soil 1-3 meters below the soil surface [22].

### 2.4 Experimental Outline and Rationale

Pyrene is a four ringed PAH causing skin, liver, and lung cancer in humans (Figure 2.5). This compound has been the target PAH for many ozonation studies. Aqueous ozonation studies include Copeland et al. [23], Bailey [12], Trapido et al. [25], Yao et al. [18], and Herner et al. [19]. Soil ozonations include Yao [3], Day [7], Hsu [6], Cole et al. [8], Eberius et al. [24], Zeng et al. [26]. Pyrene was selected for this study because the available literature provides a good foundation for understanding the ozonolysis of pyrene in aqueous and soil systems. The research conducted for this study could lead to improved use of ozone in PAH remediation. This phase of the research will investigate the effect of various conditions such as pH, temperature, soil moisture, and contamination duration have on ozone efficiency of pyrene removal from soil. Dry and moisturized soils were evaluated at various pH levels and temperatures. Soil stored for 6 months after it was contaminated was also evaluated to determine the effect of aging.

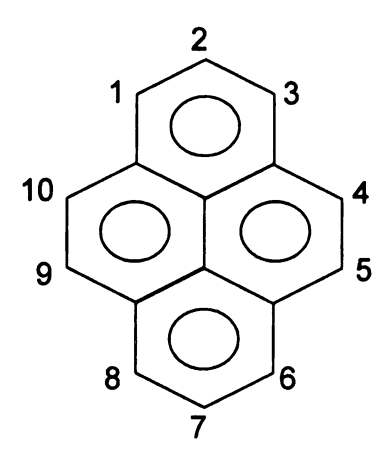


Figure 2.5. Pyrene

### Hypothesis for the effect of various conditions

The presence of water should decrease process efficiency by increasing the amount of ozone required to remove a PAH contaminant. One benefit from soil moisture, however, might be that water will directly react with ozone to form hydroxyl radicals, which will also be able to react with PAH compounds. The moisture levels evaluated were 0, 5% and 10% by weight. The pH levels of 2, 6, and 8 were selected for the soil conditions and are consistent with the pH levels used in many aqueous studies. Soil with a pH of 2 would naturally be too acidic for vegetation; however, this pH facilitates the investigation of the direct ozone reaction with pyrene. A pH of 6 was the natural pH of the Metea soil and is comparable to the pH of most natural soils and previous soil ozonation studies. A pH of 8 allows for the investigation of indirect reactions and the resulting pyrene removal and byproducts.

For the temperature studies, room temperature (25  $\pm$  4 °C) was selected to simulate spring/summer conditions and an average temperature of 13  $\pm$  2 °C was used for fall/winter conditions. It is expected that pyrene removal will improve with lower temperatures because ozone decomposition is low. The rate of pyrene removal is expected to decrease at higher temperatures.

The evaluation of soil spiked with 300 ppm pyrene and aged for 6 months at 25 °C should prove to be interesting because most soil studies have been conducted in freshly spiked soil (i.e., short contamination life). At Superfund sites, however, contamination has been present for many years. Sorption strength for PAHs is believed to increase with longer exposure times. This would result in the need to use more ozone to remediate aged soils. The aged soil studies should determine if the ozone demand

required to remove pyrene increases in soil contaminated for longer periods of time and if augmentation of conditions can improve process efficiency.

#### 2.4.1 Materials

*Chemicals*. Pyrene was purchased at a purity of 98% from Sigma Chemical (Sigma Chemical, St. Louis, MO).

Soil. A Metea soil excavated approximately 2 -3 ft below ground surface was selected for evaluations. The soil was collected from the southeast side of Michigan State University (MSU) Engineering Research Complex on research farm property. This type of soil was chosen due to its physical properties and its similarity to the soil used in previous ozonation studies conducted at MSU. The soil used was analyzed for physical and chemical characteristics by MSU Soils Testing Lab (Table 2.2).

Table 2.2. Physical and Chemical Characteristics of the Metea Soil

Soil Type:	Sandy-loam	
Soil pH:	6.2	
Sand	76.20%	
Silt	13.40%	
Clay	10.40%	
Phosphorus	58 mg/kg	
Potassium	14 mg/kg	
Calcium	238 mg/kg	
Magnesium	87 mg/kg	
Manganese	4.2 mg/kg	
Iron	15 mg/kg	
Organic Matter	0.40%	

Soil Preparation. Air-dried soil was sieved to remove any large debris such as rocks. To contaminate the soil, 0.15 g of pyrene was dissolved in < 20 mL of acetonitrile and sonicated for 10 minutes to assure complete dissolution of the solute. In a glass jar, 50 g of soil followed by a few drops of the PAH solution was added and shaken by hand. The process of adding soil and PAH solution was repeated until all of the PAH solution and a total dry weight of 500 g of soil was combined. The mixed soil was then shaken for 1 hour using a Mistral Multi-mixer (Lab-Line Instruments, Inc., Melrose Park, Ill). The soil was dried at room temperature and then stored in an airtight jar in the dark. Each batch of soil was used within one week of contamination. A concentration of 300 mg pyrene/kg soil (ppm pyrene) in soil was used for all experiments.

#### 2.4.2 Methods

Ozonation Experiments. Figure 2.6 shows a schematic of the experimental set-up. Ozone was generated in dried oxygen using a Polymetrics Model T-408 ozone generator (San Jose, CA). The experiments were conducted in a 2.5 cm (i.d.) x 15 cm reactor equipped with Teflon caps containing glass fiber filter paper at the inlet and outlet to uniformly distribute the gas flow. The flow of ozone into the reactor was regulated using a mass flow meter (Aalborg Instruments & Controls, Inc., Orangeburg, New York). The concentrations of ozone in the influent and effluent gas streams were measured spectrophotometrically at 258 nm using a UV-Visible light spectrophotometer (Model 1201, Shimadzu Scientific Instruments, Japan). The absorbance values for ozone were converted to concentration using a molar absorptivity coefficient for ozone of 3000 M<sup>-1</sup> cm<sup>-1</sup> [27]. Before entering the soil column, the gas stream was passed through a gas

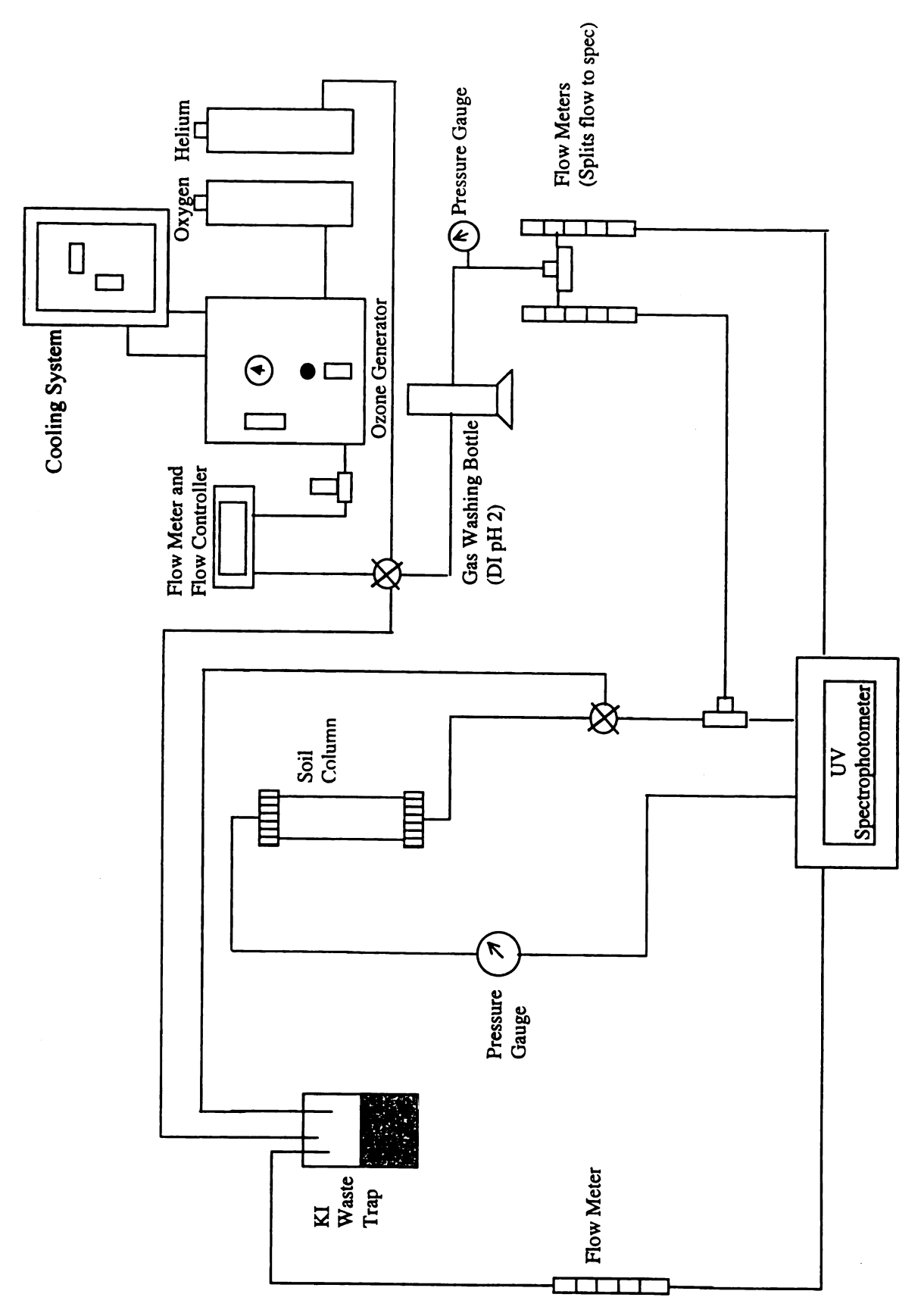


Figure 2.6. Schematic of the ozonation system.

washing bottle containing deionized water acidified to a pH of 2 using phosphoric acid. This provided a moisturized gas stream and prevented the soil in the columns from drying out. After each experiment, helium gas was used to purge ozone from the system. Excess ozone was destroyed in a 2% potassium iodide (KI) solution. Ozonation studies were conducted in triplicate and excess ozone experiments (ozonation time > 4 hours) were either duplicated or run in triplicate.

Dry Soil and Aged Soil Experiments. The soil was added to the column in 1 cm increments and packed level before the addition of more soil. The final bulk density for the dry soil after packing and settling was 1.1 g/cm<sup>3</sup>. The aged soil was contaminated using the same procedure described for soil preparation and stored for 6 months at room temperature in the dark. The conditions for packing and ozonation were identical to those used for the dry soil experiments.

Moisture Experiments. The column was wet packed with soil containing either 5% or 10% moisture to a uniform height in the column in the same manner described above. After packing, the bulk density was 1.05 g/cm<sup>3</sup> for the 5% moisture soil and 1.1 g/cm<sup>3</sup> for the soil containing 10% moisture. A wet packing method was chosen, as opposed to saturating the column and draining to the desired moisture content, to prevent the loss of residual pyrene that may dissolve in water and to assure reproducibility of the soil moisture content for the experiments. The moisture content of the soil was determined gravimetrically prior to ozonation and directly following ozonation using a 10 g sample of the test soil.

Experiments for pH. The soil was acidified to pH 2 using a 0.5 M H<sub>2</sub>SO<sub>4</sub> solution. For basic conditions, a pH of 8 was obtained using 0.01 M NaOH. The pH of the soil was tested prior to and directly following the ozonation process using two pH testing methods (pHydrion paper, Micro Essential Laboratory, Inc., Brooklyn, NY and Rapidest pH Soil Tester, Luster Leaf Products, Inc., Woodstock, IL).

Experiments for Temperature. An ambient temperature ( $25 \pm 4$  °C) was used to represent spring and summer time soil temperature. To represent fall and winter conditions, an average reactor temperature of  $13 \pm 2$  °C was maintained using the same ozonation system design in Figure 2.4 with modifications to the soil column. The column was wrapped with tubing forming a jacket for circulating chilled water down the length of the column (Figure 2.7a and 2.7b). After packing the column, the column and soil temperature were allowed to stabilize for 30 minutes. Ice in an insulated bucket was used to chill the glass bottle containing the recycled jacket water and was refilled as needed. The goal for the colder temperature experiments was to maintain a reactor temperature range from 10 - 15°C to represent fall or winter conditions.

Extraction. For this study, two factors influenced the extraction method selected. First, a mixture of byproducts, both polar and non-polar, was expected from the ozonation process. Therefore, a portion of the byproducts would be water-soluble and a portion would be soluble in organic solvents. Second, for future toxicology studies, the sensitivity of the biological assay to solvents must be considered. The types of solvents used for extraction should be non-toxic and kept at a minimum, so that samples from this

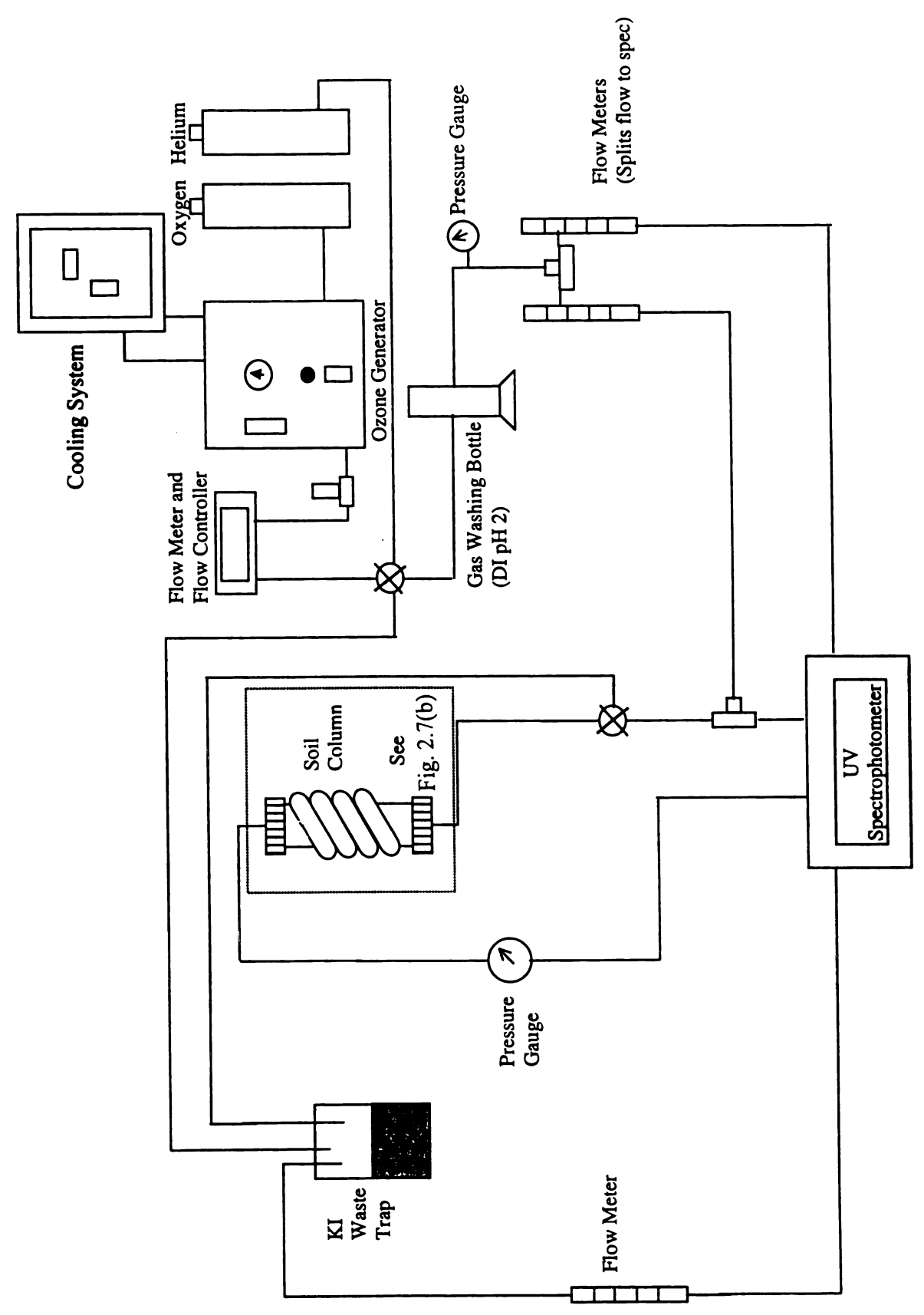


Figure 2.7 (a) Experimental set-up for 13°C ozonation system.

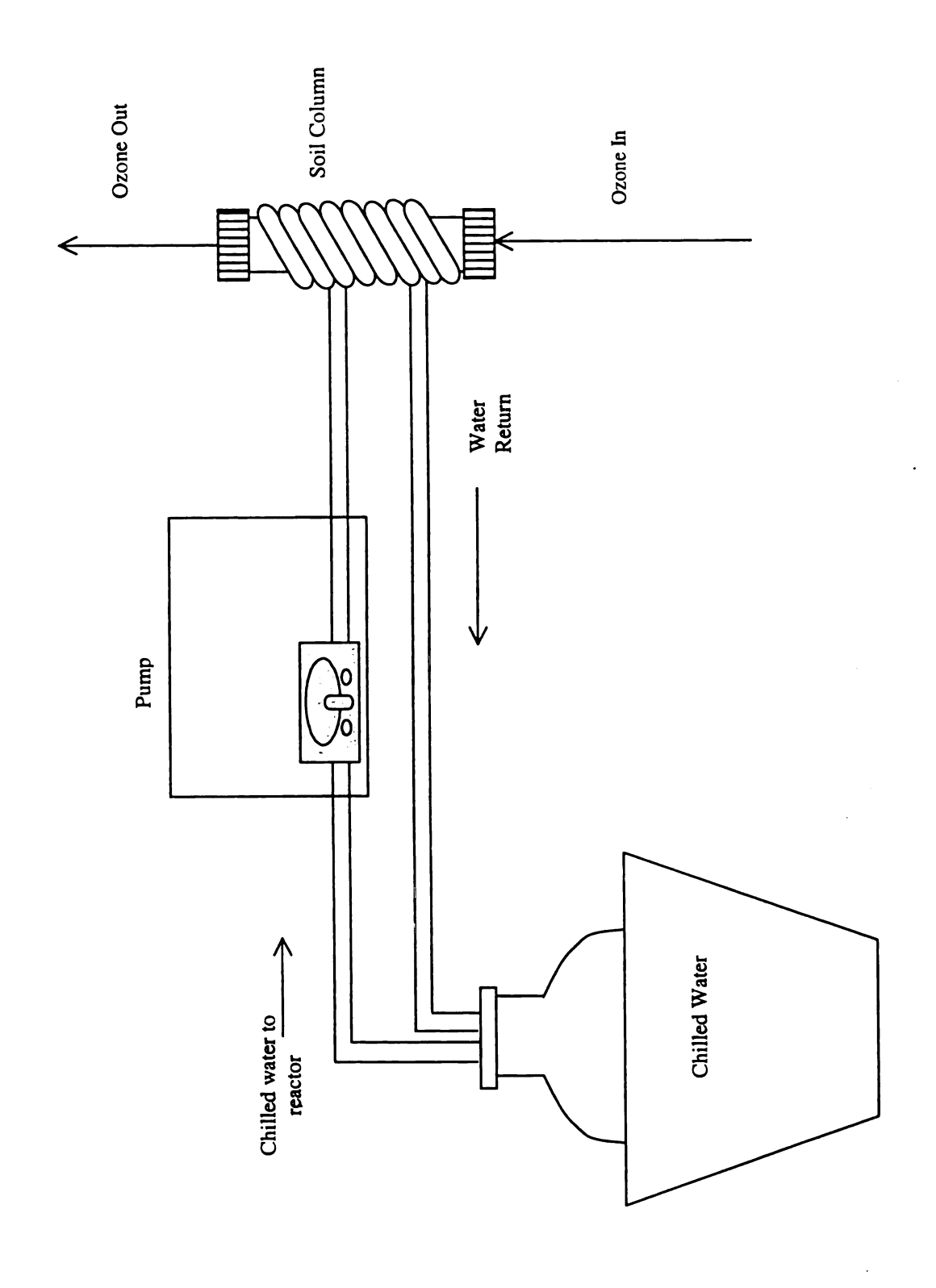


Figure 2.7 (b) Cooling system for column in the 13 ° C ozonation systems.

research could be dried and sent for toxicological evaluation. These reasons led to the selection of the direct-solvent extraction method. The extraction method was adapted from a method described by Grimmer et al. [28] and similar to Martens et al. [29]. Direct extraction is reported to result in removal efficiencies statistically similar to the Soxhlet extraction method for PAH compounds from coal-tar contaminated soil [30].

Pyrene was extracted using a dry weight of 7.6 g of soil washed in either 200 mL of DI water or acetonitrile. The DI extraction allowed for the determination of the water-soluble byproducts and the acetonitrile extraction determined the organically bound byproducts that would remain persistent in the soil. The flasks were shaken in the solvent for 3 hours at 150 cycles per minute. Following the extraction procedure, 1 mL of 1 M H<sub>2</sub>SO<sub>4</sub> was added to the flask to encourage settling of the suspended solids. The flasks were then allowed to settle for 24 hours. Mass balances for the pyrene extraction procedure yielded between 95 – 98% pyrene recoveries from soil. For each experiment, pyrene was extracted from contaminated soil that was not ozonated, to use as a soil control.

RP-HPLC Analysis. A Gilson HPLC unit (Worthington, OH), UV detector (Model 116), and an Altima C18 reverse phase column (5 μM) with dimensions 4.6 x 250 mm was used for HPLC Analysis (Alltech Co., Deerfield, IL). The effluent was monitored at 254 nm wavelength. Pure ACN (99.8% purity) and HPLC grade water was used as the mobile phases. The linear gradient used for the mobile phase was 25%/75% ACN/H<sub>2</sub>O at the time of injection and held for 3 minutes. It was then linearly increased to 90%/10% ACN/H<sub>2</sub>O over 5 minutes, held at 90%/10% ACN/H<sub>2</sub>O for 10 minutes, and linearly

decreased to 25%/75% ACN/H<sub>2</sub>O over 5 minutes. The mobile phase was held for an additional 5 minutes at this ratio. The total run time was 28 minutes. All extracts were run in triplicate.

Statistical Analysis. Experiments were conducted in triplicate and the data were analyzed using a t-test and an f-test. These analyses were used to compare the results at the 95% confidence level.

#### 2.5 Results and Discussion

The Metea soil used in this study was a sandy-loam with a natural pH of 6.2. This soil has also been used in three PAH previous ozonation studies [3, 6-8]. An additional pyrene soil ozonation study is available using soil collected from Wurtsmith AFB in Michigan [8]. In related PAH ozonation studies, Choi et al. [31] investigated phenanthrene contaminated sand ozonations using a system similar to the system used for this research. Lim et al. [32] evaluated ozone decomposition in soil slurries using 5 – 50 g soil/L of deionized water.

Clean soil and soil contaminated with pyrene (300 ppm) was ozonated using several combinations for test conditions. The experiments for the study evaluated three different pHs (2, 6, 8), two temperatures (25°C, 13°C), and three moisture content levels (dry, 5%, 10%). Contaminated soil stored for 6 months was also ozonated at room temperature at the three pH levels. Preliminary experiments determined that neither airstripping nor oxygen stripping for 24 hours was able to degrade pyrene in the soil (HPLC chromatograph in Appendix B). The ozone doses of  $2.22 \pm 0.06$  mg ozone/ppm pyrene (mg O<sub>3</sub>/ppm Pyr),  $3.85 \pm 0.11$  mg O<sub>3</sub>/ppm Pyr, and  $16.21 \pm 0.45$  mg O<sub>3</sub>/ppm Pyr were used in all tests. These doses are reported at the 95% confidence interval. The data collected evaluated the ozone breakthrough curve (BTC) and the degree of pyrene removal in contaminated soil. The list of ozonation experiments conducted is provided in Table 2.3. Plots of the data are provided in Appendix A.

Table 2.3 Summary of Ozonation Experiments

	Pyrene Concen.			
Sample	(ppm)	pН	Ozonation duration	Variable
dry soil	Clean	2,6,8	4 hours	pH, 25℃
dry soil	Clean	2,6,8	4 hours	pH, 13 <b>°</b> C
5% moisture	Clean	2,6,8	4 hours	pH, 25°C
5% moisture	Clean	2,6,8	4 hours	pH, 13 <b>º</b> C
10% moisture	Clean	2,6,8	4 hours	pH, 25°C
10% moisture	Clean	2,6,8	4 hours	pH, 13ºC
dry soil	300	2	35 minutes, 1 hour, 4 hours	pH, 25°C
dry soil	300	6	35 minutes, 1 hour, 4 hours	pH, 25°C
dry soil	300	8	35 minutes, 1 hour, 4 hours	pH, 25℃
5% moisture	300	2	35 minutes, 1 hour, 4 hours	moisture, pH, 25°C
5% moisture	300	6	35 minutes, 1 hour, 4 hours	moisture, pH, 25°C
5% moisture	300	8	35 minutes, 1 hour, 4 hours	moisture, pH, 25°C
10% moisture	300	2	35 minutes, 1 hour, 4 hours	moisture, pH, 25°C
10% moisture	300	6	35 minutes, 1 hour, 4 hours	moisture, pH, 25°C
10% moisture	300	8	35 minutes, 1 hour, 4 hours	moisture, pH, 25°C
dry soil	300	2	35 minutes, 1 hour, 4 hours	pH, 13°C
dry soil	300	6	35 minutes, 1 hour, 4 hours	pH, 13⁰C
dry soil	300	8	35 minutes, 1 hour, 4 hours	pH, 13°C
5% moisture	300	2	35 minutes, 1 hour, 4 hours	pH, moisture, 13°C
5% moisture	300	6	35 minutes, 1 hour, 4 hours	pH, moisture, 13°C
5% moisture	300	8	35 minutes, 1 hour, 4 hours	pH, moisture, 13°C
10% moisture	300	2	35 minutes, 1 hour, 4 hours	pH, moisture, 13°C
10% moisture	300	6	35 minutes, 1 hour, 4 hours	pH, moisture, 13°C
10% moisture	300	8	35 minutes, 1 hour, 4 hours	pH, moisture, 13°C
dry soil	300	2	35 minutes, 1 hour, 4 hours	pH, 25°C,aged
dry soil	300	6	35 minutes, 1 hour, 4 hours	pH, 25°C,aged
dry soil	300	8	35 minutes, 1 hour, 4 hours	pH, 25°C,aged

## 2.5.1 Dry soil Ozonation studies

### a. Non-contaminated, dry soil studies

Ozone breakthrough curves (BTC) are produced by monitoring the concentration of ozone in the effluent gas stream. Figure 2.8 is a representative BTC for clean Metea soil at pH 6. Experiments conducted in the clean soils showed that the effluent ozone concentration reached levels > 80% within 3 – 6 minutes. The effluent ozone concentration remained relatively constant in the clean soil from 5 minutes to 4 hours of ozonation time. This result is similar to the BTC trends seen in previous studies at pH 6 [6-8, 32].

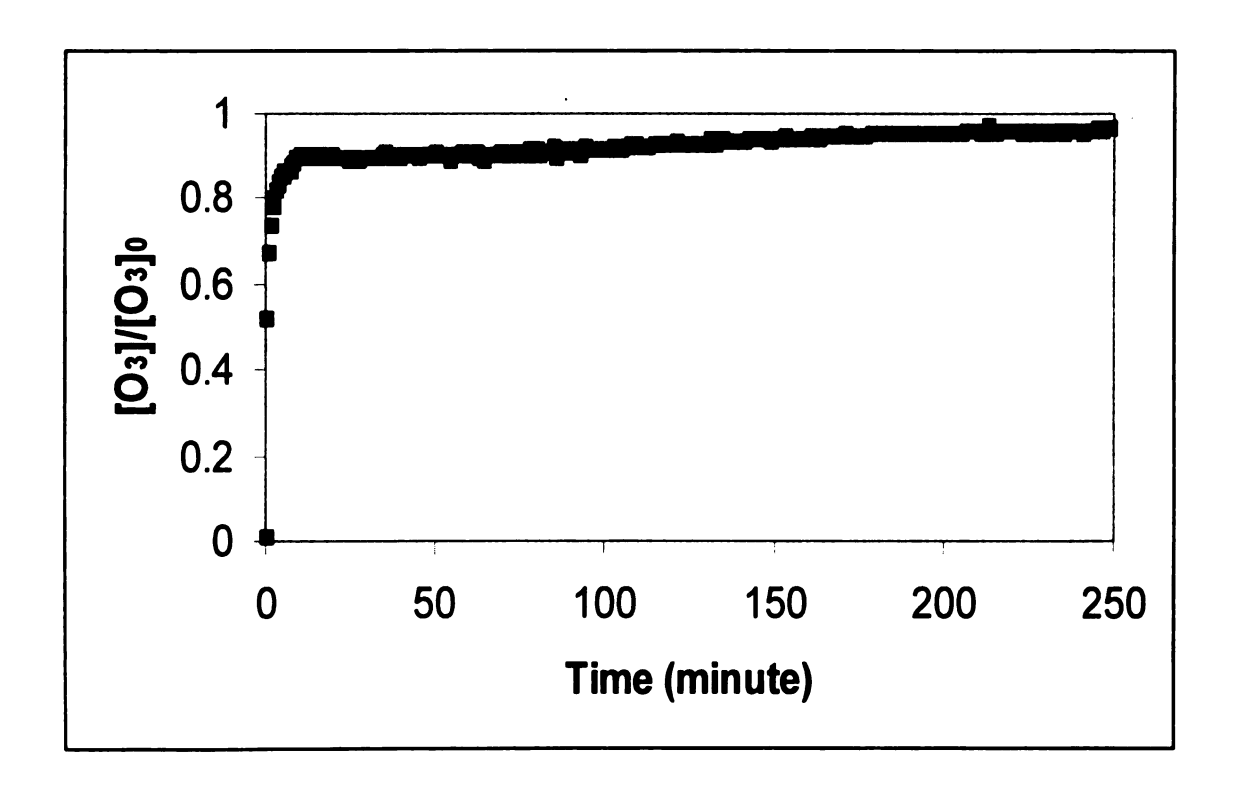


Figure 2.8. Representative ozone breakthrough curve for clean soil at 25°C.

The constant level seen in the BTCs, or "tailing" effect, is defined as the point where the slope of the effluent BTC becomes essentially zero or the ozone concentration in the column reaches steady-state [6-8]. The ozone concentration in the effluent never reaches the influent ozone concentration despite long ozonation times [8]. The tailing effect results in the effluent recovery reaching 95% – 98% of the influent concentration. Day [7] suggested this result might be due to a constant ozone demand exerted by the Metea soil and auto-decomposition of ozone. Hsu [6] attributes the tailing effect to pressure differences between the inlet and outlet of the column.

## b. Pyrene remediation in Dry soils

Compared to clean soils, ozone breakthrough occurred at a slower rate in the pyrene contaminated soils. Figure 2.9 is the BTC for dry, pyrene soil at pH 2, pH 6 and pH 8 at 25°C. Ozone breakthrough was the slowest in the pH 8 soil. The slower ozone breakthrough in the effluent stream indicated that more ozone was reacting or decomposing in the pH 8 soil. As the pH decreased, the amount of ozone present in the effluent stream increased and ozone breakthrough occurred faster. Breakthrough occurred the fastest for pH 2 soil effluent stream.

A notable observation was seen in the dry soil ozonation experiments. In these soils, the effluent stream showed ozone breakthrough initially increasing and then reaching a region where the effluent ozone concentration would either decrease (pH 2) or plateau for a period of time (pH 6 and pH 8). This phenomenon was highly reproducible.

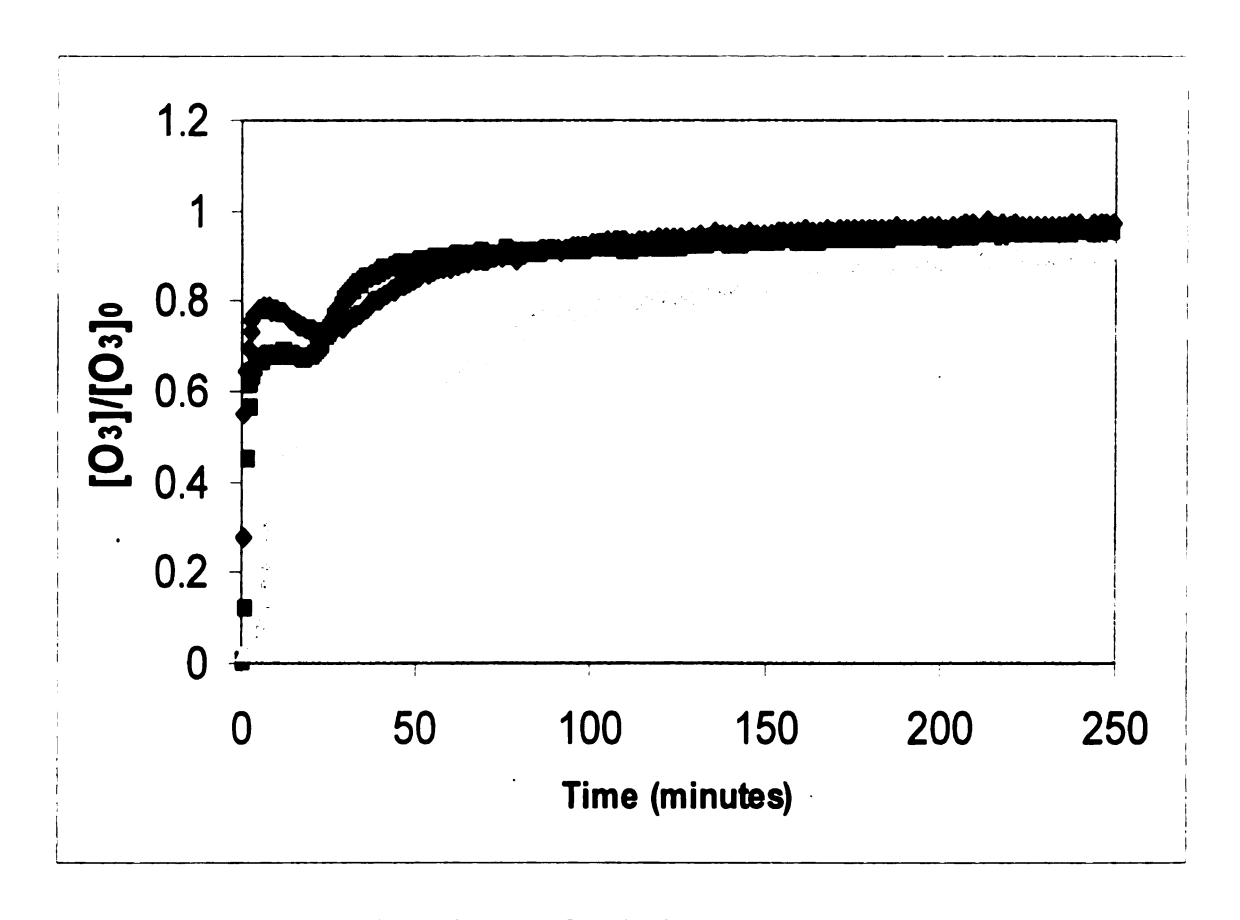


Figure 2.9. Ozone breakthrough curve for air-dried, pyrene soil at 25°C: ◆ pH 2, ■ pH 6, △ pH 8

The decline in the effluent ozone (pH 2) suggested that the ozone demand for the soil had increased compared to that observed during the early ozonation times. The plateau region suggests that the ozone demand exerted by the soil has leveled to a constant rate of ozone uptake. Once the ozone demand for the region was fulfilled, the BTCs began to increase to 95 – 98% ozone breakthrough. These regions might indicate the occurrence of parallel reactions where ozone is reacting with both soil organic matter and pyrene.

The variance in ozone demand seen in the dry soils might be similar to the observations by Day [7]. A plot of the effluent ozone concentration in pyrene contaminated Metea (250 ppm Pyr) showed an initial increase in ozone breakthrough followed by a reduction in ozone detected in the effluent. The ozone concentration increased to 20 mg/L ozone within 3 minutes and then decreased to approximately 2 mg/L ozone detected in the effluent. The total experiment time was 16 minutes. If the experiment had been conducted for longer ozonation time, the effluent ozone concentration might have increased to reach concentrations similar to the influent stream. Lim et al. (2002) also noted the presence of two phases during phenanthrene ozonation in soil slurries and asymmetry in the BTC.

Masten [33] has shown that ozone can react with both humic acid and volatile organic compounds (VOC). In the series of batch experiments, a known volume of water and humic acid solution were added to a 20 mL headspace vial. The samples were chilled in a water bath for one hour. Aqueous ozone and a stock solution of VOC were added to the vial and were allowed to react overnight in the water bath. In the

experiments without contaminant, humic acid solutions (40 mg/L as TOC) reacted with ozone resulting in a 13% decrease of the TOC concentration.

In the experiments for VOCs, the extent to which VOCs were oxidized by ozone was affected by the concentration of humic acid and by pH. At constant ozone dosage, as humic acid concentration increased the extent of TCE reacting within the system decreased. For example, an initial humic acid concentration of 60 mg/L, a 3- to 4-fold increase in the ozone concentration resulted in a larger extent of trichloroethylene (TCE) reacting within the system. At concentrations less than 60 mg/L and the same ozone dose, TCE oxidation was such that < 10% of the initial TCE concentration was detected. In contrast, concentrations greater than 60 mg/L demonstrated a linear decrease in TCE oxidation. In increasing the pH from 2 to 6.3, similar results were observed and a slight increase in the amount of TCE which reacted. Masten [33] suggested that for TCE oxidation, changing from pH 2 to 6.3, the direct reaction between ozone and TCE might not be the sole reaction.

The ability to remediate pyrene from dry soil appears to increase with increasing pH (Table 2.4). The amount of pyrene removed from the soil is consistent with the data from the BTCs. The BTC for pH 8 demonstrated higher level of pyrene removal and the slowest ozone breakthrough. The pH 2 soil had the lowest level of pyrene remediation and the fastest ozone breakthrough. At an applied dose of 660 ± 18 mg O<sub>3</sub>, pyrene removal reached 39.9% at pH 2, 94.9% at pH 6, and 96.4% at pH 8. Pyrene removal from the pH 2 soil reached 94.8% after using 4860 mg O<sub>3</sub>. These results show that less ozone was required at pH 6 and pH 8 to achieve removal of > 90% of the pyrene. This finding is

interesting because in aqueous systems, pyrene removal decreased with increasing pH [18, 19].

Table 2.4. Percentage of pyrene removed from air-dried Metea soil at 25°C.

	Ozonation Time				
Sample	35 minute ozonation <sup>a</sup>	1 hour ozonation <sup>b</sup>	4 hour ozonation <sup>c</sup>		
	% Pyrene removed	% Pyrene removed	% Pyrene removed		
Dry, pH 2	39.9 ±2.8	46.4 ± 3.8	94.8 ± 1.7		
Dry, pH 6	$94.9 \pm 3.0$	$95.5 \pm 1.02$	$97.7 \pm 0.2$		
Dry, pH 8	$96.4 \pm 2.7$	$98.0 \pm 1.5$	$98.9 \pm 0.5$		

a.  $2.22 \pm 0.06$  mg O<sub>3</sub>/ppm Pyr ozone dose reported at 95% C.I.

Previous pyrene ozonation studies in Metea soil were conducted in dry soils at a pH range from pH 5.4 – 6.6 and organic matter contents of  $0.4 \pm 0.1\%$ . In dry Metea soil (pH 6, OM = 0.5%), pyrene was reduced by 83% using 582 mg O<sub>3</sub> [3]. A 91% removal was achieved at a dose of 2392 mg O<sub>3</sub> [3]. In soil from Wurtsmith Air Force Base (pH 7.3 to 8; OM = 0.1- 0.22%), ozonation yielded an average pyrene removal of 90% using 998 mg O<sub>3</sub> and 97% using 1995 mg O<sub>3</sub> [8]. In these studies, the pyrene concentrations were 100 ppm and 200 ppm, respectively. The results for these studies appear to be consistent. Day [7] reported effective pyrene removal using ozone in dry Ottawa soils and Metea (pH 5.4  $\pm$  0.87; OM = 0.4  $\pm$  0.1), but the ozone doses (20.1 – 33.1 mg O<sub>3</sub>) are significantly lower in comparison to the studies discussed above.

b.  $3.85 \pm 0.11$  mg O<sub>3</sub>/ppm Pyr ozone dose reported at 95% C.I.

c.  $16.21 \pm 0.45$  mg O<sub>3</sub>/ppm Pyr ozone dose reported at 95% C.I.

### 2.5.2 Moisturized soil ozonation studies

### a. Non-contaminated, 5% moisturized soil

Soils with various moisture contents were evaluated to determine the effect moist soils can have on ozone efficiency and pyrene removal. The data indicate that clean soil with 5% moisture by weight exerted a greater ozone demand than dry soil (Figure 2.10). The increase in ozone demand is attributed to the dissolution of gaseous ozone and the subsequent decomposition reactions due to water present in the soil. These results are consistent with the BTCs obtained for Wurtsmith soils with 4.4% and 6.9% moisture contents by Cole [8] and Ottawa sand (no organic matter) by Day [7]. Moisturized Metea demonstrated an increase in ozone demand compared to Ottawa sand containing a radical scavenger (0.08 M tertiary-butyl alcohol) [7]. In the Day [7] study, experimental difficulties with the dry, Metea experiments precluded the ability to compare BTCs for dry Metea soil and moisturized soils.

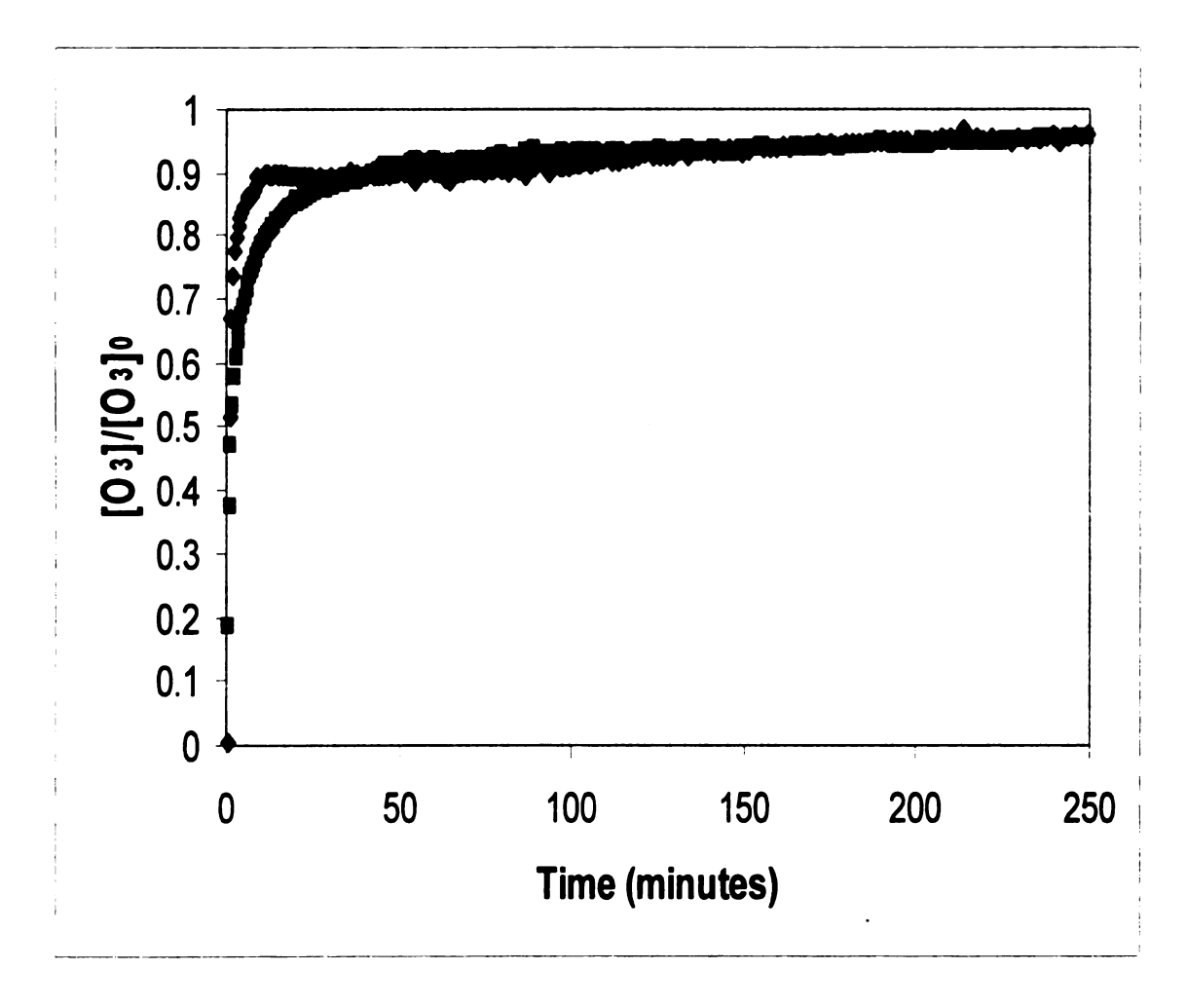


Figure 2.10. Breakthrough curve for clean Metea Soil at pH 6 (25°C): ♦ dry, ■ 5% moisture

# b. Pyrene remediation in 5% moisture content soils

Pyrene removal was less in the 5% moisturized soil compared to the dry soil. Table 2.5 lists the pyrene removal in the 5% moisture content soils. This observation suggests that more ozone would be needed to remediate moist contaminated soils. The results from the 1 hour and 4 hour ozonations followed the same trend of pyrene removal increasing at higher pHs. The order for pyrene removal was pH 2 < pH 6 < pH 8.

Table 2.5. Percentage of pyrene removed from Metea soil at 5% moisture content and 25°C.

	Ozonation Time				
Sample	35 minute ozonation <sup>a</sup>	1 hour ozonation <sup>b</sup>	4 hour ozonation <sup>c</sup>		
	% Pyrene removed	% Pyrene removed	% Pyrene removed		
5% moisture, pH 2	$54.1 \pm 3.37$	$63.2 \pm 3.6$	$86.2 \pm 1.04$		
5% moisture, pH 6	$55.5 \pm 2.2$	$65.9 \pm 0.2$	$91.3 \pm 1.0$		
5% moisture, pH 8	$36.7 \pm 3.8$	$75.8 \pm 2.0$	$95.4 \pm 0.9$		
_					

a.  $2.22 \pm 0.06$  mg O<sub>3</sub>/ppm Pyr reported at 95% C.I.

An interesting result seen in the BTC is that at the  $2.22 \pm 0.11$  mg O<sub>3</sub>/ppm Pyr dose (35 minute ozonation time), pyrene removal was higher in the pH 2 soil than the pH 8 soil. From the BTC, one can observe that for the pH 2 soil, the concentration of ozone present in the effluent for the first 40 minutes is less than the pH 6 and pH 8 BTC. For the ozonation time > 40 minutes, the effluent concentration of ozone at pH 2 increased to 98% of the influent concentration, while at pH 6 and pH 8, the concentrations of the effluent ozone were approximately 95- 96% of the influent stream (Figure 2.11).

b.  $3.85 \pm 0.11$  mg O<sub>3</sub>/ppm Pyr reported at 95% C.I.

c.  $16.21 \pm 0.45$  mg O<sub>3</sub>/ppm Pyr reported at 95% C.I.

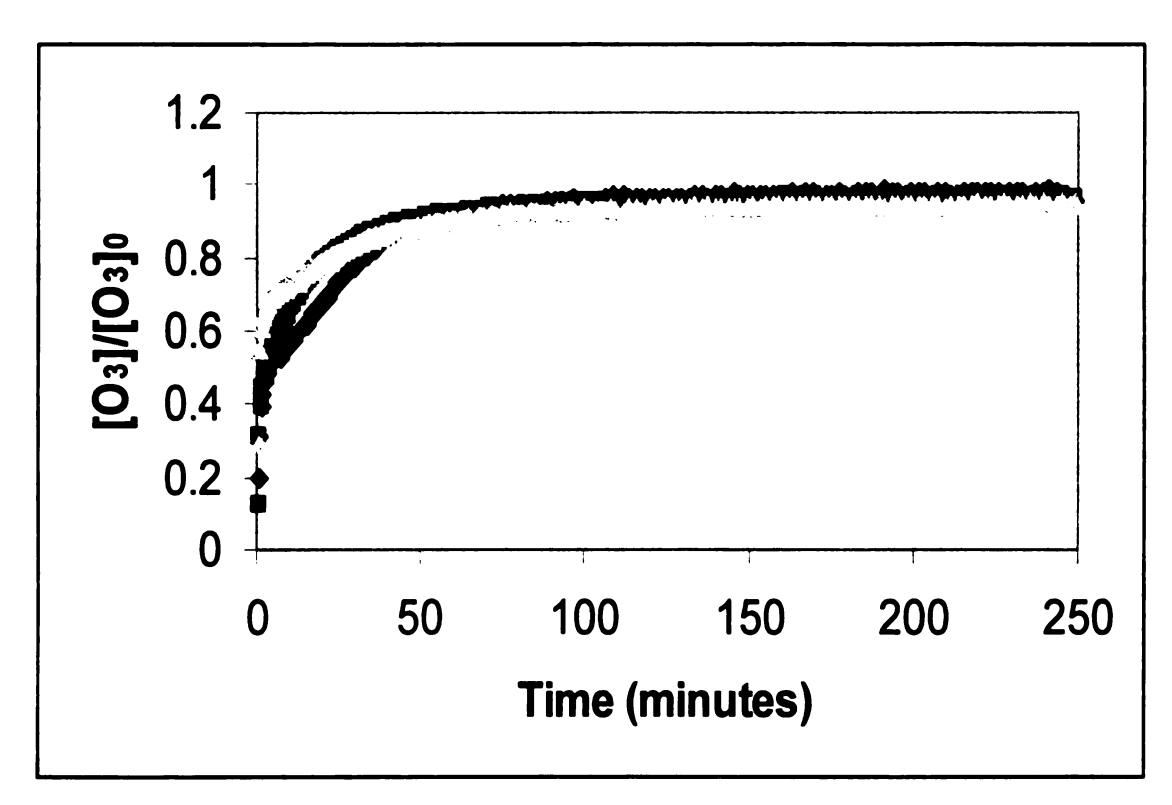


Figure 2.11. Ozone breakthrough curve for 5% moisture, pyrene soil at 25°C: ◆ pH 2, ■ pH 6, △ pH 8

## c. Non-contaminated, 10% moisturized soil

A comparison of the BTC for non-contaminated, dry, 5% moisture and 10% moisture soils at pH 2 is presented in Figure 2.12. At pH 2 and early in the ozonation process (time < 25 minutes), ozone breakthrough was lower in both the 5% and 10% moisturized soils. For the remaining 4 hour ozonation, the dry soil ultimately exhibited a higher ozone demand and lower BTC. As mentioned earlier for the dry, pyrene soil, the clean dry soil at pH 2 also demonstrated an increase in ozone demand after the initial breakthrough. The effluent ozone then rebounded to levels consistent with the other BTCs over the 4 hour ozonation period.

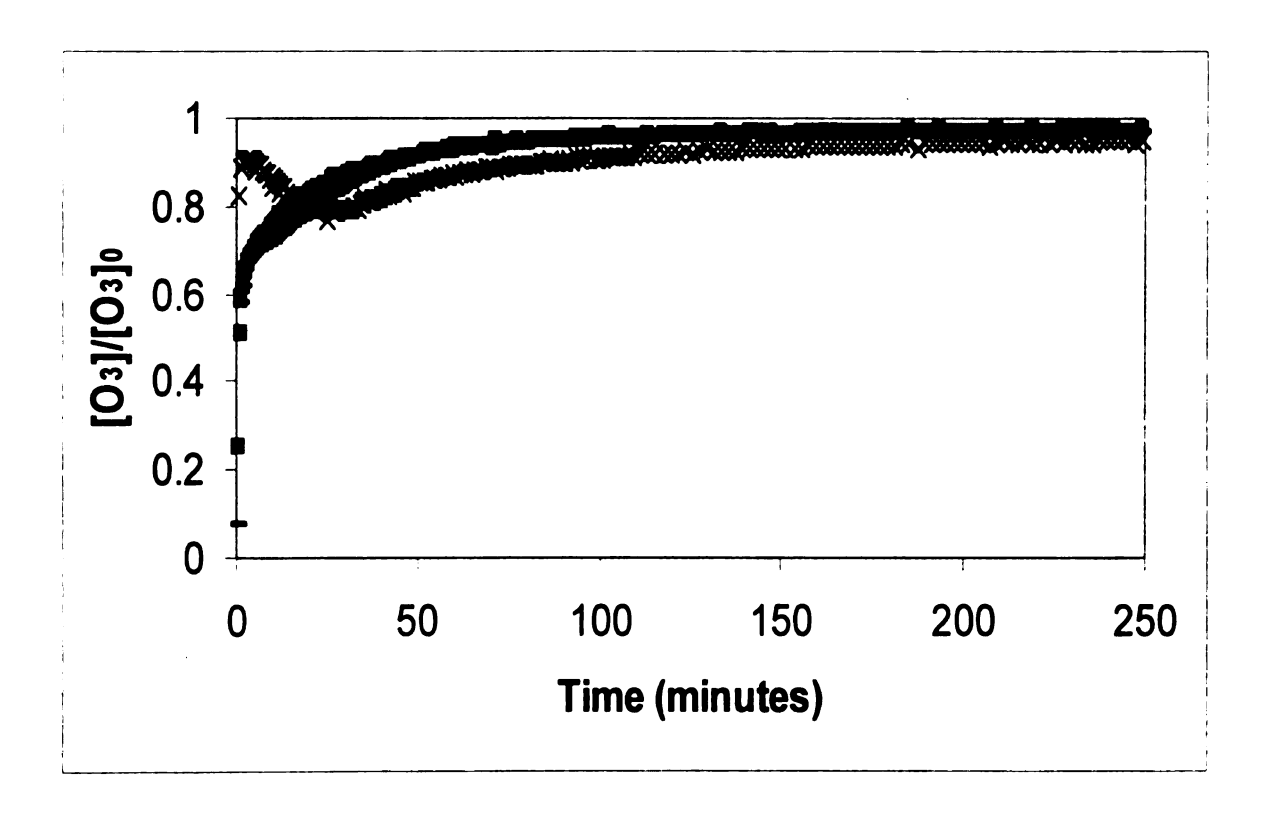


Figure 2.12. Ozone breakthrough curve for non-contaminated Meta at pH 2 (25°C):

X dry soil, 5% moisture soil, -10% moisture soil

Ozone breakthrough occurred faster in the 10% moisture soil than the 5% moisture soil. The dry soil also ultimately had the highest ozone demand. This observation is consistent with the results presented in Choi et al. [32]. As the water content increased in clean sand and fixed gas flux, the ozone breakthrough time was seen to decrease [32]. The ozone breakthrough from fastest to slowest was 26% > 16% > 6% > 0% moisture content. Choi et al. [32] hypothesized that water molecules were able to cover the sand surface leading to fluid interfering with the ozone reactions with organic matter. The BTC was more retarded in the dry column than in the other conditions evaluated.

At pH 6 and pH 8, the BTCs for the dry soil and 10% moisture soil did not significantly differ in the rate of ozone breakthrough. The 5% moisture soil was consistently the slowest. The BTCs for clean Metea at pH 6 and pH 8, respectively, are shown in Figures 2.13 and 2.14.

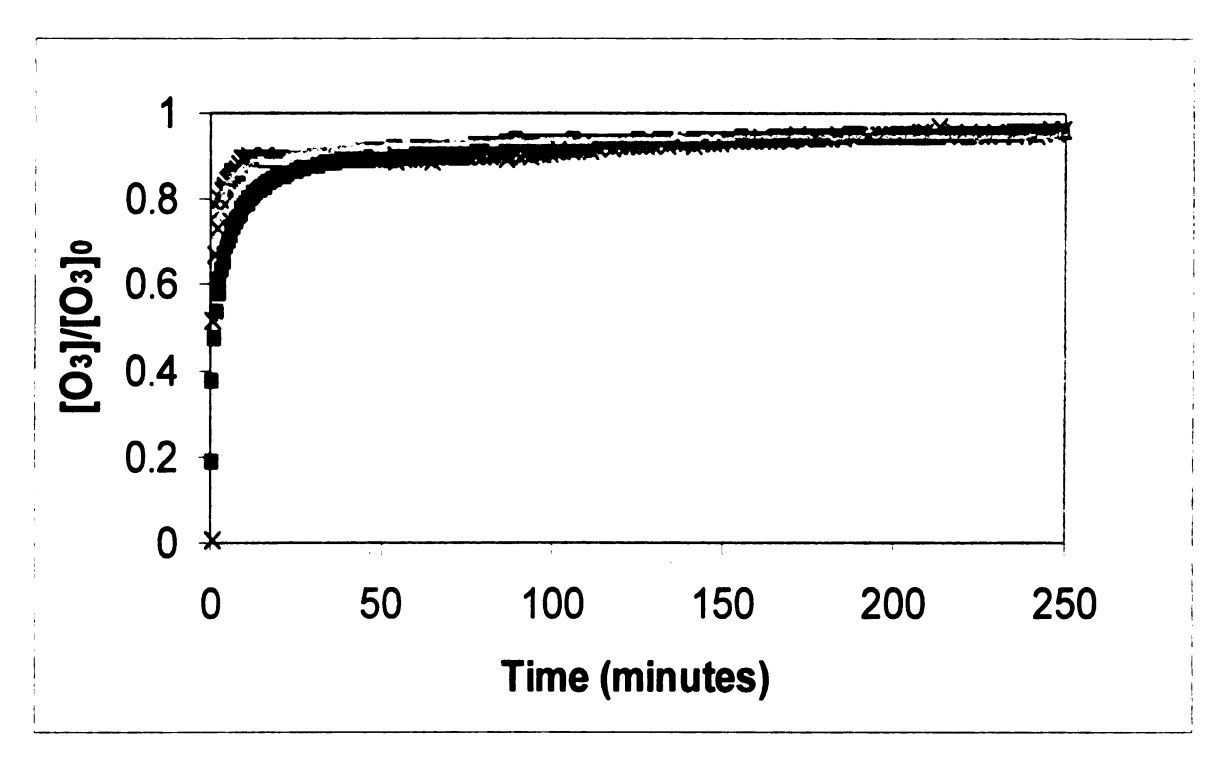


Figure 2.13. Ozone breakthrough curve for non-contaminated Meta at pH 6 (25°C):

X dry soil, 5% moisture soil, - 10% moisture soil

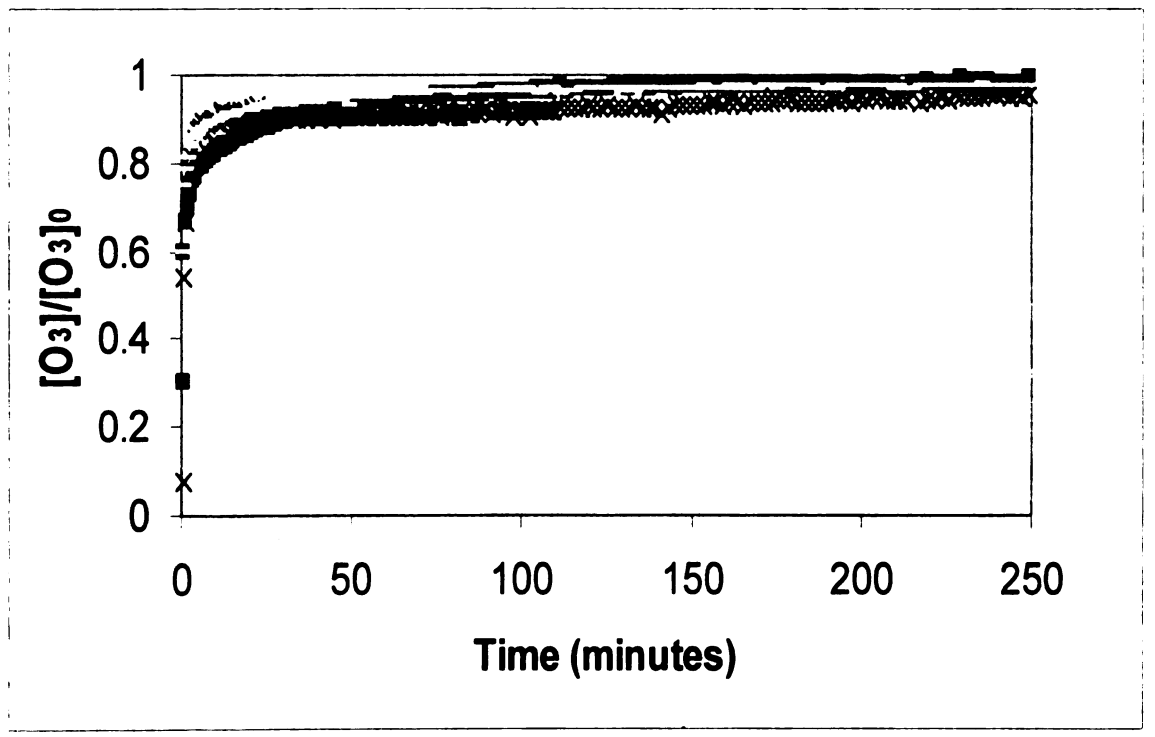


Figure 2.14. Ozone breakthrough curve for non-contaminated Meta at pH 8 (25°C):

X dry soil, 5% moisture soil, -10% moisture soil

#### d. Pyrene remediation in 10% moisture soils

For the soils containing 10% moisture, as the pH increased, pyrene removal decreased. This observation is consistent with the results seen in aqueous solutions. In ozonation studies where pyrene was dissolved in 90%/10% acetonitrile/water, the ozone demand increased and pyrene removal efficiency decreased with increasing pH [18, 19]. The 10% moisture, pH 8 soils showed high ozone demand in the BTC but the amount of pyrene removed from the soil was the lowest in the data set. Pyrene removal was pH 8 < pH 6 < pH 2 in the 10% moisture soils (Table 2.6). The 10% moisture soil at pH 2 had the lowest ozone demand and the highest level of pyrene removal reaching  $80.7 \pm 0.8\%$ . The BTC for 10% moisture, pyrene soil at pH 2, 6, and 8 are given in Figure 2.15.

Table 2.6. Percentage of pyrene removed from 10% moisture content soil at 25°C.

	Ozonation Time			
Sample 35 minute ozonation <sup>a</sup>		1 hour ozonation <sup>b</sup>	4 hour ozonation <sup>c</sup>	
	% Pyrene removed	% Pyrene removed	% Pyrene removed	
10% moisture, pH 2	$29.91 \pm 4.7$	59.7 ± 1.5	$80.7 \pm 0.8$	
10% moisture, pH 6	$33.78 \pm 3.7$	$44.6 \pm 5.9$	$50.3 \pm 1.0$	
10% moisture, pH 8	$24.6 \pm 5.5$	$49.5 \pm 6.8$	$52.9 \pm 1.2$	

a.  $2.22 \pm 0.06$  mg O<sub>3</sub>/ppm Pyr ozone dose delivered to the soil. Reported at 95% C.I.

b.  $3.85 \pm 0.11$  mg O<sub>3</sub>/ppm Pyr ozone dose delivered to the soil. Reported at 95% C.I.

c.  $16.21 \pm 0.45$  mg O<sub>3</sub>/ppm Pyr ozone dose delivered to the soil. Reported at 95% C.I.

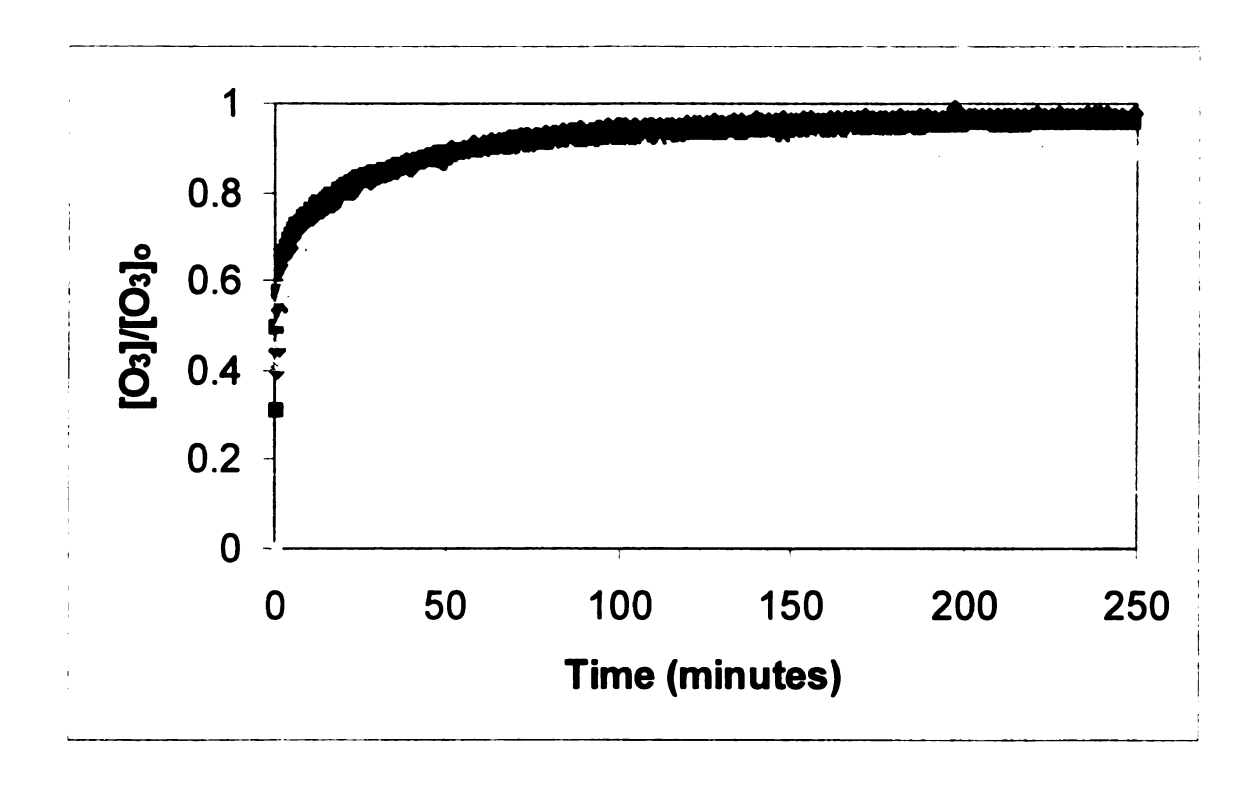


Figure 2.15. Ozone breakthrough curve for 10% moisturized, pyrene soil at 25°C: ◆ pH 2, ■ pH 6, △ pH 8

The degree of saturation in the soils (5% versus 10%) might explain the different results obtained for pyrene remediation. The 5% moisture soil appeared to have a mix of both dry and wet soil particles and was not as saturated as 10% moisture soil. It is possible that the saturation level affects the rate of direct reactions and the indirect OH radical reactions occurring in the soil. Day [7] addressed the issue of monolayer coverage in Metea soils. Monolayer coverage is assumed in Metea soil for a relative humidity between 26 - 90% and based on the amount of water in the soil. Water uptake in the Metea soil and the monolayer coverage assumption is considerably favorable due to the mineral content and high surface area that can act as a water-holding reservoir [7]. The 10% moisture soil would have more water in soil pores and larger surface area coverage than soil at 5% moisture. This difference in water saturation might alter the results seen for ozonation efficiency. A 2700 BET surface area analysis conducted on Metea soil calculated the total surface area to be 36.34 m<sup>2</sup>/g [7]. The Day [7] study determined that monolayer coverage existed in the Metea at moisture contents ≥ 11%. Day did not evaluate soils having moisture contents < 11%.

The removal of pyrene might be more favorable in dry soils and unsaturated soils with low water content (0 - 5%) than in soils with higher moisture contents due to the availability of water-free areas on the soil particle. Choi et al. [32] concluded that water molecules cover the sand surface even at lower moisture contents. The degree of wetting and amount of pore water would block the reactive sites on the sand surface, thus subduing catalytic reactions with ozone. In the 10% moisturized soils, water might have coated the soil surface and inhibited ozone from reacting with soil organic matter and

pyrene. The hydrophobic nature of PAHs suggests that pyrene would preferably remain sorbed to the soil particle and orient away from water [7].

Saturation level within the soil appears to play a significant role in ozone efficiency and pyrene removal. If this is true, then dry soil would exhibit the ideal soil condition for PAH ozonation. In dry soil, ozone would be able to directly react with organic matter and pyrene. This theory is supported by the result seen in the dry soil ozonations. In the soils containing 5% moisture, ozone would react with organic matter, soil pore water, and pyrene not blocked by soil water. In the 10% moisture soils, ozone appears to react directly with soil pore water and organic matter and not as extensively with pyrene, leading to decreased pyrene remediation.

# 2.5.3 Ozonation at Colder Temperature

The removal efficiency for pyrene in the 13°C soil is shown in Table 2.7. The BTC for the 13°C soils showed the same trend as the dry soils at 25°C where pH 8 < pH 6 < pH 2 (Figure 2.16). Within a treatment set for the 5% and 10% moisturized soils, the effect pH had on pyrene removal differed. In the 5% moisture soils, pyrene removal was pH 6  $\approx$  pH 8 and both pH 6 and pH 8 were < pH 2. In the 10% moisture soils, increasing the pH appeared to decrease pyrene removal yielding pH 8 < pH 6 < pH 2. This result is consistent with the trend seen at 25°C.

Table 2.7. Percentage of pyrene removed from soils at 13°C.

		Ozonation Time	
Sample	35 minute ozonation <sup>a</sup>	1 hour ozonation <sup>b</sup>	4 hour ozonation <sup>c</sup>
	% Pyrene removed	% Pyrene removed	% Pyrene removed
DII 2	21.0 . 0.0	47.7 + 2.7	01.0 . 1.6
Dry, pH 2	$31.8 \pm 8.8$	47.7 ± 2.7	$81.8 \pm 1.6$
Dry, pH 6	$95.2 \pm 2.9$	$96.0 \pm 0.8$	$98.4 \pm 0.6$
Dry, pH 8	$97.3 \pm 0.8$	$97.6 \pm 0.6$	98.7 ± 0.2
5% moisture, pH 2	$48.1 \pm 4.6$	$64.0 \pm 0.86$	92.1 ± 2.5
5% moisture, pH 6	$33.4 \pm 3.3$	59.7 ± 1.5	88.5 ± 1.3
5% moisture, pH 8	$35.6 \pm 4.5$	$49.4 \pm 3.5$	$88.9 \pm 1.5$
10% moisture, pH 2	$25.1 \pm 1.5$	$54.8 \pm 2.8$	93.2 ± 3.4
10% moisture, pH 6	$21.7 \pm 2.6$	$34.2 \pm 3.6$	$87.6 \pm 1.0$
10% moisture, pH 8	$38.3 \pm 1.0$	$48.5 \pm 1.3$	$82.8 \pm 7.0$

a.  $2.22 \pm 0.06$  mg O<sub>3</sub>/ppm Pyr reported at 95% C.I.

b.  $3.85 \pm 0.11$  mg O<sub>3</sub>/ppm Pyr reported at 95% C.I.

c.  $16.21 \pm 0.45$  mg O<sub>3</sub>/ppm Pyr reported at 95% C.I.

The pyrene removal efficiency decreased slightly in dry soil at  $13 \pm 0.2$  °C compared to the dry soil at 25°C (Table 2.8). In the moisturized soils, the lower temperature improved pyrene removal for the 10% moisturized soil. This observation might support the hypothesis that pyrene remediation may improve at lower temperatures. The rationale for this is that ozone decomposition would be reduced at lower temperature and direct ozonation would predominate.

Table 2.8. A comparison of pyrene removal in the soils at 13°C and 25°C

Table 2.8. A comparison of py	Pyrene removal				
	Ozone dose: $16.2 \pm 0.11$ mg O <sub>3</sub> /ppm Pyr				
Sample	13°C	25°C			
Dry, pH 2	81.8 ± 1.6%	94.8 ± 1.7%			
Dry, pH 6	$98.4 \pm 0.6\%^{a}$	$97.7 \pm 0.2\%^{a}$			
Dry, pH 8	$98.7 \pm 0.2\%^{a,b}$	$98.9 \pm 0.5\%^{a,b}$			
5% moisture, pH 2	92.1 ± 2.5%	86.2 ± 1.04%			
5% moisture, pH 6	$88.5 \pm 1.3\%^{c}$	91.3 ± 1.0%			
5% moisture, pH 8	$88.9 \pm 1.5\%^{c}$	95.4 ± 0.9%			
10% moisture, pH 2	$93.2 \pm 3.4\%$	80.7 ± 0.8%			
10% moisture, pH 6	$87.6 \pm 1.0\%$	50.3 ± 4.3%			
10% moisture, pH 8	$82.8 \pm 7.0\%$	52.9 ± 1.2%			

a. Statistically similar at 95% C.I.

b. Statistically similar at 95% C.I.

c. Statistically similar at 95% C.I.

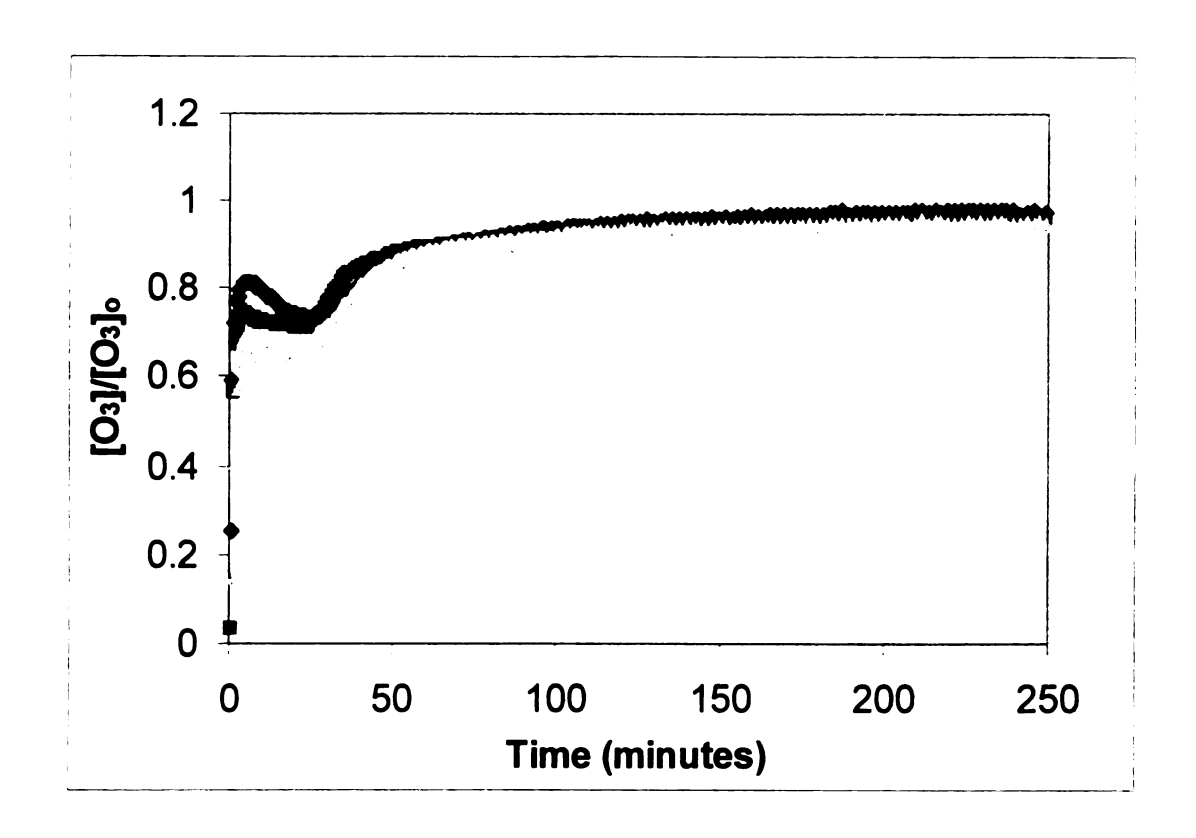


Figure 2.16. Ozone breakthrough curve for air-dried, pyrene soil at 13°C: ◆ pH 2, ■ pH 6, △ pH 8

Pyrene reduction for pH 6 and pH 8 at 13°C were not statistically different at the 95% C.I. This suggests ozonation efficiency in pyrene removal did not change significantly when comparing reduction in the pH 6 and pH 8.

The BTC for the 5% moisture soils at 13°C is shown in Figure 2.17. A higher ozone demand was observed at pH 2, along with the highest level of pyrene removal.

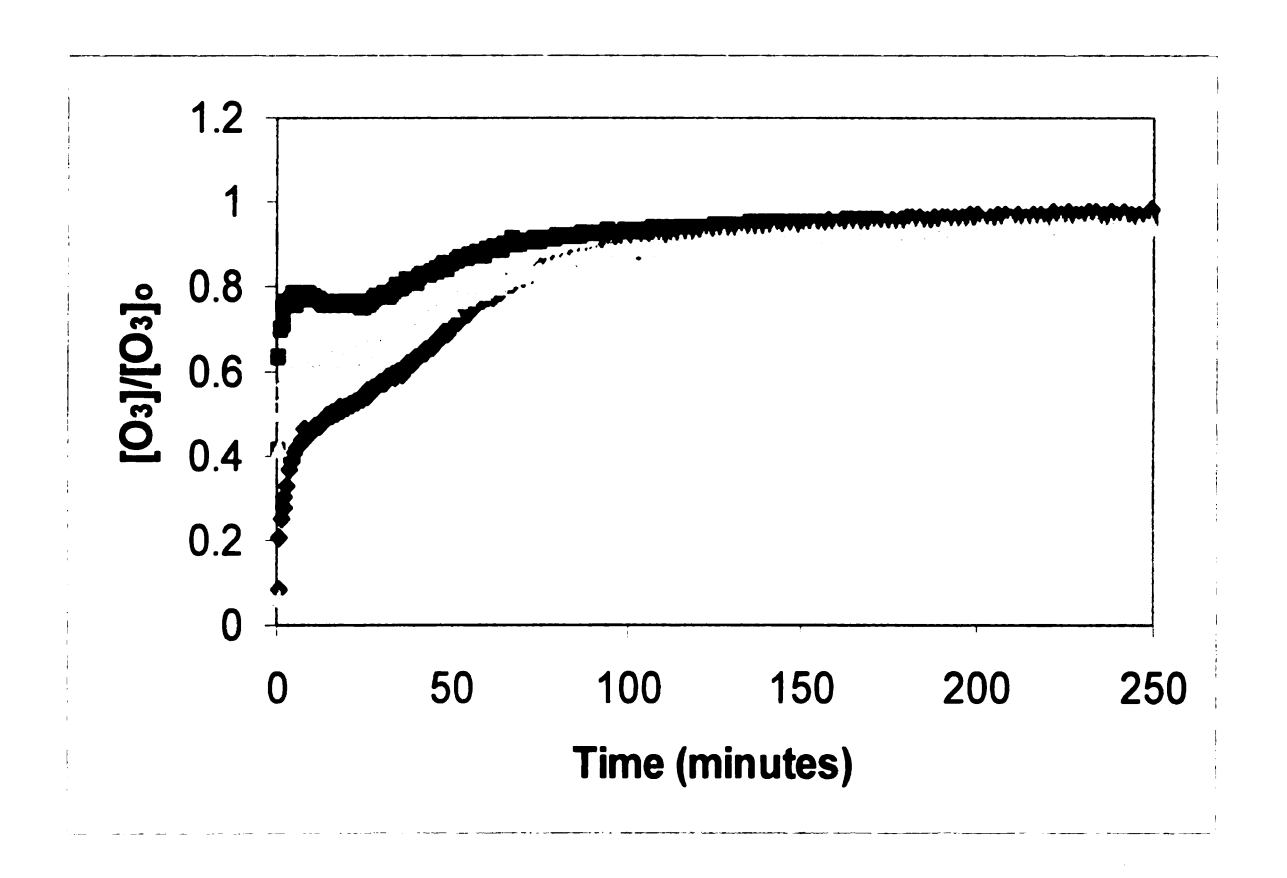


Figure 2.17. Ozone breakthrough curve for 5% moisture, pyrene soil at 13°C: ◆ pH 2, ■ pH 6, △ pH 8

The BTC for 10% moisture soils at 13°C is shown in Figure 2.18. The breakthrough of ozone was slower in the pH 8 soils, but the BTCs were similar for pH 2, 6, and 8. A table for the pyrene removal at  $2.2 \pm 0.06$ ,  $3.85 \pm 0.11$ , and  $16.2 \pm 0.45$  mg  $O_3$ /ppm Pyr is provided in the Appendix.

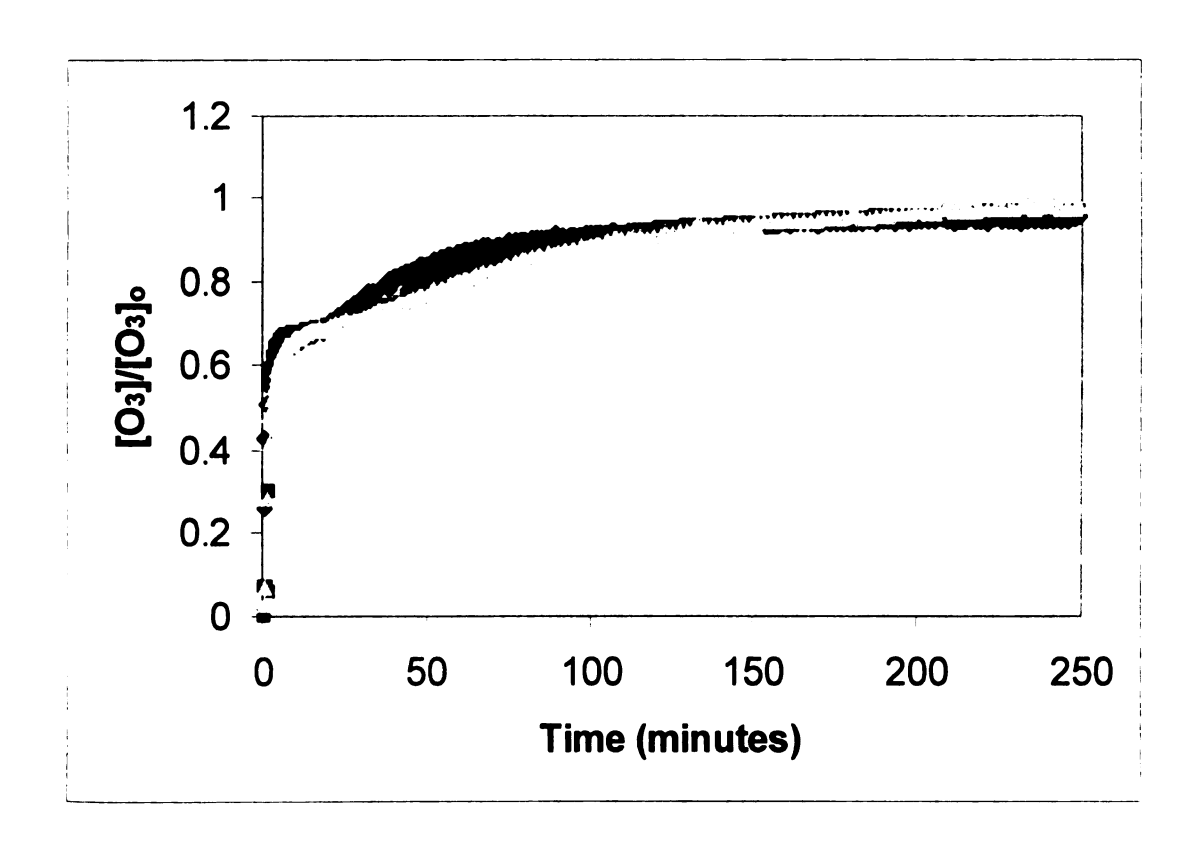


Figure 2.18. Ozone breakthrough curve for 10% moisutre, pyrene soil at 13°C: ◆ pH 2, ■ pH 6, △ pH 8

### 2.5.5 Ozonation of Aged soil

For the aged soil experiments, only dry soil ozonation studies were performed due to the limited amount of soil. Because dry soil demonstrated the highest extent of pyrene removal in the previous studies, the difference in removal efficiency between newly contaminated soil (less than 2 weeks of contamination) and soil contaminated for 6 months could be easily compared. In the aged soil experiments, the efficiency of pyrene oxidation was greatly reduced. Extracts from the control (aged contaminated soil/non-ozonated) indicated that between 89 – 92% of the pyrene could be extracted from the soil. This is only a slight decrease in removal efficiency compared to freshly contaminated controls using the direct extraction technique.

The pyrene removal efficiency in the aged soil decreased by 3-4 times compared to short-term contaminated soil. The order for pyrene removal was consistent with the previous dry soil studies where pH 2 < pH 6 < pH 8 (Table 2.9).

Table 2.9. Percentage of pyrene removed from air-dried Metea soil at 25°C.

	Ozonation Time				
Sample	35 minute ozonation <sup>a</sup>	1 hour ozonation <sup>b</sup>	4 hour ozonation <sup>c</sup>		
	% Pyrene removed	% Pyrene removed	% Pyrene removed		
Dry, pH 2	$9.09 \pm 1.6$	$13.5 \pm 2.1$	$21.1 \pm 3.3$		
Dry, pH 6	$5.3 \pm 4.2$	$24.4 \pm 1.3$	$24.9 \pm 5.1$		
Dry, pH 8	$19.8 \pm 2.1$	$23.1 \pm 5.5$	$25.3 \pm 2.3$		

a.  $2.22 \pm 0.06$  mg O<sub>3</sub>/ppm Pyr ozone dose reported at 95% C.I.

b.  $3.85 \pm 0.11$  mg O<sub>3</sub>/ppm Pyr ozone dose reported at 95% C.I.

c.  $16.21 \pm 0.45$  mg O<sub>3</sub>/ppm Pyr ozone dose reported at 95% C.I.

A comparison of the BTCs and the extent of pyrene removal in the aged soil show interesting results. At pH 2, both the short-term and aged soils exhibited the same characteristic shape for the BTC (Figure 2.19). The aged, pH 2 soil shows a higher ozone demand than the freshly contaminated soil. The total pyrene removal in the aged soil at an ozone dose of  $16.2 \pm 0.11$  mg O<sub>3</sub>/ppm Pyr was  $21.1 \pm 3.3\%$  in the aged soil compared to  $94.8 \pm 1.7\%$  in the short-term soil. A similar result is seen in the BTC for pH 6 short-term and aged soils (Figure 2.20). The pH 6, aged soil exhibited  $24.9 \pm 5.1\%$  removals at the same ozone dose. The pH 8, aged soil reached  $25.3 \pm 2.3\%$  removal and had a lower ozone demand than newly contaminated soil (Figure 2.21). The pyrene removal efficiency for the pH 6 and pH 8 soils were statistically similar at the 95% C.I.

These results support the hypothesis that pyrene would have stronger sorption after 6 months of contamination and would require higher doses of ozone to reduce PAH concentrations. Therefore, the results obtained from lab ozonation studies using short-term contaminated soil will over-estimate the ability to remediate soils with long-term contamination. This finding would suggest that aged soil experiments might be a better measure of ozonation processes for laboratory studies.

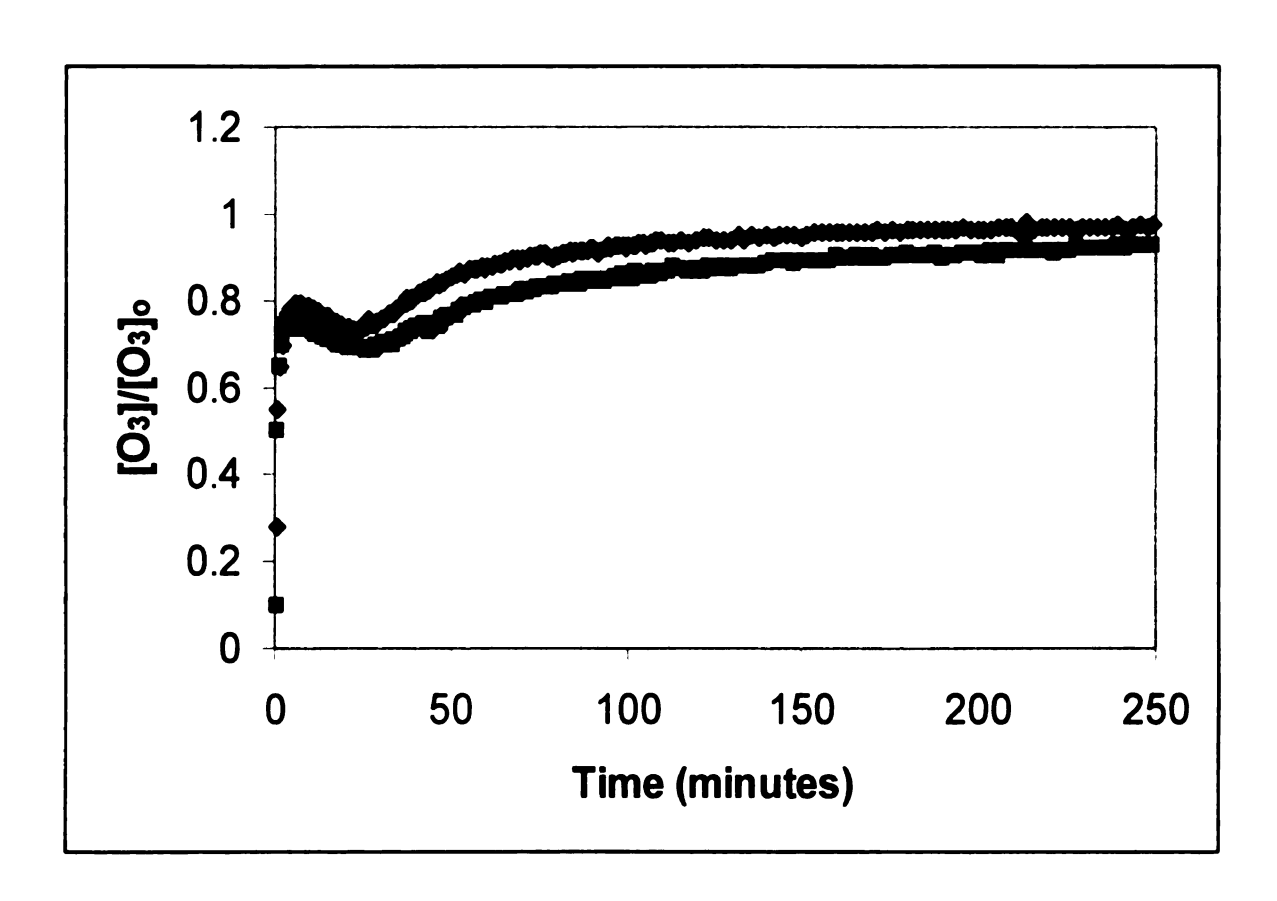


Figure 2.19. Ozone breakthrough curve for short-term and long term contaminated soil at pH 2 and 25°C: ◆ Short-term soil, ■ long-term soil.

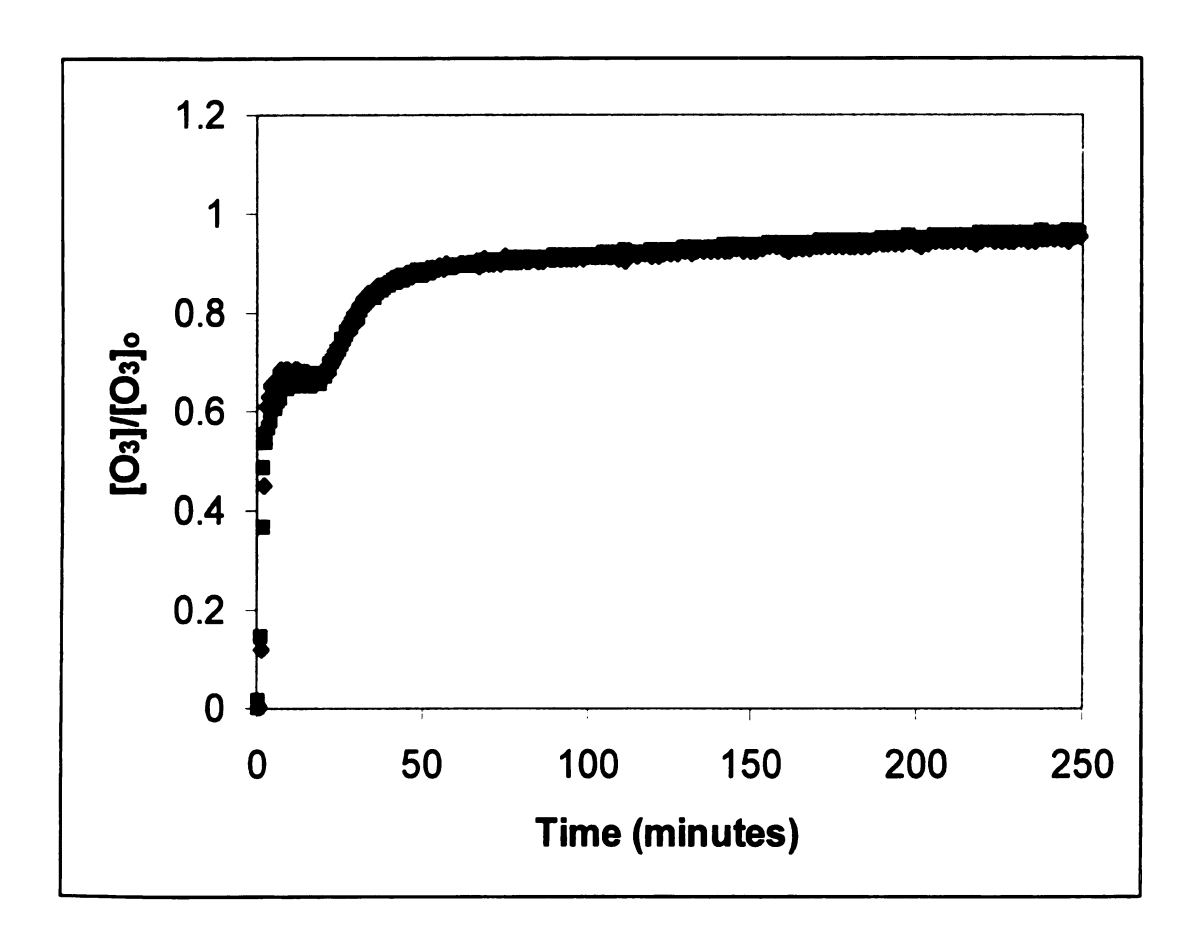


Figure 2.20. Ozone breakthrough curve for short-term and long term contaminated soil at pH 6 and 25°C: 

Short-term soil, long-term soil.

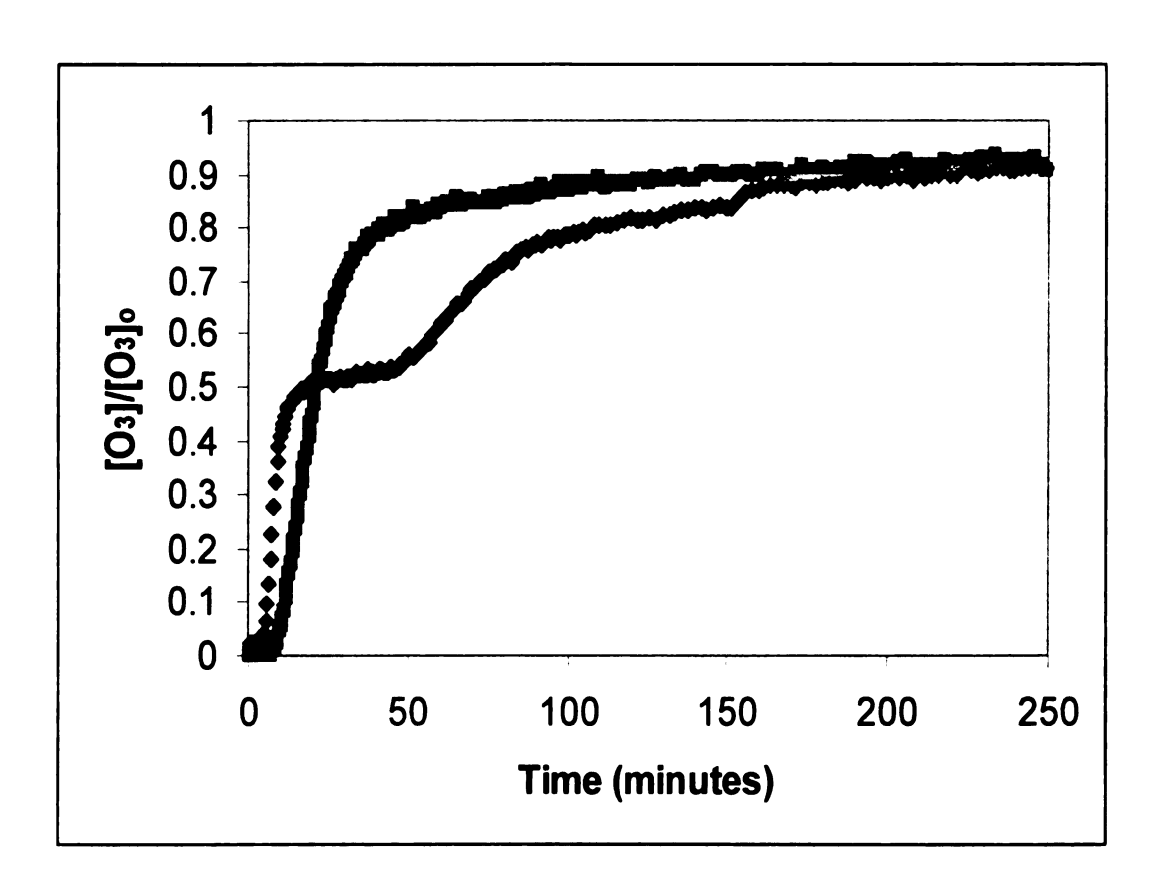


Figure 2.21. Ozone breakthrough curve for short-term and long term contaminated soil at pH 8 and 25°C: ◆ Short-term soil, ■ long-term soil.

### 2.6 Conclusions

Dry soil ozonation resulted in the highest level of pyrene removal. In the dry soils, as pH increased, removal increased such that pyrene removal efficiencies at pH 6 and pH 8 reached 95 – 97% at a dose of 2.22 mg O<sub>3</sub>/mg Pyr (35 minute ozonation time).

Ozonation for 4 hours resulted in 81 – 98% removal for the soils at all pH levels tested.

The improvement in ozonation efficiency with respect to increasing pH is contrary to the results seen in aqueous systems.

The degree of saturation (i.e. dry versus, 5% or 10% moisture) also appeared important. The original hypothesis expected the presence of water to increase ozone demand and increase pyrene oxidation especially with the 10% saturated soil. It was also hypothesized that the increase in moisture and pH would increase the production of OH radicals that would facilitate pyrene reduction. This hypothesis was not supported by the results. The moisturized soils had slower removal of pyrene with the efficiency decreasing as the moisture content increased. The 5% moisturized soils exhibited lower ozonation efficiency, but increasing the pH improved pyrene remediation. In the 10% moisture soil, as pH increased, pyrene removal decreased. The results seen in the 10% water content soils are synonymous with the results seen in aqueous ozonation studies.

At lower temperatures, the pyrene removal improved for the moisturized soils but followed the same trends seen in the ambient temperature experiments. The dry soil ozonations yielded between 81 - 98% pyrene removals. The moisturized soils had pyrene removal from 82 - 93%. The higher pyrene conversion seen in the moisturized soils could be the result of changes in the soil properties. Ozonating the 5% and 10% moisturized soils were more difficult at the lower temperature. Soil packing and the

hardening of the soil at 13°C often prevented the ozone gas from being able to move through the column. Therefore, despite the improvements seen for pyrene removal, the difficulty in ozone delivery to moisturized soils might warrant not using lower temperatures to ozonate wet soils *in-situ*.

The aged soil experiments support the hypothesis that PAH adsorption to soil increases with longer exposure times. One of the more surprising observations from the experiments is that the ozone breakthrough curves in the aged soil matched the curves produced in the freshly contaminated soil (pH 2 and pH 6). The pyrene removal however was only 21 – 25% after 4 hours of ozonation. Therefore, soil that has been contaminated for long periods of time will require higher levels of ozone to reduce the PAH contamination.

#### 2.7 References

- 1. US Environmental Protection Agency. Workshop on Chemical Oxidation in the Vadose Zone. 1995.
- 2. Masten, S. and Davies, S.; "The Use of Ozonation to Degrade Organic Contaminants in Wastewaters." *Enviro. Sci. Technol.* **1994**, 28(4), 181A 185A.
- 3. Yao, J.J.; "Ozonation of Soils Contaminated with Polycyclic Aromatic Hydrocarbons (PAHs)", M.S. Thesis, Department of Civil and Environmental Engineering, Michigan State University, 1991.
- 4. Leahy. M.; Nelson, C.; Florentine, A.; Schmitz, R.; Ozonation as a Polish Technology for in-situ Bioremediation. *Manufactured Gas Plant Site Remediation. Fourth International In-situ and On-site Bioremeidation Symposium.* April 28 May 1, 1997. Volume 3, 479 483.
- 5. Nelson, C; Seaman, M.; Peterson, D.; Nelson, S.; Buschnom. R.; Ozone Sparging for the Remediation of MGP Contaminants. *Manufactured Gas Plant Site Remediation.* Fourth International In-situ and On-site Bioremeidation Symposium. April 28 May 1, 1997. Volume 3, 457 462.
- 6. Hsu, I.; The Use of Gaseous Ozone to Remediation the Organic Contaminants in the Unsaturated Soils, Ph.D. Thesis, Department of Civil and Environmental Engineering, Michigan State University, 1995.
- 7. Day, J.E.; "The Effect of Soil Moisture on the Ozonation of Pyrene in Soils", M.S. Thesis, Department of Civil and Environmental Engineering, Michigan State University, 1994.
- 8. Cole, D.; Masten, S.; Use of In-situ Ozonation for the Remediation of Contaminated Wurtsmith Soils. Report to the Great Lakes and Mid-Atlantic Hazardous Substance Research Center R2D2 Program. 1997.
- 9. Nimmer, M.; Wayner, B.; Morr, A.; In-situ Ozonation of Contaminated Groundwater. Environmental Progress. 19(3). 2000. 183 196.
- 10. US EPA Record of Decision. EPA 541-R01-503. Rasmussen's Dump, Brighton, MI. **2001**.
- 11. US EPA Record of Decision. EPA RO5-R84-008. 1984.
- 12. Bailey, P. "Chapter 5: Ozonation of Aromatic Compounds: Bond Attack versus Atom Attack on Benz-fused Carbocyclics." <u>Ozonation in Organic Chemistry, Volume II.</u>
  Non-Olefinic Compounds. Academic Press: New York, **1982**.

- 13. Trapido, M.; Veressinina, Y.; Munter, R.; "Ozonation and Advanced Oxidation Processes of Polycyclic Aromatic Hydrocarbons in Aqueous Solutions- A Kinetic Study." *Environ. Technol.* **1995**, 16, 729-740.
- 14. Langlais, B; Reckhow, D; Brink, D. Editors. Ozone in Water Treatment: Application and Engineering. Lewis Publihers, Inc., 1991. 11 43.
- 15. Staehelin, J. and Hoigné, J.; "Decomposition of Ozone in Water in the Presence of Organic Solutes Acting as Promoter and Inhibitors of Radical Chain Reactions." *Environ. Sci. Technol.* **1985**, 19, 1206 1213.
- 16. Lindsey, M.; Tarr, M.; "Inhibition of Hydroxyl Radical Reaction with Aromatics by Dissolved Natural Organic Matter." *Environ. Sci. Technol.* 2000, 34, 444 449.
- 17. Xiong, F. and Legube, B.; "Enhancement of Radical Chain Reactions of Ozone In Water In the Presence of An Aquatic Fulvic Acid." *Ozone Sci. & Technol.* 1991, 13(3), 349-363.
- 18. Yao, J.; Ph.D. Dissertation. "The Mechanism of the Reaction of Ozone with Pyrene and Benz[a]anthracene in Acetonitrile/water Mixture." Michigan State University: Department of Civil and Environmental Engineering. 1997.
- 19. Herner, H, Trosko, J.; Masten, S.; "The Reaction of Ozone with Pyrene: The Byproducts and Their Toxicological Implication". *Environ. Sci. Technol.* **2001**, 32(10), 3001 -3012.
- 20. Atkinson, R. and Carter, W.; "Kinetics and Mechanisms of the Gas-Phase Reactions of Ozone with Organic Compounds under Atmospheric Conditions." *Chem. Rev.* 1984, 84, 437–470.
- 21. Sotelo, J; Beltran, F.; Benitez, F.; Beltranheredia J.; Ozone Decomposition in Water Kinetic Study. *Industrial and Engineering Chemistry Research.* 1987, 26(1), 39 43.
- 22. Hillel, D.; Environmental Soil Physics. Academic Press: New York, 1998, 327.
- 23. Copeland, P.; Dean, R.; McNeil, D.; "The Ozonolysis of Polycyclic Hydrocarbons: Part II". J. Chem. Soc. 1961, 1232 1236.
- 24. Eberius, M; Berns, A; Schuphan, I.; "Ozonation of pyrene and benzo[a]pyrene in silica and soil- C<sup>14</sup> balances and chemical analysis of oxidation products as a first step to ecotoxicological evaluation." Fresnius Z. Anal., 1997, 359, 274-279.
- 25. Trapido, M.; Veressinina, Y.; Munter, R.; "Ozonation and Advanced Oxidation Processes of Polycyclic Aromatic Hydrocarbons in Aqueous Solutions- A Kinetic Study". *Environ. Technol.* **1995**, 16, 729-740.

- 26. Zeng, Y.; Hong, P.; Wavrek, D. "Chemical-Biological Treatment of Pyrene". Water Res. 2000, 34(4), 1157-1172.
- 27. Bader, H.; Hoigne, J.; J. Ozone Sci. Technol. 1983, 4, 169-176.
- 28. Grimmer, G.; Bohnke, H.; Borwitzky, H.; "Gas-chromatographische Profilanalyse der polycyclischen aromatischen Kohlenwasserstoffe in Klarschlammproben," *Fresenius Z. Anal. Chem.* 1978, 289, 91 95.
- 29. Martens, D.; Frankenberger Jr., W; "Enhanced Degradation of Polycyclic Aromatic Hydrocarbons in Soil Treated with an Advanced Oxidated Process – Fenton's Reagent (Article number 340072)" http://www.crcpress.com/jour/sss/arts/340072.html
- 30. Lee, P.; Ong, S.; Golchin, J.; Nelson, G.; "Extraction Method for Analysis of PAHs in Coal-Tar-Contaminated Soils". *Practice Periodical of Hazardous, Toxic, and Radioactive waste Management.* October 1999, 155-162.
- 31. Choi, H.; Lim, H.-N.; Hwang, T.M.; Kang, J.; "Transport characteristics of gas phase ozone in unsaturated porous media for in-situ chemical oxidation." *Journal of Contaminant Hydrology.* 2002. 57, 81 98.
- 32. Lim, H.; Choi, H.; Hwang, T.; Kang, J.; "Characterization of Ozone decomposition in a soil slurry: kinetics and mechanisms." Water Res. 2002, 219 229.
- 33. Masten, S.; "Ozonation of VOC's in the presence of Humic Acid". Ozone. Sci. Eng. 1991, 13(3), 287-312.

# Chapter 3

## HPLC and GC/MS Identification of Pyrene Ozonation Byproducts

### 3.1 Introduction

Five significant studies have identified pyrene ozonation byproducts. Three aqueous ozonation studies have identified at least 16 pyrene byproducts [1-4]. The proposed structures in aqueous systems are consistent with the byproducts detected in subsequent pyrene ozonation studies [5]. Two published papers have addressed pyrene ozonation byproducts in soil and on glass beads [6-7]. In the solid media studies, at least 33 byproducts were presented. Criticism of the methods used for the solid media, however, has lead to doubt of the validity of the byproducts produced.

## a. Pyrene ozonation byproducts in aqueous systems

In non-participating solvents, ozone is theorized to react with pyrene at the 4, 5 and then the 9, 10 bonds. The byproducts first formed are phenanthrene-like compounds followed by biphenyl-like compounds [2-4]. Figure 3.1 is the pathway proposed for pyrene ozonation [2]. The work by Bailey [2] summarized the byproducts produced from many ozonation studies in various solvents. Figure 3.2 presents a summary the 16 byproducts identified during ozonation in 90%: 10% acetonitrile: water (v/v) mixture [4]. The byproducts detected by Yao et al. [4] included many of the byproducts presented by Bailey [2] and 8 additional compounds.

a: R = Hb: R = OH

Figure 3.1 Pyrene ozonation pathways (Bailey, 1982)

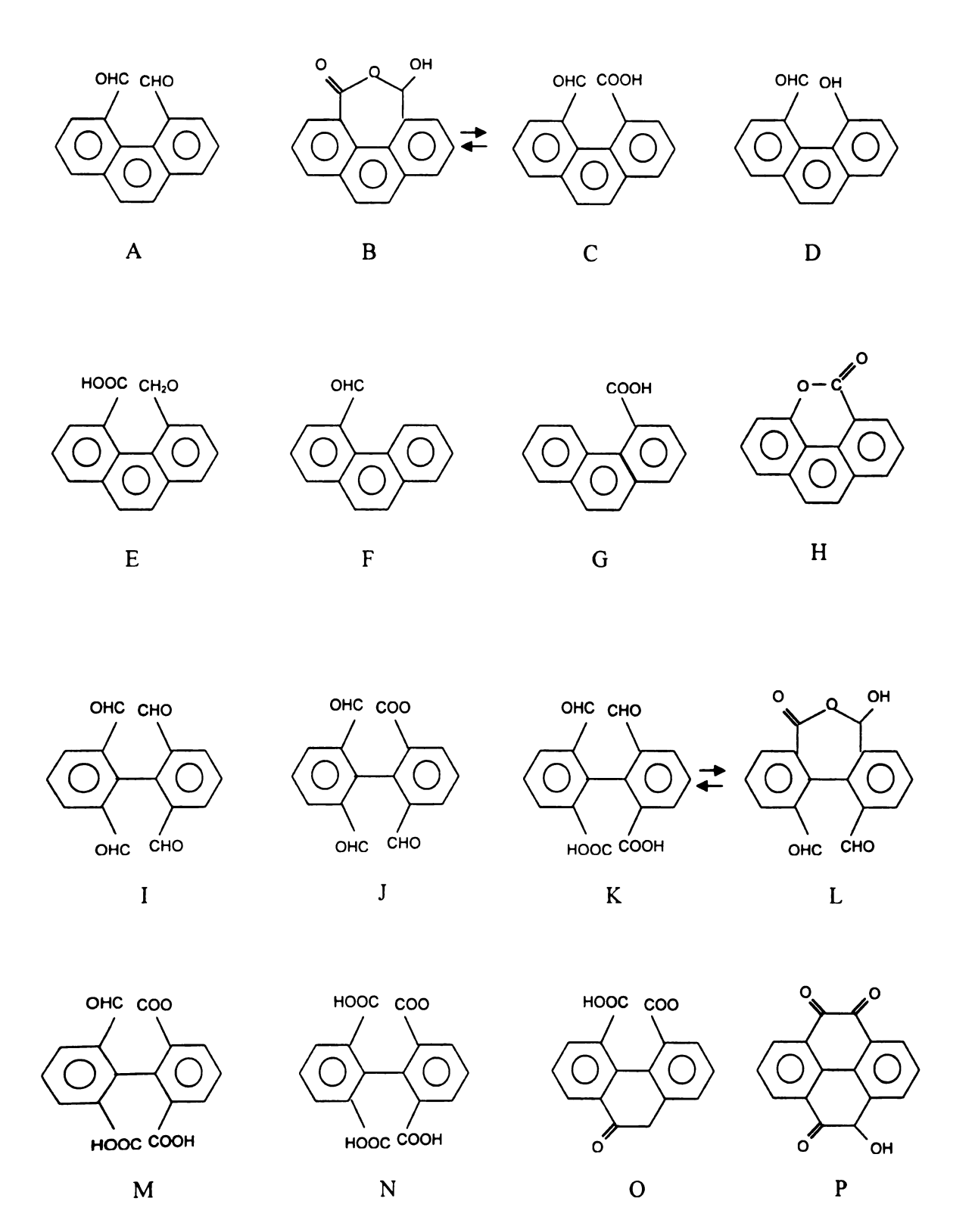


Figure 3.2 Byproducts from pyrene ozonation in 90% acetonitrile/10% water (Yao et al., 1998)

### b. Pyrene ozonation Byproducts formed in Solid media

#### Ozonation in Soil/Silica Sand

Eberius et al. [6] investigated the ozonation of pyrene and benzo[a]pyrene in silica and soil to determine the oxidation byproducts. This study hypothesized that, like the previous aqueous ozonation studies, the soil ozonation byproducts produced would be similar to the pyrene ozonation pathway described by Bailey [2]. The byproducts produced during the soil study were phenanthrene, biphenyls, and quinone-like compounds. This evidence coincides with the pathway hypothesized to occur in aqueous systems. Water-soluble byproducts accounted for 20-30%, non-extractable bound residues accounted for 10%, and the balance for the byproducts produced was extractable in organic solvents.

The compounds identified in the Eberius et al. study differed from the predictions by Bailey [2] and Yao et al. [4]. The difference was primarily due to the functional groups attached. Eberius et al. [6] modified the original hypothesis for the two ozonation pathways by suggesting that the functional groups attached to the phenanthrene, biphenyl, and quinone structures should include -COOCH<sub>3</sub>, in addition to the -COOH and -CHO groups described by Bailey [2]. Figure 3.3 depicts the Eberius et al. [6] pathways. Critiques of the study argued that the use of methanol as an extraction solvent might have caused methylation of the byproducts [6]. In studies conducted by Herner [5], methylated compounds were observed when methanol was used in the extraction procedure. The methylation of the compounds could explain the difference between the byproducts detected in aqueous system ozonation and the ones produced in the soil. The author also conceded to the pre-publication critiques of the paper by agreeing that methylation may

have corrupted the results. Table 3.1 presents the list of PAH-quinones and eight ring fission products identified in the soil study.

Table 3.1. Byproducts Identified following Pyrene Ozonation in Silica

Compound	Molecular Weight
Phenanthrene-dimethylester	294
Formyl-phenanthrene-methylester	264
Triformyl-biphenyl-methylester	282ª
Biphenyl-tetramethylester	386
Dimethoxy-pyrene	262
Carboxy-naphthalene-trimethylester	346
Triformyl-benzene-methylester	220
Benzene-tetramethylester	310

a. The paper reported the molecular weight as 282. The correct molecular weight should be MW 296.

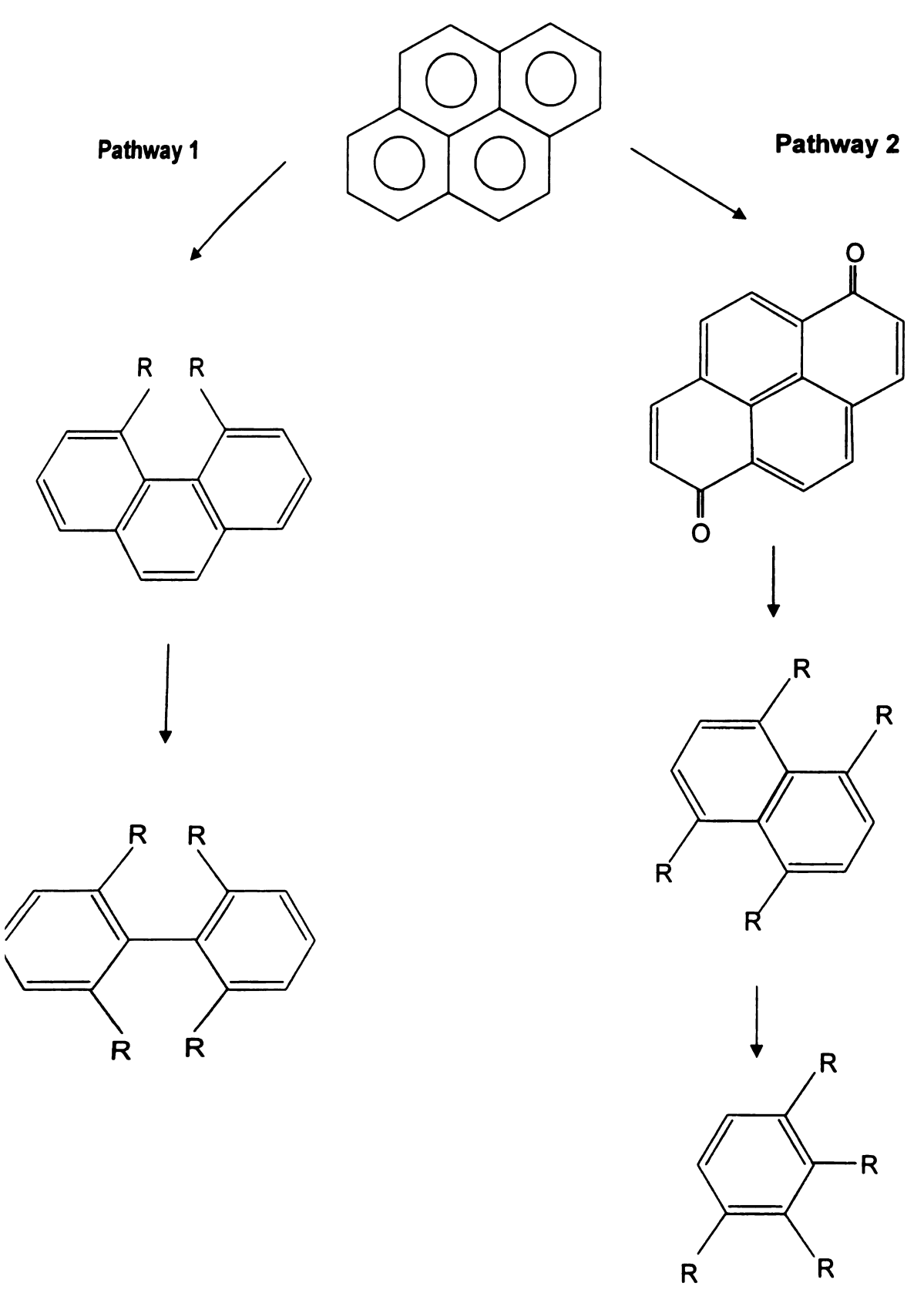


Figure 3.3 Proposed pyrene ozonation Pathway 1 and Pathway 2 R = COOH, CHO, and COOCH<sub>3</sub> (after methylation)

### Ozonation of pyrene coated glass beads

Zeng et al. [7] investigated the efficacy of combining ozone treatment and biological treatment for pyrene removal. In the first study, water was ozonated to saturation and supplied to a packed column containing glass beads coated with recrystallized pyrene. The pyrene was then extracted from the beads and used for biological treatment. The second study evaluated ozonation of 1 g of pyrene added to water in either a batch reactor or serum bottles. Following ozonation, Zeng et al. [7] identified 25 byproducts. Two intermediates (4, 5-phenanthrenedialdehyde and 2, 2', 6, 6'-biphenyltetraaldehyde) were produced in the column, but not in the batch reactor. These two compounds directly correlate to two of the compounds produced in aqueous ozonations [2, 4]. Table 3.2 is a listing of the 25 compounds detected in the study. Table 3.3 lists the byproducts removed by biotreatment following ozonation [7]. Since publication, the Zeng et al. [7] byproducts have also been challenged [8]. Buser et al. [8] noted that many of the predicted byproducts could not to be the result of ozonation, but are possibly artifacts from plastic and the solvents used.

## 3.2 Significance of ozonation byproduct studies

Both identifying and understanding the toxicity of pyrene ozonation compounds remains open for research. The 20-30% water-soluble substances detected in Eberius et al. [6] would be important to chemically identify because these compounds are likely to soluble and mobile in groundwater. At the time of publication for the soil study,

Table 3.2 Byproducts produced in the ozonated column effluent ● found, ○ not found (Zeng et al., 2000)

Recention	Compound	Betore	OZOIIS	Ozonated efficient at interval	it interval		CHISC
time (min)	•	ozonation	15-30 min	30-60 min	60-90 min	60-90 min 90-120 min (120 min after)	(120 min after)
14.6	Unknown (m/z 154)	•	•	•	•	•	•
15.3	Unknown (m/z 139)	•	•	•	•	•	•
20.2	Ethanol, 2-[2-butoxyethoxy]-	•	0	0	0	0	0
22.5	Phthalic anhydride	•	•	•	•	0	•
23.2	Propanoic acid, 2-methyl-, butyl ester	•	•	•	•	0	•
25.3	Tetradecane	•	•	•	•	0	•
28.1	Pentadecane	•	•	0	0	0	0
28.2	Butylated hydroxytoluene	•	•	0	0	0	•
29.5	Diethyl phthalate	•	0	0	0	0	0
30.7	Hexadecane	•	•	•	0	0	0
33.0	Nonyl phenol	•	•	•	0	0	•
37.6	4H-cyclopenta[def]phenanthrene	•	•	•	•	•	•
37.9	Dibutyl phthalate	•	•	•	•	•	•
38.3	Hexadecanoic acid	•	•	•	0	0	•
38.8	Xanthone	0	0	•	•	•	•
41.6	Henicosane	•	•	•	•	•	•
41.7	Pyrene	•	•	•	•	•	•
43.3	2,2',6,6'-biphenyltetraaldehyde	0	•	•	•	•	•
45.1	Docosane	•	•	•	•	•	•
45.3	Tricosane	•	•	•	•	•	•
46.8	Benzylbutyl phthalate	•	•	•	•	•	•
46.9	4, 5-Phenanthrenedialdehyde	0	•	•	•	•	•
48.4	Tetracosane	•	•	•	•	•	•
48.7	Cyclopenta[def]phenanthrene	•	•	•	•	•	•
48.8	1,2-Benzenedicarboxylic acid	•	•	•	•	•	•
50.4	Hexacosane	•	•	•	•	•	•
53.6	6-Pronvl tridecane	•	•	•	•	•	•

Table 3.3 Intermediates and products in ozonated effluent after various degrees of biotreatment; ● found, ○ not found (Zeng et al., 2000)

Retention	Compound	Biological incubation of ozonated effluent (Days)				
time		0 5 10 15				ys) 20
(min)	77.1		<u> </u>	10		
14.6	Unknown (m/z 154)	•	-		•	. •
15.3	Unknown (m/z 139)	•	•	•	•	0
20.2	Ethanol, 2-[2-butoxyethoxy]-	0	0	0	0	U
22.5	Phthalic anhydride	•	0	0	0	0
23.2	Propanoic acid, 2-methyl-, butyl ester	•	0	0	0	0
25.3	Tetradecane	•	•	•	•	•
28.1	Pentadecane	0	0	0	0	0
28.2	Butylated hydroxytoluene	•	•	•	•	•
29.5	Diethyl phthalate	0	0	0	0	0
30.7	Hexadecane	•	0	0	0	0
31.0	Phosphoric acid tributyl ester	0	0	0	•	•
33.0	Nonyl phenol	•	0	0	0	0
37.6	4H-cyclopenta[def]phenanthrene	•	0	0	0	0
37.9	Dibutyl phthalate	•	•	•	•	•
38.3	Hexadecanoic acid	•	0	0	0	0
38.8	Xanthone	•	0	0	0	0
41.6	Henicosane	•	0	0	0	0
41.7	Pyrene	•	0	0	0	0
43.0	Biological culture (m/z 226)	•	•	•	•	•
43.3	2,2',6,6'-biphenyltetraaldehyde	•	0	0	0	0
45.1	Docosane	•	0	0	0	0
45.3	Tricosane	•	•	•	•	•
46.8	Benzylbutyl phthalate	•	•	•	•	•
46.9	4, 5-Phenanthrenedialdehyde	•	•	•	•	•
48.4	Tetracosane	•	•	•	•	•
48.7	Cyclopenta[def]phenanthrene	•	•	•	•	•
48.8	1,2-Benzenedicarboxylic acid	•	•	•	•	•
48.9	Pentacosane	•	•	•	•	•
50.4	Hexacosane	•	•	•	•	•
53.6	6-Propyl tridecane	•	•	•	•	•

Eberius et al. [6] noted that no information existed on the toxicity or mutagenicity of the aromatic ozonation products containing carboxyl-groups and formyl-groups, especially the reactive aldehydes that are under suspect of exhibiting possible negative biological effects. Recent publications presented findings that the presence of aldehyde or carboxylic acid functional groups attached to PAH ozonation byproducts affected toxicity [9-11].

The Zeng et al. [7] study evaluated only the acute toxicity of the treated soil to *E. coli* and not the potential for carcinogenic behavior to humans or animals. Identifying products and understanding toxicity is also important because at least five days of bioremediation was required in the Zeng et al. [7] to remove 10 of the 25 byproducts produced (40%). As such, water-soluble byproducts could, potentially, be transported through groundwater before bioremediation could effectively reduce toxicity. Bioremediation could not remove the remaining 60% from the Zeng et al. [7] product list even after 20 days of treatment.

### 3.3 Research Focus

The goal for this research was to identify the byproducts produced during pyrene soil ozonation. One major area of interest was to determine if environmental conditions such as temperature, soil moisture, and pH would affect pyrene decomposition and byproduct formation. The study consisted of two phases. Phase 1 was the HPLC analyses of dry, 5% moisture, and 10% moisturized soil at various conditions. The pH levels tested were pH 2, 6, and 8 and the temperatures evaluated were 13°C and 25°C. Extracts using a polar solvent were used to remove from the soil, products that would become mobile in

groundwater. A non-polar solvent was used to extractable products that would remain bound to the soil. In phase 2, the soil extracts were fractionated using the HPLC and the fraction components were identified using GC/MS.

### 3.3.1 Materials

Chemicals. Pyrene was purchased at a purity of 98% from Sigma Chemical (Sigma Chemical, St. Louis, MO). Two compounds, 2,2',6,6'-biphenyl tetraaldehyde and 2,2',6,6' -biphenyl tetra carboxylic acid, were synthesized by Joseph Ward (MSU Department of Organic Chemistry, East Lansing, MI). The synthesis method for the compounds is discussed in detail in Chapter 4.

Soil. Metea soil with a 300 ppm pyrene concentration was ozonated using the methods described in Chapter 2. This treated soil was then used for HPLC and GC/MS studies.

#### 3.3.2 Methods

Extraction. Direct extraction was used to reclaim pyrene and ozonation byproducts from soil [11, 12]. Direct extraction is reported to result in removal efficiencies statistically similar to or better than the Soxhlet extraction method for PAH compounds from coal tar contaminated soil [13]. A dry weight of 7.6 g of soil was washed in 200 ml of acetonitrile (ACN) or DI water. The purpose for the ACN extract was to remove for analysis any organic compounds that would remain bound to soil particles after ozonation. The DI extract was used to remove from the soil any compounds that would be able to dissolve into groundwater and potentially travel to nearby aquifer systems. The flasks were shaken in the solvent for 3 hours at 150 cycles per minute. Following the extraction procedure, 1

ml of 1 M H<sub>2</sub>SO<sub>4</sub> was added to the flask to encourage settling of the suspended solids. The contents of the flasks were then allowed to settle for 24 hours. Mass balances for the pyrene extraction procedure yielded between 95 – 97% pyrene recoveries from soil. For each experiment, pyrene was extracted from untreated contaminated soil for use as a soil control. Both ACN and DI extracts were analyzed using reverse-phase high pressure liquid chromatography (RP-HPLC).

RP-HPLC Analysis. A Gilson HPLC unit (Worthington, OH), UV detector (Model 116), and an Altima C18 reverse phase column (5 μM) with dimensions 4.6 x 250 mm was used for HPLC Analysis (Alltech Co., Deerfield, IL). The effluent was monitored at 254 nm wavelength. Pure ACN (99.8% purity) and HPLC grade water were used as the mobile phases. The linear gradient used for the mobile phase was 25%:75% ACN: deionized (DI) water at the time of injection and held for 3 minutes. It was then linearly increased to 90%: 10% ACN: DI water over 5 minutes, held at 90%: 10% ACN: DI water for 10 minutes, and linearly decreased to 25%: 75% ACN: DI water over 5 minutes. The mobile phase was held for an additional 5 minutes at this ratio. The total run time was 28 minutes. All extracts were run in triplicate.

### Gas Chromatography/Mass Spectra (GC/MS)

Sample Preparation. Soil extracts were fractionated to separate significant peaks using the HPLC method described above. The ozonated samples and fractions were then rotary evaporated (Buchi WaterBath with Rotavapor, Westbury, NY) and dried to recover the solid byproduct. The byproduct fractions were re-suspended in ACN and injected into a

Varian Chrompack 2000 Saturn GC/MS. The temperature program for the GC/MS is presented in Table 3.4.

Table 3.4. Temperature profile for GC/MS method

Temperature	Increment Rate (°c/min)	Hold Time (minutes)	Total Run Time (minutes)
100°c	-	2	2
220°c	20°c	0	8
260°c	5°c	2	18
300°c	20°	2	22

### 3.4 Results and Discussion

### 3.4.1 Pyrene and control HPLC chromatograms

The RP-HPLC method eluted the more polar compounds from the column first by starting with a 25%:75% acetonitrile: water mobile phase at the time of injection. The mobile phase was linearly increased to a solvent mixture of 90%:10% acetonitrile: water to elute the more polar organic compounds. Two synthesized pyrene ozonation byproducts (MSU Department of Organic Chemistry, East Lansing, MI) and a pyrene standard were available to use as controls. The first synthesized compound (2,2',6,6' biphenyl tetra carboxylic acid) was biphenyl-like with four –COOH functional groups and eluted after 2.0 ± 0.1 minutes (Figure 3.4a). The second synthesized compound, 2,2',6,6' biphenyl tetraaldehyde, was biphenyl-like with four –CHO functional groups.

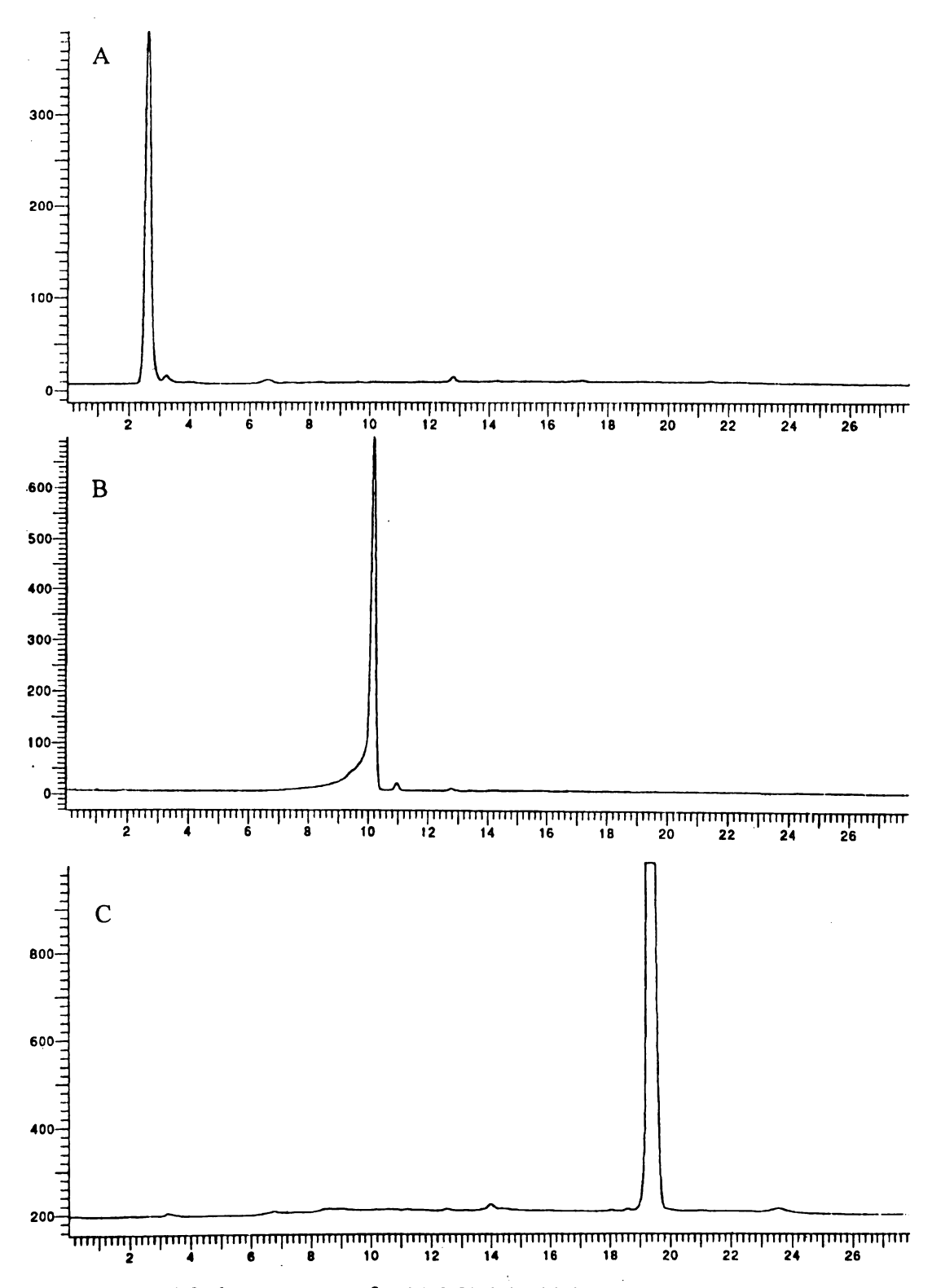


Figure 3.4 HPLC chromatograms for (a) 2,2',6,6' -biphenyl tetra carboxylic acid, (b) 2,2',6,6'-biphenyl tetra aldehyde, (c) pyrene standard.

This compound eluted from the column after 9.8 - 10.2 minutes (Figure 3.4b). The pyrene standard (98% pure, Sigma Chemical) had a retention time of approximately 18.6  $\pm$  0.4 minutes (Figure 3.4c).

Air stripping and oxygen stripping control experiments were conducted to determine if either of the gases could reduce the pyrene concentration in soil. The gases were sparged through the soil reactor for 24 hours at conditions identical to the ozonation system. Chromatograms from the oxygen-sparged and the air-sparged soil matched the pyrene control (soil extract). Figure 3.5a – c and Figure 3.6a – c show the chromatograms for the ACN and the DI extracts for pyrene soil control, oxygen stripped pyrene soil and air-stripped pyrene soil, respectively. These experiments indicated that neither air nor oxygen was able to reduce the pyrene the in soil.

### 3.4.2 HPLC Chromatograms

#### **Ozonated Soil**

The chromatogram for the 5% moisture soil (pH 6) is a good representation of the DI extract chromatograms obtained for the various soil conditions evaluated (Figure 3.7). In the chromatogram, a large peak eluted after 2 minutes. As higher ozone doses were applied to the soil, this peak is observed to increase in area. The second notable peak eluted after 4 minutes and decreased with increasing ozone. In the DI extract for pyrene soil (non-ozonated), the same two peaks were detected (Refer to Figure 3.6 a). The peak eluting at 2 minutes in the non-ozonated soil was significantly smaller than the 2 minute peak in the ozonated soil. The peak in the non-ozonated soil at 4 minutes was similar in

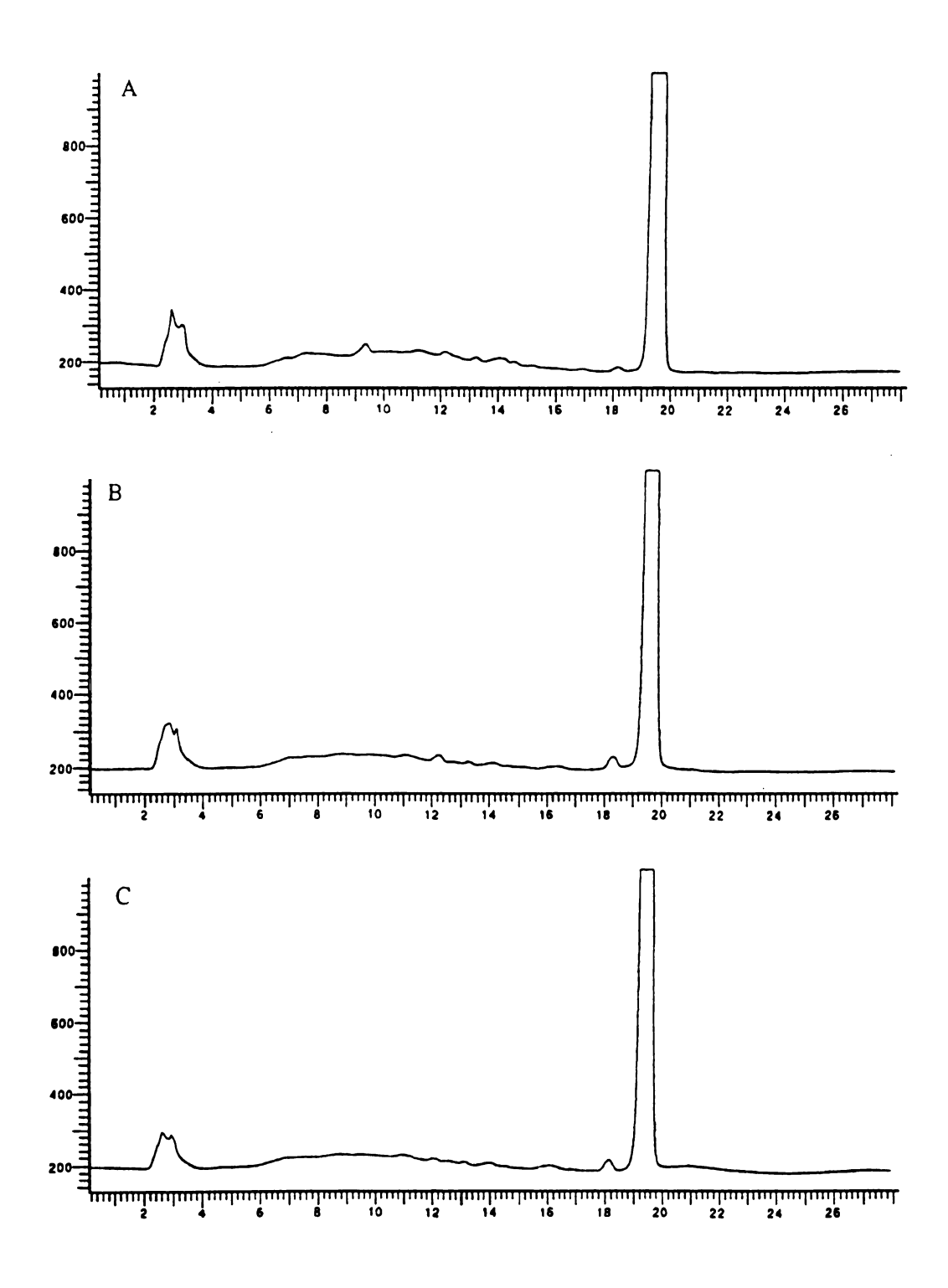


Figure 3.5 Acetonitrile extracts from 24 hour oxygen and air sparged pyrene contaminated soil (a) pyrene soil, (b) oxygen-sparged pyrene soil, (c) air-sparged pyrene soil.

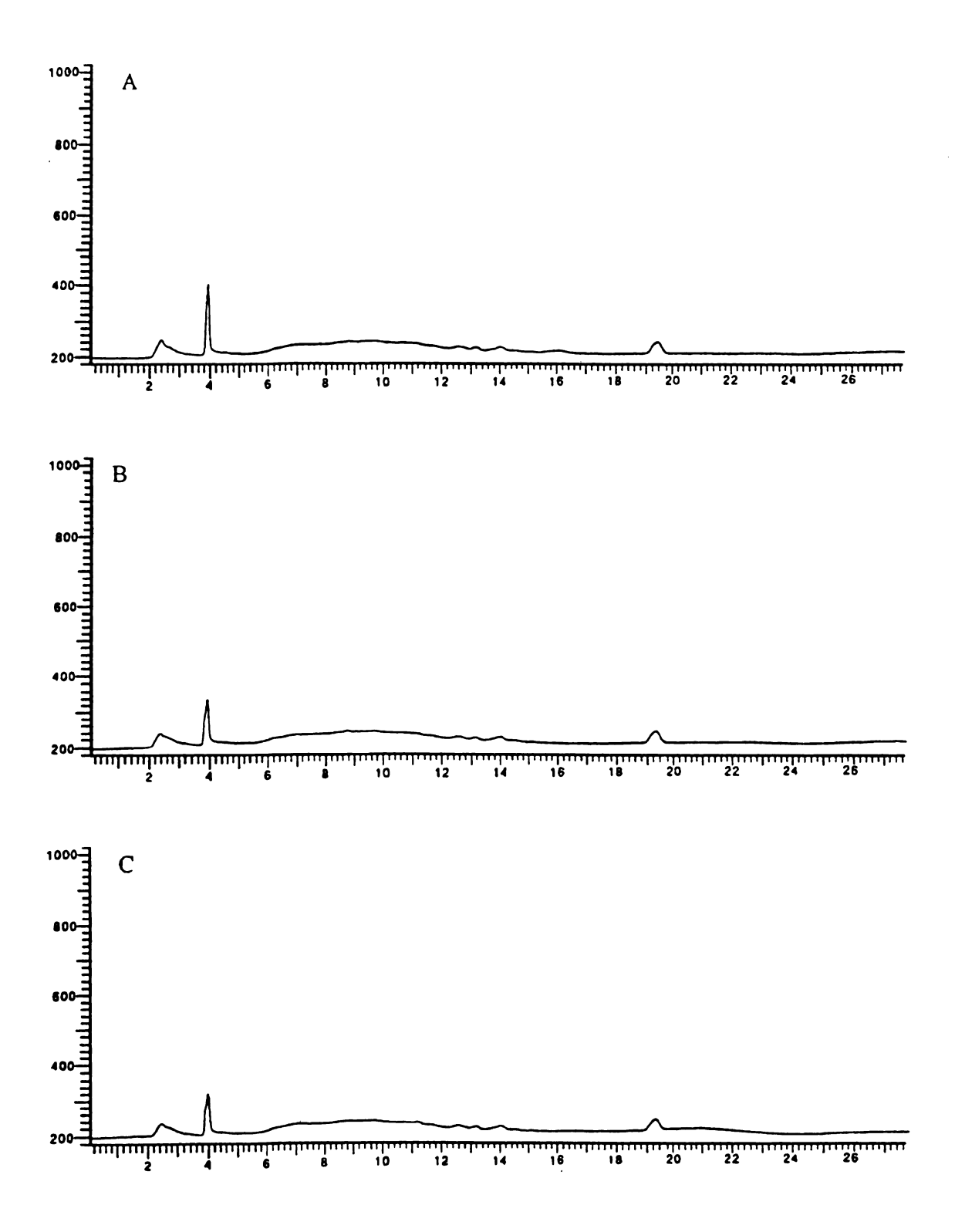


Figure 3.6 Deionized water extracts from 24 hour oxygen and air sparged pyrene contaminated soil (a) pyrene soil, (b) oxygen-sparged pyrene soil, (c) air-sparged pyrene soil.

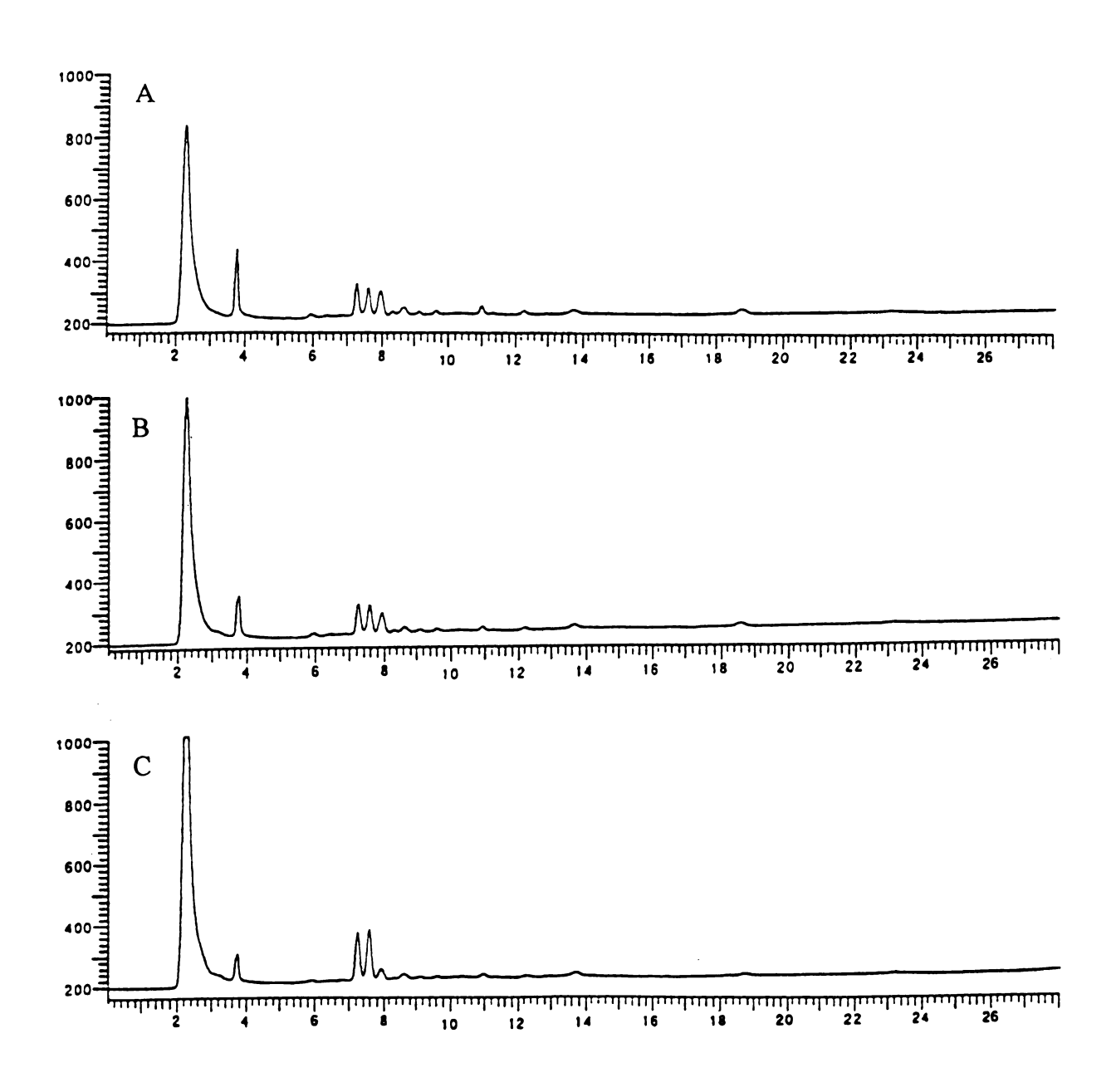


Figure 3.7 DI extract chromatogram for 5% moisture (pH 6) pyrene contaminated soil. (a) 2.2 mg  $O_3$ /ppm pyr, (b) 3.85 mg  $O_3$ /ppm pyr, (c) 16 mg  $O_3$ /ppm pyr.

size to the low  $O_3$  dose (2.2 mg  $O_3$ /mg Pyr) soil but larger than the 4 minute peaks in the ozonated soils > 3.85 mg  $O_3$ /mg Pyr dose.

A set of peaks eluting at 7.2, 7.6, and 7.8 minutes in the ozonated DI extracts are identified as the triplet peaks in the chromatograms. The triplet peaks are interesting because the peaks were consistently present in the moisturized soil extracts and the dry soil (pH 2). The third peak in the triplet set decreased in area with increasing ozone, while the remaining two had a small increase in area. The triplet peaks were the most prominent in the 10% moisturized soils and were either not detected, or were very small, in the dry soil chromatograms (pH 6, pH 8). Figures 3.8 and 3.9 are the DI extract chromatograms for dry and 10% moisture soil at pH 6, respectively.

Figure 3.10 is an example of the HPLC chromatogram for the 5% moisture soil (pH 6) ACN extract. In the ACN extract, the most prominent peak was the pyrene peak occurring at  $18.6 \pm 0.2$  minutes. The area for this peak decreased as ozonation time increased. The dry soil (pH 6) exhibited the fastest reduction in pyrene while the 10% moisture soil (pH 6) had the slowest pyrene removal (Figure 3.11 and Figure 3.12). Minor peaks eluted after 2 minutes and between 6 – 14 minutes retention time. In the moisturized soils, a peak at 11.8 minutes was also present in the chromatograms.

Due to the similarity in the extract chromatograms for the soils tested, all of the chromatograms are provided in Appendix B. The chromatograms included in the appendix are for the soils at three saturation levels (0, 5% and 10%), the three pH levels of pH 2, 6 and 8, and the two temperatures evaluated (13°C and 25°C).

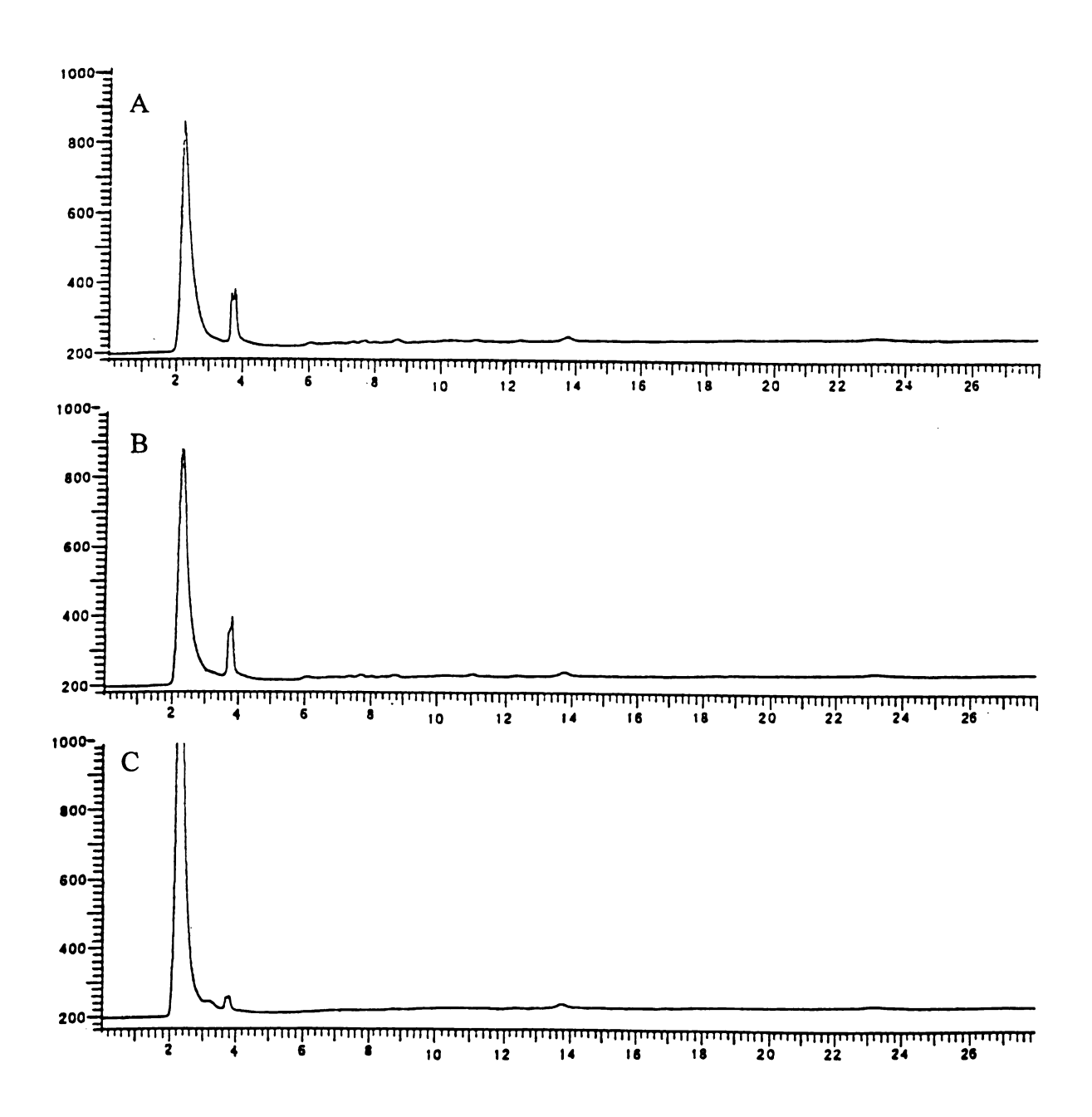


Figure 3.8 DI extract chromatogram for dry (pH 6) pyrene contaminated soil. (a) 2.2 mg  $O_3$ /ppm pyr, (b) 3.85 mg  $O_3$ /ppm pyr, (c) 16 mg  $O_3$ /ppm pyr.

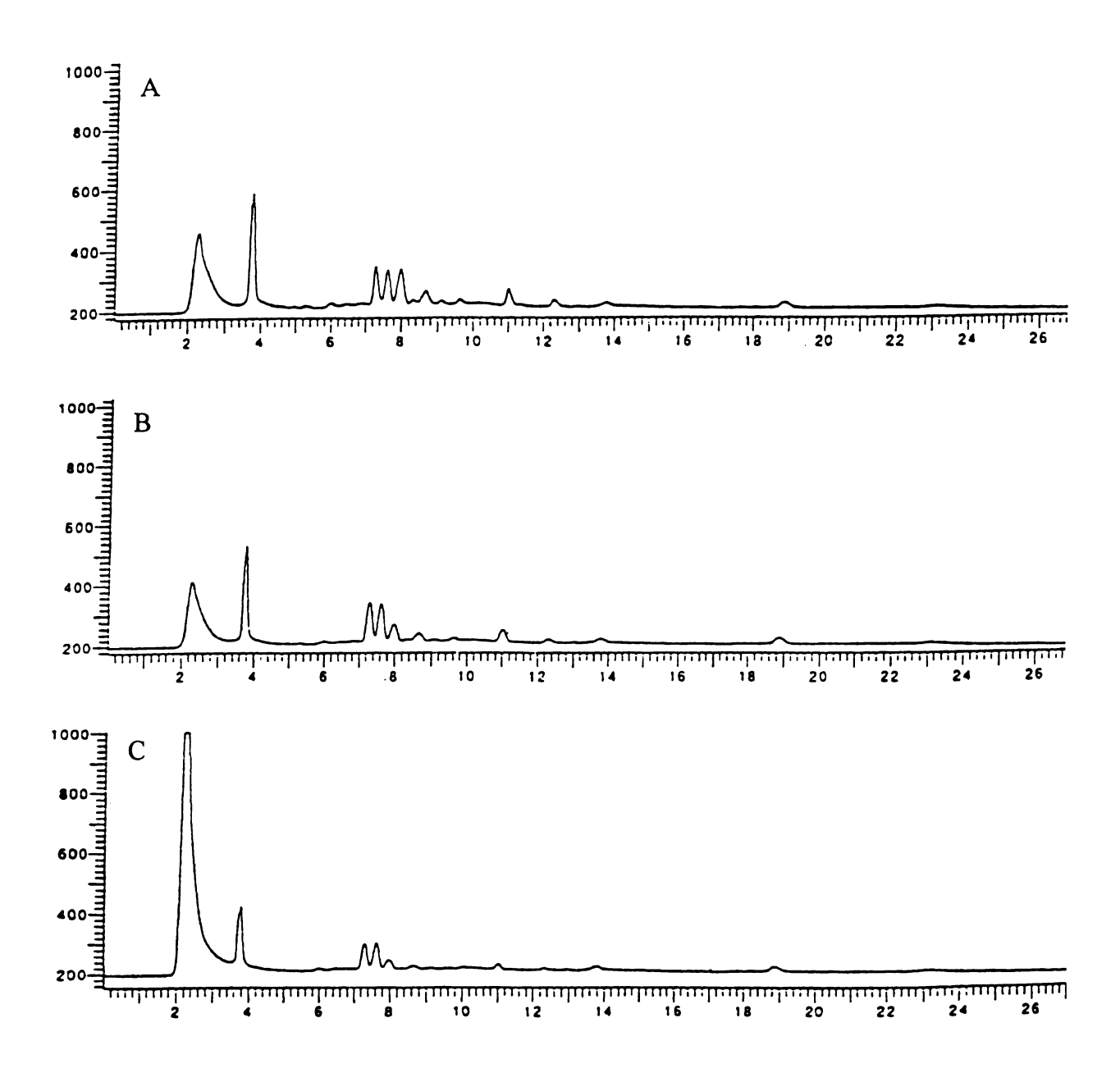


Figure 3.9 DI extract chromatogram for 10% moisture (pH 6) pyrene contaminated soil. (a) 2.2 mg  $O_3$ /ppm pyr, (b) 3.85 mg  $O_3$ /ppm pyr, (c) 16 mg  $O_3$ /ppm pyr.

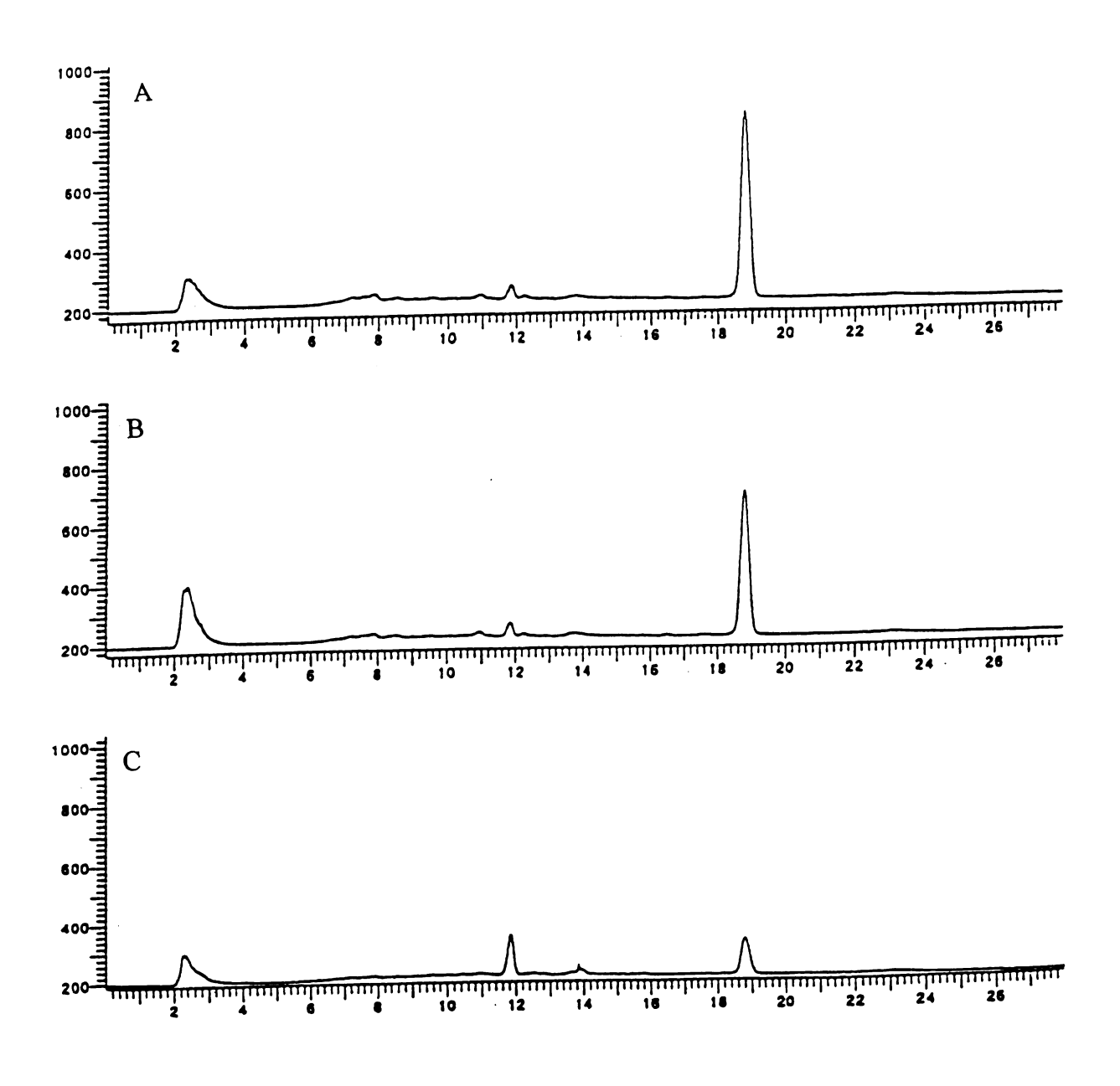


Figure 3.10 ACN extract chromatogram for 5% moisture (pH 6) pyrene contaminated soil. (a) 2.2 mg  $O_3$ /ppm pyr, (b) 3.85 mg  $O_3$ /ppm pyr, (c) 16 mg  $O_3$ /ppm pyr.

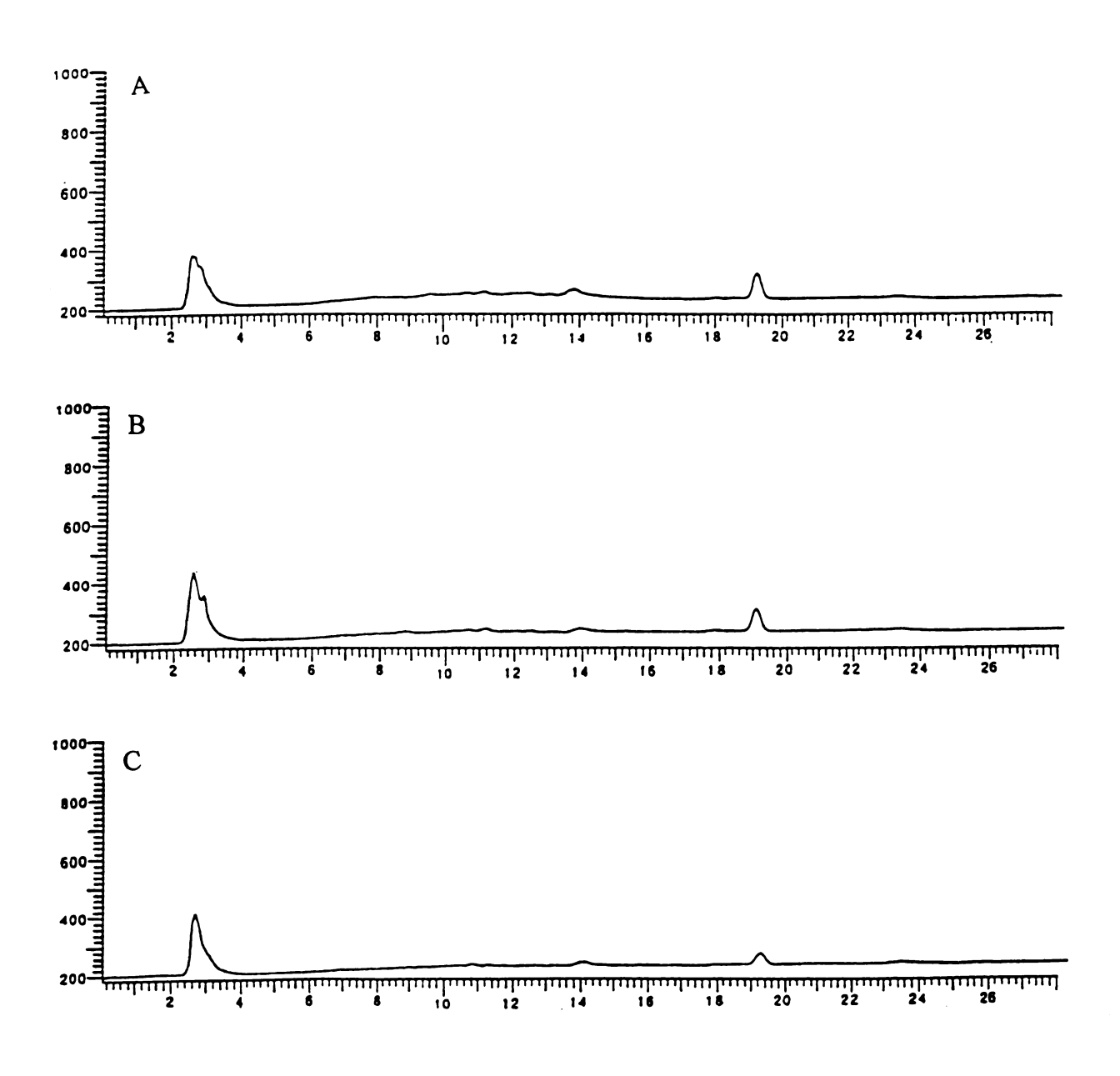


Figure 3.11 ACN extract chromatogram for dry (pH 6) pyrene contaminated soil. (a) 2.2 mg  $O_3$ /ppm pyr, (b) 3.85 mg  $O_3$ /ppm pyr, (c) 16 mg  $O_3$ /ppm pyr.

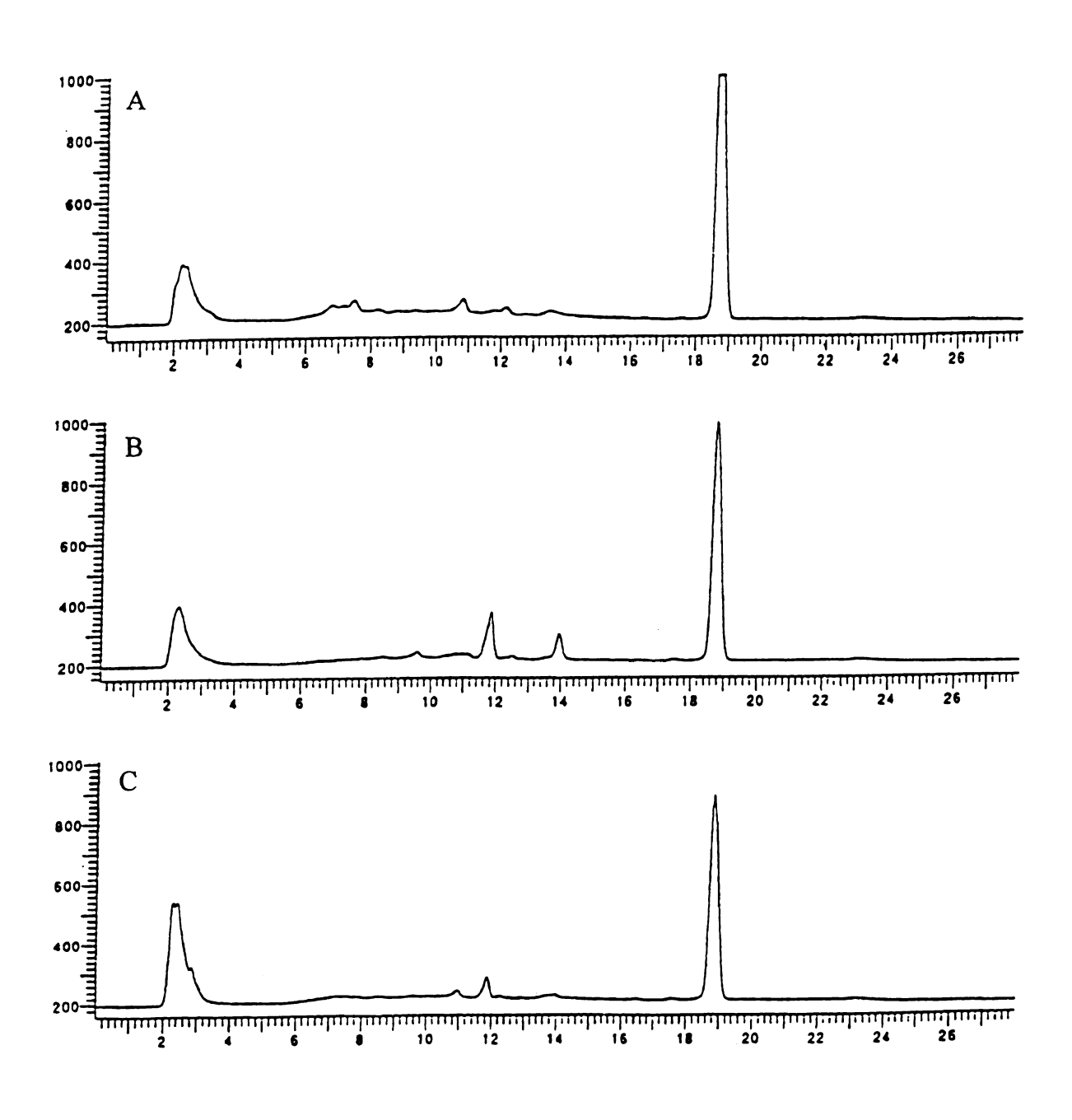


Figure 3.12 ACN extract chromatogram for 10% moisture (pH 6) pyrene contaminated soil. (a) 2.2 mg  $O_3$ /ppm pyr, (b) 3.85 mg  $O_3$ /ppm pyr, (c) 16 mg  $O_3$ /ppm pyr.

# 3.4.3 GC/MS Analysis

GC/MS analysis was conducted by fractionating the ACN and DI extracts from ozonated samples. During this phase of the research, attempts were made to fractionate the peaks to isolate individual compounds. For some of the smaller peaks, recovering sufficient quantities for analysis and obtaining pure fractions was extremely difficult. Therefore, collecting groups of peaks improved recovery efforts and allowed for the identification of several compounds. A pyrene standard GC/MS reference spectrum was available in the Saturn GC/MS database. Yao [3] dissertation research was an extensive study identifying pyrene ozonation byproducts in 90%: 10% acetonitrile: water and provided GC/MS spectra. This research could be used as a reference for the ozonation byproducts.

The HPLC peaks were fractionated into 15 sections (Figure 3.13). The compounds identified were consistent with Pathway 1 pyrene soil ozonation byproducts and possibly two new compounds originating from Pathway 2 (Figure 3.14; Table 3.5). Three of the byproducts proposed for aqueous ozonation [3-5] were not found in this study. The GC/MS spectra for all compounds detected are presented in Appendix C.

Fraction 1 (F1) and F8 eluted after 2 minutes from the HPLC column. The compounds in this peak were important to identify because this peak appeared to contain the major pyrene oxidation byproduct or byproducts produced. The GC/MS detected the presence of two compounds with the molecular weights of MW 282 and MW 330. The polarity of these compounds would suggest that they will readily dissolve into ground-



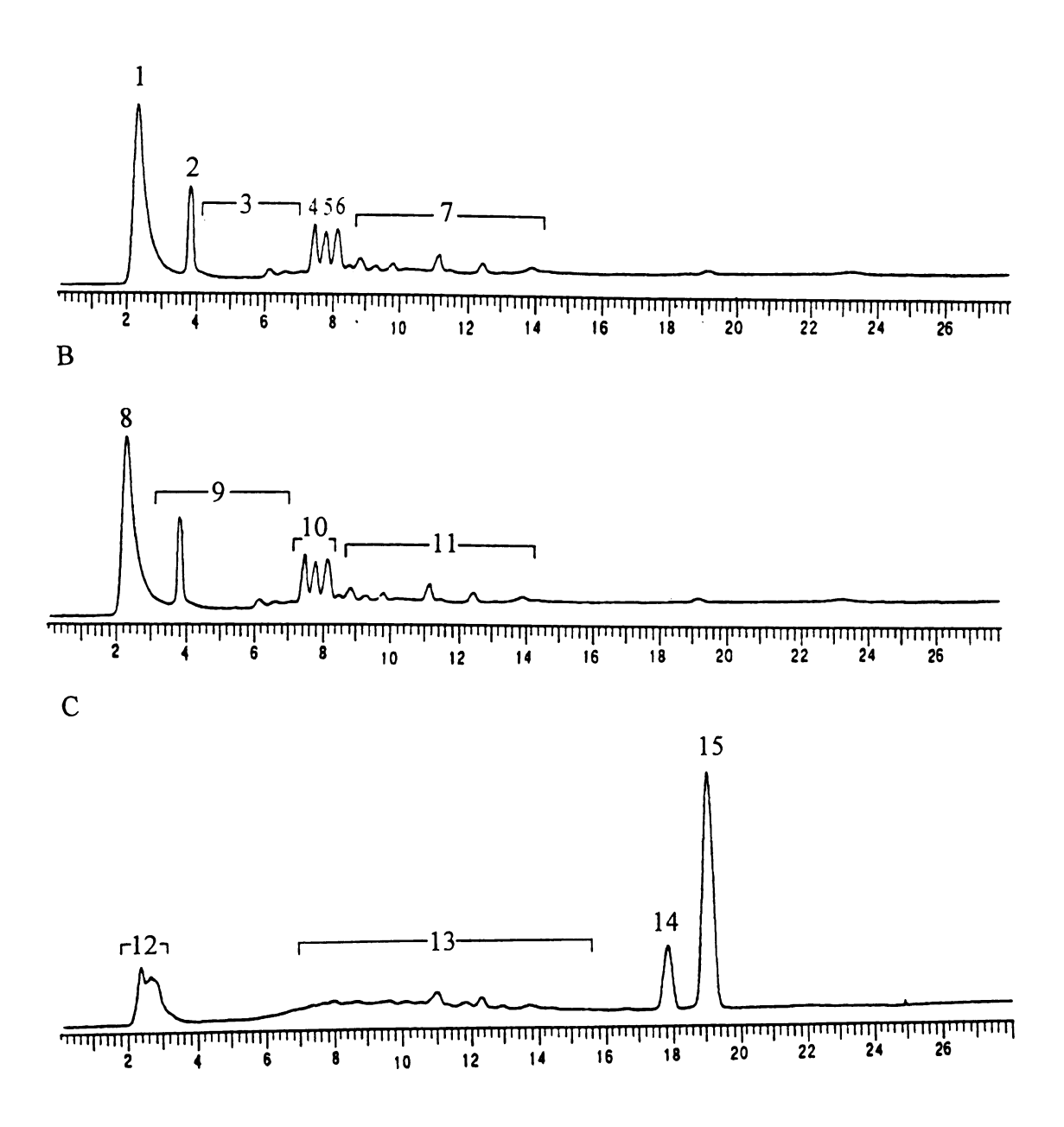


Figure 3.13 Fractions collected for GC/MS analysis. (a) DI extracts fraction scheme 1; (b) DI extracts fraction scheme 2; (c) ACN extracts.

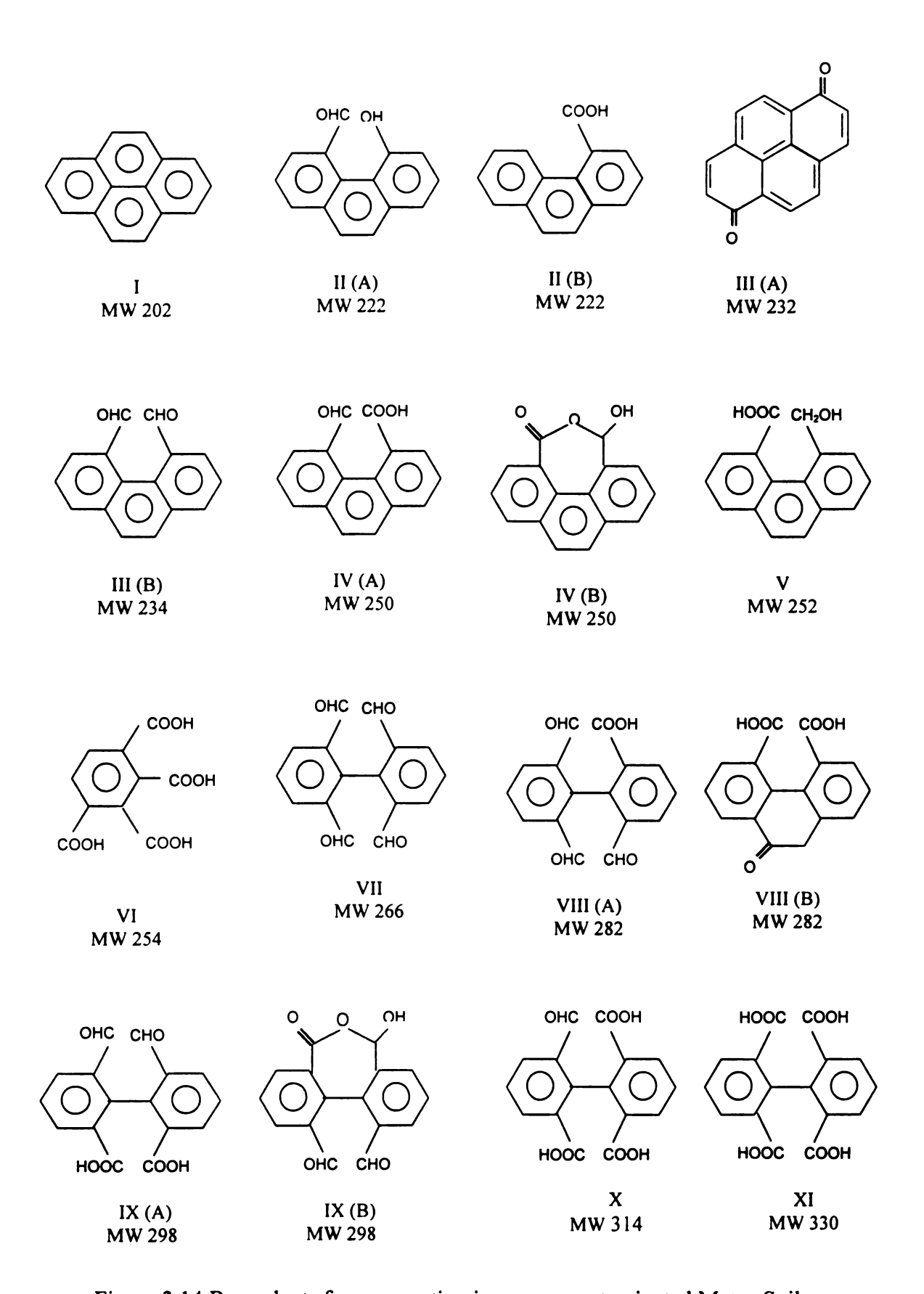


Figure 3.14 Byproducts from ozonation in pyrene contaminated Metea Soil

Table 3.5. GC/MS ion peaks for the soil ozonation byproducts

Compound ID	MW	Retention Time (minutes)	Major Ion Peaks
I	202	16.599 <sup>a</sup> 15.537	202, 101(m/z = 100%) 202, 101(100%)
IIA/B	222	11.964	222, 221(100%), 207, 143
III (A) III (B)	232 234	16.231	232, 117(100%) 234, 232, 117(100%)
IV A/B	250	4.650	250, 248(100%), 234, 221, 206, 196
v	252	15.846	252(100%), 237, 225, 207, 184, 119
VI	254	6.258	254, 253(100%), 223, 207, 119
VII	266	7.081 18.64 <sup>a</sup>	267(100%), 253, 237, 223, 207, 193, 119 267, 237(100%), 207, 181, 153,73
VIII A/B	282	9.376 15.551	282 (100%), 267, 252, 221, 147 282, 267, 250, 234, 221(100%), 147
IX A/B	298	3.969 21.074	298, 297(100%), 265, 250, 239, 223, 113,105 298, 294(100%), 281, 267, 253, 225, 207
х	314	10.861 15.846	314, 311, 281, 221(100%), 147 314, 313, 281, 252(100%), 207, 184, 134,119
XI	330	7.680 7.684ª	330, 328(100%), 296, 282, 266, 253, 223,208 330, 327(100%), 311, 297, 281, 267, 253,239

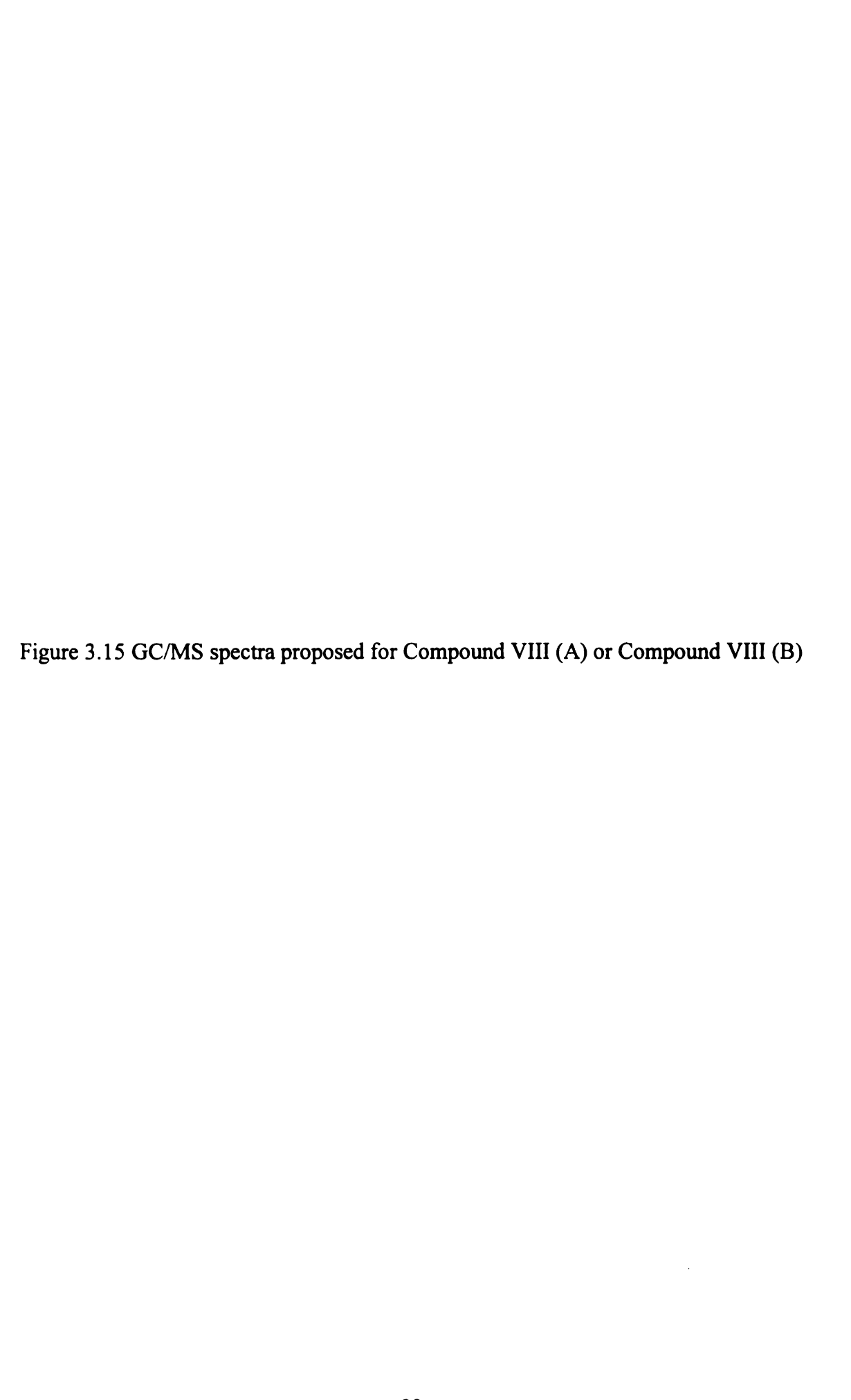
a. GC/MS retention time for the standard or synthesized compound

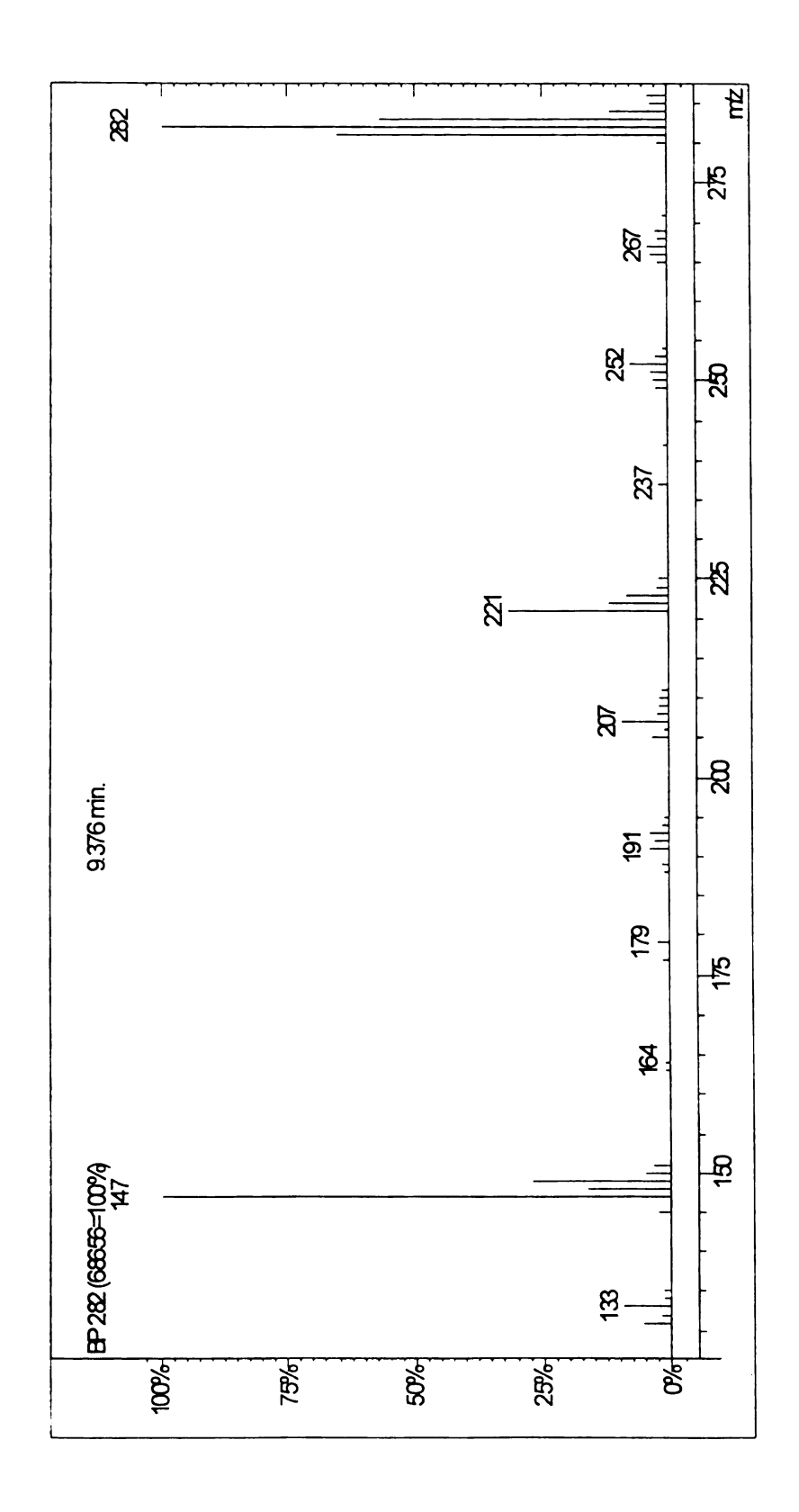
water and would be transported through the aquifer. The toxicity of these compounds may also determine the efficacy of remediating the site to non-toxic levels.

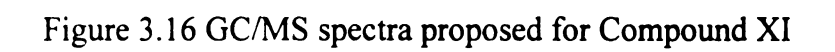
Compound VIII A and Compound VIII B are the two possible configurations for MW 282. Figure 3.15 is the GC/MS spectra. The polarity of the mobile phase at the 2 minute time point, however, would suggest that Compound VIII B is the more logical choice. Compound VIII A is a biphenyl compound and was detected in a peak where the mobile phase was more non-polar had a higher concentration of ACN. This compound will be addressed later in the discussion.

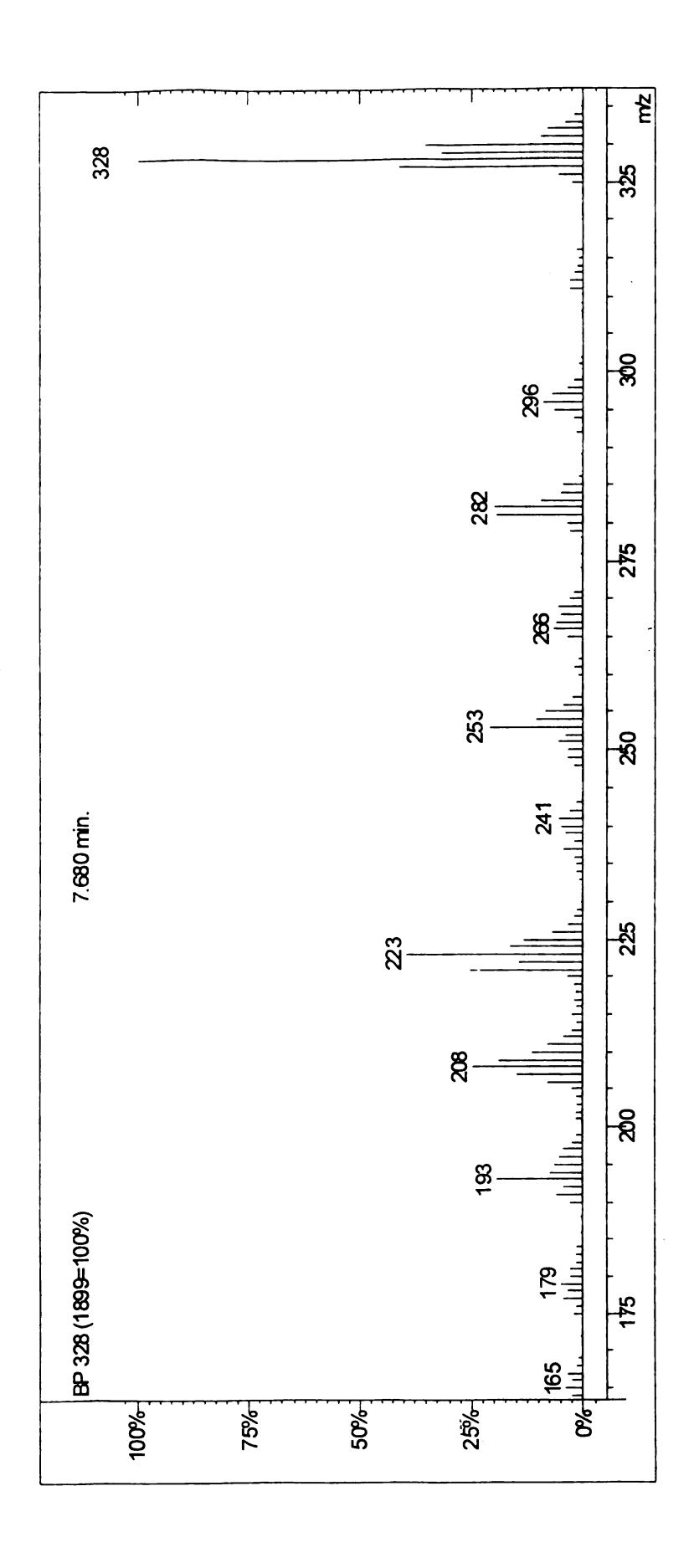
Identification of Compound XI (2,2',6,6'-biphenyl tetracarboxylic acid) in F1 and F8 was further verified by the HPLC chromatogram for the standard presented earlier in the chapter (Refer to Figure 3.4 a) and the GC/MS spectra for the synthesized standard. 2,2',6,6'-biphenyl tetracarboxylic acid was detected in aqueous ozonation as a byproduct formed at high ozone doses > 4.5 mol O<sub>3</sub>/mol pyr [4]. This compound was also a product produced by ozonation followed by the addition of hydrogen peroxide in solution [2]. Eberius et al. [6] identified in soil, biphenyl-tetramethylester (MW 386), which is the methylated form of 2,2',6,6'-biphenyl tetra carboxylic acid. Compound XI was one of the synthesized pyrene ozonation byproducts evaluated for toxicity in Chapter 4. Figure 3.16 is the GC/MS spectra.

Ozonation byproducts with the MW range from 222 to 314 were detected in the fractions from F2 to F11. These compounds consisted of the phenanthrene-like and biphenyl-like compounds. The triplet peaks contained three of the biphenyl-like compounds having MW of 282 (Compound VIII A), 298 (Compound IX A), and 314





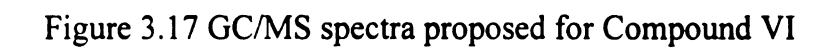


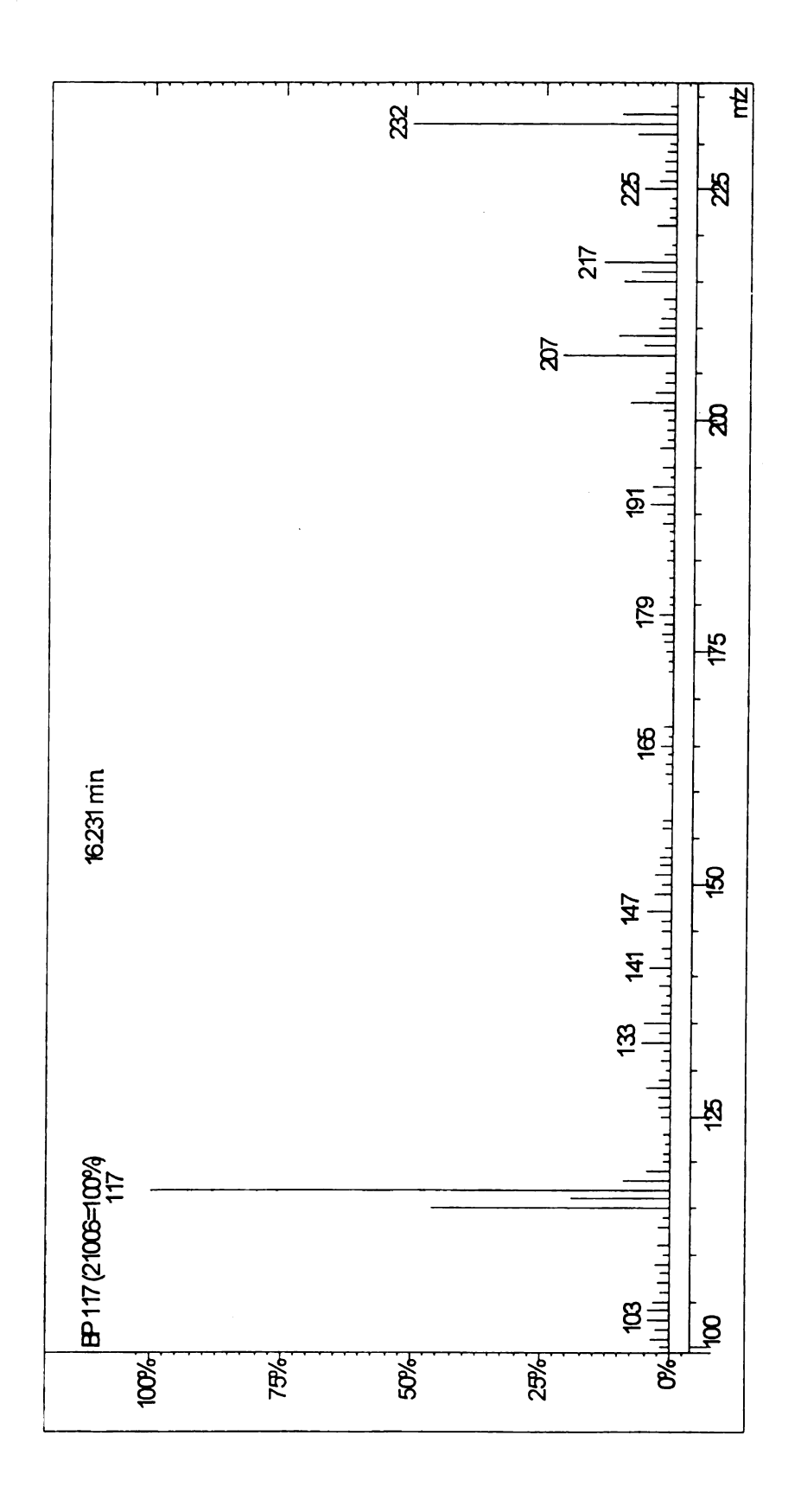


(Compound X). The biphenyl compounds detected are consistent with ozonation byproducts generated in various solvents [2, 4]. In comparison to the results from Eberius et al. (1997), the methylated form of Compound VIII(A) would be triformyl-biphenyl-methylester (MW 296).

Compound VI (benzene-tetracarboxylic acid MW 254) was detected within the in F5 (Figure 3.17). This compound was predicted to occur in soil via Pathway 2 but has not been reported in aqueous systems [6]. Benezene-tetramethylester (MW 310) is the methylated form of Compound VI identified in the previous sand/silica study. For many of the GC/MS spectra, m/z 206 – 207 was detected as a major ion fragment but did not conclusively present itself as an individual byproduct peak. The chemical structure for this molecular weight would be similar to Compound VI but with three aldehyde functional groups and one carboxylic acid group. The fragment for m/z 206 - 207 in the methylated form would match triformyl-benzene-methylester (MW 220) identified in Eberius et al. [6].

In F6, a compound with the MW of either 232 or 234 was detected. The two possible configurations are Compound III(A) from Pathway 2 or Compound III(B) from Pathway 1. Both of these compounds have been detected in pyrene ozonation studies. Eberius et al. [6] reported identification of dimethoxy-pyrene (MW 262) which is the methylated form of Compound III(A). Yao et al. [4] detected Compound P (Refer to Figure 3.2) at high ozone doses. Herner [5] also detected a new compound which has four quinone-groups (MW 262) instead of the two quinone-groups as in Compound III(A). Yao et al. [4] reported the presence of 4,5-phenanthrene dialdehdye (Compound IIIB)

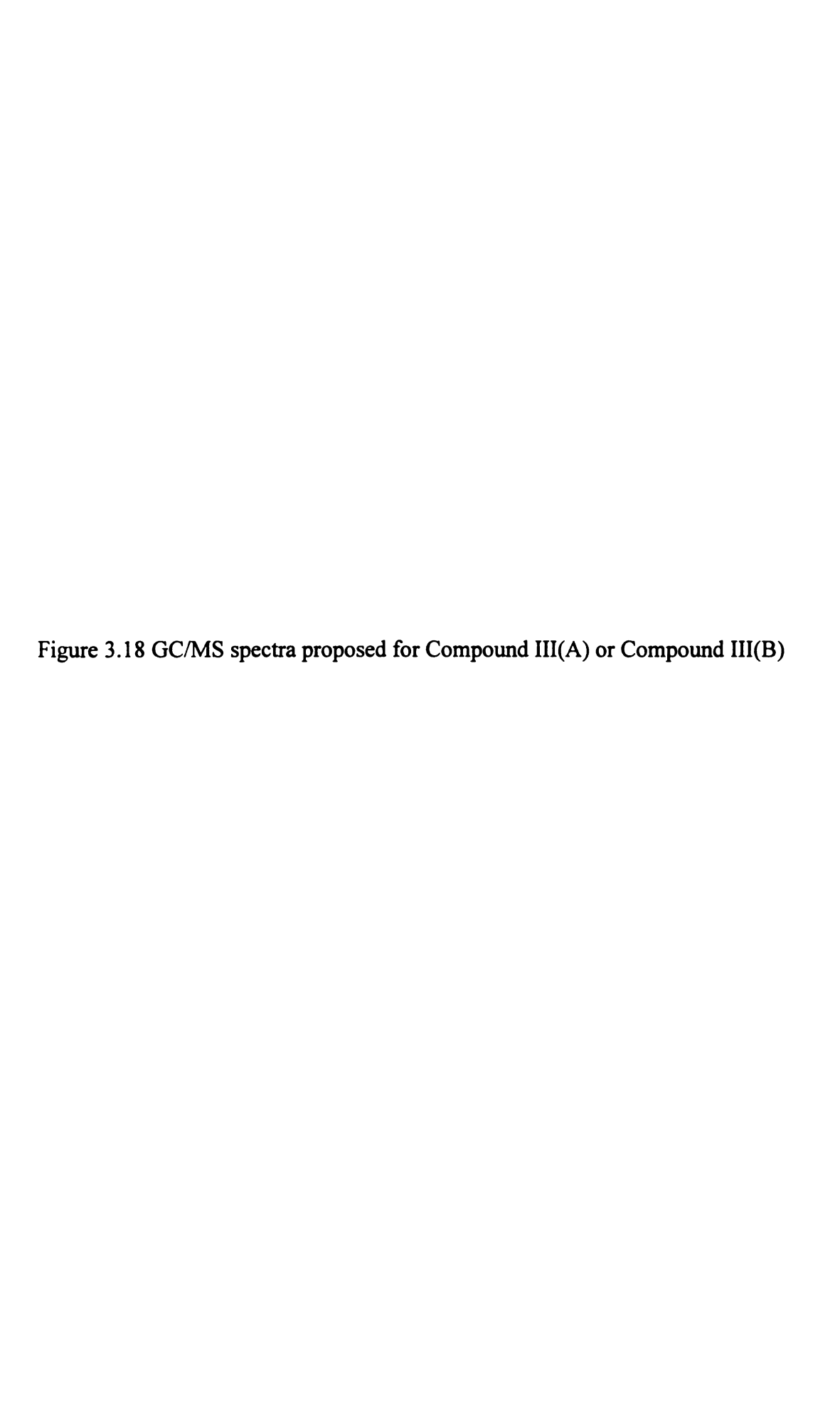




in aqueous solution for low ozone doses. Zeng et al. [7] also detected 4, 5-phenanthrene dialdehyde in ozonation on glass beads and in the batch reactor. The GC/MS spectra showed a major ion peak (m/z(100%) = 117) which might suggest a fragmentation pattern for Compound III(B) (Figure 3.18). A strong peak for m/z(50%) = 232 is present in the spectra, therefore, Compound III(A) could not be eliminated as a possible structure for the spectra.

In F7 and F13, Compound VII (2,2',6,6'-biphenyl tetraaldehyde) was detected among the byproducts. The standard for 2,2',6,6'-biphenyl tetraaldehyde eluted from the HPLC column between 10.2 – 10.6 minutes (Refer to Figure 3.4 b), which is within the time range for the effluent collected for F7 and F13. Both Bailey [2] and Yao et al. [4] reported 2,2',6,6'-biphenyl tetraaldehyde at low doses in solution. Zeng et al. [7] detected 2,2',6,6'-biphenyl tetraaldehyde as a byproduct from ozonation of glass beads coated with pyrene. The GC/MS spectrum is provided in Figure 3.19 and is consistent with the spectra for the synthesized 2,2',6,6'-biphenyl tetraaldehyde.

The remaining individual peaks successfully fractionated were fraction numbers F14 and F15. Fraction 14 eluted from the column at 17.4 minutes. GC/MS detected a compound with the MW of 298 in F14. This compound is interesting because it was detected occasionally in both non-ozonated soil and ozonated soil during experiments with identical handling and storage conditions for the soils. This compound may also be a naturally occurring degradation product seen in the pyrene standard. From the HPLC chromatograms, the peak collected in F14 was easily removed by ozonation and appears to degrade even faster than pyrene (Figure 3.20). The structure for Compound IX (B) is



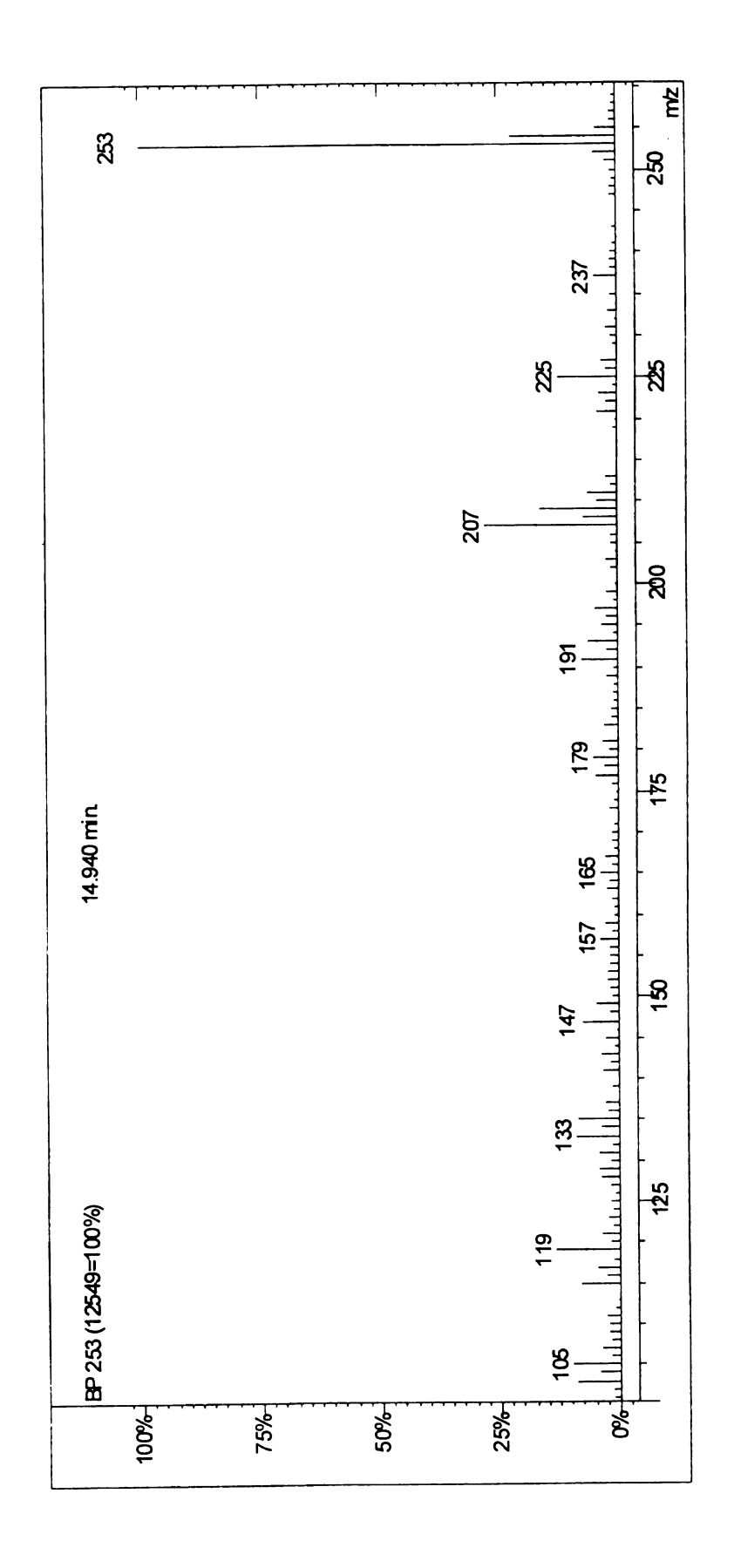
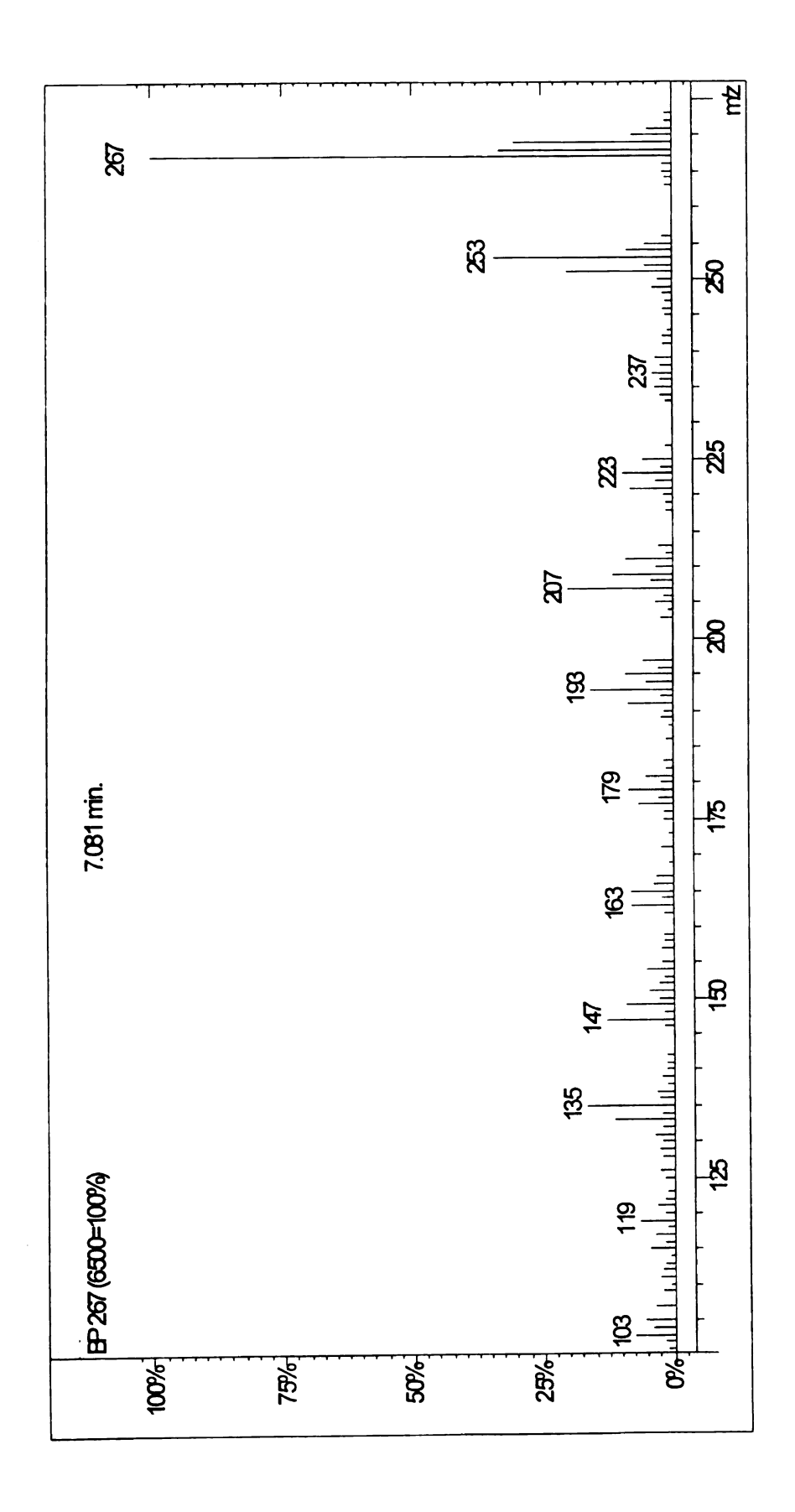


Figure 3.19 GC/MS spectra proposed for Compound VII



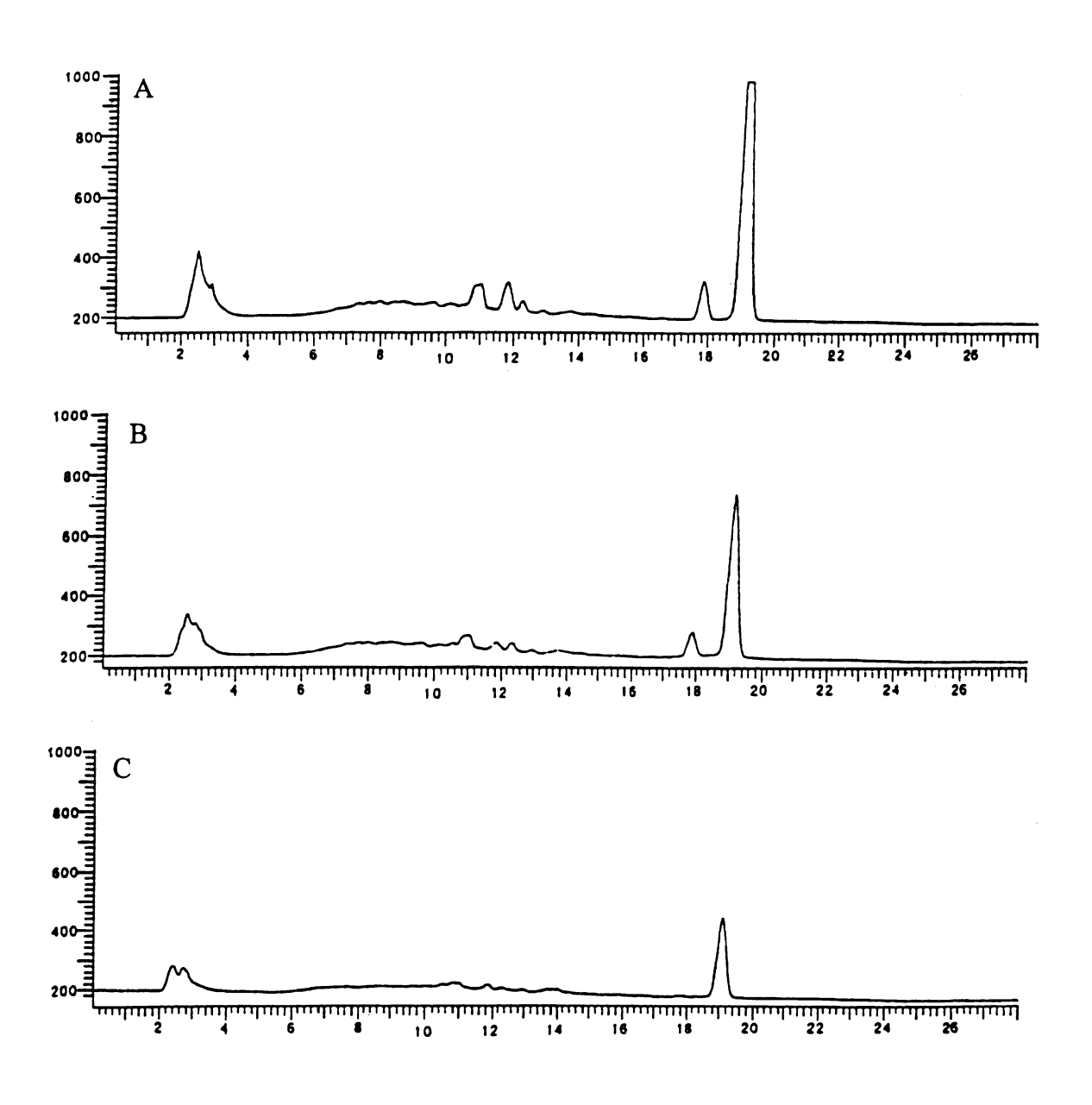


Figure 3.20 ACN extract for 10% moisture (pH 2) pyrene soil. (a) 2.2 mg  $O_3$ /ppm pyr, (b) 3.85 mg  $O_3$ /ppm pyr, (c) 16 mg  $O_3$ /ppm pyr.

the

pyr

309

App

that

bipl whi

proc

com

3.5

aque

bypr The

VII(

conv

more

comi

phen

comp

the better candidate for the MW 298 eluting at 17.4 minutes. Fraction 15 contained pyrene with a MW 202.

Two unidentified compounds were detected with major ion peaks (m/z= 100%) at 309 and 340 - 342. The GC/MS spectra for these two compounds are included in Appendix C. No structural information is available for identification of these compounds. Based on the proposed pathway 1 and pathway 2 compounds, it is possible that these fragments could be compounds with the naphthalene-like structures or biphenyl-like. Eberius et al. [6] detected carboxy-napthlalene-trimethylester (MW 346) which would suggest the possibility that naphthalene –based compounds may have been produced. Further study is needed to verify the results and proposed structures for these compounds.

## 3.5 Conclusions

Ozonation in geological material resulted in similar byproducts as those from aqueous systems. This finding suggests that the literature available for aqueous ozonation byproducts might be applicable in other byproducts being investigated for soil ozonation. The final pyrene oxidation products appear to be two polar compounds, Compound VII(B) and Compound XI. Pyrene removal was most complete in dry soil with conversion of pyrene to Compounds VIII(B) and Compound XI. In the moisturized soils, more intermediate byproducts such as the phenanthrene-like and biphenyl-like compounds were produced in addition to the two polar compounds. The presence of the phenanthrene-like and biphenyl-like compounds would suggest that non-polar compounds are produced and that these compounds would remain bound in the soil.

Toxicology evaluation of the ozonation byproducts is important to identify if ozonation is effective treatment for soil and groundwater. Evaluation, specifically of the polar compounds, is important because these compounds would be able to dissolve into groundwater and reach local aquifers. Compound XI (2,2',6,6' – biphenyl tetracarboxylic acid) is one of the compounds addressed in the toxicology study (Chapter 4). The toxicology research also evaluated Compound VII (2,2',6,6'- biphenyl tetraaldehyde). These two compounds are examples of how the functional groups attached to the byproduct can have extremely different effects on the cellular level.

#### 3.7 References

- 1. Copeland, P.; Dean, R.; McNeil, D.; "The Ozonolysis of Polycyclic Hydrocarbons: Part II." J. Chem. Soc. 1961, 1232 1236.
- 2. Bailey, P. "Chapter 5: Ozonation of Aromatic Compounds: Bond Attack versus Atom Attack on Benz-fused Carbocyclics". <u>Ozonation in Organic Chemistry</u>, <u>Volume II.</u> Non-Olefinic Compounds. Academic Press: New York, **1982**.
- 3. Yao, J.; Ph.D. Dissertation. "The Mechanism of the Reaction of Ozone with Pyrene and Benz[a]anthracene in Acetonitrile/water Mixture." Michigan State University: Department of Civil and Environmental Engineering. 1997.
- 4. Yao, J.J; Huang, Z.; Masten, S.; "The Ozonation of Pyrene: Pathway and Product Identification". Wat. Res. 1998, 32(10), 3001-3012.
- 5. Herner, H.; "The Reaction of Ozone with Pyrene: The Byproducts and Their Toxicological Implications". Ph.D. Dissertation, Department of Civil and Environmental Engineering, Michigan State University, 1999.
- 6. Eberius, M; Berns, A; Schuphan, I.; "Ozonation of pyrene and benzo[a]pyrene in silica and soil- C<sup>14</sup> balances and chemical analysis of oxidation products as a first step to ecotoxicological evaluation". Fresnius Z. Anal., 1997, 359, 274-279.
- 7. Zeng, Y.; Hong, P.; Wavrek, D. "Chemical-Biological Treatment of Pyrene". Water Res. 2000, 34(4), 1157-1172.
- 8. Buser, H.; Poiger, T.; Muller, M.; "Comment on Integrated Chemical-Biological Treatment of Benzo[a]pyrene." *Environ. Sci., Technol.* **2000**, 34, 4255.
- 9. Upham, B.; Yao, J.; Trosko, J.; Masten, S.; "The Determination of the Efficacy of Ozone Treatment Systems Using Gap Junctional Intercellular Communication Bioassay". *Environ. Sci. Technol.* **1995**, 29(12), 2923 2928.
- 10. Herner, H.; Trosko, J.; Masten, S.: "The Reaction of Ozone with Pyrene: The Byproducts and Their Toxicological Implications". *Environ. Sci. Technol.* **2001**, 32(10), 3001 -3012.
- 11. Luster-Teasley, S; Yao, J.; Herner, H.; Trosko, J.; Masten, S.; "Ozonation of Chrysene: Evaluation of Byproduct Mixtures and Identification of Toxic Constituent." *Environ. Sci. Technol.* **2002**, 36(5), 869 876.
- 12. Grimmer, G.; Bohnke, H.; Borwitzky, H.; "Gas-chromatographische Profilanalyse der polycyclischen aromatischen Kohlenwasserstoffe in Klarschlammproben," *Fresenius Z. Anal. Chem.* **1978**, 289, 91 95.

- 13. Martens, D.; Frankenberger Jr., W; "Enhanced Degradation of Polycyclic Aromatic Hydrocarbons in Soil Treated with an Advanced Oxidated Process Fenton's Reagent (Article number 340072)" 1998
  http://www.crcpress.com/jour/sss/arts/340072.html
- 14. Lee, P.; Ong, S.; Golchin, J.; Nelson, G.; "Extraction Method for Analysis of PAHs in Coal-Tar-Contaminated Soils". *Practice Periodical of Hazardous, Toxic, and Radioactive waste Management.* October 1999, 155-162.

### **CHAPTER 4**

An evaluation of Pyrene ozonation byproducts 2,2',6,6'-biphenyltetraldehyde and 2,2',6,6'-biphenyl tetra carboxylic acid

S. Luster-Teasley<sup>1</sup>, P. Ganey<sup>4</sup>, M. DiOrio<sup>4</sup>, J. Ward<sup>2</sup>, R. Malescka<sup>2</sup>, J. Trosko<sup>3</sup>, and S. Masten<sup>1\*</sup>

<sup>1</sup>Department of Civil and Environmental Engineering
<sup>2</sup>Department of Chemistry
<sup>3</sup>Department of Pediatric Medicine and Human Development
<sup>4</sup>Department of Pharmacology and Toxicology

# Michigan State University East Lansing, MI 48824

\*Corresponding Author: Phone number: (517) 353-8539; Fax: (517) 355-0250; e-mail: masten@msu.edu

#### **Abstract**

In this study, 2,2',6,6'-biphenyl tetraaldehyde, an initial byproduct formed from the ozonation of pyrene, and 2,2',6,6'-biphenyl tetracarboxylic acid, a subsequent pyrene ozonation byproduct were evaluated using two toxicology assays to compare the toxicity of ozonation byproducts with that of the parent compound. The first assay measured the potential for the compounds to block gap junctional intercellular communication (GJIC) using the scrape loading/dye transfer (SL/DT) technique in normal WB-344 rat liver epithelial cells. The second assay evaluated the ability for the compounds to affect neutrophil function by measuring the production of superoxide in a human cell line (HL60). 2,2',6,6'-biphenyl tetraaldehyde was determined to show adverse effects in both toxicity analyses. 2,2',6,6'-biphenyl tetraaldehyde was inhibitory to GJIC at low

concentrations (5  $\mu$ M) and irreversible damage resulted when cells were exposed to this compound for 30 minutes. In the human neutrophil assay, 2,2',6,6'-biphenyl tetraaldehyde reduced the ability for human cells to produce superoxide. 2,2',6,6'-biphenyl tetra carboxylic acid did not exhibit any significant effect in either assays.

**Keywords:** Ozone, ozonation, oxidation, pyrene, polycyclic aromatic hydrocarbons, PAH, Gap Junctional Intercellular Communication, GJIC, superoxide, Human neutrophil assay

## 4.1 Introduction

The need for effective *in-situ* treatment technologies has led to the increased use of ozone treatment to remediate PAH contamination in groundwater and soil [1-3]. Though ozone is effective in oxidizing parent PAH compounds, numerous byproducts are produced. The lack of information available identifying these byproducts and on individual byproduct toxicity present a serious deficiency in research. PAH compounds are known to posses mutagenic and carcinogenic characteristics [4-13]. Therefore the potential for the byproducts to continue to have carcinogenic or mutagenic characteristics is a consideration that must be addressed.

Pyrene (Figure 4.1 A) is an example of a four ringed, PAH causing skin, liver, and lung cancer in humans [14]. Since 1937, pyrene ozonation studies in various participating and non-participating solvents have lead to the identification of at least 28 byproducts [15-17]. Pyrene ozonation proceeds via ozone attack at the bonds of lowest localization energy, which are the 4, 5 bonds followed by attack at the 9, 10 bonds [16]. Ozonolysis of pyrene initially promotes the formation of phenanthrene-like compounds followed by the formation of biphenyl-like compounds [16,17]. These byproducts can be substituted with hydroxyl, aldehyde, and carboxylic acid functional groups [1, 16]. When pyrene was treated with excess ozone in a nonparticipating solvent, the predominant byproducts were either 2,2', 6,6'-biphenyl tetraaldehyde or 2,2', 6,6'-biphenyl tetracarboxylic acid. 2,2', 6,6'-biphenyl tetracarboxylic acid was produced using only ozonation treatment and 2,2',6,6'-biphenyl tetracarboxylic acid was produced using ozonation followed by the addition of hydrogen peroxide [15,16].

Only a few toxicology studies have evaluated the carcinogenic potential of PAH ozonation byproducts [18-24]. Upham et al. [19] investigated the ozonation of pyrene and the potential for the byproduct mixture produced to disrupt intercellular communication. This study suggested that the early ozonation byproducts of pyrene in aqueous systems are more toxic than the parent compound, pyrene. At  $1.6 \pm 0.1$  mol O<sub>3</sub>/mol PAH, pyrene had completely disappeared but the disruption of cellular communication was higher for the ozonated mixture than that observed with pyrene. Yao et al. [17] determined that at this ozone concentration, the predominant compounds were  $2.2^{\circ},6.6^{\circ}$  -biphenyl tetraaldehyde and 2-carboxy- $2^{\circ},6.6^{\circ}$  biphenyl trialdehyde.

A total of 4.5 mol ozone/mol pyrene was required to destroy all of the intermediate products inhibitory to GJIC [20]. At concentrations greater than 4.5 mol O<sub>3</sub>/mol pyrene, Yao et al. [17] reported that the concentrations of 2,2',6,6' biphenyl tetraaldehyde and 2-carboxy-2',6,6' biphenyl trialdehyde had significantly decreased. The remaining compounds were found to be biphenyls substituted with three or four carboxylic acid groups or oxygen bonds such as 2,2',6,6'-biphenyl tetra carboxylic acid and 2,6-carboxy-2',6' biphenyl dialdehyde predominated.

For the present work, pyrene ozonation byproducts were evaluated using two different toxicology assays. This study focused on evaluating the toxicity of two pyrene ozonation byproducts: 2,2',6,6'-biphenyl tetraaldehyde (Figure 4.1 B) and 2,2',6,6'-biphenyl tetracarboxylic acid (Figure 4.1 C).

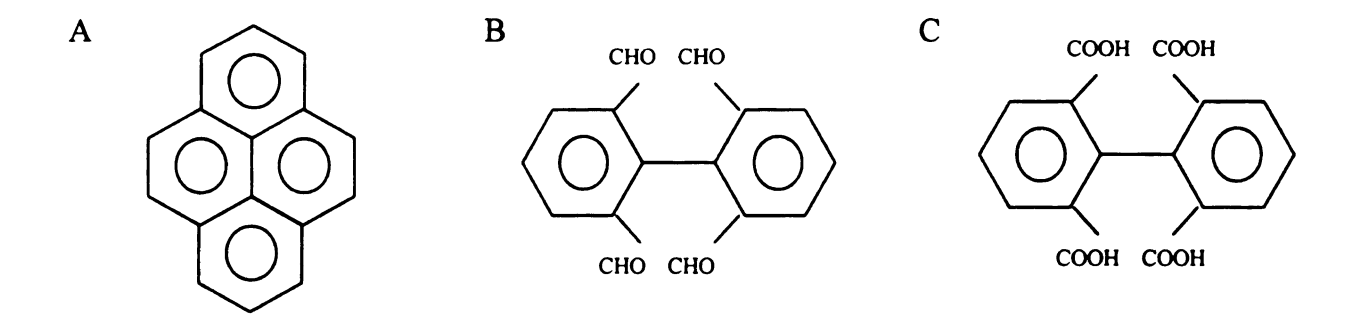


Figure 4.1. A. Pyrene; B. 2,2',6,6'-biphenyltetraaldehyde and C. 2,2'6,6'-biphenyl tetracarboxylic acid

The assays were chosen based on a collaborative effort between engineering and toxicology research groups. Each of the toxicology assays represents a cellular function that results from integration of cellular signaling and changes in each can be associated with effects on the whole organism. The first study evaluated the compounds for their potential to block gap junctional intercellular communication (GJIC) in WB-344 rat liver epithelial cells using the scrape/load dye transfer assay (SL/DT).

The GJIC assay is a non-genotoxic assay that measures the ability for cells to transfer information, low molecular weight molecules, and small regulatory and macromolecular substances through the cytoplasm of one cell to the next cell through channels called gap junctions. GJIC controls cell homeostasis and cell synchronization. Some PAH compounds are epigenetically toxic, however, only a few studies have investigated epigenetic toxicity of ozonation byproducts using the GJIC assay [19-25]. Epigenetic toxicity refers to the altering of the expression of the genetic information of cells at the transcription, translation, or posttranslational level. Transcription is the turning off of genes. Translation is the modification of the stability of the gene message

and the post translation is the modification of the protein coded by the gene [26]. Most cancer cells have dysfunctional gap junctional intercellular communication because cells are no longer communicating to prevent uncontrolled growth [27, 28].

The second assay evaluated the ability for the compounds to affect neutrophil production of superoxide anion in a human cell line (HL60). Generation of reactive oxygen species by neutrophils is critical to their function to kill bacteria. Molecular oxygen is reduced by the enzyme NADPH oxidase to form superoxide anion, which in turn can be reduced to other reactive oxygen species, some of which are potentially toxic. Multiple pathways lead to the activation of NADPH oxidase and production of superoxide anion in neutrophils, and the pathways activated are dependent on the stimulus. Thus, generation of superoxide anion by neutrophils results from activation of a complex network of intracellular signals and represents an integrated cellular function. Previous studies have demonstrated alteration in neutrophil production of reactive oxygen species by environmental chemicals and their products of remediation [29-34].

Neutrophils are involved in nonspecific immunity and represent the first line of defense against invading pathogens. They become activated by stimuli to produce reactive oxygen species and release degradative enzymes that kill infecting bacteria. Alteration in function of neutrophils can affect host immunity as well as cause tissue injury. For example, inappropriate activation of neutrophils leads to tissue injury in a variety of models [35-38]. Conversely, inhibition of activation of neutrophils, such as was observed with 2,2',6,6'-biphenyltetraaldehyde, could lead to impaired ability of these cells to respond effectively to bacteria. The consequence of this effect would be an increased susceptibility to infection. Inhibition of neutrophil activation in response to

another stimulus has been observed with polychlorinated biphenyls [29]. This response is dependent on the presence of ortho-substituted chlorines on the phenyl rings.

# 4.2 Experimental Section

## 4.2.1 Materials

Chemicals. Pyrene (98% purity, Sigma Chemical) was used for all of the toxicology studies. The two byproducts, 2,2',6,6'-biphenyl tetraaldehyde and 2,2',6,6'-biphenyl tetracarboxylic acid, were synthesized by Joseph Ward and Dr. Robert Malescka from the Department of Chemistry at Michigan State University (East Lansing, MI).

Synthesis of Pyrene ozonation byproducts. Biphenyl-2,6,2',6'-tetracarbaldehyde (or 2,2',6,6'-biphenyl tetraaldehyde) [39]<sup>i</sup> and biphenyl-2,6,2',6'-tetracarboxylic acid (or 2,2',6,6'-biphenyl tetracarboxylic acid) [40]<sup>ii</sup> are have been previously reported, however, their preparations are poorly described and lack characterization data. As such, modified procedures were developed and the compounds fully characterized to ensure the fidelity of the toxicological studies.

Biphenyl-2,6,2',6'-tetracarbaldehyde was prepared by dissolving pyrene in a 2:1 CH<sub>2</sub>Cl<sub>2</sub>/MeOH solution, triethylamine (1 mL) was then added, and the solution was purged with nitrogen for 15 min and cooled to -78 °C. Ozone was then bubbled through the solution for 1.5 h after which time the solution was greenish-blue. Nitrogen was then bubbled through the solution for 15 min to remove the excess ozone. Dimethylsulfide (7 mL) was added drop wise to reduce the ozonide. The solution was allowed to warm slowly to room temperature overnight. The solvent was removed *in vacuo* and the

residue dissolved in ethyl acetate. The organic layer was washed with water and brine, and dried over MgSO<sub>4</sub>. The solution was decolorized with Norit–A charcoal. After filtration the solvent was removed *in vacuo* and the resulting residue was subjected to flash silica gel chromatography (50% ethyl acetate/hexanes). This afforded 2.1 g (54%) of the desired product as a white solid. mp 155-156°C (lit. 162-163). IR (KBr) 3076 (m), 2831 (s), 2737 (s), 1695 (s), 1572 (s), 1450 (2), 1383 (m), 1238 (s), 1159 (m), 958 (s), 794 (s). <sup>1</sup>H NMR (300 MHz, CDCl<sub>3</sub>)  $\delta$  7.88 (t, J = 7.69 Hz, 2 H), 8.28 (d, J = 7.69 Hz, 4 H), 9.72 (s, 4 H); <sup>13</sup>C NMR (75 MHz, CDCl<sub>3</sub>)  $\delta$  189.5, 135.6, 135.5, 129.7. Anal. Calcd for C<sub>16</sub>H<sub>10</sub>O<sub>4</sub>: C, 72.18; H, 3.79. Found: C, 72.23; H, 3.98.

Biphenyl-2.6,2',6'-tetracarboxylic acid was prepared by suspending biphenyl-2,6,2',6'-tetracarbaldehyde (3.7 mmol, 1.0 g) in water (20 mL) followed by addition of potassium stearate (0.403 mmol, 0.130 g) and KMnO<sub>4</sub> (11.1 mmol, 1.75 g) [34]. The reaction was heated to 50 °C and allowed to stir overnight. It was then cooled to room temperature and filtered thru a pad of NaCl. The filtrate was then acidified to pH 2.5, filtered, and the solid dried *in vacuo* to afford 950 mg (79%) as a white solid. IR (KBr) 2997 (br. s), 1684(s), 1583(s), 1464(s), 1404(s), 1267(s), 929(s), 761(s), 684(s), 534(w). <sup>1</sup>H NMR (300 MHz, DMSO-d6)  $\delta$  7.43 (t, J = 7.69, 2 H), 7.9 (d, J = 7.69 4 H); <sup>13</sup>C NMR (74.5 MHz, DMSO-d6)  $\delta$  167.3 ,142.1, 137.7, 132.2, 131.6, 126.4.  $\lambda_{max}$  = 292 nm (EtOH). LRMS (direct probe EI) m/z 330 (M+). Anal. Calcd for C<sub>16</sub>H<sub>10</sub>O<sub>8</sub>: C, 58.19; H, 3.05. Found: C, 58.10; H, 3.10.

# 4.2.2 Methods: Toxicology Assays

4.2.2.1 Gap Junctional Intercellular Communication Assay. The GJIC assays consist of 4 tests to evaluate the effect a compound can have on cellular communication. These tests consist of dose response, time response, time recovery, and cytoxicity. In the GJIC assay, rat liver epithelial cells (WB-F344) were used from a strain of rat on which many environmental toxicants and chemical carcinogenesis studies are tested. This is a diploid, non-tumorigenic cell line on which a large database of toxicity/cancer information for other in vivo tested chemicals can be used to compare results.

Science, Gibbstown, NJ) and sonicated for 5 minutes to insure complete dissolution. 2,2',6,6'-biphenyl tetraaldehyde was dissolved in ACN (99.8% purity, EM Science, Gibbstown, NJ). Acetonitrile (ACN) was selected as the solvent because it has little effect on GJIC at a final ACN concentration up to 1.75% in cell culture medium [20]. All experiments were conducted at an ACN concentration of 1% or less in cell culture medium. 2,2',6,6'-biphenyl tetracarboxylic acid was dissolved in a 30: 60 ACN/ DDI water solution because the compound was more polar.

Cell Culture. WB-F344 rat epithelial cell lines were obtained from Dr. J.W. Grisham and M. S. Tsao of the University of North Carolina (Chapel Hill, NC). Cells were cultured in 25 ml of D medium (Formula No. 78-5470EG, GIBCO Laboratories, Grand Island, NY) containing 5% fetal bovine serum (FBS) (GIBCO Laboratories, Grand Island, NY) and 0.2% gentamycin. The cells were incubated at 37°C in a humidified atmosphere

containing 5% CO<sub>2</sub> and 95% air. The cells were grown in 150 mm plastic flasks, and the culture was split and new medium was added every other day. WB-F344 is a diploid, non-tumorigenic cell line on which a large database of toxicity/cancer information for other in vivo tested chemicals can be used to compare results [26].

Bioassay for GJIC. Bioassays were conducted in 35 mm<sup>2</sup> Petri dishes with confluent cultures grown for 2 days in 2 ml of D medium supplemented with 5% fetal bovine serum. The procedure for the scrape loading/dye transfer (SL/DT) technique was adapted from the method used by El-Fouly et al. [42] and is described in detail by Herner et al. (23). All tests were run in triplicate and at non-cytotoxic levels determined by the neutral red uptake assay kit (Sigma Chemical Co., St. Louis, MO). Under fluorescent light, the Lucifer yellow dye will fluoresce to indicate the distance the dye travels from the scrape. This distance was measured and compared to a control group of cells that were exposed to acetonitrile only (vehicle controls), but assayed using the identical SL/DT method. Three photographs were taken for each concentration tested and the area coverage of the dye was measured. All photographs were taken within 1 hour of experiment completion. The area of fluorescence was measured and calculated using a GelDoc Program produced by NeucleoTech, Inc. The area of each picture was averaged together to obtain a representative fraction of control (f). The results were reported as an average  $\pm$  standard deviation determined at the 95% confidence interval (C.I.).

GJIC was assessed by the decrease in communication of the cells exposed to the toxicant compared to the vehicle control group (acetonitrile only). Complete communication is identified as an f value of 1.0 or 100% communication as compared to

the control. GJIC f values less than 0.5 indicate a significant decrease because the cells are communicating at approximately half of normal communication levels. GJIC values between 0.0 - 0.3 are considered to correspond to no intercellular communication. These interpretations for GJIC are consistent with those of Upham et al. [19] and Herner et al. [23]. Controls were run for each experiment to standardize the measurement for normal cell-cell communication at the time of the experiment. Using the t-test it was determined that the mean f values obtained from the control cells without solvent and the vehicle controls do not differ at a 95% confidence interval (95% C.I.). Statistical analyses using the two-tailed t-test and F-test at 95% C.I. were used to compare within treatment and between treatment variations in the mean f values.

Bioassay for Cytotoxicity. Cytotoxicity was tested using the neutral red uptake assay according to the method of Borenfreund and Puerner [43]. WB-F344 cells were grown using the same method as the cells used for the GJIC assay. It is necessary to use non-cytotoxic levels of toxicants in GJIC studies, since if levels used are cytotoxic, then differentiation between decreased communication due to cell death cannot be distinguished from decreased intercellular communication due to blockage of gap junctions. Therefore to accurately measure decreased GJIC activity, only non-cytotoxic concentrations were used.

4.2.2.2 HL-60 Neutrophil Assay. Trypan Blue solution, cytochrome c, SOD (superoxide dismutase), PMA (phorbol 12-myristate 13-acetate), pyruvate substrate, NADH and DMF (N,N-dimethylformamide) were purchased from Sigma Chemical Company (St. Louis,

MO). DMSO (dimethyl sulfoxide) was purchased from J.T. Baker (Phillipsburg, NJ). Iscove's Modified Dulbecco's Medium was obtained from ATCC (American Type Culture Collection, Manassas, VA). Fetal bovine serum (FBS) was obtained from Atlanta Biologicals (Norcross, GA). Antibiotic-antimycotic (10,000 U/mL penicillin G sodium, 10,000 μg/mL streptomycin sulfate, and 25 μg/mL amphotericin B) and gentamicin (50 mg/mL) were purchased from Life Technologies (Rockville, MD). Triton X-100 (scintillation grade) was obtained from Research Products International Corp. (Mount Prospect, IL).

Cells. HL60 cells were used for the studies presented here. The human, promyelocytic cell line, HL60, can be differentiated with dimethylsulfoxide (DMSO) to cells with many of the characteristics of mature neutrophils [Yamaguchi, 1998 #335; Kargman, 1994 #339; Thompson, 1988 #342; Seino, 1998 #346; Korchak, 1998 #344]. Differentiated HL60 cells are a good model with which to study neutrophil responses in vitro because they respond like neutrophils with respect to agonist-stimulated activation of intracellular pathways and consequent changes in function, including generation of reactive oxygen species [Rane, 1997 #332; Yu, 1995 #338], [Gallois, 1998 #334], [Browning, 1997 #336]. HL-60 cells were purchased from ATCC. Cells (30x10<sup>6</sup>) were grown in suspension in 75 mL medium (Iscove's Modified Dulbecco's medium with 15% fetal bovine serum, 1% antibiotic-antimycotic and 0.1% gentamicin) in 75cm<sup>2</sup> culture flasks. Cells were kept at 37° C in a humidified incubator with 5% CO<sub>2</sub>/95% air. Differentiation to a neutrophil-like phenotype was achieved by culturing cells with 1.25% DMSO for seven days. Cells were centrifuged at 200 x g for 10 minutes, resuspended in Hanks'

balanced salt solution (HBSS), and counted using a hemacytometer. Percent viability was determined by trypan blue staining. Cells were diluted to 625,000/mL in HBSS for use in the superoxide anion assay.

Superoxide anion assay. Superoxide anion (O<sub>2</sub>') production by HL-60 cells was determined from the SOD-sensitive reduction of cytochrome C [53]. The assay was carried out in a 96-well plate; each well contained 200 μL cell suspension (125,000 cells), 25 μL of either vehicle (0.1% DMF), pyrene, 2,2',6,6'-biphenyltetracarboxylic acid or 2,2',6,6'-biphenyltetraaldehyde at the indicated concentrations, cytochrome C (135 μM) or cytochrome C with SOD (327 U/mL), and 25 μL PMA. Stock solutions of pyrene, 22'66'-biphenyltetracarboxylic acid and 22'66'-biphenyltetraaldehyde were 40, 10 and 1 μM in DMF. These were diluted with HBSS, and final concentrations in the wells were 40, 10, and 1 μM. Cytochrome C was dissolved in HBSS (10 mg/mL), and SOD was dissolved in cytochrome C solution (1960 U/mL). A 2 mg/mL stock solution of PMA in DMSO was diluted with HBSS and added at a final concentration of 1 ng/mL in the well. Each treatment was represented by triplicate wells on the same plate; the average of these triplicates was taken as n=1.

Cells were added to wells containing vehicle, pyrene, 2,2',6,6'-biphenyltetracarboxylic acid or 2,2',6,6'-biphenyltetraaldehyde, followed by addition of cytochrome C or cytochrome C plus SOD. Absorbance at 550 nm was read every 30 seconds for 30 minutes (at 37° C) using an El<sub>x</sub>808 microplate reader (BIO-TEK Instruments, Inc., Winooski, VT). PMA was then added to each well and the absorbance was recorded for an additional 30 minutes. Mean absorbance of triplicate wells

containing SOD was subtracted from the mean absorbance of the corresponding triplicate wells without SOD. O<sub>2</sub> concentration was calculated using an extinction coefficient of 18.5 cm<sup>-1</sup> mM<sup>-1</sup>.

Lactate dehydrogenase (LDH) assay. LDH was used as a measure of cytotoxicity. LDH activity was measured using pyruvate as a substrate according to Bergmeyer and Bernt (54). After determination of O<sub>2</sub> generation, the plate was spun at 650 x g for five minutes. 50 μL of supernatant was removed from each well and transferred to another plate. LDH reagent (233 :M NADH, 47.6 μM pyruvate in 200 μL 50 mM phosphate buffer) was added to each well, and the change in absorbance at 340 nm was measured over five minutes at 37° C. Total cellular LDH was measured in each experiment in triplicate wells in which cells were lysed with Triton X-100 (4 % final concentration). Cytotoxicity is expressed as the percent of total cellular LDH activity released into the medium by the cells.

Statistical analysis: Data were analyzed by one-way analysis of variance (ANOVA). The criterion for significance was p < 0.05.

### 4.3 Results and Discussion

### 4.3.2 GJIC Evaluation

Cytotoxicity. The cytotoxicity assay (Neutral Red Dye Uptake assay) for Pyrene and 2,2',6,6' biphenyl tetraaldehdye are shown in Figure 4.2. Pyrene was not cytotoxic at the concentration range evaluated (0 – 80  $\mu$ M). 2,2',6,6'-biphenyl tetraaldehyde reached

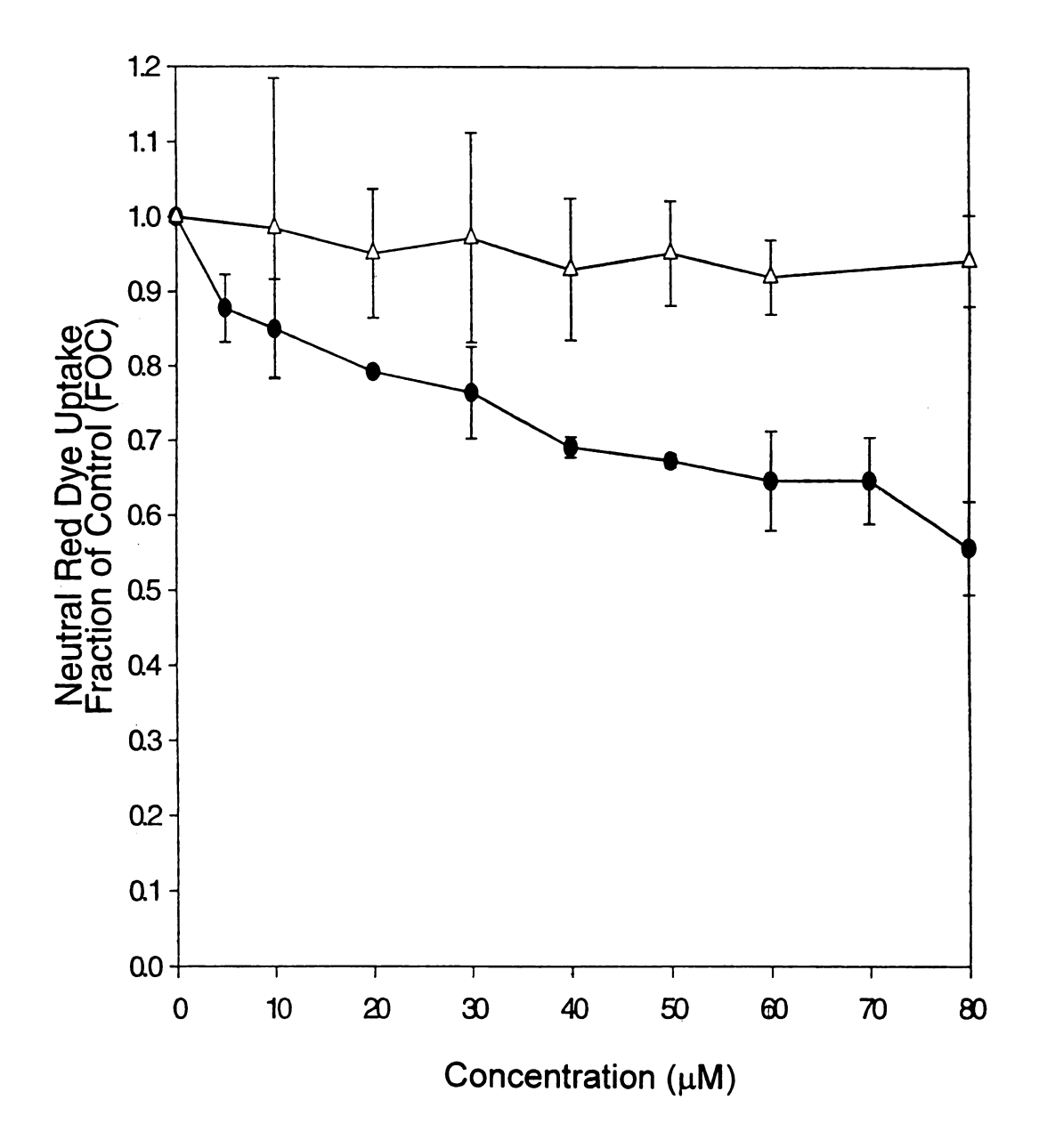


Figure 4.2. Cytotoxicity profile for △ pyrene and ● 2,2',6,6'-biphenyl tetraaldehyde

cytotoxic levels at concentrations greater than 20  $\mu$ M. To evaluate the ability of the compound to inhibit intercellular communication, non-cytotoxic levels were used. This assures that any blockage of communication seen in the assay is due to blockage of gap junctions and not due to cell death. A concentration of 5  $\mu$ M was used for the time response and time recovery experiments to account for standard deviation seen in the cytotoxicity assay and to assure the concentration was not cytotoxic (f > 0.8). 2,2',6,6' biphenyl tetracarboxylic acid was not cytotoxic at the concentrations (0 –500  $\mu$ M) evaluated (Figure 4.3).

Dose Response. For dose response experiments, cells were exposed to varying doses of a toxicant for 30 minutes and then assayed to determine GJIC levels. As shown in Figure 4.4, pyrene significantly blocked intercellular communication (f = 0.2 - 0.5) starting at 40 μM and complete inhibition of communication (f < 0.2) occurred at 50 μM. GJIC in cells exposed to 2,2',6,6'-biphenyl tetraaldehyde reached f < 0.5 at a concentration of 15 μM. At concentrations greater than 20 μM, however, cytotoxic levels were reached and GJIC blockage was caused by the inhibition of intercellular communication and cell death. 2,2',6,6'-biphenyl tetracarboxylic acid was non-inhibitory to GJIC at the concentrations tested (10 – 500 μM).

Time Response. For time response experiments, cells were exposed to a fixed dose of toxicant for varying amounts of time. As shown in Figure 4.5, 2,2',6,6'-biphenyl tetraaldehyde (5  $\mu$ M) blocked communication after 30 minutes of exposure. Complete inhibition was reached in 2 hours and 24 hour exposure led to cell death. Exposure to

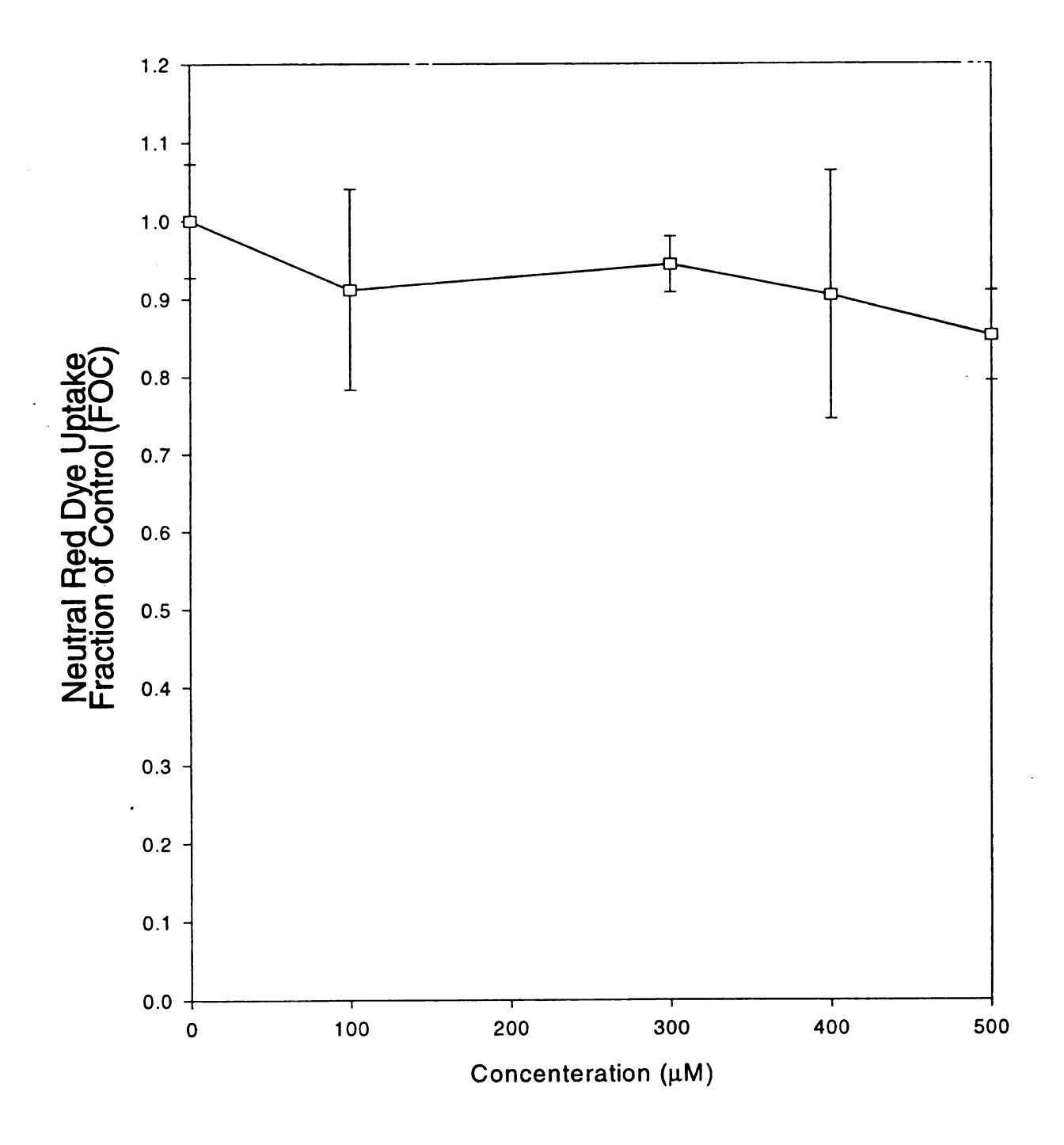


Figure 4.3. Cytotoxicity profile for 2,2',6,6'-biphenyl tetracarboxylic acid

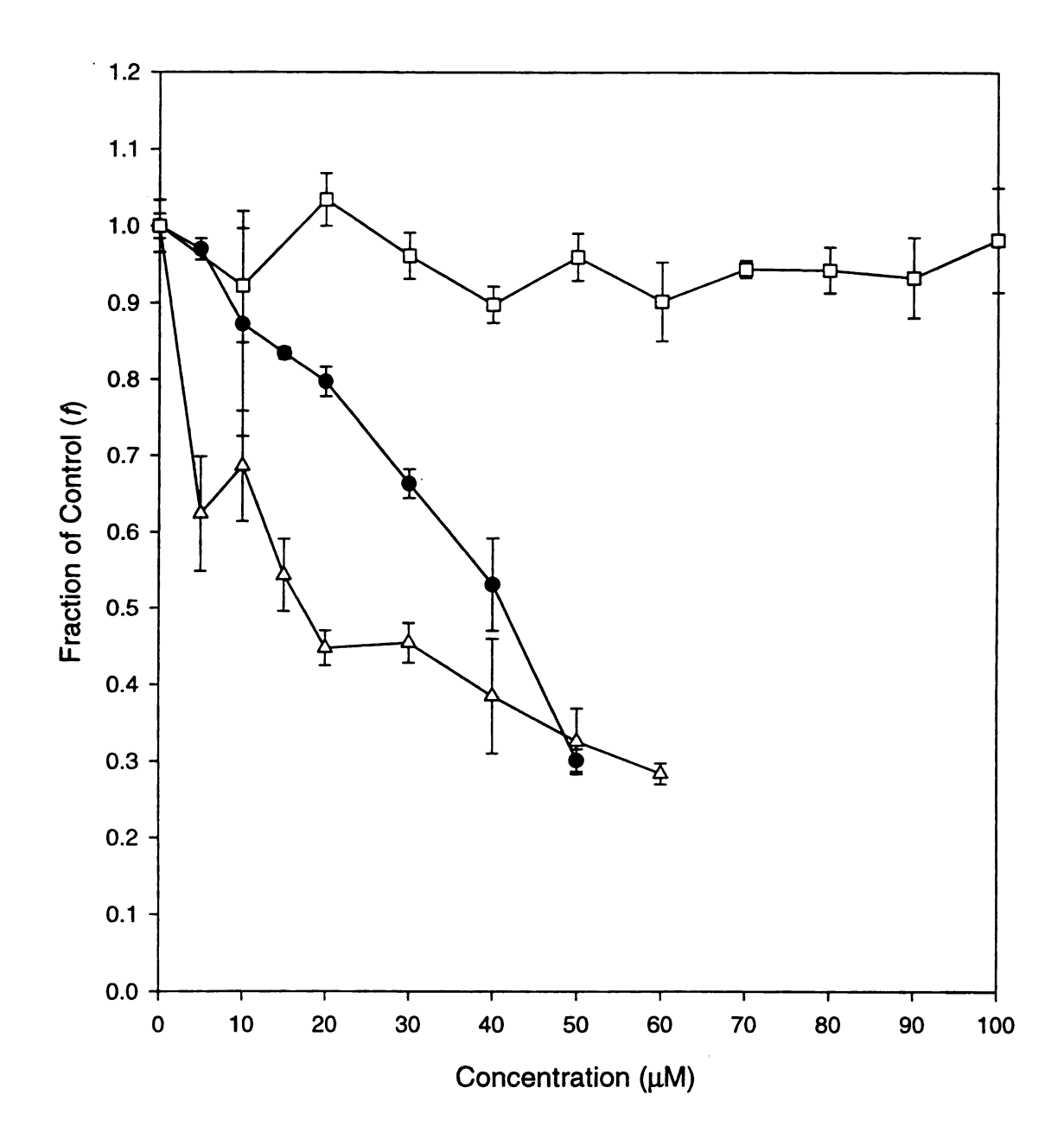


Figure 4.4. Dose response curve for cells exposed to  $\bullet$  pyrene  $(0-50 \,\mu\text{M})$ ,  $\Delta$  2,2',6,6'-biphenyl tetraaldehyde  $(0-60 \,\mu\text{M})$  and  $\Box$  2,2',6,6'-biphenyl tetracarboxylic acid  $(0-100 \,\mu\text{M})$  for 30 minutes.

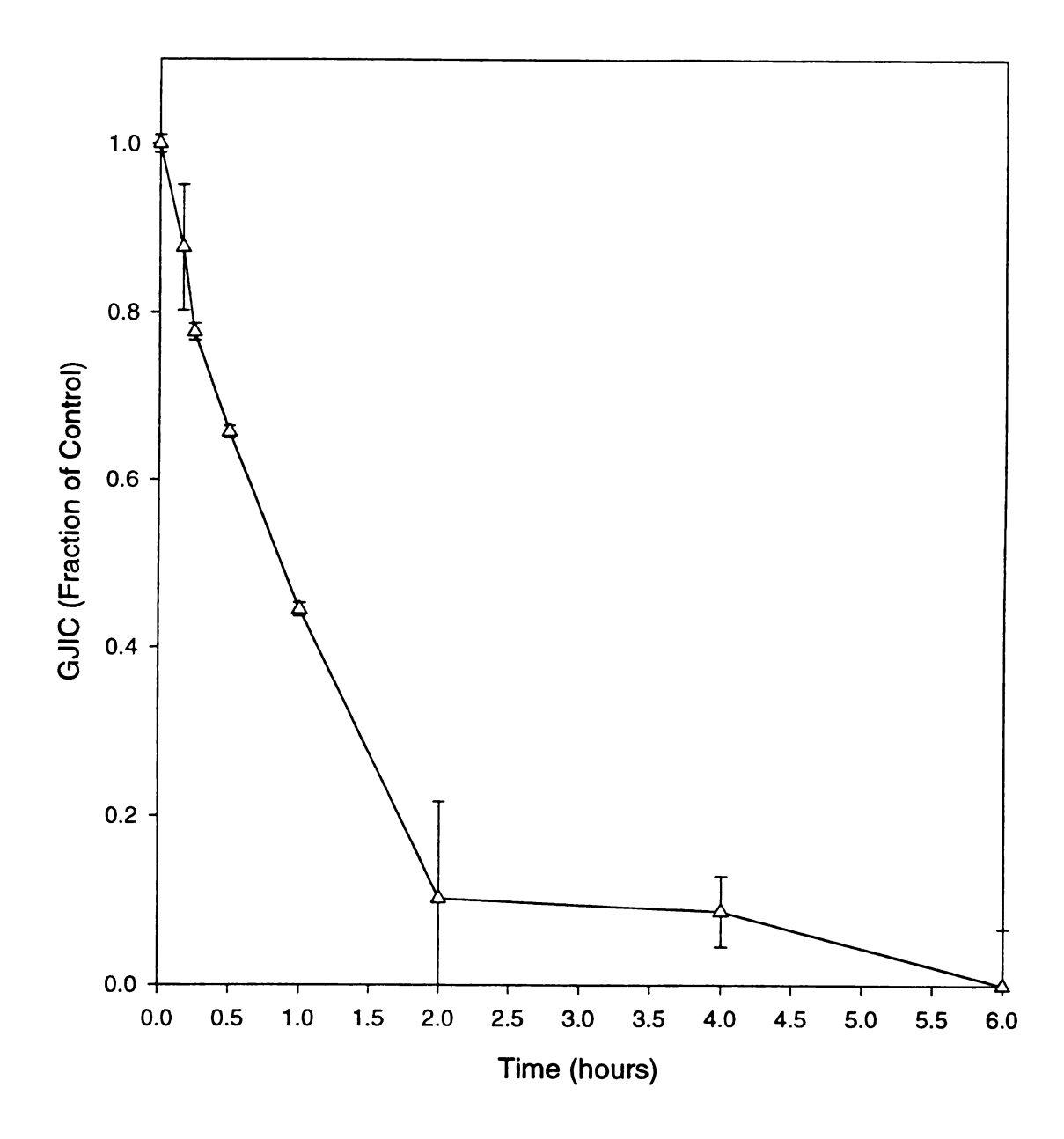


Figure 4.5. Time response for cells exposed to 5  $\mu M$  concentration of 2,2',6,6'-biphenyl tetraaldehyde.

2,2',6,6'-biphenyl tetracarboxylic acid (500  $\mu$ M) did not result in a reduction in communication even after 24 hours (Figure 4.6).

Time Recovery. The time recovery assay is used to determine if cells are able to recover full communication after the removal of the toxicant and replacement of new media. For experiments, cells were exposed to a fixed dose of toxicant for 30 minutes and then rinsed. New D-media was added to the plate and the cells were returned to the incubator. GJIC assays were then performed to determine the initial GJIC value and the subsequent GJIC values for 30 minutes, 60 minutes, 1 hour, 2 hours, 4 hours and 5.5 hours after media replacement.

After 30 minutes of exposure to 2,2',6,6'-biphenyl tetraaldehyde (5  $\mu$ M), rinsing of the plate, and replacement of new media, cellular communication continued to decrease and never recovered (Figure 4.7). No recovery of GJIC was seen and complete inhibition was reached within 1 hour despite media replacement. Time recovery was not performed for 2,2',6,6'-biphenyl tetracarboxylic acid because no significant difference in effects to GJIC were seen between the concentrations tested (10 – 500  $\mu$ M) and controls at a p < 0.01.

4.3.2 HL-60 Neutrophil Assay. Exposure of HL-60 cells to pyrene or its metabolites in the absence of PMA did not result in generation of  $O_2^-$  (data not shown). HL-60 cells stimulated with PMA produced  $O_2^-$ . The generation of  $O_2^-$  by PMA-stimulated cells was unaffected by treatment with either pyrene or the carboxylic acid derivative at concentrations up to 40  $\mu$ M (Figure 4.8). The tetraaldehyde derivative caused a

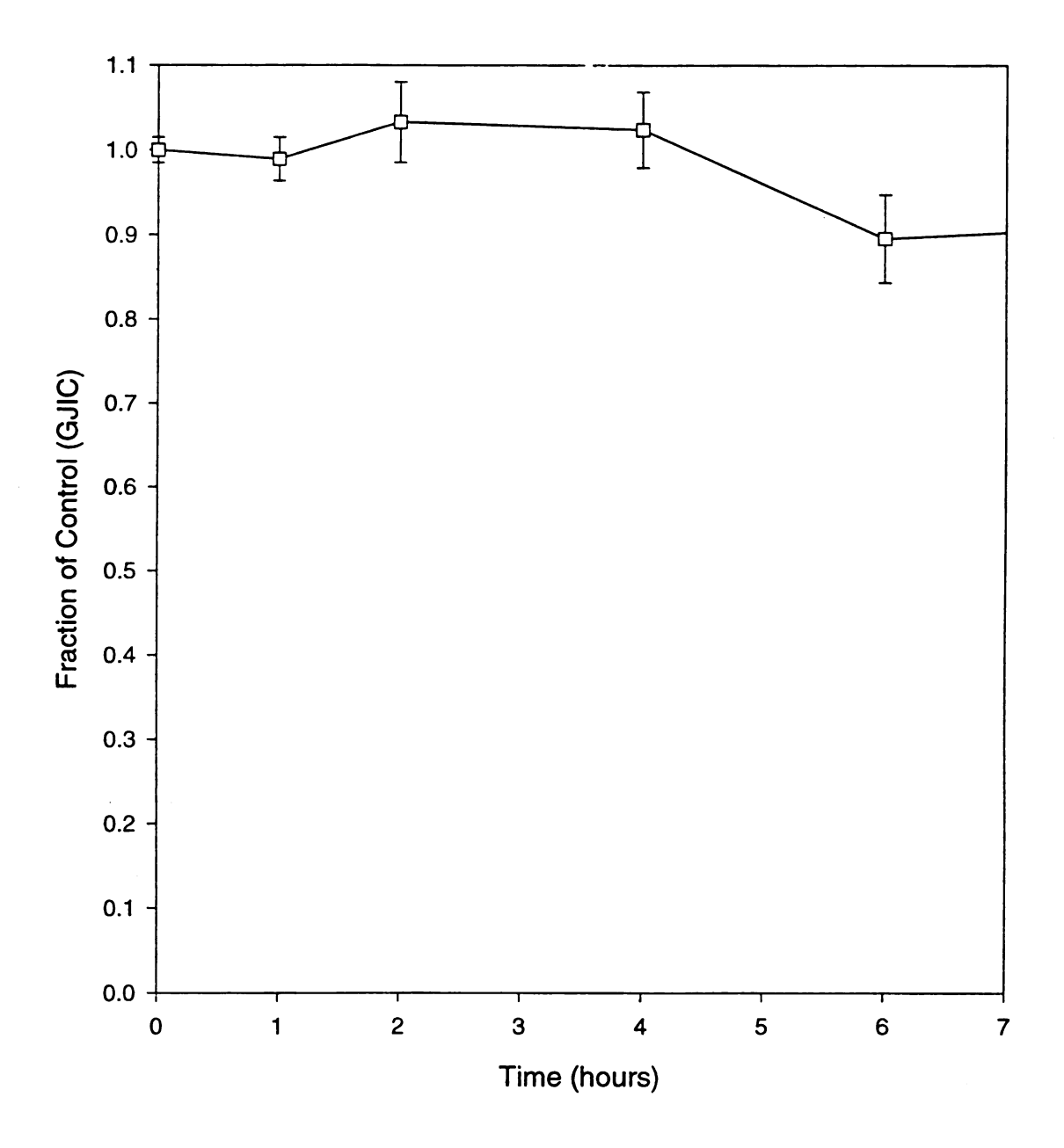


Figure 4.6. Time response 2,2',6,6'-biphenyl tetracarboxylic acid at 500 mM concentration.

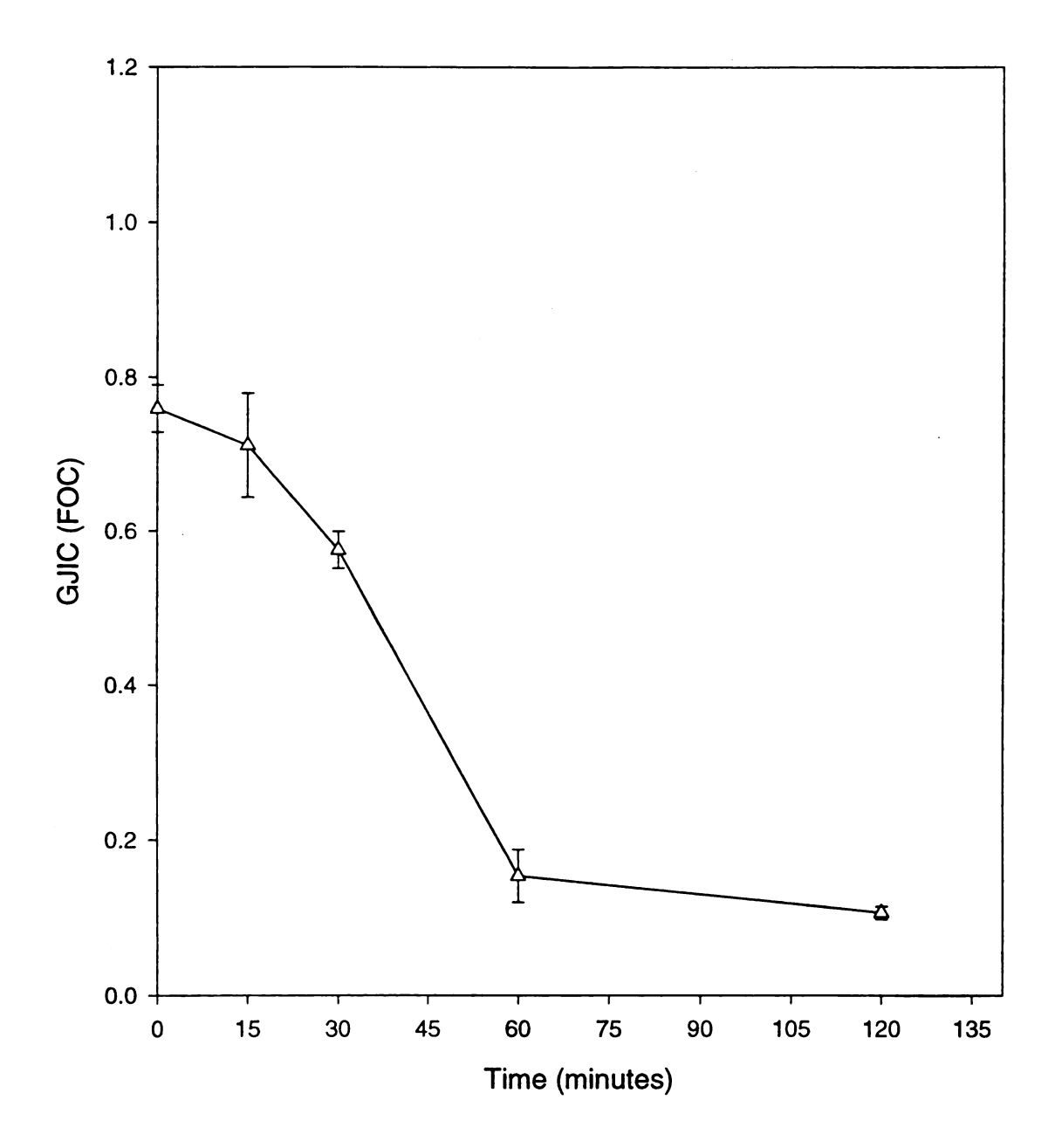


Figure 4.7. Time recovery for cells exposed to 5  $\mu$ M concentration of 2,2',6,6'-biphenyl tetraaldehyde for 30 minutes, rinsed, and allowed to recover intercellular communication in new media for various periods of time.

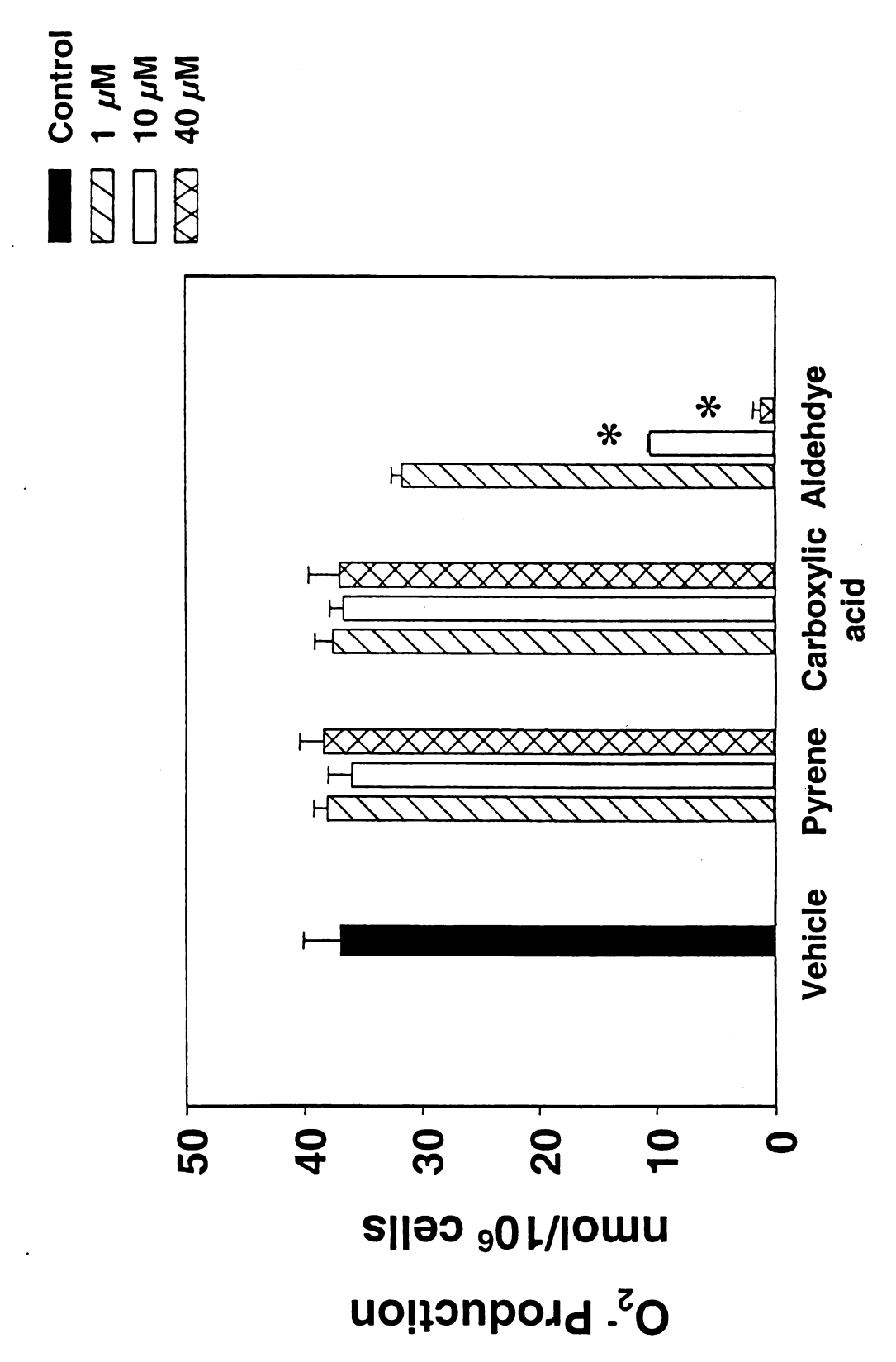
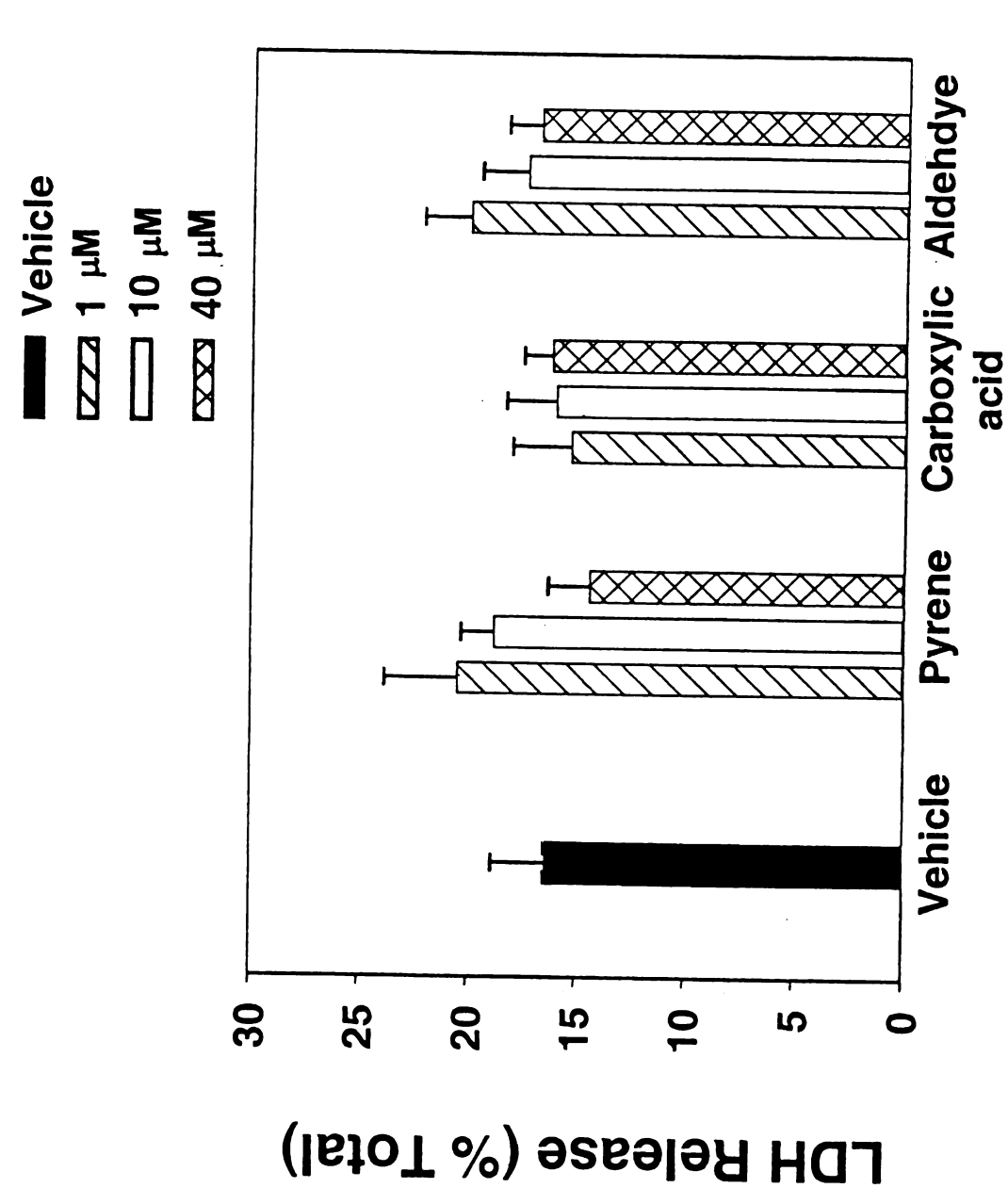


Figure 4.8 Effect of pyrene and its metabolites on PMA-stimulated superoxide anion (O<sub>2</sub>) generation by HL-60 cells. Cells were incubated with pyrene or its metabolites at the concentrations indicated for 30 minutes, after which PMA (1 ng/mL) was added. O<sub>2</sub> produced after addition of PMA was determined as described in the Methods. N = 3. \*, significantly different from vehicle (p < 0.05)

concentration-dependent decrease in PMA-stimulated O<sub>2</sub> production. LDH release by HL-60 cells was not increased by exposure to either pyrene or its metabolites (Figure 4.9), demonstrating that at the concentrations used, these chemicals are not cytotoxic to the cells.



**acid**Figure 4.9 Cytotoxicity in HL-60 cells exposed to pyrene or its metabolites. Cells were incubated with pyrene or its metabolites at the concentrations indicated as described in the legend to Figure 4.8. LDH released by the cells was measured at the end of the 60-minute incubation as described in Methods. N = 3. No significant differences observed.

### 4.4 Conclusion

It is important to identify PAH oxidation constituents and to understand the relative toxicity because these compounds. Though limited toxicology studies for PAH ozonation byproducts are available, the results obtained from the GJIC analysis are consistent with previous gap junction studies. The ability of 2,2',6,6' biphenyl tetraaldehyde more than 2,2',6,6' tetracarboxylic acid to inhibit GJIC is thought to be related to the functional groups attached at the 4, 5 or 9, 10 bonds. This conclusion is also supported in literature where various functional groups adjacent to or a part of PAH oxidation products have been shown to enhance the carcinogenic activity of PAHs [5-10, 19-24]. Herner et al. [23] analyzed three phenanthrene-like products produced during pyrene ozonation and seven commercially available products similar in structure only differing by the location and type of functional group. The phenanthrene and biphenyllike compounds with only aldehyde groups (i.e., 1,2,3,4-tetrahydro-9-phenanthrene carboxaldehyde and 2-biphenyl carboxaldehyde) were more inhibitory than biphenyl-like compounds with carboxyl groups (i.e., diphenic acid, 2-biphenyl carboxylic acid, and 2biphenyl carboxylic acid). A comparison of the biphenyl compounds showed that the biphenyl compounds with only aldehyde groups completely blocked communication (f < 10.2) at concentrations much lower than the biphenyl compounds with carboxylic acid groups (f = 0.8 - 1.0).

The effects of pyrene ozonation products were examined in two *in vitro* assays of biological activity. Each of these assays represents a cellular function that results from integration of cellular signaling and changes in each can be associated with effects on the whole organism. In this study, we determined that the functional group attached to the

oxidized bonds (i.e., aldehyde or carboxylic) appears to determine the ability of a compound to effect cellular function. The presence of aldehyde groups in all four positions led to a compound with increased toxicity while the presence of four carboxylic acid groups led to a compound that shows little to no effect in the toxicology studies at the levels tested. 2,2',6,6'-biphenyl tetraaldehyde demonstrated an increased ability to inhibit GJIC as compared to pyrene. Time response and time recovery results indicated that irreversible damage to cells resulted from exposure to this compound at very low doses and short time periods. This indicates the potential for decreased intercellular communication and an increased chance of tumor formation and disruption of normal cell function.

# **Environmental Significance**

Particulate matter, fluidized bed combustion systems, coal burning, vehicle emissions contain significant levels of PAH compounds. The incomplete combustion of fossil fuels, gasoline and coal results in polycyclic compounds that can exist in both gaseous and solid phases in air [55]. At ambient temperatures and depending on the molecular mass, PAHs with two- and three- rings (i.e. naphthalene, anthracene) are found predominantly in the gas-phase. PAHs with six or more rings (i.e. naphtha[2, 1-a]pyrene, coronene) adsorb to particles and are found in the solid-phase; and in both solid and gas-phases, four— and 5- ring (i.e. pyrene, chrysene) PAHs will exist [7, 55-56].

Gas-phase PAHs are chemically reactive in the lower troposphere and are known to yield secondary pollutants that include strongly carcinogenic and mutagenic compounds (11-12, 56-57). It has been experimentally shown that gas-phase reactions for

2 and 3 ring PAHs with hydroxyl radicals and with ozone resulted in the production of oxidized PAH compounds containing quinone and dialdehyde groups [56, 58]. As seen in the present work, the presence of dialdehyde functional groups is an indication of toxicity.

Oxidized PAH byproducts in aqueous and solid media might also correlate to compounds detected in atmospheric reactions with PAH particulate matter. More investigations identifying products of reaction of PAHs in ambient air with hydroxyl radicals and ozone could provide a link to compounds detected in aqueous ozonations where numerous studies have identified byproducts for PAH compounds.

# Acknowledgments

We would like to thank the NIEHS-Superfund Grant for funding support.

### 4.5 References

- 1. Corless, C.; Reynolds, G.; Graham, N.; Perry, R.; "Ozonation of Pyrene in Aqueous Solution". Water Research. 1990, 24(9), 1119 1123.
- 2. Trapido, M.; Veressinina, Y.; Munter, R.; "Ozonation and Advanced Oxidation Processes of Polycyclic Aromatic Hydrocarbons in Aqueous Solutions- A Kinetic Study". *Environ. Technol.* **1995**, 16, 729-740.
- 3. Masten, S. and Davies, S.; "The Use of Ozonation to Degrade Organic Contaminants in Wastewaters". *Enviro. Sci. Technol.* **1994**, 28(4), 181A 185A.
- 4. Gilula, N.; Fancett, D.; Aoki, A.; "The Sertoli Cell Occluding Junctions and Gap Junctions in Mature and Developing Mammalian Testis". *Dev. Biol.* **1976**, 50, 142-168.
- 5. Jerina, D.M.; Yagi, H.; Lehr, R.E.; Thakker, D.R.; Schaefer-Ridder, M.; Karle, J.M.; Levin, W.; Wood, A.W.; Chang, R.L.; Conney, A.H.; "The Bay Region Theory of Carcinogenesis by Polycyclic Aromatic Hydrocarbons". <u>In Polycyclic Hydrocarbons and Cancer. Volume 1. Environment, Chemistry, and Metabolism</u>. Academic Press: New York, 1978, 173 185.
- 6. Neff, J.M. "Polynuclear Aromatic Hydrocarbons in Aqueous Environment: Sources, Fates and Biological Effects". <u>Applied Science</u>. London. **1979**, 227.
- 7. Hoffmann, D.; Lavoie, E.J.; Hecht, S.S.; "Polynuclear Aromatic Hydrocarbons: Effects of Chemical Structure on Tumorgenicity". *Polynuclear Aromatic Hydrocarbons: Physical and Biological Chemistry. Sixth International Symposium.* Battelle Press: Columbus, 1982, 1-19.
- 8. Friesel, H.; Schope, K.B.; Hecker, E.; "Bay Region versus L-Region Activation of the Tumor Initiator 7, 12-Dimethyl Benz(a)anthracene". *Polynuclear Aromatic Hydrocarbons: Formation, Metabolism and Measurement. Seventh International Symposium.* Battelle Press: Columbus, 1982, 517-530.
- 9. Melikian, A.A; Lavoie, E.J.; Hecht, S.S.; Hoffmann, D.; "On the Enhancing Effect of a Bay Region Methyl Group in 5-Methyl Chrysene Carcinogenesis." *Polynuclear Aromatic Hydrocarbons: Formation, Metabolism and Measurement. Seventh International Symposium.* Battelle Press: Columbus, 1982, 861-875.
- 10. Larsen, W.; Werf, S.; Brunner, G.; "A Dramatic Loss of Cumulus Cell Gap Junctions is Correlated with Germinal Vesicle Breakdown in Rat Oocytes". *Dev. Biol*, 1986, 113, 517 521.

- 11. Hannigan, M.; Cass, G.; Penman, B.; Crespi, C.; Lafleur, A.; Busby, W.; Thilly, W.; "Human Cell Mutagens in Los Angeles Air". *Environ. Sci. Technol.* 1997. 31, 438 447.
- 12. Hannigan, M.; Cass, G.; Penman, B.; Crespi, C.; Lafleur, A.; Busby, W.; Thilly, W.; Simoneit, B.; "Bioassay-Directed Chemical Analysis of Los Angeles Airborne Particulate Matter Using a Human Cell Mutagenicity Assay". *Environ. Sci. Technol.* 1998. 32, 3502 3514.
- 13. Clemons, J.; Allan, L.; Marvin, C.; Wu, Z.; McCarry, B.; Bryant, D.; Zacharewski, T.; "Evidence of Estrogen- and TCDD-Like Activities in Crude and Fractionalted Extracts of PM<sub>10</sub> Air Particulate Material Using in Vitro Gene Expression Assays." *Environ. Sci. Technol.* **1998**, 32, 1853 1860.
- 14. American Toxic Substance Registry (ATSDR), 1997.
- 15. Copeland, P.; Dean, R.; McNeil, D.; "The Ozonolysis of Polycyclic Hydrocarbons: Part II". J. Chem. Soc. 1961, 1232 1236.
- 16. Bailey, P.; Ozonation in Organic Chemistry, Volume II. Non-Olefinic Compounds. Academic Press: New York, 1982. 43 109.
- 17. Yao, J.J; Huang, Z.; Masten, S.; "The Ozonation of Pyrene: Pathway and Product Identification". Wat. Res. 1998, 32(10), 3001-3012.
- 18. Yoshikawa, T.; Ruhr, L.; Flory, W.; Giamalva, D.; Church, D.; Pryor, W.; "Toxicity of Polycyclic Aromatic Hydrocarbons I. Effect of Phenanthrene, pyrene and their ozonized products on blood chemistry in rats". *Toxicol. Appli. Pharmacol.* 1985. 79, 218-226.
- 19. Upham, B.; Masten, S.; Lockwwok, B.; Trosko, J.; "Nongenotoxic effects of polycyclic Aromatic Hydrocarbons and Their Ozonation byproducts on the intercellular communication of Rat Liver Epithelial Cells." Fund. Appl. Tox. 1994, 23, 470-475.
- 20. Upham, B.; Yao, J.; Trosko, J.; Masten, S.; "The Determination of the Efficacy of Ozone Treatment Systems Using Gap Junctional Intercellular Communication Bioassay". *Environ. Sci. Technol.* 1995, 29(12), 2923 2928.
- 21. Upham, B.; Weis, L.; Rummel, A.; Masten, S.; Trosko, J.; "The Effects of Anthracene and Methylated Anthracenes on Gap Junctional Intercellular Communication in Rat Liver Epithelial Cells". Fund. Appli. Tox. 1996, 34, 260-264.
- 22. Upham, B.; Weis, L.; Rummel, A.; Trosko, J.; "Modulated Gap Junctional Intercellular Communication as a Biomarker of PAH Epigenetic Toxicity: Structure Function Relationship". *Env. Health Perspectives.* 1998, 106(4), 975 981.

- 23. Herner, H, Trosko, J.; Masten, S.; "The Reaction of Ozone with Pyrene: The Byproducts and Their Toxicological Implication". *Environ. Sci. Technol.* **2001**, 32(10), 3001 -3012.
- 24. Luster-Teasley, S; Yao, J.; Herner, H.; Trosko, J.; Masten, S.; "Ozonation of Chrysene: Evaluation of Byproduct Mixtures and Identification of Toxic Constituent". *Environ. Sci. Technol.* **2002**, 36(5), 869 876.
- 25. Ghoshal, S.; Weber, W.; Rummel, A.; Trosko, J.; Upham, B.; "Epigenetic Toxicity of a mixture of Polycyclic Aromatic Hydrocarbons on Gap Junctional Intercellular Communication before and after biogradation". Environ. Sci. Technol. 1999, 33(7), 1044 1050.
- 26. Trosko, J. personal communication, Michigan State University, 2001.
- 27. Trosko, J.; Chang, C.; Madhukar, B.; Klauning, J.; "Chemical Oncogene and Growth Factor Inhibition of Gap Junction Intercellular Communication: An Integrative Hypothesis of Carcinogesesis." Pathobiology. 1990, 58, 265-278.
- 28. Trosko, J.; Madhukar, B.; Chang, C.; "Endogenous and Exogenous Modulation of Gap Junction Intercellular Communication: Toxicological and Pharmacological Implications". *Life Sci.* **1993**, 53, 1-19.
- 29. Ganey, P.E., Sirois, J.E., Denison, M., Robinson, J.P. and Roth, R.A.; "Neutrophil function after exposure to polychlorinated biphenyls in vitro". Environ. Hlth. Perspect. 1993. 101: 430-434, 1993.
- 30. Voie OA, Fonnum F.; "Ortho substituted polychlorinated biphenyls elevate intracellular [Ca<sup>2+</sup>] in human granulocytes". *Environ Toxicol Pharmacol.* **1998**, 5: 105-12.
- 31. Narayanan, P.K., Carter, W.O., Ganey, P.E., Roth, R.A., Voytik-Harbin, S.L. and Robinson, J.P.; "Impairment of human neutrophil oxidative burst by polychlorinated biphenyls: Inhibition of superoxide dismutase activity". *J. Leuk. Biol.* 1998, 63: 216-224, 1998.
- 32. Tithof, P.K., Olivero, J., Ruehle, K., and Ganey, P.E.; "Activation of neutrophil calcium-dependent and -independent phospholipases A<sub>2</sub> by organochlorine compounds". *Toxicol. Sci.*, **2000**, 53: 40-47.
- 33. Ganey, P.E., Quensen, J.F., Mousa, M.A., Boyd, S.T., Wagner, M.A., and Fischer, L.J.: "Biological activity associated with noncoplanar polychlorinated biphenyls after microbial dechlorination of Aroclor 1242 and Aroclor 1254. Environ". *Toxicol. Chem.* 2000, 19: 1311-1316.

- 34. Olivero, J., and Ganey, P.E.; "A molecular motif required for the activation of rat neutrophil phospholipase A<sub>2</sub> by organochlorine compounds". *Chem. Res. Toxicol.*, **2002**, 15: 153-159.
- 35. Hewett, JA; Schultze, AE; VanCise, S; Roth, RA.; "Neutrophil depletion protects against liver injury from bacterial endotoxin." *Lab Invest*. 1992 Mar;66(3):347-61.
- 36. Yabe Y, Kobayashi N, Nishihashi T, Takahashi R, Nishikawa M, Takakura Y, Hashida M. "Prevention of neutrophil-mediated hepatic ischemia/reperfusion injury by superoxide dismutase and catalase derivatives". *J Pharmacol Exp Ther.* **2001**, 298(3):894-9.
- 37. Kiely PD, Wang JC, Kelly CJ, Condron C, Watson RG, Bouchier-Hayes DJ. "Diethylmaleate, a pro-oxidant, attenuates experimental ischaemia-reperfusion-induced lung injury". *Br J Surg.* **2002**, Apr;89(4):482-5.
- 38. Ikeda Y, Young LH, Lefer AM. Attenuation of neutrophil-mediated myocardial ischemia-reperfusion injury by a calpain inhibitor. *Am J Physiol Heart Circ Physiol*. **2002** Apr; 282(4):H1421-6.
- 39. Fieser, L. F.; Novello, F. C. "9-Methyl-3,4-benzpyrene". J. Amer. Chem. Soc. 1940, 62, 1855-1859.
- 40. Yakobson, G. G.; Vlasov, V. M.; Vorozhtsov, N. N. "Prepartion of Decafluoropyene and its Interaction with Nitric Acid". *Dokl. Chem. Engl. Transl.* 1966, 169, 762-764.
- 41. Jursic, B. "Surfactant Assisted Permanganate Oxidation of Aromatic Compounds". *Can. J. Chem.* 1989, 67, 1381-1383.
- 42. El-Fouly, M.; Trosko, J.; Chang, C.; "Scrape Loading and Dye Transfer: A Rapid and simple Technique to Study Gap Junction Intercellular Communication". *Exp. Cell Res.* 1987, 168, 422-430.
- 43. Borenfreund, E.; Prunerm J. "Toxicity Determined In Vitro by Morphological Alterations and Netural Red Absorption Toxicology". *Toxicology Letters*. **1985**, 24, 119 124.
- 44. Yamaguchi, T.; Hayakawa T.; "Granulocyte colony-stimulating factor promotes function maturation of O₂ generating system during differentiation of HL-60 to neutrophil-like cells." Archives of Biochemistry and Biophysics. 1998, 353(1): 93-100.
- 45. Kargman, S., Ali, A., Vaillancourt, J.P., Evans, J.F., and Nicholson, D.W. "Protein kinase C-dependent regulation of sulfidopeptide leukotriene biosynthesis and leukotriene C4 synthase in neutrophilic HL-60 cells". *Mol Pharmacol.* 1994, 45: 1043-1049.

- 46. Thompson, B.Y., Sivam, G., Britigan, B.E., Rosen, G.M, and Cohen, M.S.; "Oxygen metabolism of the HL-60 cell line: comparison of the effects of monocytoid and neutrophilic differentiation". *J Leukocyte Biol.* **1988**, 43: 140-147.
- 47. Senio, Y.; Ikeda, U.; Sekiguchi, H.; Morita, M, Konishi, K.; Kasahara, T.; Shimada, K.; Expression of Leukocyte Chemotactic Cytokines in Myocarduak Tissue." *Cytokine*, 1995, 7(3): 301 304.
- 48. Korchak, H.M., Rossi, M.W., and Kilpatrick, L.E.; "Selective role for beta-protein kinase C in signaling for O-2 generation but not degranulation or adherence in differentiated HL60 cells". *J Biol Chem.* 1998, 273: 27292-27299.
- 49. Rane, M.J.; Carrithers, S.L.; Arthur, J.M.; Klein, J.B.; McLeish, K.R.; "Formyl peptide receptors are coupled to multiple mitogen-activated protein kinase cascades by distinct signmal transduction pathways Role in activation of reduced nictinamide adenine dinucleotide oxidase". *J. Immunology.* 1997, 159 (10): 5070 5078.
- 50. Yu, H. Suchard, S.J., Nairn, R. and Jove, R.; "Dissociation of mitogen-activated protein kinase activation from the oxidative burst in differentiated HL-60 cells and human neutrophils". *J Biol Chem.* **1995**, 270: 15719-15724.
- 51. Gallois, A.; Bueb, J.L.; Tschirhart, E.; "Effect of SK & F96365 on extracellular Ca<sup>2+</sup>-dependent O<sub>2</sub> production in neutrophil-like HL-60 cells". *European J. of Pharmacology.* **1998**, 361 (2-3): 293 298.
- 52. Browning, D.D.; Pan, Z.K.; Prossnitz, E.R.; Ye, R.D.; "Cell type and developmental stage-specific activation of NF-kappa B by fMet-Leu-Phe in myeloid cells". *J Biological Chem.* 1997, 272 (12), 7995 8001.
- 53. Babior, B.M., Kipnes, R.S. and Curnutte, J.T.; "Biological defense mechanisms. The production by leukocytes of superoxide, a potential bactericidal agent". *J. Clin. Invest.* **1973**, 52, 741-744.
- 54. Bergmeyer, H.V. and Bernt, E.; "Lactate dehydrogenase UV assay with pyruvate and NADH". In: Methods of Enzymatic Analysis, H.V. Bergmeyer, Ed. Academic Press, New York, 1974, 524-579.
- 55. Liu, K.; Xie, W.; Zhao, Z-B.; Pan, W-P.; Riley, J.; "Investigation of Polycyclic Aromatic Hydrocarbons in Fly Ash from Fluidized Bed Combustion Systems". *Environ. Sci. Technol.* **2000**, 34, 2273 2279.
- 56. Bunce, N.; Liu, L.; Zhu, J.; Lane, D.; "Reaction of Naphtalene and Its Derivatives with Hydroxyl Radicals in the Gas Phase". *Environ. Sci. Technol.* 1997, 31, 2252 2259.

- 57. Helmig, D.; Arey, J.; Harger, W.P. Atkinson, R.; Lopezcanico, J.; Formation of Mutagenic Nitrodibenzopyranones and their occurrence in ambient Air". *Env. Sci. Tehnol.* 1992, 26 (3): 622 624.
- 58. Riesen, F.; Arey, J.; "Reactions of Hydroxyl Radicals and Ozone with Acenaphthene and Acenaphthylene. *In Press. Envion. Sci. Technol.* **2002**.

## Chapter 5

## 5.1 Introduction

This chapter is divided into two sections. Section 1 addresses reaction kinetics and Section 2 presents an application of the Hsu and Masten [1] model to experimental data.

### 5.2 Section 1: Reaction kinetics

The direct reaction between ozone and organic matter or ozone and a contaminant is considered an overall second order reaction; first order with respect to each reactant. The equation can be written as:

$$- d[O_3]/dt = k [O_3]^m [M]^n$$
 (Eqn 5.1)

where k is the second order rate constant  $(\sec^{-1} (kg/L)(mg/kg)^{-1})$ , [M] is the organic matter concentration or contaminant concentration (mg/kg), and m = n = 1 indicating that one mole of [M] reacts with one mole of ozone. This expression can be simplified to the first order expression:

$$-d[O_3]/dt = k'[O_3]$$
 (Eqn 5.2)

where k' = k[M] and is the pseudo-first order reaction constant.

Equation 5.2 can be integrated to yield,

$$-\ln [O_3]/[O_3]_0 = k t$$
 (Eqn 5.3)

In first order reactions, a plot of  $-\ln [O_3]/[O_3]_0$  versus time (t) will result in a linear plot. The slope of the line represents the first order rate constant (k) with the units of second<sup>-1</sup> (s<sup>-1</sup>). The variable  $[O_3]$  represents the experimental ozone concentration and  $[O_3]_0$  is the initial ozone concentration, both with units of (mg) or (mg/L).

Previous studies in aqueous systems with humic acid and in the presence of organic matter have used first order kinetics for the data [2-6]. These studies have also reported the presence of two distinct regions in the kinetic analysis. Day [4] noted the occurrence of two regions in the pseudo-first order plots for dry Metea. Day [4] proposed that the first region corresponded to the initial rate of the ozone reaction and the second region corresponded to the rate of ozone self-decomposition. Alebić-Juretić et al. [2] and Hsu [5] proposed that the two regions were artifacts of the surface coverage of PAHs on the soil particles. Lim et al. [6] described the first region as the instantaneous ozone demand (ID) phase exerted by the soil and the region where reactions between ozone/soil organic matter (SOM) and ozone/metal oxides predominated.

## 5.2.1 Reaction Kinetics for Experiments

First order plots were constructed using Equation 5.3, however, the experimental results did not appear to be best represented by simple first order kinetics. Hsu [5] also observed that ozonation experiments for phenanthrene contaminated soil did not fit first order kinetics.

To calculate  $-d[O_3]/dt$  using Equation 5.1, one would not only need to know the concentration of ozone, but also the change in concentration for all of the constituents reacting within the system [M]. Monitoring changes in soil constituents within the system however is not possible during an experimental run. In an attempt to re-evaluate the experimental data, a second order rate expression for ozone was proposed to describe ozone decomposition within the system. This expression would suggest that Eqn 5.1 could be re-written where m = 2 for  $[O_3]$  and n = 1 for [M]. Equation 5.1 thus becomes,

$$-d[O_3]/dt = k[O_3]^2[M]^1$$
 (Eqn 5.4)

this can be simplified to,

$$-d[O_3]/dt = k'[O_3]^2$$
 (Eqn 5.5).

where k' = k[M] and would be a pseudo-second order rate constant  $[s^{-1} \cdot (mg/L)^{-1}]$  or  $[s^{-1} \cdot (mg/kg^{-1})]$ . Use of Equation 5.5 would assume that the reaction conditions are such that the rate is essentially a function of the concentration of ozone. Integrating Equation 5.5 yields,

$$1/[O_3] - 1/[O_3]_0 = k t$$
 (Eqn 5.5).

For Equation 5.5, a plot of  $(1/[O_3] - 1/[O_3]_0)$  versus time or  $1/[O_3]$  versus time will be linear with slope k. Both of the plots will have identical slopes; but the difference between the two plots would be the location of the y-intercept. For  $(1/[O_3] - 1/[O_3]_0)$  versus time, the y-intercept would be zero. For  $1/[O_3]$  versus time, the y-intercept would equal  $1/[O_3]_0$ .

Both first order (Equation 5.3) and second order (Equation 5.5) reactions plots were constructed for the present study. The reaction order and rate constants were determined based on the best linear fit. Reported in this chapter are the k values and comparisons of a few of the first order and second order plots. In Appendix A, both first order and second order plots are provided for the experiments.

## 5.2.1.1 Non-Contaminated Dry Soil

Figure 5.1 and Figure 5.2 are examples of the first order and second order plots obtained for the dry, non-contaminated Metea (pH 6). In these soils, two regions were observed. In the dry non-contaminated soil (pH 6, 25°C), Region I appeared to follow second order kinetics ( $r^2 = 0.93$ ). Region II had the best representation as first order ( $r^2 = 0.96$ ). Table 5.1 compares first order and second order rate constants for the dry, non-contaminated soils.

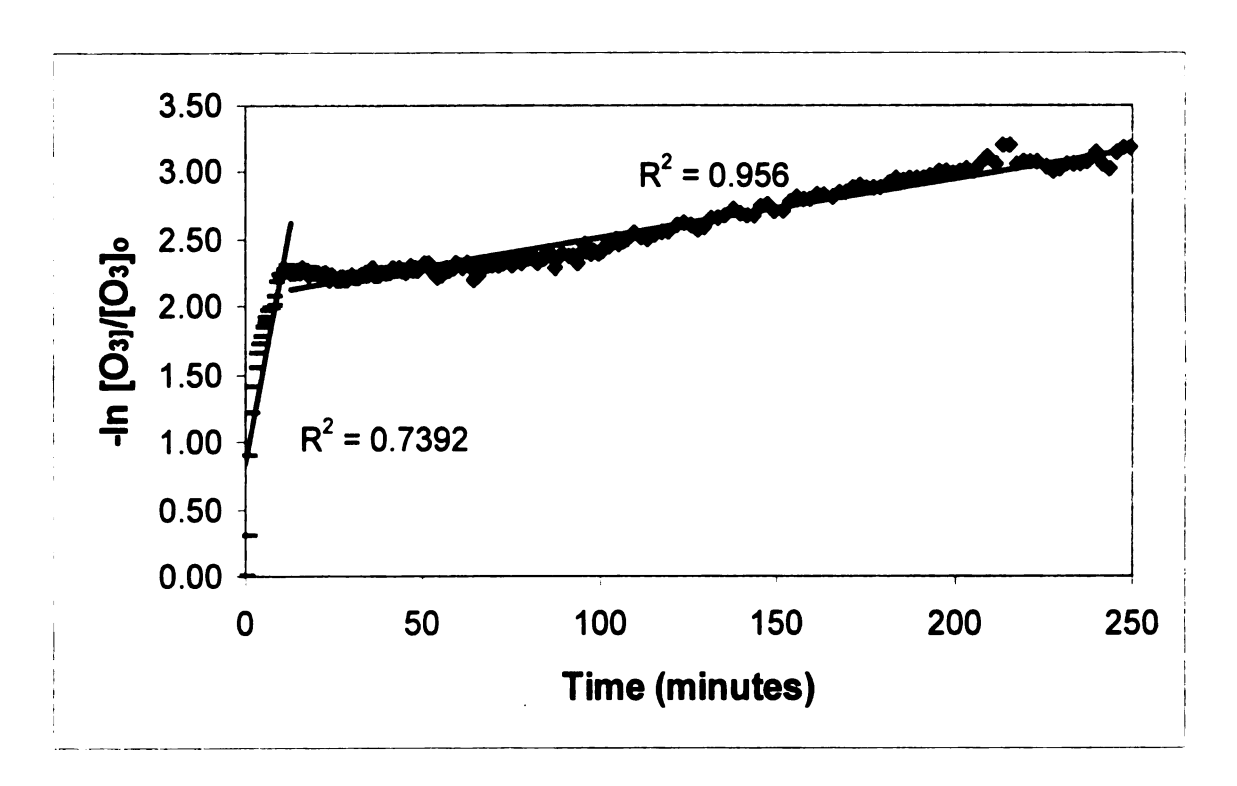


Figure 5.1 First order plot for Dry, non-contaminated Metea soil pH 6 at 25°C:

- Region I; Region II.

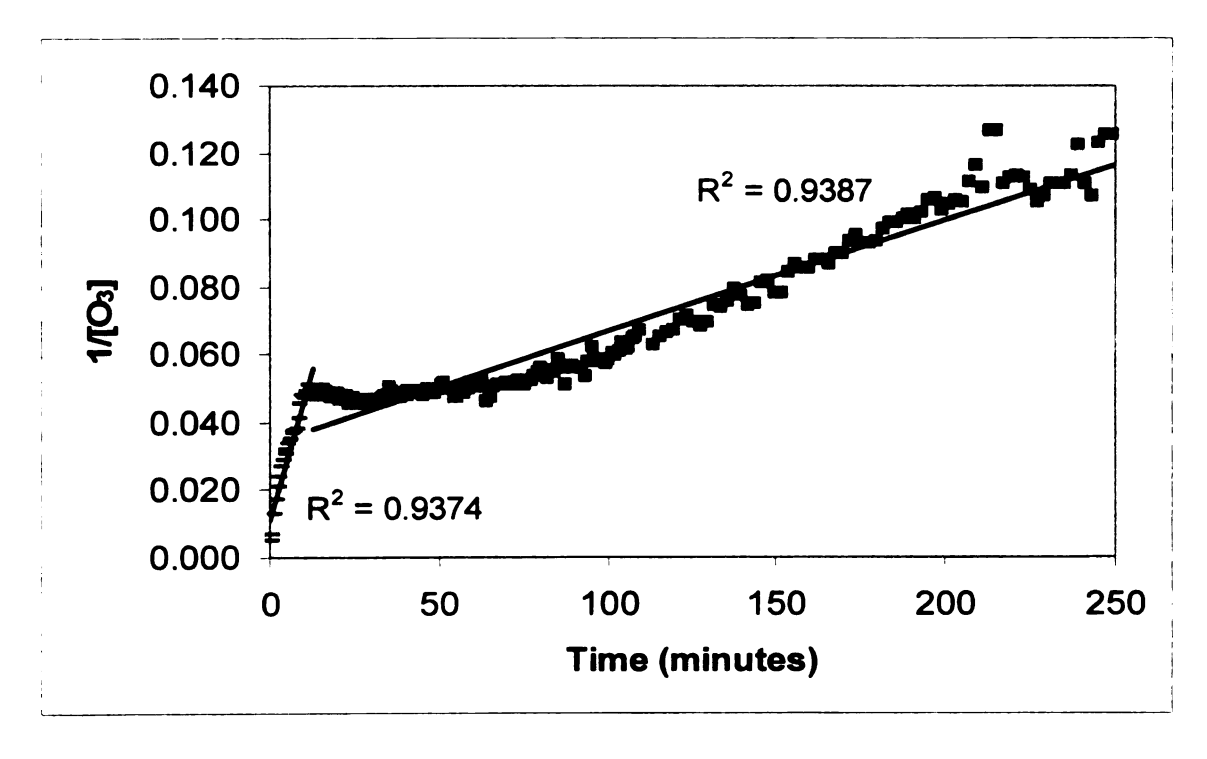


Figure 5.2 Second order plot for Dry, non-contaminated Metea soil pH 6 at 25°C:

- Region I; Region II.

Table 5.1. Rate constants for dry, non-contaminated Metea soil (values reported at 95% Confidence Interval (C.I.)).

Sample	First order Region I k <sub>1</sub> (s <sup>-1</sup> )	First order Region II k <sub>1</sub> (s <sup>-1</sup> )
Dry, clean Metea pH 2 Dry, clean Metea pH 6 Dry, clean Metea pH 8	$2.6 \pm 0.18 \times 10^{-1}$ r <sup>2</sup> = 0.44 $2.2 \pm 0.01 \times 10^{-3}$ r <sup>2</sup> = 0.73 $1.2 \pm 0.04 \times 10^{-3}$ r <sup>2</sup> = 0.61	$1.1 \pm 0.32 \times 10^{-4}  r^2 = 0.92$ $7.3 \pm 0.17 \times 10^{-5}  r^2 = 0.96$ $5.8 \pm 0.08 \times 10^{-5}  r^2 = 0.97$
Sample	Second order Region I k <sub>2</sub> (s·mg O <sub>3</sub> /kg soil) <sup>-1</sup>	Second order Region II k <sub>2</sub> (s·mg O <sub>3</sub> /kg soil) <sup>-1</sup>
Dry, clean Metea pH 2 Dry, clean Metea pH 6 Dry, clean Metea pH 8	$3.0 \pm 0.24 \times 10^{-4} \text{ r}^2 = 0.83$ $1.3 \pm 0.11 \times 10^{-4} \text{ r}^2 = 0.93$ $1.0 \pm 0.02 \times 10^{-4} \text{ r}^2 = 0.94$	$5.4 \pm 0.44 \times 10^{-6} \text{ r}^2 = 0.98$ $5.3 \pm 0.43 \times 10^{-6} \text{ r}^2 = 0.94$ $3.6 \pm 0.29 \times 10^{-6} \text{ r}^2 = 0.92$

# **5.2.2.1 Non-Contaminated Moisturized Soils**

Table 5.2 and Table 5.3 presents the first order rate and second order rate constants, respectively. The non-contaminated, moisturized Metea demonstrated better r<sup>2</sup> values using second order kinetics for Region I. For Region II, first order and second order did not show significant differences in the r<sup>2</sup> values.

Table 5.2 The first order reaction rate constants for 5% and 10% moisture, non-contaminated Metea soil at 25°C (values reported at 95% C.I.)

Sample	First order Region I k <sub>1</sub>	First order Region II
	(s) <sup>-1</sup>	(s) <sup>-1</sup>
5%,clean Metea pH 2 5%,clean Metea pH 6 5%,clean Metea pH 8	$5.4 \pm 0.41 \times 10^{-4}  r^2 = 0.93$ $8.9 \pm 0.07 \times 10^{-4}  r^2 = 0.85$ $5.5 \pm 0.01 \times 10^{-4}  r^2 = 0.85$	$6.8 \pm 0.04 \times 10^{-5}$ r <sup>2</sup> = 0.97
10%,clean Metea pH 2 10%,clean Metea pH 6 10%,clean Metea pH 8	$6.0 \pm 0.36 \times 10^{-4} \text{ r}^2 = 0.90$ $3.8 \pm 0.11 \times 10^{-4} \text{ r}^2 = 0.64$ $5.1 \pm 0.22 \times 10^{-4} \text{ r}^2 = 0.75$	$6.7 \pm 0.14 \times 10^{-5}$ $r^2 = 0.91$ $3.3 \pm 0.11 \times 10^{-5}$ $r^2 = 0.86$ $6.2 \pm 0.22 \times 10^{-5}$ $r^2 = 0.89$

Table 5.3 The second order reaction rate constant for 5% and 10% moisture, non-contaminated Metea soil (values reported at 95% C.I.)

Sample	Second order Region I k <sub>2</sub> (s·mg O₃/kg soil) <sup>-1</sup>	Second order Region II k₂ (s·mg O₃/kg soil) <sup>-1</sup>
5%,clean Metea pH 2	$1.2 \pm 0.20 \times 10^{-5}$ $r^2 = 0.94$	$1.2 \pm 0.12 \times 10^{-5}$ r <sup>2</sup> = 0.94
5%,clean Metea pH 6	$1.5 \pm 0.52 \times 10^{-5}$ $r^2 = 0.97$	$3.8 \pm 0.09 \times 10^{-6}$ r <sup>2</sup> = 0.92
5%,clean Metea pH 8	$2.1 \pm 0.05 \times 10^{-5}$ $r^2 = 0.98$	$2.1 \pm 0.17 \times 10^{-5}$ r <sup>2</sup> = 0.98
10%,clean Metea pH 2	$1.7 \pm 0.05 \times 10^{-5} \text{ r}^2 = 0.99$	$6.5 \pm 0.52 \times 10^{-6}$ $r^2 = 0.94$
10%,clean Metea pH 6	$1.3 \pm 0.28 \times 10^{-5} \text{ r}^2 = 0.93$	$2.3 \pm 0.19 \times 10^{-6}$ $r^2 = 0.92$
10%,clean Metea pH 8	$2.7 \pm 0.03 \times 10^{-5} \text{ r}^2 = 0.94$	$6.5 \pm 0.58 \times 10^{-6}$ $r^2 = 0.82$

# 5.2.2 Reaction kinetics for pyrene contaminated soils at 25°C

Table 5.4 summarizes the first order reaction rate constants for pyrene-contaminated soil. First order kinetics offers an acceptable fit for the experimental data  $(r^2 = 0.82 - 0.97)$ . Two regions were observed for the moisturized soils and for dry, pH 6 soil.

Using second order kinetics, the linear representation of the data improved (Table 5.5). In the pH 2 soils, the two regions present in the first-order plots became one region in a second order plot of the data. For example, in the moisturized soils, two regions were present in the first-order reaction plot for 5% moisture, pH 2 soil (Figure 5.3(a)). A second order plot of the data, however, does not show the two-phase region (Figure 5.3(b)). The 10% moisture, pH 2 soil also demonstrates this difference in first order (Figure 5.4(a)) and second order (Figure 5.4(b)). Table 5.5 lists the reaction rate constants for second order.

Table 5.4 First order ozone decomposition rates for pyrene contaminated soils at 25°C (values reported at 95% C.I.).

Sample	First order Region I k <sub>1</sub> (s) <sup>-1</sup>	First order Region II k <sub>1</sub> (s) <sup>-1</sup>
Dry, pH 2, 25°C Dry, pH 6, 25°C Dry, pH 8, 25°C 5%, pH 2,25 °C 5%, pH 6, 25°C 5%, pH 8, 25°C 10%, pH 2, 25°C	$1.8 \pm 0.16 \times 10^{-4}  r^2 = 0.95$ $5.4 \pm 0.45 \times 10^{-4}  r^2 = 0.82$ $9.3 \pm 0.27 \times 10^{-4}  r^2 = 0.95$ $5.8 \pm 0.75 \times 10^{-4}  r^2 = 0.99$ $6.0 \pm 0.50 \times 10^{-4}  r^2 = 0.95$ $3.8 \pm 0.13 \times 10^{-4}  r^2 = 0.93$ $3.8 \pm 0.51 \times 10^{-4}  r^2 = 0.99$	$6.9 \pm 0.20 \times 10^{-6}  r^{2} = 0.97$ $\star$ $1.2 \pm 0.05 \times 10^{-4}  r^{2} = 0.89$ $6.8 \pm 0.26 \times 10^{-5}  r^{2} = 0.90$ $4.7 \pm 0.03 \times 10^{-5}  r^{2} = 0.88$
10%, pH 6, 25°C 10%, pH 8, 25°C	$3.7 \pm 0.14 \times 10^{-4}$ $r^2 = 0.99$ $3.4 \pm 0.39 \times 10^{-4}$ $r^2 = 0.94$	

<sup>\*</sup>Only one region observed

Table 5.5 Second order ozone decomposition rates for pyrene contaminated soils at 25°C (values reported at 95% C.I.).

Sample	Second order Region I k <sub>2</sub> (s·mg O <sub>3</sub> /kg soil) <sup>-1</sup>	Second order Region II k <sub>2</sub> (s·mg O <sub>3</sub> /kg soil) <sup>-1</sup>
Dry, pH 2, 25°C Dry, pH 6, 25°C Dry, pH 8, 25°C	1.1 $\pm$ 0.09 x 10 <sup>-5</sup> r <sup>2</sup> = 0.98 9.4 $\pm$ 0.77 x 10 <sup>-6</sup> r <sup>2</sup> = 0.95 3.6 $\pm$ 0.29 x 10 <sup>-6</sup> r <sup>2</sup> = 0.98	$4.2 \pm 0.33 \times 10^{-6} \text{ r}^2 = 0.97$
5%, pH 2,25 °C 5%, pH 6, 25°C 5%, pH 8, 25°C	$1.9 \pm 0.15 \times 10^{-5}  r^2 = 0.98$ $1.4 \pm 0.02 \times 10^{-5}  r^2 = 0.99$ $1.1 \pm 0.1 \times 10^{-5}  r^2 = 0.98$	$5.1 \pm 0.07 \times 10^{-6}$ $r^2 = 0.95$ $3.0 \pm 0.24 \times 10^{-6}$ $r^2 = 0.88$
10%, pH 2, 25°C 10%, pH 6, 25°C 10%, pH 8, 25°C	1.4 ± 0.11 x 10 <sup>-5</sup> $r^2 = 0.99$ 8.8 ± 0.71 x 10 <sup>-6</sup> $r^2 = 0.99$ 6.1 ± 0.49 x 10 <sup>-6</sup> $r^2 = 0.97$	t $5.0 \pm 0.4 \times 10^{-6}$ $r^2 = 0.97$ $1.7 \pm 0.14 \times 10^{-6}$ $r^2 = 0.98$

<sup>\*</sup> Only one region observed

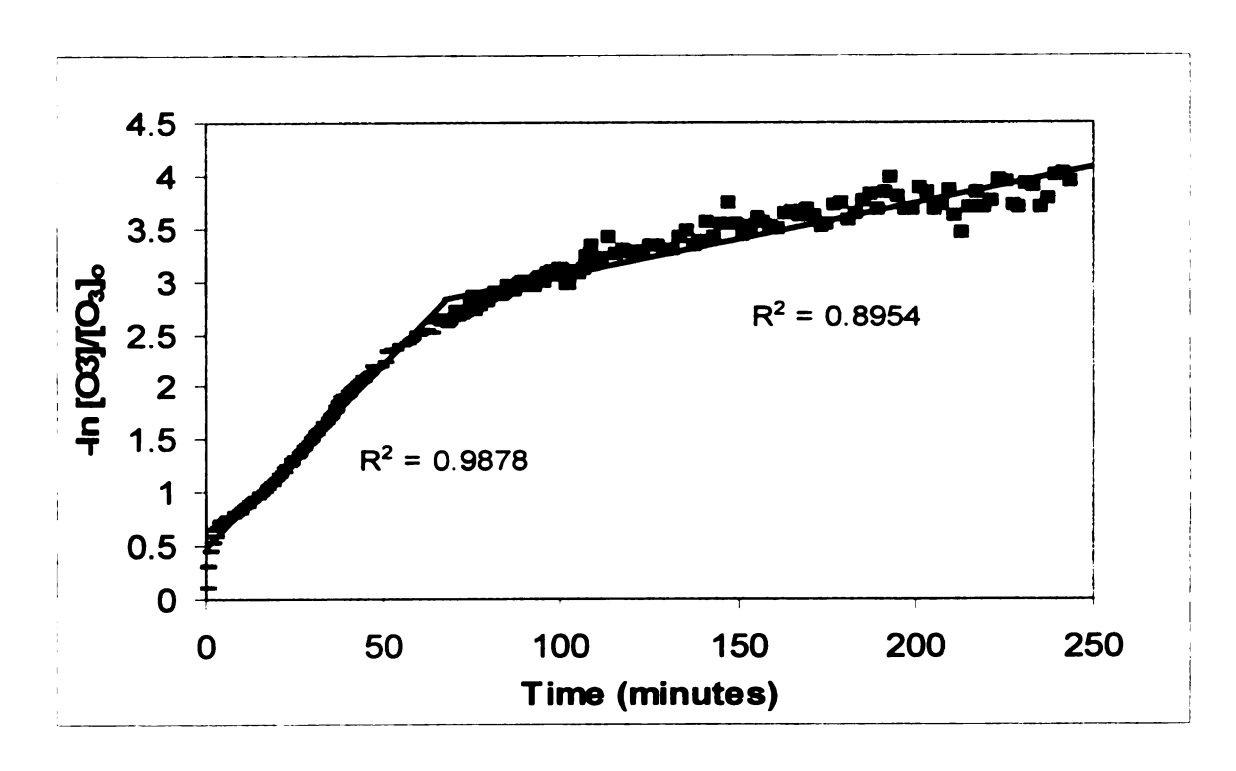


Figure 5.3 (a). First-order plot of 5% moisturized soil at pH 2 at 25°C:: Region I;

Region II

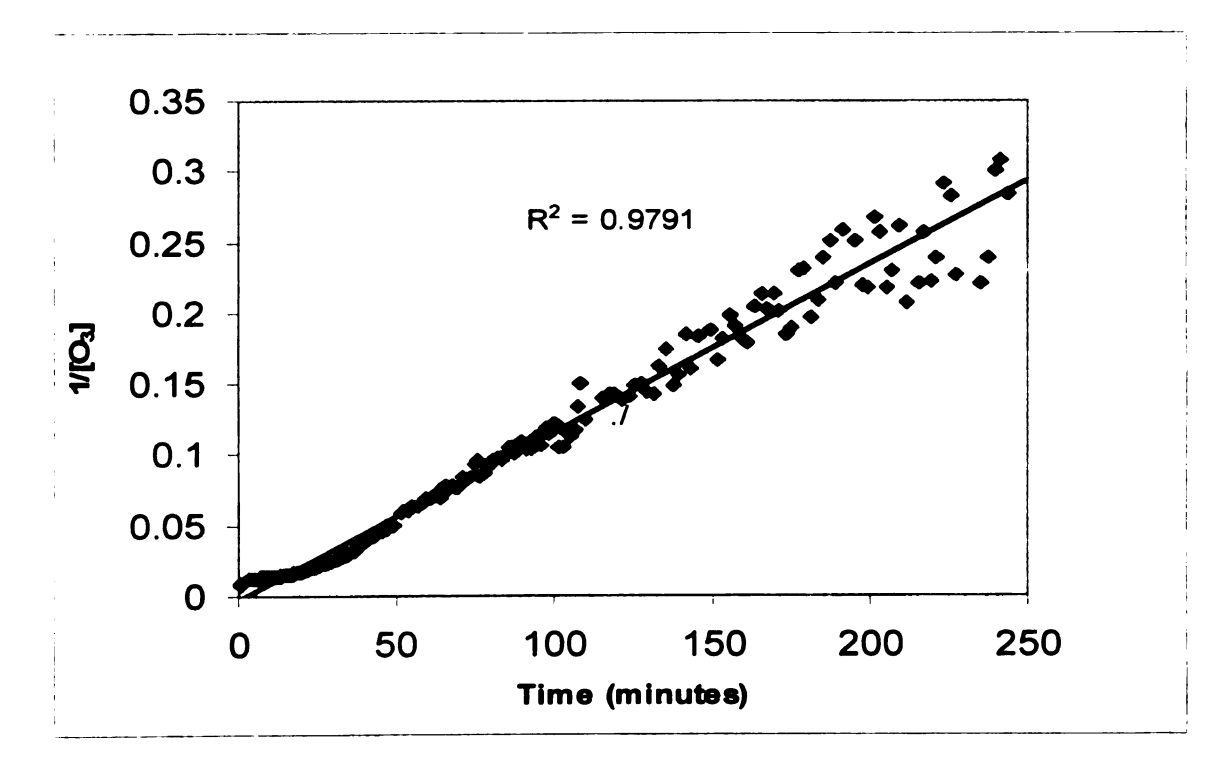


Figure 5.3(b). Second-order plot of 5% moisturized soil at pH 2 at 25°C.

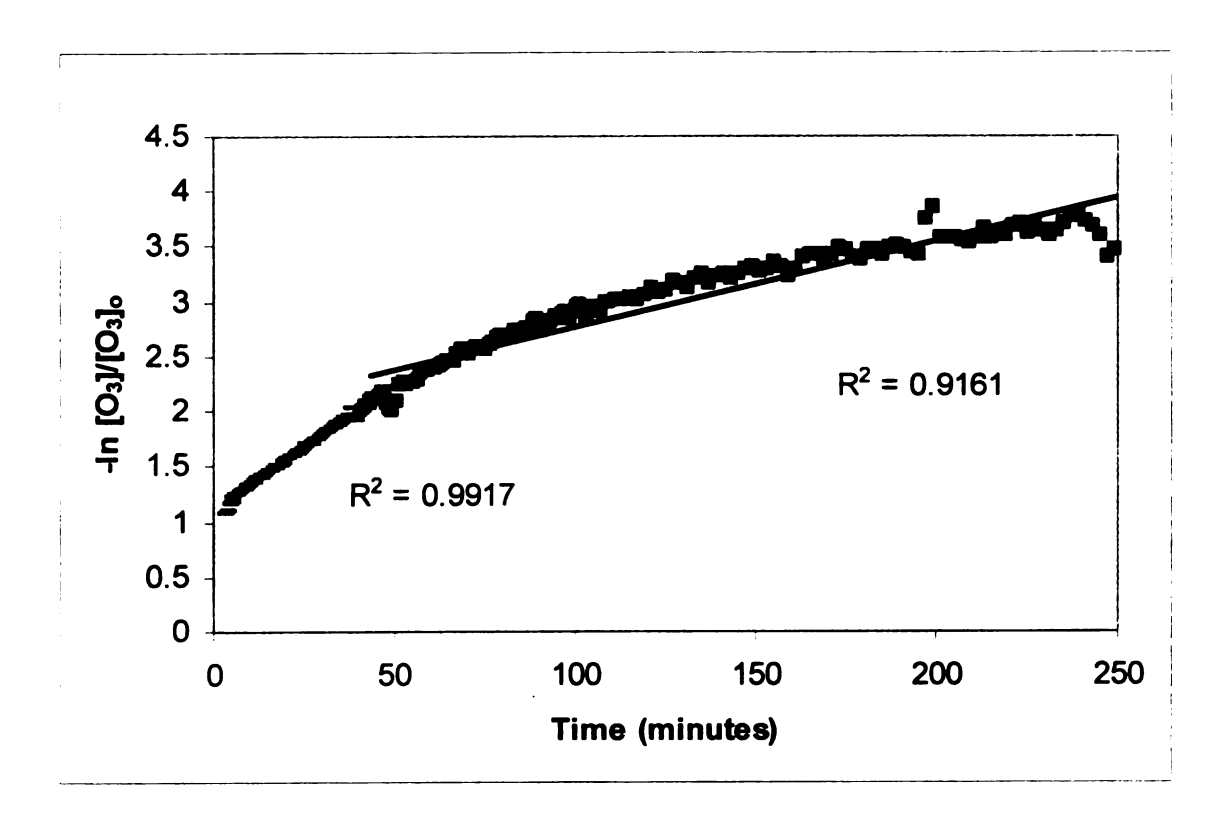


Figure 5.4(a). First-order plot of 10% moisturized soil at pH 2 at 25°C.

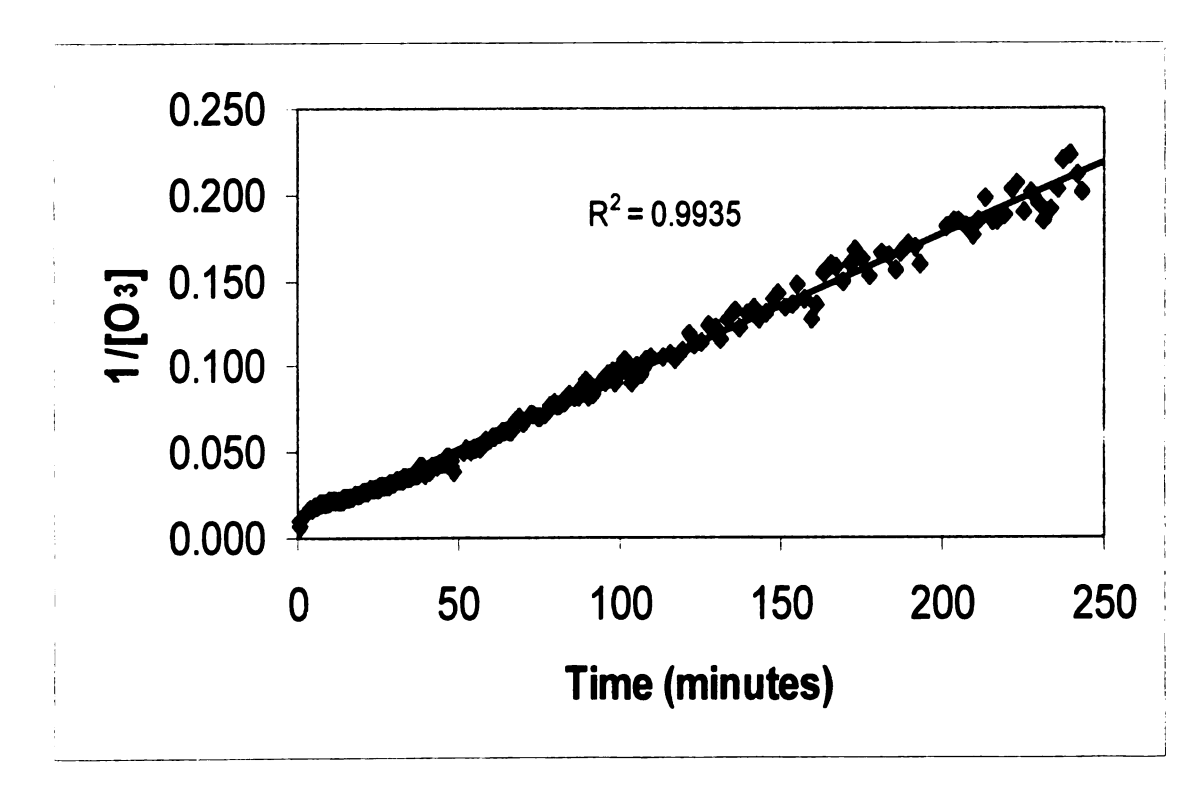


Figure 5.4(b). Second-order plot of 10% moisturized soil at pH 2 at 25°C.

Figure 5.5 lists the pseudo-first order rate constants  $(k_I)$  in order from smallest to the largest. Evaluation of the first order reaction rate constants for the dry soils shows that the pseudo-first order rate constant  $(k_I)$  increased as the pH increased. In the dry soils, the value for  $k'_I$  pH 2 <  $k'_I$  pH 6 <  $k'_I$  pH 8. In the 10% moisturized soils, the opposite observation is seen where  $k'_I$  decreased as the pH increased. The rate constants for 10% moisture soil pH 2, pH 6, and pH 8 were statistically similar. The same observation can be made for the 5%, pH 2 and pH 6 soils. For the 5% moisturized soil, the  $k_I$  value is such that pH 8 < pH 2 < pH 6.

	FIRST ORDER RATE CONSTANT k <sub>1</sub> (s <sup>-1</sup> )
Dry, pH 8 (25°C)	9.3 x 10 <sup>-4</sup> ↑
5%, pH 6 (25°C)	6.0 x 10 <sup>-4</sup>
5%, pH 2 (25°C)	5.8 x 10 <sup>-4</sup>
Dry, pH 6 (25°C)	5.4 x 10 <sup>-4</sup>
10%, pH 2 (25°C) ; 5%, pH 8 (25°C	) 3.8 x 10 <sup>-4</sup>
10%, pH 6 (25°C)	3.7 x 10 <sup>-4</sup>
10%, pH 8 (25°C)	3.4 x 10 <sup>-4</sup>
Dry, pH 2 (25°C)	1.8 x 10 <sup>-4</sup>

Figure 5.5 The first order rate constants listed in increasing order for Metea soil ozonated at 25°C.

Figure 5.6 lists the second order rate constants  $(k_2)$  in increasing order. A notable trend seen in the second order rate constants is that  $k_2$  decreased as the pH increased for all of the soil conditions. For example in the 5% moisture soils, the rate constants are such that  $k_2$  pH 2 >  $k_2$  pH 6 <  $k_2$  pH 8. This observation is also consistent for the dry and 10% moisture soils.

	SECOND ORDER RATE CONSTANT k <sub>2</sub> (s·mg O <sub>3</sub> /kg soil) <sup>-1</sup>
5%, pH 2 (25°C)	1.9 x 10 <sup>-5</sup>
5%, pH 6 (25°C) ; 10%, pH 2 (25°C)	1.4 x 10 <sup>-5</sup>
5%, pH 8 (25°C) ; Dry, pH 2 (25°C)	1.1 x 10 <sup>-5</sup>
Dry, pH 6 (25°C)	9.4 x 10 <sup>-6</sup>
10%, pH 6 (25°C)	8.8 x 10 <sup>-6</sup>
10%, pH 8 (25°C)	6.1 x 10 <sup>-6</sup>
Dry, pH 8 (25°C)	3.6 x 10 <sup>-6</sup>

Figure 5.6 The second order rate constants listed in increasing order for Metea soil ozonated at 25°C.

## 5.2.3 Reaction kinetics for ozonation at 13°C in pyrene contaminated soils

Table 5.6 and Table 5.7 lists the first order and second order rate constants for ozonation at the colder temperature. The second order plots appear to better represent the kinetics for the experiments except for the 10% (pH 8) soil. In the 10% (pH 8) soil, first-order kinetics appeared to result in a better linear representation of the data. Figure 5.7(a) and 5.7(b) show the first order versus second order plots for 10% moisture, pH 8 soil.

Table 5.6 First order Reaction rate constants for 13°C temperature experiments (values reported at 95% C.I.)

Sample	First orde Region k <sub>1</sub> (s) <sup>-1</sup>		First orde Region I k <sub>1</sub> (s) <sup>-1</sup>	
Dry, pH 2, 13°C Dry, pH 6, 13°C Dry, pH 8, 13°C 5%, pH 2, 13°C 5%, pH 6, 13°C 5%, pH 8, 13°C 10%, pH 2, 13°C 10%, pH 6, 13°C 10%, pH 6, 13°C	$2.0 \pm 0.35 \times 10^{-4}$ $1.7 \pm 0.13 \times 10^{-4}$ $3.4 \pm 0.04 \times 10^{-4}$ $2.3 \pm 0.33 \times 10^{-4}$ $1.6 \pm 0.06 \times 10^{-4}$ $1.6 \pm 0.48 \times 10^{-4}$ $3.2 \pm 0.17 \times 10^{-4}$ $1.8 \pm 0.71 \times 10^{-4}$ $4.0 \pm 0.22 \times 10^{-3}$	$r^{2} = 0.95$ $r^{2} = 0.64$ $r^{2} = 0.97$ $r^{2} = 0.95$ $r^{2} = 0.93$ $r^{2} = 0.97$ $r^{2} = 0.94$	$3.3 \pm 0.51 \times 10^{-5}$ $3.3 \pm 0.38 \times 10^{-6}$ $5.8 \pm 0.05 \times 10^{-5}$ $2.1 \pm 0.22 \times 10^{-4}$	$r^2 = 0.92$ $r^2 = 0.92$

<sup>\*</sup> Only one region observed

Table 5.7 Second order reaction rate constants for 13°C temperature experiments (values reported at 95% C.I.)

Sample	Second order Region I k <sub>2</sub> (s·mg O <sub>3</sub> /kg soil) <sup>-1</sup>		Second order Region II k <sub>2</sub> (s·mg O₃/kg soil) <sup>-1</sup>
Dry, pH 2, 13°C Dry, pH 6, 13°C Dry, pH 8, 13°C 5%, pH 2, 13°C 5%, pH 6, 13°C 5%, pH 8, 13°C 10%, pH 2, 13°C 10%, pH 6, 13°C 10%, pH 6, 13°C	$1.6 \pm 0.14 \times 10^{-5}$ $7.4 \pm 0.61 \times 10^{-6}$ $7.2 \pm 0.41 \times 10^{-6}$ $1.6 \pm 0.04 \times 10^{-5}$ $8.2 \pm 0.1 \times 10^{-6}$ $8.0 \pm 0.2 \times 10^{-6}$ $8.4 \pm 0.68 \times 10^{-6}$ $8.7 \pm 0.71 \times 10^{-6}$ $7.0 \pm 0.57 \times 10^{-6}$	$r^{2} = 0.98$ $r^{2} = 0.96$ $r^{2} = 0.95$ $r^{2} = 0.95$ $r^{2} = 0.98$ $r^{2} = 0.98$ $r^{2} = 0.98$	*  *  4.2 ± 0.34 × 10 <sup>-6</sup> $r^2 = 0.93$ 1.9 ± 0.15 × 10 <sup>-5</sup> $r^2 = 0.92$

<sup>\*</sup>Only one region observed

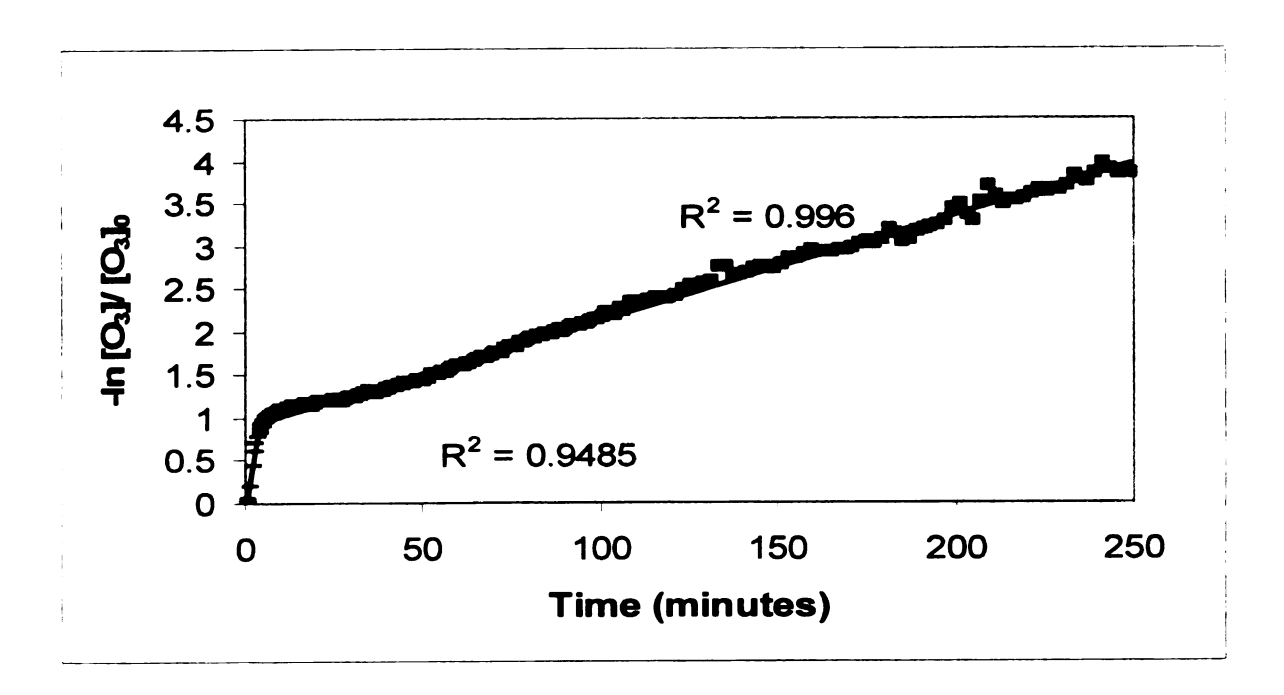


Figure 5.7(a). First order plot for 10% moisture soil, pH 8 at 13°C.

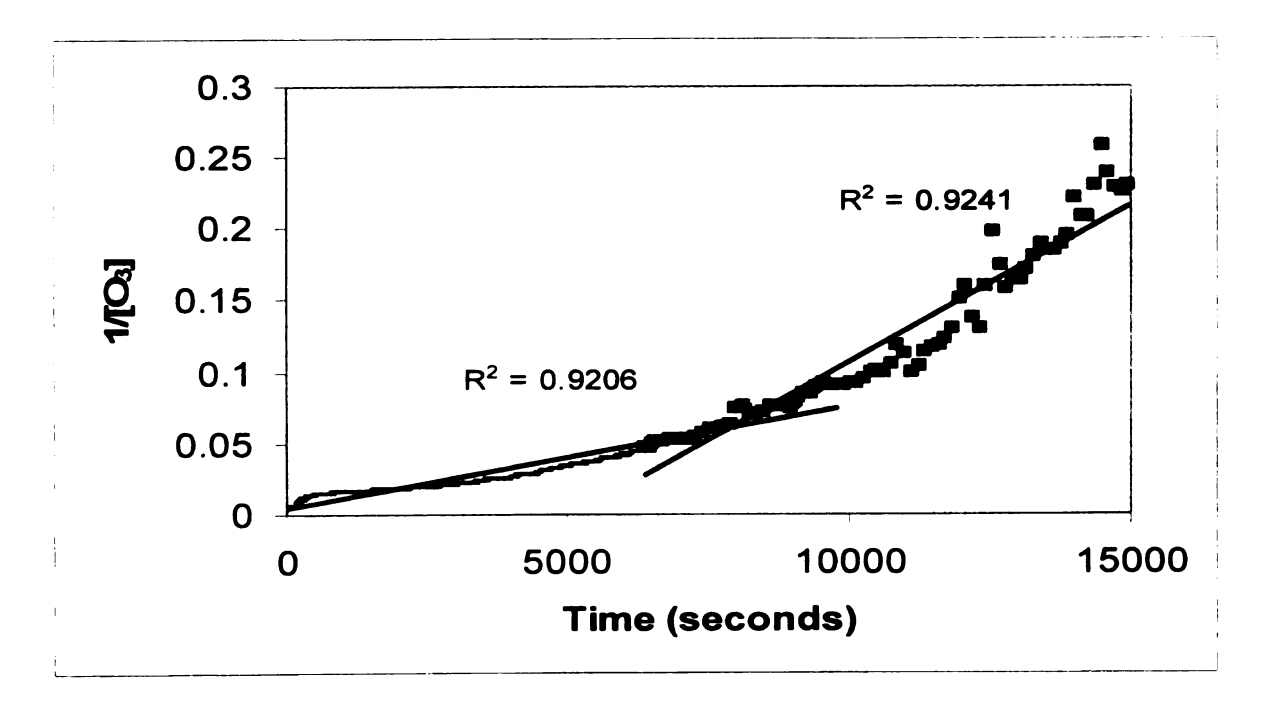


Figure 5.7(b). Second order plot for 10% moisture soil, pH 8 at 13°C: Region I;

Region II.

Figure 5.8 lists the first order rate constants in increasing order. At 13°C, the range for the rate constant  $(k_I)$  was from  $1.6 \times 10^{-4} - 4.0 \times 10^{-3}$ . The 5% (pH 6 and pH 8), dry (pH 6), and 10% (pH 6) the rate constants were statistically similar. The  $k_I$  values did not appear to follow a trend of increasing or decreasing with respect to changes in pH. For the dry soil at 13°C, the  $k_I$  values were pH 6 < pH 2 < pH 8. In the 5% moisture soil,  $k_I$  pH 8 =  $k_I$  pH 6 < pH 2. For the 10% moisture soils, the order for  $k_I$  was pH 6 < pH 2 < pH 8.

	FIRST ORDER RATE CONSTANT k <sub>1</sub> (s <sup>-1</sup> )
10%, pH 8 (13°C)	4.0 x 10 <sup>-3</sup>
Dry, pH 8 (13°C)	3.4 x 10 <sup>-4</sup>
10%, pH 2 (13°C)	3.2 x 10 <sup>-4</sup>
5%, pH 2(13°C)	2.3 x 10 <sup>-4</sup>
Dry, pH 2 (13°C)	2.0 x 10 <sup>-4</sup>
10%, pH 6 (13°C)	1.8 x 10 <sup>-4</sup>
Dry, pH 6 (13°C)	1.7 x 10 <sup>-4</sup>
5%, pH 8 (13°C) ; 5%, pH 6 (13°C)	1.6 x 10 <sup>-4</sup>

Figure 5.8 The first order rate constants listed in increasing order for Metea soil ozonated at 13°C.

Figure 5.9 lists the second order rate constants in increasing order. For the dry and 5% moisture soils,  $k_2$  decreased as the pH increased. This observation is consistent with the results seen in the 25°C experiments. In the 10% moisture soils, the order for the second order rate constants was pH 8 < pH 2 < pH 6.

	SECOND ORDER RATE CONSTANT $k_2$ (s·mg O <sub>3</sub> /kg soil) <sup>-1</sup>	
	<b>†</b>	
5%, pH 2 (13°C) ; Dry, pH 2 (13°C)	1.6 x 10 <sup>-5</sup>	
10%, pH 6 (13°C)	8.7 x 10 <sup>-6</sup>	
10%, pH 2 (13°C)	8.4 x 10 <sup>-6</sup>	
5%, pH 6 (13°C)	8.2 x 10 <sup>-6</sup>	
5%, pH 8 (13°C)	8.0 x 10 <sup>-6</sup>	
Dry, pH 6 (13°C)	7.4 x 10 <sup>-6</sup>	
Dry, pH 8 (13°C)	7.2 x 10 <sup>-6</sup>	
10%, pH 8 (13°C)	7.0 x 10 <sup>-6</sup>	

Figure 5.9 The second order rate constants listed in increasing order for Metea soil ozonated at 13°C.

# 5.2.4 Reaction kinetics Ozonation in Aged soil

Figure 5.10 presents a comparison of first order rate constants for the aged soils and the short-term contamination soils. In both the aged soils and the short-term soils, the  $k_l$  value increased as the pH increased.

	FIRST ORDER RATE CONSTANT k <sub>1</sub> (s <sup>-1</sup> )
Dry, pH 8 (25°C)	9.3 x 10 <sup>-4</sup> ♠
Dry, pH 8 Aged (25°C)	7.9 x 10 <sup>-4</sup>
Dry, pH 6 Aged (25°C)	5.7 x 10 <sup>-4</sup>
Dry, pH 6 (25°C)	5.4 x 10 <sup>-4</sup>
Dry, pH 2 (25°C)	1.8 x 10 <sup>-4</sup>
Dry, pH 2 Aged (25°C)	1.1 x 10 <sup>-4</sup>

Figure 5.10 Comparison of the rate constants for aged soils and short-term contaminated soils at 25°C.

For the second order analysis, however, the reaction rates did not significantly improve for the linear regression compared to the first order  $r^2$  values (Table 5.8). This result might indicate that first order kinetics describes the reaction occurring in the aged soils. Figure 5.11 compares the second order rate constants for the aged soil and the short-term contaminant soils. The data plotted using second order did not appear to follow the trends seen in the previous second order analyses. For the aged soils, the order for the rate constants was pH 2 < pH 8 < pH 6.

	SECOND ORDER RATE CONSTANT k <sub>2</sub> (s·mg O <sub>3</sub> /kg soil) <sup>-1</sup>	
	(cg cgg cc)	
Dry, pH 2 (25°C)	1.1 x 10 <sup>-5</sup>	
Dry, pH 6 (25°C)	9.4 x 10 <sup>-6</sup>	
Dry, pH 6 Aged (25°C)	8.1 x 10 <sup>-6</sup>	
Dry, pH 8 Aged (25°C)	6.7 x 10 <sup>-6</sup>	
Dry, pH 2 Aged (25°C)	5.8 x 10 <sup>-6</sup>	
Dry, pH 8 (25°C)	3.6 x 10 <sup>-6</sup>	

Figure 5.11 Comparison of the rate constants for aged soils and short-term contaminated soils at 25°C.

Table 5.8 Comparison of first order rate constants and second order rate constants for ozonation in Metea soil aged for 6 months (values reported at 95% C.I.)

Sample	First order Region I k (s) <sup>-1</sup>	First order Region II k (s) <sup>-1</sup>
Dry, pH 2 Dry, pH 6 Dry, pH 8	$1.1 \pm 0.29 \times 10^{-4}  r^2 = 0.91$ $5.7 \pm 0.07 \times 10^{-4}  r^2 = 0.88$ $7.9 \pm 0.40 \times 10^{-4}  r^2 = 0.96$	9.7 ± 0.64 x 10 <sup>-5</sup> $r^2$ = 0.99 7.7 ± 0.73 x 10 <sup>-5</sup> $r^2$ = 0.94
	Second order Region I k (s·mg O <sub>3</sub> /kg soil) <sup>-1</sup>	Second Order Region II k (s·mg O <sub>3</sub> /kg soil) <sup>-1</sup>
Dry, pH 2 Dry, pH 6 Dry, pH 8	$5.8 \pm 0.09 \times 10^{-6}$ $r^2 = 0.97$ $8.1 \pm 0.13 \times 10^{-6}$ $r^2 = 0.98$ $6.7 \pm 0.11 \times 10^{-6}$ $r^2 = 0.96$	$^{*}$ $^{*}$ $^{*}$ $^{2.4 \pm 0.4 \times 10^{-4}}$ $r^{2} = 0.97$

<sup>\*</sup>Only one region detected

#### 5.3 Discussion of Reaction Kinetics and Introduction of the Model

The experimental data collected for this project could be represented using first order kinetics. The pseudo-first order reaction rate constants in the Metea soil are consistent with the values reported by Day (1994). The presence of the two regions is also consistent with previous studies and demonstrates the complexity in evaluating ozone decomposition kinetics in contaminated soil [2 - 6].

The improvement in the linear representation of the data using pseudo second order proves interesting. It is unknown as to why using second order improved the correlation coefficients for r<sup>2</sup>. In literature, Gurol et al. [7] also observed that ozone decomposed by a second-order reaction with respect to ozone concentration. In aqueous system batch experiments, distilled and deionized water was ozonated at 20°C in the pH

range of 2 - 10. In Gurol et al. [7], the kinetics for ozone decomposition in the system could be expressed by the relationship

$$-d[O_3]/dt = k[O_3]^2[OH^-]^{0.55}$$

where [OH] is the hydroxide ion concentration of the solution. For the experiments, second order kinetics represented the data much better than first order and 3/2 order kinetics.

### 5.3.1 Section 2: Modeling

The data in this may study support the findings of Hsu [5] where the data phenanthrene ozonation in soil did not fit simple first order kinetics. Hsu and Masten [1] theorized that reactions in the soil could occur either in series or in parallel based on surface area coverage of the contaminant of soil particles. Hsu and Masten [1] observed that when the soil was completely coated with phenanthrene, the reaction between phenanthrene and ozone predominated until the concentration of phenanthrene reached less than 40 ppm phenanthrene. Once the phenanthrene concentration was reduced to 40 ppm phenanthrene, the ozone/organic matter reaction began. Parallel reactions for ozone/phenanthrene and ozone/organic matter were thought to occur if the phenanthrene unevenly coated the soil surface. In the Hsu and Masten study, two distinct kinetic regions were also observed.

Hsu and Masten [1] presented a mathematical model describing the reactions of ozone/ soil organic matter and ozone/ PAH contaminant in soil. In Hsu and Masten [1],

the rate expression for the gaseous ozone reaction with organic matter and phenanthrene was defined as,

$$\frac{\partial [\rho_{o_3}]}{\partial t} = -v_z \frac{\partial [\rho_{o_3}]}{\partial z} - \left(\frac{\rho_b}{ns_a}\right) [\rho_{o_3}] (k_{om}[OM] + k_c[C])$$
 (Eqn. 5.6)

where  $\rho_{O3}$  = gaseous ozone mass density (mg/L), t = time (s),  $\nu_z$  = gas velocity (cm/s),  $\rho_b$  = bulk density of soil, n = total porosity of soil,  $s_a$  = degree of gas saturation,  $k_{om}$  = second order reaction rate constant (s<sup>-1</sup> · (mg organic matter/kg soil)<sup>-1</sup> · (L gas/kg soil), [OM] = soil organic matter concentration (mg/kg),  $k_c$  = second-order rate constant for the reaction of gaseous ozone and phenanthrene in soil (s<sup>-1</sup>· (mg phenanthrene/kg soil)<sup>-1</sup> · (L gas/kg soil)), and C = phenanthrene concentration in soil (mg phenanthrene/kg soil).

Hsu and Masten [1] predicted that the distribution of phenanthrene in the soil would affect the reaction and considered two possible reaction mechanisms. The first reaction considered the possibility that phenanthrene completely coated the soil particles. In this case, the reaction between phenanthrene and ozone would predominate during the early stages of the reaction. Once the phenanthrene reached a concentration of 40 ppm, the ozone and soil organic matter reaction would proceed. The result would be two sequential reactions occurring within the system. The value for k<sub>om</sub> would be zero until the point where organic matter would start to react with ozone. The second possible mechanism considered the case where phenanthrene only partially coated the soil surface. In this case, the reactions of ozone/ phenanthrene and ozone/ soil organic matter would occur in parallel, both starting at time zero.

Assuming that soil organic matter is immobile, the rate expression for organic matter was written as,

$$\frac{\partial OM}{\partial t} = \left(\frac{k_{om}}{\zeta_{om}}\right) \rho_{O_3}[OM]$$
 (Eqn. 5.7)

where  $\zeta_{om}$  = stoichiometric coefficient (g of ozone/g of soil organic matter).

The rate expression describing the reaction of ozone with a contaminant in could be written as,

$$\frac{\partial C}{\partial t} = \left(\frac{k_c}{\zeta_c}\right) \rho_{o_3} C \tag{Eqn. 5.8}$$

where  $\zeta_c$  = stiochiometric coefficient (g of ozone/g of phenanthrene).

The pressure decrease along the flow path of the column would affect ozone gas velocity and mass concentration. The equation was represented as,

$$P(z) = \left[ P^{2}_{in} - \frac{P^{2}_{in} - P^{2}_{out}}{L} z \right]^{1/2}$$
 (Eqn. 5.9)

where P = gas pressure (cm  $H_2O$ );  $P_{in}$  and  $P_{atm}$  are the inlet and outlet gas pressure, respectively; and L = length of the gas flow path (cm). The gas velocity along the flow path could be described as,

$$v(z) = \frac{Kd(P^{2}_{in} - P^{2}_{out})}{2L} \left[ P^{2}_{in} - \frac{P^{2}_{in} - P^{2}_{out}}{L} z \right]^{-1/2}$$
 (Eqn. 5.10)

where  $K_d$  = gas conductivity (cm/s). Therefore, the correction for the ozone mass concentration becomes,

$$\rho_{O_3}|_P = \rho_{O_3}|_{atm} \left(\frac{P}{P_{atm}}\right)$$
 (Eqn. 5.11)

where  $P_{atm} = atmospheric pressure (1033.6 cm H<sub>2</sub>O).$ 

Hsu and Masten [1] developed a solution for the gaseous ozone concentration using finite differencing on the mass-balance for gaseous ozone and soil organic matter. Eqns 5.4 and 5.6, thus become,

$$\frac{\rho^{j} o_{3,i+1} - \rho^{j} o_{3,i}}{\Delta t} = -\nu_{z} \frac{\rho^{j+1} o_{3,i} - \rho^{j} o_{3,i}}{\Delta z} - \frac{\rho_{b} k_{om}}{n s_{a}} \rho^{j} o_{3,i} [OM]^{j}_{i}$$
 (Eqn. 5.12)

$$\frac{OM_{i+1}^{j} - OM_{i}^{j}}{\Delta t} = \left(\frac{1}{\zeta_{om}}\right) k_{om} \rho_{o_{3},i} [OM]^{j}_{i}$$
 (Eqn. 5.13)

The model predictions were reported to exhibit a reasonable fit to the experimental data in 10 cm and 30 cm columns. It was observed that the initial unsteady-state conditions for the gas pressure resulted in minor deviations between the simulated and experimental results [1]. Both parallel and series reactions for ozone with soil organic matter and phenanthrene could be simulated using the model.

Kim et al. [8] recently developed three models to described gaseous ozone transport. The work presents an equilibrium model, a kinetic model and a model called the "lump model" which was similar to Hsu and Masten [1]. The Kim lump model and the Hsu model differ in some parameter definitions and the inclusion of the dispersion term. Hsu and Masten [1] explained the ability to omit the dispersion term in the equation based on work by Carberry (1976). The work noted that the dispersion term in a packed-bed reactor was negligible if the ratio of the bed length to the particle diameter is greater than 50. Since the ratio of the bed length for the experiments conducted by Hsu [5] was 10 - 30 cm and the diameter of the largest soil grain was 1.19 mm, the dispersion term was neglected.

In Kim et al. [8], the lump model expressed the gaseous ozone mass balance as

$$\frac{\partial}{\partial t}(ns_aC_0) = \frac{\partial}{\partial z} \left[ D_0 \frac{\partial(ns_aC_0)}{\partial z} \right] - v \frac{\partial(ns_aC_0)}{\partial z} - ns_aC_0(k_{d,1} + k_{s,1}C_s + k_{c,1}C_c) \quad \text{(Eqn. 5.14)}$$

where  $k_{d,1}$  = lumped first order ozone self-decomposition constant;  $k_{s,1}$  = lumped secondorder reaction constant for organic matter; and  $k_{c,1}$  is the lumped second order reaction constant for the contaminant. The mass balance equations for organic matter and the contaminant can be expressed as follows,

$$\frac{\partial(\rho_b C_s)}{\partial t} = -\frac{1}{y_{o,c}} n s_a k_{s,1} C_s C_o$$
 (Eqn. 5.15)

$$\frac{\partial (\rho_b C)_c}{\partial t} = -\frac{1}{\gamma_{o,c}} n s_a k_{c,1} C_c C_o$$
 (Eqn. 5.16)

where  $C_s$  = concentration of organic matter,  $C_o$  = concentration of ozone, and  $C_c$  = concentration of contaminant.

## **Experimental Basis for Modeling**

This phase of the research was designed to test the applicability of the Hsu and Masten model to the experimental data. For the modeling, an attempt was made to construct an ozonation system using a 3.5 foot column and to apply the model to the experimental data. Data from the 15 cm column ozonation experiments were also available to apply the model.

#### 5.3.2 Materials and methods

Soil. Two types of soil were evaluated in the large soil column. Ottawa sand, which contained no organic matter, was the first soil evaluated. The second was Metea soil excavated from the southeast side of Michigan State University (MSU) campus on research farm property. All of the experiments in the smaller column were conducted using Metea soil and the experimental methods are presented in Chapter 2.

Ozonation Experiments. Ozone was generated by dried oxygen electric discharge using a Polymetrics Model T-408 ozone generator (San Jose, CA). The bench scale experiments were conducted in a 2.5 cm (i.d.) x 15 cm reactor. The pilot scale experiments were conducted in a column with dimensions of 2" (i.d.) x 3.5 ft in height. The glass column had ports at 6 inch increments that needed to be sealed to prevent gas leakage. The ports were sealed by first closing the openings using 12 mm Teflon®-lined

aluminum HPLC vial crimp seals. Each seal was then surrounded with a thick layer of parafilm around the crimp top and on the exterior of the port. Finally, PVC pipe end cap fittings were secured to each port. The column successfully passed a leak test when filled with water and allowed to sit overnight.

The flow of ozone into the reactors was regulated at using an Aalborg mass flow meter (Aalborg Instruments & Controls, Inc., Orangeburg, New York). The concentration of ozone in the influent and effluent gas streams was measured spectrophotometrically at 258 nm using an UV-Visible light spectrophotometer (Model 1201, Shimadzu Scientific Instruments, Japan). The absorbance values for ozone converted to the concentration using a molar absorptivity coefficient for ozone of 3000 M<sup>-1</sup> cm<sup>-1</sup> (Bader and Hoigné, 1982). Figure 5.12 shows a schematic of the experimental set-up for the 3.5 foot column. Before entering the soil column, the gas stream was passed through a gas-washing bottle containing deionized water acidified to a pH of 2 using phosphoric acid. This provided a moisturized gas stream and prevented the soil in the columns from drying out. After the ozonation time was completed, helium gas was used to purge ozone from the system. All waste ozone was destroyed in a 2% potassium iodide (KI) solution.

Column Packing. A method combining the recommendations of Dr. Simon Davies [9] and Tim Mayotte [10] was used to pack the column. Column packing is important to prevent channeling through the column, which can distort the performance of the experiments. The column was packed in 1 cm increments by pouring sand into the top of the column. A stream of Helium gas was passed through the bottom of the column (~350 ml/min) during the packing process. A device able to vibrate the column (Hompedics

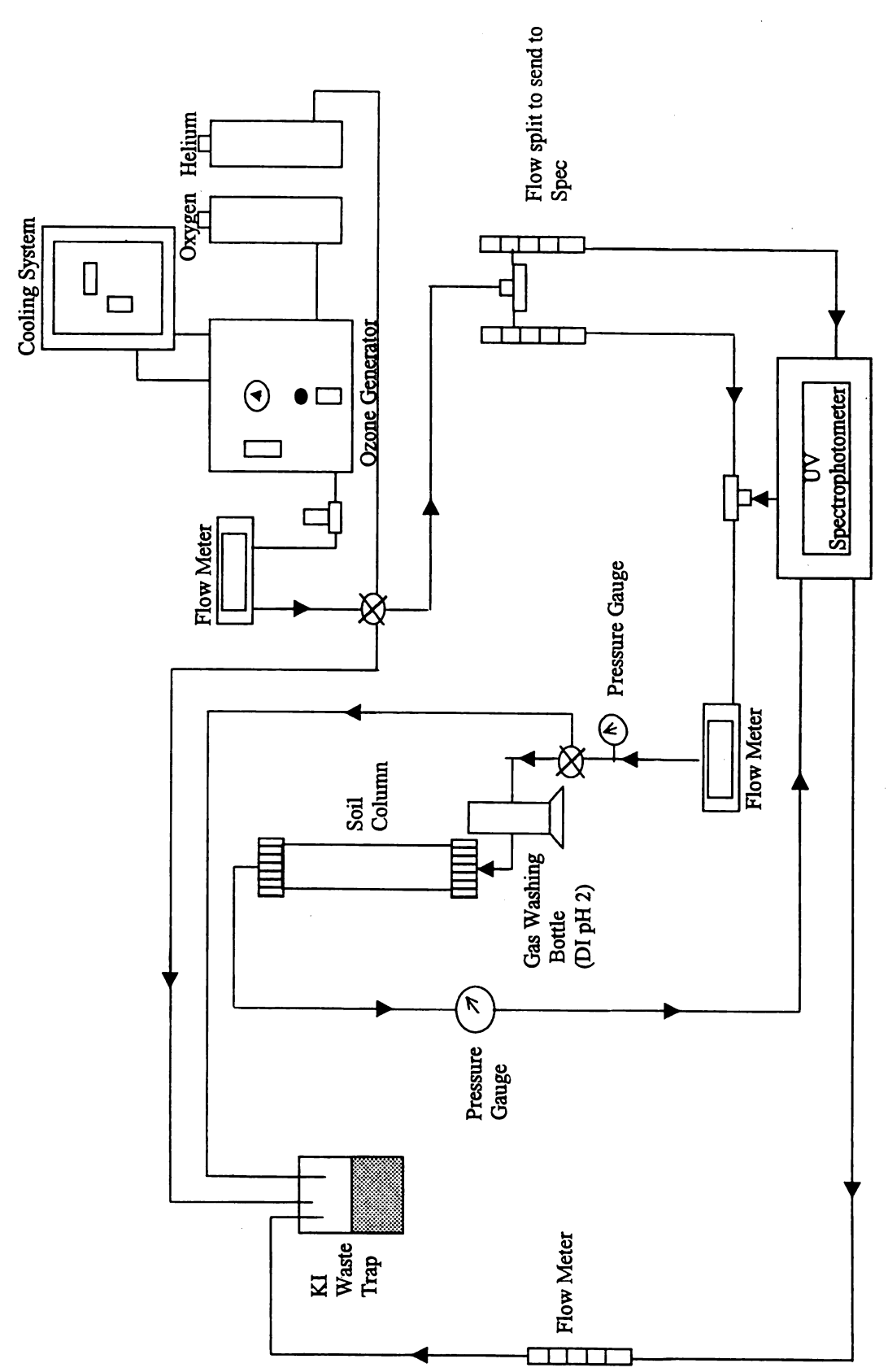


Figure 5.12. Schematic of the ozonation system for the 3.5 foot column

massager) was placed against the wall of the column at the location being filled soil. The massager was then moved up the length of the column as the soil height increased in the column. This procedure was done to help facilitate settling of the soil particles in the column.

Modeling Software. The Excel Solver function and MathCAD 2000 (Mathsoft, Inc. Cambridge, MA) was used to calculate the model parameters and to solve the models. Solutions using finite differencing and a fourth order Runge-Kutta were developed and compared to the experimental data.

### 5.4 Results

## 5.4.1 The 3.5 foot column ozonation Experiments

#### Method 1

The original goal for this portion of the research was to apply the Hsu [5] model to experimental data collected from a 3.5 foot column. Initially, the system was designed identical to the ozonation set-up for the 15 cm column including the use of a gas wash bottle to create a moisturized gas stream. The system run with an empty column produced the BTC presented in Figure 5.13. The tailing point was observed at 50% of the influent concentration. This may have been due to the pressure drop affecting the ozone concentration in the effluent gas stream.

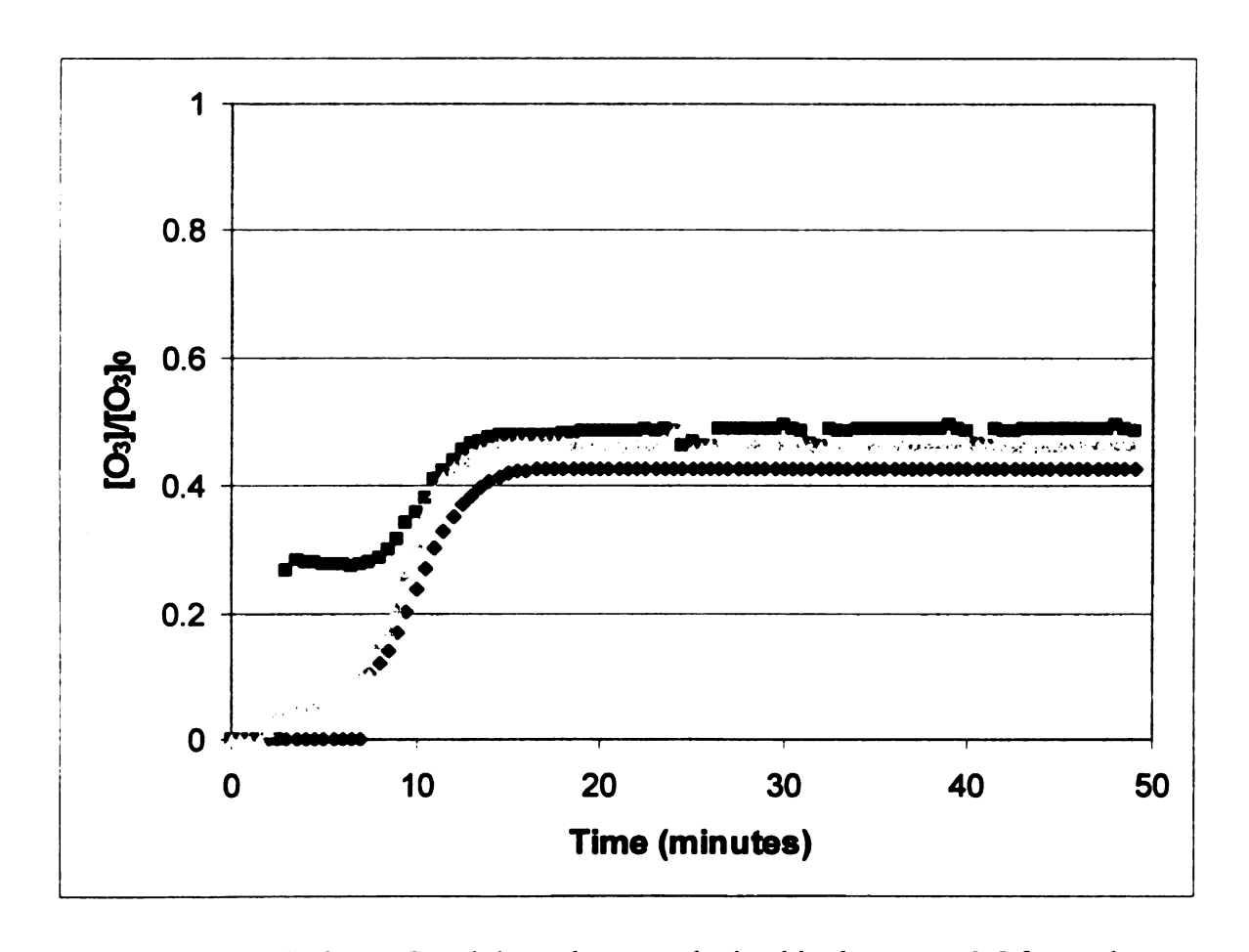


Figure 5.13. Ozone Breakthrough curve obtained in the empty 3.5 foot column

Similar BTCs were obtained in the 3.5 foot column using Ottawa sand. The maximum [O<sub>3</sub>]/[O<sub>3</sub>]<sub>0</sub> reached was 40% of the influent (Figure 5.14). Figure 5.14 compares the BTC for the column filled with 12 inches, 24 inches, and 36 inches of Ottawa sand.

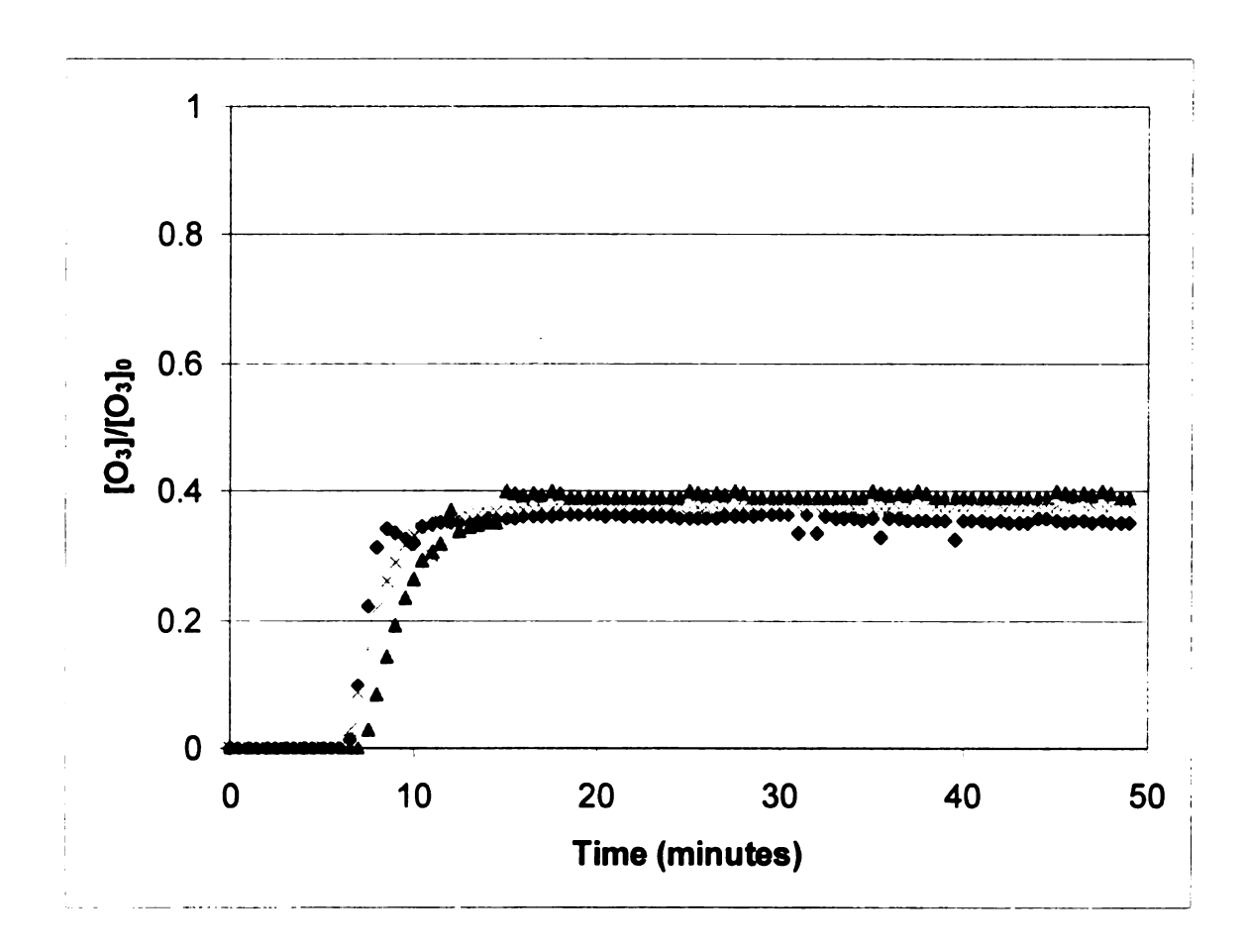


Figure 5.14 Ozone BTC for 3.5 foot column with gas wash bottle. Column filled with 12 inches, × 24 inches, and • 36 inches of Ottawa geologic material.

Using the ozonation system with this set-up, several experiments with Metea soil were attempted without success. The following experiments were conducted:

- 1. Column with 3.5 ft of Metea soil
- 2. Column with 10 cm Metea soil
- 3. Column with 10 cm support layer of Ottawa and 10 cm layer of Metea
- 4. 1 cm support layer of clean, 6 mm glass beads and 10 cm layer of Metea. The glass beads were washed with deionized water followed by washing with acetonitrile. The beads were oven dried and allowed to cool before use.
- 5. Column with 50/50 Ottawa/Metea soil retained by 40 mesh

In these experiments, either no gas flow was detected in the effluent stream or the gas flow was found to decrease until no gas flow was detected during the experiment run. In an effort to improve the system performance, the gas wash bottle was removed to increase the pressure within the system.

#### Method 2

The removal of the gas wash bottle significantly improved the system performance. The BTC for the empty column and the column packed with 42 inches of Ottawa geologic material resulted in a curve that did not demonstrate tailing (Figure 5.15).

The Metea soil experiments, however, continued to exhibit problems with the effluent ozone stream. The column full of Metea resulted in no gas being detected in the effluent stream. A 12 inch layer of Metea initially demonstrated gas breakthrough that stopped in less than 2 minutes. Limited success was obtained initially in the column containing 10 cm of Metea. Ozone breakthrough was detected, however, after 10 - 15 minutes, the ozone breakthrough curve decreased to the point where either no ozone was detected or the gas flow stopped (Figure 5.16).

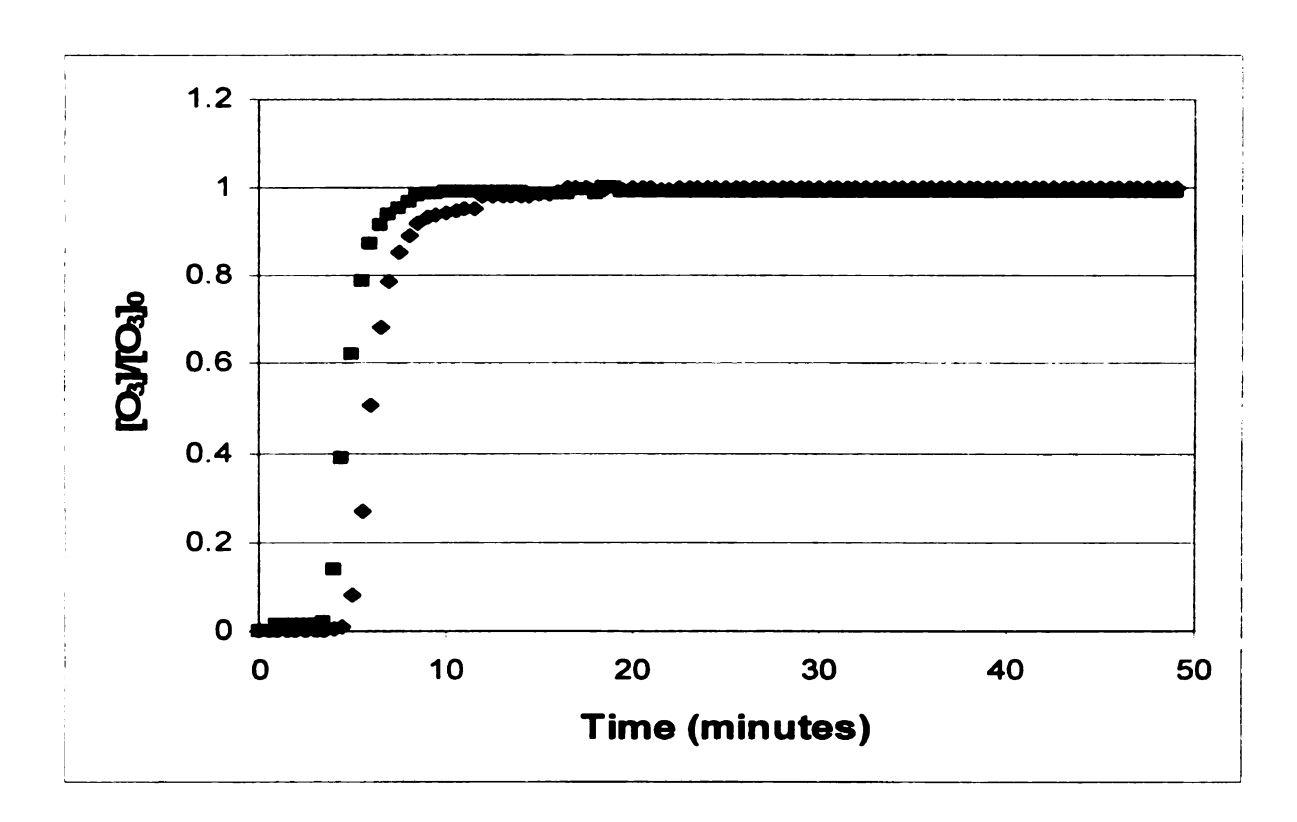


Figure 5.15 Ozone BTC in the 3.5 foot column without the gas washing bottle.

• Empty; • 42 inches of Ottawa geologic material

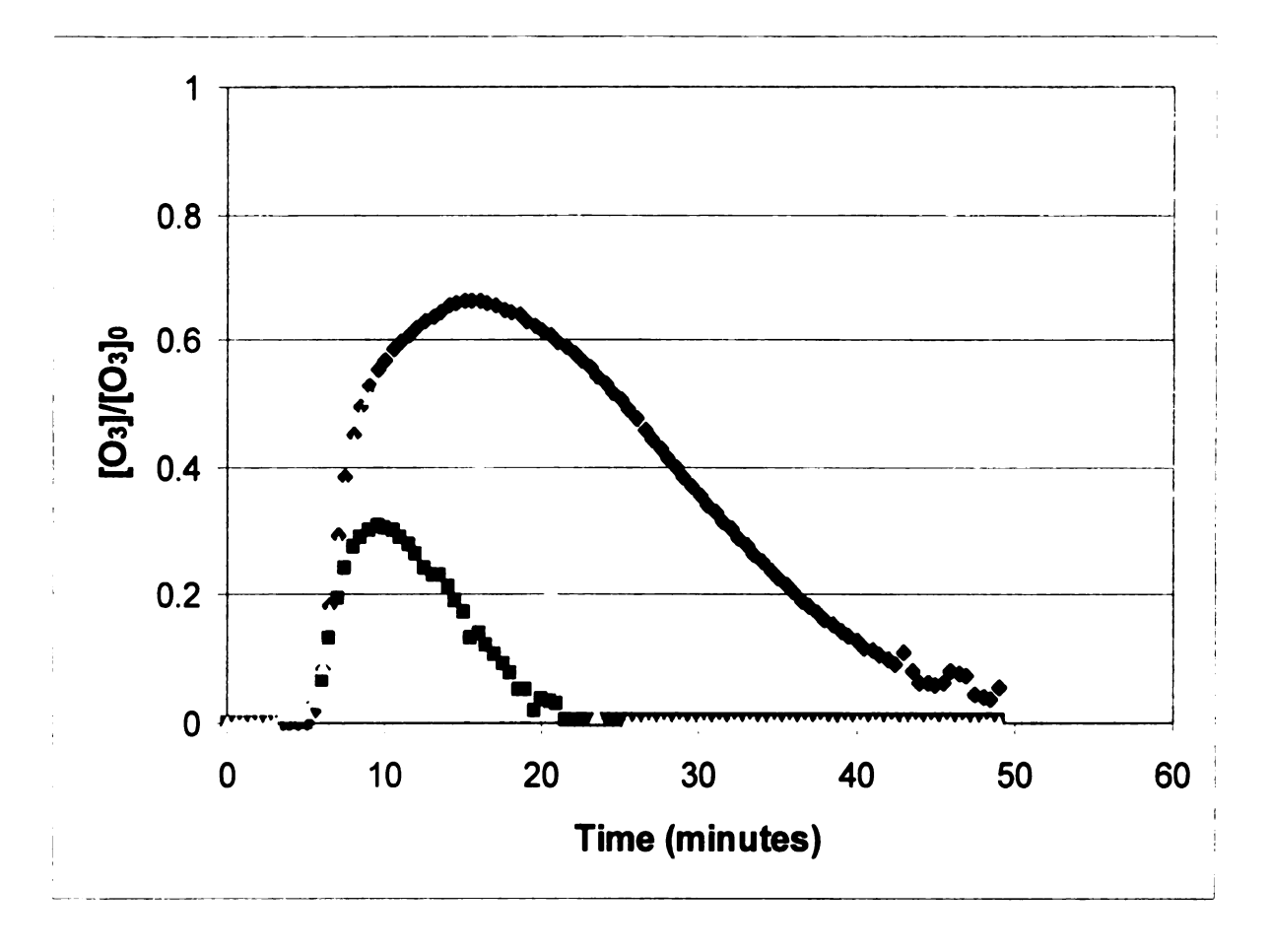


Figure 5.16. Ozone breakthrough curves for Experiments 1, 2, and 3 in the 3.5 foot column without the gas wash bottle and containing 10 cm of Metea soil.

## **5.4.2 Model Application**

Due to the difficulty with the experiments conducted in the 3.5 foot columns, the model was first applied to the data collected from in the 15 cm soil column experiments. The governing equations from the Hsu model were solved using two methods. The finite-difference method was implemented using Eqn. (5.12) and Eqn. (5.13). A method using a fourth-order Runge-Kutta to solve Eqn. 5.4 was also used to compare the models results. Examples of the MathCAD programs are provided in Appendix D.

### 5.4.2.1 Experiments in the 15 cm column

The experimental conditions used in the model for the dry, non-contaminated soil (pH 6) were as follows: L = 15 cm;  $\rho_b$  = 1.1 kg/L; n = 0.4;  $s_a$  = 1.0; k = 1.4 x 10<sup>-4</sup> (s<sup>-1</sup> · (mg O<sub>3</sub>/kg soil)<sup>-1</sup>;  $k_d$  = 0.0798,  $[O_3]_0$  = 55 mg/L;  $OM_0$  = 4000 mg/kg;  $\zeta_{om}$  = 4.7 ± 0.8 mg O<sub>3</sub>/mg OM was the ozone dose where the soil organic matter had completely reacted. Hsu and Masten (1997) calculated the second order rate constant for organic matter as  $k_{om}$  = 8.8 x 10<sup>-6</sup> [s<sup>-1</sup> (mg of soil organic carbon/kg of dry soil)<sup>-1</sup> (L of gas/kg of soil)] using a series of equations to solve for  $k_{om}$  implicitly. The reaction rate constants discussed in sections 5. 2 of this study, however, had the units (s<sup>-1</sup> · (mg O<sub>3</sub>/kg soil)<sup>-1</sup>. Therefore, the k value was calculated to conform to the units needed for the model. The value for  $k_{om}$  was solved using equations (3-14 through 3-17) in Hsu's dissertation [5] and the "solver" function in Excel. The spreadsheet calculation is provided in Appendix D. The  $k_{om}$  was calculated to be 5.7 x 10<sup>-7</sup> [s<sup>-1</sup> (mg of soil organic carbon/kg of dry soil)<sup>-1</sup> (L of gas/kg of soil)].

Figure 5.17 is the finite difference solution for dry, non-contaminated soil. The model predicted slower breakthrough for ozone compared to the experimental data. Adaptation of the model using a "tailing factor" ranging from 90% - 95% breakthrough of the influent concentration was necessary to fit the model to the data.

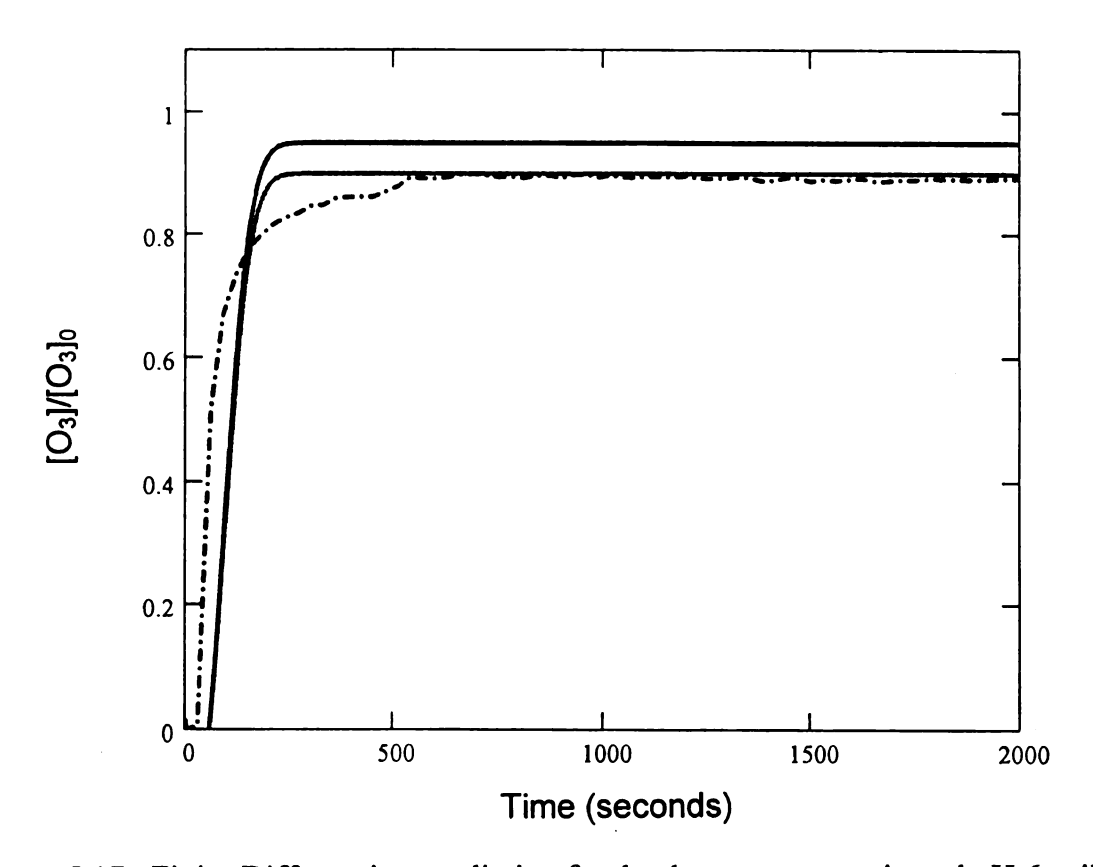


Figure 5.17. Finite-Differencing prediction for the dry, non-contaminated pH 6 soil:

- • - Experimental data BTC; — Hsu model with 95% breakthrough; — Hsu model with 90% breakthrough.

A second method used a Runge-Kutta solution to calculate the ozone decomposition. Figure 5.18 shows the solution generated by MathCAD. Finite differencing was used to solve for the reaction with organic matter. The Runge-Kutta solution was used for ozone decomposition. The program limitations prevented the use of a variable organic matter concentration in the final governing equation, however, due to the large amount of organic matter present in the soil, the organic matter concentration calculated by the finite differencing step was used in the Runge-Kutta solution. The model gives a prediction close to the experimental data. The model required the use of a "tailing factor".

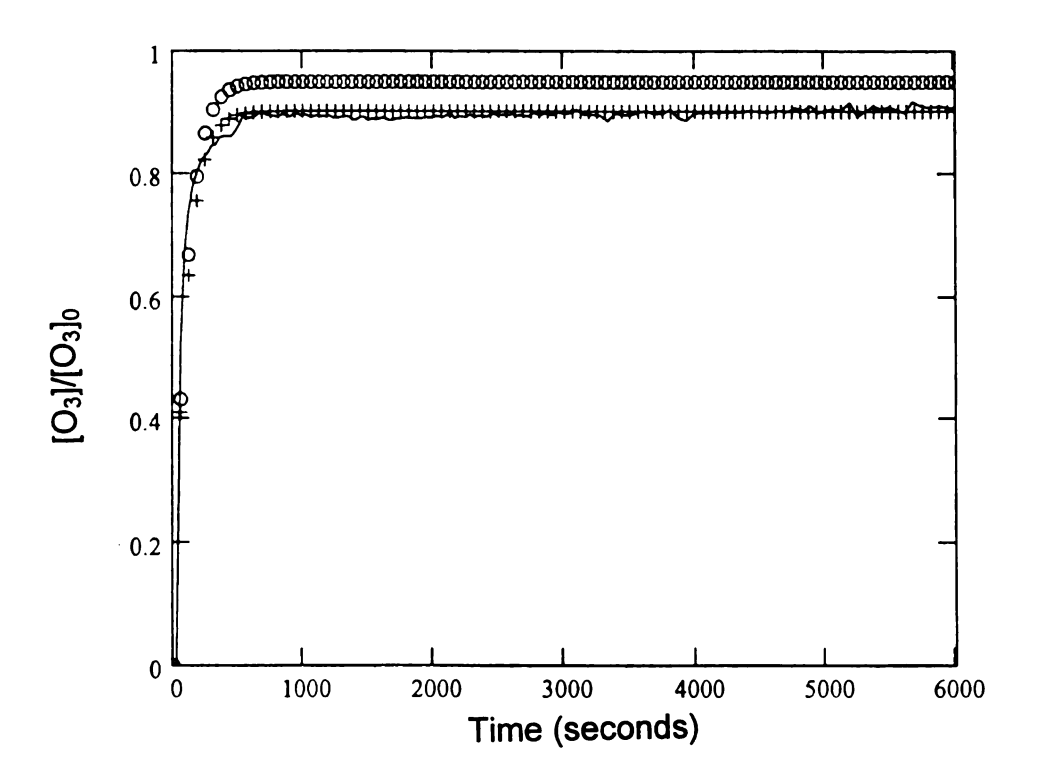


Figure 5.18. Runge-Kutta prediction for the dry, non- contaminated soil at pH 6:

— Experimental Data BTC; O Hsu model with 95% breakthrough; + Hsu model with 90% breakthrough.

## 5.4.2.2 Model application in the 3.5 foot column

In these experiments with Ottawa sand, no organic matter was present in the system therefore  $k_{om}$  and  $k_c$  can be neglected. The Hsu model in equation 5.6 therefore simplifies to first order. The model predictions using the Runga-Kutta solution appears to have an adequate prediction of the data. The time delay was not predicted by the curve and some of the same parameters that were used in the model from the small soil column were assumed to apply to the larger column. Figure 5.19 is the curve predicted for the empty system and the column with 42 inched of Ottawa sand.

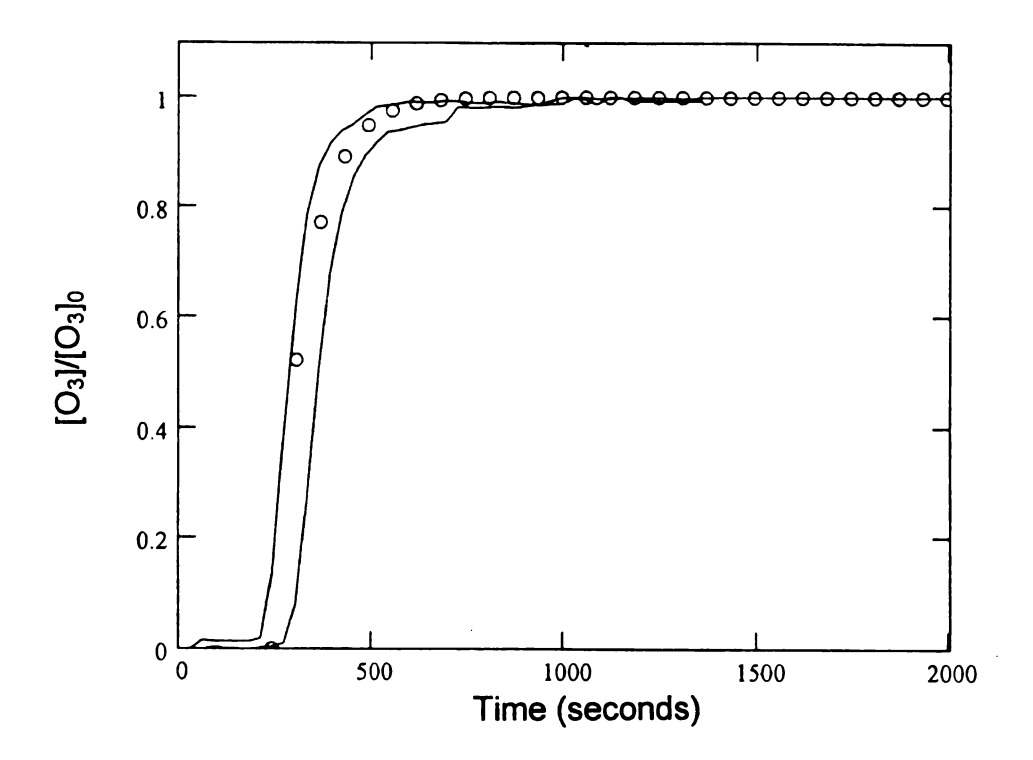
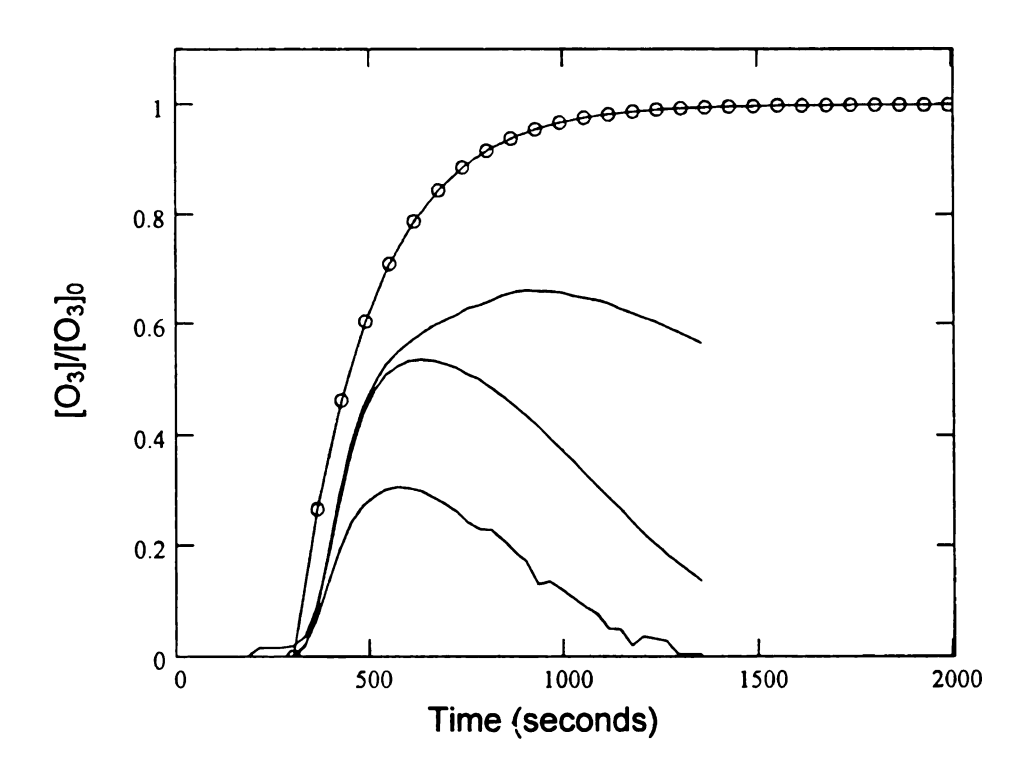


Figure 5.19. Model prediction for the 3.5 column empty and with 42 inches of Ottawa sand: —— BTC for Empty Column; —— BTC for Ottawa Sand; O Model prediction.

The model applied to the experimental data for the 10 cm of Metea soil generated a curve that may represent the BTC that would have been produced if the experiment had proceeded to completion. A large pressure drop was hypothesized to occur between the inlet and outlet. The outlet pressure observed in the column was unstable due to the experimental error. However, using the initial inlet and outlet pressures observed, Figure 5.20 shows a curve that appears to have a similar slope as the experimental data.



### 5.5 Modeling Discussion and Conclusions

Both Hsu and Kim presented models that are similar in development. Kim et al. [8] compared the predictions from both the lump model and the Hsu model using data from Hsu's dissertation [5]. After attempting to apply the experimental conditions published in Hsu [5], Kim et al. [8] observed that the lump model and the Hsu model yielded predictions that did not acceptably describe the experiment BTCs. The model results were improved slightly using different parameters for the reaction rate constants and the stoichiometric coefficient ( $\zeta_{om}$ ). The kinetic parameters reported in Kim et al. [8]

and the original kinetic parameters presented in Hsu's dissertation are inconsistent, which may have caused the problems in the results developed by Kim et al.

Even though, Kim et al. [8] published results that do not support the Hsu model, the Hsu model does appear to calculate adequate predictions for ozone decomposition. The Hsu model appears to adequately fit the experimental data in the 15 cm column and possibly the 3.5 foot column. In the smaller column, a tailing factor was necessary. As seen in the 3.5 foot columns, however, removal of the gas wash bottle resulted in BTCs where the effluent concentration reached the influent concentration. Intuitively, one would think that removal of the gas wash bottle in the smaller system would improve results. In experiments conducted in the smaller system without the gas wash bottle, however, the system and became an ozone destruct unit. In this system, all ozone entering the column was catalytically oxidized on the dry soil surface. This occurrence was observed by Hsu [5] and during preliminary experiments conducted for the present study (See Appendix D for BTC in the system without gas wash bottle). This might also explain the curves produced in the 3.5 foot columns containing 10 cm of Metea (Figure 5.15).

The model was sensitive to the pressure changes in the larger column, such that, pressure differences between the inlet pressure and outlet pressure had a large impact on the curves generated. In varying the outlet pressure, the larger the pressure drop, the smaller the slope of the curve generated by the model and the longer predicted time for [O<sub>3</sub>] to reach 100% breakthrough. Some parameter conditions, such as the k<sub>om</sub> value, appear to be soil and system specific. For the soil used in this study, the k<sub>om</sub> calculated using the experimental data was a key factor in the model prediction. The organic matter

concentration (mg/kg) and the stoichiometric coefficient  $\zeta_{om}$  are also system specific and important aspects for the model prediction.

#### 5.6 References

- 1. Hsu, I. and Masten, S.J.; "The Kinetics of the reaction of ozone with phenanthrene in unsaturated soils." *Journal of Environ. Eng. Sci.*, 1997. 14(4), 207 217.
- 2. Alebić-Juretić, A; Cvităs, T; Klasnic, L; "Heterogeneous Polycyclic Aromatic Hydrocarbon Degradation with Ozone on Silca Gel Carrier." *Environ. Sci. Technol.* 1990, 24, 62-66.
- 3. Masten, S.; "Ozonation of VOC's in the presence of Humic Acid". Ozone. Sci. Eng. 1991, 13(3), 287-312.
- 4. Day, J.E.; "The Effect of Soil Moisture on the Ozonation of Pyrene in Soils." M.S. Thesis, Department of Civil and Environmental Engineering, Michigan State University, 1994.
- 5. Hsu, I.; "The Use of Gaseous Ozone to Remediate the Organic Contaminants in the Unstaturated Soils, Ph.D. Thesis, Department of Civil and Environmental Engineering, Michigan State University, 1995.
- 6. Lim, H-N.; Choi, H.; Hwang, T-M.; Kang, J-W.; "Characterization of ozone decomposition in a soil slurry: kinetics and mechanism." *Water Research.* **2002**. 36, 219 229.
- 7. Gurol, M.; Singer, P.; "Kinetics of Ozone Decomposition: A Dynamic Approach". Env. Sci. Technol. 1982, 16(7), 377 383.
- 8. Kim, J.; Choi, H.; :Modeling in sity ozonation for the remediation of nonvolatile PAH-contaminated unsaturated soils." *Journal of Contaminant Hydrology.* **2002**. 55(3-4), 261-285.
- 9. Davies, Simon. Personal communication (2002).
- 10. Mayotte, Tim. Personal communication (2002).

#### **CHAPTER 6**

### **Summary and Recommendations**

### 6.1 Summary

The primary focus of this study was to investigate the use of gaseous ozone in the remediation of pyrene contaminated soil. The affect soil conditions, such as soil moisture content, pH, soil temperature, and soil contaminant age, would have on pyrene oxidation was evaluated. The study identified pyrene ozonation byproducts produced in soil. Two synthesized ozonation byproducts were evaluated for the ability to inhibit Gap Junctional Intercellular Communication (GJIC). In collaboration with the Department of Pharmacology and Toxicology, the synthesized compounds were also evaluated for the ability to affect netrophil function by measuring the production of superoxide in a human cell line (HL60). Scale-up of the ozonation system from the 15 cm column to a 3.5 foot column was attempted to generate data that could verify the use of the Hsu and Masten (1997) model in larger soil columns.

Ozonation studies were conducted in 15 cm soil columns containing pyrene contaminated soil (300 ppm). Soil moisture and pH appeared to be significant environmental conditions that influenced the reduction of pyrene concentrations. The experiment variables for soil moisture were dry soil, soil with 5% moisture content, and soil with 10% moisture content. The pH levels evaluated were pH 2, pH 6 and pH 8. Dry soil with high pH (pH 6, pH 8) resulted in the highest level of contaminant removal. In the presence of soil moisture, the reduction of pyrene concentrations in soil required longer treatment times compared to the dry soils.

Ozonation experiments were conducted in soil at ambient temperature (25°C) and in soil chilled to 13°C. This experiment was designed to determine the affect temperature would have on contaminant removal. Temperature was determined to not significantly improve the reduction of pyrene concentration in the dry soils. Pyrene removal in the moisturized soils improved compared to the ambient temperature studies. The lower temperature (13°C), however, made conducting the ozonation experiments harder to consistently perform. The colder temperature appeared to harden the packed soil and inhibited gas flow through the soil.

The aged soil experiments demonstrated the difficulty in remediating soils contaminated with PAHs for long periods of time. Soil contaminated with pyrene and stored for 6 months was ozonated using the identical experiment procedures. These experiments were conducted to determine if contaminant age in soil affects the efficiency of PAH removal using ozone. The sorption strength of PAH to soil is believed to increase over time; however, most laboratory studies are performed using freshly contaminated, spiked soils. In the ozonation experiments for the aged soils, the reduction of pyrene concentrations was found to be 3 - 4 times less in the aged soils compared to the freshly contaminated. This would suggest that the ozone required to remove contamination from soil in freshly contaminated soil would differ from soil that has had longer periods of PAH contamination.

The pyrene ozonation byproducts produced in soil are consistent with the compounds produced from aqueous pyrene ozonation. The byproducts detected were phenanthrene-like and biphenyl-like with hydroxyl, aldehyde, and carboxylic acid functional groups. Two new compounds were identified, benzene-tetracarboxylic acid

and a quinone. These two compounds were consistent with the compounds identified in previous soil ozonation studies.

Two synthesized pyrene ozonation byproducts were evaluated using toxicology assays. Synthesized compounds were used due to the difficulty in purifying byproducts from ozonated mixtures and because the compounds are not commercially available. 2,2',6,6'-biphenyl tetraaldehyde was determined to show adverse effects in both toxicity analyses. 2,2',6,6'-biphenyl tetraaldehyde was inhibitory to GJIC at low concentrations (5 μM) and irreversible damage resulted when cells were exposed to this compound for 30 minutes. In the human neutrophil assay, 2,2',6,6'-biphenyl tetraaldehyde reduced the ability for human cells to produce superoxide. 2,2',6,6'-biphenyl tetra carboxylic acid did not exhibit any significant effect in either assays.

The reaction of ozone with organic matter is considered second order overall and first order with respect to each reactant. The rate expression can be simplified to a pseudo-first order expression. The experimental data in this study did not appear to be represented using first-order kinetics. The reaction kinetics was therefore evaluated using both pseudo-first order and pseudo-second order kinetics for the experimental data. The data plotted using a second-order rate expression showed better r<sup>2</sup> values compared to the first-order representation of the data.

An ozonation system using a 3.5 foot column was designed to evaluate ozone transport. The system was initially designed based on the bench-scale ozonation system which used a 15 cm soil column and a gas wash bottle containing deionized water (pH 2). The experiments conducted using this system produced ozone breakthrough curves for the column filled with 12, 24, and 36 inches of Ottawa sand. The breakthrough curves

however had a tailing factor where the effluent concentration stabilized at 40% of the influent concentration. Several experiments were attempted using Metea soil without success. In these experiments, either no gas flow was detected in the effluent stream or the gas flow in the effluent slowly decreased over time. The gas wash bottle was removed from the system design with the hope of increasing the pressure and the gas flow to the column. Using the modified design, the system performance improved significantly. The experiments conducted with an empty column and with the column filled with 42 inches of Ottawa sand produced breakthrough curves that did not demonstrate tailing and the effluent concentration reached the influent concentration. The Metea soil ozonation experiments in the modified systems produced breakthrough curves that initially showed detection of ozone in the effluent stream. During the course of the experiment, however, the effluent ozone concentration began to decline until no ozone was detected in the effluent stream. Due to the difficulties in obtaining data in the 3.5 foot column, the Hsu and Masten (1997) model was also applied to the Metea soil data collected from the 15 cm column.

#### 6.2 Recommendations

Ozonation processes are increasing being implemented for *in-situ* remediation of groundwater and soil. The results from this study therefore provide relevant information that can be applied to process implementation. Based upon this investigation, gaseous ozone can be used to remediate soils contaminated with PAHs such as pyrene. The ability for ozone to reduce PAH contamination is dependent on the soil conditions and the length of time the PAH has been present in the soil. Many remediation projects

choose not to use ozonation processes due to the lack of information on the byproducts produced. The results from this study, however, show that the ozonation byproducts produced in soil are consistent with aqueous ozonation byproducts. The detection of similar byproducts is important because a large amount of literature is readily available for aqueous PAH ozonation byproducts. This finding will help in identifying potential compounds that could be produced in soil if ozonation is used *in-situ* for PAH remediation.

The recommendations for future studies are as follows:

- (1) Ozonation studies should be performed using both freshly contaminated soils and soils contaminated with the target compound for at least 6 months.
- (2) Further study using soils with different soil proprieties, or soils from contaminated sites, is recommended to investigate ozonation efficiency and the subsequent PAH removal.
- (3) The results from the bench scale ozonation experiments should be compared to results obtained in field studies.
- (4) Soil ozonation studies including byproduct identification and toxicology evaluations using PAH compounds, such as phenanthrene and chrysene are needed.
- (5) A study should identify the byproducts present in samples obtained from a field experiment or from a site where in-situ ozonation was implemented. A toxicology study using these samples would also be interesting to perform.



## PLACE IN RETURN BOX to remove this checkout from your record. TO AVOID FINES return on or before date due. MAY BE RECALLED with earlier due date if requested.

DATE DUE	DATE DUE	DATE DUE
		-

6/01 c:/CIRC/DateDue.p65-p.15

## THE USE OF GASEOUS OZONE TO REMEDIATE PYRENE CONTAMINATED SOILS: A STUDY OF BYPRODUCT PRODUCTION, ENVIRONMENTAL EFFECTS ON REMEDIATION EFFORTS, AND SCALE-UP

**VOLUME II** 

By

Stephanie Luster-Teasley

## A DISSERTATION

Submitted to
Michigan State University
in partial fulfillment of the requirements
for the degree of

**DOCTOR OF PHILOSOPHY** 

Department of Civil and Environmental Engineering

2003

## APPENDIX A

Appendix A includes an example of one of the Excel spreadsheets generated for the ozone raw data. Hard copies of the breakthrough curves, first order, and second order plots for the ozonation experiments are also provided in Appendix A.

Table A1. Summary of Ozonation Experiments

	Pyrene Concen.			
Sample	(ppm)	рН	Ozonation duration	Variable
dry soil	Clean	2,6,8	4 hours	pH, 25 <b>°</b> C
dry soil	Clean	2,6,8	4 hours	pH, 13⁰C
5% moisture	Clean	2,6,8	4 hours	pH, 25⁰C
5% moisture	Clean	2,6,8	4 hours	pH, 13 <b>°</b> C
10% moisture	Clean	2,6,8	4 hours	pH, 25 <b>°</b> C
10% moisture	Clean	2,6,8	4 hours	pH, 13ºC
dry soil	300	2	35 minutes, 1 hour, 4 hours	pH, 25°C
dry soil	300	6	35 minutes, 1 hour, 4 hours	pH, 25℃
dry soil	300	8	35 minutes, 1 hour, 4 hours	pH, 25℃
5% moisture	300	2	35 minutes, 1 hour, 4 hours	moisture, pH, 25°C
5% moisture	300	6	35 minutes, 1 hour, 4 hours	moisture, pH, 25°C
5% moisture	300	8	35 minutes, 1 hour, 4 hours	moisture, pH, 25°C
10% moisture	300	2	35 minutes, 1 hour, 4 hours	moisture, pH, 25°C
10% moisture	300	6	35 minutes, 1 hour, 4 hours	moisture, pH, 25°C
10% moisture	300	8	35 minutes, 1 hour, 4 hours	moisture, pH, 25°C
dry soil	300	2	35 minutes, 1 hour, 4 hours	pH, 13°C
dry soil	300	6	35 minutes, 1 hour, 4 hours	pH, 13℃
dry soil	300	8	35 minutes, 1 hour, 4 hours	pH, 13℃
5% moisture	300	2	35 minutes, 1 hour, 4 hours	pH, moisture, 13°C
5% moisture	300	6	35 minutes, 1 hour, 4 hours	pH, moisture, 13°C
5% moisture	300	8	35 minutes, 1 hour, 4 hours	pH, moisture, 13°C
10% moisture	300	2	35 minutes, 1 hour, 4 hours	pH, moisture, 13°C
10% moisture	300	6	35 minutes, 1 hour, 4 hours	pH, moisture, 13°C
10% moisture	300	8	35 minutes, 1 hour, 4 hours	pH, moisture, 13°C
dry soil	300	2	35 minutes, 1 hour, 4 hours	pH, 25°C,aged
dry soil	300	6	35 minutes, 1 hour, 4 hours	pH, 25°C,aged
dry soil	300	8	35 minutes, 1 hour, 4 hours	pH, 25°C,aged

Table A2. Example of spreadsheet generated for raw data OZONATION RAW DATA DRY (25 C), 300 ppm pyr soil (Ph6)

0 0 0 0.005 0.93223 0.002145 0.003 0.005 0.93323 0.002145 0.003 0.005 0.937234 0.120746 0.005 0.937234 0.120746 0.005 0.937234 0.120746 0.005 0.937234 0.120746 0.005 0.937234 0.120746 0.005 0.937234 0.120746 0.005 0.937234 0.120746 0.005 0.937234 0.120746 0.005 0.937234 0.120746 0.005 0.937234 0.120746 0.005 0.937234 0.120746 0.005 0.937234 0.120746 0.005 0.937234 0.120746 0.005 0.937234 0.120746 0.005 0.937234 0.120746 0.005 0.937234 0.120746 0.005 0.937234 0.120746 0.005 0.937234 0.120746 0.005 0.937234 0.120746 0.005 0.944307 0.450537 0.007 0.944307 0.450537 0.007 0.944307 0.450537 0.007 0.944307 0.450537 0.007 0.944307 0.450537 0.007 0.944307 0.450537 0.0010 0.955784 0.560877 0.007 0.0010 0.955784 0.560877 0.007 0.007 0.0010 0.955784 0.560877 0.007 0.007 0.007 0.007 0.007 0.007 0.944307 0.450537 0.007		Time	Time	Influent Ozone	Effluent Ozone	O3 reacted (mg O3/kg soil)	First order -In(C/Co)	Second order	BTC Influent pH 6 dry	BTC Effluent pH 6 dry
1         0         0         0.000         0.000         0.000           2         30         0.5         9.517         0.017         189.994         0.002         0.005         0.93228         0.002145           3         60         1         9.722         0.027         193.900         0.003         0.005         0.93233         0.02145           4         90         1.5         9.811         0.604         184.142         0.064         0.005         0.937234         0.120746           5         120         2         9.869         2.825         140.882         0.337         0.007         0.944307         0.450537           6         150         2.5         9.967         5.044         98.462         0.705         0.010         0.955784         0.56053           8         210         3.5         10.093         6.275         76.370         0.972         0.013         0.95592         0.632406           9         240         4         10.042         6.829         72.268         1.022         0.014         0.95592         0.632406           10         270         4.5         10.038         6.541         69.944         1.054	Tape ID#	(sec)	(min)	(mg O3)	(mg O3)	absorbed		1/C	BTC	BTC
1         0         0         0.000         0.000         0.000           2         30         0.5         9.517         0.017         189.994         0.002         0.005         0.93228         0.002145           3         60         1         9.722         0.027         193.900         0.003         0.005         0.93233         0.02145           4         90         1.5         9.811         0.604         184.142         0.064         0.005         0.937234         0.120746           5         120         2         9.869         2.825         140.882         0.337         0.007         0.944307         0.450537           6         150         2.5         9.967         5.044         98.462         0.705         0.010         0.955784         0.56053           8         210         3.5         10.093         6.275         76.370         0.972         0.013         0.95592         0.632406           9         240         4         10.042         6.829         72.268         1.022         0.014         0.95592         0.632406           10         270         4.5         10.038         6.541         69.944         1.054		0	0	0.000	0.000	0.000				
2         30         0.5         9.517         0.017         189.994         0.002         0.005         0.920285         0.003483           3         60         1         9.722         0.027         193.900         0.003         0.005         0.933234         0.02146           4         90         1.5         9.811         0.604         184.142         0.064         0.005         0.937234         0.120746           5         120         2         9.869         2.825         140.882         0.337         0.007         0.944307         0.450537           6         150         2.5         9.967         5.044         98.462         0.705         0.010         0.955784         0.560877           7         180         3         10.074         5.904         83.398         0.882         0.012         0.964725         0.611011           8         210         3.5         10.038         6.245         72.268         1.022         0.014         0.9584983         0.647988           10         270         4.5         10.038         6.541         69.944         1.054         0.014         0.9584983         0.647988           11         300 <t< td=""><td>1</td><td></td><td></td><td></td><td></td><td></td><td></td><td></td><td></td><td></td></t<>	1									
3         60         1         9.722         0.027         193.900         0.003         0.005         0.93323         0.002145           5         120         2         9.869         2.825         140.882         0.337         0.007         0.944307         0.450537           6         150         2.5         9.967         5.044         98.462         0.705         0.010         0.955784         0.560877           7         180         3         10.074         5.904         83.398         0.882         0.012         0.964725         0.611011           8         210         3.5         10.093         6.275         76.370         0.972         0.013         0.95952         0.632406           9         240         4         10.042         6.429         72.268         1.022         0.014         0.95872         0.655206           11         300         5         10.100         6.653         68.936         1.075         0.015         0.966727         0.66233           13         360         6         10.237         6.823         68.78         1.091         0.015         0.975801         0.667386           14         390         6.5 <td></td> <td></td> <td></td> <td></td> <td>0.017</td> <td>189.994</td> <td>0.002</td> <td>0.005</td> <td>0.920285</td> <td>0.00348</td>					0.017	189.994	0.002	0.005	0.920285	0.00348
4         90         1.5         9.811         0.604         184.142         0.064         0.005         0.937234         0.120746           5         120         2         9.869         5.044         98.462         0.337         0.007         0.944307         0.450537           7         180         3         10.074         5.904         83.398         0.882         0.012         0.964725         0.611011           8         210         3.5         10.093         6.275         76.370         0.972         0.013         0.95952         0.632406           9         240         4         10.042         6.429         72.268         1.022         0.014         0.954932         0.6552           11         300         5         10.100         6.653         68.936         1.075         0.015         0.958672         0.652203           12         330         5.5         10.193         6.751         68.852         1.086         0.015         0.975801         0.66218           14         390         6.5         10.241         6.890         68.278         1.098         0.015         0.975801         0.665618           14         390         6			1	9.722	0.027	193.900	0.003	0.005	0.93323	0.002145
6         150         2.5         9.967         5.044         98.462         0.705         0.010         0.955784         0.560877           7         180         3         10.074         5.904         83.398         0.882         0.012         0.964725         0.611011           8         210         3.5         10.093         6.275         76.370         0.972         0.013         0.95952         0.632406           9         240         4         10.042         6.429         72.268         1.022         0.014         0.954983         0.647988           10         270         4.5         10.038         6.541         69.944         1.054         0.014         0.956727         0.662503           11         300         5         10.100         6.653         68.936         1.075         0.015         0.966727         0.662203           12         330         5.5         10.293         6.823         68.278         1.098         0.015         0.975801         0.665208           13         360         6         10.241         6.895         68.278         1.098         0.015         0.977803         0.678393           15         420		90	1.5	9.811	0.604	184.142	0.064	0.005	0.937234	0.120746
6         150         2.5         9.967         5.044         98.462         0.705         0.010         0.955784         0.560877           7         180         3         10.074         5.904         83.398         0.882         0.012         0.964725         0.611011           8         210         3.5         10.093         6.275         76.370         0.972         0.013         0.95592         0.632406           9         240         4         10.042         6.429         72.268         1.022         0.014         0.954983         0.647988           10         270         4.5         10.038         6.541         69.944         1.054         0.014         0.956727         0.652203           11         300         5         10.100         6.653         68.936         1.075         0.015         0.966227         0.662233           13         360         6         10.241         6.806         68.824         1.091         0.015         0.975801         0.665618           14         390         6.5         10.237         6.823         68.278         1.098         0.015         0.975801         0.667396           15         420	5	120	2	9.869	2.825	140.882	0.337	0.007	0.944307	0.450537
7         180         3         10.074         5.904         83.398         0.882         0.012         0.964725         0.611011           8         210         3.5         10.093         6.275         76.370         0.972         0.013         0.9594983         0.647988           10         270         4.5         10.038         6.541         69.944         1.054         0.014         0.954983         0.647988           11         300         5         10.100         6.653         68.936         1.075         0.015         0.966727         0.662203           12         330         5.5         10.193         6.751         68.852         1.086         0.015         0.976602         0.662333           13         360         6         10.247         6.800         68.824         1.091         0.015         0.975801         0.666518           14         390         6.5         10.237         6.823         68.278         1.098         0.015         0.975801         0.667396           15         420         7         10.247         6.893         67.046         1.117         0.015         0.977803         0.682679           15         420		150	2.5	9.967	5.044	98.462	0.705	0.010	0.955784	0.560877
9 240 4 10.042 6.429 72.268 1.022 0.014 0.954983 0.647988 10 270 4.5 10.038 6.541 69.944 1.054 0.014 0.95872 0.655206 11 300 5 10.100 6.653 68.936 1.075 0.015 0.966727 0.662203 12 330 5.5 10.193 6.751 68.852 1.086 0.015 0.976602 0.662338 13 360 6 10.241 6.800 68.824 1.091 0.015 0.975801 0.665618 14 390 6.5 10.237 6.823 68.278 1.098 0.015 0.975801 0.667396 15 420 7 10.247 6.895 67.046 1.117 0.015 0.977803 0.678313 16 450 7.5 10.229 6.961 65.366 1.141 0.015 0.972065 0.681906 17 480 8 10.199 6.959 64.806 1.147 0.015 0.972065 0.681906 18 510 8.5 10.244 6.989 65.100 1.146 0.015 0.980873 0.682585 19 540 9 10.259 7.010 64.988 1.150 0.015 0.975001 0.683958 20 570 9.5 10.201 6.968 64.666 1.149 0.015 0.97530 0.682125 21 600 10 10.195 6.947 64.960 1.144 0.015 0.98387 0.682585 22 630 10.5 10.257 6.968 65.786 1.137 0.015 0.981673 0.687795 23 660 11 10.323 7.017 66.122 1.139 0.015 0.98543 0.681505 24 690 11.5 10.343 7.066 65.548 1.149 0.015 0.98543 0.684766 25 720 12 10.300 7.059 64.820 1.156 0.015 0.98543 0.684766 25 720 12 10.300 7.059 64.820 1.156 0.015 0.98543 0.684766 26 750 12.5 10.231 7.024 64.134 1.150 0.015 0.97380 0.682439 28 810 13.5 10.178 6.926 65.044 1.141 0.015 0.9738 0.682439 30 870 14.5 10.256 6.993 65.576 1.136 0.015 0.97396 0.682439 31 900 15 10.215 6.968 65.506 1.137 0.015 0.97380 0.682439 32 930 15.5 10.276 6.968 65.576 1.136 0.015 0.97380 0.682439 33 960 16 10.311 6.975 6.968 65.704 1.137 0.015 0.97380 0.682439 34 990 16.5 10.296 6.968 66.570 1.130 0.015 0.983275 0.675489 33 960 16 10.311 6.975 6.968 65.504 1.137 0.015 0.982474 0.67934 34 990 16.5 10.296 6.968 66.570 1.129 0.015 0.983275 0.6756489 35 1020 17 10.266 6.940 66.514 1.127 0.015 0.983275 0.6756489 36 1050 17.5 10.261 6.992 66.990 1.120 0.015 0.9861673 0.6726123 37 1080 18 10.307 6.926 67.620 1.115 0.015 0.9861673 0.6726123 38 1110 18.5 10.317 6.940 67.550 1.117 0.015 0.985677 0.672623 38 1110 18.5 10.317 6.940 67.550 1.117 0.015 0.981673 0.6725123 39 1140 19 10.297 6.940 67.144 1.121 0.015 0.981673 0.672512		180	3	10.074	5.904	83.398	0.882	0.012	0.964725	0.611011
9 240 4 10.042 6.429 72.268 1.022 0.014 0.954983 0.647988 10 270 4.5 10.038 6.541 69.944 1.054 0.014 0.95872 0.555206 11 300 5 10.100 6.653 68.936 1.075 0.015 0.966727 0.662203 12 330 5.5 10.193 6.751 68.852 1.086 0.015 0.976602 0.662339 13 360 6 10.241 6.800 68.824 1.091 0.015 0.975801 0.665618 14 390 6.5 10.237 6.823 68.278 1.098 0.015 0.975801 0.665618 14 390 6.5 10.237 6.823 68.278 1.098 0.015 0.975801 0.667396 15 420 7 10.247 6.895 67.046 1.117 0.015 0.977803 0.678313 16 450 7.5 10.229 6.961 65.366 1.141 0.015 0.972332 0.682679 17 480 8 10.199 6.959 64.806 1.147 0.015 0.972332 0.682585 19 540 9 10.259 7.010 64.988 1.150 0.015 0.972065 0.681906 19 540 9 10.259 7.010 64.988 1.150 0.015 0.975001 0.683958 19 540 9 10.259 7.010 64.988 1.150 0.015 0.975001 0.683958 19 540 9 10.259 6.966 64.666 1.144 0.015 0.975001 0.683958 19 540 9 10.259 6.967 64.966 1.144 0.015 0.975001 0.683958 19 540 9 10.257 6.968 64.666 1.149 0.015 0.969796 0.682125 10 600 10 1.095 6.947 64.960 1.144 0.015 0.986873 0.67795 12 630 10.5 10.257 6.968 65.786 1.137 0.015 0.986844 0.681505 12 690 11.5 10.343 7.066 65.548 1.149 0.015 0.986344 0.681505 12 600 12 10.300 7.059 64.820 1.156 0.015 0.986344 0.681505 12 600 12 10.300 7.059 64.820 1.156 0.015 0.97807 0.685905 12 10.231 7.024 64.134 1.160 0.016 0.97332 0.682732 12 88 810 13.5 10.178 6.926 65.044 1.141 0.015 0.97399 0.678508 12 9 840 14 10.212 6.933 65.576 1.136 0.015 0.97380 0.69343 1 900 15 10.215 6.940 65.506 1.137 0.015 0.97380 0.67932 1 930 15.5 10.276 6.940 65.506 1.137 0.015 0.983275 0.675489 1 990 16.5 10.296 6.968 66.570 1.129 0.015 0.982474 0.67924 1 190 0.015 0.982474 0.67924 1 190 0.015 0.982474 0.67934 1 190 0.15 0.98602 0.676004 1 1.140 0.015 0.982677 0.67268 1 1.150 0.015 0.983275 0.676488 1 1.10 0.015 0.982677 0.67268 1 1.10 0.015 0.982677 0.67268 1 1.10 0.015 0.982677 0.67268 1 1.10 0.015 0.982677 0.67268 1 1.10 0.015 0.982677 0.67268 1 1.10 0.015 0.982677 0.67260 1 1.10 0.015 0.982677 0.67260 1 1.110 0.015 0.981673 0.67261 1 1.110 0.015 0.981673 0.67261 1 1.110 0.015 0.98			3.5	10.093	6.275	76.370	0.972	0.013	0.95952	0.632406
11         300         5         10.100         6.653         68.936         1.075         0.015         0.966727         0.662203           12         330         5.5         10.193         6.751         68.852         1.086         0.015         0.976602         0.662339           13         360         6         10.241         6.800         68.824         1.091         0.015         0.975801         0.665618           14         390         6.5         10.237         6.823         68.278         1.098         0.015         0.977803         0.678313           15         420         7         10.249         6.956         65.366         1.141         0.015         0.977803         0.678313           16         450         7.5         10.229         6.961         65.366         1.141         0.015         0.977803         0.6826196           18         510         8.5         10.244         6.989         65.100         1.146         0.015         0.977901         0.682958           19         540         9         10.259         7.010         64.988         1.150         0.015         0.979001         0.683958           20         570		240	4	10.042	6.429	72.268	1.022	0.014	0.954983	0.647988
12         330         5.5         10.193         6.751         68.852         1.086         0.015         0.976602         0.662339           13         360         6         10.241         6.800         68.824         1.091         0.015         0.975801         0.665618           14         390         6.5         10.237         6.823         68.278         1.098         0.015         0.975801         0.667366           15         420         7         10.247         6.895         67.046         1.117         0.015         0.977803         0.678313           16         450         7.5         10.229         6.961         65.366         1.141         0.015         0.972065         0.682679           17         480         8         10.199         6.959         64.806         1.147         0.015         0.972065         0.681906           18         510         8.5         10.244         6.989         65.100         1.146         0.015         0.975001         0.682585           19         540         9         10.259         7.010         64.988         1.150         0.015         0.97332         0.682125           21         600	10	270	4.5	10.038	6.541	69.944	1.054	0.014	0.95872	0.655206
13         360         6         10.241         6.800         68.824         1.091         0.015         0.975801         0.665618           14         390         6.5         10.237         6.823         68.278         1.098         0.015         0.975801         0.667396           15         420         7         10.247         6.895         67.046         1.117         0.015         0.977803         0.678313           16         450         7.5         10.229         6.961         65.366         1.141         0.015         0.972065         0.682679           17         480         8         10.199         6.959         64.806         1.147         0.015         0.972065         0.682685           18         510         8.5         10.244         6.989         65.100         1.146         0.015         0.980873         0.682585           19         540         9         10.259         7.010         64.988         1.150         0.015         0.98378         0.682585           20         570         9.5         10.201         6.968         64.666         1.149         0.015         0.969796         0.682125           21         600		300	5	10.100	6.653	68.936	1.075	0.015	0.966727	0.662203
14         390         6.5         10.237         6.823         68.278         1.098         0.015         0.975801         0.667396           15         420         7         10.247         6.895         67.046         1.117         0.015         0.977803         0.678313           16         450         7.5         10.229         6.961         65.366         1.141         0.015         0.972065         0.682679           17         480         8         10.199         6.959         64.806         1.147         0.015         0.972065         0.682685           19         540         9         10.259         7.010         64.988         1.150         0.015         0.975001         0.682585           20         570         9.5         10.201         6.968         64.666         1.149         0.015         0.969796         0.682125           21         600         10         10.195         6.947         64.960         1.144         0.015         0.9733         0.680691           22         630         10.5         10.257         6.968         65.786         1.137         0.015         0.981673         0.67795           23         660	12	330	5.5	10.193	6.751	68.852	1.086	0.015	0.976602	0.662339
15         420         7         10.247         6.895         67.046         1.117         0.015         0.977803         0.678313           16         450         7.5         10.229         6.961         65.366         1.141         0.015         0.972332         0.682679           17         480         8         10.199         6.959         64.806         1.147         0.015         0.972065         0.681906           18         510         8.5         10.244         6.989         65.100         1.146         0.015         0.980873         0.682585           19         540         9         10.259         7.010         64.988         1.150         0.015         0.975001         0.683958           20         570         9.5         10.201         6.968         64.666         1.149         0.015         0.969796         0.682125           21         600         10         10.195         6.947         64.960         1.144         0.015         0.9738         0.680691           22         630         10.5         10.237         7.017         66.122         1.137         0.015         0.986344         0.681505           24         690	13	360	6	10.241	6.800	68.824	1.091	0.015	0.975801	0.665618
16         450         7.5         10.229         6.961         65.366         1.141         0.015         0.972332         0.682679           17         480         8         10.199         6.959         64.806         1.147         0.015         0.972065         0.681906           18         510         8.5         10.244         6.989         65.100         1.146         0.015         0.980873         0.682585           19         540         9         10.259         7.010         64.988         1.150         0.015         0.975001         0.683958           20         570         9.5         10.201         6.968         64.666         1.149         0.015         0.99796         0.682125           21         600         10         10.195         6.947         64.960         1.144         0.015         0.9733         0.680691           22         630         10.5         10.257         6.968         65.786         1.137         0.015         0.985343         0.680691           24         690         11.5         10.343         7.066         65.548         1.149         0.015         0.985543         0.684766           25         720	14	390	6.5	10.237	6.823	68.278	1.098	0.015	0.975801	0.667396
17         480         8         10.199         6.959         64.806         1.147         0.015         0.972065         0.681906           18         510         8.5         10.244         6.989         65.100         1.146         0.015         0.980873         0.682585           19         540         9         10.259         7.010         64.988         1.150         0.015         0.975001         0.683958           20         570         9.5         10.201         6.968         64.666         1.149         0.015         0.969796         0.682125           21         600         10         10.195         6.947         64.960         1.144         0.015         0.9738         0.680691           22         630         10.5         10.257         6.968         65.786         1.137         0.015         0.981673         0.67795           23         660         11         10.323         7.017         66.122         1.139         0.015         0.986344         0.681505           24         690         11.5         10.343         7.066         65.548         1.149         0.015         0.97807         0.685905           26         750	15	420	7	10.247	6.895	67.046	1.117	0.015	0.977803	0.678313
18         510         8.5         10.244         6.989         65.100         1.146         0.015         0.980873         0.682585           19         540         9         10.259         7.010         64.988         1.150         0.015         0.975001         0.683958           20         570         9.5         10.201         6.968         64.666         1.149         0.015         0.969796         0.682125           21         600         10         10.195         6.947         64.960         1.144         0.015         0.9738         0.680691           22         630         10.5         10.257         6.968         65.786         1.137         0.015         0.981673         0.67795           23         660         11         10.323         7.017         66.122         1.139         0.015         0.986344         0.681505           24         690         11.5         10.300         7.059         64.820         1.156         0.015         0.97807         0.685905           25         720         12         10.300         7.059         64.820         1.156         0.015         0.97807         0.685905           26         750	16	450	7.5	10.229	6.961	65.366	1.141	0.015	0.972332	0.682679
19         540         9         10.259         7.010         64.988         1.150         0.015         0.975001         0.683958           20         570         9.5         10.201         6.968         64.666         1.149         0.015         0.969796         0.682125           21         600         10         10.195         6.947         64.960         1.144         0.015         0.9738         0.680691           22         630         10.5         10.257         6.968         65.786         1.137         0.015         0.981673         0.67795           23         660         11         10.323         7.017         66.122         1.139         0.015         0.986344         0.681505           24         690         11.5         10.343         7.066         65.548         1.149         0.015         0.986344         0.681505           25         720         12         10.300         7.059         64.820         1.156         0.015         0.97807         0.685905           26         750         12.5         10.231         7.024         64.134         1.155         0.016         0.97332         0.687208           27         780	17	480	8	10.199	6.959	64.806	1.147	0.015	0.972065	0.681906
20         570         9.5         10.201         6.968         64.666         1.149         0.015         0.969796         0.682125           21         600         10         10.195         6.947         64.960         1.144         0.015         0.9738         0.680691           22         630         10.5         10.257         6.968         65.786         1.137         0.015         0.981673         0.67795           23         660         11         10.323         7.017         66.122         1.139         0.015         0.986344         0.681505           24         690         11.5         10.343         7.066         65.548         1.149         0.015         0.986344         0.681505           25         720         12         10.300         7.059         64.820         1.156         0.015         0.97807         0.685905           26         750         12.5         10.231         7.024         64.134         1.160         0.016         0.97232         0.687208           27         780         13         10.178         6.926         65.044         1.141         0.015         0.97384         0.682439           28         810	18	510	8.5	10.244	6.989	65.100	1.146	0.015	0.980873	0.682585
21         600         10         10.195         6.947         64.960         1.144         0.015         0.9738         0.680691           22         630         10.5         10.257         6.968         65.786         1.137         0.015         0.981673         0.67795           23         660         11         10.323         7.017         66.122         1.139         0.015         0.986344         0.681505           24         690         11.5         10.343         7.066         65.548         1.149         0.015         0.985543         0.684766           25         720         12         10.300         7.059         64.820         1.156         0.015         0.97807         0.685905           26         750         12.5         10.231         7.024         64.134         1.160         0.016         0.97232         0.687208           27         780         13         10.175         6.968         64.134         1.155         0.016         0.97232         0.682439           28         810         13.5         10.178         6.926         65.044         1.141         0.015         0.972999         0.678508           29         840	19	540	9	10.259	7.010	64.988	1.150	0.015	0.975001	0.683958
22       630       10.5       10.257       6.968       65.786       1.137       0.015       0.981673       0.67795         23       660       11       10.323       7.017       66.122       1.139       0.015       0.986344       0.681505         24       690       11.5       10.343       7.066       65.548       1.149       0.015       0.985543       0.684766         25       720       12       10.300       7.059       64.820       1.156       0.015       0.97807       0.685905         26       750       12.5       10.231       7.024       64.134       1.160       0.016       0.972332       0.687208         27       780       13       10.175       6.968       64.134       1.155       0.016       0.967394       0.682439         28       810       13.5       10.178       6.926       65.044       1.141       0.015       0.972999       0.678508         29       840       14       10.212       6.933       65.576       1.136       0.015       0.9738       0.67932         30       870       14.5       10.205       6.933       65.436       1.137       0.015       0.975801	20	570	9.5	10.201	6.968	64.666	1.149	0.015	0.969796	0.682125
23       660       11       10.323       7.017       66.122       1.139       0.015       0.986344       0.681505         24       690       11.5       10.343       7.066       65.548       1.149       0.015       0.985543       0.684766         25       720       12       10.300       7.059       64.820       1.156       0.015       0.97807       0.685905         26       750       12.5       10.231       7.024       64.134       1.160       0.016       0.972332       0.687208         27       780       13       10.175       6.968       64.134       1.155       0.016       0.967394       0.682439         28       810       13.5       10.178       6.926       65.044       1.141       0.015       0.972999       0.678508         29       840       14       10.212       6.933       65.576       1.136       0.015       0.9738       0.67932         30       870       14.5       10.205       6.933       65.436       1.137       0.015       0.971664       0.67944         31       900       15       10.215       6.940       65.506       1.137       0.015       0.983275	21	600	10	10.195	6.947	64.960	1.144	0.015	0.9738	0.680691
24       690       11.5       10.343       7.066       65.548       1.149       0.015       0.985543       0.684766         25       720       12       10.300       7.059       64.820       1.156       0.015       0.97807       0.685905         26       750       12.5       10.231       7.024       64.134       1.160       0.016       0.972332       0.687208         27       780       13       10.175       6.968       64.134       1.155       0.016       0.967394       0.682439         28       810       13.5       10.178       6.926       65.044       1.141       0.015       0.972999       0.678508         29       840       14       10.212       6.933       65.576       1.136       0.015       0.9738       0.67932         30       870       14.5       10.205       6.933       65.436       1.137       0.015       0.971664       0.67944         31       900       15       10.215       6.940       65.506       1.137       0.015       0.975801       0.679294         32       930       15.5       10.276       6.961       66.304       1.131       0.015       0.983275	22	630	10.5	10.257	6.968	65.786	1.137	0.015	0.981673	0.67795
25         720         12         10.300         7.059         64.820         1.156         0.015         0.97807         0.685905           26         750         12.5         10.231         7.024         64.134         1.160         0.016         0.972332         0.687208           27         780         13         10.175         6.968         64.134         1.155         0.016         0.967394         0.682439           28         810         13.5         10.178         6.926         65.044         1.141         0.015         0.972999         0.678508           29         840         14         10.212         6.933         65.576         1.136         0.015         0.9738         0.67932           30         870         14.5         10.205         6.933         65.436         1.137         0.015         0.971664         0.67944           31         900         15         10.215         6.940         65.506         1.137         0.015         0.975801         0.679294           32         930         15.5         10.276         6.961         66.304         1.131         0.015         0.982474         0.677397           34         990	23	660	11	10.323	7.017	66.122			0.986344	0.681505
26         750         12.5         10.231         7.024         64.134         1.160         0.016         0.972332         0.687208           27         780         13         10.175         6.968         64.134         1.155         0.016         0.967394         0.682439           28         810         13.5         10.178         6.926         65.044         1.141         0.015         0.972999         0.678508           29         840         14         10.212         6.933         65.576         1.136         0.015         0.9738         0.67932           30         870         14.5         10.205         6.933         65.436         1.137         0.015         0.971664         0.67944           31         900         15         10.215         6.940         65.506         1.137         0.015         0.975801         0.679294           32         930         15.5         10.276         6.961         66.304         1.131         0.015         0.983275         0.675489           33         960         16         10.311         6.975         66.724         1.128         0.015         0.982474         0.677397           34         990 <td>24</td> <td>690</td> <td>11.5</td> <td>10.343</td> <td>7.066</td> <td>65.548</td> <td>1.149</td> <td>0.015</td> <td>0.985543</td> <td>0.684766</td>	24	690	11.5	10.343	7.066	65.548	1.149	0.015	0.985543	0.684766
27       780       13       10.175       6.968       64.134       1.155       0.016       0.967394       0.682439         28       810       13.5       10.178       6.926       65.044       1.141       0.015       0.972999       0.678508         29       840       14       10.212       6.933       65.576       1.136       0.015       0.9738       0.67932         30       870       14.5       10.205       6.933       65.436       1.137       0.015       0.971664       0.67944         31       900       15       10.215       6.940       65.506       1.137       0.015       0.975801       0.679294         32       930       15.5       10.276       6.961       66.304       1.131       0.015       0.983275       0.675489         33       960       16       10.311       6.975       66.724       1.128       0.015       0.982474       0.677397         34       990       16.5       10.296       6.968       66.570       1.129       0.015       0.980472       0.676058         35       1020       17       10.266       6.940       66.514       1.127       0.015       0.976602	25	720	12	10.300		64.820				0.685905
28 810 13.5 10.178 6.926 65.044 1.141 0.015 0.972999 0.678508 29 840 14 10.212 6.933 65.576 1.136 0.015 0.9738 0.67932 30 870 14.5 10.205 6.933 65.436 1.137 0.015 0.971664 0.67944 31 900 15 10.215 6.940 65.506 1.137 0.015 0.975801 0.679294 32 930 15.5 10.276 6.961 66.304 1.131 0.015 0.983275 0.675489 33 960 16 10.311 6.975 66.724 1.128 0.015 0.982474 0.677397 34 990 16.5 10.296 6.968 66.570 1.129 0.015 0.980472 0.676058 35 1020 17 10.266 6.940 66.514 1.127 0.015 0.976602 0.676004 36 1050 17.5 10.261 6.912 66.990 1.120 0.015 0.979672 0.671162 37 1080 18 10.307 6.926 67.620 1.115 0.015 0.985277 0.672762 38 1110 18.5 10.317 6.940 67.550 1.117 0.015 0.981406 0.675415	26	750	12.5							
29       840       14       10.212       6.933       65.576       1.136       0.015       0.9738       0.67932         30       870       14.5       10.205       6.933       65.436       1.137       0.015       0.971664       0.67944         31       900       15       10.215       6.940       65.506       1.137       0.015       0.975801       0.679294         32       930       15.5       10.276       6.961       66.304       1.131       0.015       0.983275       0.675489         33       960       16       10.311       6.975       66.724       1.128       0.015       0.982474       0.677397         34       990       16.5       10.296       6.968       66.570       1.129       0.015       0.980472       0.676058         35       1020       17       10.266       6.940       66.514       1.127       0.015       0.976602       0.676004         36       1050       17.5       10.261       6.912       66.990       1.120       0.015       0.985277       0.672762         37       1080       18       10.307       6.926       67.620       1.115       0.015       0.981673	27	780	13	10.175						
30       870       14.5       10.205       6.933       65.436       1.137       0.015       0.971664       0.67944         31       900       15       10.215       6.940       65.506       1.137       0.015       0.975801       0.679294         32       930       15.5       10.276       6.961       66.304       1.131       0.015       0.983275       0.675489         33       960       16       10.311       6.975       66.724       1.128       0.015       0.982474       0.677397         34       990       16.5       10.296       6.968       66.570       1.129       0.015       0.980472       0.676058         35       1020       17       10.266       6.940       66.514       1.127       0.015       0.976602       0.676004         36       1050       17.5       10.261       6.912       66.990       1.120       0.015       0.979672       0.671162         37       1080       18       10.307       6.926       67.620       1.115       0.015       0.985277       0.672762         38       1110       18.5       10.317       6.940       67.550       1.117       0.015       0.981406	28	810	13.5							
31       900       15       10.215       6.940       65.506       1.137       0.015       0.975801       0.679294         32       930       15.5       10.276       6.961       66.304       1.131       0.015       0.983275       0.675489         33       960       16       10.311       6.975       66.724       1.128       0.015       0.982474       0.677397         34       990       16.5       10.296       6.968       66.570       1.129       0.015       0.980472       0.676058         35       1020       17       10.266       6.940       66.514       1.127       0.015       0.976602       0.676004         36       1050       17.5       10.261       6.912       66.990       1.120       0.015       0.979672       0.671162         37       1080       18       10.307       6.926       67.620       1.115       0.015       0.985277       0.672762         38       1110       18.5       10.317       6.940       67.550       1.117       0.015       0.981673       0.672512         39       1140       19       10.297       6.940       67.144       1.121       0.015       0.981406		840								
32     930     15.5     10.276     6.961     66.304     1.131     0.015     0.983275     0.675489       33     960     16     10.311     6.975     66.724     1.128     0.015     0.982474     0.677397       34     990     16.5     10.296     6.968     66.570     1.129     0.015     0.980472     0.676058       35     1020     17     10.266     6.940     66.514     1.127     0.015     0.976602     0.676004       36     1050     17.5     10.261     6.912     66.990     1.120     0.015     0.979672     0.671162       37     1080     18     10.307     6.926     67.620     1.115     0.015     0.985277     0.672762       38     1110     18.5     10.317     6.940     67.550     1.117     0.015     0.981406     0.675415       39     1140     19     10.297     6.940     67.144     1.121     0.015     0.981406     0.675415	30	870	14.5							
33     960     16     10.311     6.975     66.724     1.128     0.015     0.982474     0.677397       34     990     16.5     10.296     6.968     66.570     1.129     0.015     0.980472     0.676058       35     1020     17     10.266     6.940     66.514     1.127     0.015     0.976602     0.676004       36     1050     17.5     10.261     6.912     66.990     1.120     0.015     0.979672     0.671162       37     1080     18     10.307     6.926     67.620     1.115     0.015     0.985277     0.672762       38     1110     18.5     10.317     6.940     67.550     1.117     0.015     0.981673     0.672512       39     1140     19     10.297     6.940     67.144     1.121     0.015     0.981406     0.675415	31	900	15							
34     990     16.5     10.296     6.968     66.570     1.129     0.015     0.980472     0.676058       35     1020     17     10.266     6.940     66.514     1.127     0.015     0.976602     0.676004       36     1050     17.5     10.261     6.912     66.990     1.120     0.015     0.979672     0.671162       37     1080     18     10.307     6.926     67.620     1.115     0.015     0.985277     0.672762       38     1110     18.5     10.317     6.940     67.550     1.117     0.015     0.981673     0.672512       39     1140     19     10.297     6.940     67.144     1.121     0.015     0.981406     0.675415	32	930								
35     1020     17     10.266     6.940     66.514     1.127     0.015     0.976602     0.676004       36     1050     17.5     10.261     6.912     66.990     1.120     0.015     0.979672     0.671162       37     1080     18     10.307     6.926     67.620     1.115     0.015     0.985277     0.672762       38     1110     18.5     10.317     6.940     67.550     1.117     0.015     0.981673     0.672512       39     1140     19     10.297     6.940     67.144     1.121     0.015     0.981406     0.675415										
36     1050     17.5     10.261     6.912     66.990     1.120     0.015     0.979672     0.671162       37     1080     18     10.307     6.926     67.620     1.115     0.015     0.985277     0.672762       38     1110     18.5     10.317     6.940     67.550     1.117     0.015     0.981673     0.672512       39     1140     19     10.297     6.940     67.144     1.121     0.015     0.981406     0.675415										
37     1080     18     10.307     6.926     67.620     1.115     0.015     0.985277     0.672762       38     1110     18.5     10.317     6.940     67.550     1.117     0.015     0.981673     0.672512       39     1140     19     10.297     6.940     67.144     1.121     0.015     0.981406     0.675415										
38 1110 18.5 10.317 6.940 67.550 1.117 0.015 0.981673 0.672512 39 1140 19 10.297 6.940 67.144 1.121 0.015 0.981406 0.675415										
39 1140 19 10.297 6.940 67.144 1.121 0.015 0.981406 0.675415										
40 1170 19.5 10.291 6.954 66.738 1.126 0.015 0.980472 0.676058										
	40	1170	19.5	10.291	6.954	66.738	1.126	0.015	0.980472	U.676058

Table A1. (cont'd)

41	1200	20	10.273	6.940	66.668	1.126	0.015	0.97807	0.67499
42	1230	20.5	10.263	6.933	66.612	1.125	0.015	0.978604	0.675985
43	1260	21	10.276	6.968	66.164	1.133	0.015	0.980472	0.680142
44	1290	21.5	10.266	7.017	64.974	1.151	0.015	0.976602	0.686936
45	1320	22	10.231	7.059	63.434	1.171	0.016	0.9738	0.693025
46	1350	22.5	10.228	7.087	62.818	1.181	0.016	0.976068	0.692781
47	1380	23	10.281	7.150	62.622	1.189	0.016	0.983942	0.698088
48	1410	23.5	10.331	7.262	61.376	1.214	0.016	0.985543	0.707786
49	1440	24	10.338	7.381	59.136	1.252	0.017	0.985277	0.720168
50	1470	24.5	10.309	7.437	57.442	1.278	0.017	0.980072	0.722631
51	1500	25	10.306	7.479	56.546	1.293	0.018	0.984743	0.72869
52	1530	25.5	10.343	7.584	55.188	1.321	0.018	0.987145	0.737732
53	1560	26	10.347	7.682	53.312	1.356	0.019	0.985543	0.747055
54	1590	26.5	10.341	7.773	51.366	1.393	0.019	0.985944	0.756226
55	1620	27	10.360	7.871	49.784	1.426	0.020	0.989147	0.763222
56	1650	27.5	10.357	7.941	48.314	1.456	0.021	0.985277	0.770283
57	1680	28	10.329	8.004	46.508	1.491	0.022	0.983942	0.779466
58	1710	28.5	10.321	8.102	44.380	1.537	0.023	0.983675	0.79053
59	1740	29	10.303	8.151	43.036	1.566	0.023	0.980472	0.791752
60	1770	29.5	10.280	8.186	41.888	1.591	0.024	0.979405	0.80079
61	1800	30	10.280	8.263	40.348	1.628	0.025	0.980472	0.806724
62	1830	30.5	10.307	8.319	39.760	1.646	0.025	0.984476	0.80751
63	1860	31	10.344	8.389	39.102	1.666	0.026	0.987545	0.814459
64	1890	31.5	10.363	8.473	37.800	1.702	0.026	0.988079	0.820773
65	1920	32	10.389	8.529	37.212	1.720	0.027	0.992616	0.821054
66	1950	32.5	10.385	8.564	36.414	1.741	0.027	0.987145	0.828309
67	1980	33	10.358	8.592	35.322	1.769	0.028	0.987545	0.830676
68	2010	33.5	10.380	8.634	34.930	1.782	0.029	0.991415	0.832817
69	2040	34	10.395	8.683	34.244	1.804	0.029	0.990348	0.837758
70	2070	34.5	10.434	8.732	34.048	1.813	0.029	0.998889	0.835939
71	2100	35	10.440	8.767	33.460	1.831	0.030	0.991415	0.843586
72	2130	35.5	10.399	8.788	32.228	1.865	0.031	0.991148	0.846506
73	2160	36	10.402	8.823	31.584	1.885	0.032	0.991949	0.849859
74	2190	36.5	10.381	8.837	30.884	1.905	0.032	0.987145	0.852643
7 <b>5</b>	2220	37	10.339	8.830	30.184	1.924	0.032	0.983942	0.855418
76	2250	37.5	10.333	8.830	30.058	1.928	0.033	0.985944	0.853682
77	2280	38	10.372	8.858	30.282	1.924	0.033	0.991415	0.854355
78	2310	38.5	10.440	8.935	30.100	1.937	0.033	0.998889	0.857315
79	2340	39	10.465	8.984	29.624	1.955	0.034	0.99622	0.859612
80	2370	39.5	10.461	8.998	29.260	1.967	0.034	0.998088	0.860677
81	2400	40	10.452	9.026	28.518	1.992	0.035	0.994485	0.866479
82	2430	40.5	10.450	9.047	28.070	2.008	0.036	0.997821	0.864919
83	2460	41	10.430	9.061	27.762	2.019	0.036	0.994218	0.869396
84	2490	41.5	10.420	9.054	27.314	2.032	0.037	0.992216	0.86846
	2 <del>49</del> 0 2520	42	10.425	9.047	27.160	2.032	0.037	0.991415	0.870507
85 86	2520 2550	42.5	10.405	9.054	26.642	2.054	0.037	0.988613	0.870307
87	2550 2580	42.5 43	10.364	9.047	26.334	2.063	0.038	0.987145	0.872973
88	2610	43 43.5	10.364	9.047	26.334	2.063	0.038	0.988613	0.872975
89	2640	43.5 44	10.304	9.047	26.488	2.063	0.038	0.995285	0.872486
	2670	44.5	10.400	9.117	26.082	2.078	0.038	0.993265	0.877238
90	20/0	<del>44</del> .3	10.421	<del>5</del> .117	20.002	2.070	0.030	U.33 14 13	0.011230

Table A1. (cont'd)

91	2700	45	10.386	9.124	25.242	2.108	0.040	0.988613	0.879725
92	2730	45.5	10.333	9.103	24.612	2.128	0.041	0.981406	0.882105
93	2760	46	10.301	9.068	24.668	2.122	0.041	0.982474	0.87843
94	2790	46.5	10.329	9.061	25.368	2.097	0.039	0.986745	0.875981
95	2820	47	10.368	9.096	25.452	2.098	0.039	0.989947	0.878539
96	2850	47.5	10.401	9.152	24.990	2.119	0.040	0.993017	0.881199
97	2880	48	10.424	9.201	24.458	2.143	0.041	0.994218	0.884161
98	2910	48.5	10.399	9.194	24.108	2.155	0.041	0.988346	0.884013
99	2940	49	10.370	9.163	24.136	2.151	0.041	0.988613	0.883234
1	3030	50.5	31.364	27.752	72.240	2.161		1.004494	0.886409
2	3090	51.5	20.979	18.630	46.984	2.189	0.043	0.995285	0.889649
3	3150	52.5	20.920	18.616	46.088	2.206	0.043	0.998889	0.890047
4	3210	53.5	20.955	18.638	46.340	2.202	0.043	0.998622	0.888815
5	3270	54.5	21.010	18.689	46.424	2.203	0.043	1.004093	0.890218
6	3330	55.5	21.031	18.777	45.080	2.233	0.044	1.000624	0.895439
7	3390	56.5	20.989	18.761	44.548	2.243	0.045	1.00009	0.892314
8	3450	57.5	20.930	18.749	43.624	2.261	0.046	0.995019	0.899276
9	3510	58.5	20.839	18.718	42.420	2.285	0.047	0.991415	0.89716
10	3570	59.5	20.854	18.686	43.372	2.263	0.046	0.996487	0.894871
11	3630	60.5	20.987	18.775	44.240	2.250	0.045	1.004093	0.894338
12	3690	61.5	21.083	18.929	43.064	2.281	0.046	1.005561	0.901393
13	3750	62.5	21.102	19.025	41.552	2.318	0.048	1.005962	0.901698
14	3810	63.5	21.087	19.013	41.468	2.319	0.048	1.004093	0.901648
15	3870	64.5	21.004	18.925	41.580	2.313	0.048	0.998088	0.900388
16	3930	65.5	20.968	18.879	41.776	2.306	0.048	1.000624	0.900373
17	3990	66.5	21.000	18.934	41.328	2.319	0.048	1.001157	0.902826
18	4050	67.5	21.034	18.921	42.252	2.298	0.047	1.003826	0.896304
19	4110	68.5	21.014	18.955	41.188	2.323	0.049	0.999289	0.907719
20	4170	69.5	20.943	18.967	39.508	2.361	0.051	0.99702	0.903627
21	4230	70.5	20.947	18.903	40.880	2.327	0.049	0.999689	0.901215
22	4290	71.5	21.021	18.956	41.300	2.320	0.048	1.004093	0.902313
23	4350	72.5	21.010	18.987	40.460	2.340	0.049	0.998622	0.905118
24	4410	73.5	20.990	18.970	40.404	2.341	0.050	1.002225	0.902397
25	4470	74.5	21.017	18.999	40.348	2.344	0.050	1.001157	0.905625
26	4530	75.5	20.971	19.074	37.940	2.403	0.053	0.997821	0.913468
27	4590	76.5	20.889	19.027	37.240	2.418	0.054	0.993417	0.908248
28	4650	77.5	20.803	18.893	38.192	2.388	0.052	0.989547	0.908159
29	4710	78.5	20.703	18.805	37.968	2.389	0.053	0.983942	0.90845
30	4770	79.5	20.707	18.787	38.416	2.378	0.052	0.989947	0.906039
31	4830	80.5	20.745	18.812	38.668	2.373	0.052	0.987545	0.907568
32	4890	81.5	20.745	18.780	38.724	2.370	0.052	0.987145	0.905502
33	4950	82.5	20.710	18.833	39.396	2.357	0.052	0.995819	0.905119
	5010	83.5	20.880	18.946	38.668	2.379	0.051	0.994485	0.909689
34 35	5070	84.5	20.825	18.969	37.128	2.37 <del>9</del> 2.418	0.052	0.990615	0.91203
36	5130	85.5	20.823	18.917	38.052	2.393	0.053	0.993951	0.905209
36 37	5130	86.5	20.919	18.936	39.340	2.363	0.053	0.998622	0.906588
	5250	87.5	20.964	19.041	38.444	2.389	0.051	0.999689	0.910025
38 30			20.987	19.041	37.940	2.30 <del>9</del> 2.404	0.052	1.00089	0.910025
39 40	5310 5370	88.5 80.5	20.967	19.090	37.548	2.40 <del>4</del> 2.414	0.053	0.998889	0.9092
40	5370	89.5						1.003826	0.909731
41	5430	90.5	21.010	19.135	37.492	2.417	0.053	1.003020	0.808731

Table A1. (cont'd)

42	5490	91.5	21.069	19.174	37.884	2.409	0.053	1.004494	0.910456
43	5550	92.5	21.087	19.188	37.968	2.408	0.053	1.005561	0.909489
44	5610	93.5	21.119	19.230	37.772	2.414	0.053	1.007563	0.911656
45	5670	94.5	21.192	19.330	37.240	2.432	0.054	1.012501	0.912614
46	5730	95.5	21.155	19.274	37.632	2.420	0.053	1.004093	0.90949
47	5790	96.5	21.064	19.174	37.800	2.411	0.053	1.003826	0.911061
48	5850	97.5	21.010	19.177	36.652	2.439	0.055	0.998889	0.914496
49	5910	98.5	21.024	19.173	37.016	2.430	0.054	1.005161	0.909453
50	5970	99.5	21.083	19.212	37.408	2.422	0.053	1.004494	0.913113
51	6030	100.5	21.014	19.216	35.952	2.459	0.056	0.998622	0.915809
52	6090	101.5	21.010	19.211	35.980	2.458	0.056	1.004093	0.912945
53	6150	102.5	21.126	19.291	36.708	2.443	0.054	1.009698	0.913296
54	6210	103.5	21.175	19.358	36.344	2.456	0.055	1.008764	0.915068
55	6270	104.5	21.155	19.383	35.448	2.480	0.056	1.00783	0.917373
56	6330	105.5	21.143	19.363	35.588	2.475	0.056	1.007563	0.914305
57	6390	106.5	21.108	19.284	36.484	2.449	0.055	1.004494	0.912847
58	6450	107.5	21.168	19.331	36.736	2.444	0.054	1.013301	0.913605
59	6510	108.5	21.294	19.496	35.952	2.472	0.056	1.016504	0.917553
60	6570	109.5	21.398	19.569	36.568	2.460	0.055	1.023177	0.911569
1	6690	111.5	42.997	39.096	78.008	2.400		1.026113	0.90701
2	6810	113.5	42.946	39.200	74.928	2.439	0.053	1.020775	0.918551
3	6930	115.5	42.868	39.298	71.400	2.486	0.056	1.022376	0.914894
4	7050	117.5	42.731	39.239	69.832	2.505	0.057	1.014236	0.921711
5	7170	119.5	42.568	39.141	68.544	2.519	0.058	1.014636	0.917269
6	7290	121.5	42.678	39.127	71.008	2.487	0.056	1.01944	0.91635
7	7410	123.5	42.756	39.214	70.840	2.491	0.056	1.018373	0.917966
8	7530	125.5	42.812	39.312	70.000	2.504	0.057	1.022109	0.918527
9	7650	127.5	42.890	39.480	68.208	2.532	0.059	1.022109	0.922444
10	7770	129.5	42.952	39.640	66.248	2.562	0.060	1.025045	0.923317
11	7890	131.5	43.137	39.746	67.816	2.543	0.059	1.030917	0.919482
12	8010	133.5	43.238	39.844	67.872	2.545	0.059	1.02985	0.923545
13	8130	135.5	43.215	39.950	65.296	2.583	0.061	1.02985	0.92536
14	8250	137.5	43.193	39.990	64.064	2.602	0.062	1.028782	0.92632
15	8370	139.5	43.224	39.998	64.512	2.595	0.062	1.031318	0.924431
16	8490	141.5	43.364	40.149	64.288	2.602	0.062	1.035455	0.92731
17	8610	143.5	43.532	40.272	65.184	2.592	0.061	1.039325	0.922958
18	8730	145.5	43.613	40.362	65.016	2.596	0.062	1.039325	0.927966
19	8850	147.5	43.778	40.575	64.064	2.615	0.062	1.047198	0.925704
20	8970	149.5	44.036	40.799	64.736	2.610	0.062	1.051602	0.927284
21	9090	151.5	44.024	40.827	63.952	2.622	0.063	1.046665	0.927451
22	9210	153.5	43.949	40.849	61.992	2.652	0.065	1.047999	0.931491
23	9330	155.5	43.778	40.849	58.576	2.705	0.068	1.038524	0.934721
24	9450	157.5	43.358	40.494	57.288	2.717	0.070	1.027981	0.933143
25	9570	159.5	43.005	40.082	58.464	2.689	0.068	1.021709	0.930904
26	9690	161.5	42.983	39.934	60.984	2.646	0.066	1.026914	0.927225
27	9810	163.5	42.868	39.830	60.760	2.647	0.066	1.016237	0.931057
28	9930	165.5	42.829	39.855	59.472	2.667	0.067	1.025045	0.930087
29	10050	167.5	43.036	40.060	59.528	2.671	0.067	1.026113	0.931591
30	10170	169.5	43.075	40.191	57.680	2.704	0.069	1.026914	0.934503
31	10290	171.5	43.193	40.354	56.784	2.722	0.070	1.031718	0.934032

Table A1. (cont'd)

32	10410	173.5	43.392	40.575	56.336	2.735	0.071	1.036389	0.936132
33	10530	175.5	43.375	40.592	55.664	2.746	0.072	1.030917	0.935534
34	10650	177.5	43.294	40.466	56.560	2.728	0.071	1.032519	0.933824
35	10770	179.5	43.282	40.435	56.952	2.721	0.070	1.030383	0.934594
36	10890	181.5	43.221	40.452	55.384	2.748	0.072	1.029583	0.937265
37	11010	183.5	43.204	40.452	55.048	2.753	0.073	1.029583	0.935321
38	11130	185.5	43.095	40.340	55.104	2.750	0.073	1.024378	0.936816
39	11250	187.5	42.820	40.214	52.136	2.799	0.077	1.016504	0.941447
40	11370	189.5	42.666	40.144	50.456	2.828	0.079	1.017038	0.940297
41	11490	191.5	42.636	40.068	51.352	2.810	0.078	1.015036	0.939258
42	11610	193.5	42.624	40.020	52.080	2.795	0.077	1.016504	0.938558
43	11730	195.5	42.594	40.051	50.848	2.819	0.079	1.013568	0.942067
44	11850	197.5	42.610	40.186	48.496	2.866	0.082	1.017305	0.944116
45	11970	199.5	42.689	40.216	49.448	2.849	0.081	1.017305	0.94005
46	12090	201.5	42.974	40.250	54.488	2.758	0.073	1.030917	0.933204
47	12210	203.5	42.941	40.258	53.648	2.773	0.075	1.015704	0.941926
48	12330	205.5	42.790	40.345	48.888	2.862	0.082	1.023711	0.943814
49	12450	207.5	42.991	40.589	48.048	2.885	0.083	1.025312	0.944423
50	12570	209.5	43.120	40.706	48.272	2.883	0.083	1.02985	0.943631
1	12690	211.5	43.154	40.757	47.936	2.891	0.083	1.026914	0.945289
2	12810	213.5	43.075	40.723	47.040	2.908	0.085	1.026113	0.945507
3	12930	215.5	42.535	40.295	44.800	2.944	0.089	1.001157	0.949214
4	13050	217.5	42.874	40.491	47.656	2.890	0.084	1.042261	0.939821
5	13170	219.5	43.392	40.886	50.120	2.852	0.080	1.025846	0.944712
6	13290	221.5	43.047	40.748	45.976	2.930	0.087	1.025846	0.948484
7	13410	223.5	43.176	40.914	45.248	2.949	0.088	1.031985	0.946722
8	13530	225.5	43.243	40.914	46.592	2.921	0.086	1.029049	0.945532
9	13650	227.5	43.148	40.782	47.320	2.903	0.085	1.027447	0.944798
10	13770	229.5	43.126	40.774	47.040	2.909	0.085	1.027981	0.946125
11	13890	231.5	43.170	40.916	45.080	2.952	0.089	1.029583	0.949449
12	14010	233.5	43.285	41.034	45.024	2.956	0.089	1.033453	0.946539
13	14130	235.5	43.336	41.023	46.256	2.931	0.086	1.031985	0.946722
14	14250	237.5	43.193	40.933	45.192	2.950	0.089	1.026647	0.948655
15	14370	239.5	43.159	41.009	43.008	2.999	0.093	1.030383	0.95169
16	14490	241.5	43.226	41.143	41.664	3.033	0.096	1.02985	0.951924
17	14610	243.5	43.260	41.121	42.784	3.007	0.093	1.031985	0.949179
18	14730	245.5	43.316	41.051	45.304	2.951	0.088	1.032519	0.946232
19	14850	247.5	43.403	41.222	43.624	2.991	0.092	1.036122	0.953246
20	14970	249.5	43.540	41.527	40.264	3.074	0.099	1.039058	0.954277

Figure A1. Breakthrough curve, first order and second order plots for dry, clean Metea soil (pH 2) at 25°C

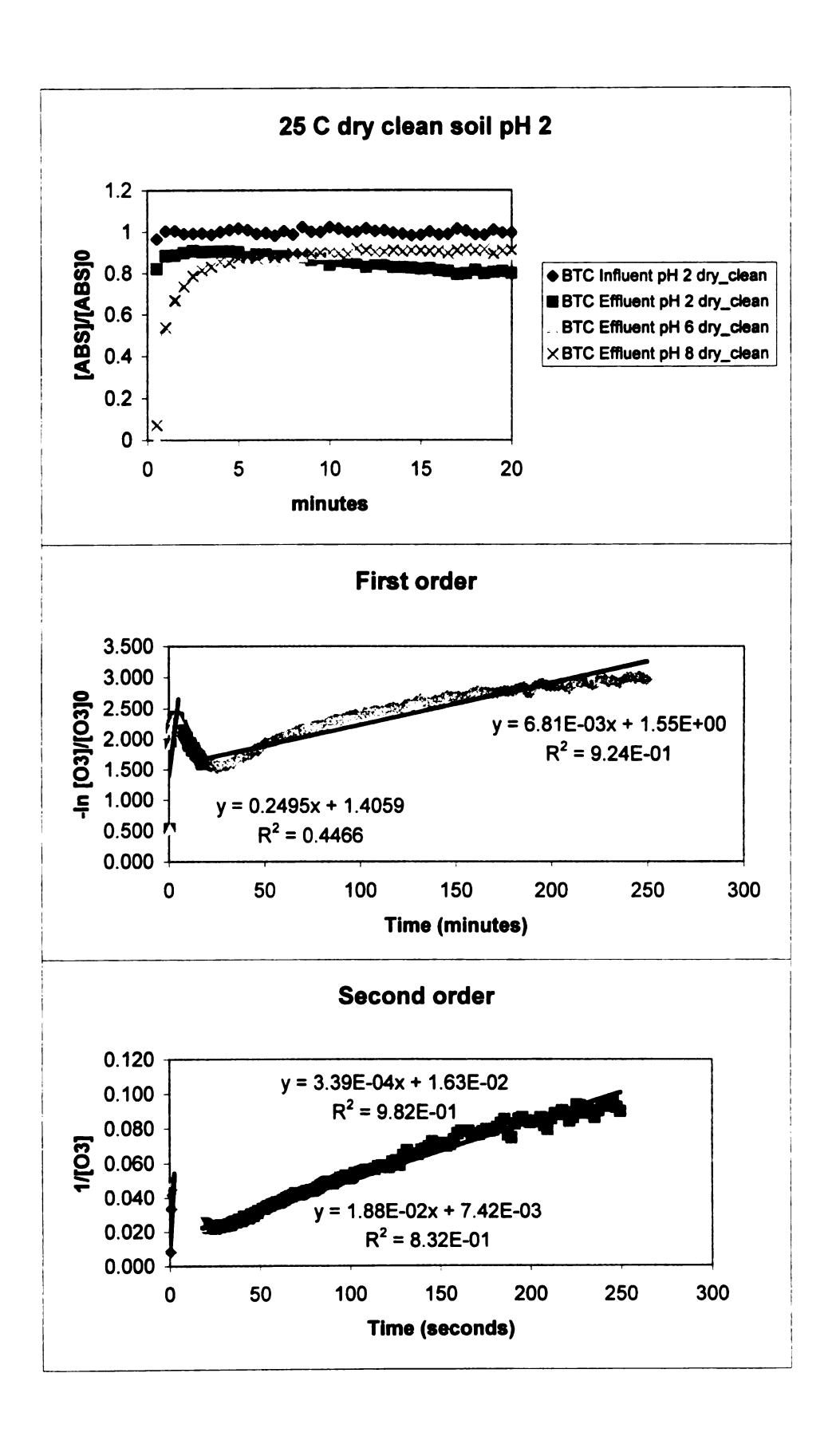
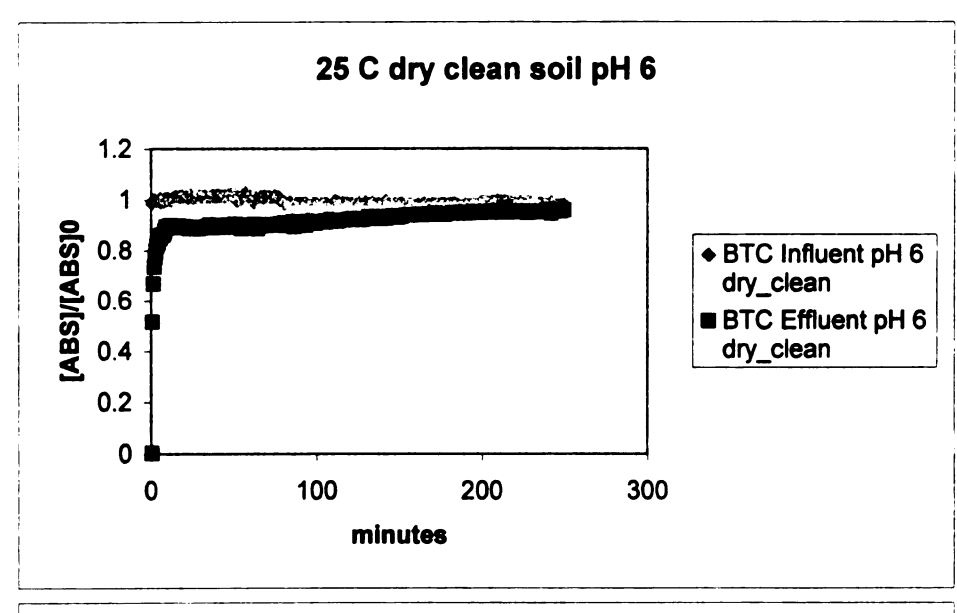
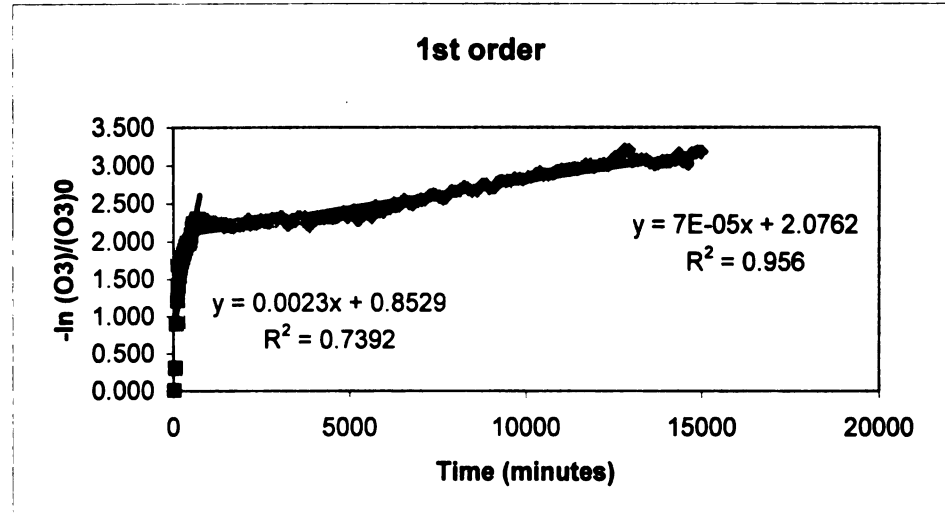


Figure A2. Breakthrough curve, first order and second order plots for dry, clean Metea soil (pH 6) at 25°C





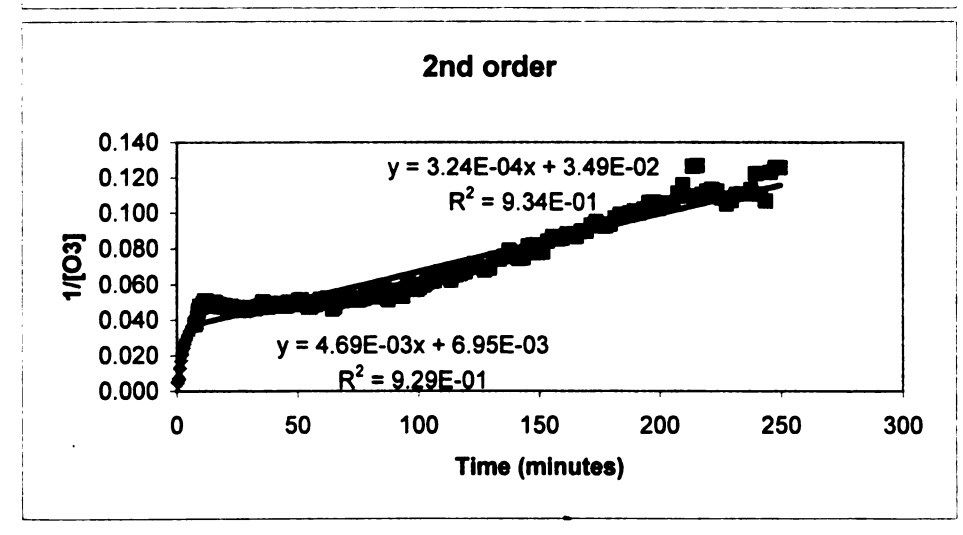


Figure A3. Breakthrough curve, first order and second order plots for dry, clean Metea soil (pH 8) at 25°C

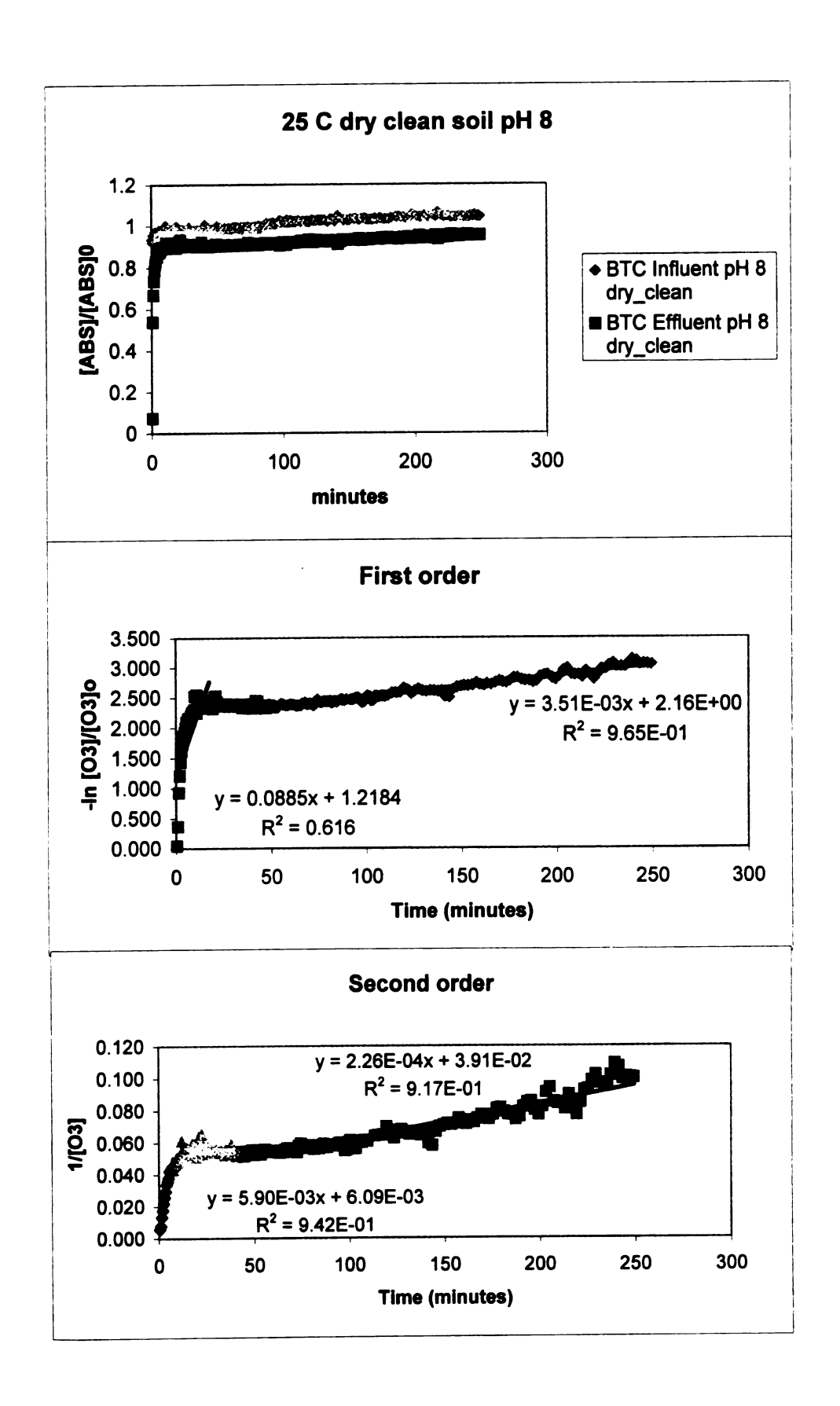
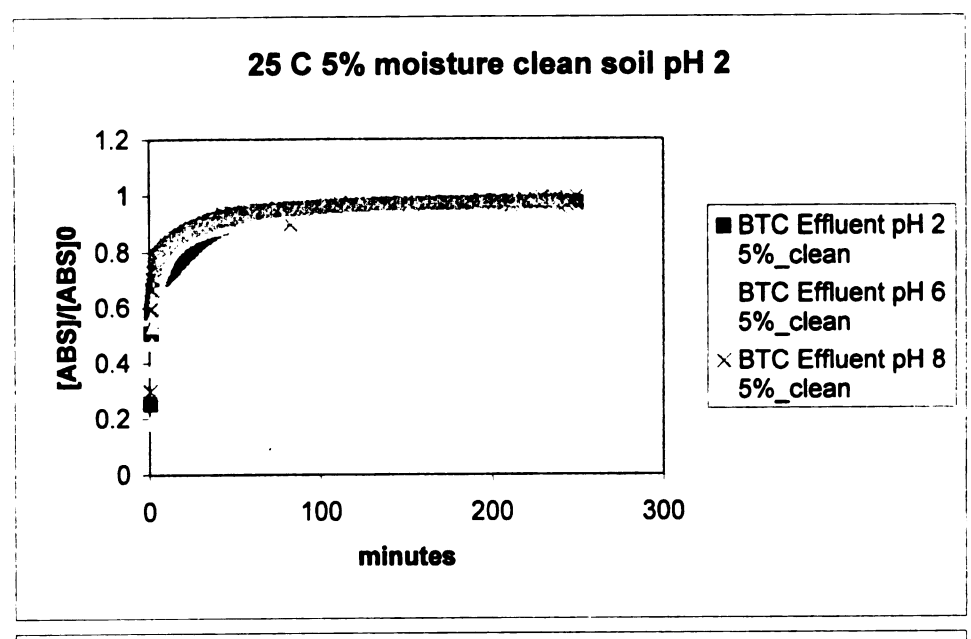
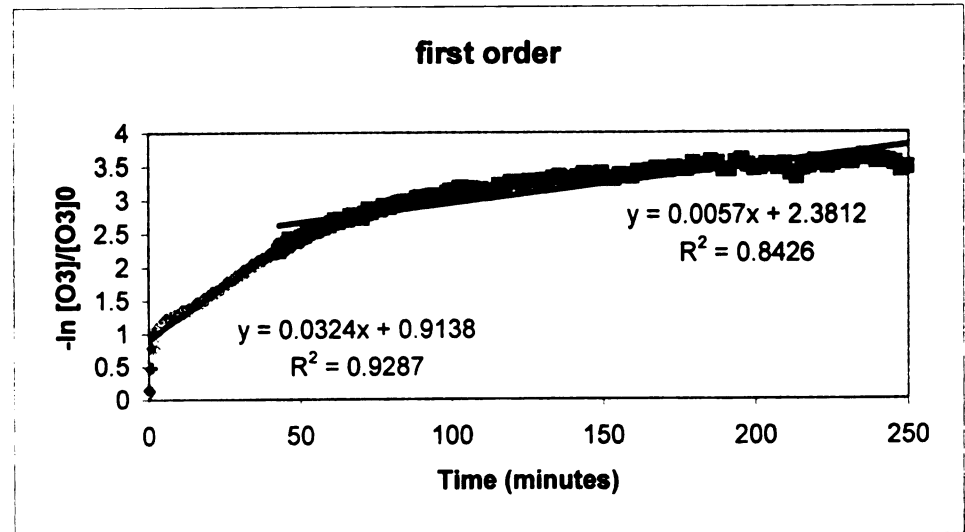


Figure A4. Breakthrough curve, first order and second order plots for 5% moisture, clean Metea soil (pH 2) at 25°C





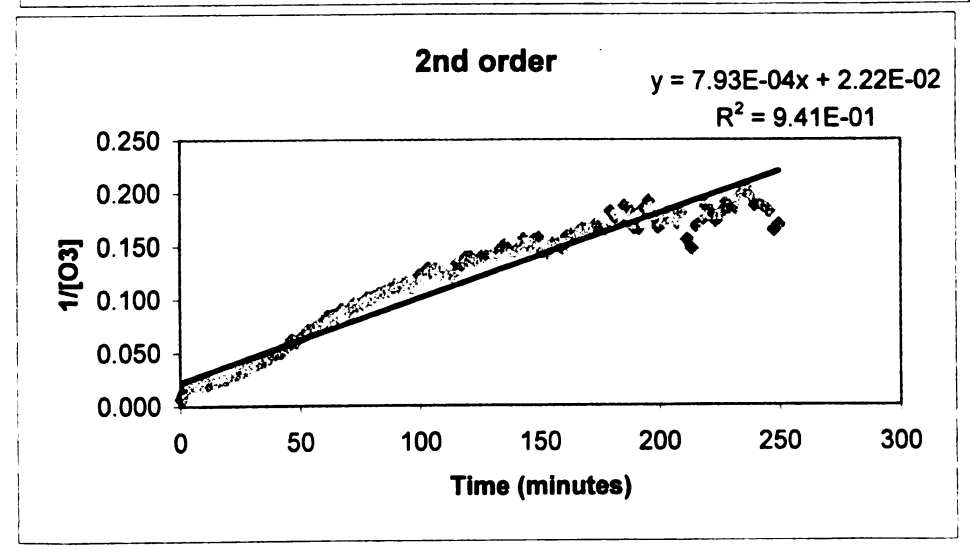
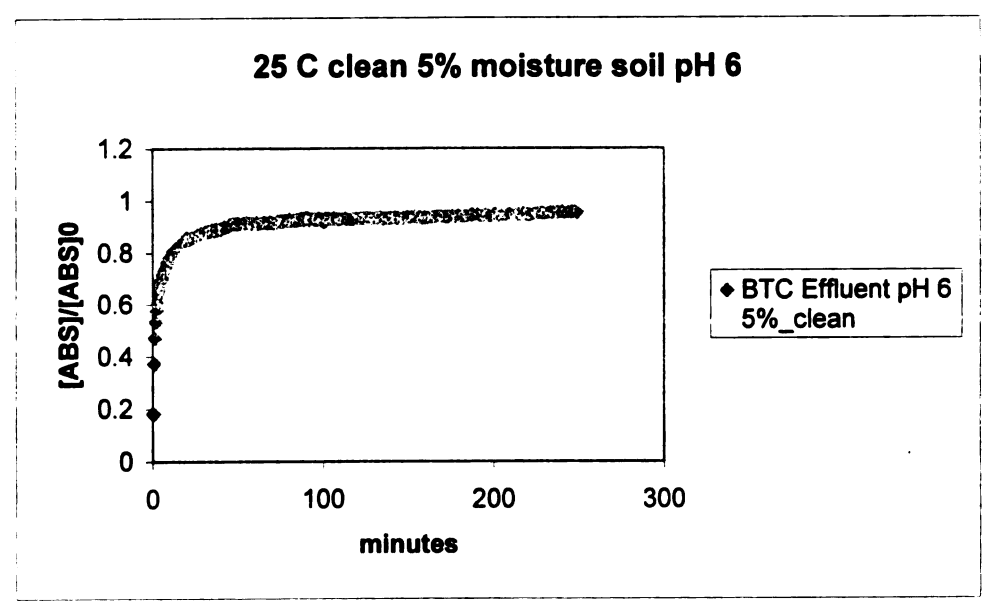
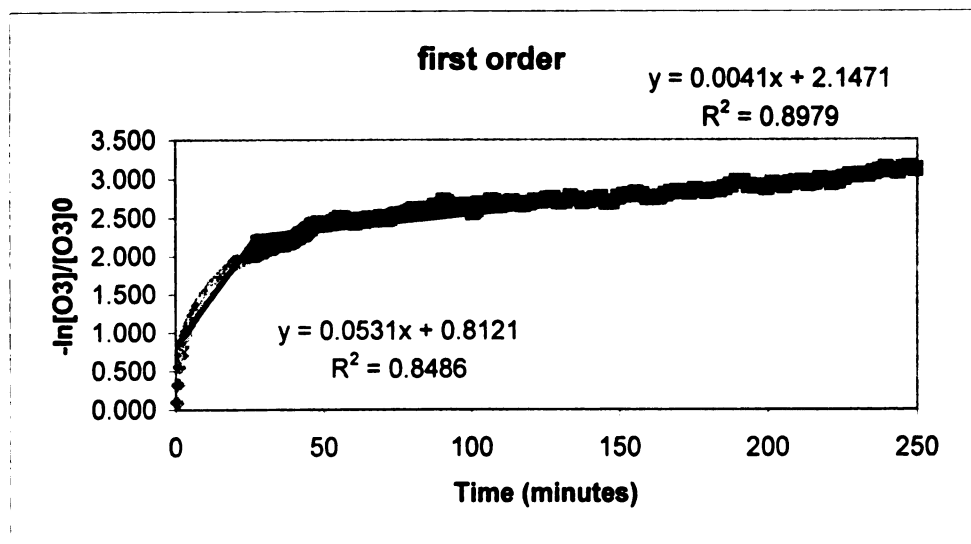


Figure A5. Breakthrough curve, first order and second order plots for 5% moisture, clean Metea soil (pH 6) at 25°C





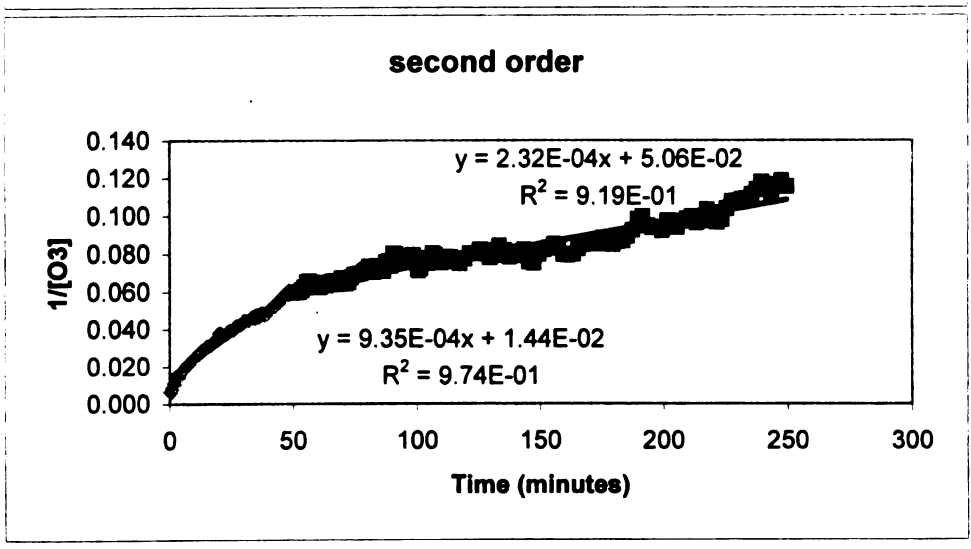
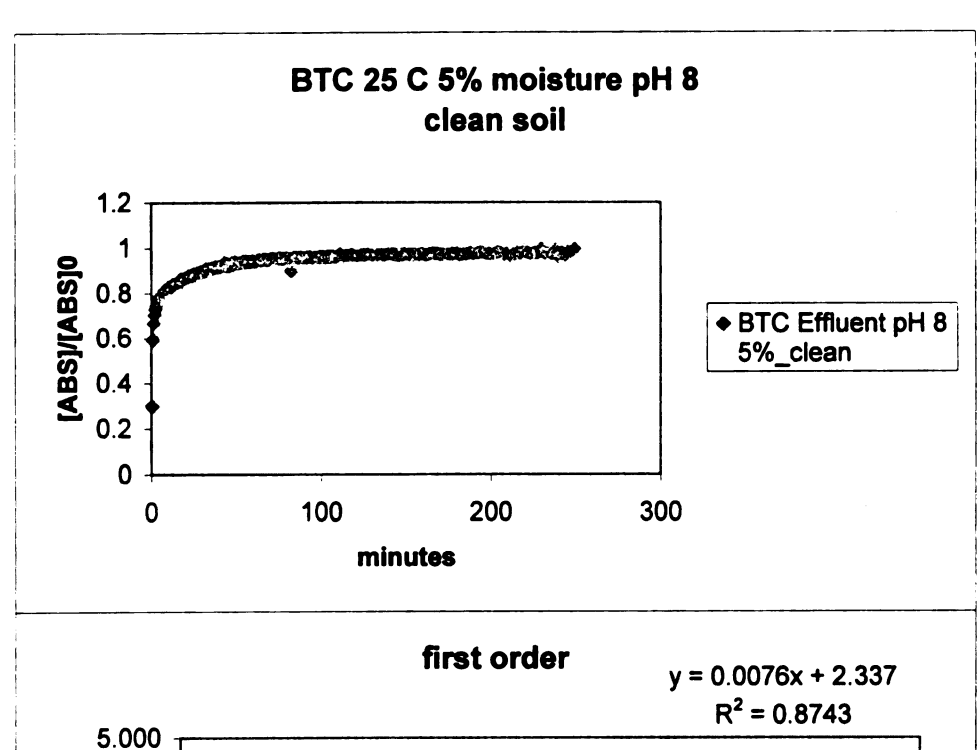
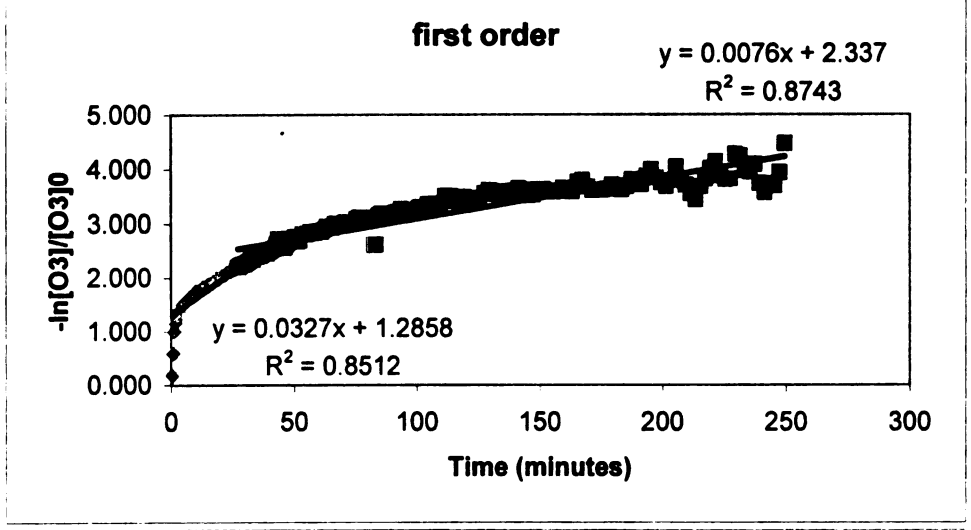


Figure A6. Breakthrough curve, first order and second order plots for 5% moisture, clean Metea soil (pH 8) at 25°C





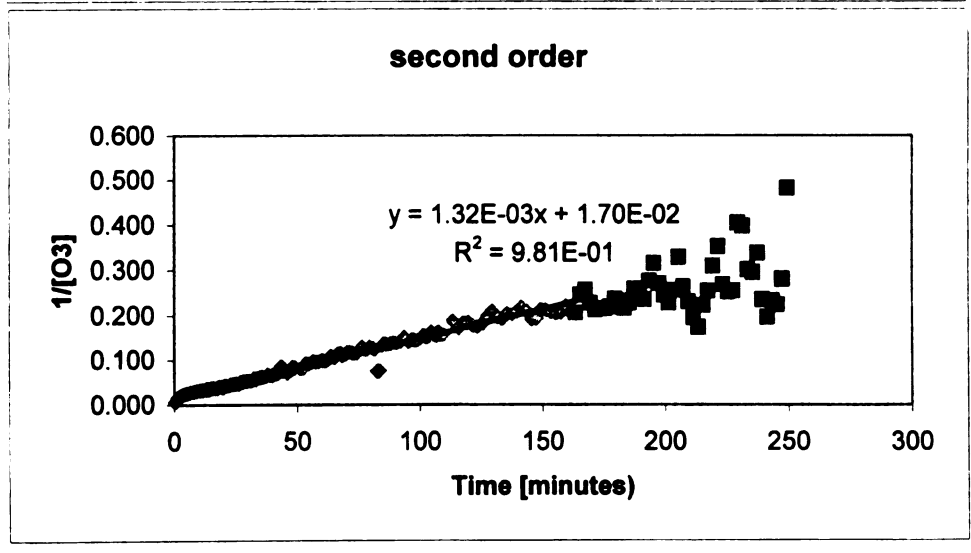


Figure A7. Breakthrough curve, first order and second order plots for 10% moisture, clean Metea soil (pH 2) at 25°C

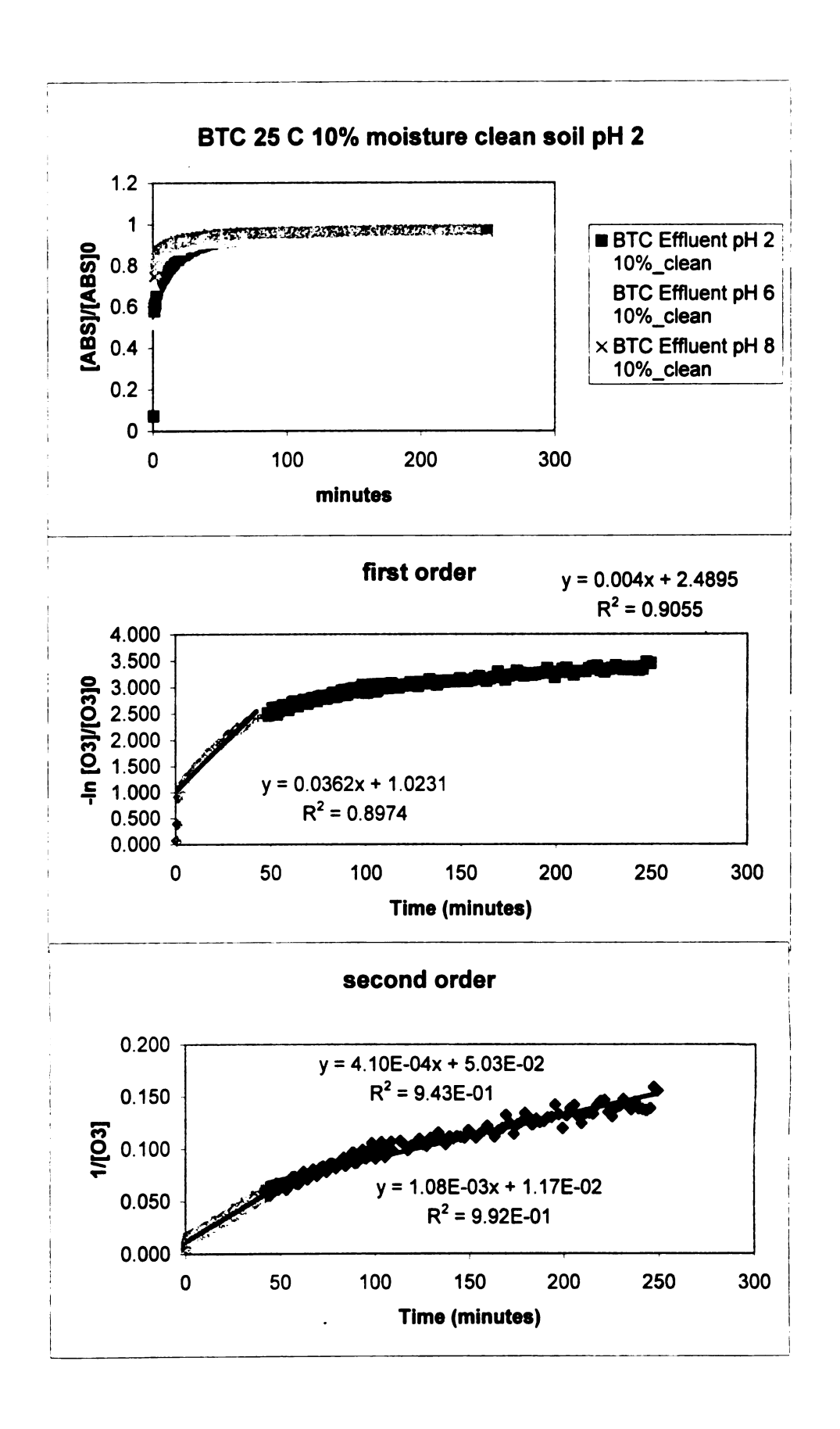


Figure A8. Breakthrough curve, first order and second order plots for 10% moisture, clean Metea soil (pH 6) at 25°C

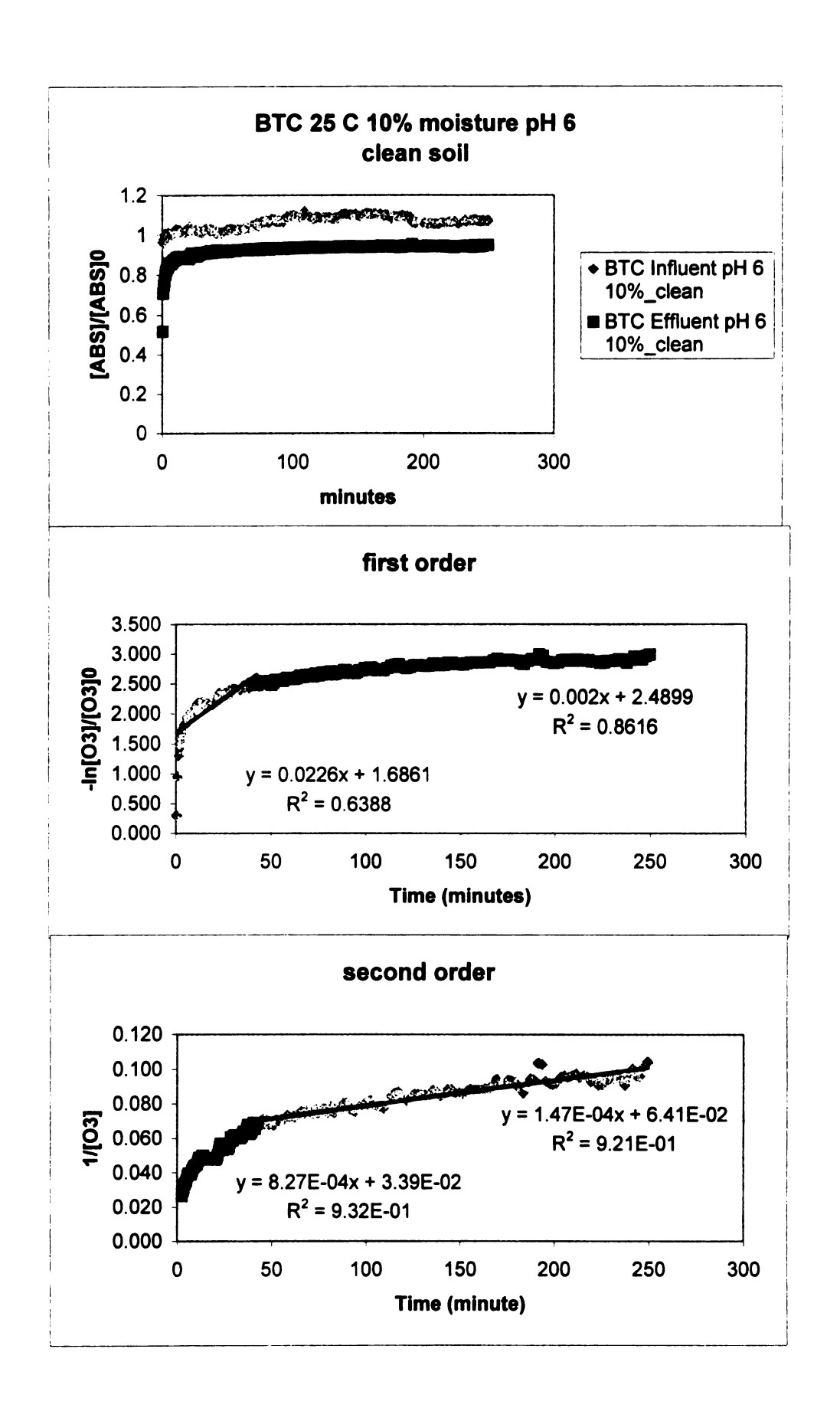
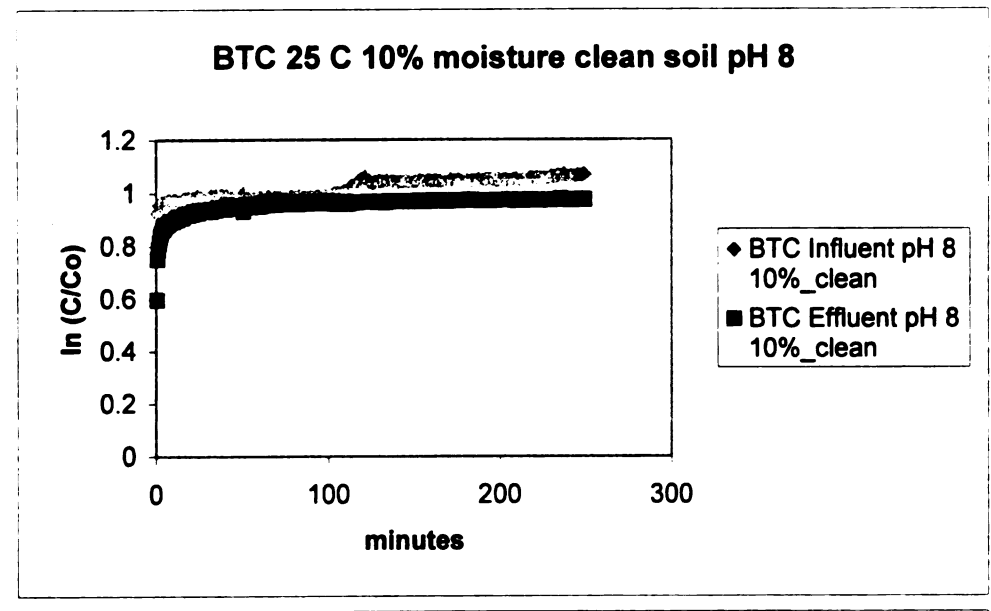
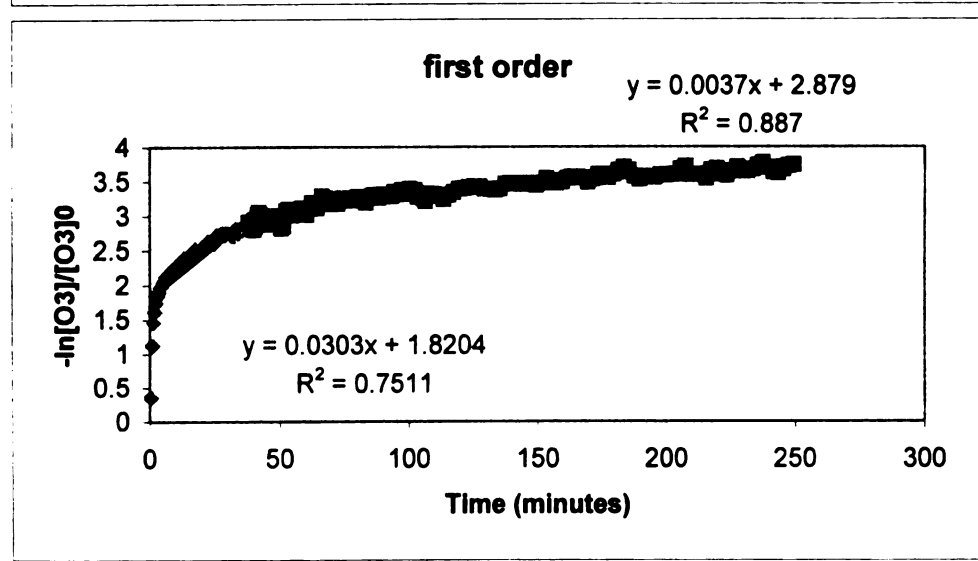


Figure A9. Breakthrough curve, first order and second order plots for 10% moisture, clean Metea soil (pH 8) at 25°C





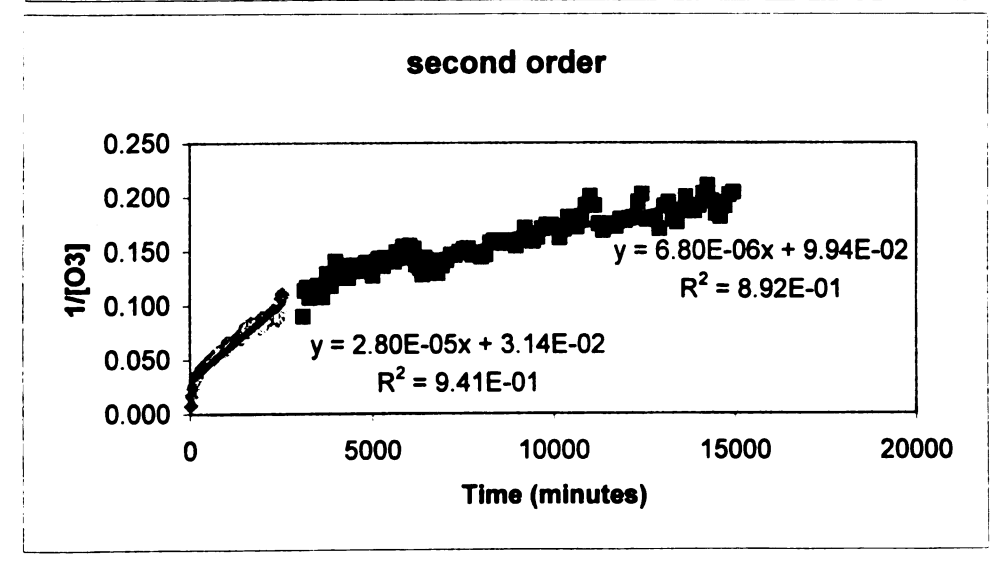


Figure A10. Breakthrough curve, first order and second order plots for dry, pyrene contaminated Metea soil (pH 2) at 25°C

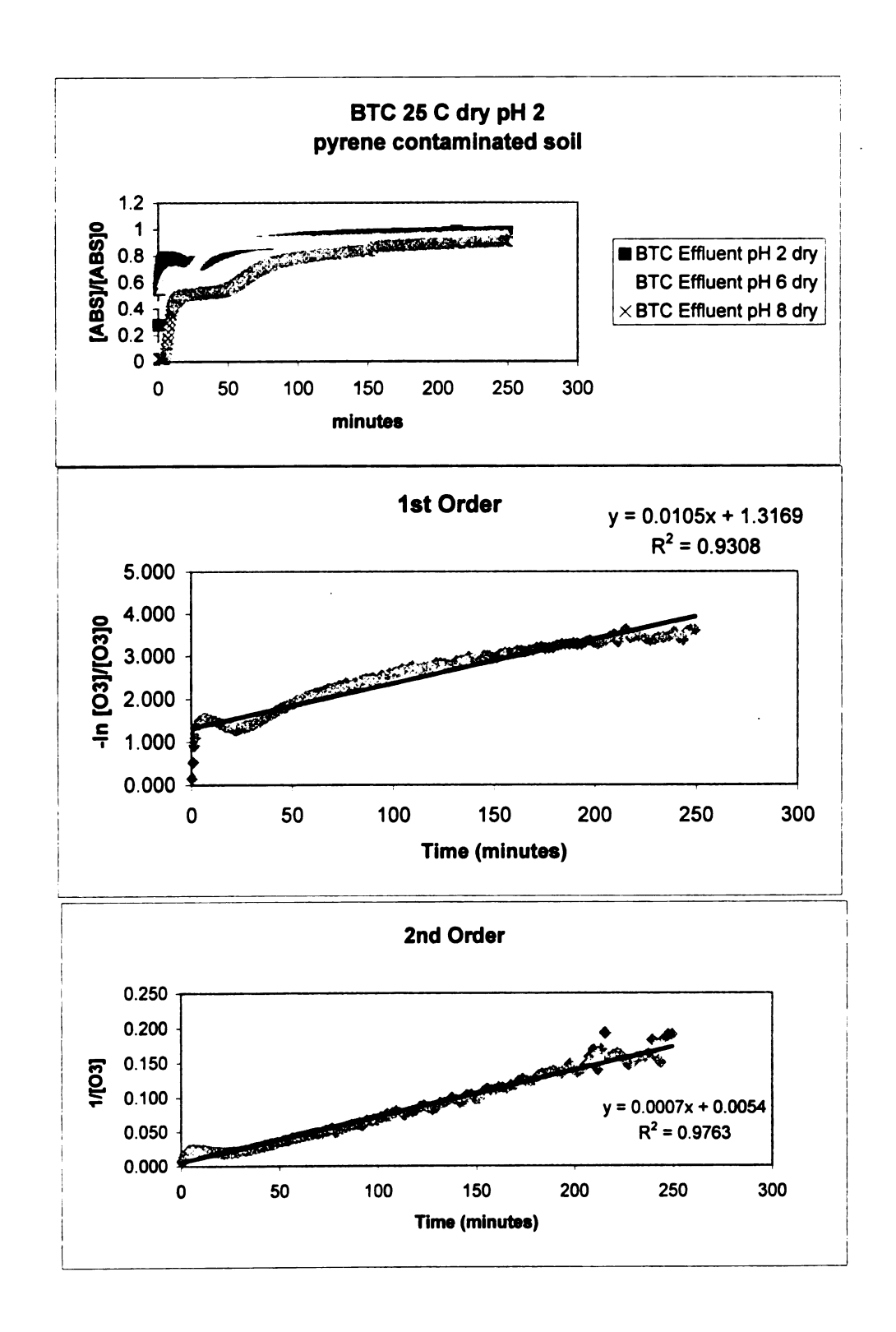


Figure A11. Breakthrough curve, first order and second order plots for dry, pyrene contaminated Metea soil (pH 6) at 25°C

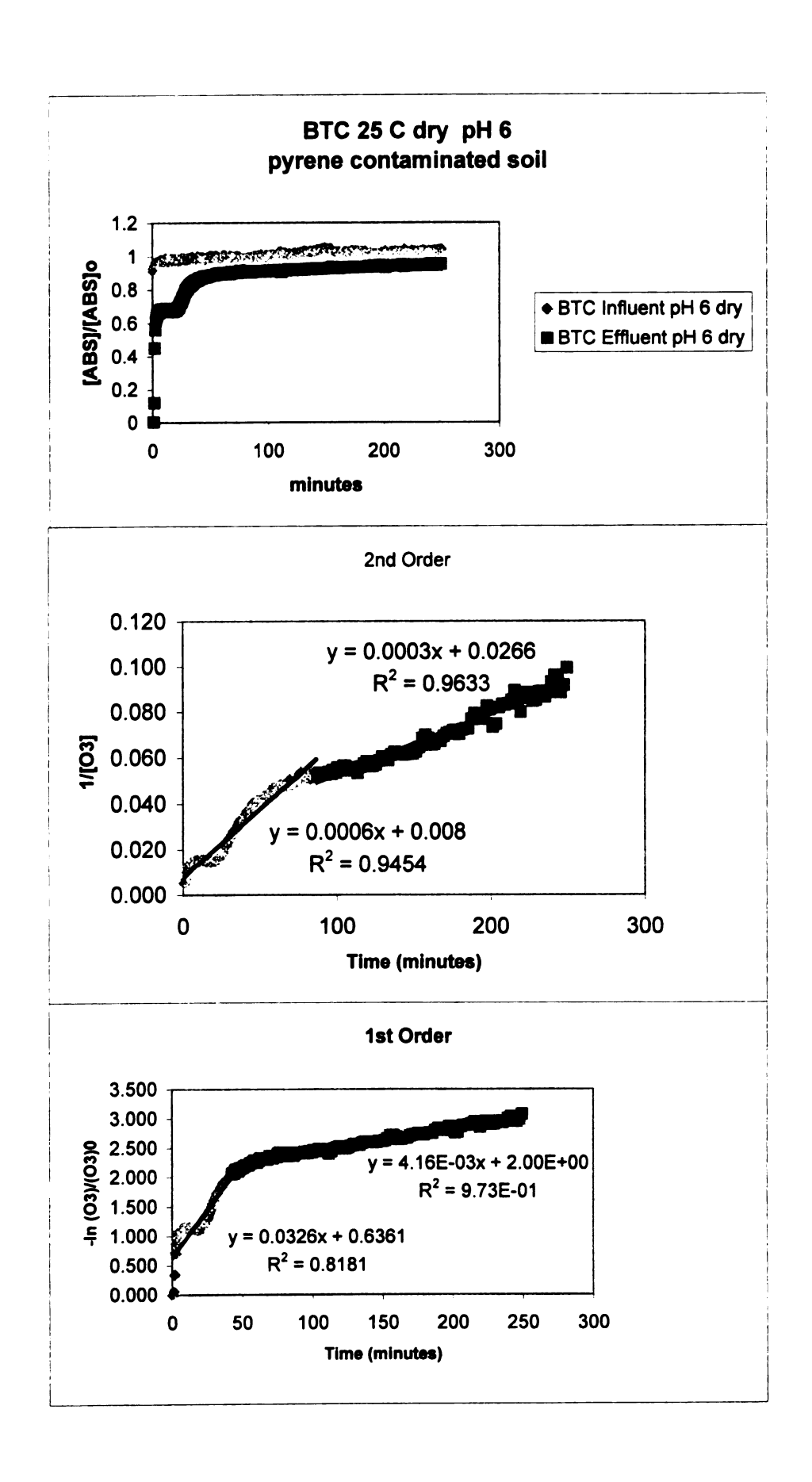


Figure A12. Breakthrough curve, first order and second order plots for dry, pyrene contaminated Metea soil (pH 8) at 25°C

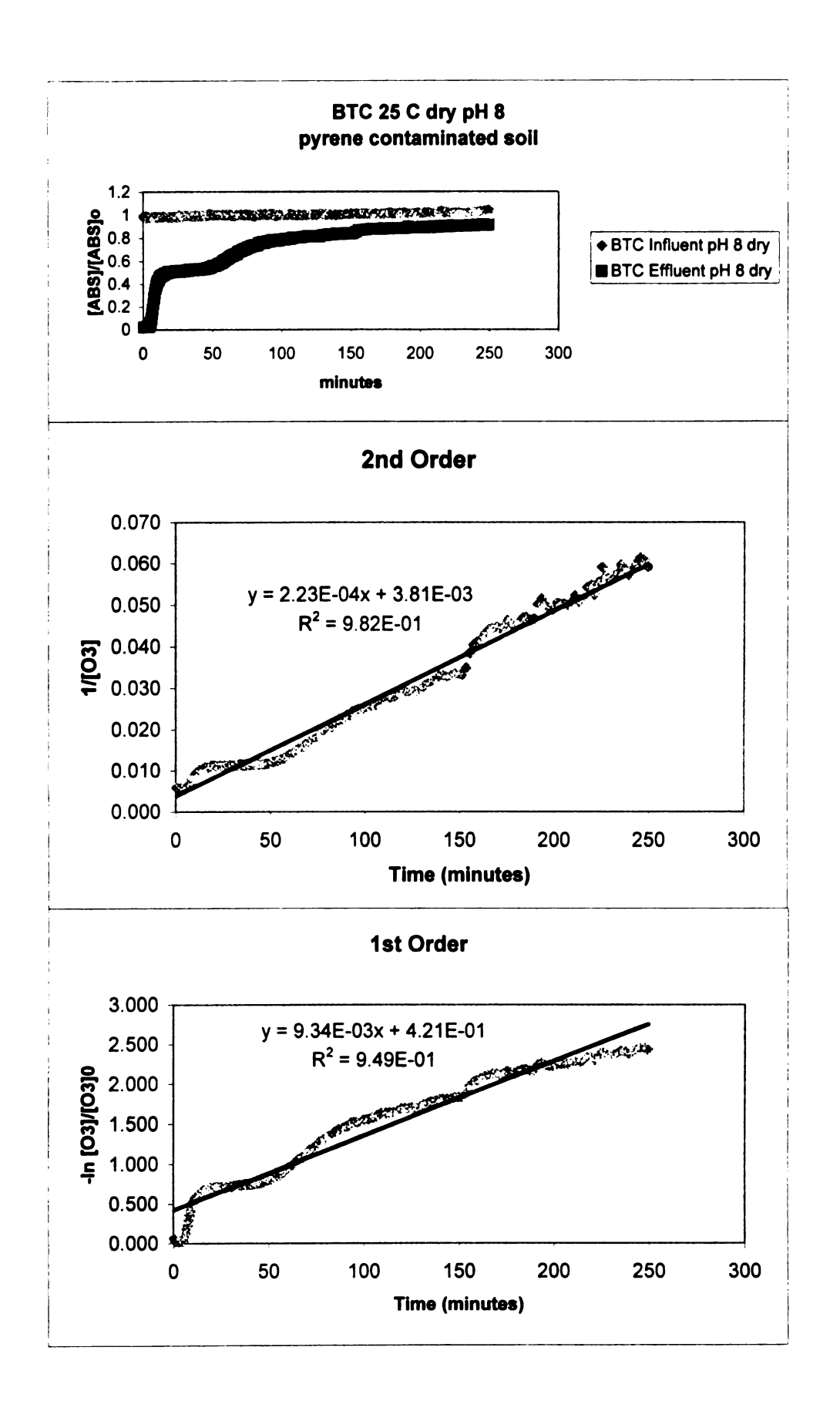


Figure A13. Breakthrough curve, first order and second order plots for 5% moisture, pyrene contaminated Metea soil (pH 2) at 25°C

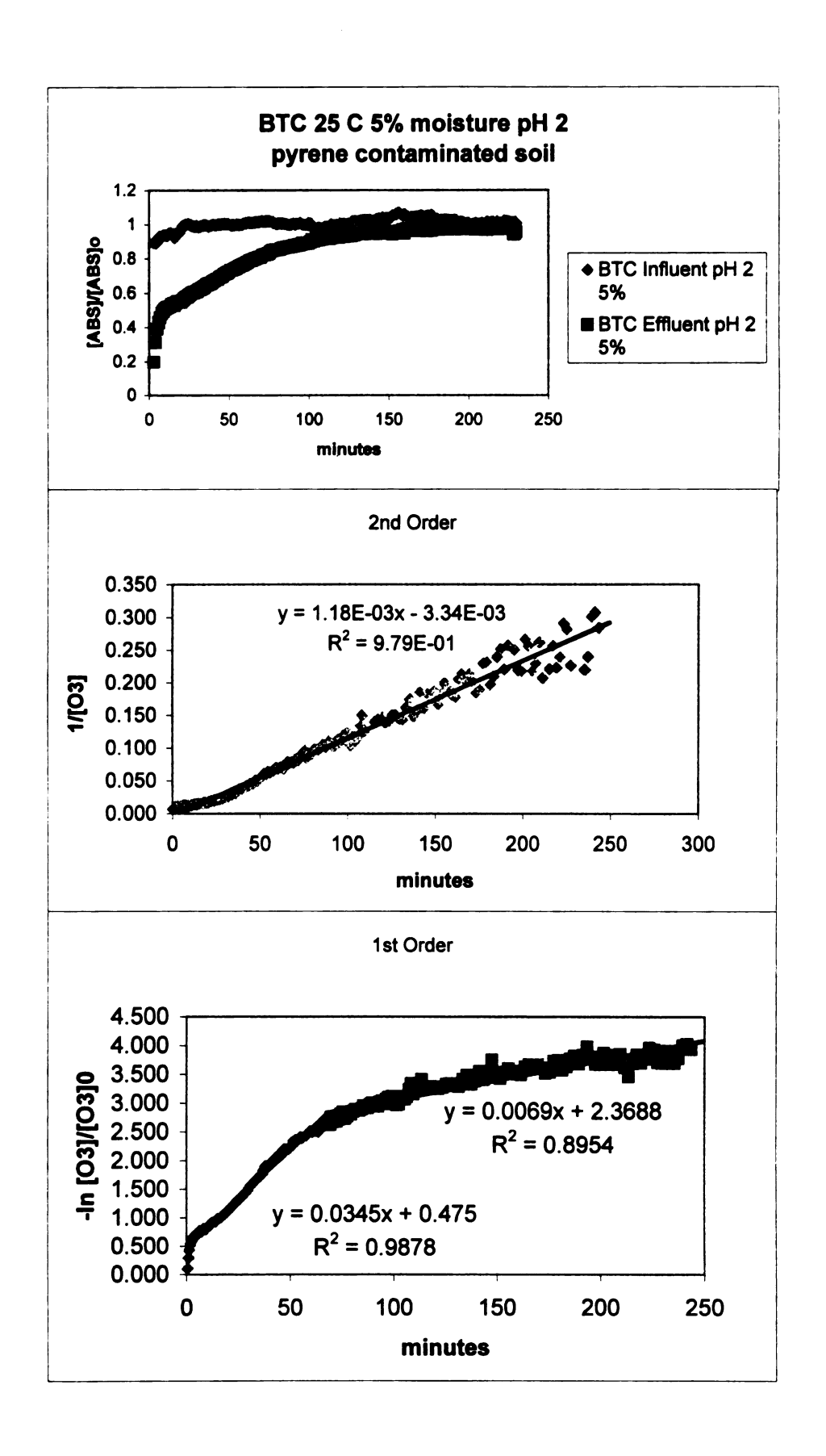
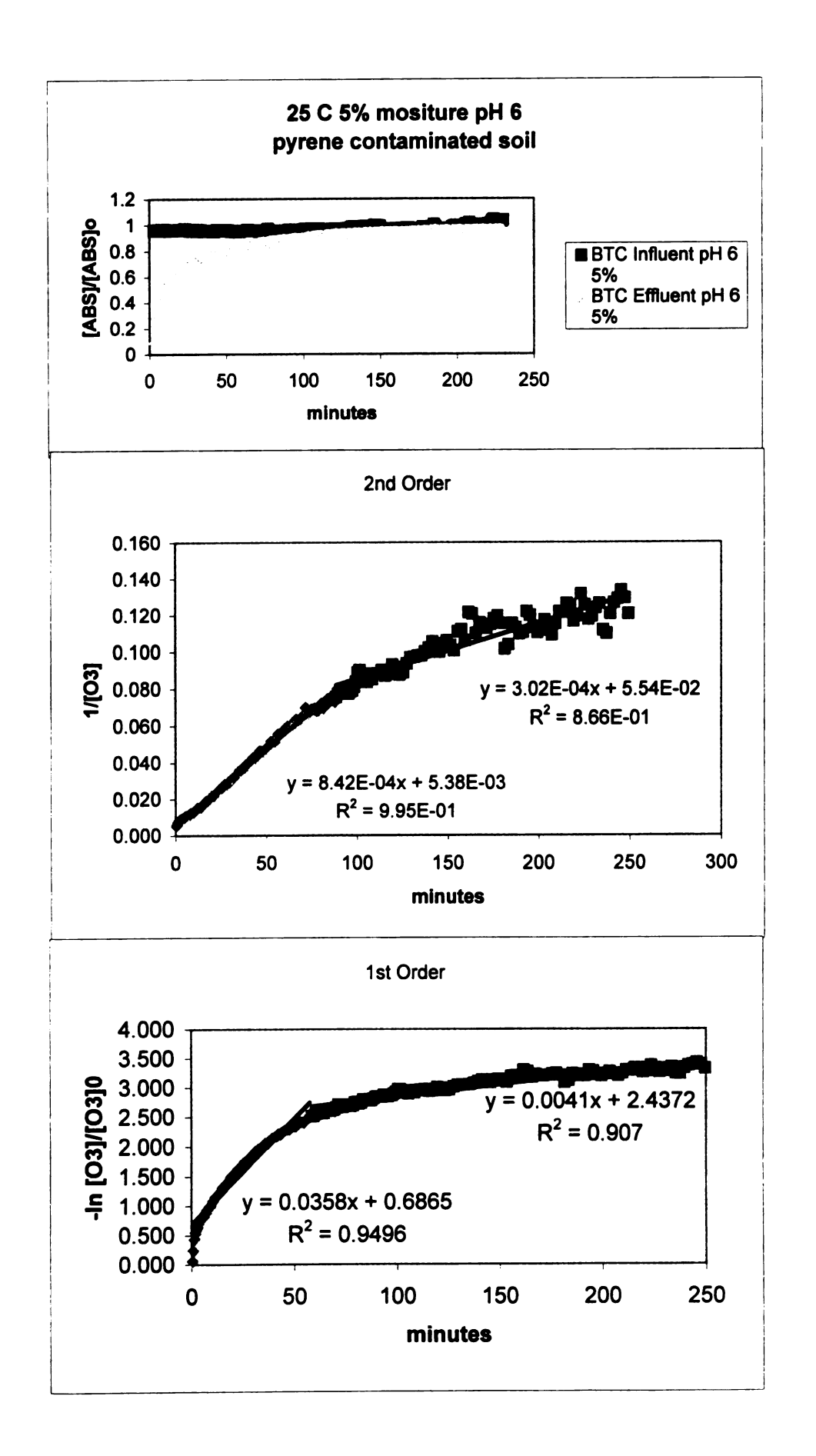
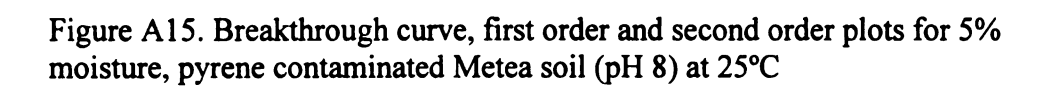


Figure A14. Breakthrough curve, first order and second order plots for 5% moisture, pyrene contaminated Metea soil (pH 6) at 25°C





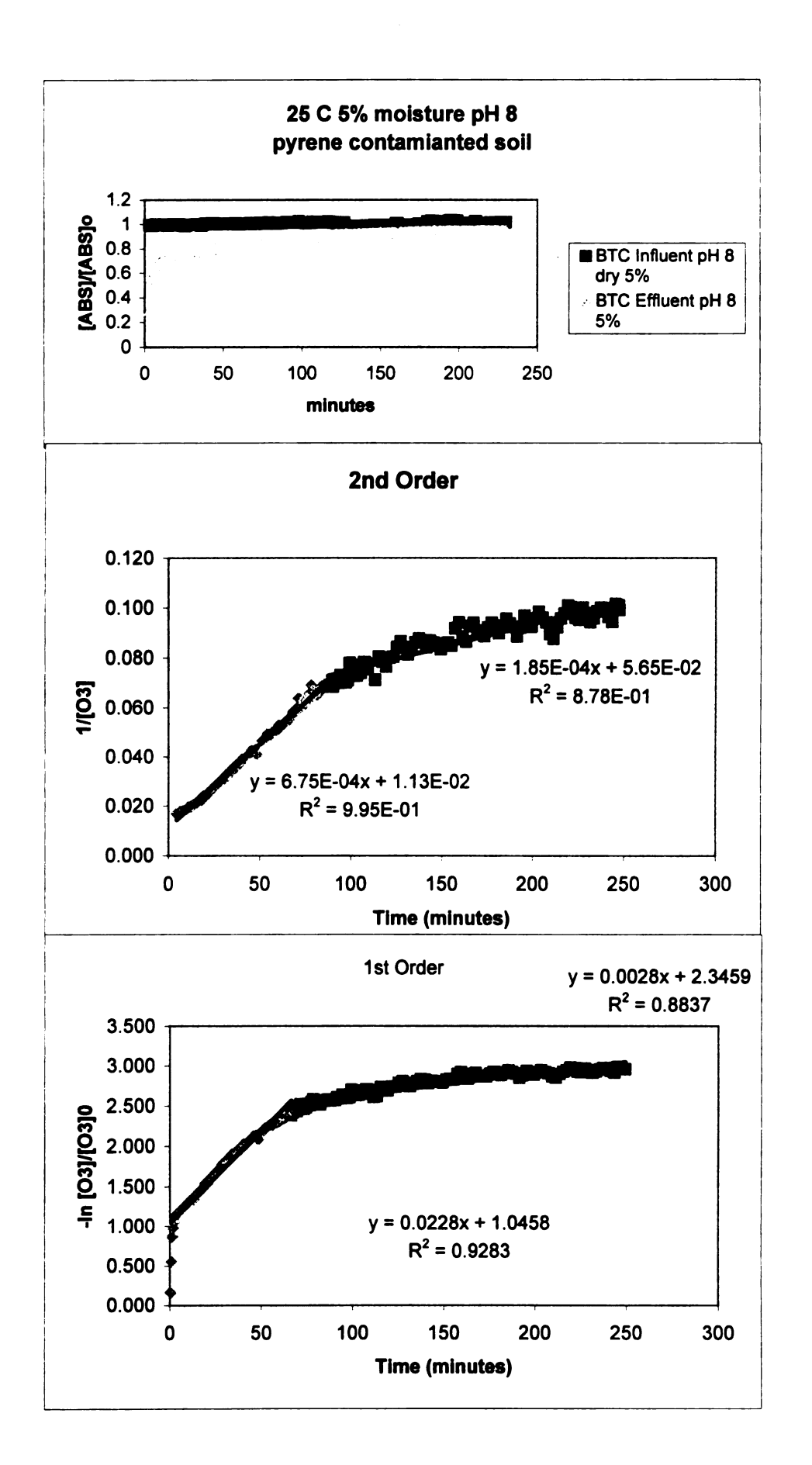


Figure A16. Breakthrough curve, first order and second order plots for 10% moisture, pyrene contaminated Metea soil (pH 2) at 25°C

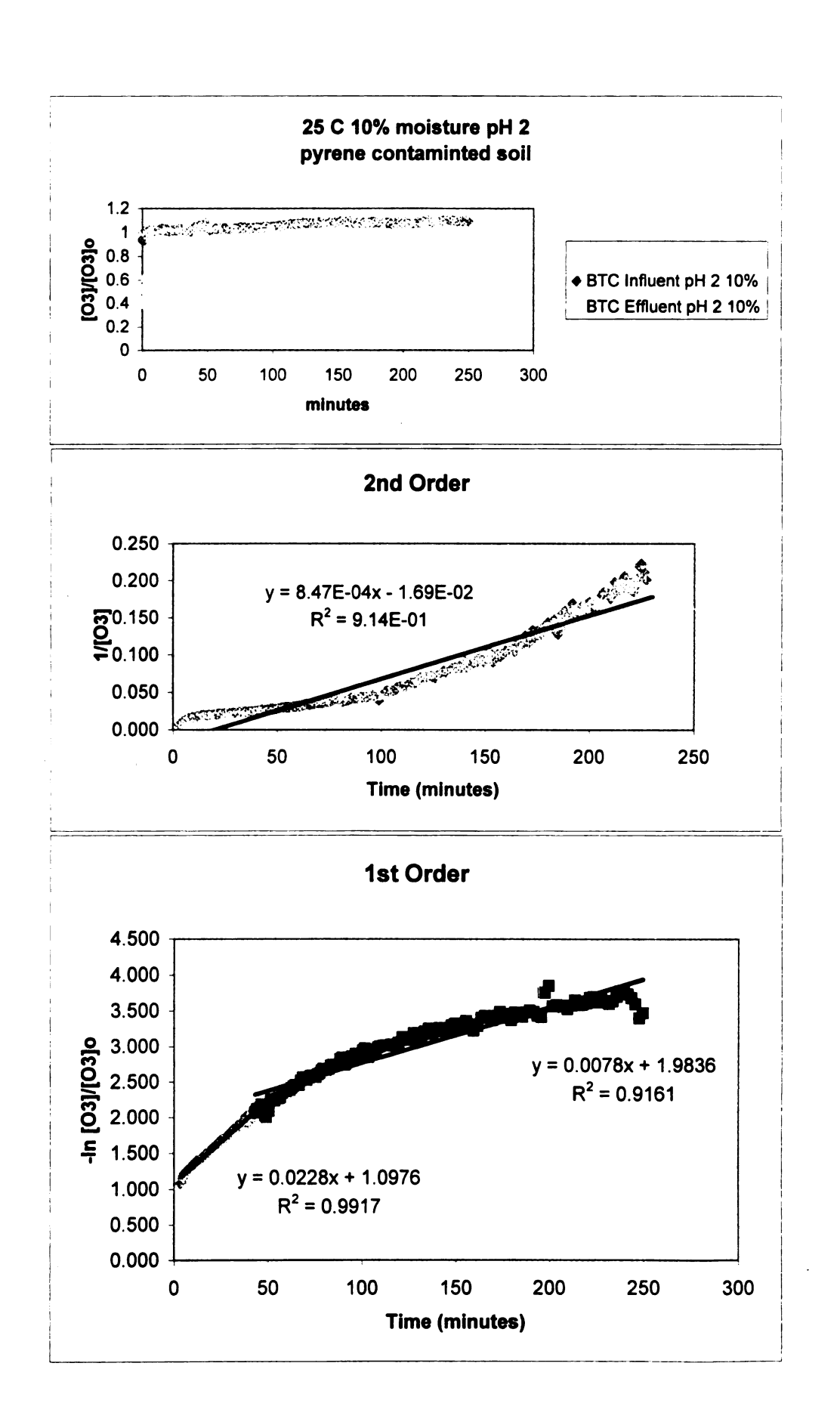


Figure A17. Breakthrough curve, first order and second order plots for 10% moisture, pyrene contaminated Metea soil (pH 6) at 25°C

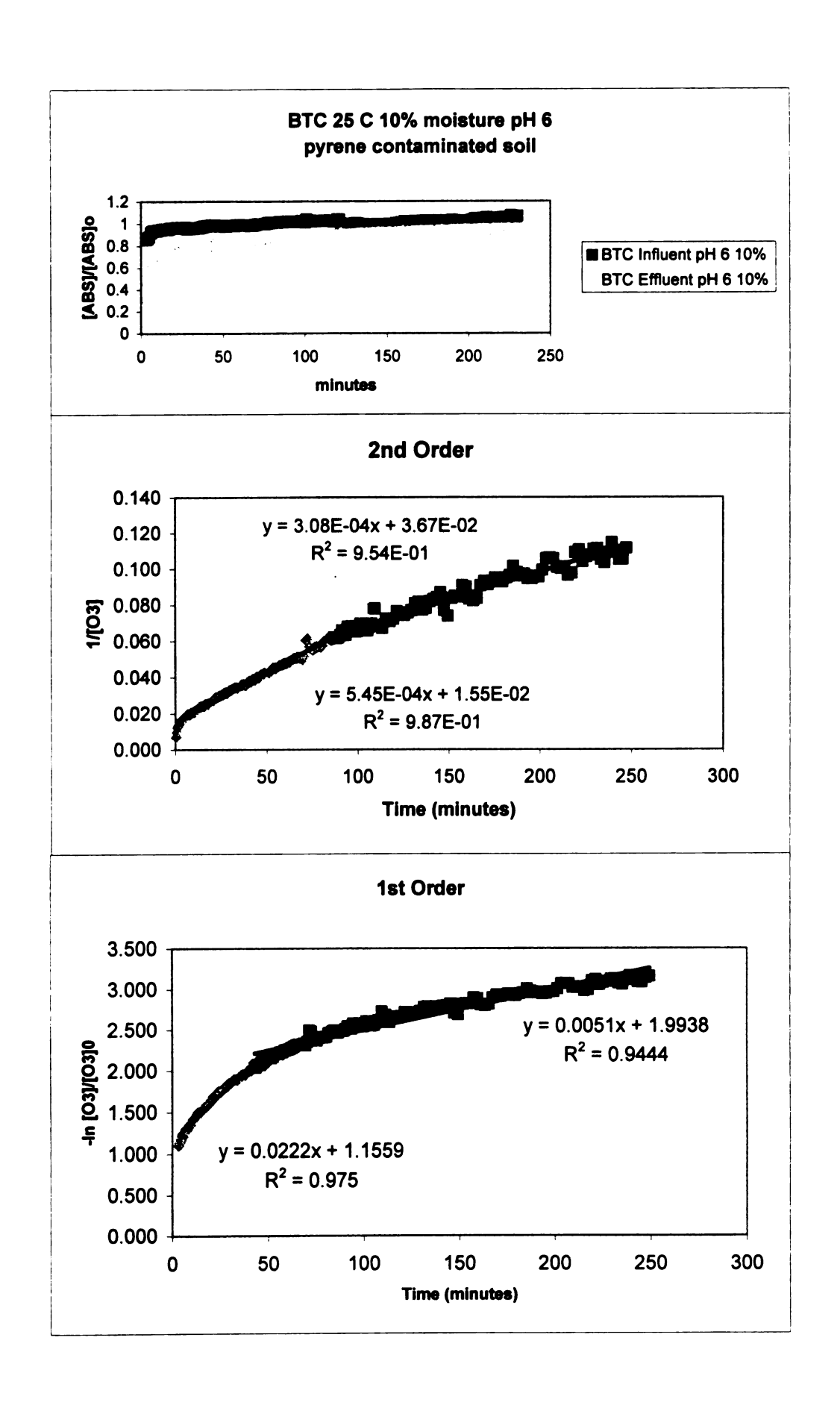
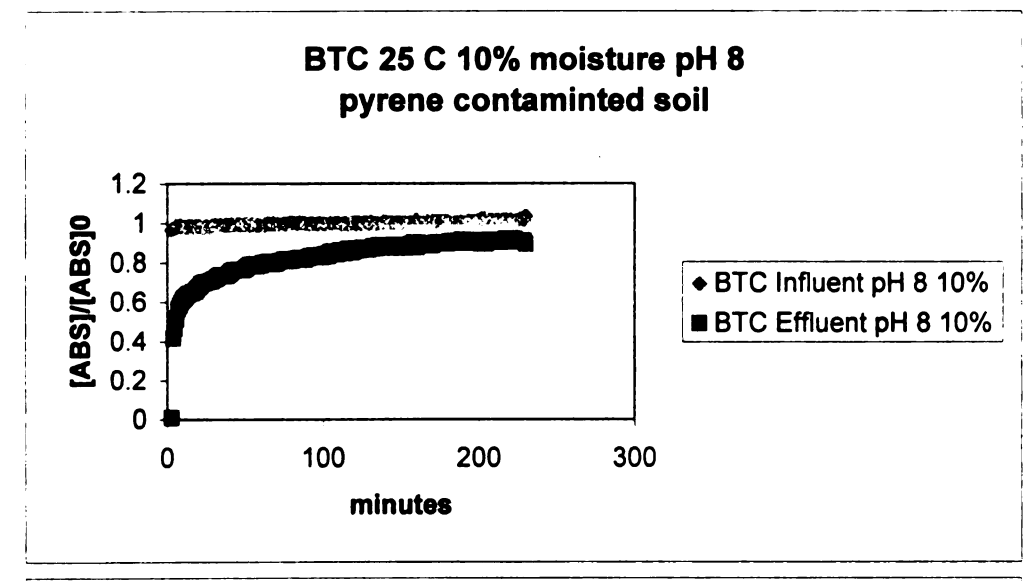
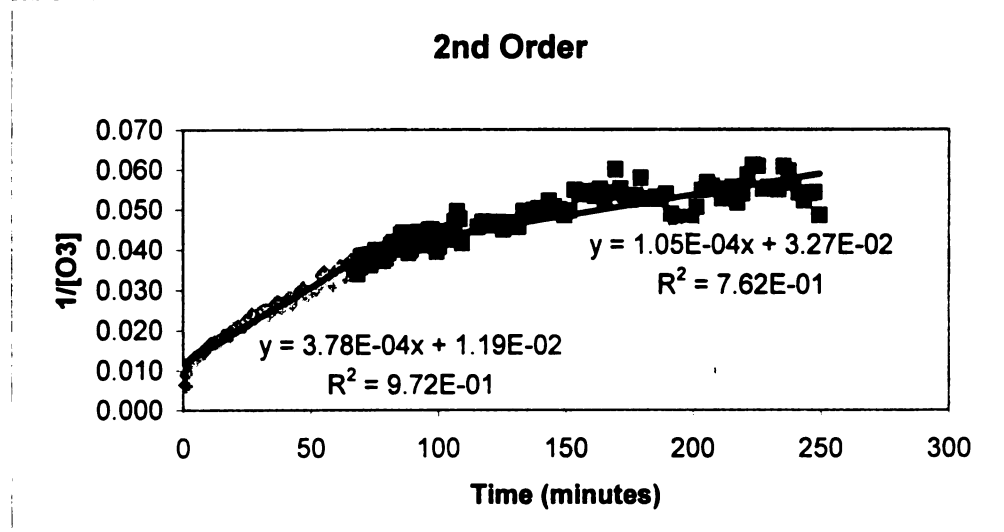


Figure A18. Breakthrough curve, first order and second order plots for 10% moisture, pyrene contaminated Metea soil (pH 8) at 25°C





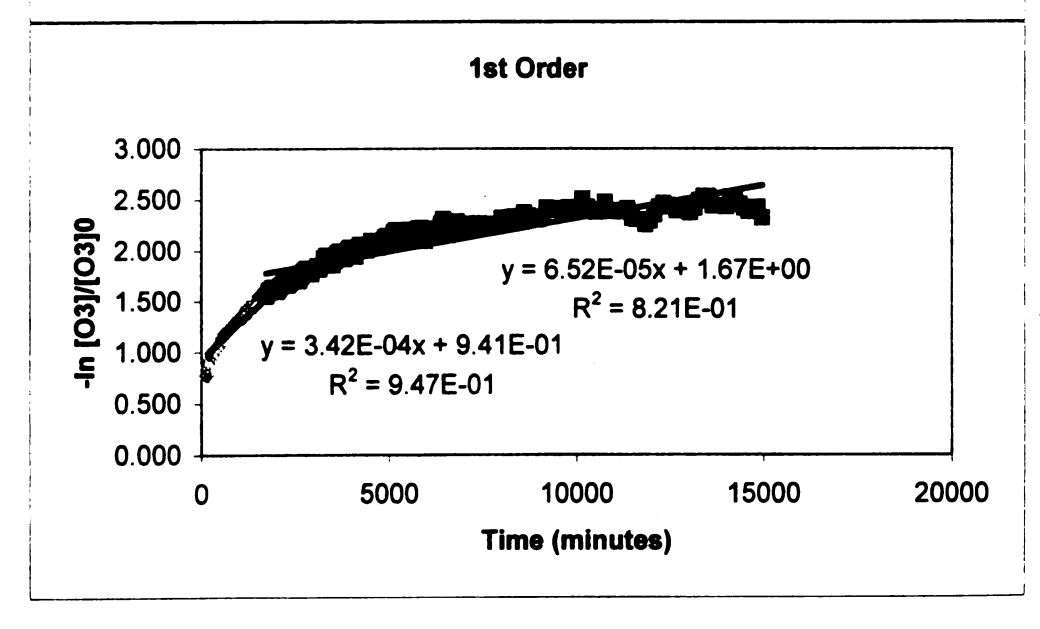


Figure A19. Breakthrough curve, first order and second order plots for dry, pyrene contaminated Metea soil (pH 2) at 13°C

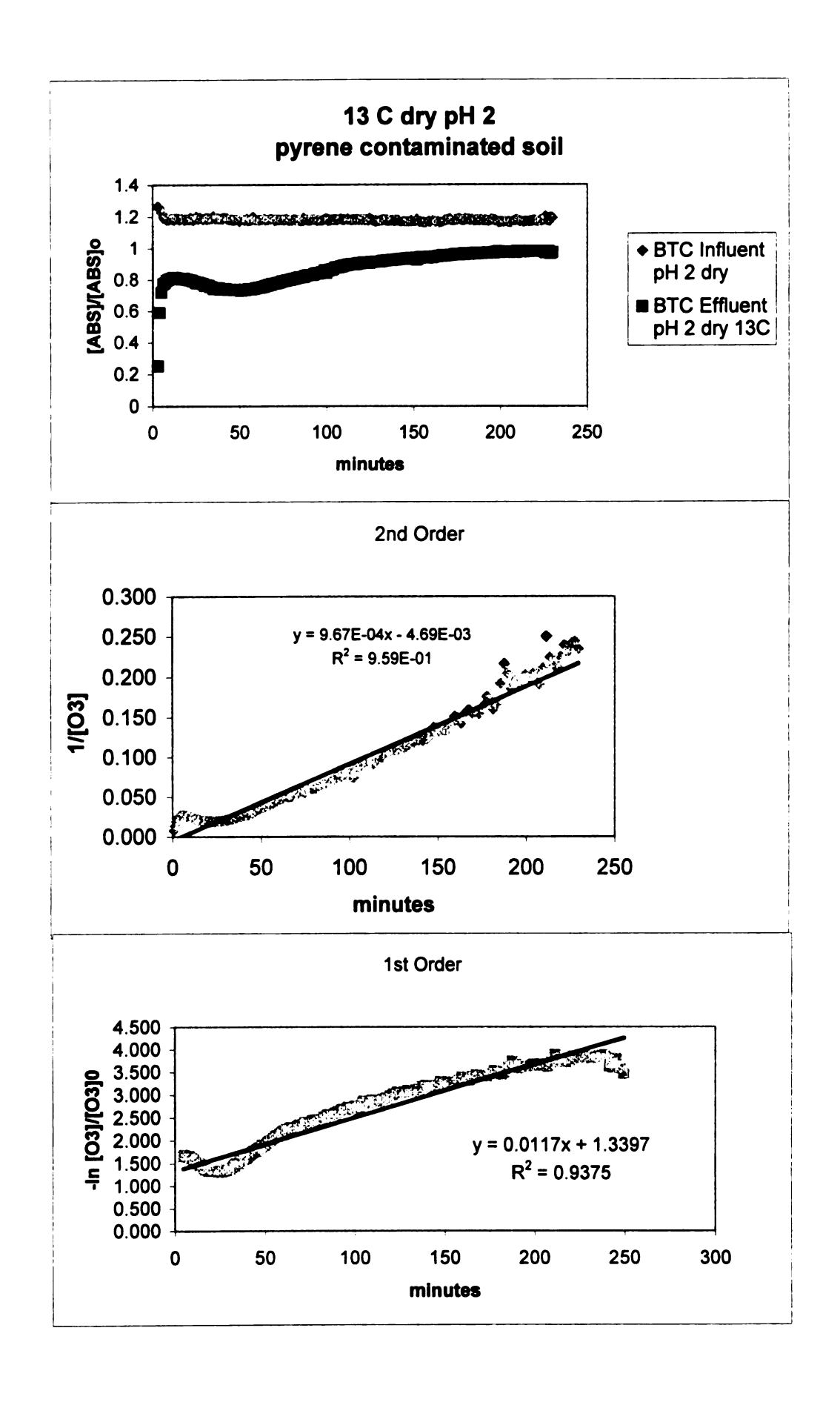


Figure A20. Breakthrough curve, first order and second order plots for dry, pyrene contaminated Metea soil (pH 6) at 13°C

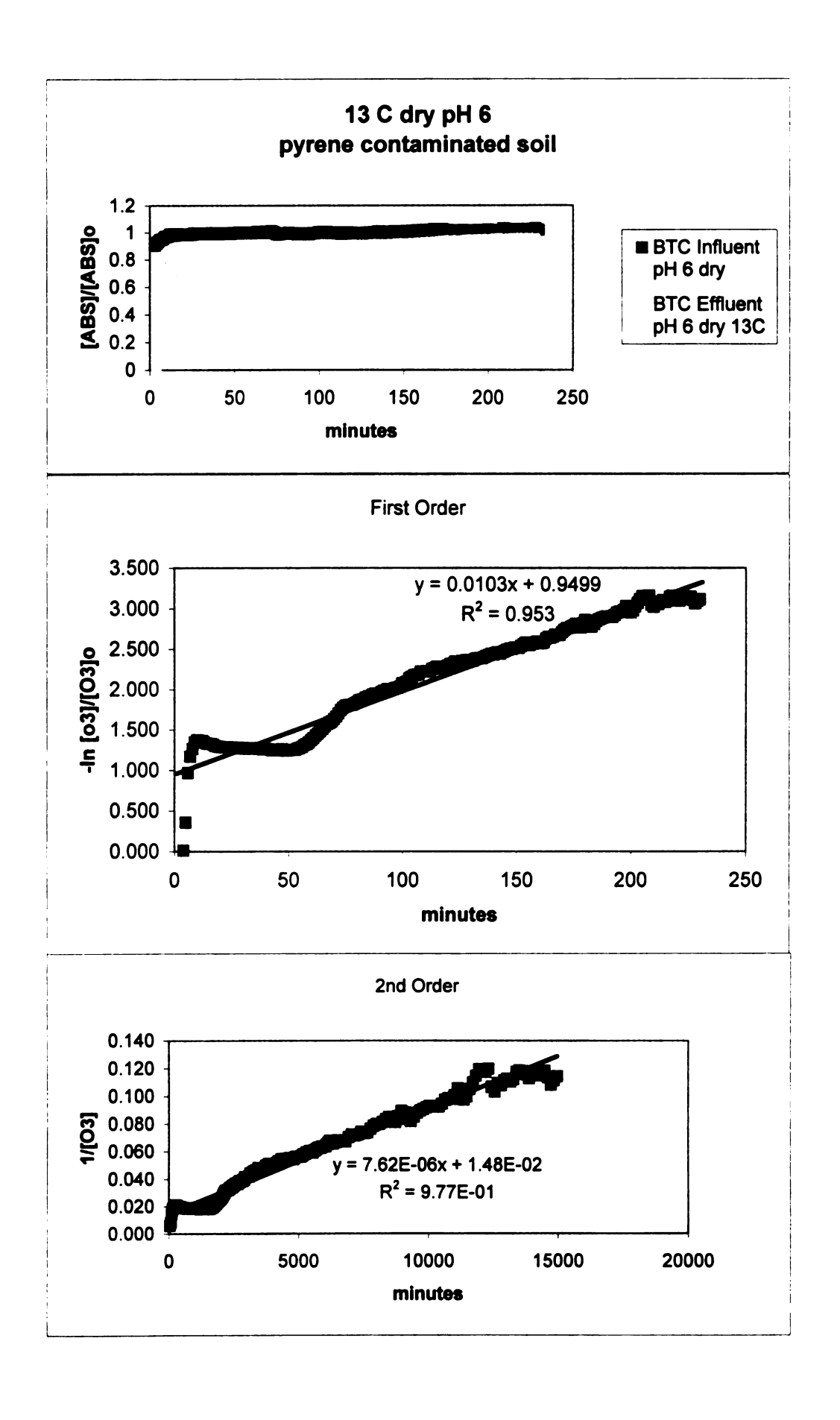
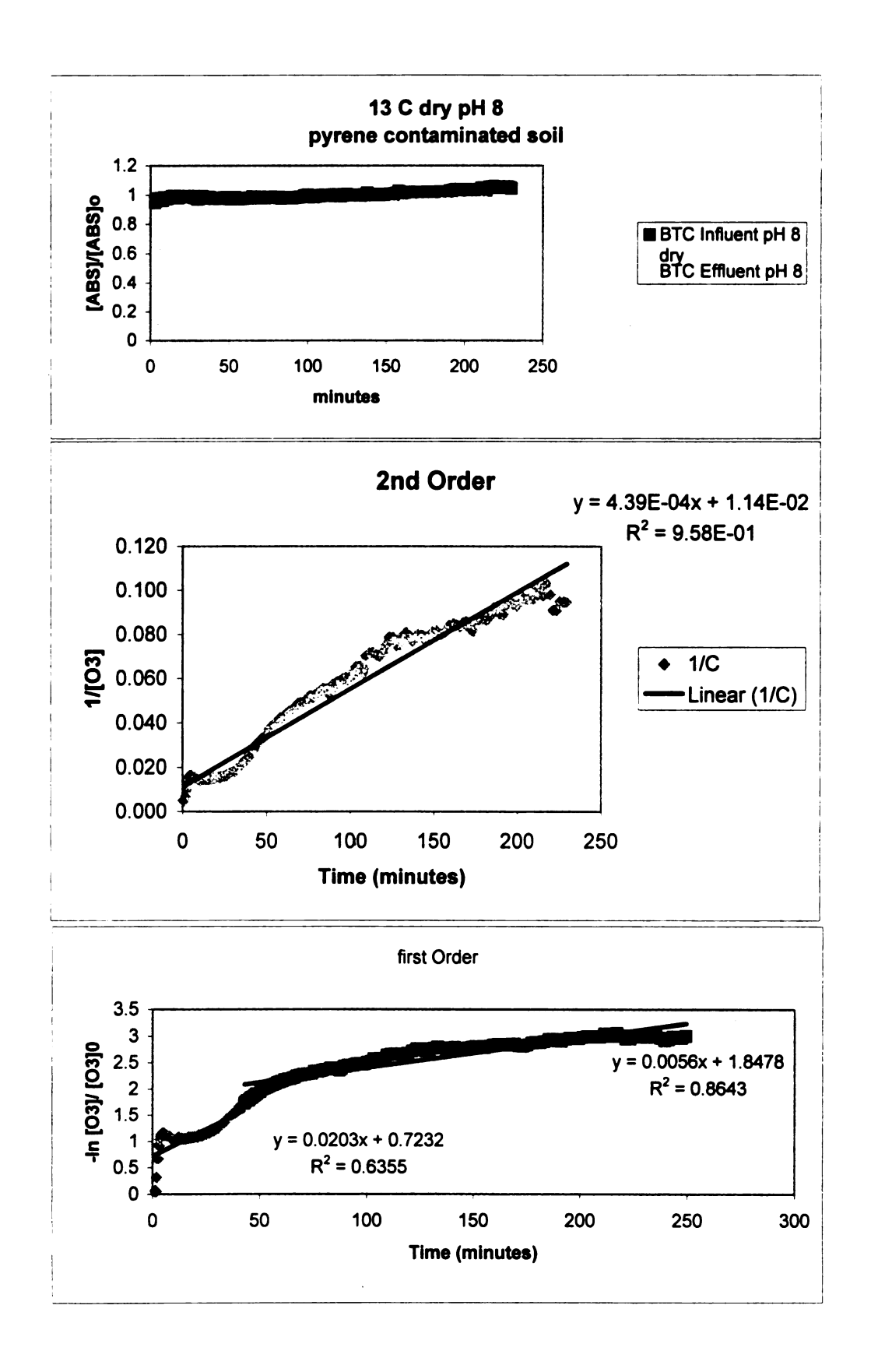
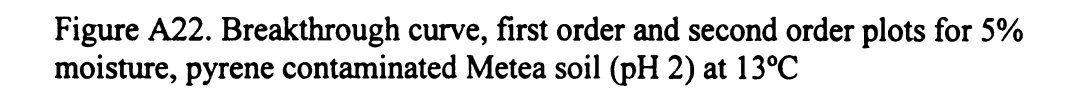


Figure A21. Breakthrough curve, first order and second order plots for dry, pyrene contaminated Metea soil (pH 8) at 13°C





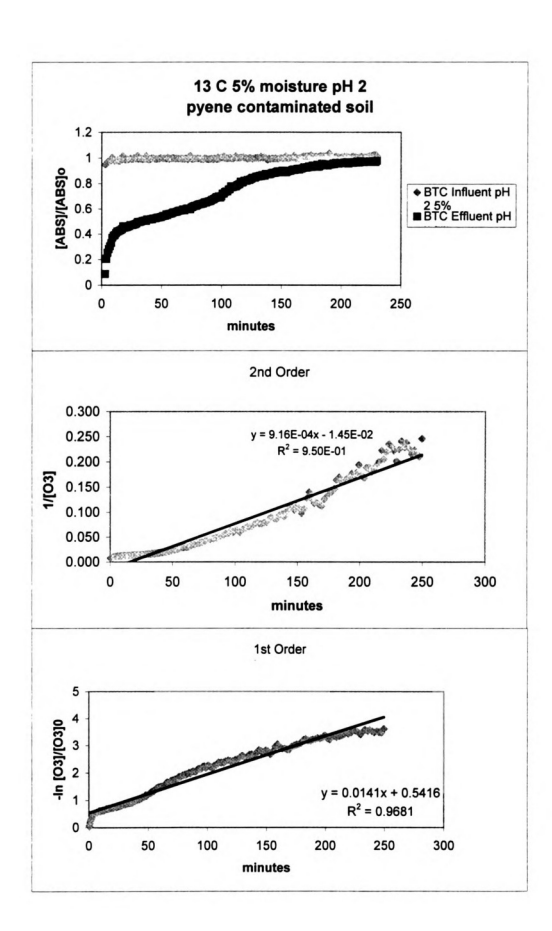


Figure A23. Breakthrough curve, first order and second order plots for 5% moisture, pyrene contaminated Metea soil (pH 6) at 13°C

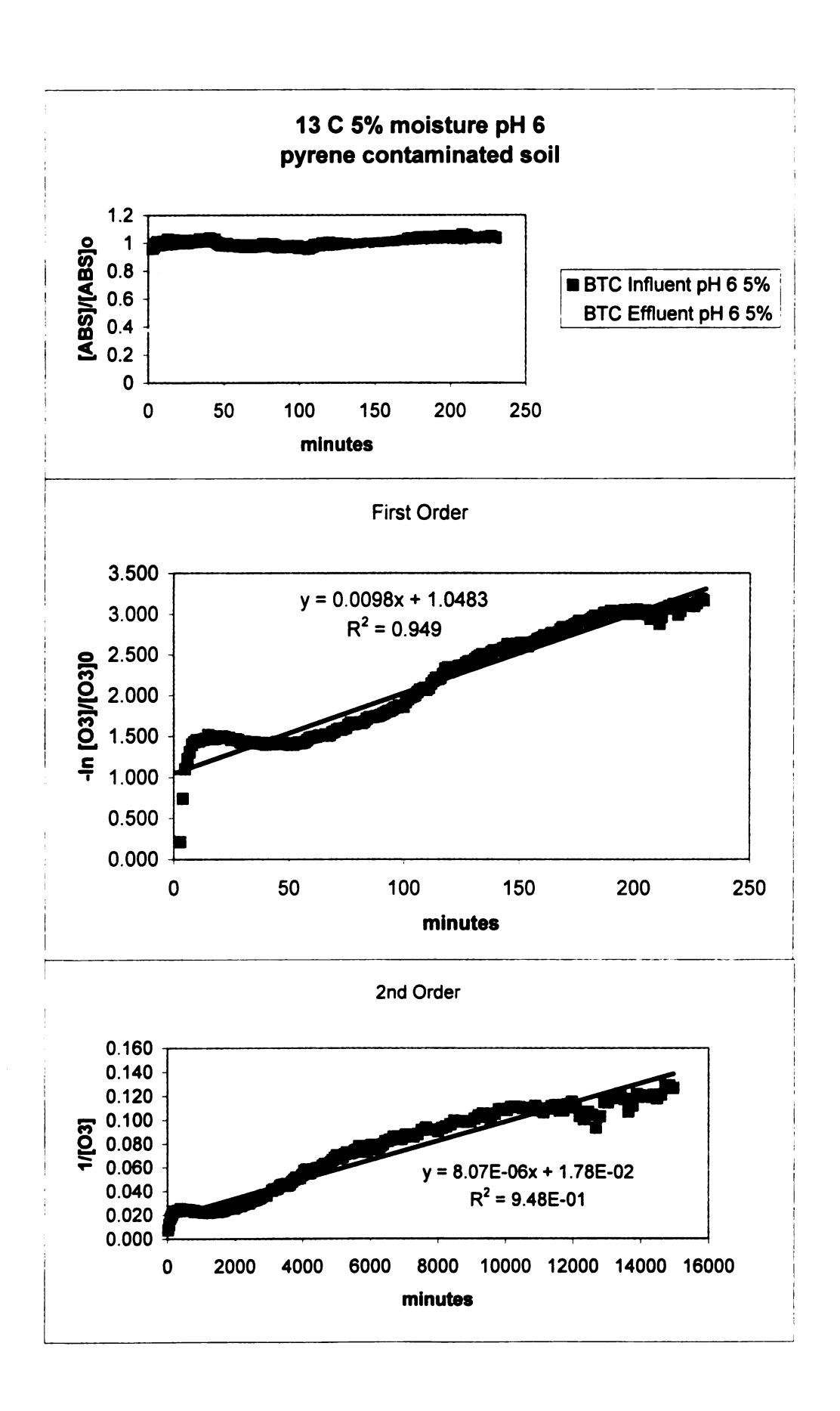
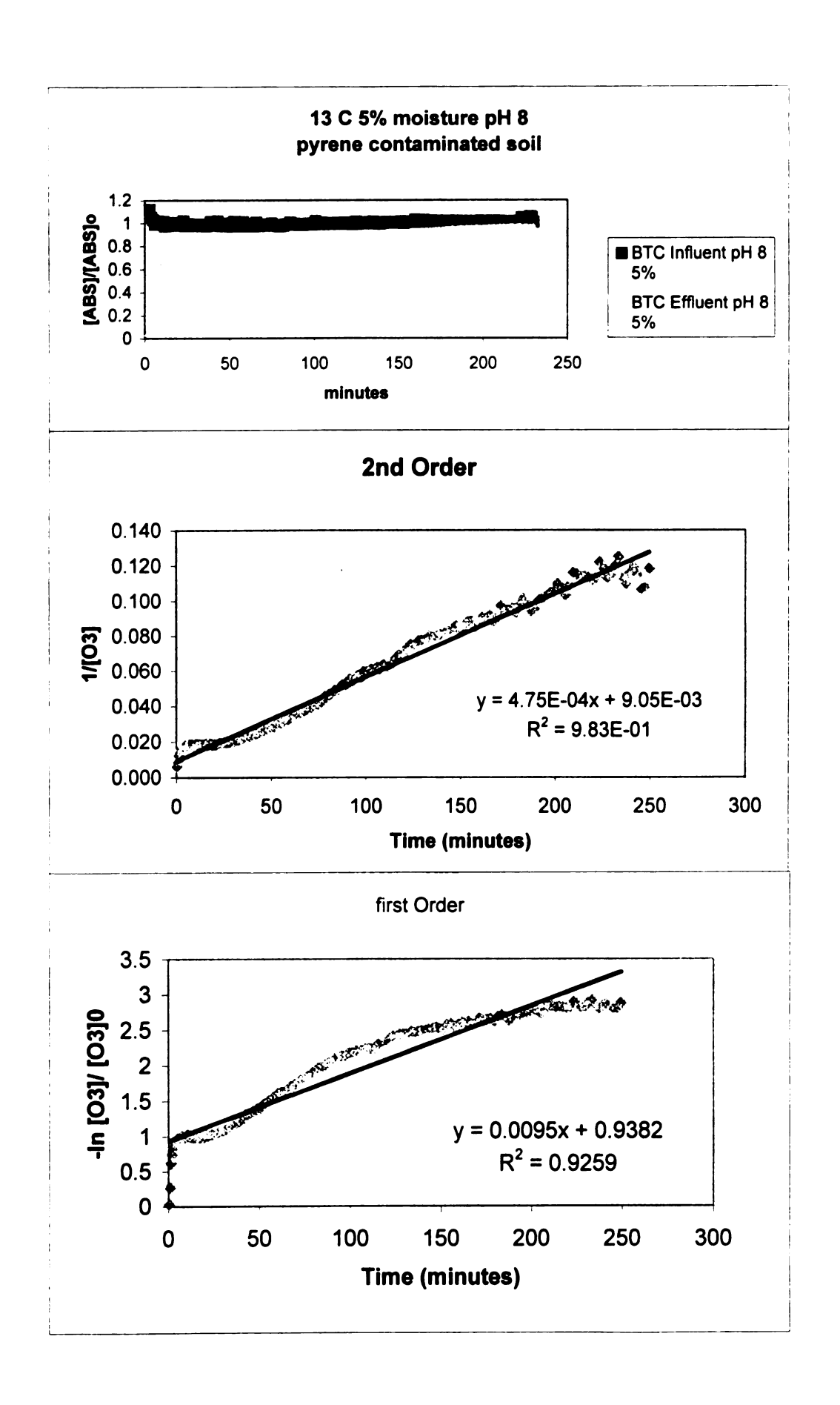
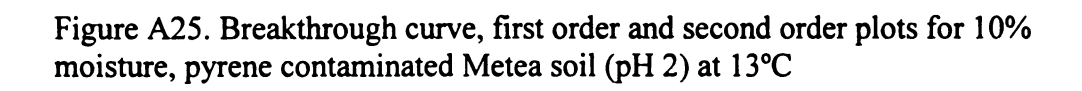


Figure A24. Breakthrough curve, first order and second order plots for 5% moisture, pyrene contaminated Metea soil (pH 8) at 13°C





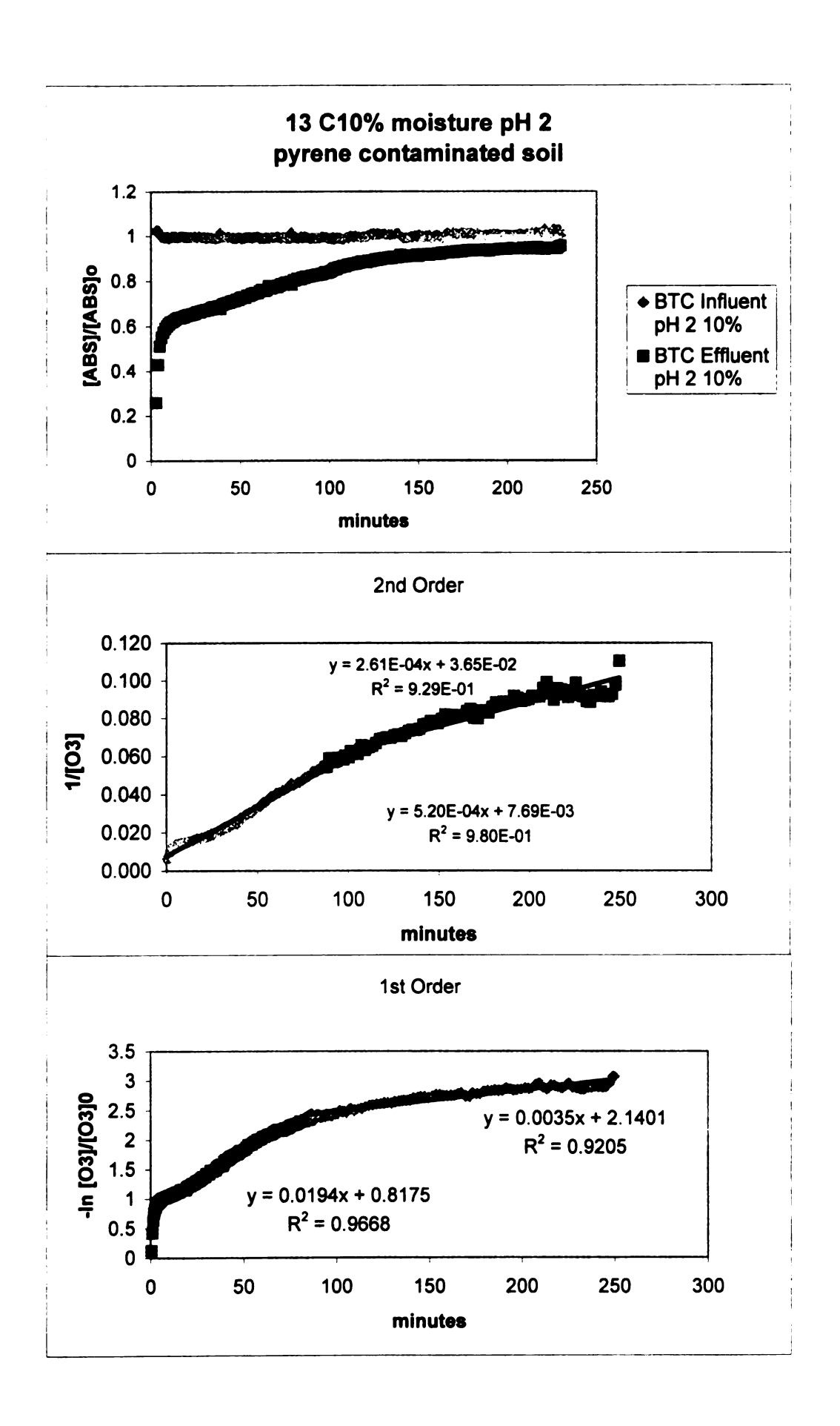


Figure A26. Breakthrough curve, first order and second order plots for 10% moisture, pyrene contaminated Metea soil (pH 6) at 13°C

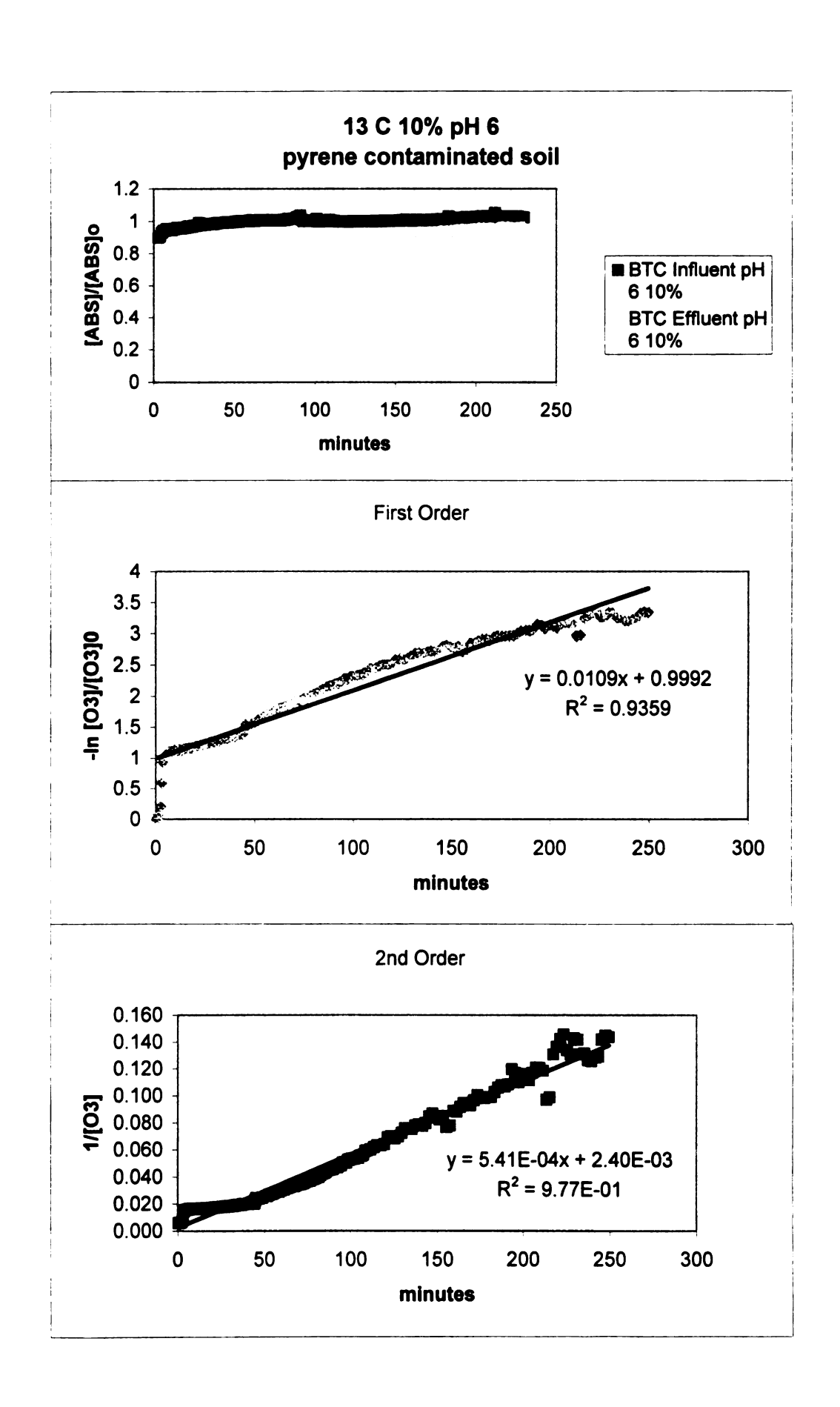


Figure A27. Breakthrough curve, first order and second order plots for 10% moisture, pyrene contaminated Metea soil (pH 8) at 13°C

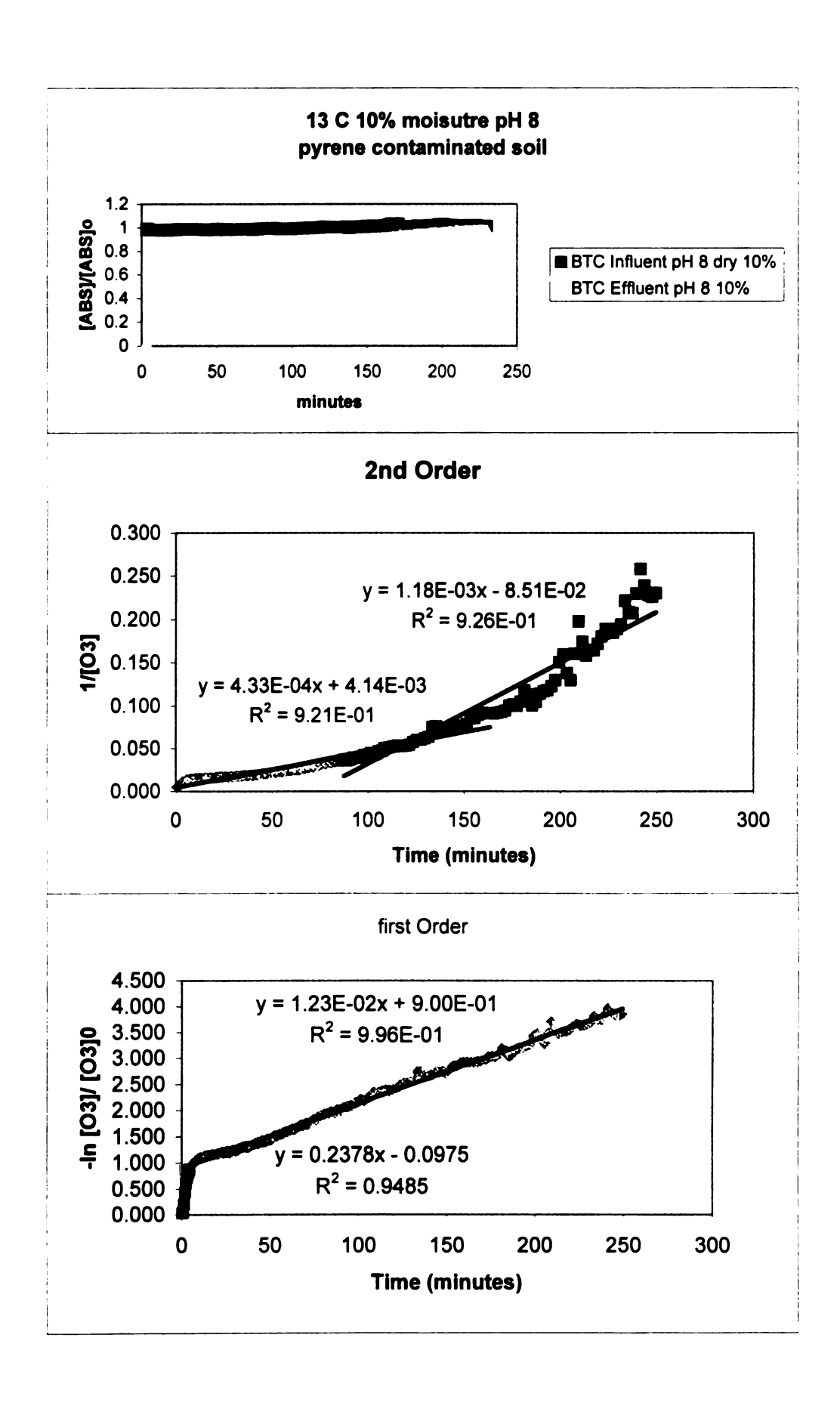


Figure A28. Breakthrough curve, first order and second order plots for aged, pyrene contaminated Metea soil (pH 2) at 25°C

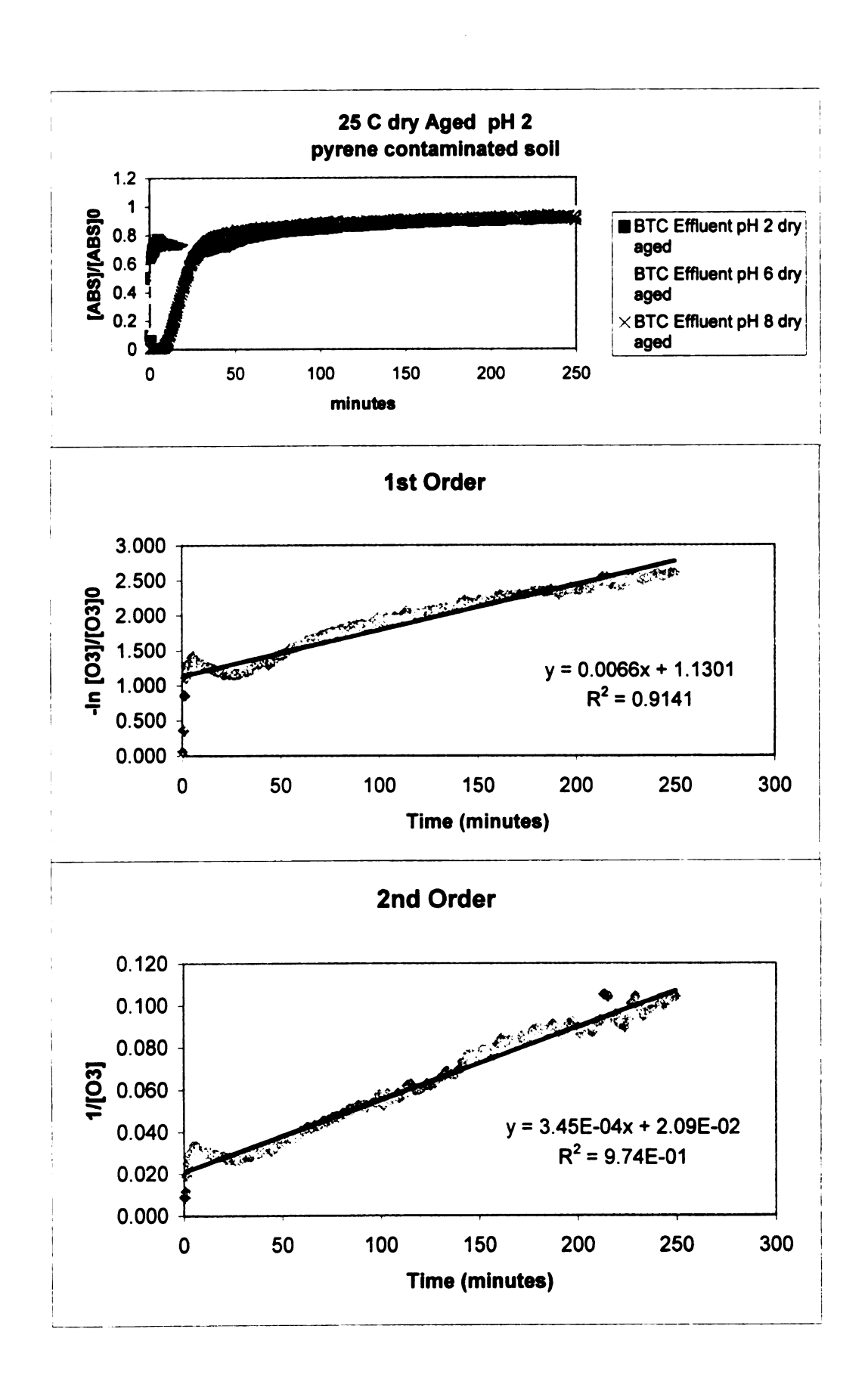


Figure A29. Breakthrough curve, first order and second order plots for aged, pyrene contaminated Metea soil (pH 6) at 25°C

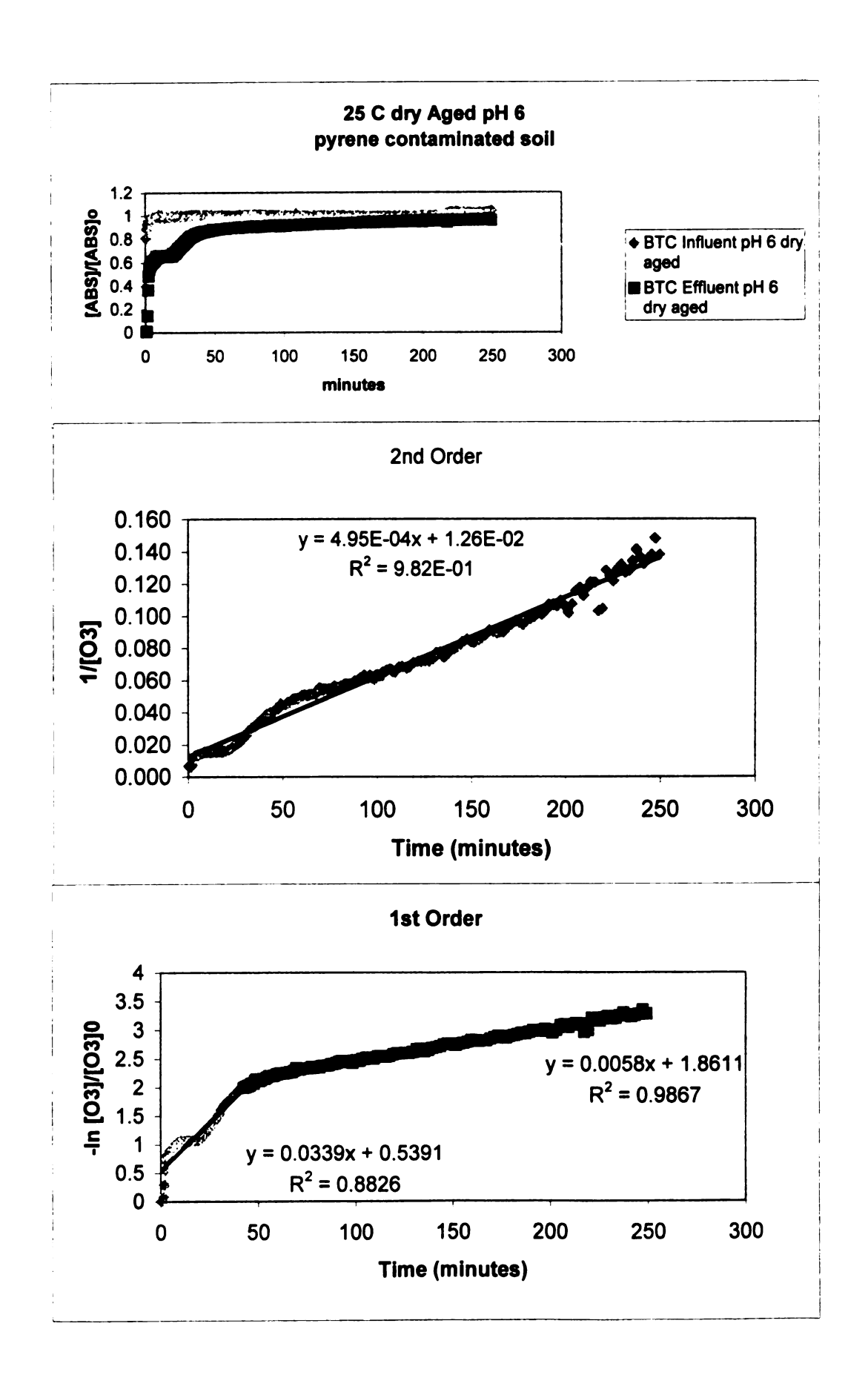
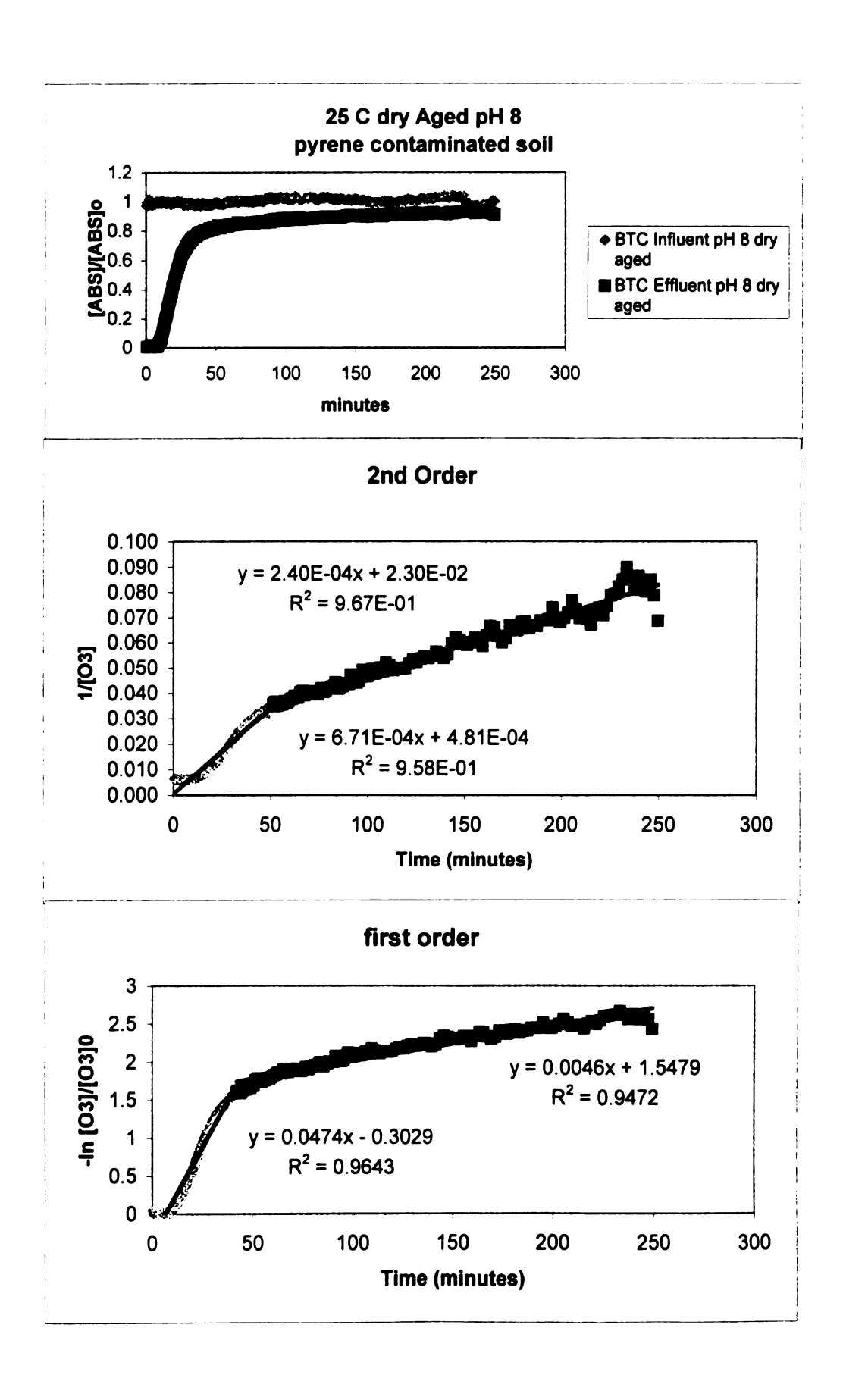


Figure A30. Breakthrough curve, first order and second order plots for aged dry, pyrene contaminated Metea soil (pH 8) at 25°C

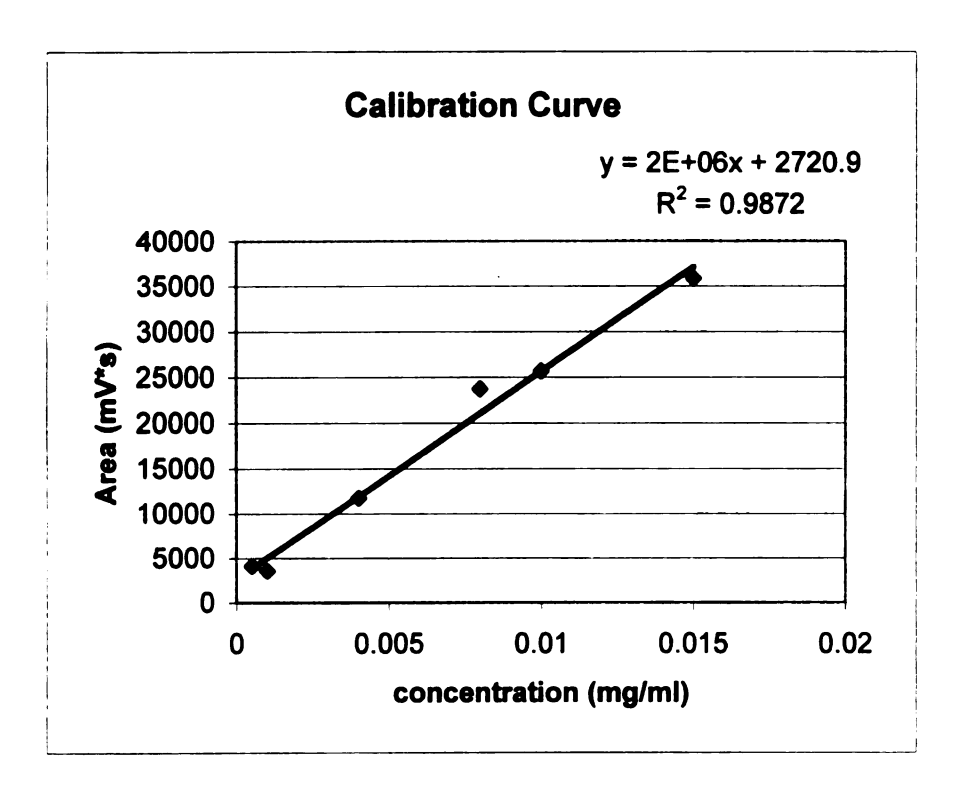


## APPENDIX B

Table B1. Spreadsheet for pyrene calibration

Evaluation of Pyrene recovery from soil Calibration curve using Pyrene standard at various concentrations

mg/ml	Area (mV*s	
0.0005	4108	
0.001	3575	
0.004	11721	
0.008	23737	
0.01	25661	
0.015	35851	



pyrene concentration in soil	300 mg/kg
amount of soil in extraction	0.0076 kg
mass of pyr in soil extraction	2.28 mg
volume of extraction solution	200 ml
concentration of pyrene in solution	0.0114 mg/ml

Calculated mass					
Pyrene extracted from soils (Area from HPLC) mV*s	of pyrene in extract	Calculated Concentration	Percent recovery		
26420	0.01184955	311.8302632	103.9434		
25800	0.01153955	303.6723684	101.2241		
25154	0.01121655	295.1723684	98.39079		

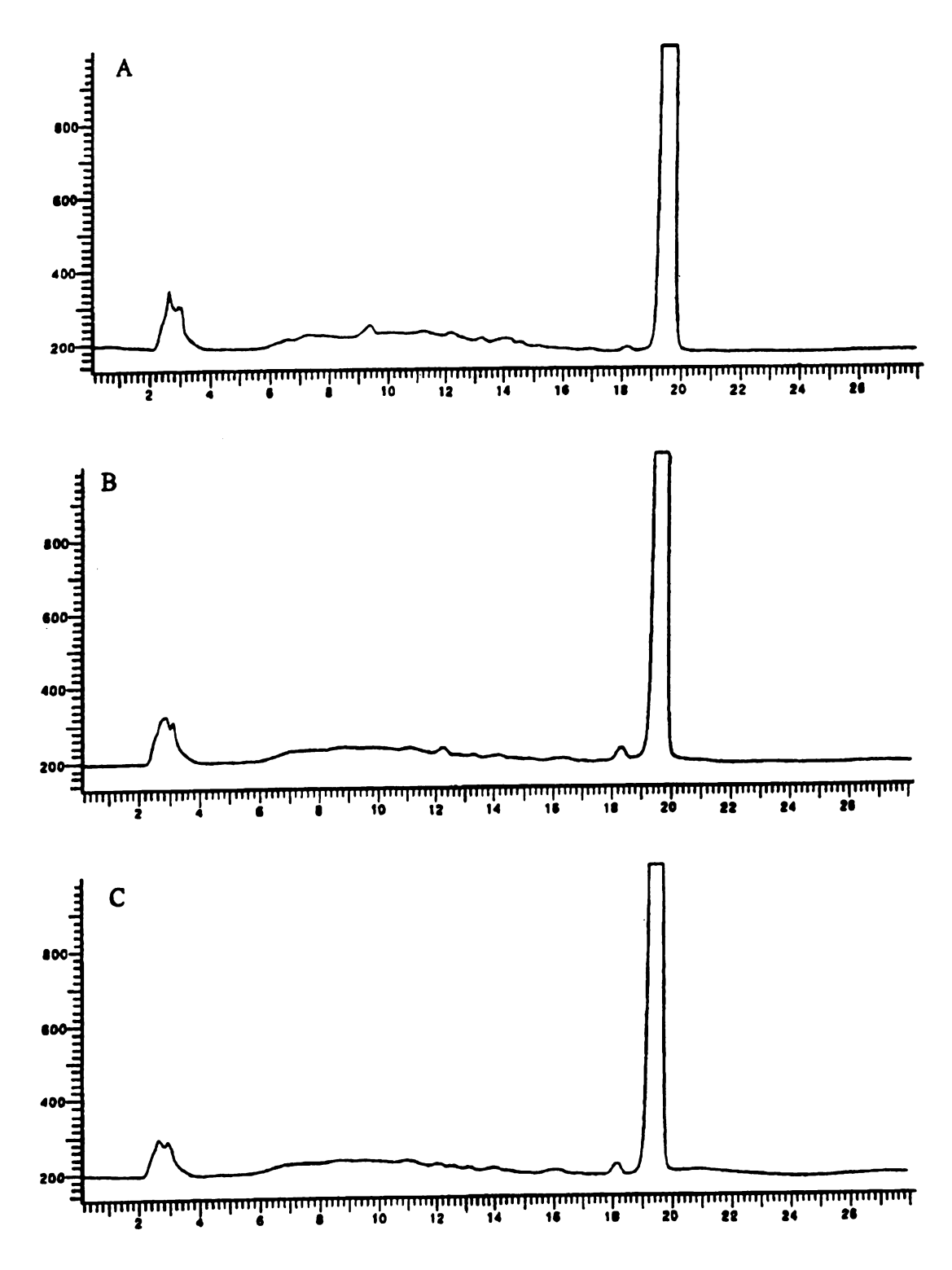
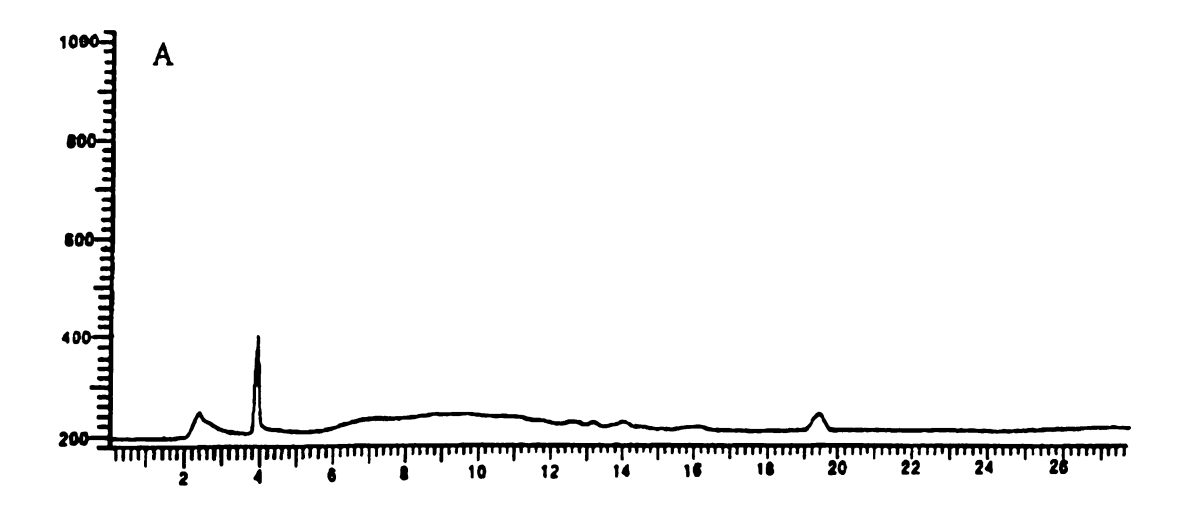
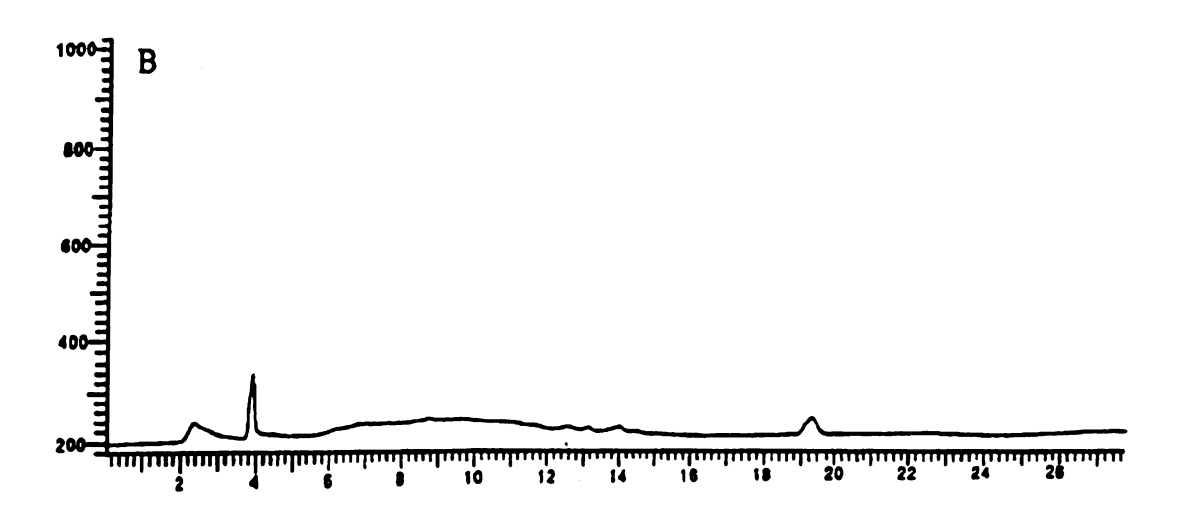


Figure B1. HPLC chromatograms of acetonitrile extracts. (a) Pyrene soil (control), (b) air-sparged through pyrene soil for 24 hours, (c) oxygen-sparged through pyrene soil for 24 hours.





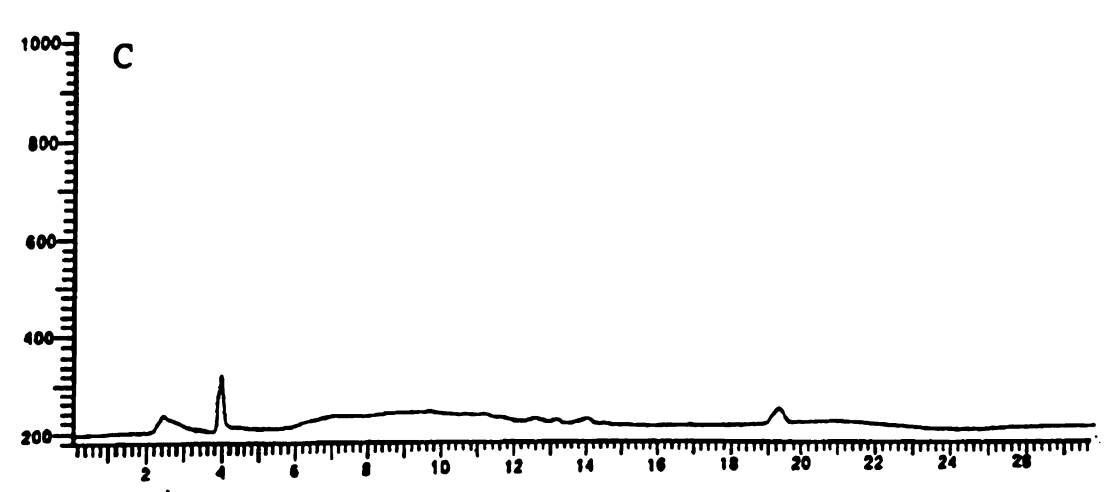
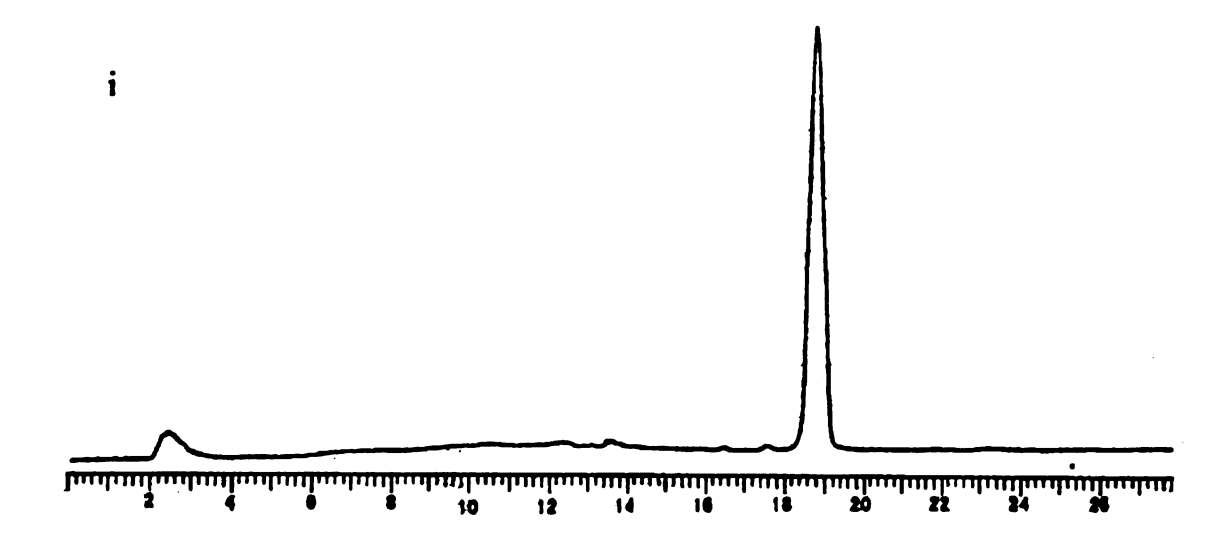


Figure B2. HPLC chromatograms of deionized water extracts. (a) Pyrene soil (control), (b) air-sparged through pyrene soil for 24 hours, (c) oxygen-sparged through pyrene soil for 24 hours.



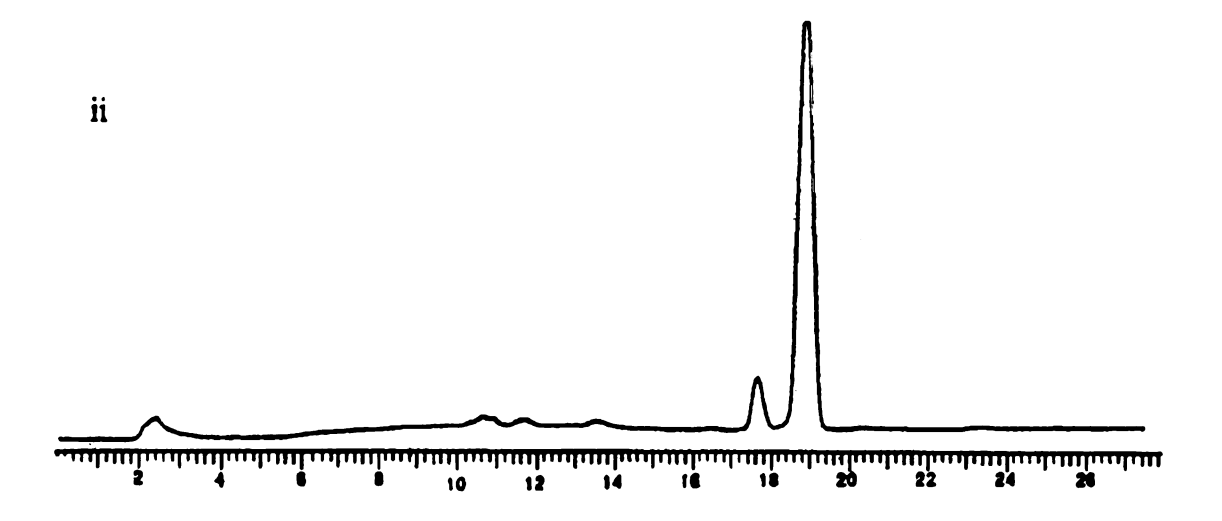


Figure B3. Examples of the two chromatograms for acetonitrile extracts from pyrene soil

Figure Control O<sub>3</sub>/p

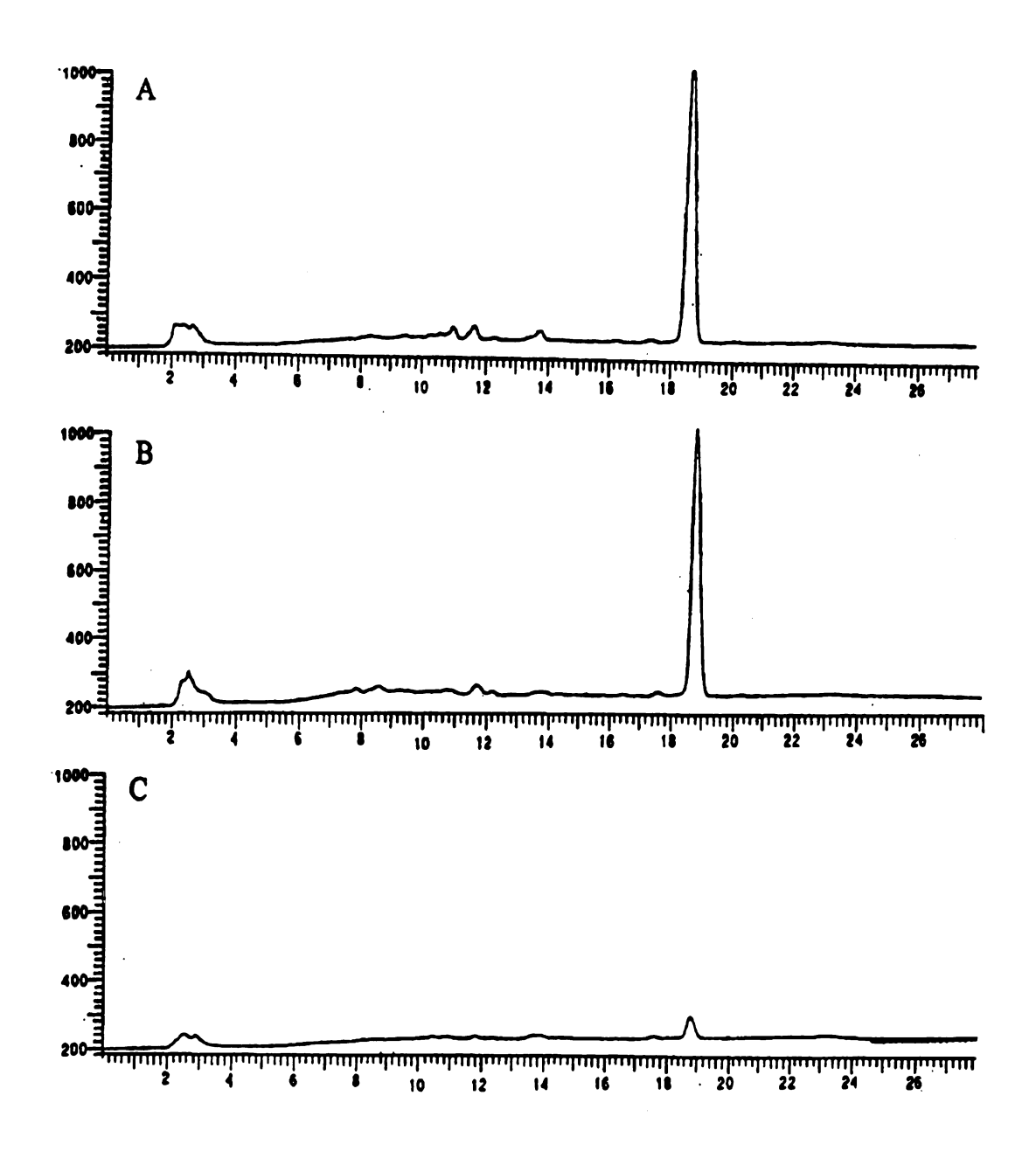


Figure B4. Acetonitrile extract chromatogram for dry, 25°C (pH 2) pyrene contaminated soil. (a) 2.2 mg  $O_3$ /ppm pyr, (b) 3.85 mg  $O_3$ /ppm pyr, (c) 16 mg  $O_3$ /ppm pyr.

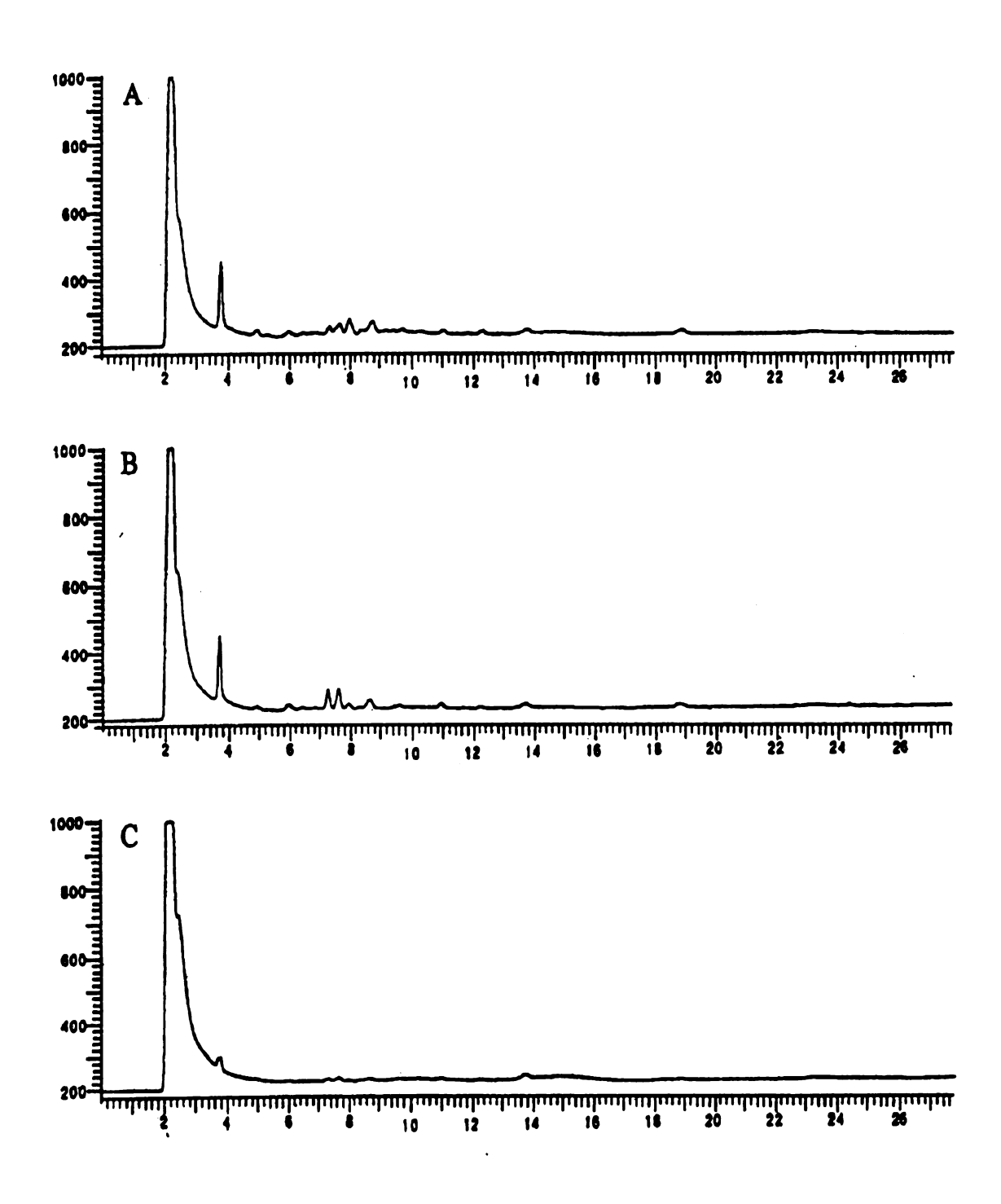


Figure B5. Deionized water extract chromatogram for dry, 25°C (pH 2) pyrene contaminated soil. (a) 2.2 mg O<sub>3</sub>/ppm pyr, (b) 3.85 mg O<sub>3</sub>/ppm pyr, (c) 16 mg O<sub>3</sub>/ppm pyr.

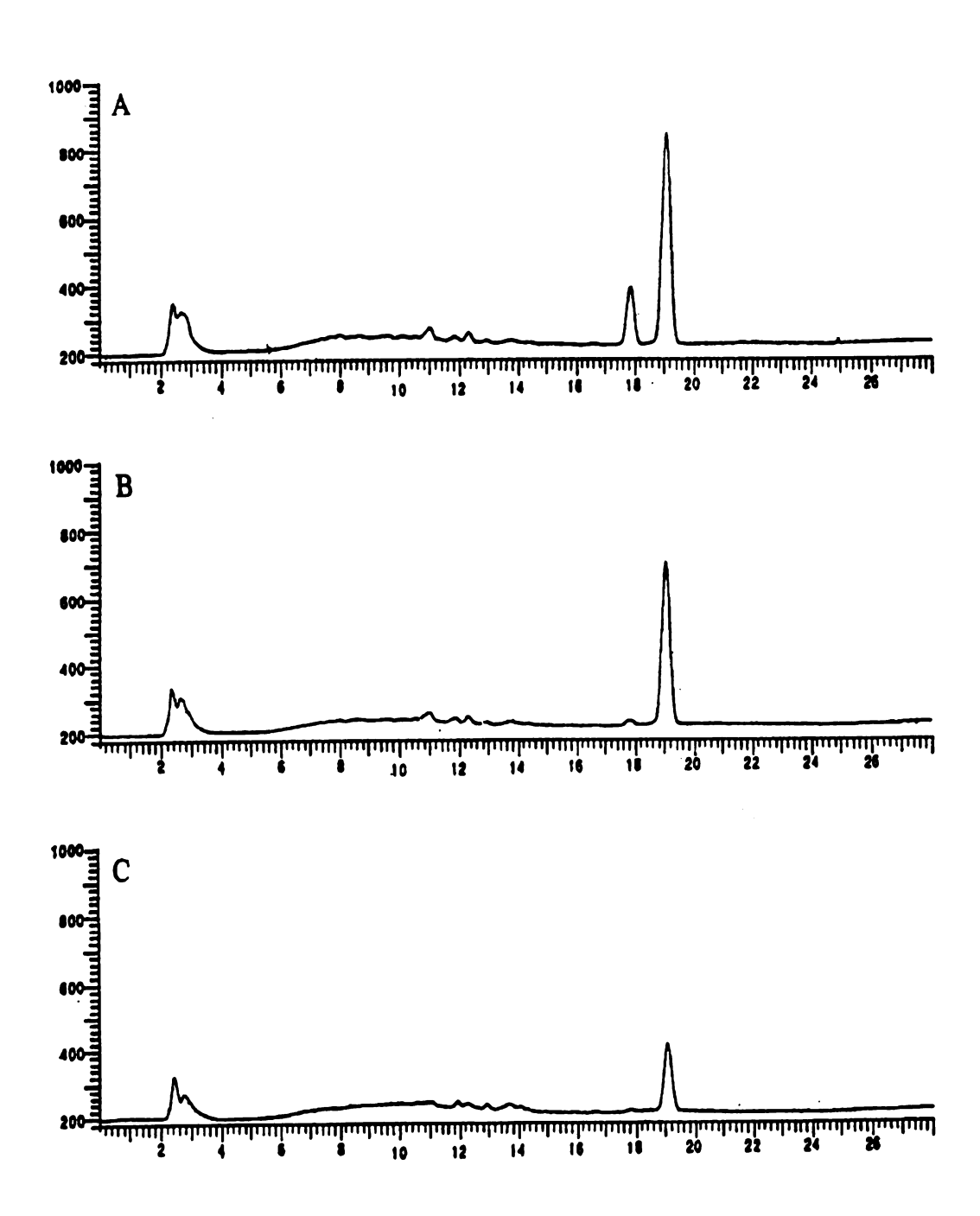


Figure B6. Acetonitrile extract chromatogram for 5% moisture, 25°C (pH 2) pyrene contaminated soil. (a) 2.2 mg O<sub>3</sub>/ppm pyr, (b) 3.85 mg O<sub>3</sub>/ppm pyr, (c) 16 mg O<sub>3</sub>/ppm pyr.

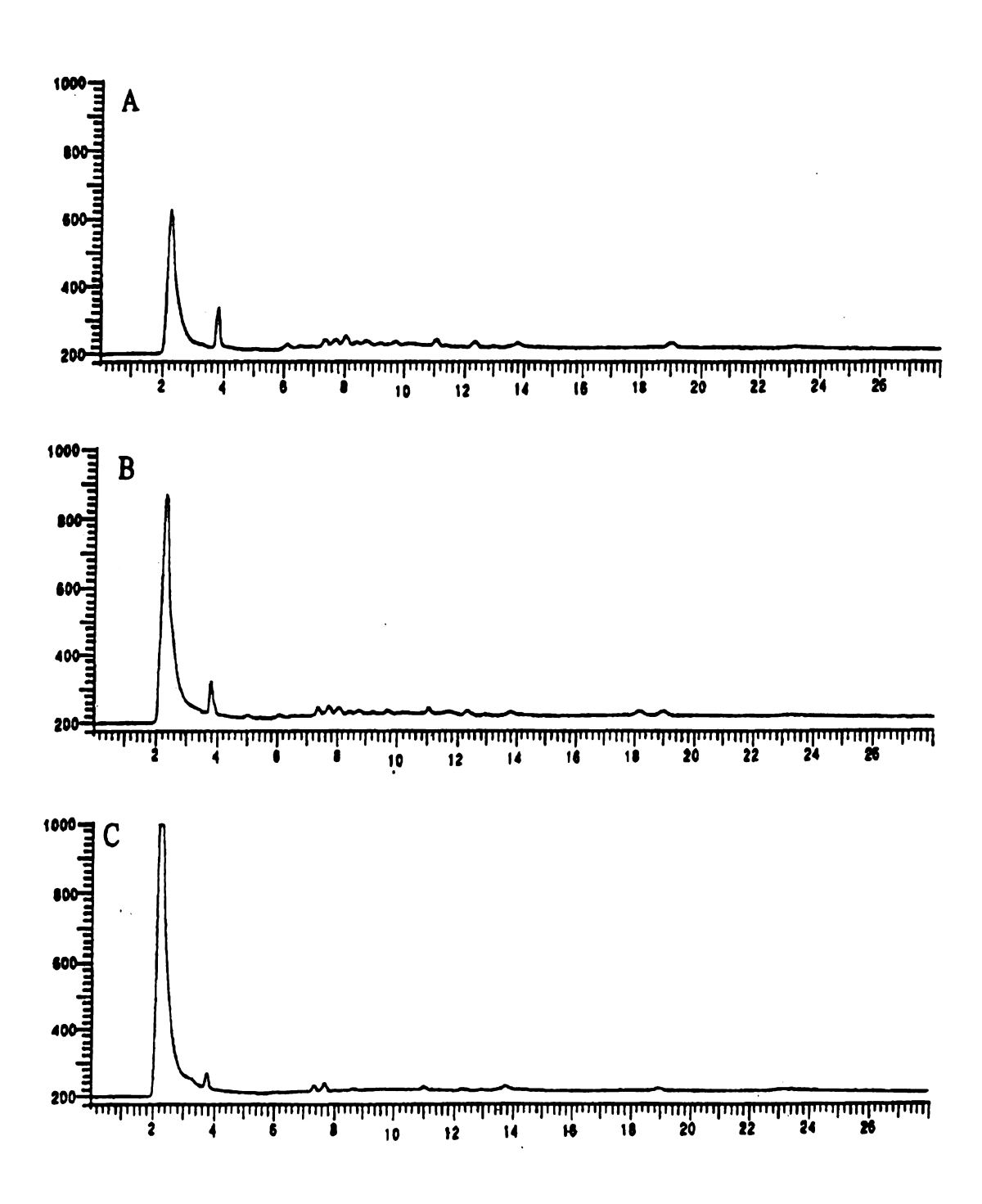


Figure B7. Deionized water extract chromatogram for 5% moisture, 25°C (pH 2) pyrene contaminated soil. (a) 2.2 mg O<sub>3</sub>/ppm pyr, (b) 3.85 mg O<sub>3</sub>/ppm pyr, (c) 16 mg O<sub>3</sub>/ppm pyr.

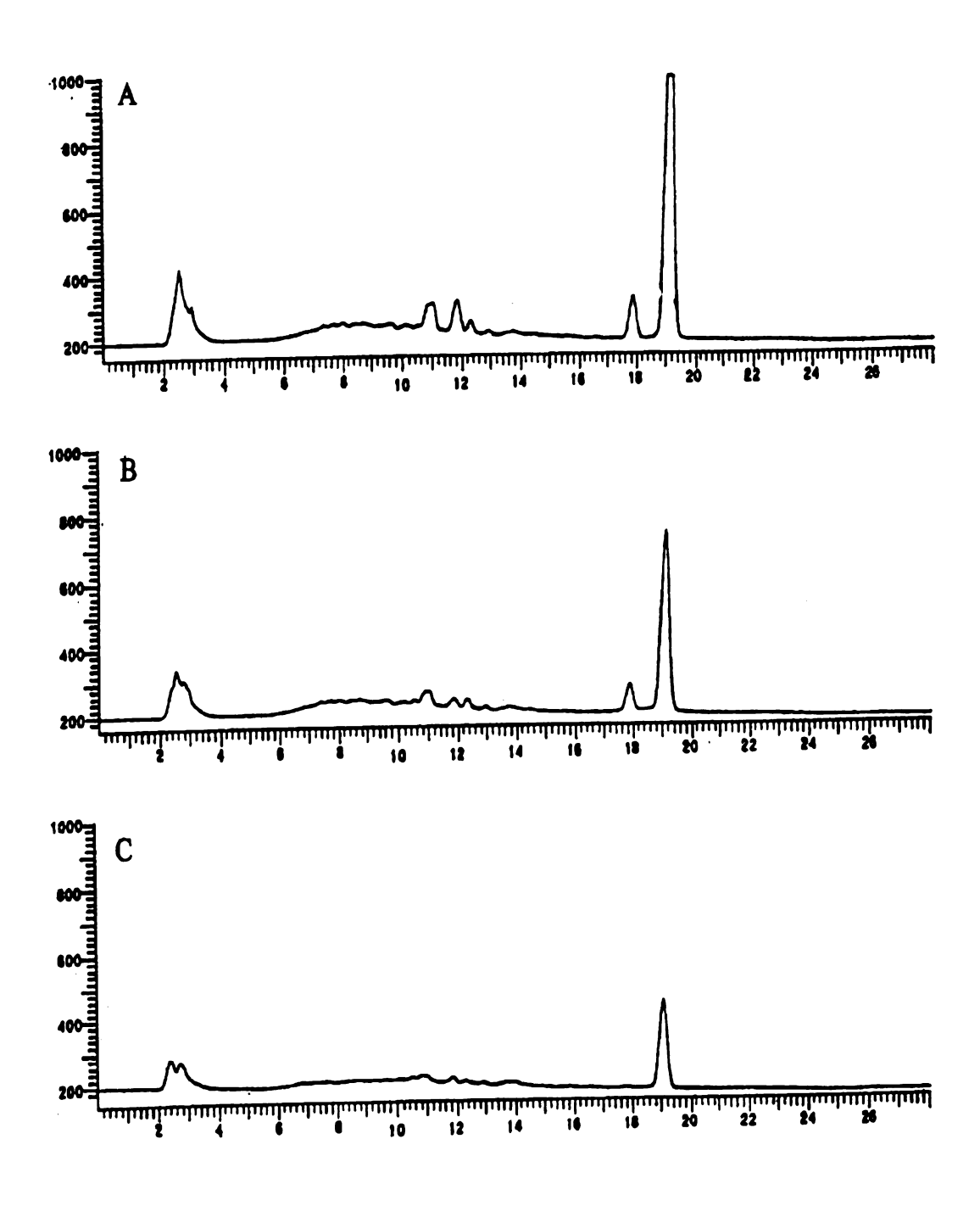


Figure B8. Acetonitrile extract chromatogram for 10% moisture, 25°C (pH 2) pyrene contaminated soil. (a) 2.2 mg O<sub>3</sub>/ppm pyr, (b) 3.85 mg O<sub>3</sub>/ppm pyr, (c) 16 mg O<sub>3</sub>/ppm pyr.

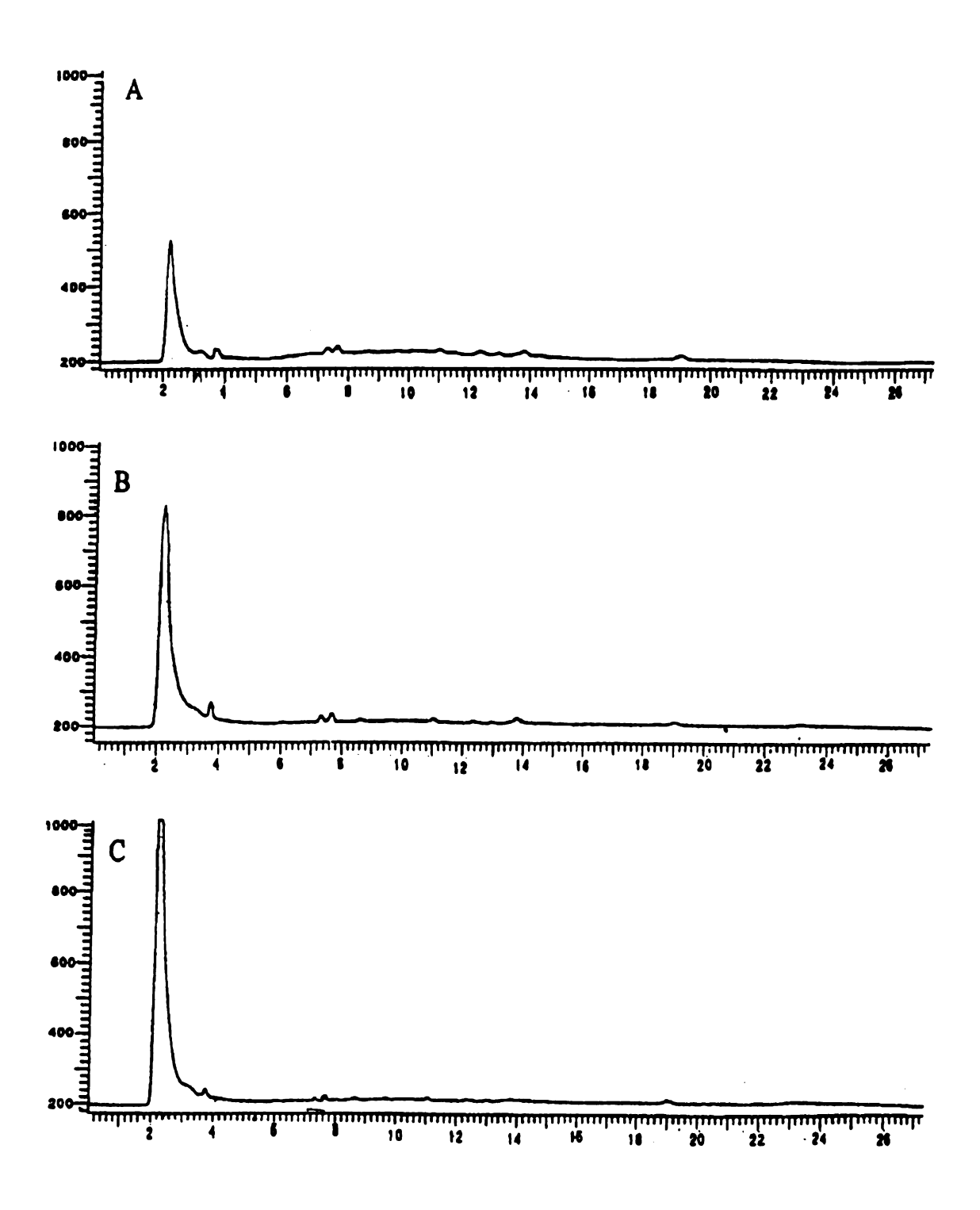


Figure B9. Deionized water extract chromatogram for 10% moisture, 25°C (pH 2) pyrene contaminated soil. (a) 2.2 mg O<sub>3</sub>/ppm pyr, (b) 3.85 mg O<sub>3</sub>/ppm pyr, (c) 16 mg O<sub>3</sub>/ppm pyr.

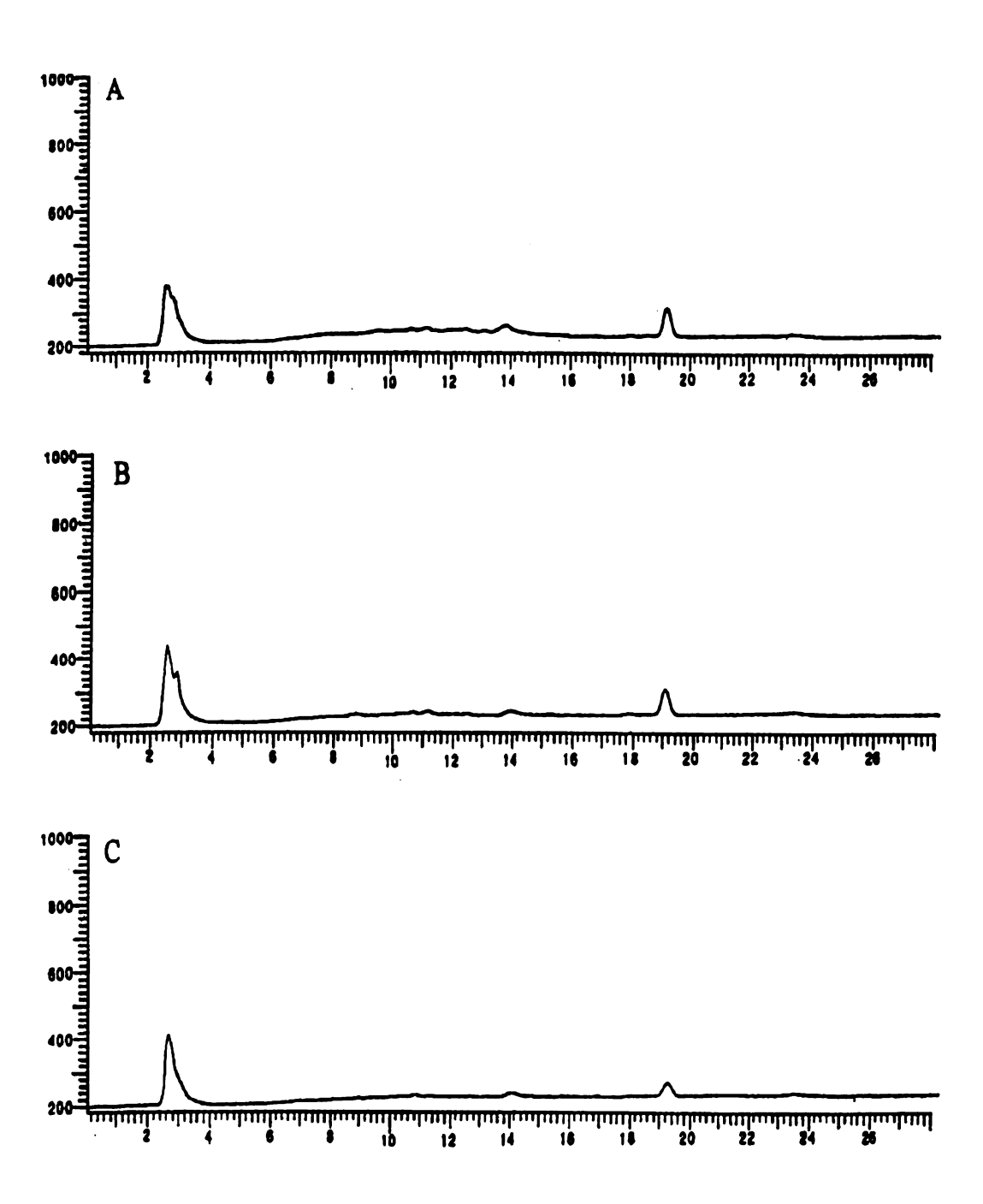


Figure B10. Acetonitrile extract chromatogram for dry, 25°C (pH 6) pyrene contaminated soil. (a) 2.2 mg O<sub>3</sub>/ppm pyr, (b) 3.85 mg O<sub>3</sub>/ppm pyr, (c) 16 mg O<sub>3</sub>/ppm pyr.

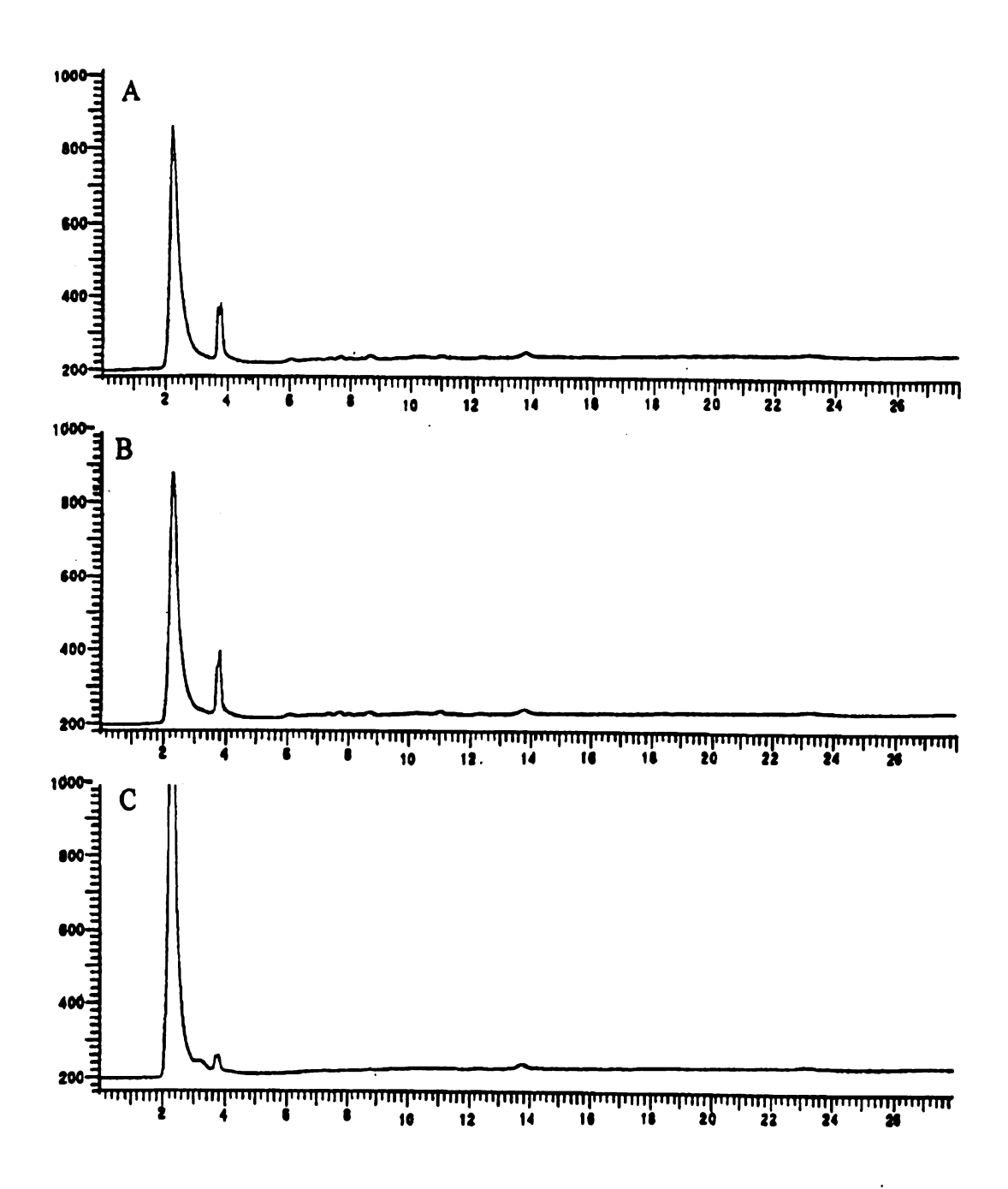


Figure B11. Deionized water extract chromatogram for dry, 25 °C (pH 6) pyrene contaminated soil. (a) 2.2 mg  $O_3$ /ppm pyr, (b) 3.85 mg  $O_3$ /ppm pyr, (c) 16 mg  $O_3$ /ppm pyr.

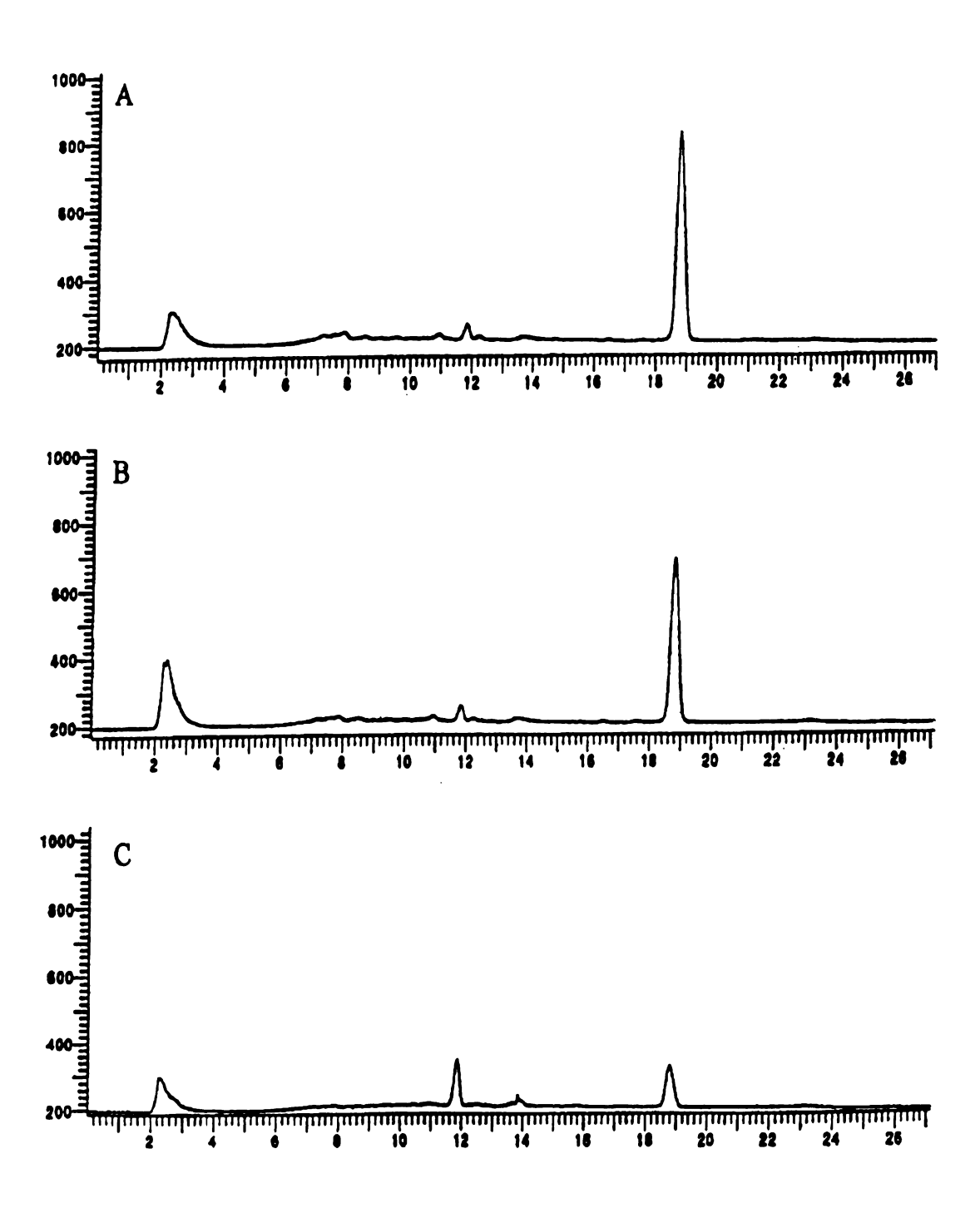


Figure B12. Acetonitrile extract chromatogram for 5% moisture, 25°C (pH 6) pyrene contaminated soil. (a) 2.2 mg O<sub>3</sub>/ppm pyr, (b) 3.85 mg O<sub>3</sub>/ppm pyr, (c) 16 mg O<sub>3</sub>/ppm pyr.

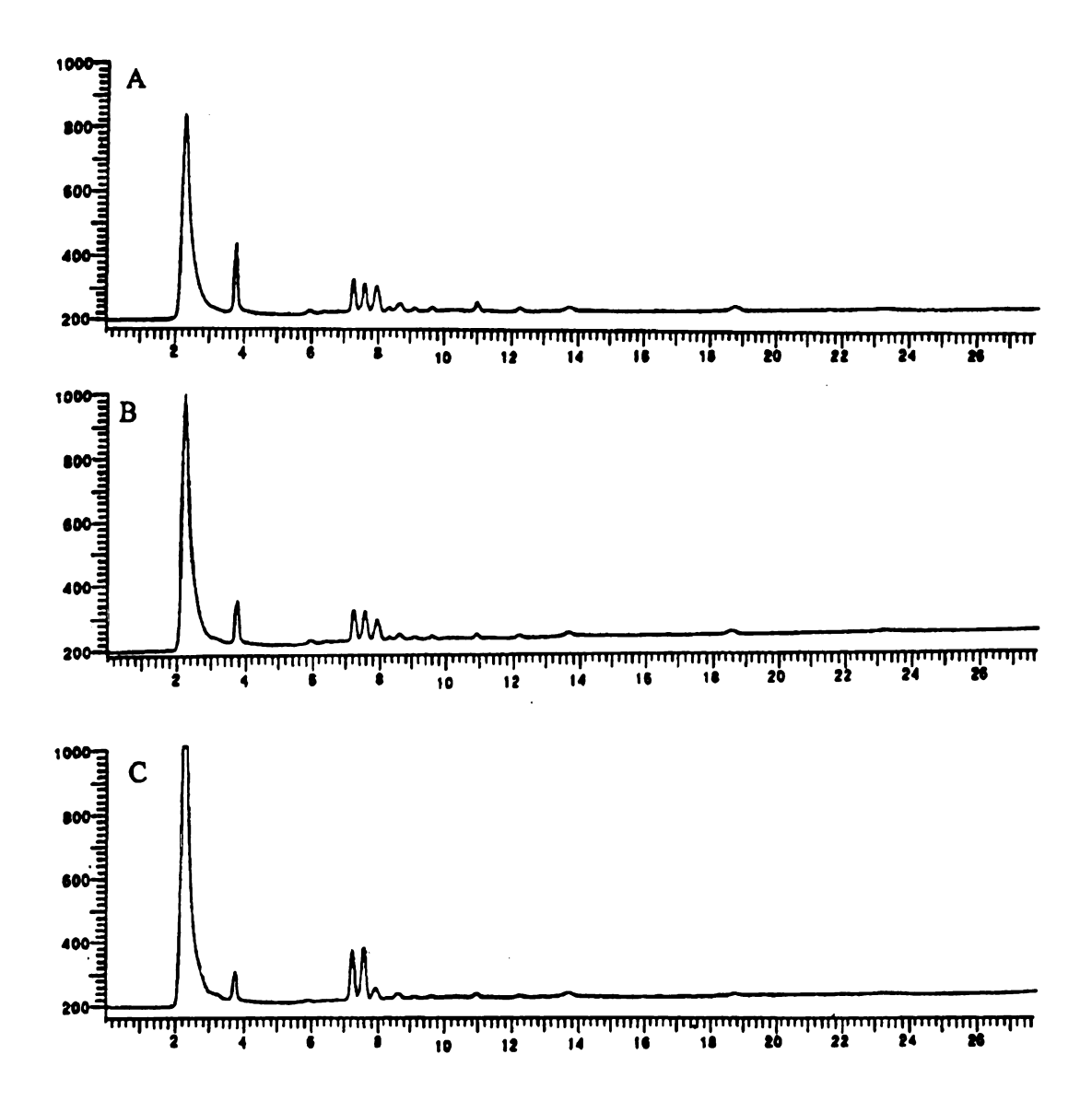


Figure B13. Deionized water extract chromatogram for 5% moisture, 25°C (pH 6) pyrene contaminated soil. (a) 2.2 mg O<sub>3</sub>/ppm pyr, (b) 3.85 mg O<sub>3</sub>/ppm pyr, (c) 16 mg O<sub>3</sub>/ppm pyr.

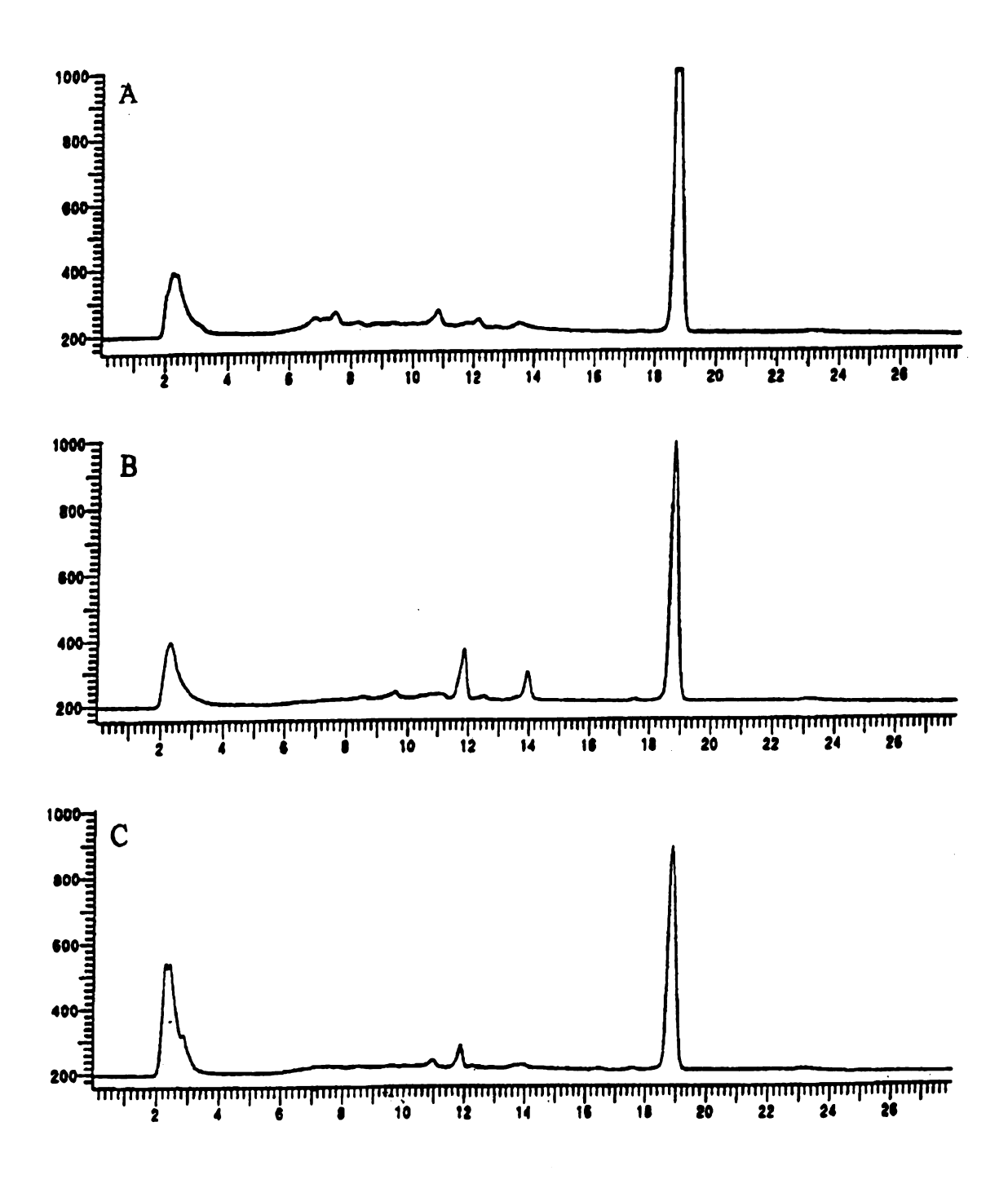


Figure B14. Acetonitrile extract chromatogram for 10% moisture, 25°C (pH 6) pyrene contaminated soil. (a) 2.2 mg O<sub>3</sub>/ppm pyr, (b) 3.85 mg O<sub>3</sub>/ppm pyr, (c) 16 mg O<sub>3</sub>/ppm pyr.

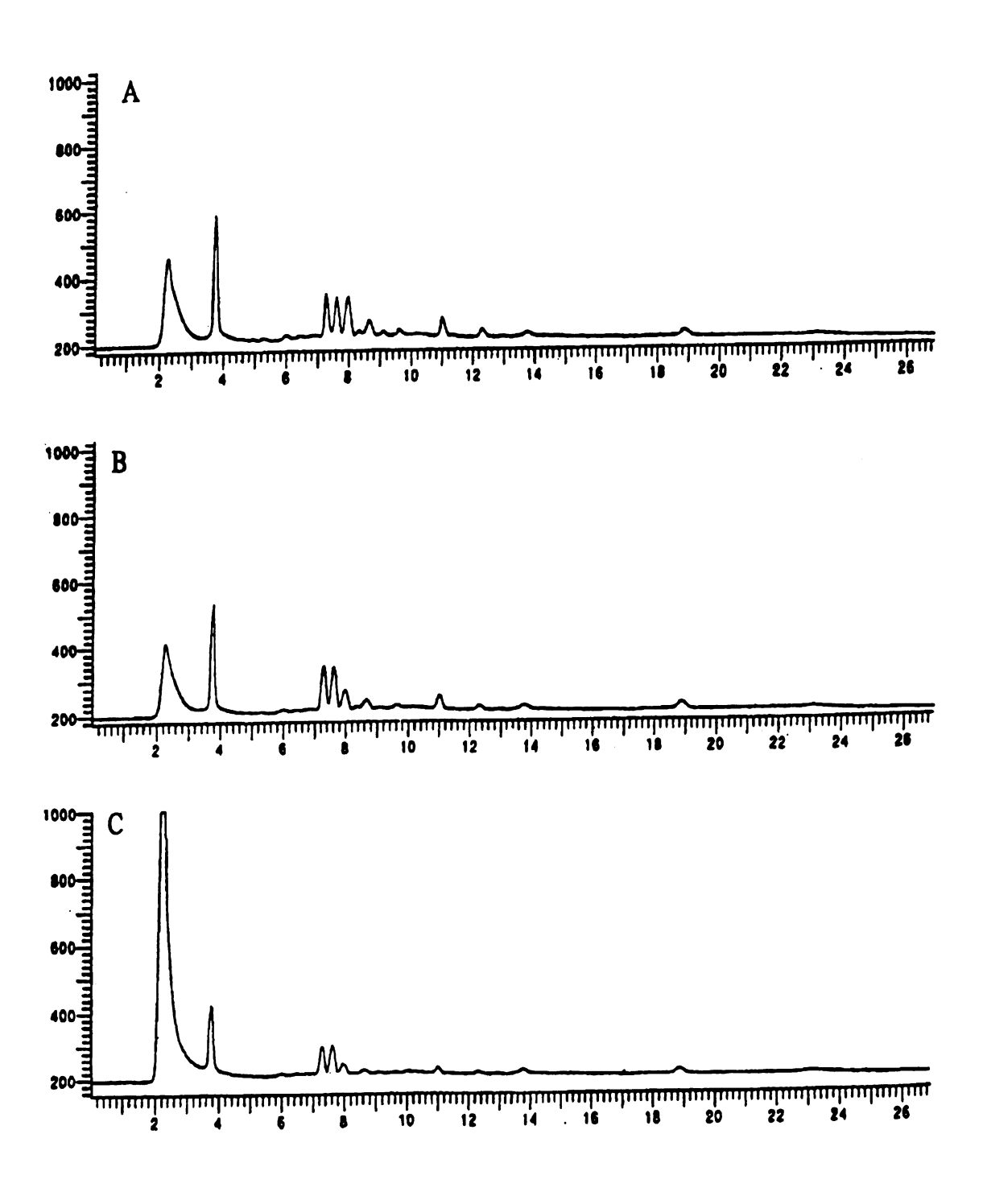


Figure B15. Deionized water extract chromatogram for 10% moisture, 25°C (pH 6) pyrene contaminated soil. (a) 2.2 mg O<sub>3</sub>/ppm pyr, (b) 3.85 mg O<sub>3</sub>/ppm pyr, (c) 16 mg O<sub>3</sub>/ppm pyr.

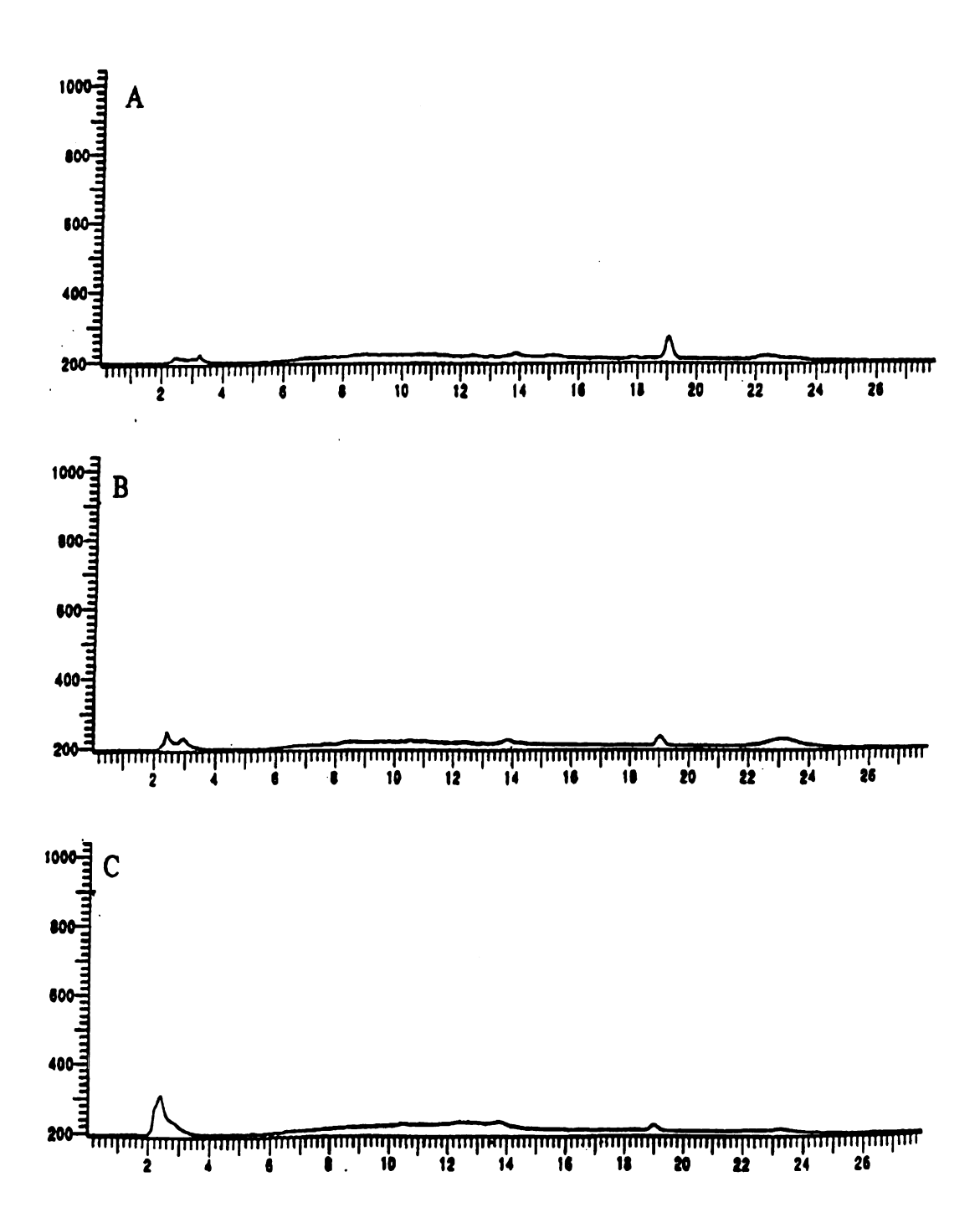


Figure B16. Acetonitrile extract chromatogram for dry, 25°C (pH 8) pyrene contaminated soil. (a) 2.2 mg O<sub>3</sub>/ppm pyr, (b) 3.85 mg O<sub>3</sub>/ppm pyr, (c) 16 mg O<sub>3</sub>/ppm pyr.

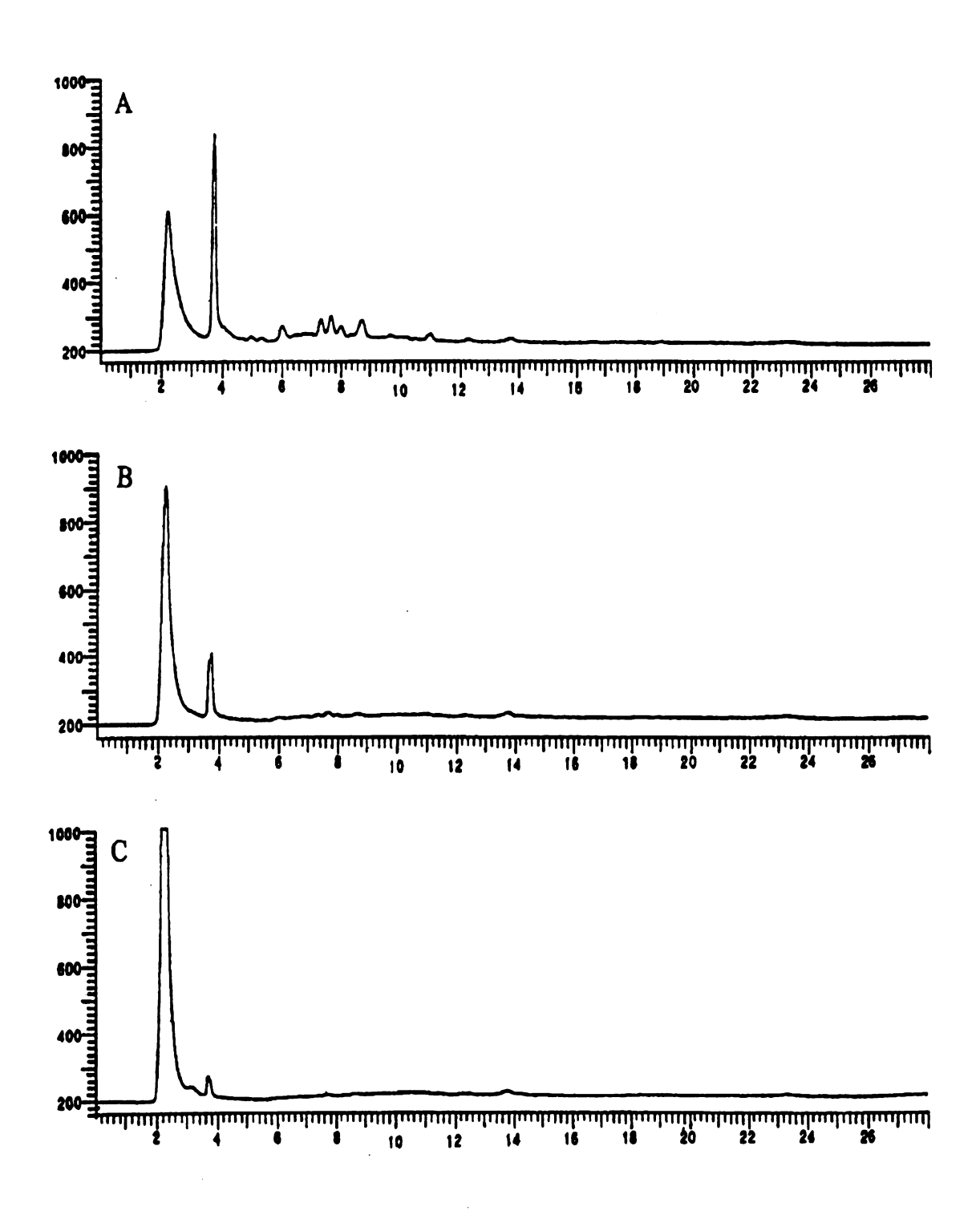


Figure B17. Deionized water extract chromatogram for dry, 25°C (pH 8) pyrene contaminated soil. (a) 2.2 mg O<sub>3</sub>/ppm pyr, (b) 3.85 mg O<sub>3</sub>/ppm pyr, (c) 16 mg O<sub>3</sub>/ppm pyr.

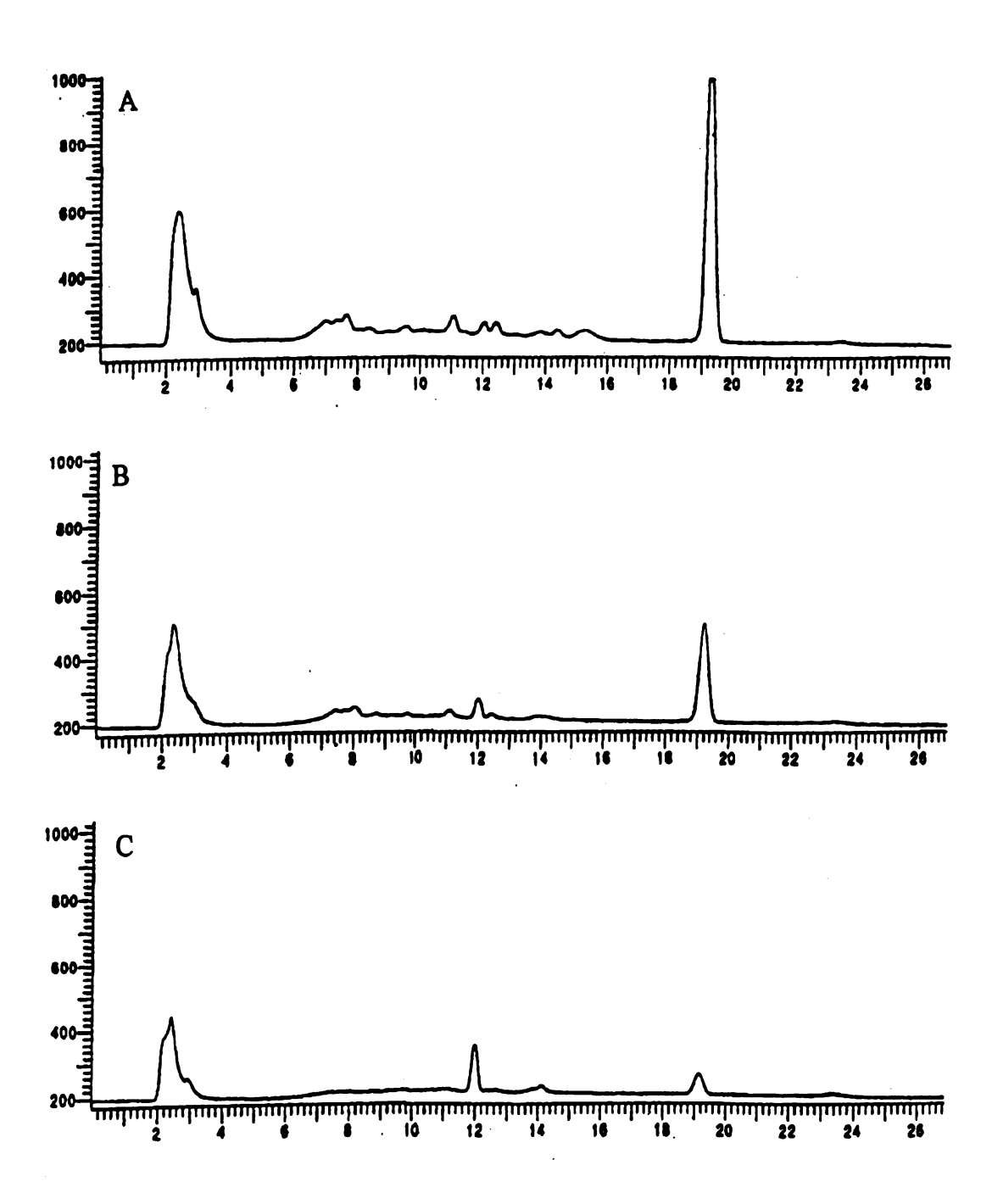


Figure B18. Acetonitrile extract chromatogram for 5% moisture, 25°C (pH 8) pyrene contaminated soil. (a) 2.2 mg O<sub>3</sub>/ppm pyr, (b) 3.85 mg O<sub>3</sub>/ppm pyr, (c) 16 mg O<sub>3</sub>/ppm pyr.

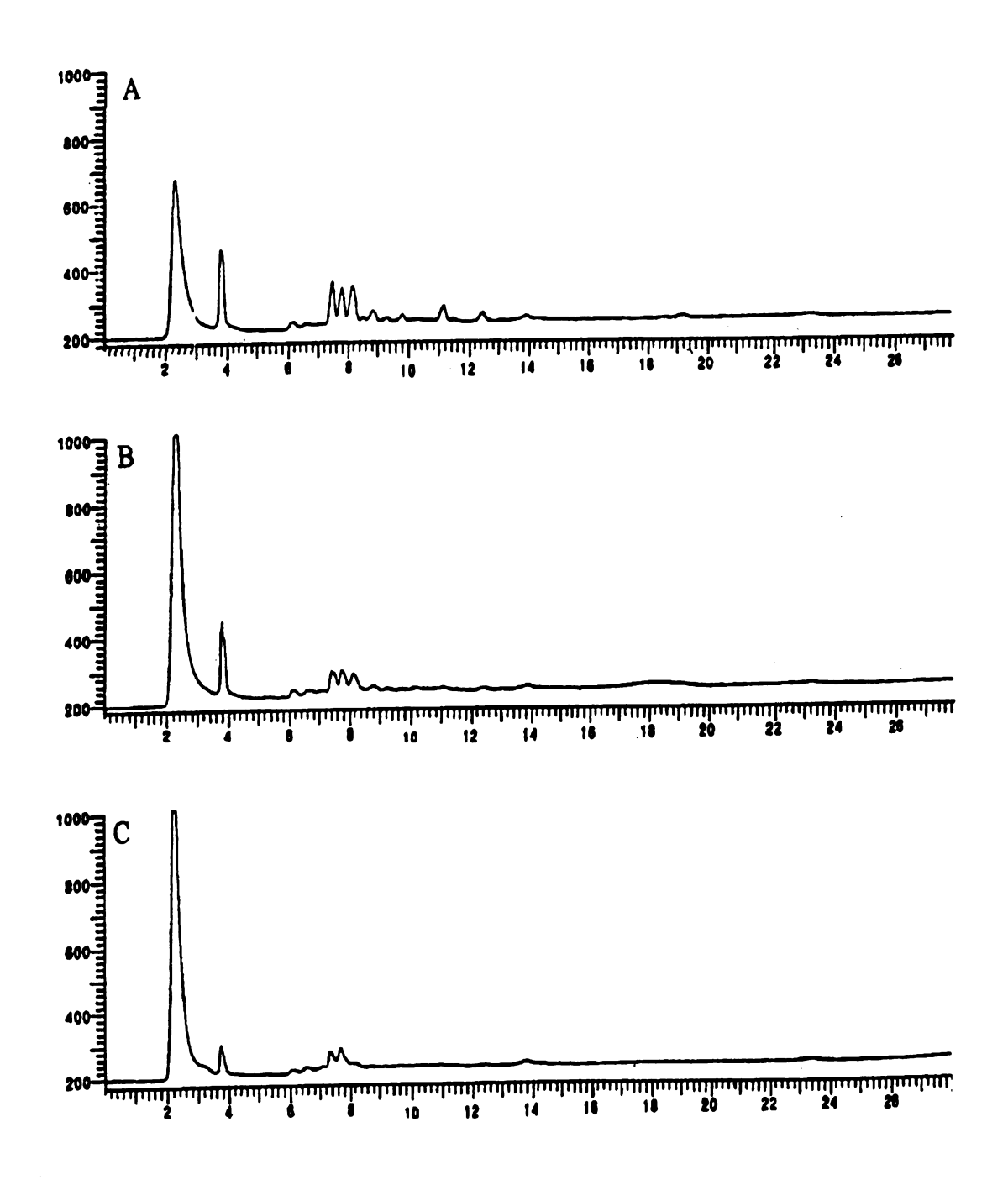


Figure B19. Deionized water extract chromatogram for 5% moisture, 25°C (pH 8) pyrene contaminated soil. (a) 2.2 mg  $O_3$ /ppm pyr, (b) 3.85 mg  $O_3$ /ppm pyr, (c) 16 mg  $O_3$ /ppm pyr.

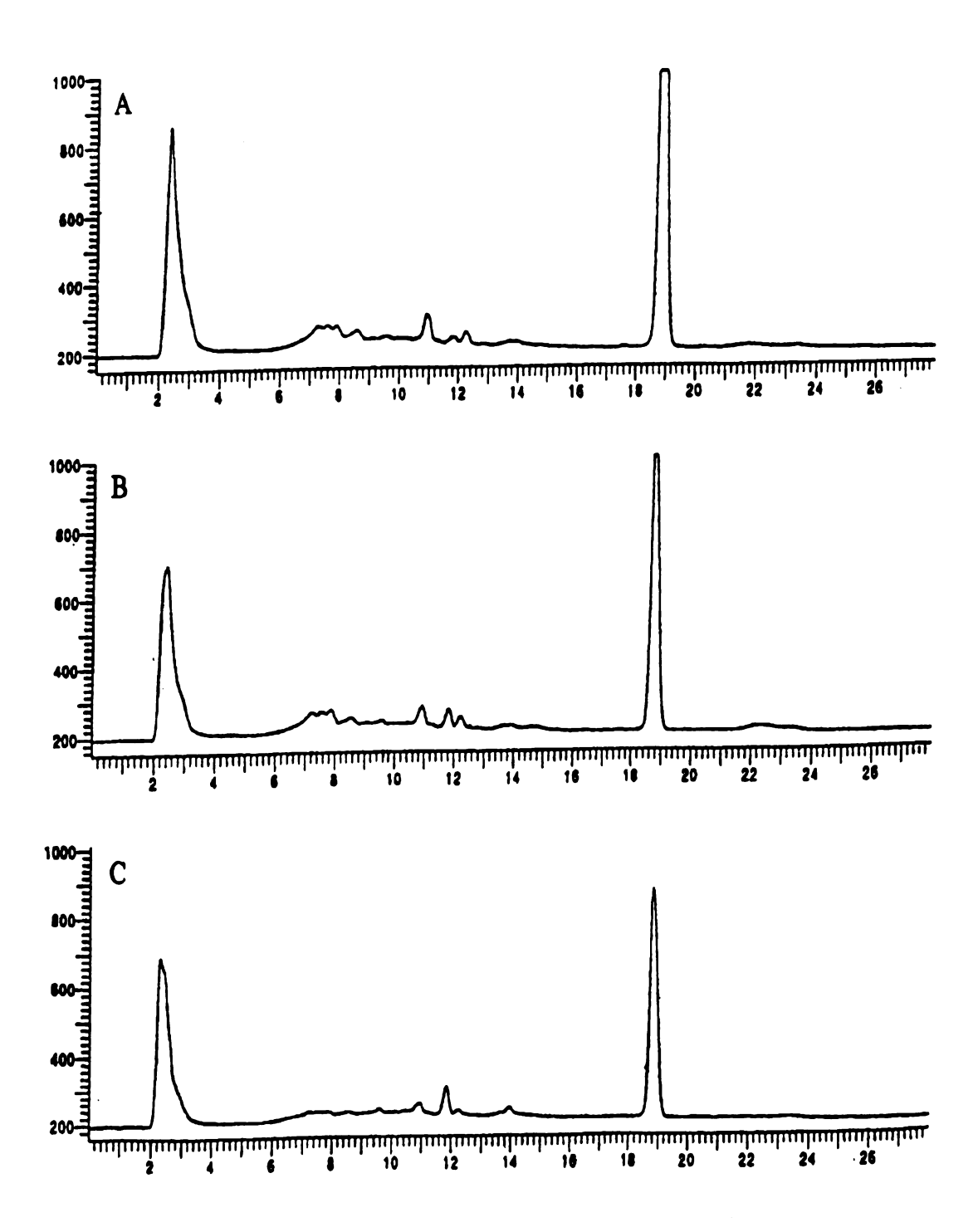


Figure B20. Acetonitrile extract chromatogram for 10% moisture, 25°C (pH 8) pyrene contaminated soil. (a) 2.2 mg O<sub>3</sub>/ppm pyr, (b) 3.85 mg O<sub>3</sub>/ppm pyr, (c) 16 mg O<sub>3</sub>/ppm pyr.

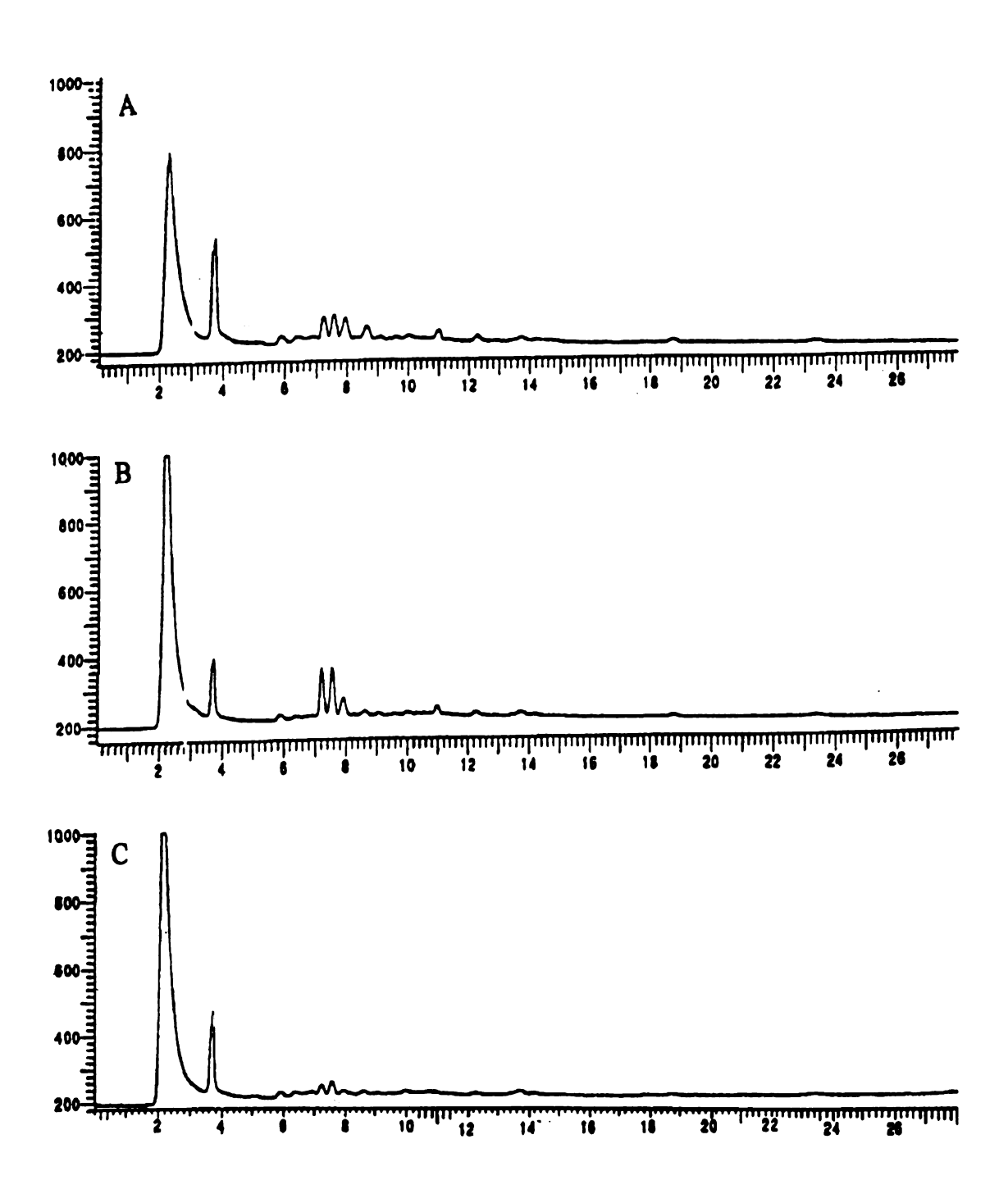


Figure B21. Deionized water extract chromatogram for 10% moisture, 25°C (pH 8) pyrene contaminated soil. (a) 2.2 mg O<sub>3</sub>/ppm pyr, (b) 3.85 mg O<sub>3</sub>/ppm pyr, (c) 16 mg O<sub>3</sub>/ppm pyr.

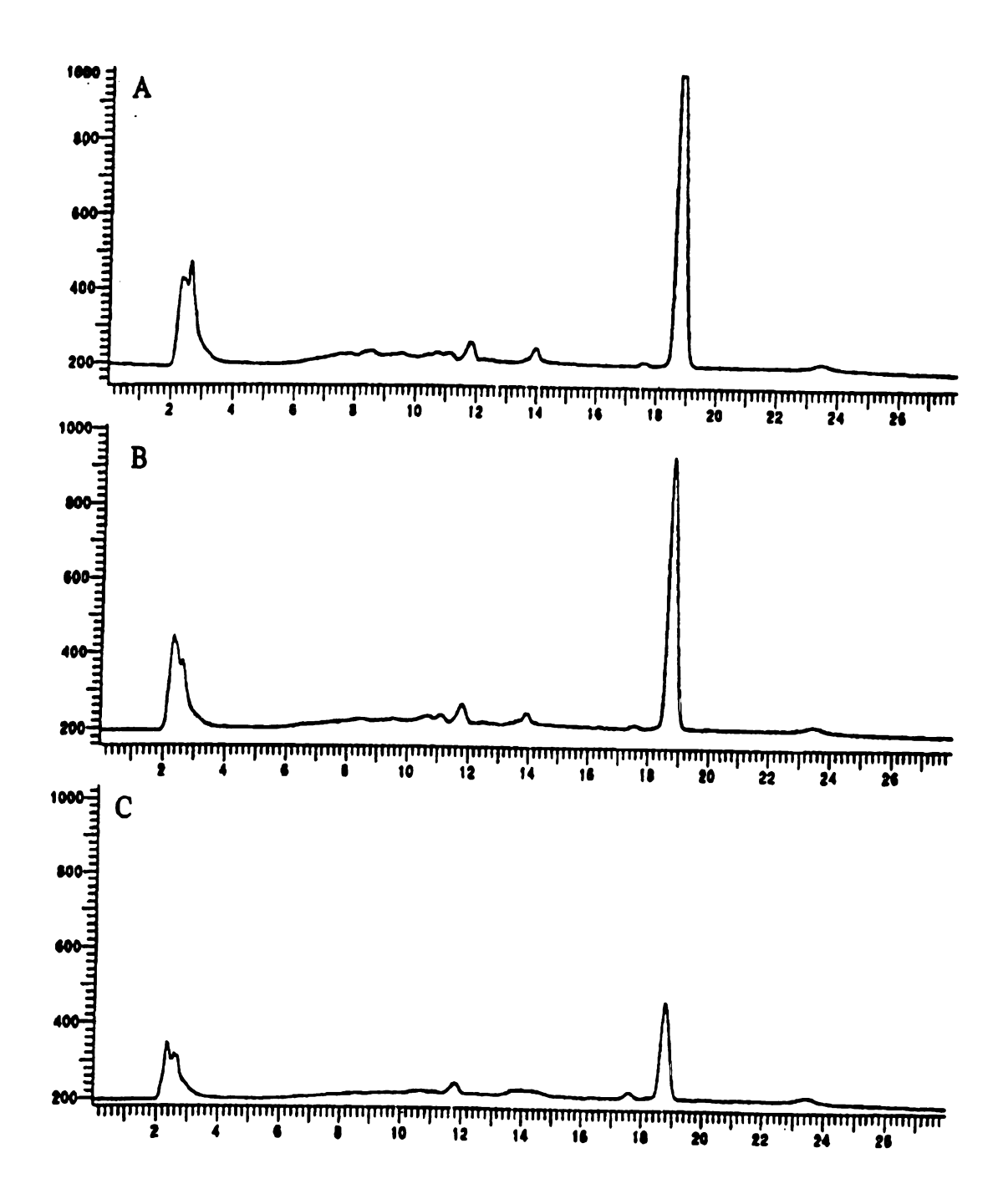


Figure B22. Acetonitrile extract chromatogram for dry, 13°C (pH 2) pyrene contaminated soil. (a) 2.2 mg  $O_3$ /ppm pyr, (b) 3.85 mg  $O_3$ /ppm pyr, (c) 16 mg  $O_3$ /ppm pyr.

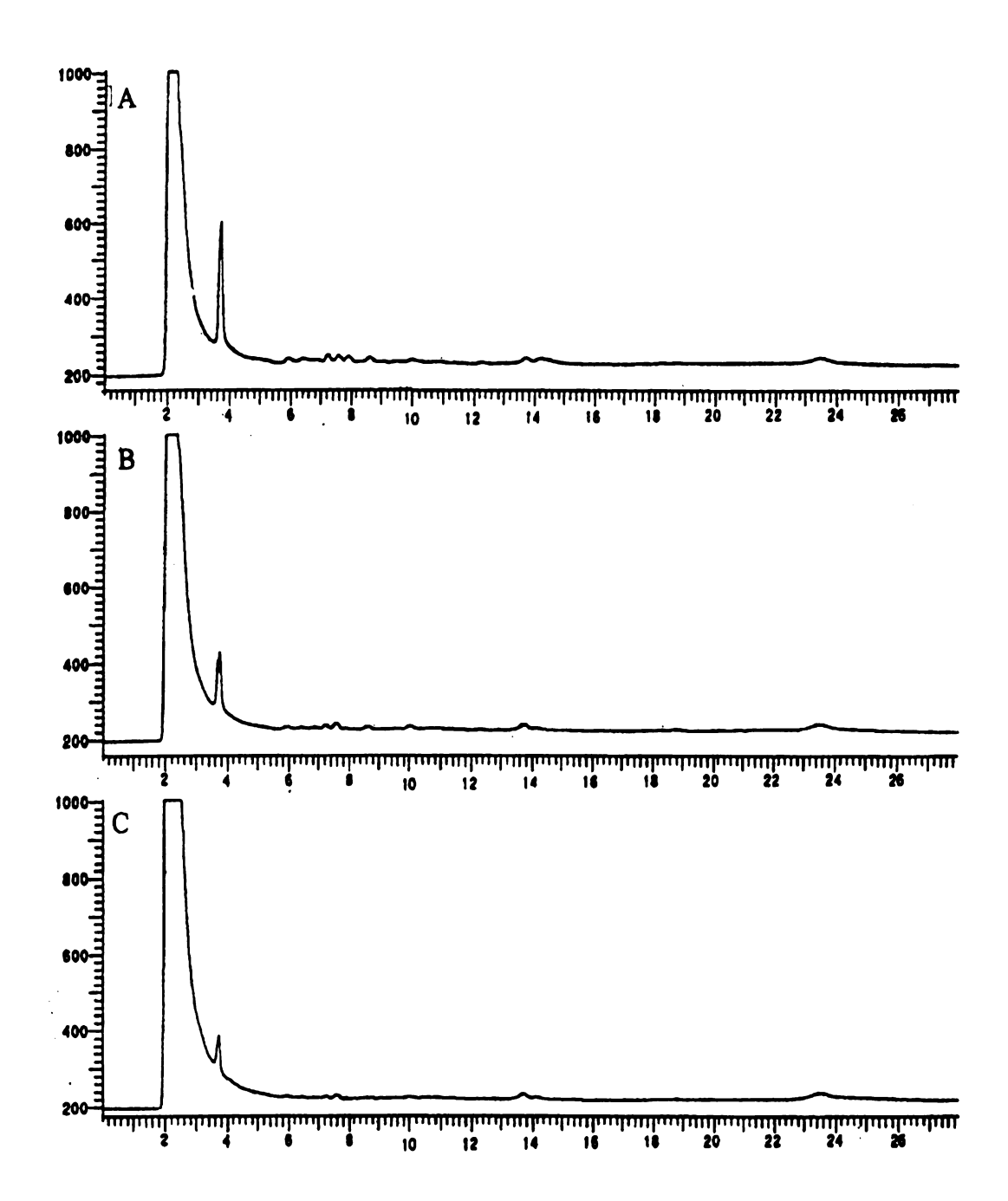


Figure B23. Deionized water extract chromatogram for dry, 13°C (pH 2) pyrene contaminated soil. (a) 2.2 mg O<sub>3</sub>/ppm pyr, (b) 3.85 mg O<sub>3</sub>/ppm pyr, (c) 16 mg O<sub>3</sub>/ppm pyr.

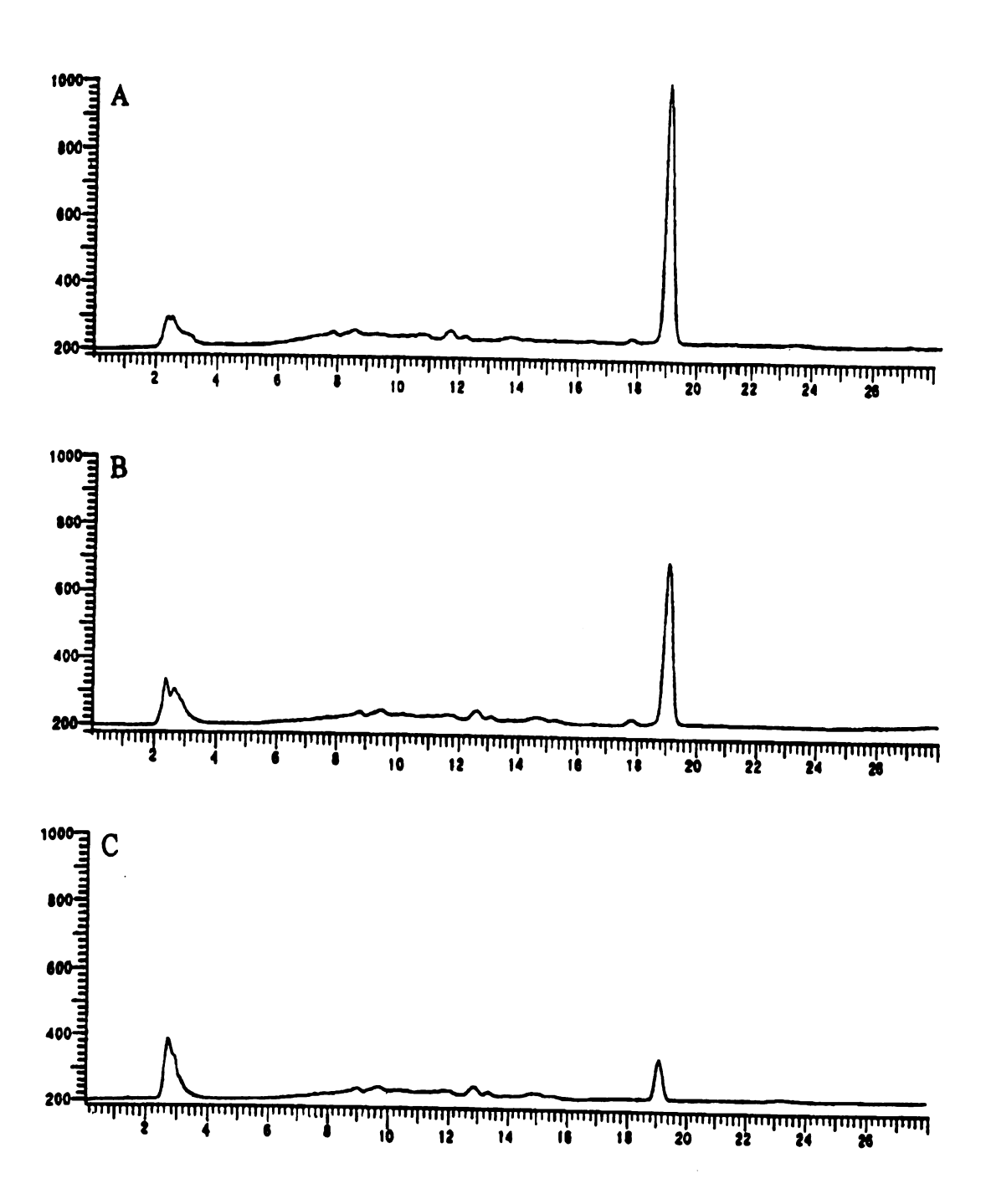


Figure B24. Acetonitrile extract chromatogram for 5% moisture, 13°C (pH 2) pyrene contaminated soil. (a) 2.2 mg O<sub>3</sub>/ppm pyr, (b) 3.85 mg O<sub>3</sub>/ppm pyr, (c) 16 mg O<sub>3</sub>/ppm pyr.

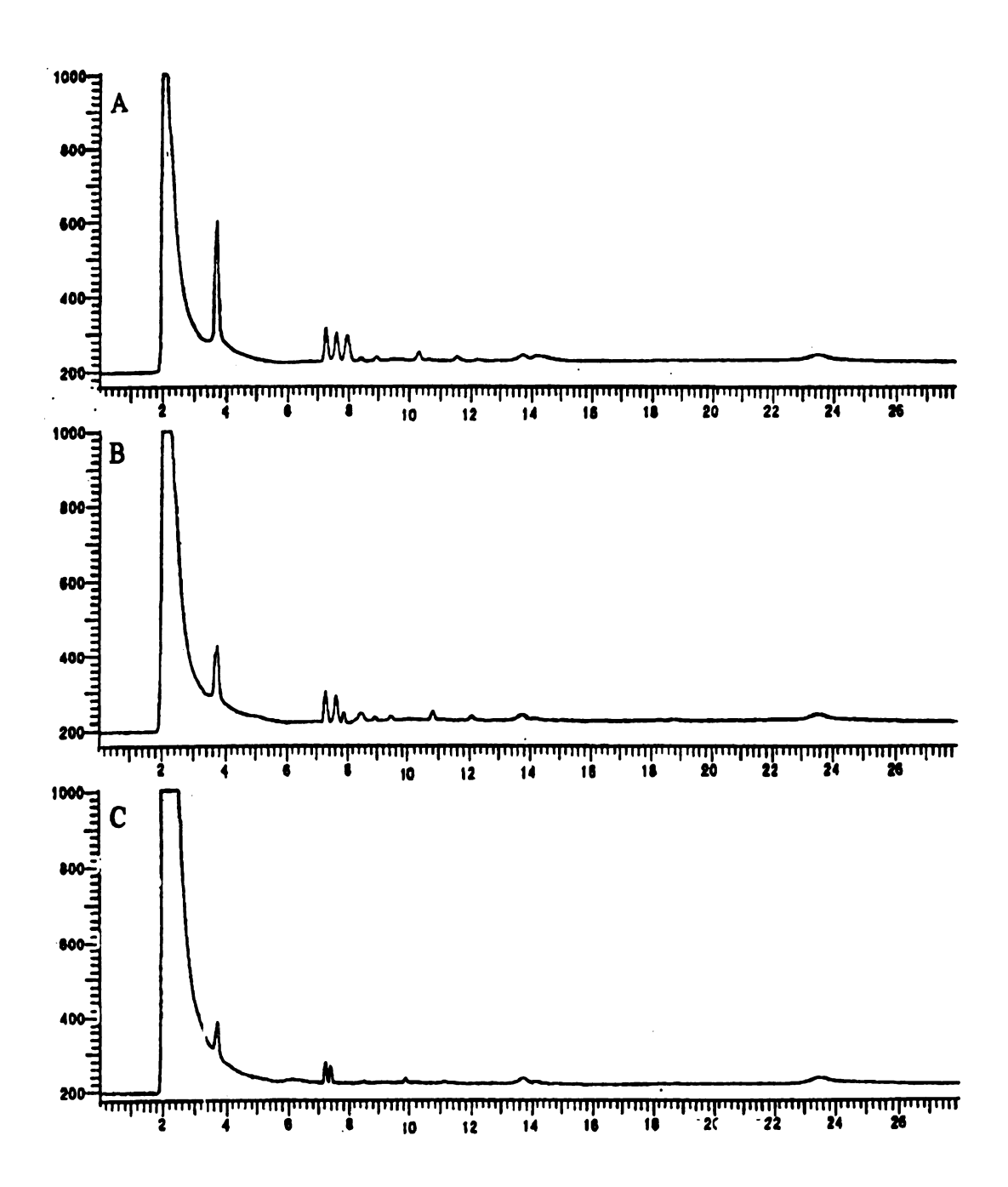


Figure B25. Deionized water extract chromatogram for 5% moisture, 13°C (pH 2) pyrene contaminated soil. (a) 2.2 mg O<sub>3</sub>/ppm pyr, (b) 3.85 mg O<sub>3</sub>/ppm pyr, (c) 16 mg O<sub>3</sub>/ppm pyr.

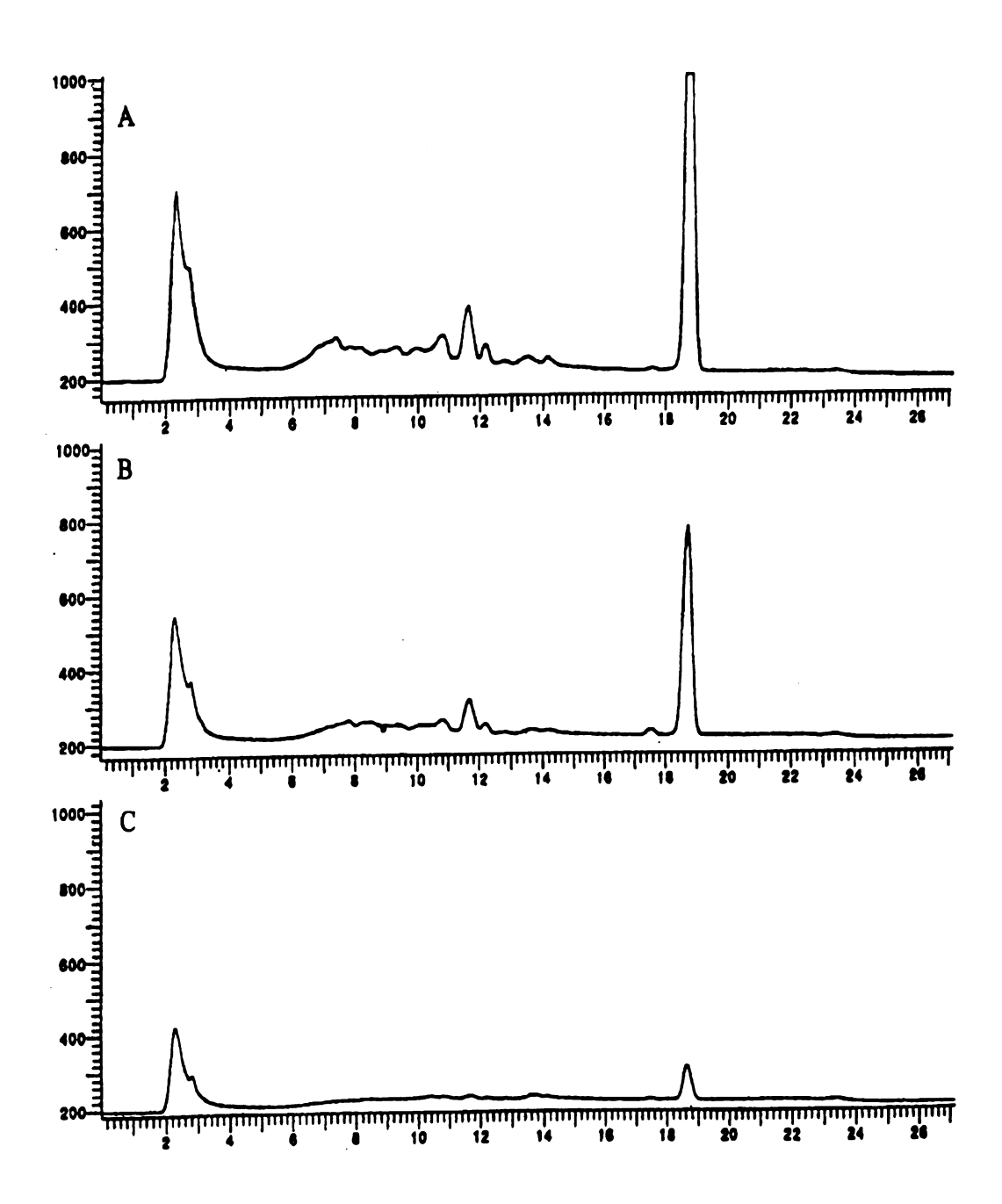


Figure B26. Acetonitrile extract chromatogram for 10% moisture, 13°C (pH 2) pyrene contaminated soil. (a) 2.2 mg O<sub>3</sub>/ppm pyr, (b) 3.85 mg O<sub>3</sub>/ppm pyr, (c) 16 mg O<sub>3</sub>/ppm pyr.

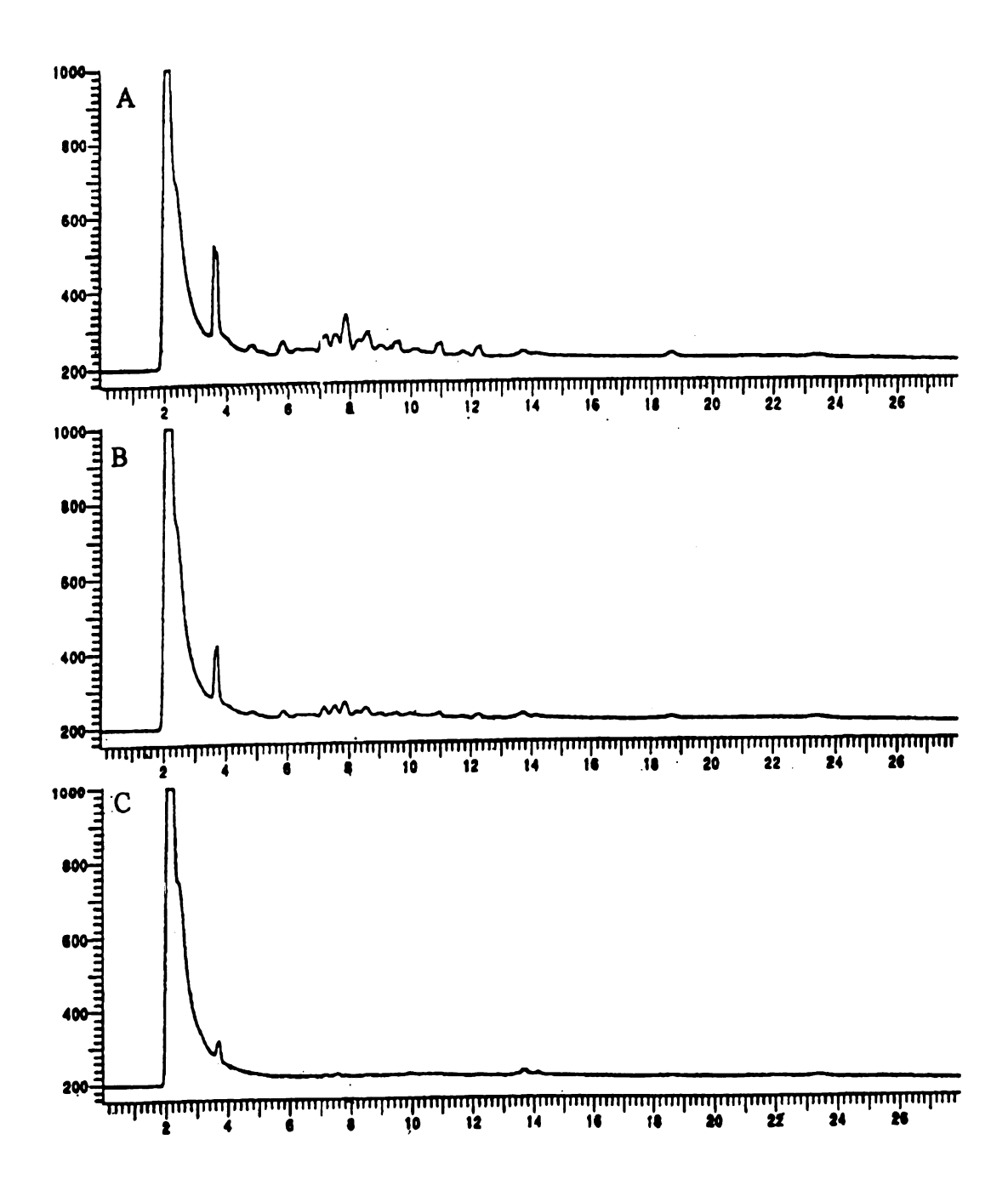


Figure B27. Deionized water extract chromatogram for 10% moisture, 13°C (pH 2) pyrene contaminated soil. (a) 2.2 mg O<sub>3</sub>/ppm pyr, (b) 3.85 mg O<sub>3</sub>/ppm pyr, (c) 16 mg O<sub>3</sub>/ppm pyr.

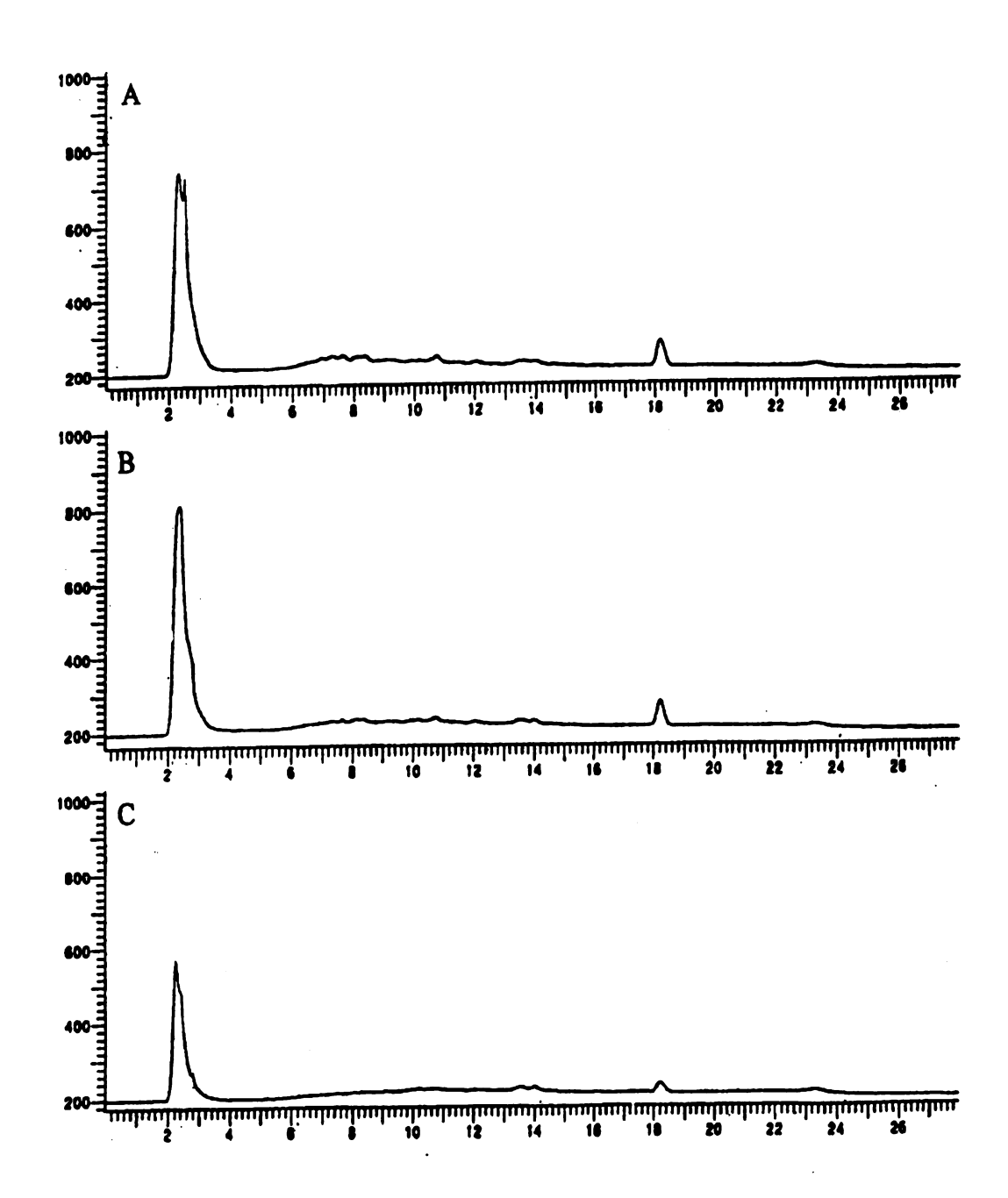


Figure B28. Acetonitrile extract chromatogram for dry, 13°C (pH 6) pyrene contaminated soil. (a) 2.2 mg O<sub>3</sub>/ppm pyr, (b) 3.85 mg O<sub>3</sub>/ppm pyr, (c) 16 mg O<sub>3</sub>/ppm pyr.

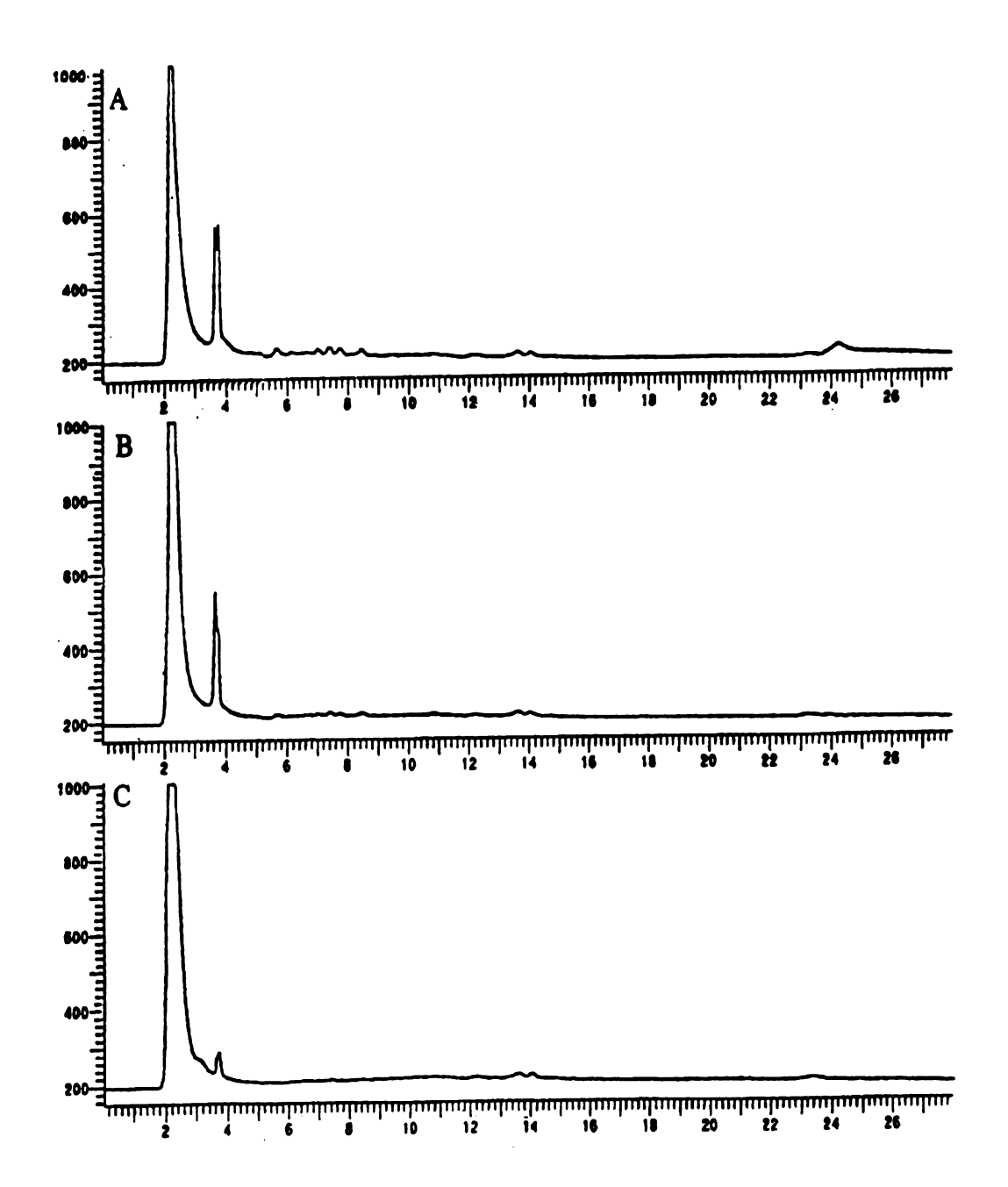


Figure B29. Deionized water extract chromatogram for dry, 13 °C (pH 6) pyrene contaminated soil. (a) 2.2 mg O<sub>3</sub>/ppm pyr, (b) 3.85 mg O<sub>3</sub>/ppm pyr, (c) 16 mg O<sub>3</sub>/ppm pyr.

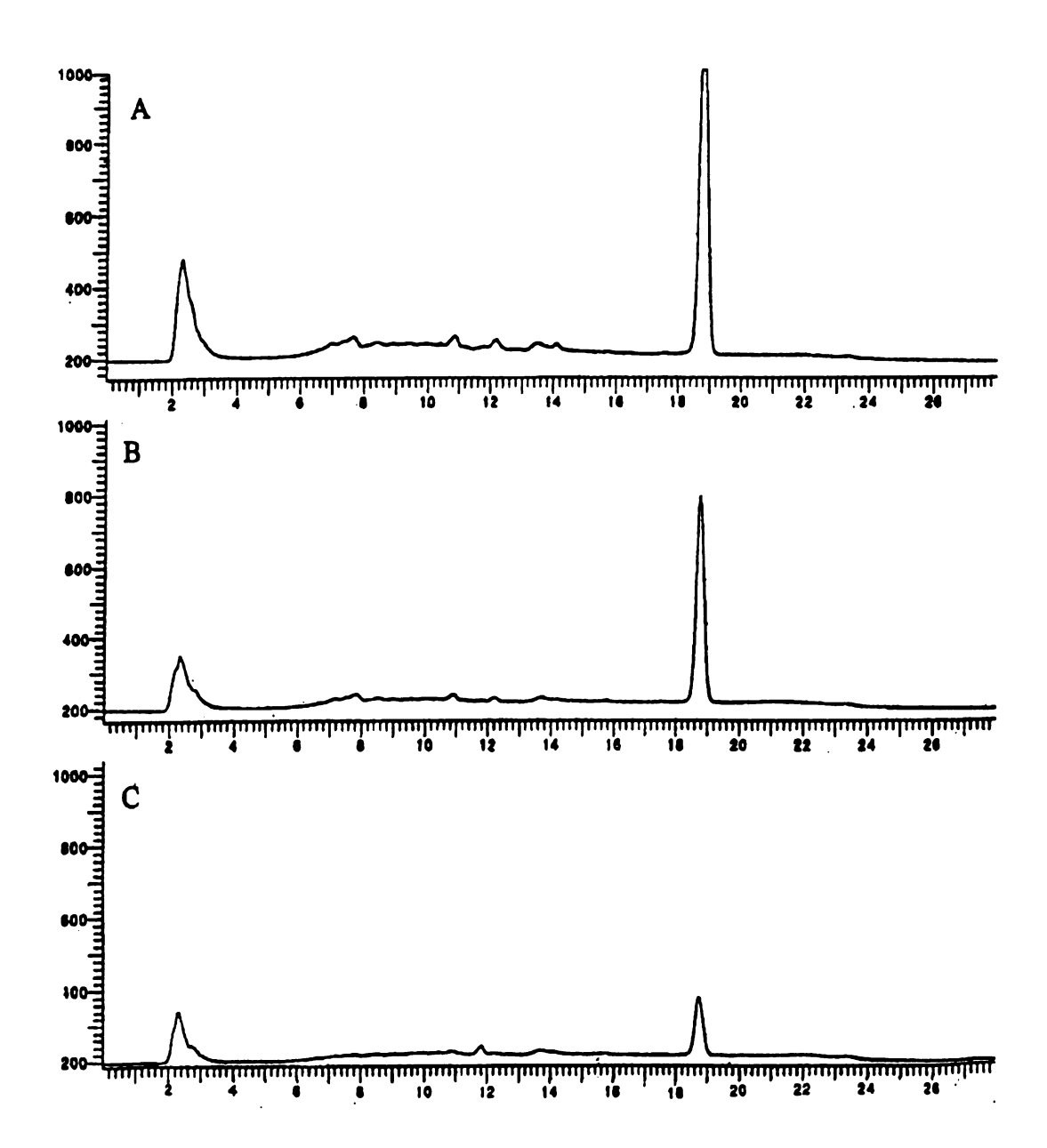


Figure B30. Acetonitrile extract chromatogram for 5% moisture, 13°C (pH 6) pyrene contaminated soil. (a) 2.2 mg O<sub>3</sub>/ppm pyr, (b) 3.85 mg O<sub>3</sub>/ppm pyr, (c) 16 mg O<sub>3</sub>/ppm pyr.

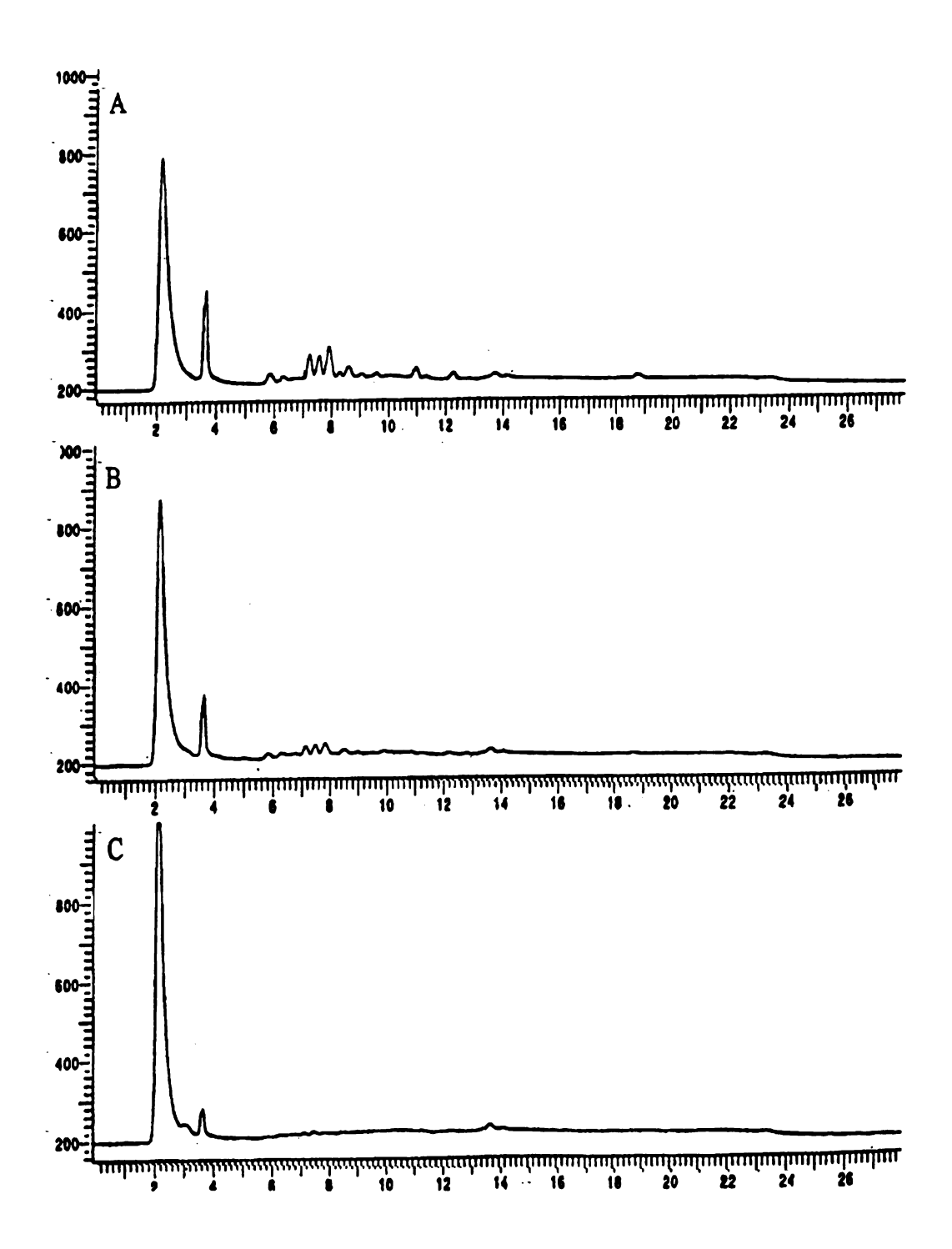


Figure B31. Deionized water extract chromatogram for 5% moisture, 13°C (pH 6) pyrene contaminated soil. (a) 2.2 mg O<sub>3</sub>/ppm pyr, (b) 3.85 mg O<sub>3</sub>/ppm pyr, (c) 16 mg O<sub>3</sub>/ppm pyr.

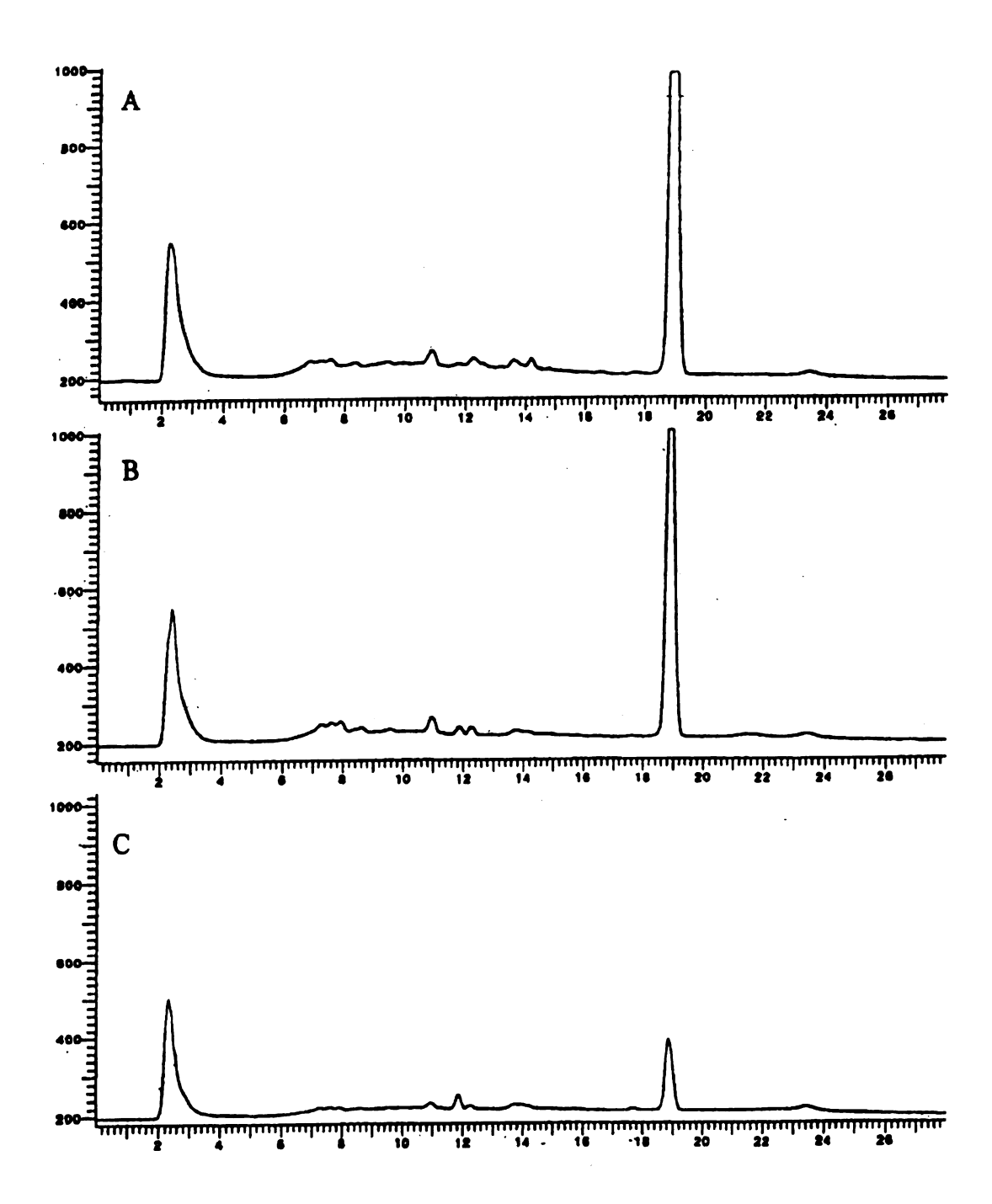


Figure B32. Acetonitrile extract chromatogram for 10% moisture, 13°C (pH 6) pyrene contaminated soil. (a) 2.2 mg O<sub>3</sub>/ppm pyr, (b) 3.85 mg O<sub>3</sub>/ppm pyr, (c) 16 mg O<sub>3</sub>/ppm pyr.

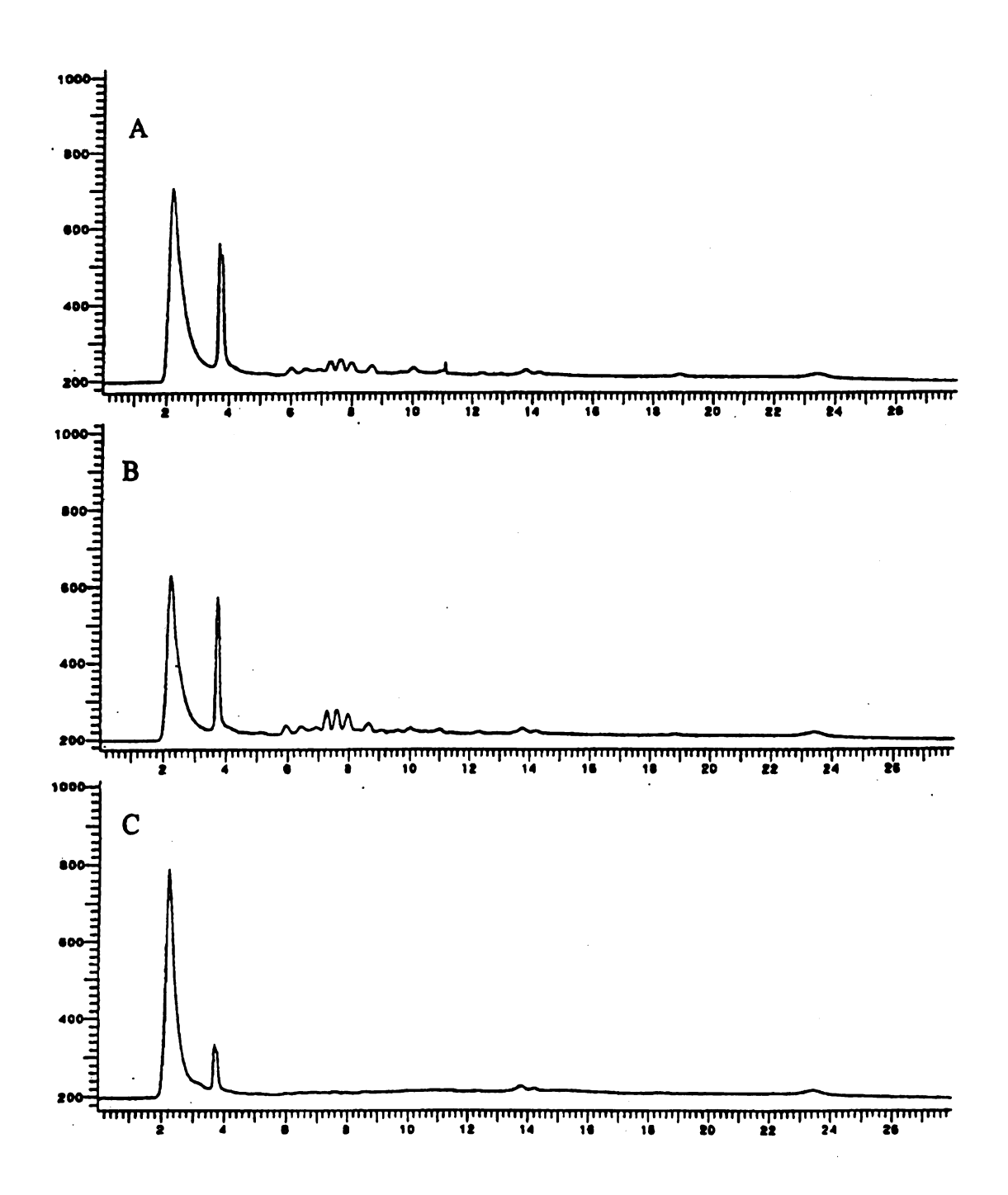


Figure B33. Deionized water extract chromatogram for 10% moisture, 13°C (pH 6) pyrene contaminated soil. (a) 2.2 mg O<sub>3</sub>/ppm pyr, (b) 3.85 mg O<sub>3</sub>/ppm pyr, (c) 16 mg O<sub>3</sub>/ppm pyr.

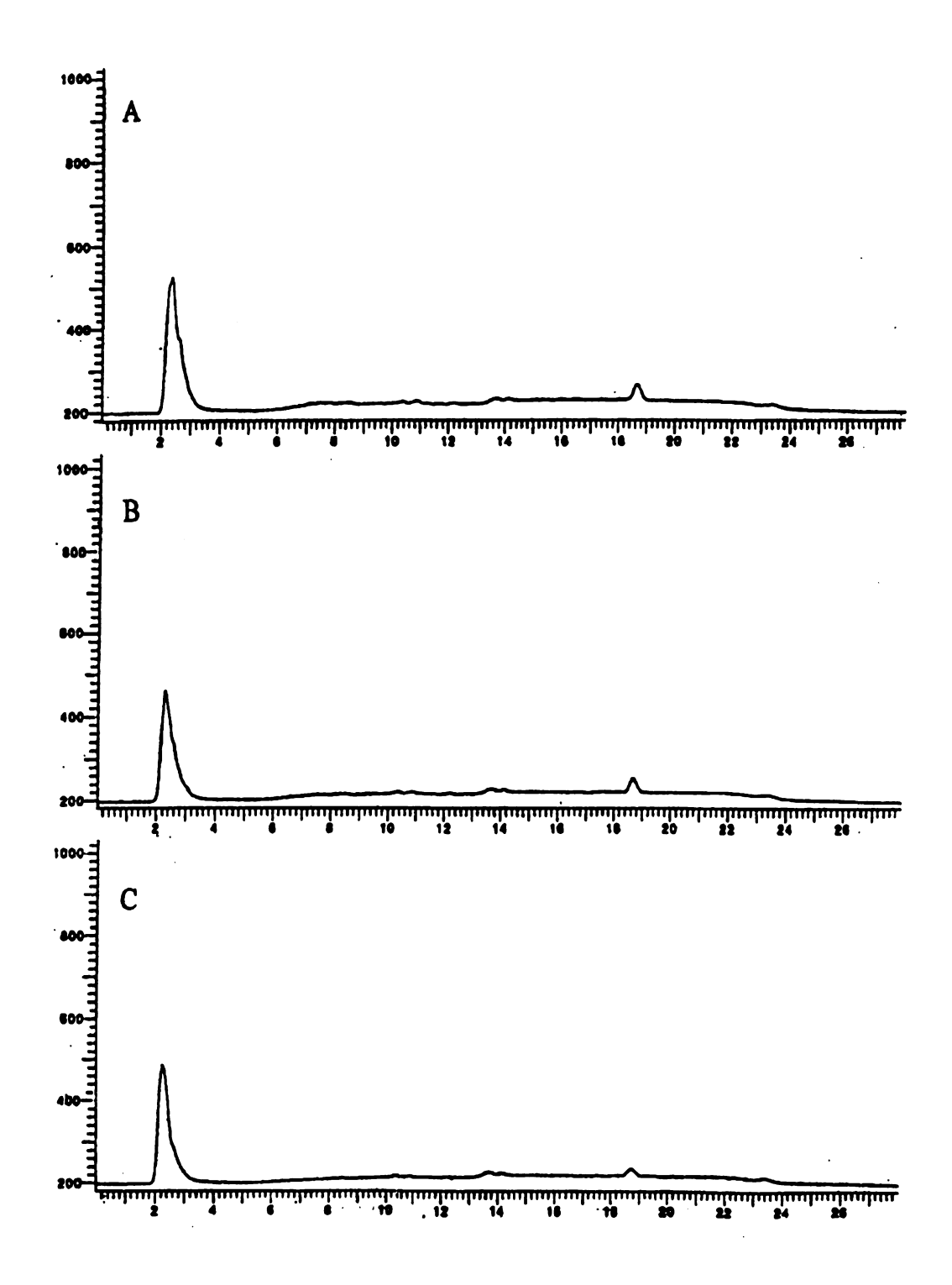


Figure B34. Acetonitrile extract chromatogram for dry, 13°C (pH 8) pyrene contaminated soil. (a) 2.2 mg O<sub>3</sub>/ppm pyr, (b) 3.85 mg O<sub>3</sub>/ppm pyr, (c) 16 mg O<sub>3</sub>/ppm pyr.

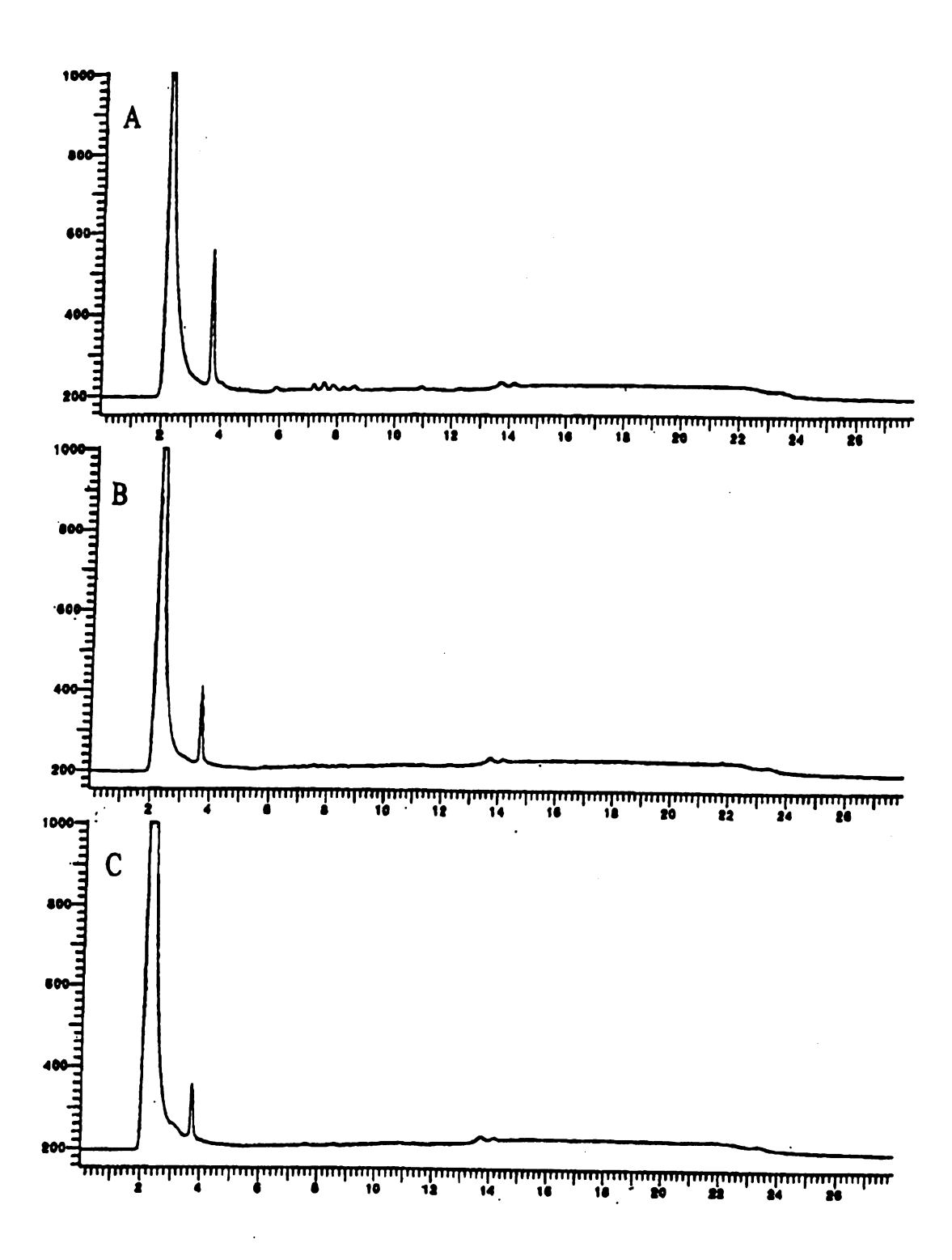


Figure B35. Deionized water extract chromatogram for dry, 13°C (pH 8) pyrene contaminated soil. (a) 2.2 mg  $O_3$ /ppm pyr, (b) 3.85 mg  $O_3$ /ppm pyr, (c) 16 mg  $O_3$ /ppm pyr.

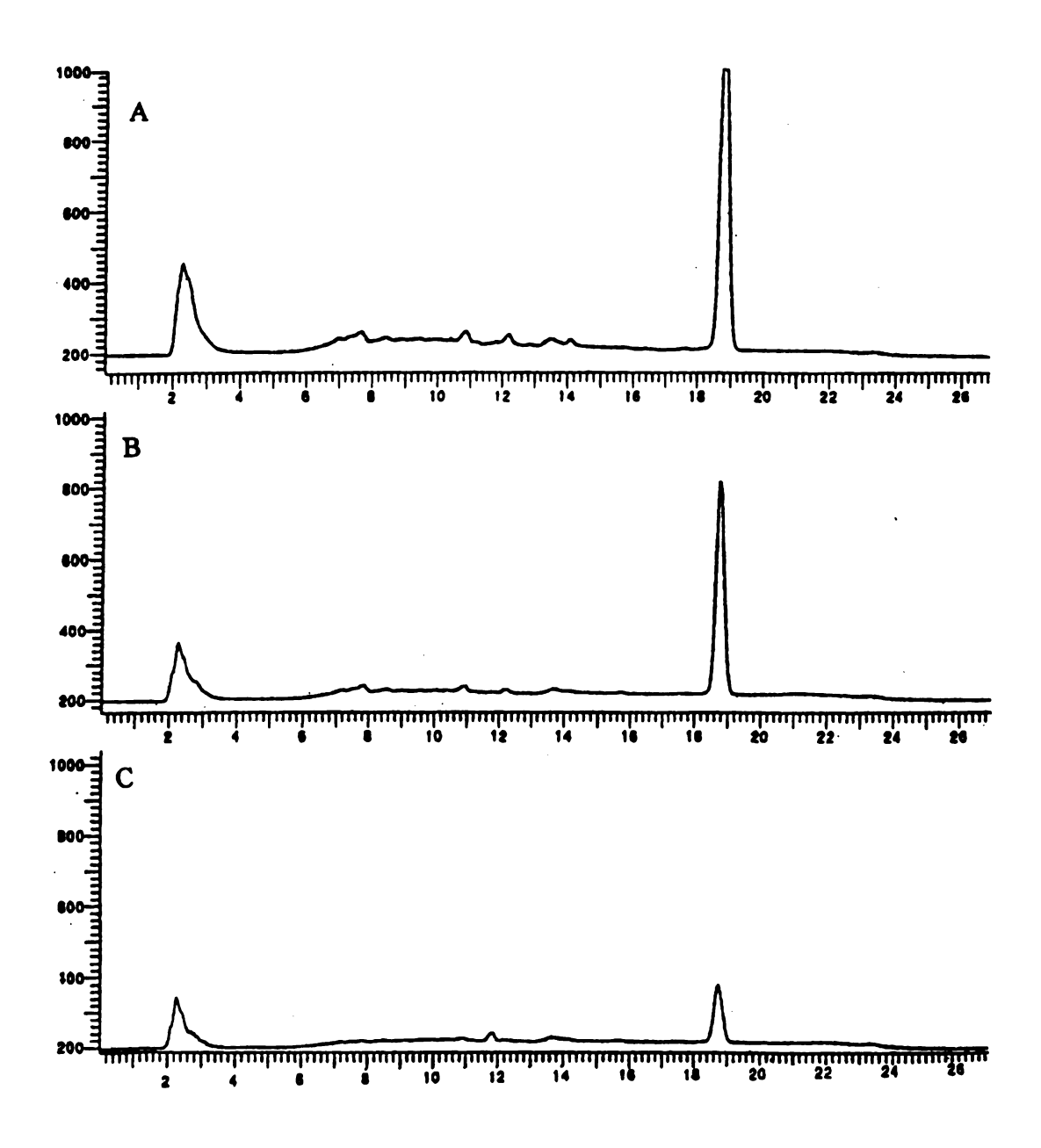


Figure B36. Acetonitrile extract chromatogram for 5% moisture, 13°C (pH 8) pyrene contaminated soil. (a) 2.2 mg O<sub>3</sub>/ppm pyr, (b) 3.85 mg O<sub>3</sub>/ppm pyr, (c) 16 mg O<sub>3</sub>/ppm pyr.

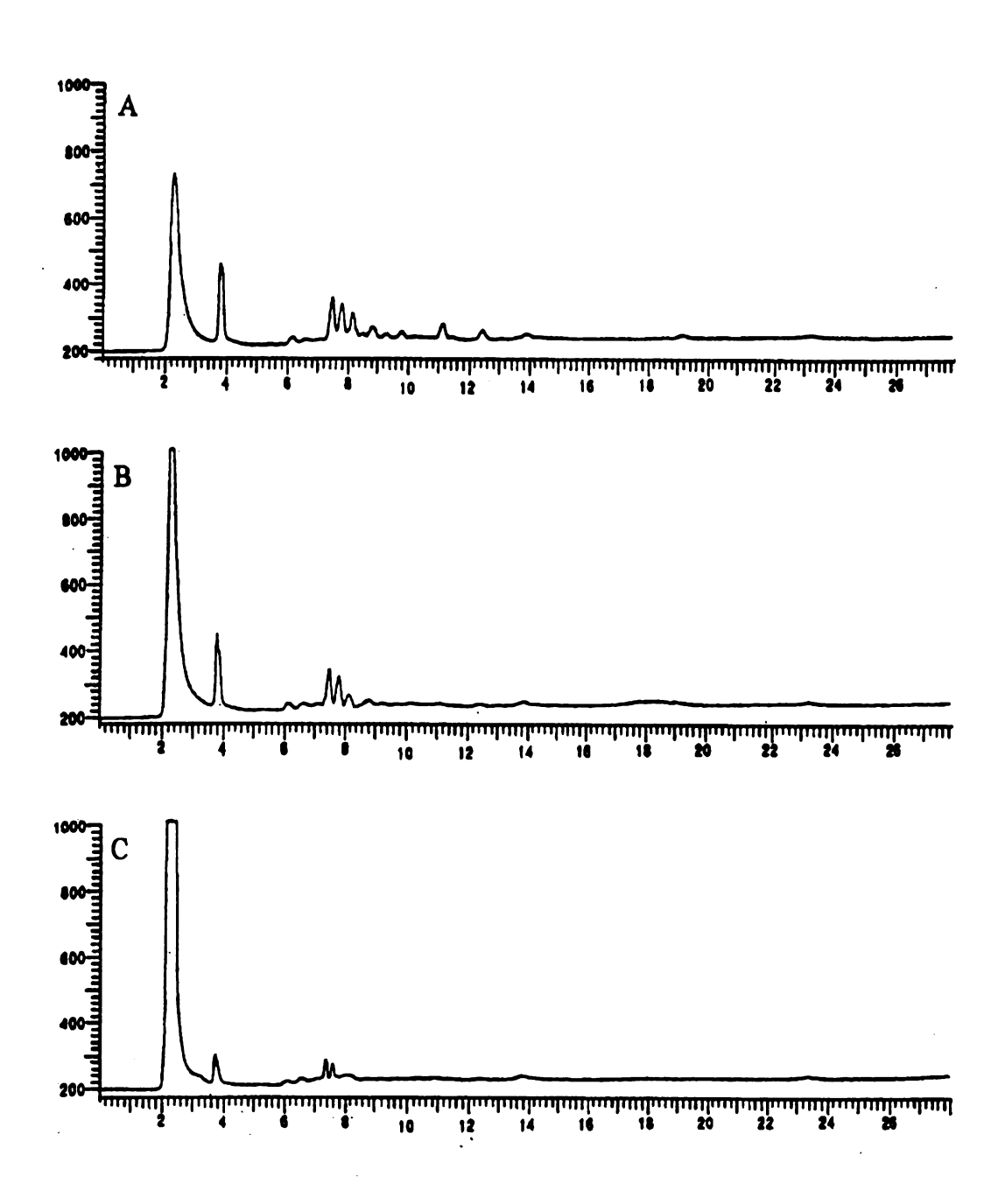


Figure B37. Deionized water extract chromatogram for 5% moisture, 13°C (pH 8) pyrene contaminated soil. (a) 2.2 mg O<sub>3</sub>/ppm pyr, (b) 3.85 mg O<sub>3</sub>/ppm pyr, (c) 16 mg O<sub>3</sub>/ppm pyr.

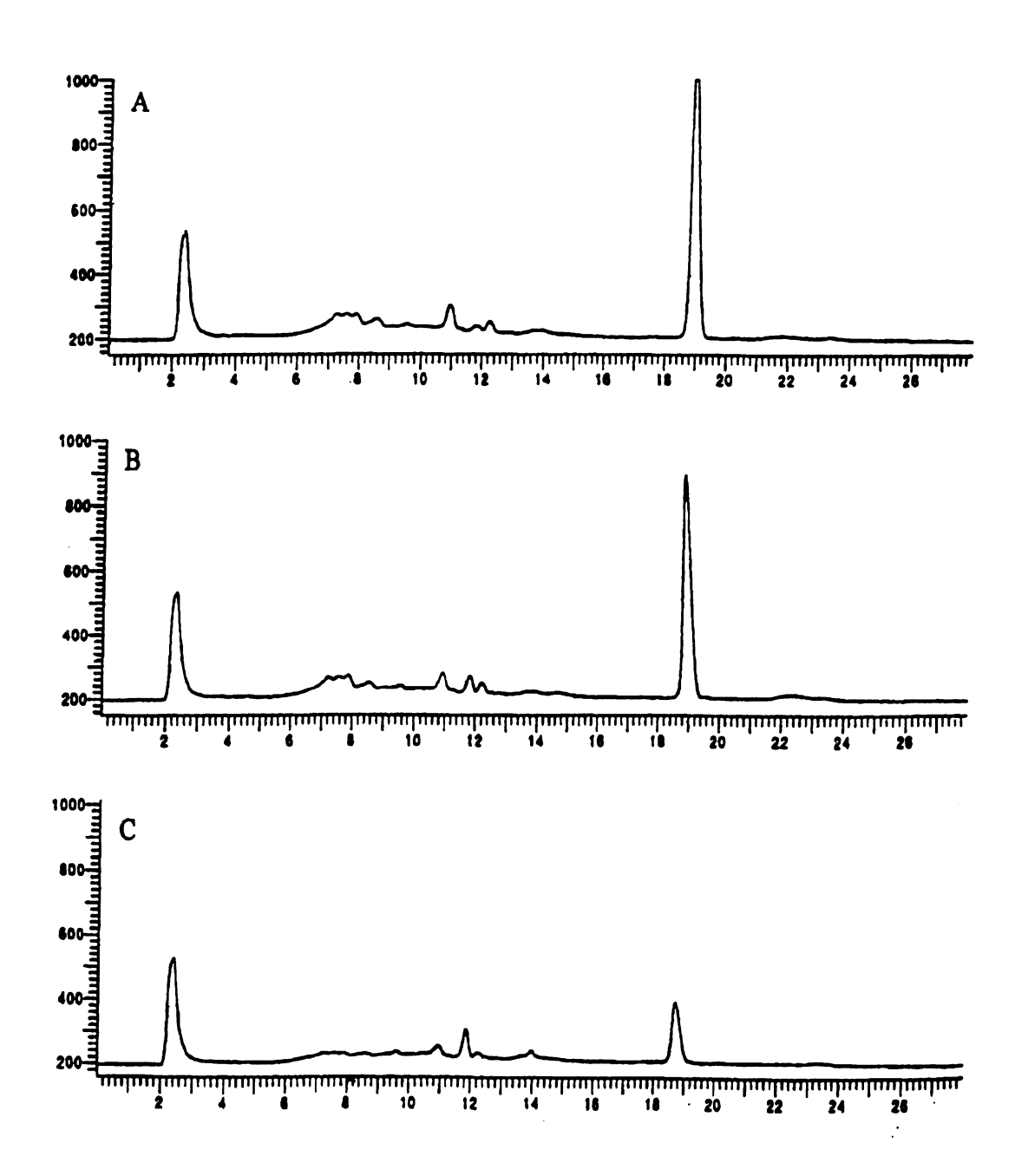


Figure B38. Acetonitrile extract chromatogram for 10% moisture, 13°C (pH 8) pyrene contaminated soil. (a) 2.2 mg  $O_3$ /ppm pyr, (b) 3.85 mg  $O_3$ /ppm pyr, (c) 16 mg  $O_3$ /ppm pyr.

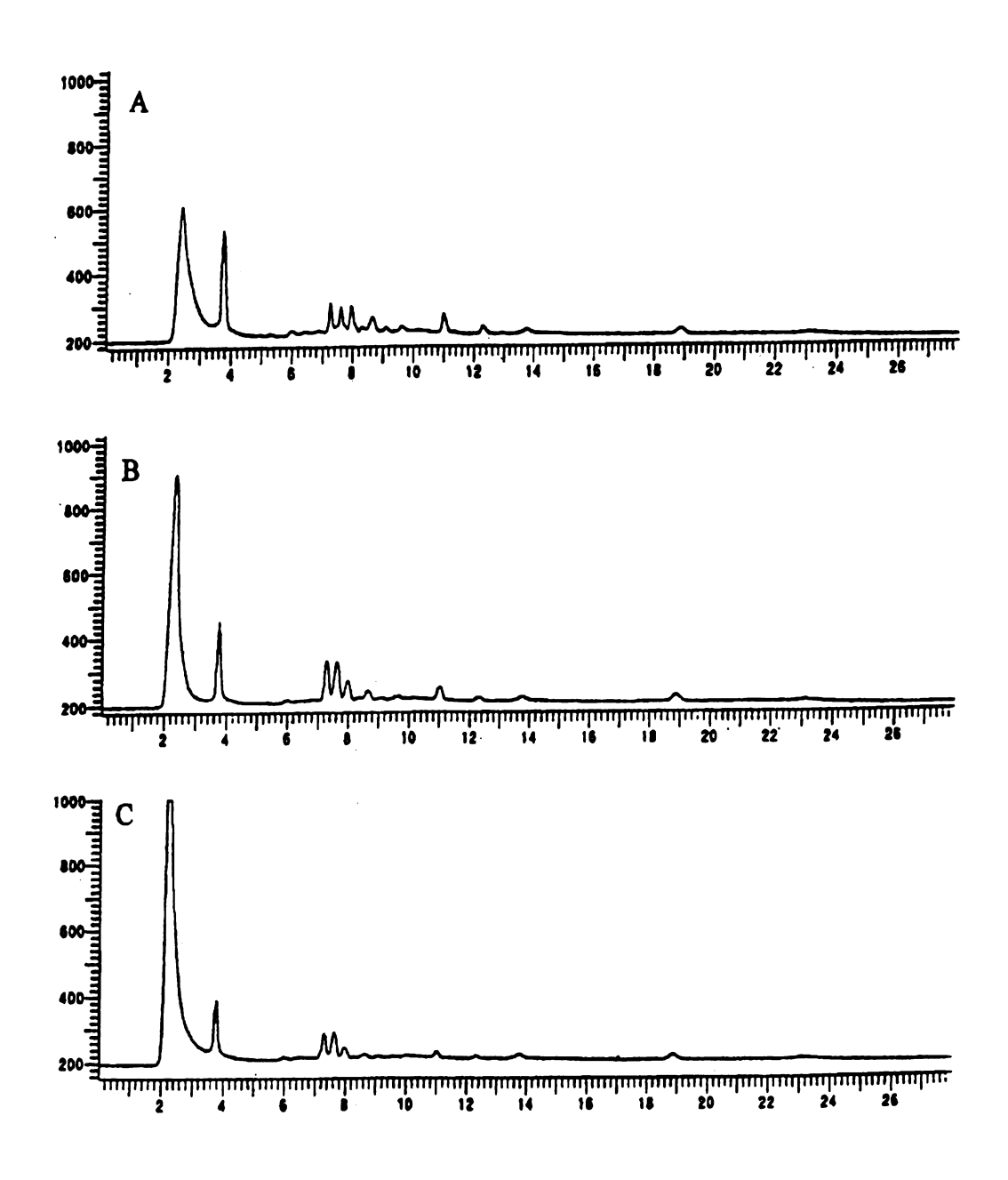


Figure B39. Deionized water extract chromatogram for 10% moisture, 13°C (pH 8) pyrene contaminated soil. (a) 2.2 mg O<sub>3</sub>/ppm pyr, (b) 3.85 mg O<sub>3</sub>/ppm pyr, (c) 16 mg O<sub>3</sub>/ppm pyr.

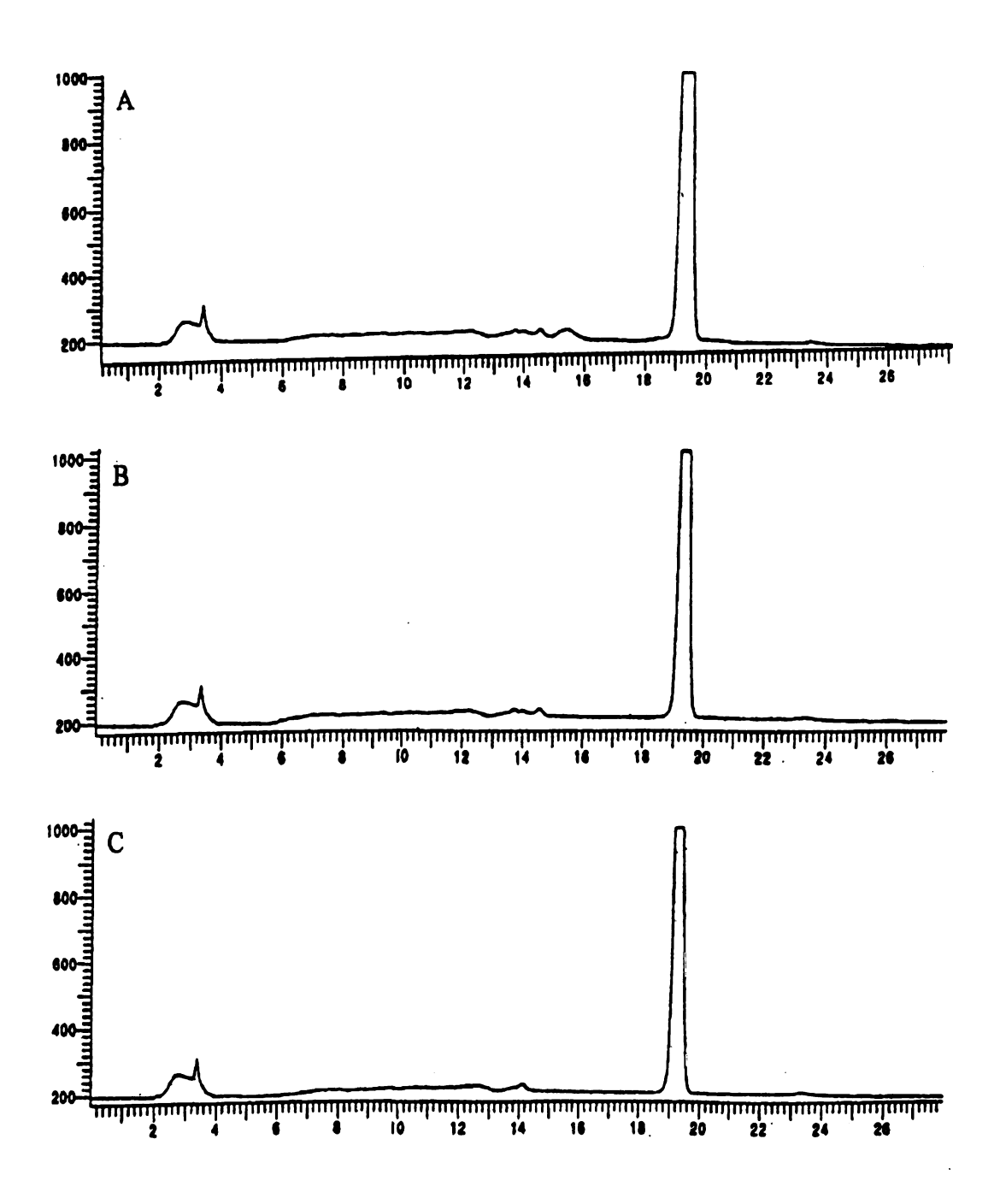


Figure B40. Acetonitrile extract chromatogram for aged, dry, 25°C (pH 2) pyrene contaminated soil. (a) 2.2 mg O<sub>3</sub>/ppm pyr, (b) 3.85 mg O<sub>3</sub>/ppm pyr, (c) 16 mg O<sub>3</sub>/ppm pyr.

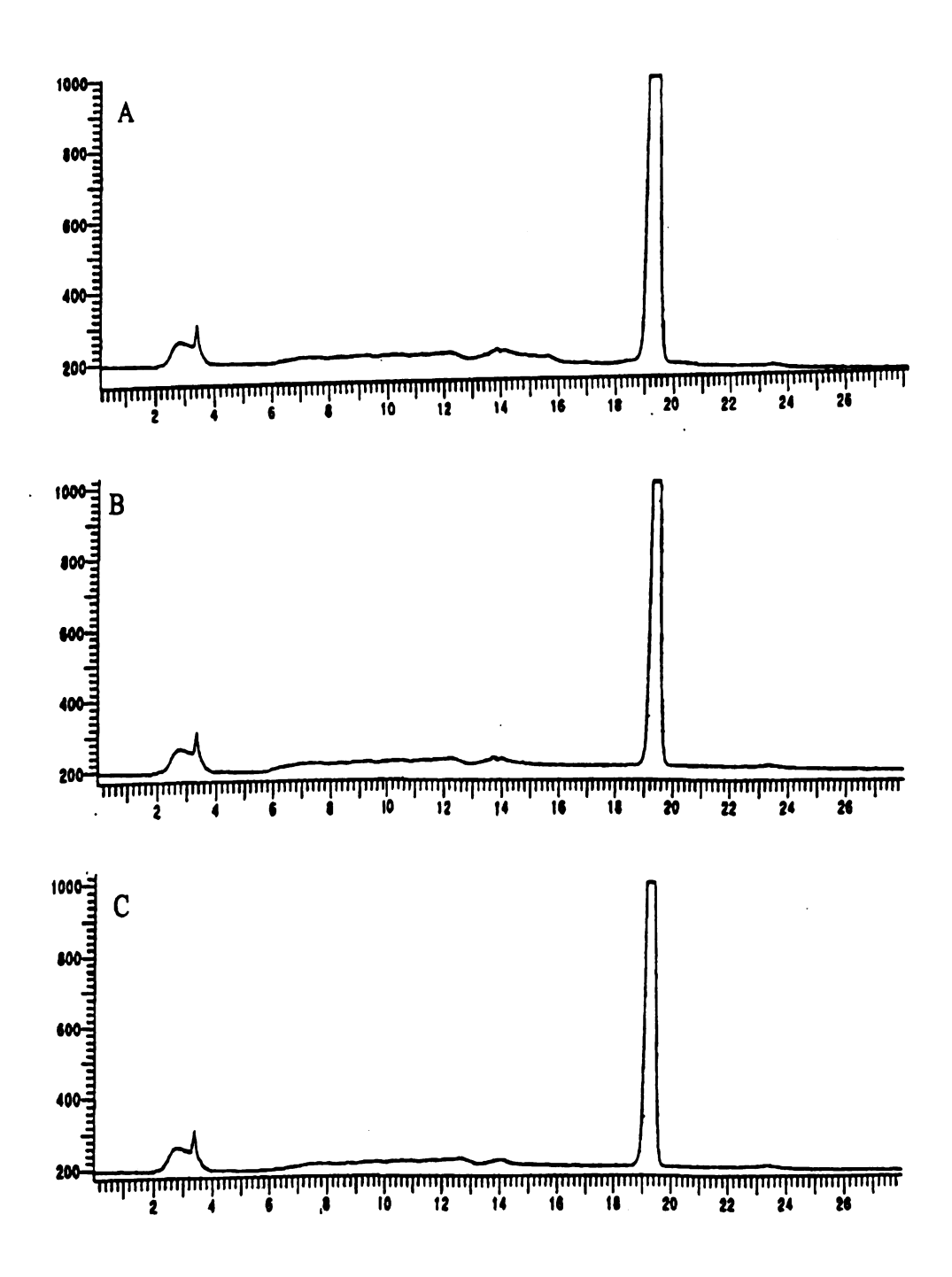


Figure B41. Acetonitrile extract chromatogram for aged, dry, 25°C (pH 6) pyrene contaminated soil. (a) 2.2 mg O<sub>3</sub>/ppm pyr, (b) 3.85 mg O<sub>3</sub>/ppm pyr, (c) 16 mg O<sub>3</sub>/ppm pyr.

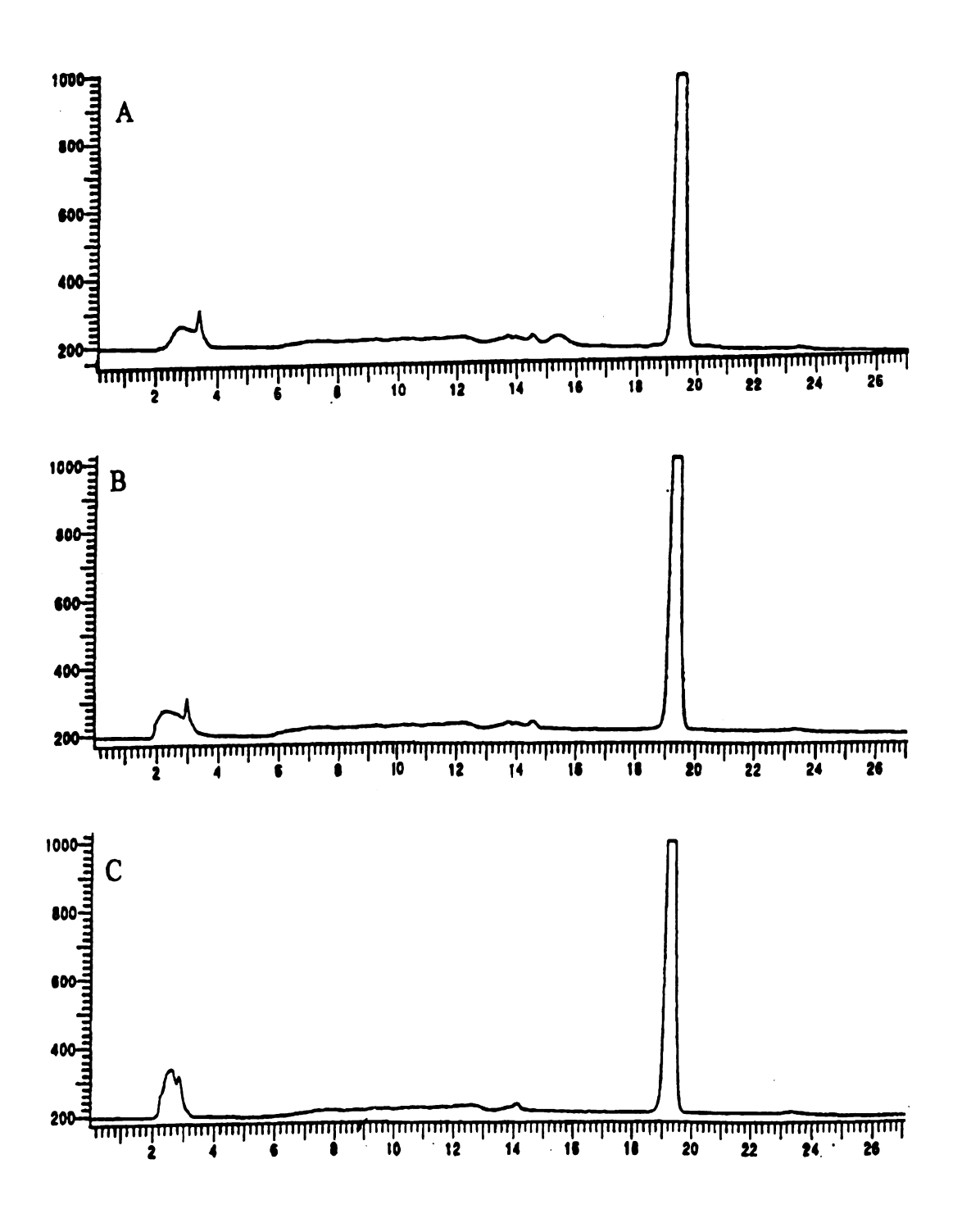


Figure B42. Acetonitrile extract chromatogram for age, dry, 25°C (pH 8) pyrene contaminated soil. (a) 2.2 mg O<sub>3</sub>/ppm pyr, (b) 3.85 mg O<sub>3</sub>/ppm pyr, (c) 16 mg O<sub>3</sub>/ppm pyr.

## APPENDIX C

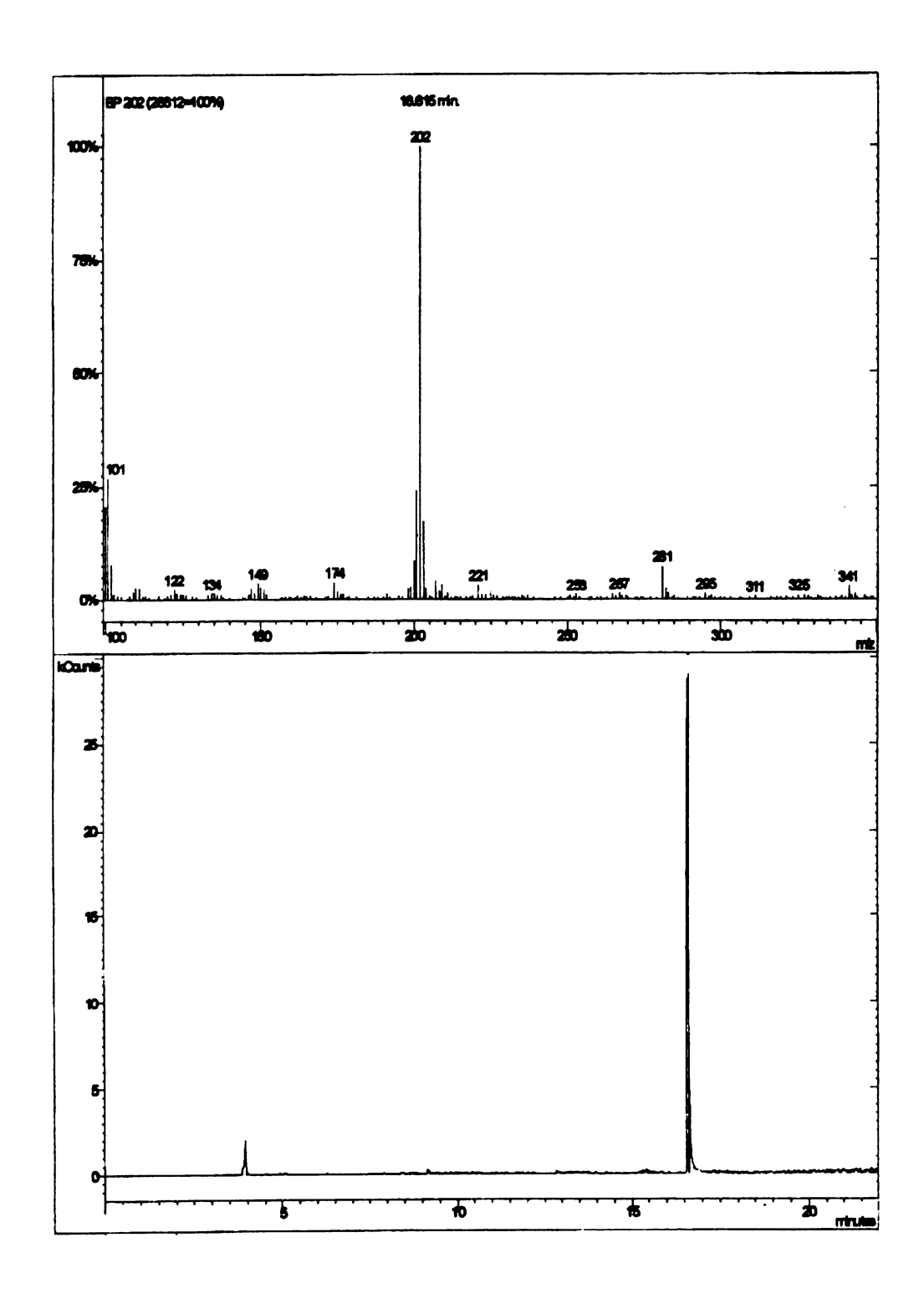


Figure C1. GC/MS spectra for pyrene standard (Compound I)

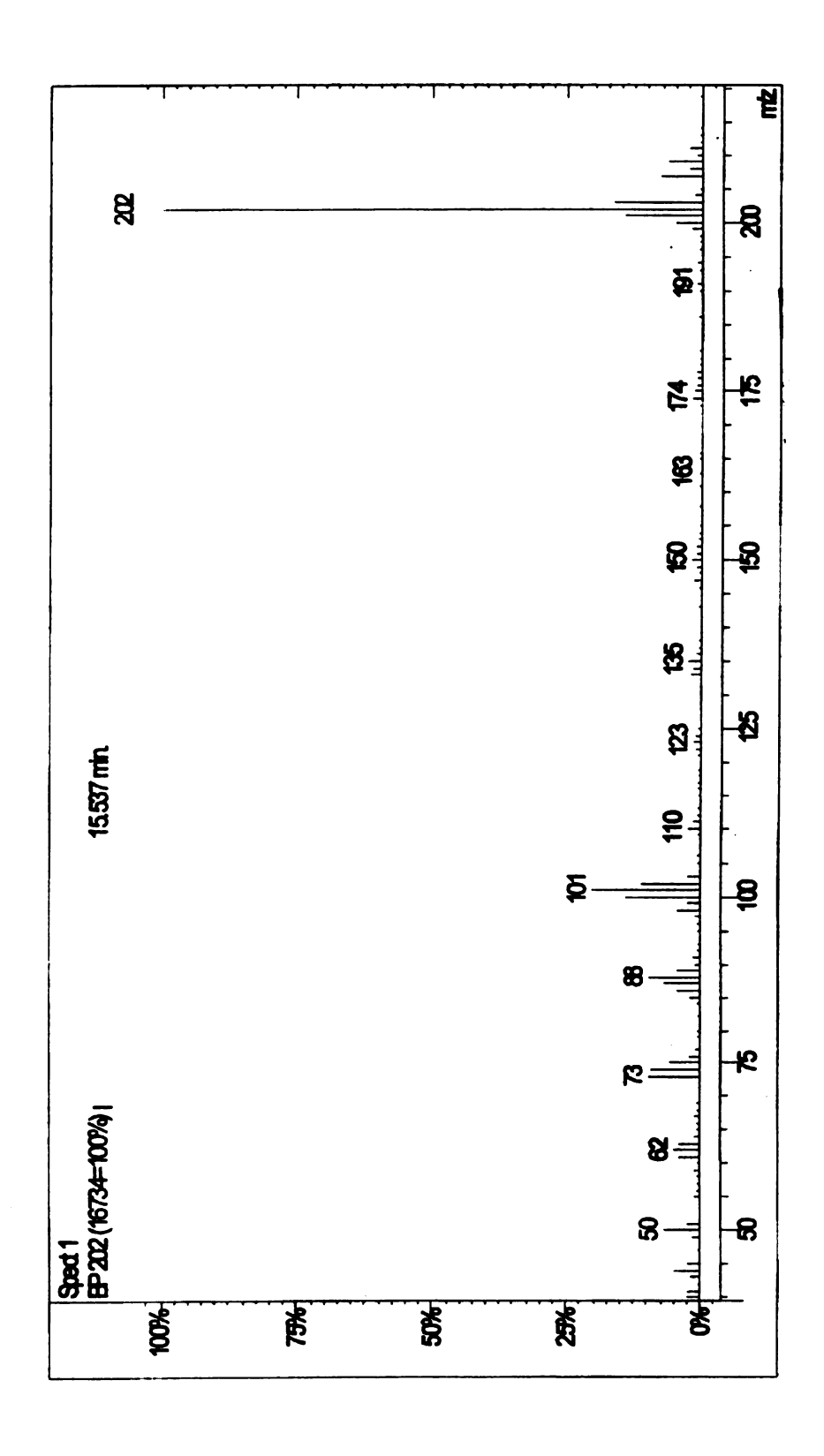


Figure C2. GC/MS spectra proposed for Compound I

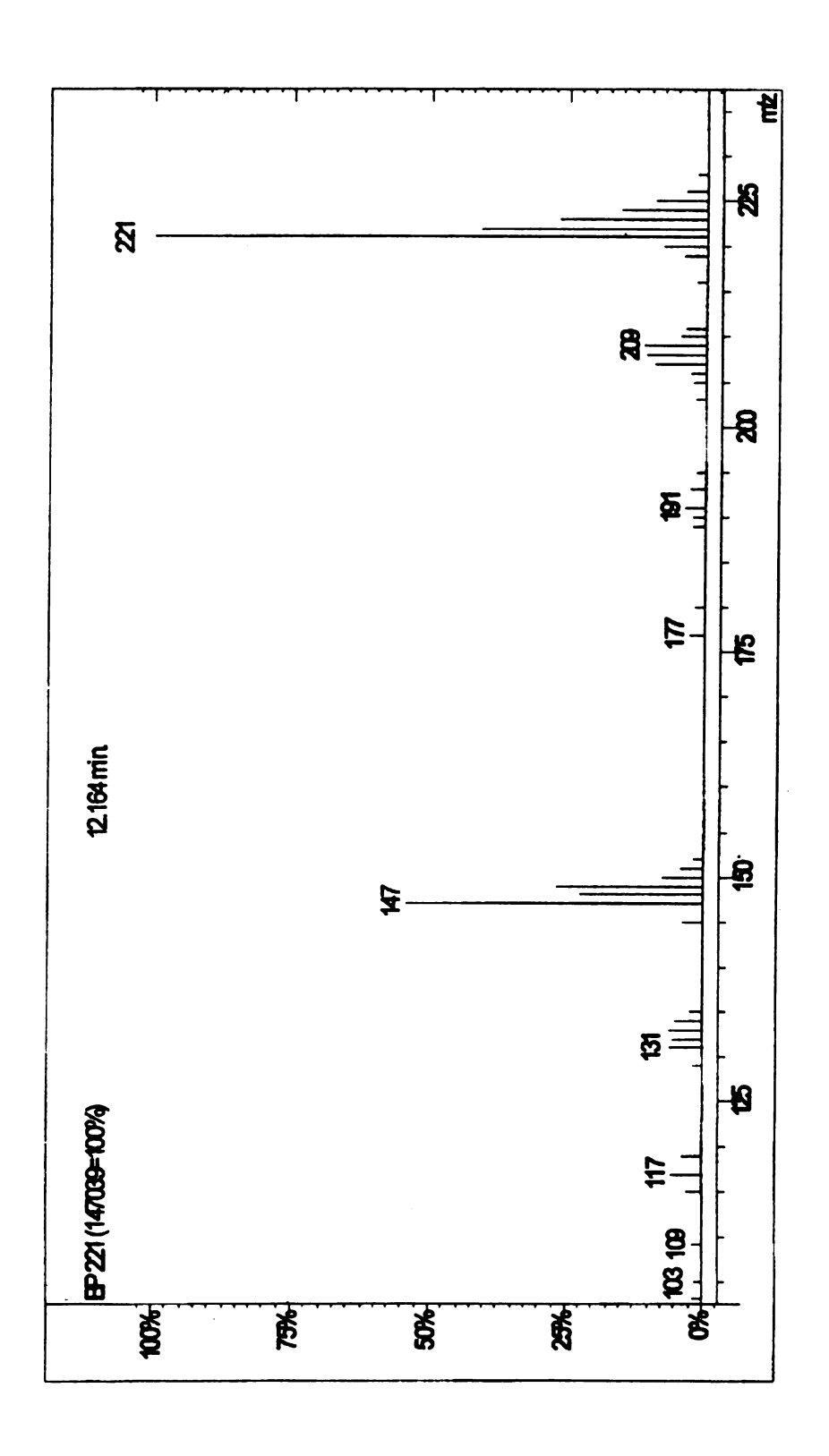


Figure C3. GC/MS spectra proposed for Compound II A/B

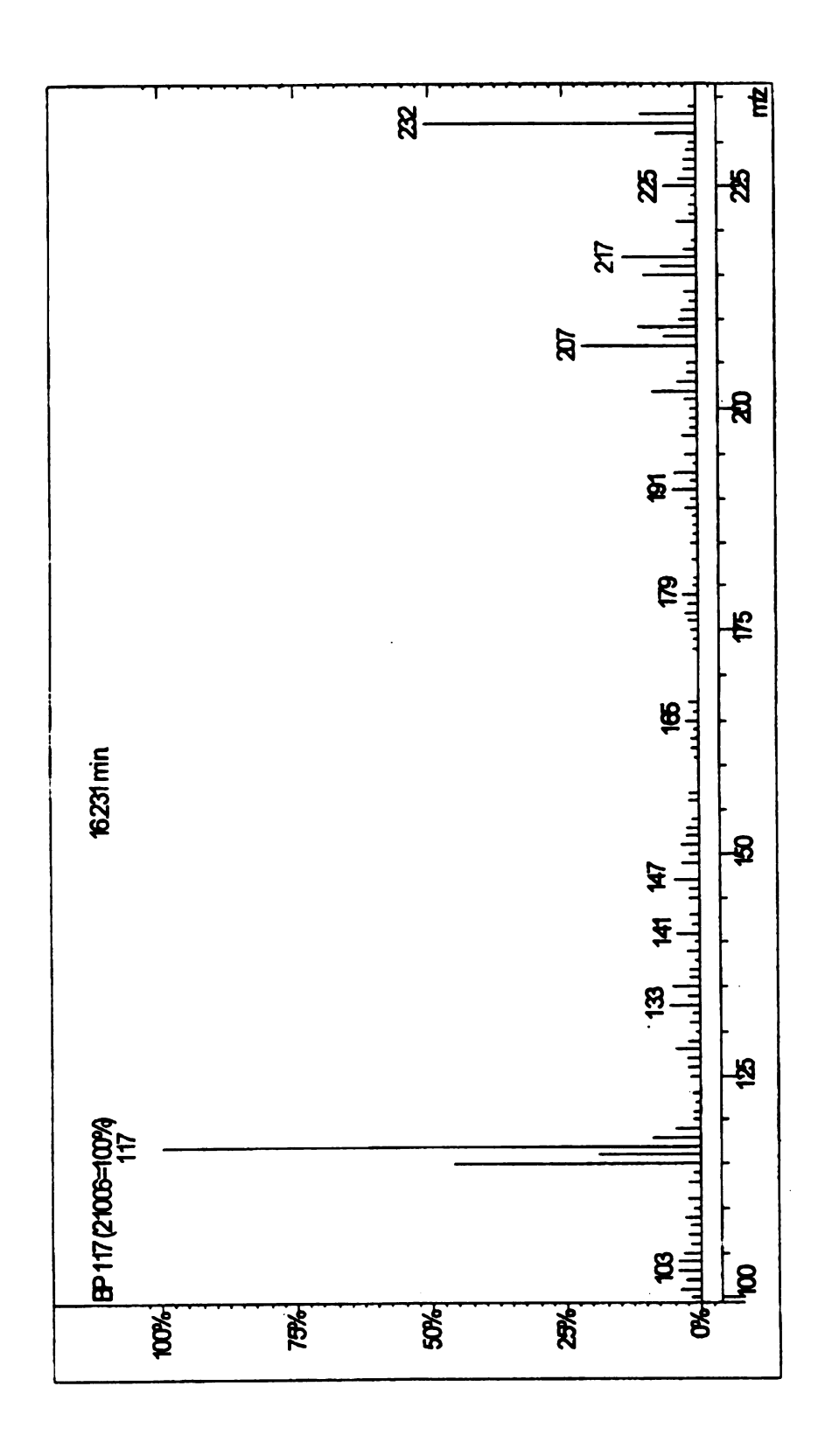


Figure C4. GC/MS spectra proposed for Compound III (A)

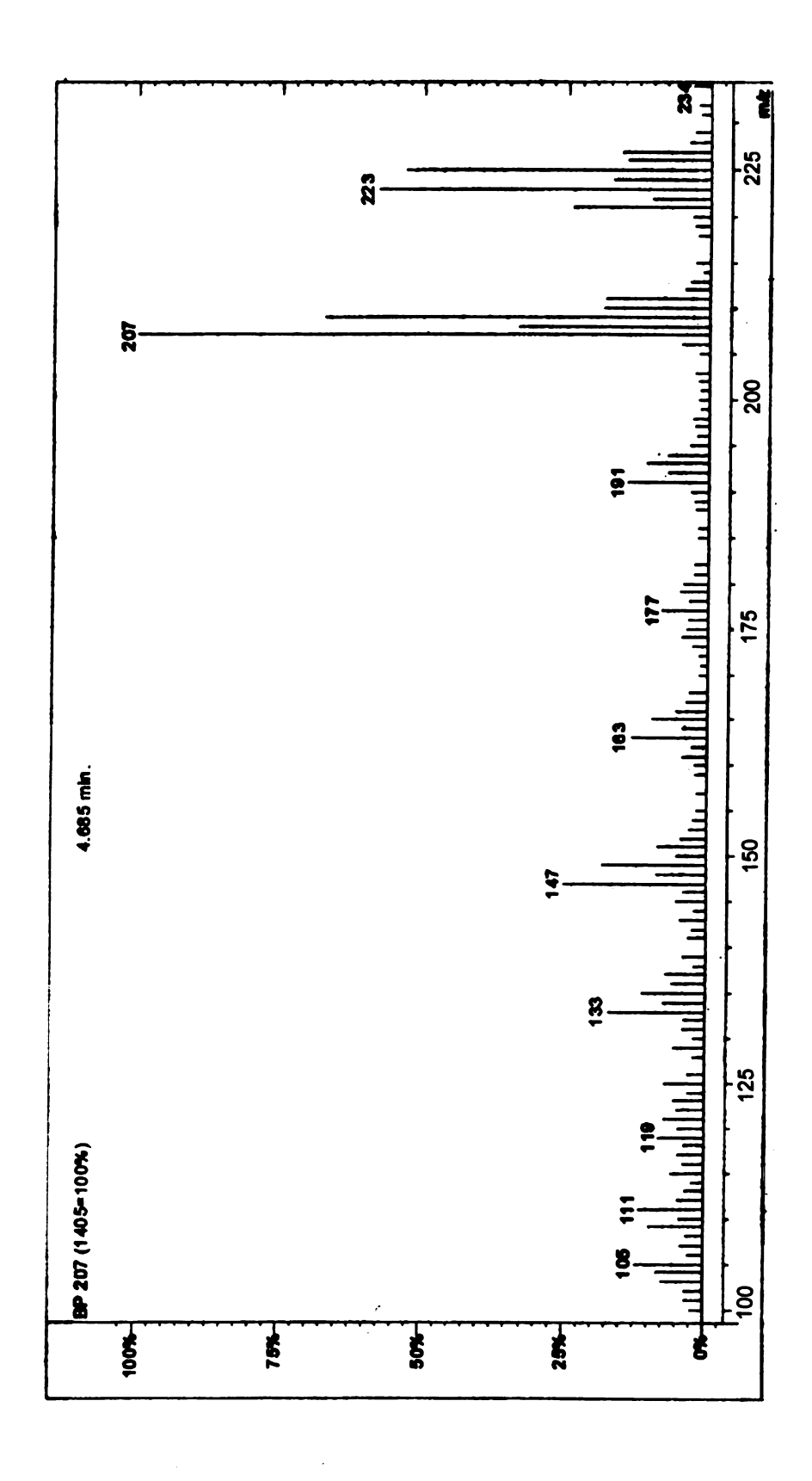


Figure C5. GC/MS spectra proposed for Compound III (B)

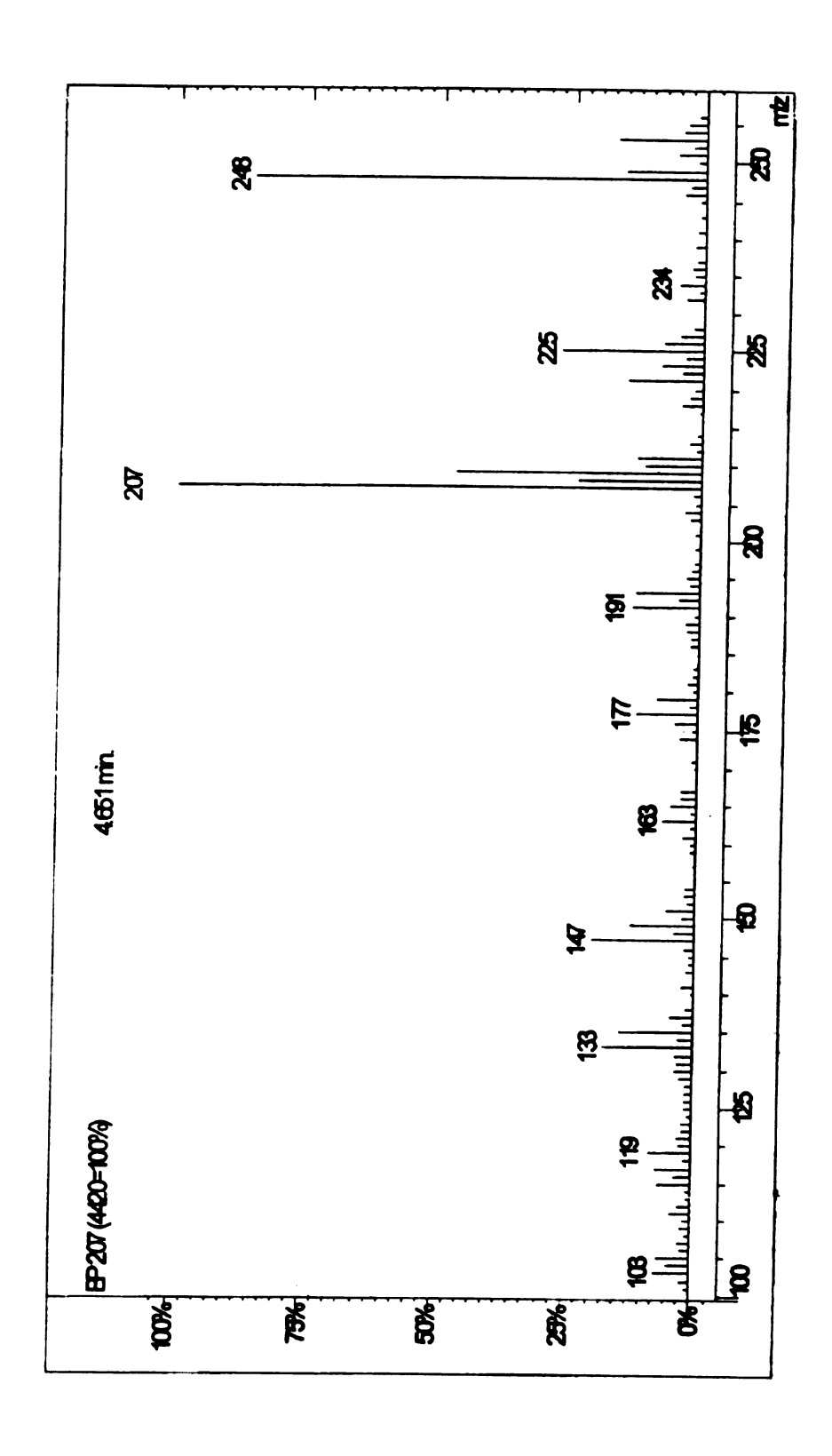


Figure C6. GC/MS spectra proposed for Compound IV A/B

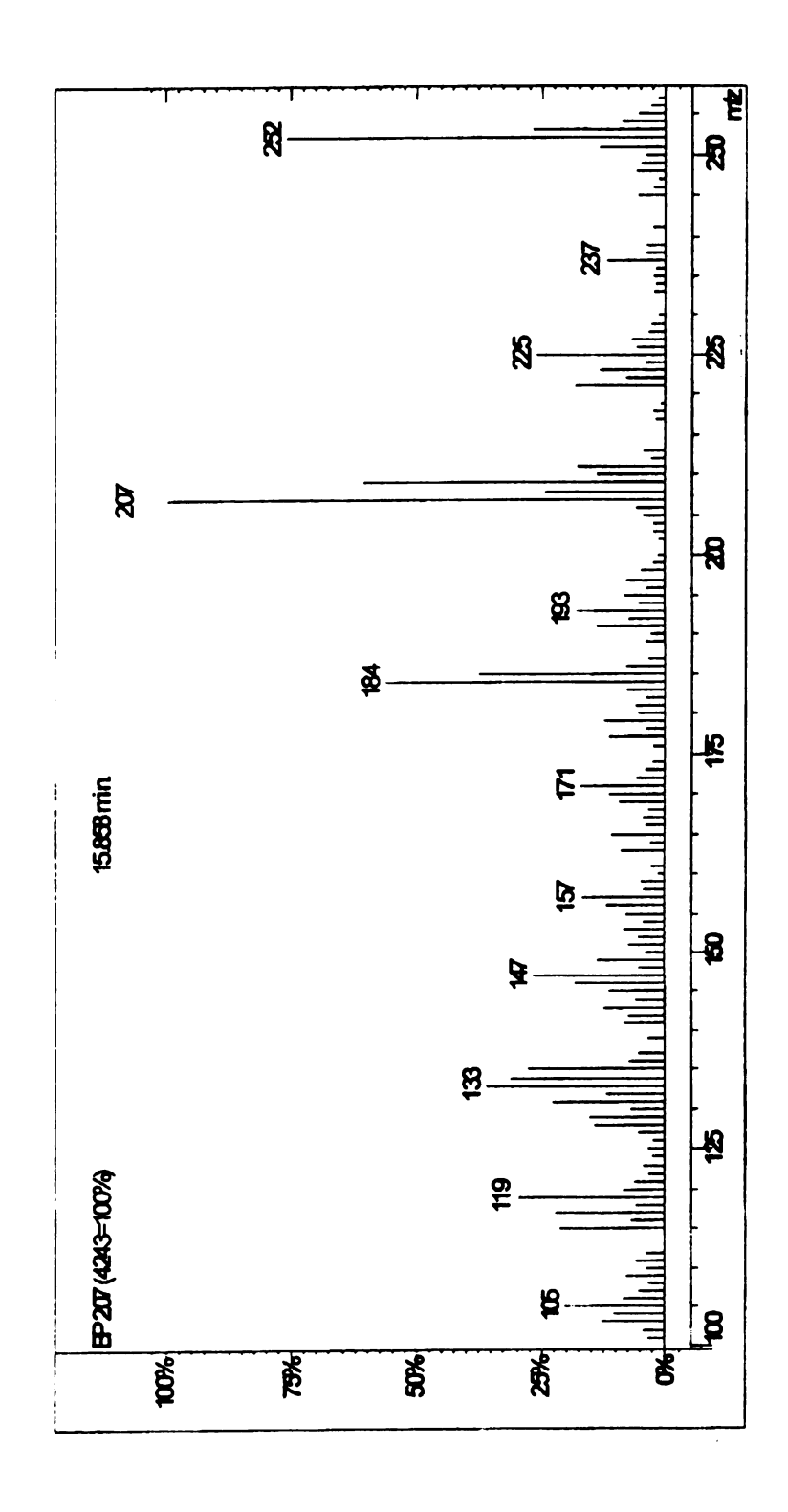


Figure C7. GC/MS spectra proposed for Compound V

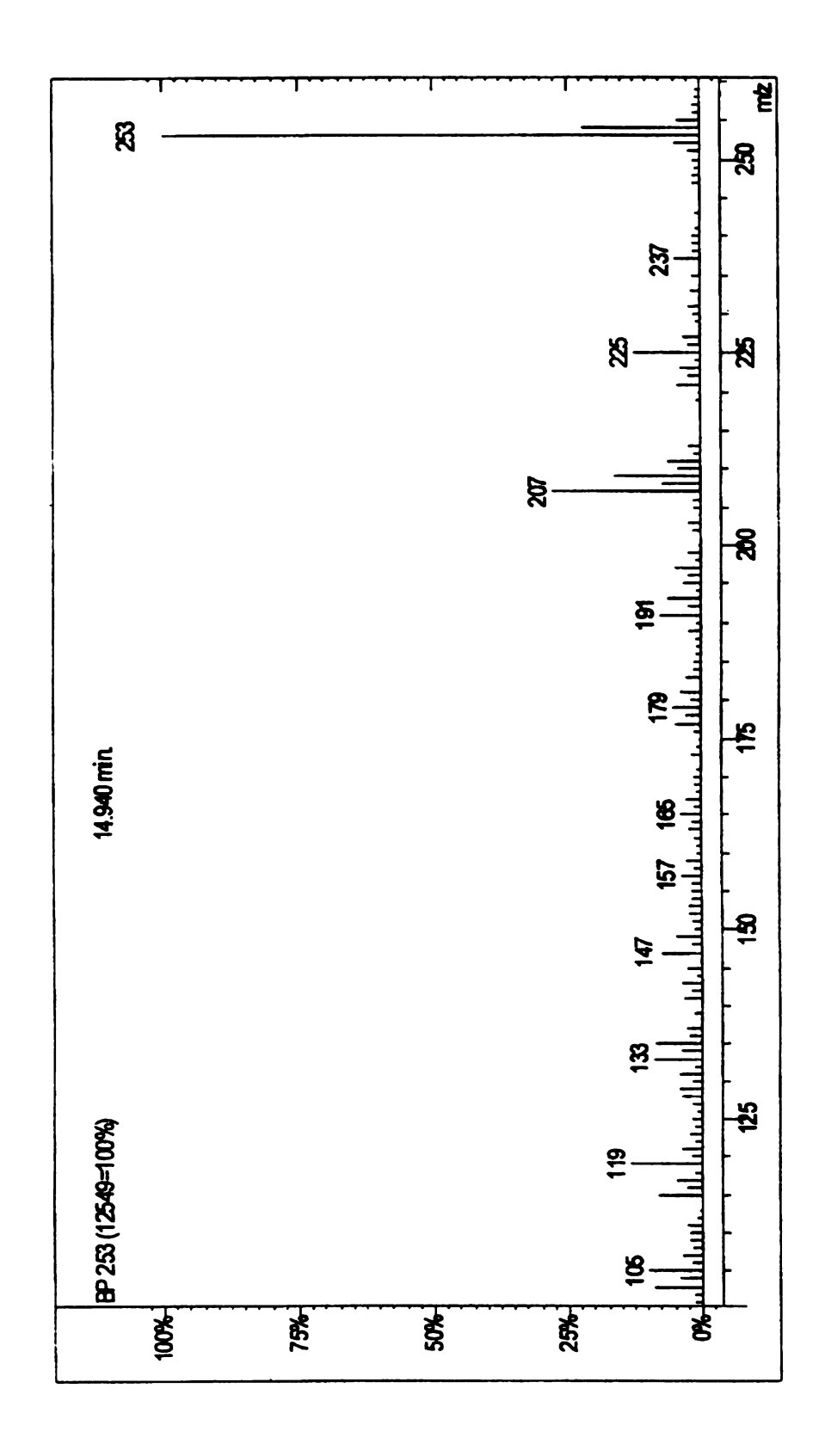


Figure C8. GC/MS spectra for Compound VI

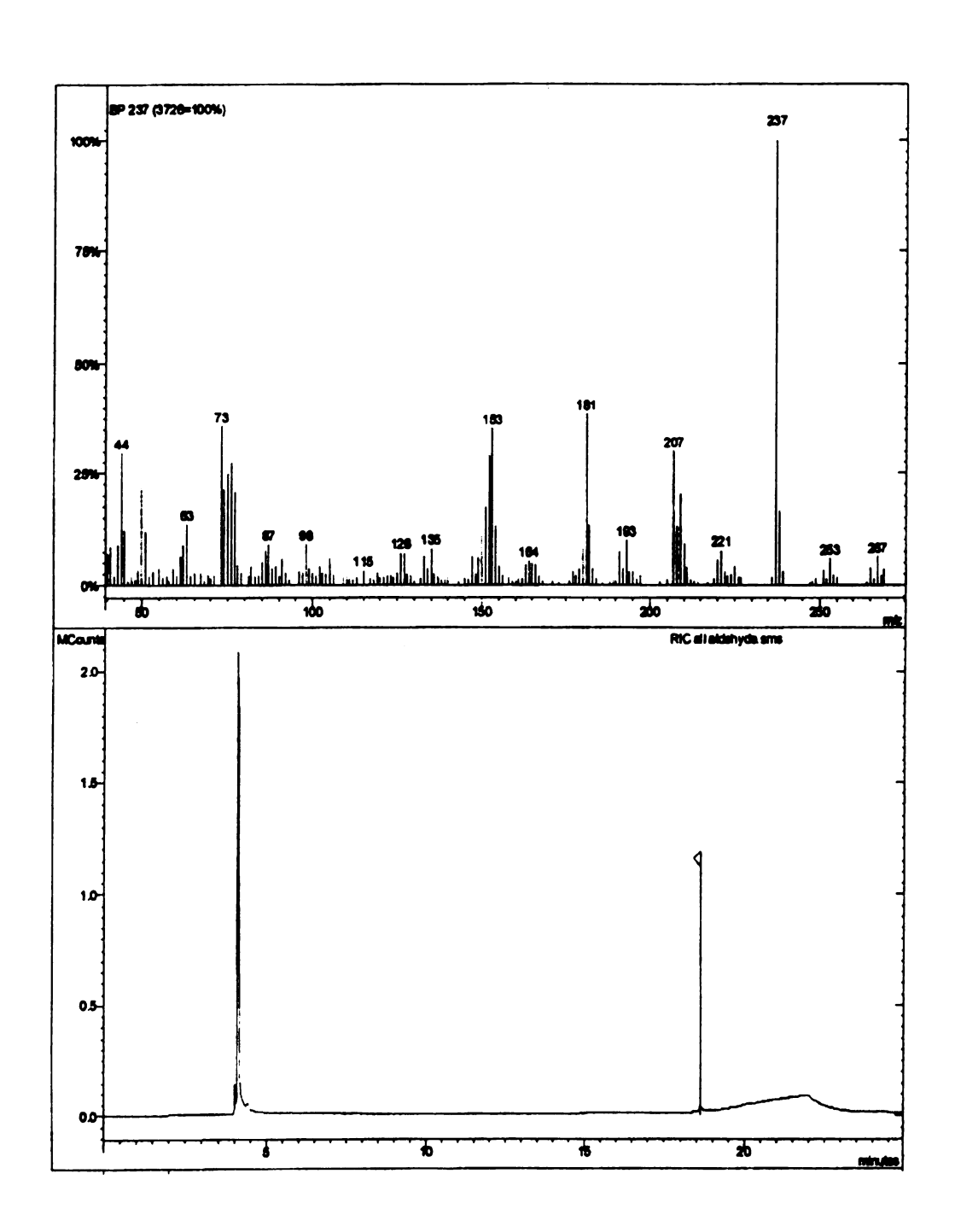


Figure C9. GC/MS spectra for 2,2',6,6'-biphenyl tetraaldehyde standard (Compound VII)

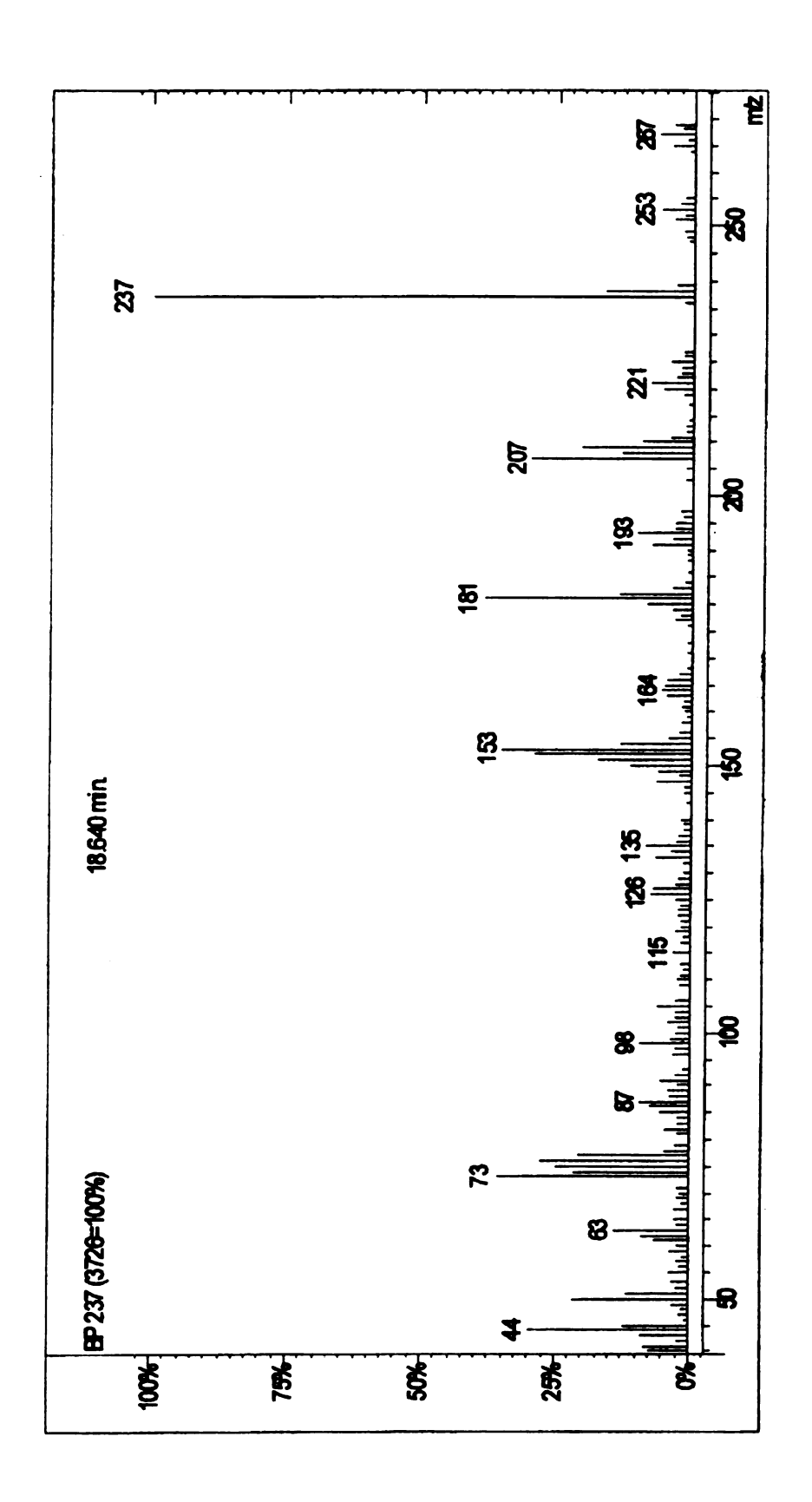


Figure C10 (a). GC/MS spectra #1 proposed for Compound VII

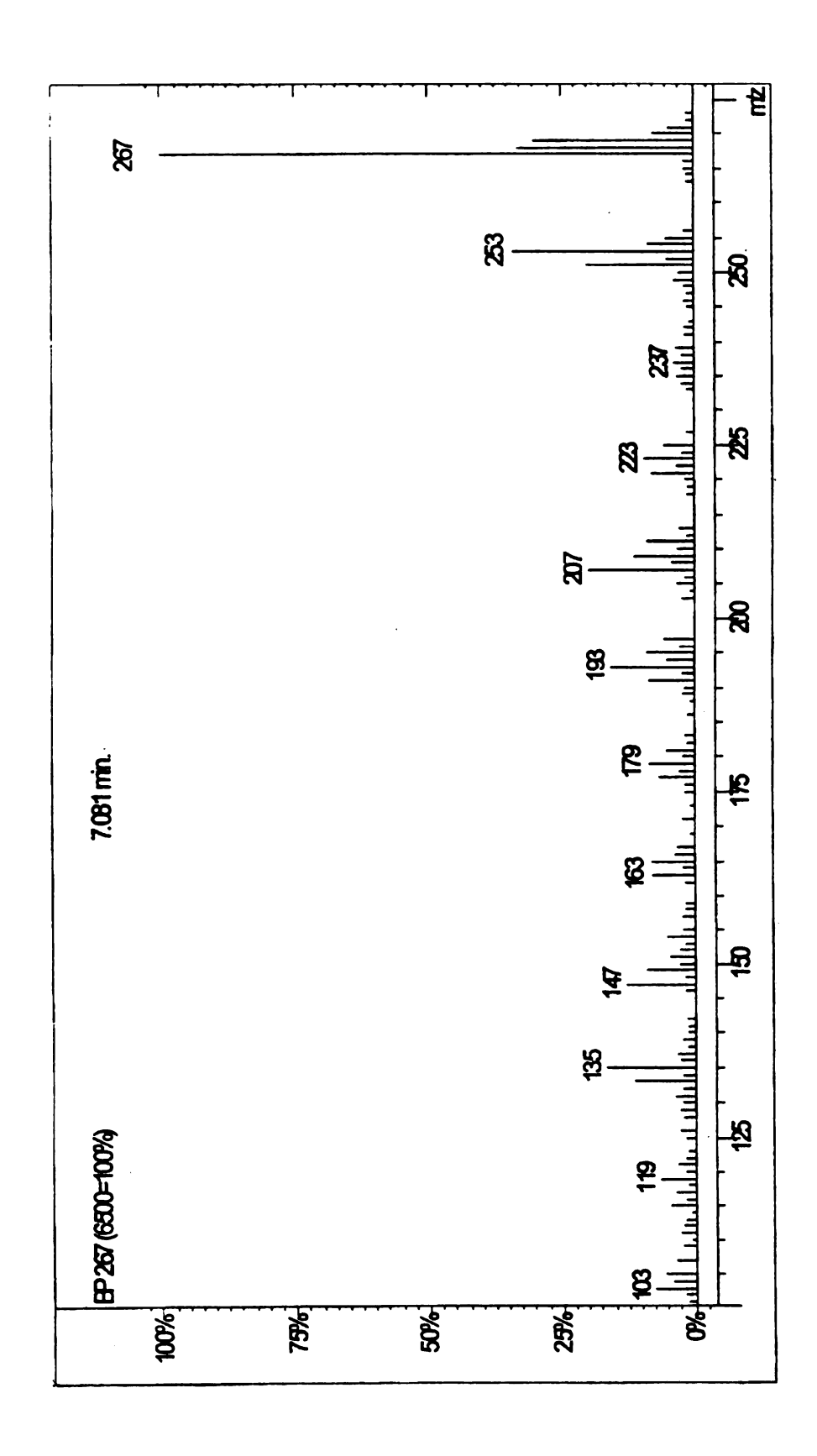


Figure C10 (b). GC/MS spectra #2 proposed for Compound VII

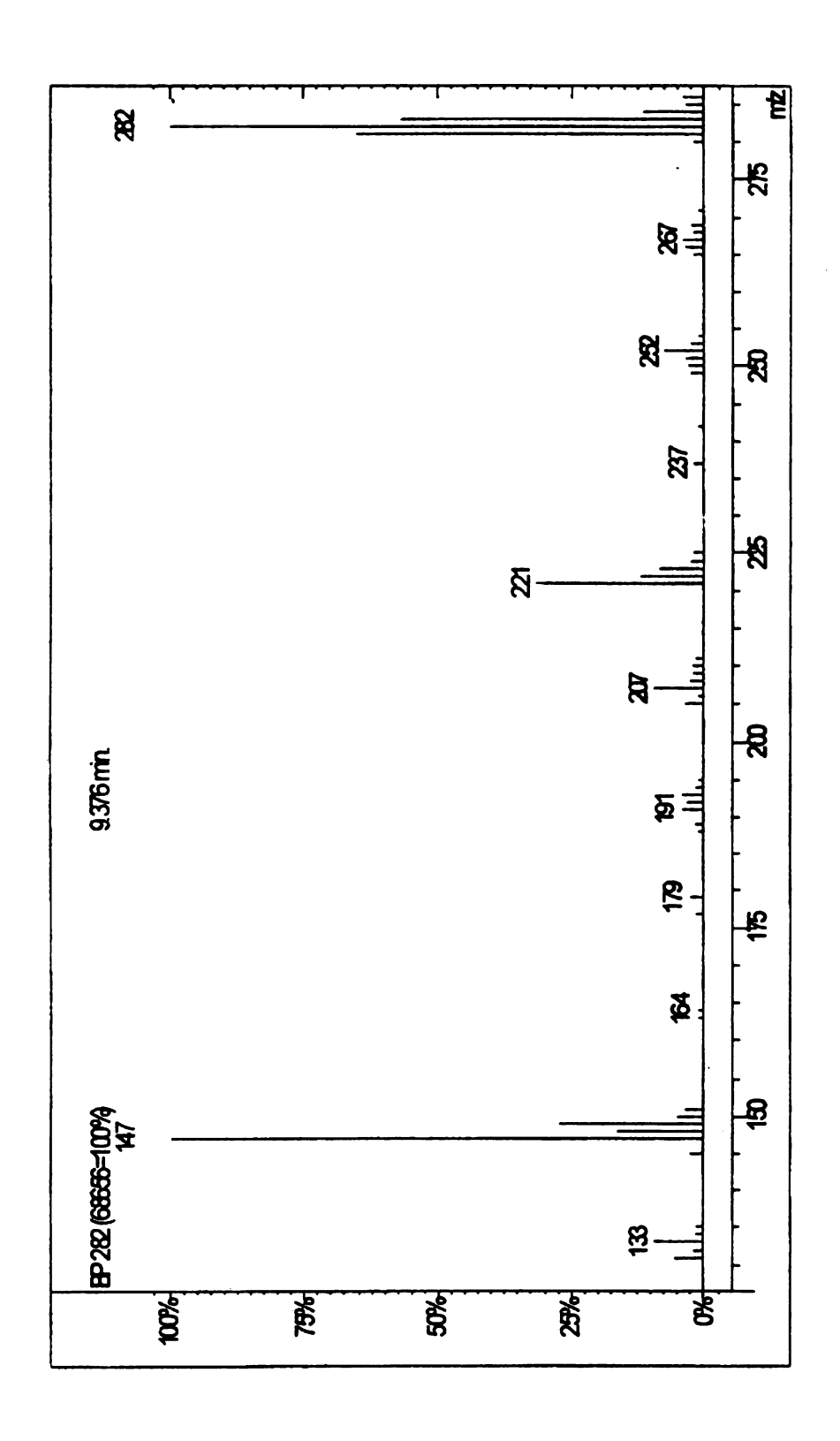


Figure C11 (a). GC/MS spectra #1 proposed for Compound VIII A/B

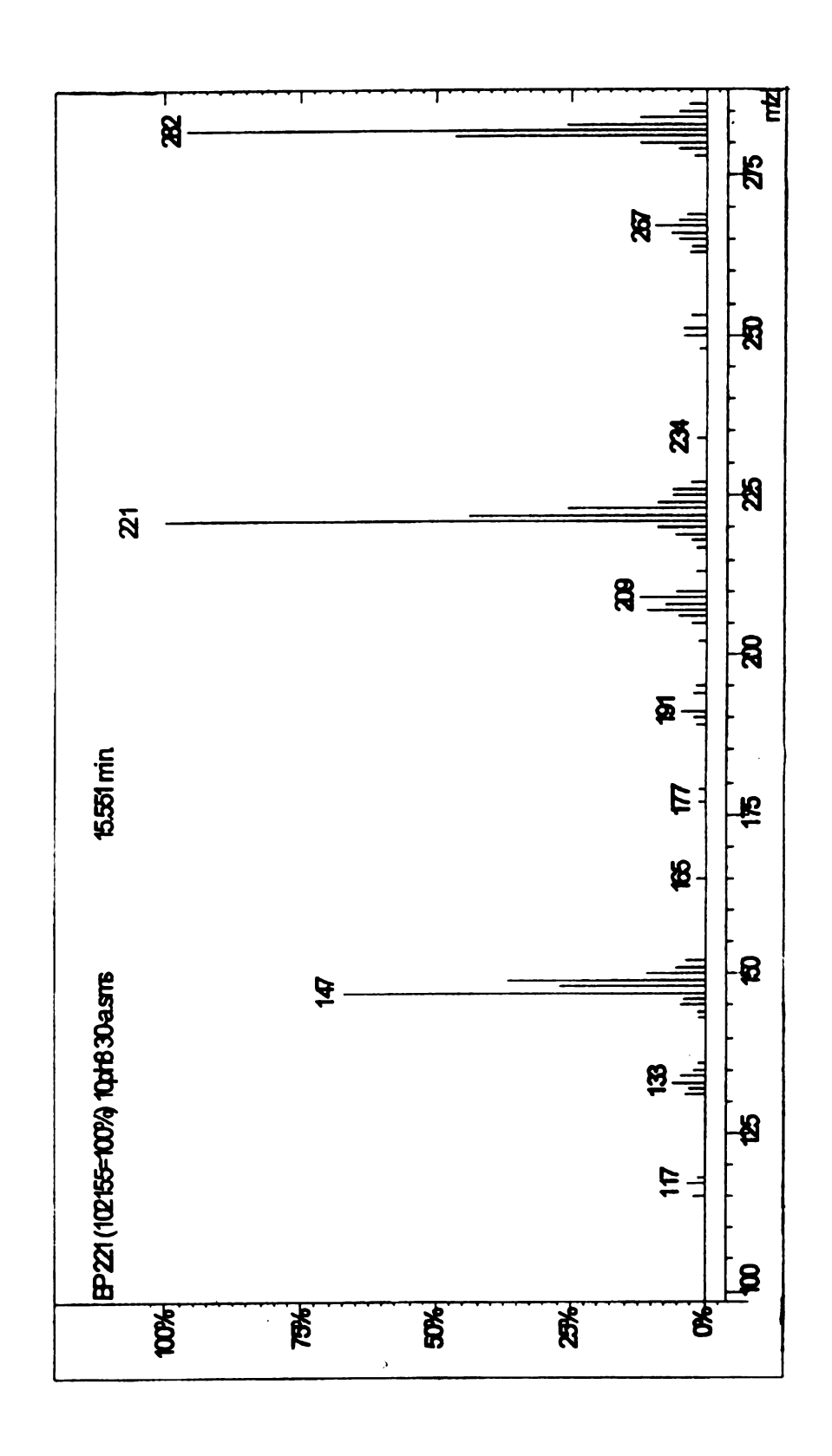


Figure C11 (b). GC/MS spectra #2 proposed for Compound VIII A/B

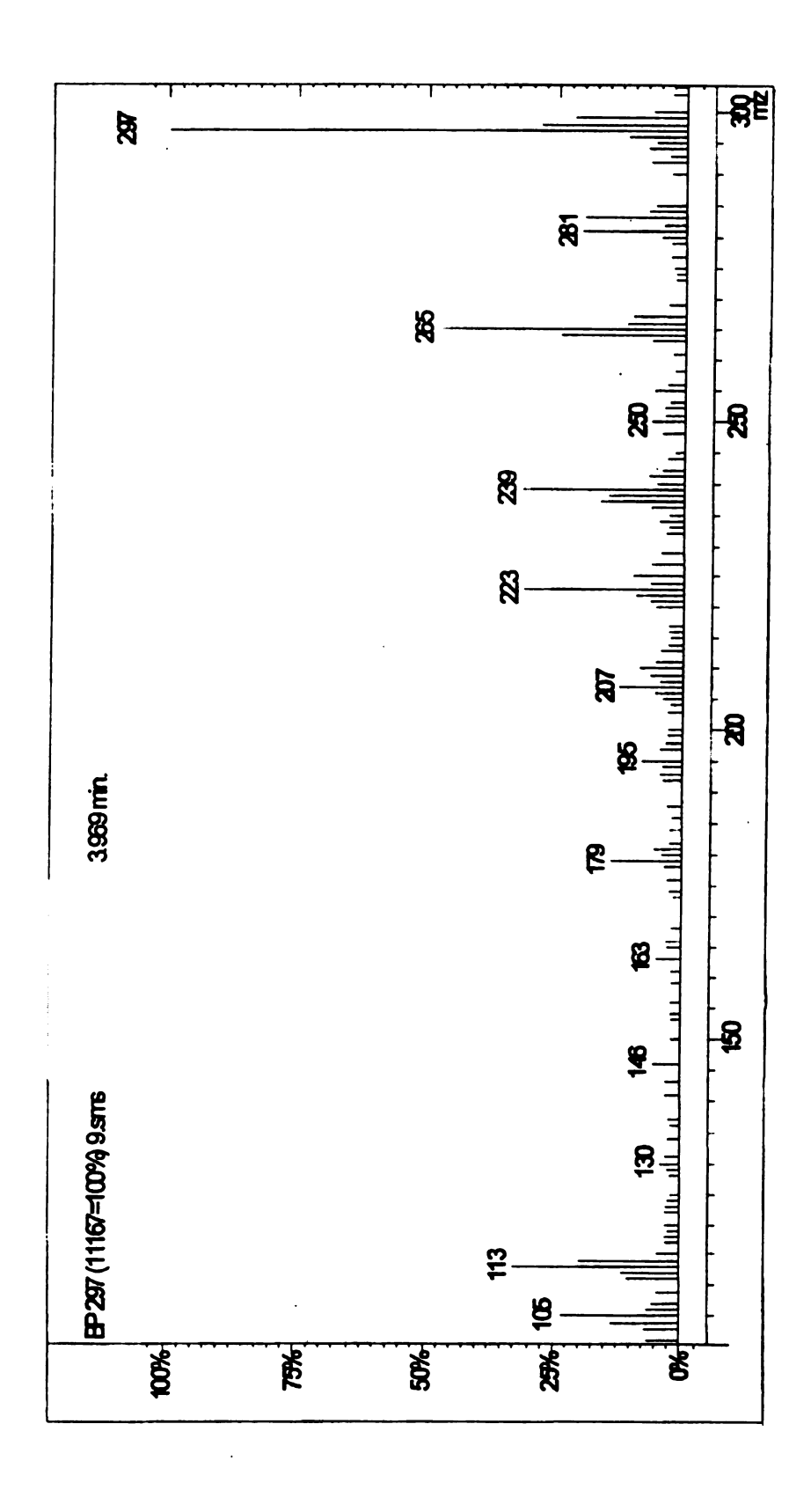


Figure C12 (a). GC/MS spectra #1 proposed for Compound IX A/B

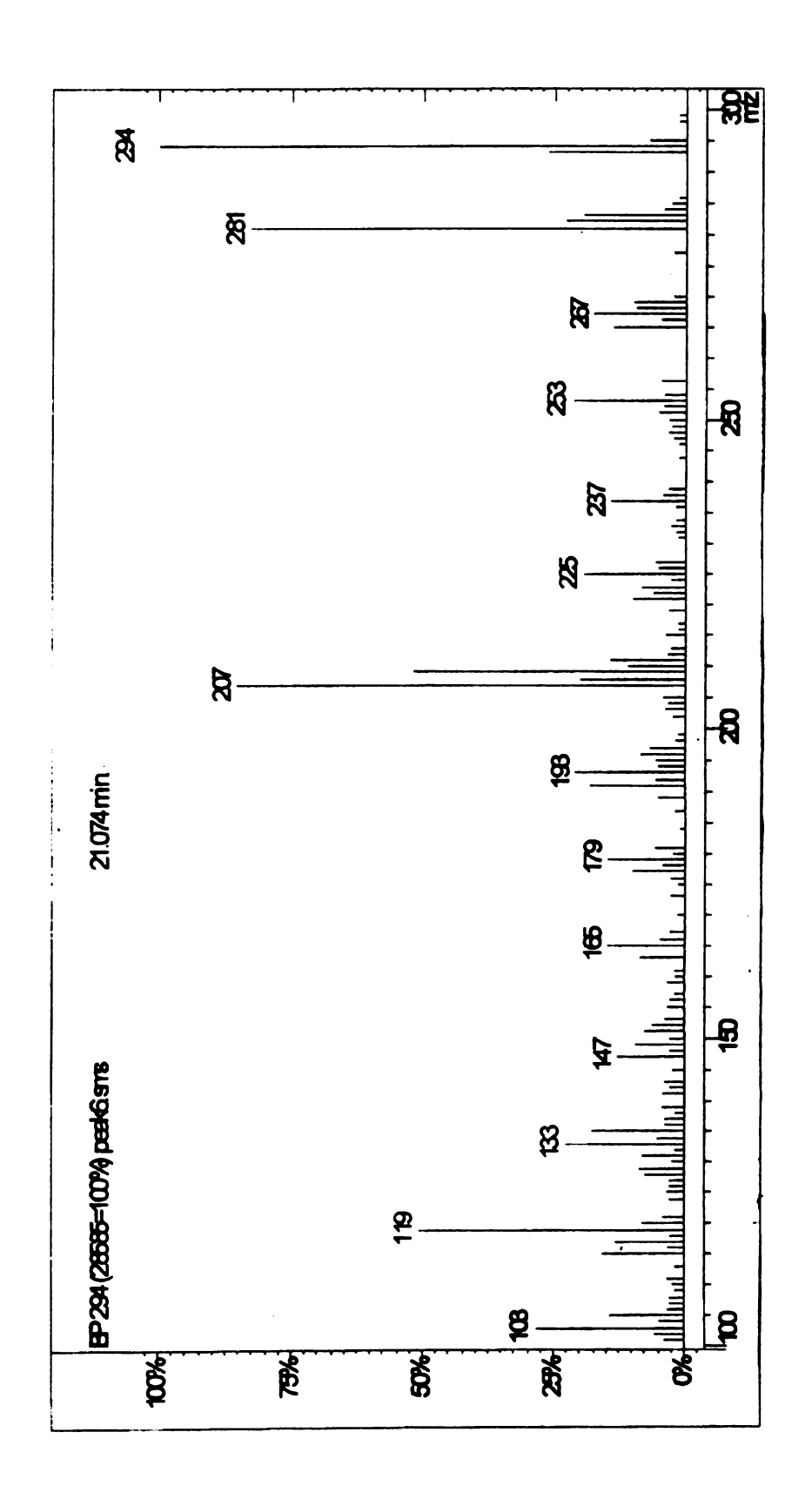


Figure C12(b). GC/MS spectra #2 proposed for Compound IX A/B

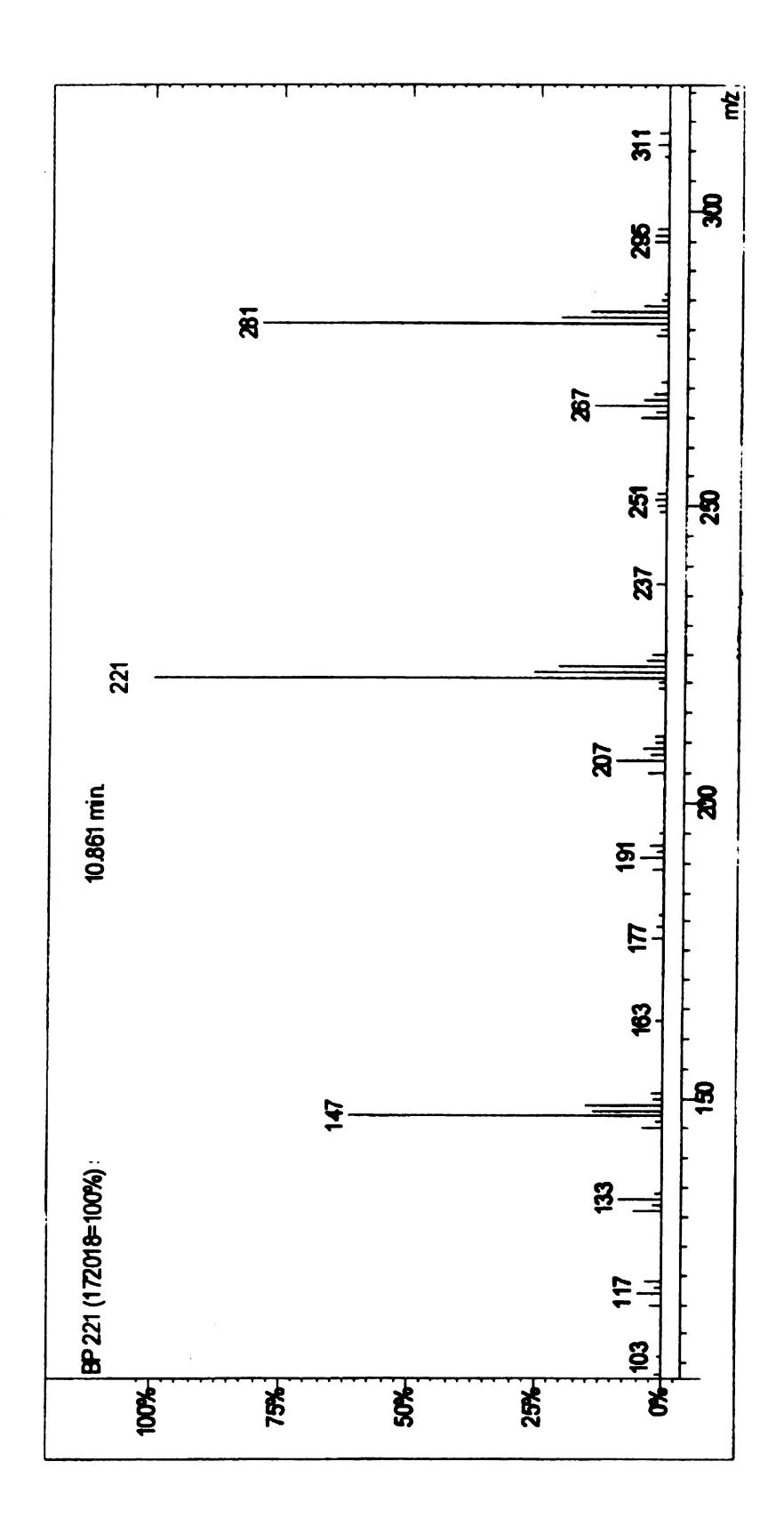


Figure C13(a). GC/MS spectra #1 proposed for Compound X

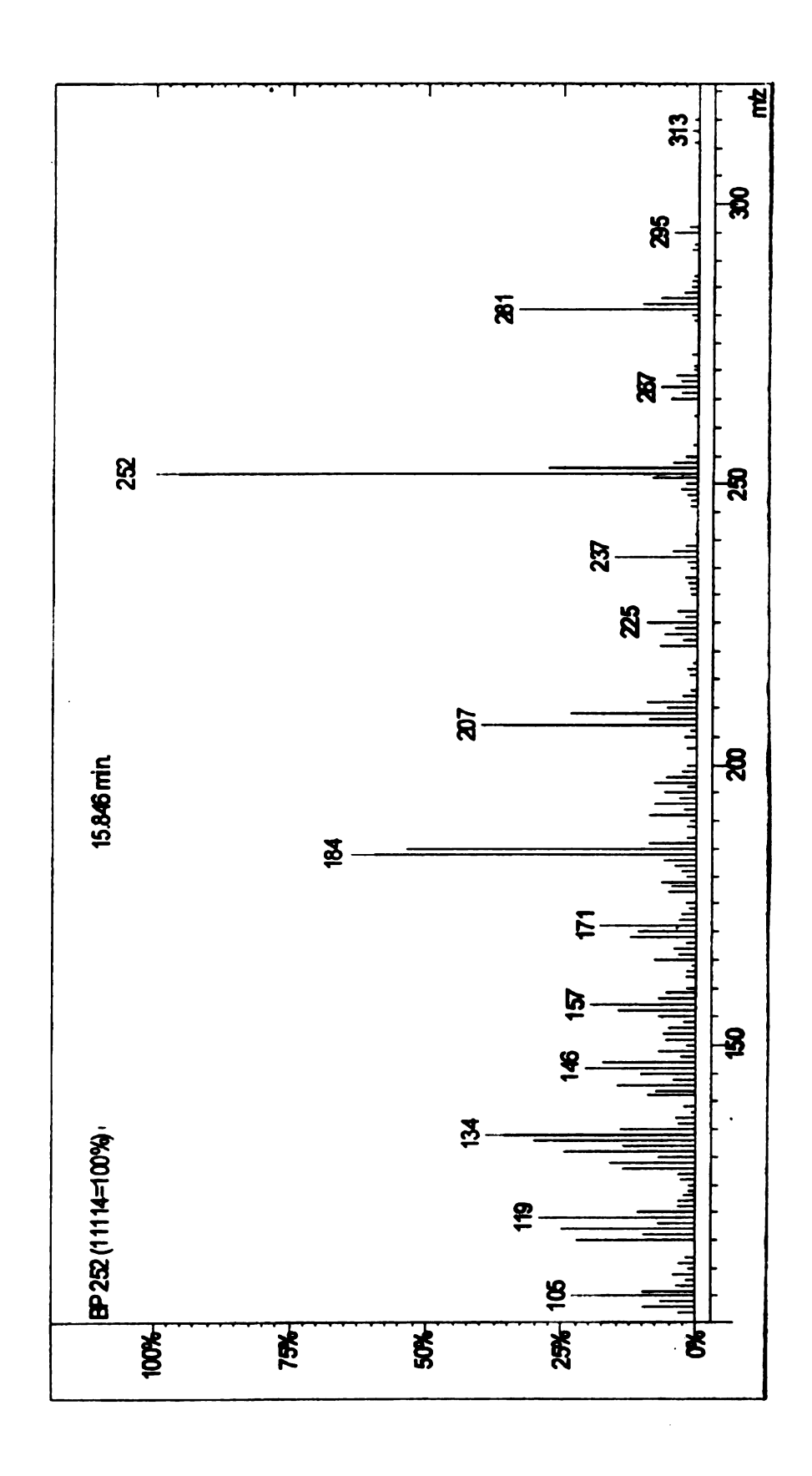


Figure C13(b). GC/MS spectra #2 for Compound X

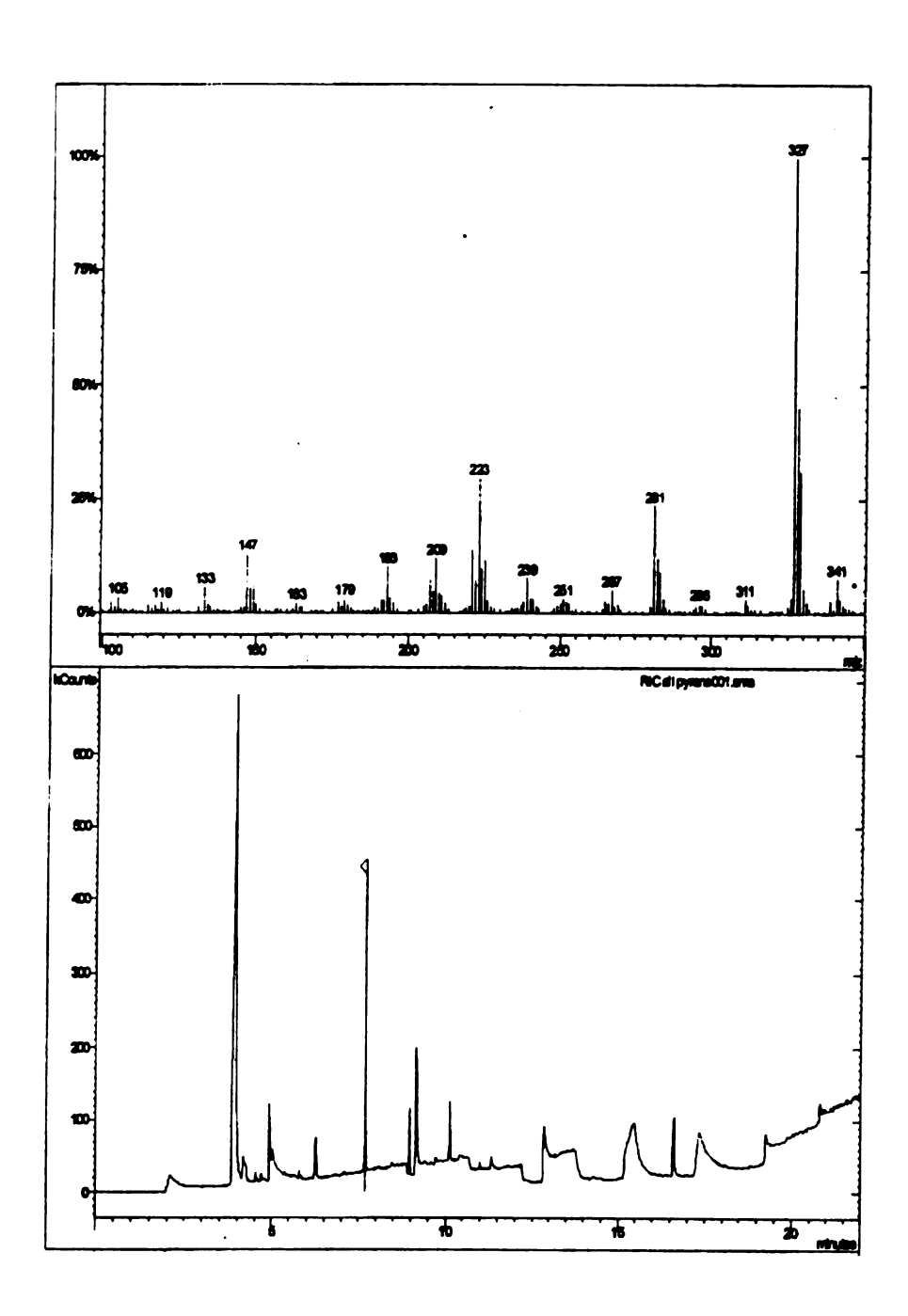


Figure C14. GC/MS spectra for 2,2',6,6'-biphenyl tetracarboxylic acid standard (Compound XI)

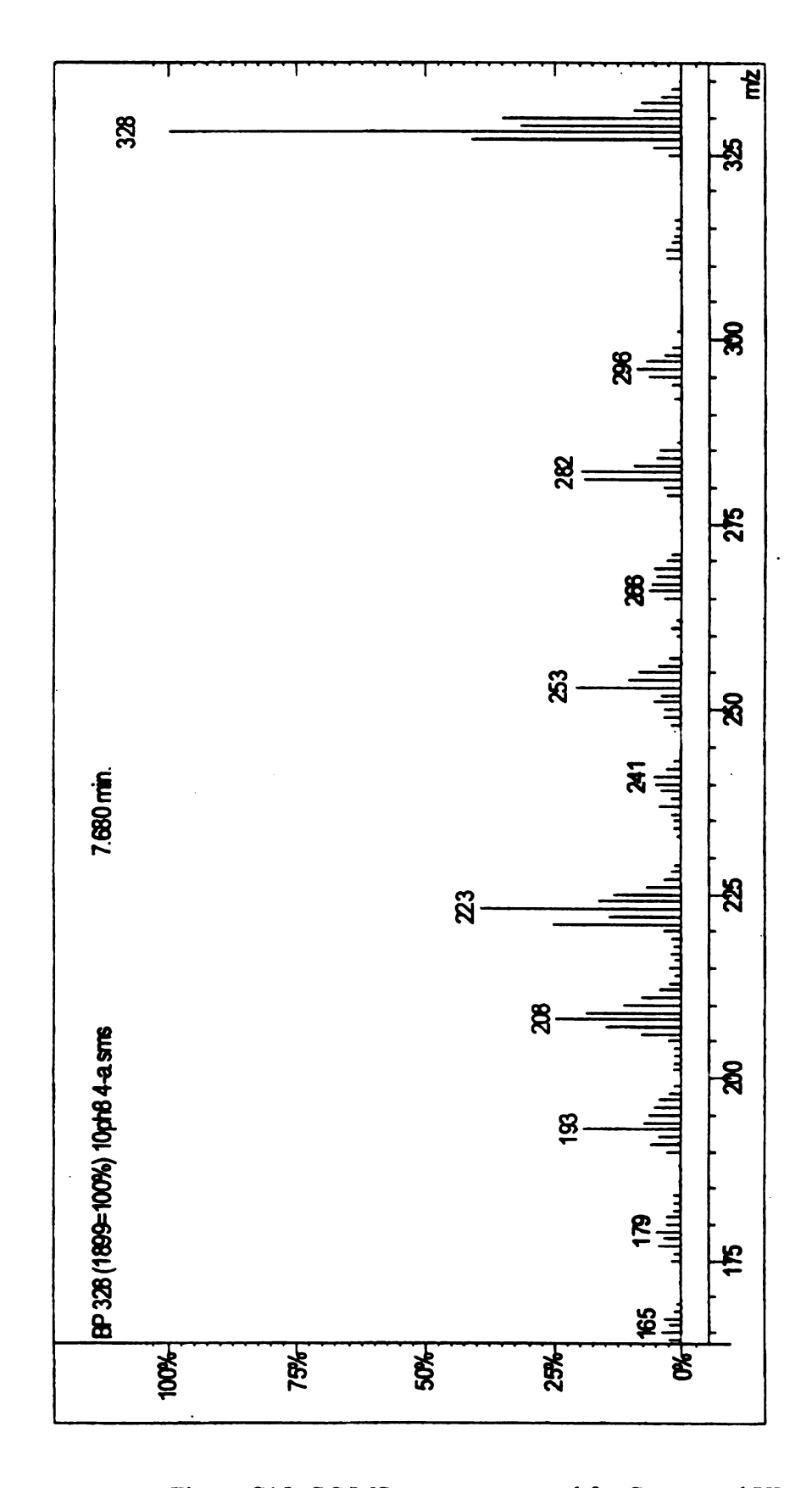


Figure C15. GC/MS spectra proposed for Compound XI

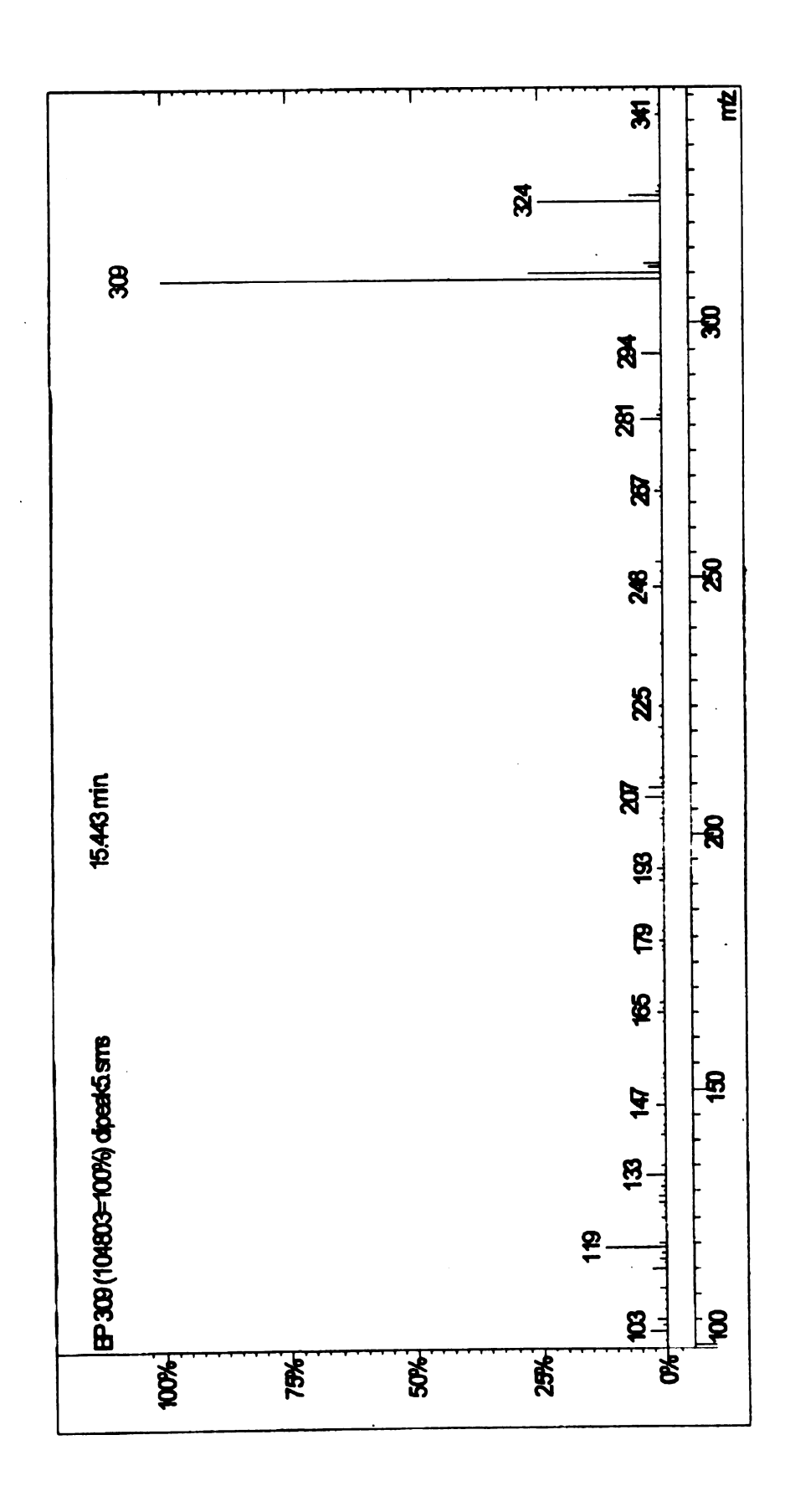


Figure C16. GC/MS spectra for unknown compound #1 (m/z 309)

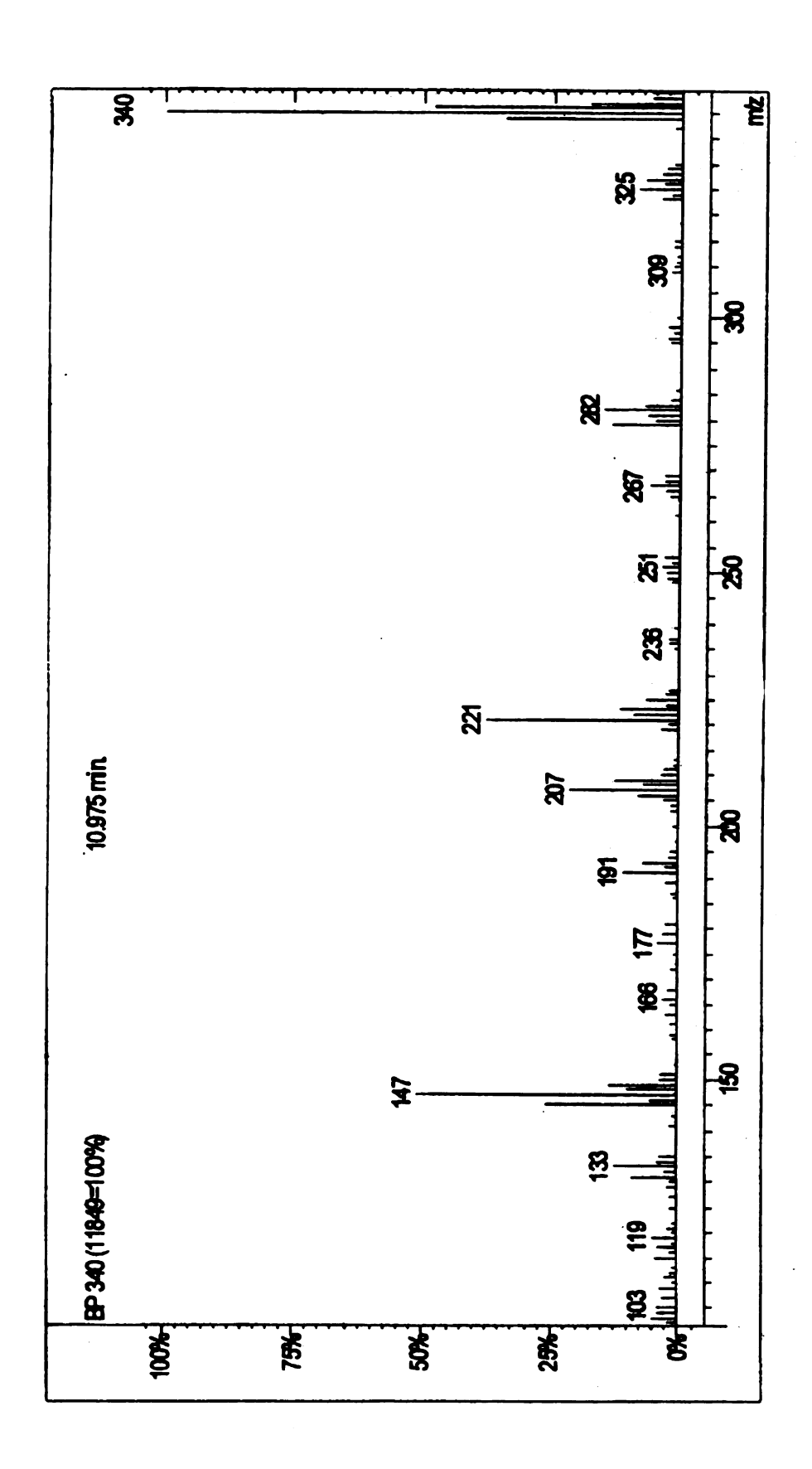


Figure C17 (a). GC/MS spectra #1 for unknown compound #2 (m/z 340)

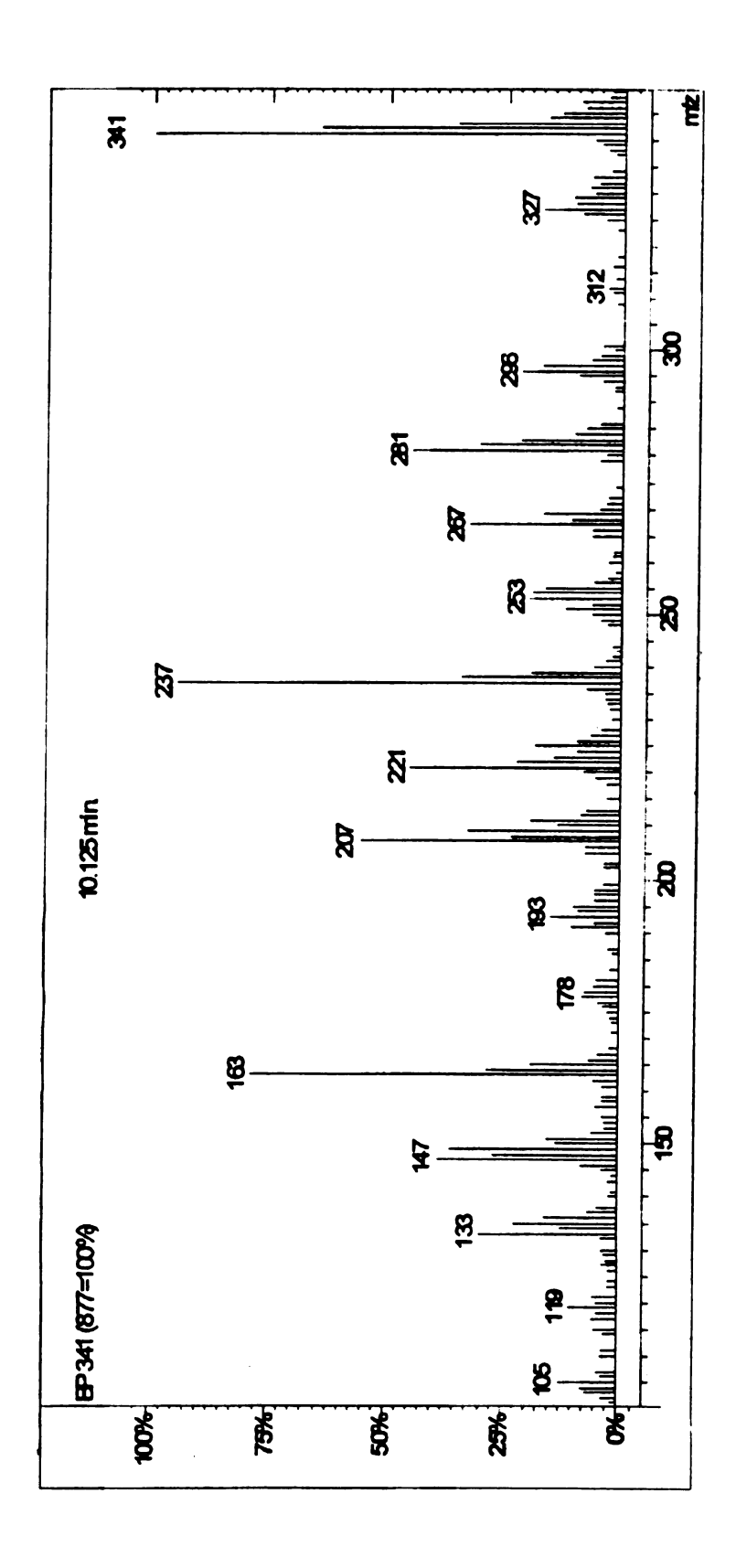


Figure C17 (b). GC/MS spectra #2 for unknown compound #2 (m/z 341)

## APPENDIX D

Modeling Note: The arrays in MathCad have a default setting where the first row and first column in the array is denoted as (0,0) and not (1,1). In this program, the rows and columns start at 0, the second column or the second row is therefore denoted by 1.

$$L := 15 \qquad \text{Column length (cm)} \qquad \text{soilmass} := \frac{50}{1000} \quad \text{kg of soil}$$
 
$$\rho b := 1.1 \qquad \text{Bulk density (g/cm^3)}$$
 
$$n := 0.42 \qquad \text{total porosity (From HSU)}$$
 
$$sa := 1 \qquad \text{gas saturation}$$
 
$$yos := 5.8 \qquad \text{stoichiometric ratio of ozone to OM}$$
 
$$Q \text{ Ozone/g OM}$$
 
$$K := 1.4 \times 10^{-4} \quad \text{second order rate constant for ozone reaction in Metea (1/s)(mg/kg)^-1}$$
 
$$OMpercent := 0.4 \qquad \text{Percentage of OM}$$
 
$$OMmgkg := \frac{0.004 \cdot 50 \cdot 1000}{\text{soilmass}} \quad \text{Organic matter concentration (mg/kg)} \quad \text{OMmgkg} = 4 \times 10^3$$
 
$$kd := 0.0798 \qquad \text{Gas conductivity}$$
 
$$kom := 5.7 \cdot 10^{-7} \quad \text{second order organic matter rate constant for OM (calculated) (s^-1)((mg OC/kg soil)^-1)(L gas/kg soil)}$$
 
$$Inlet gas concentration (mg/L)$$
 
$$Pin := 1525 \qquad Inlet pressure (cm H20)$$
 
$$Pout := 1494 \qquad \text{Outlet pressure (cm H20)}$$

**Loops and Interations** 

$$C := 0..(L - 1)$$
 $m := 0..499$  miterations := 500

 $O3_{0.1} = 55$  initialization of array for ozone concentration

OM<sub>0,1</sub> := OMmgkg initialization of arrary for Organic Matter

Pressure distribution through the column

$$P2_{m,0} := \left[ Pin^2 - \left( \frac{Pin^2 - Pout^2}{L} \cdot m \right) \right]^{0.5}$$

Assuming immobile OM available to react over 4 hour runtime

Gas velocity calculation along flow path through the column in 1 cm increments

$$dt := \frac{15000}{\text{miterations}}$$
 Time divided by iterations

$$v_{m,0} := kd \cdot \frac{\left(Pin^2 - Pout^2\right)}{2L} \left[ Pin^2 - \frac{\left(Pin^2 - Pout^2\right)}{L} \cdot m \right]^{-0.5}$$

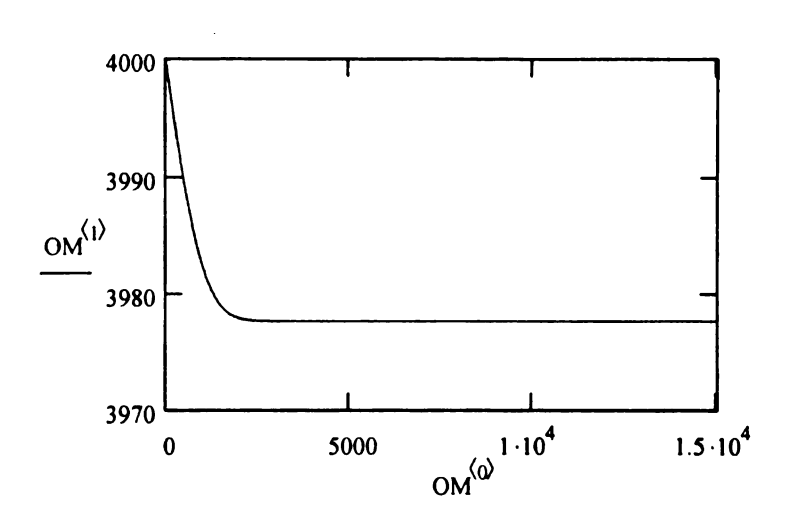
$$O32_{0,0} := 55$$
  $OM_{0,0} := 0$  Initialize OM time step

$$O32_{m+1,0} := O32_{m,0} \cdot \frac{P2_{m,0}}{Pin}$$

$$OM_{m+1,1} := OM_{m,1} - \left(\frac{kom}{yos} \cdot OM_{m,1} \cdot O32_{m,0}\right) \cdot dt$$
 Fin

 $OM_{m+1,0} := OM_{m,0} + dt$ 

Finite difference Equation Hsu 4-7



$$dz := \frac{L}{miterations}$$

$$O32_{0,0} := 55$$
  $O3hsu_{0,1} := 55$ 

Gas velocity calculation along flow path through the column in 1 cm increments

Modeltime := 1200

Miterations := 500

Miterations = m iterations in the finite difference

 $dt := \frac{Modeltime}{Miterations}$ 

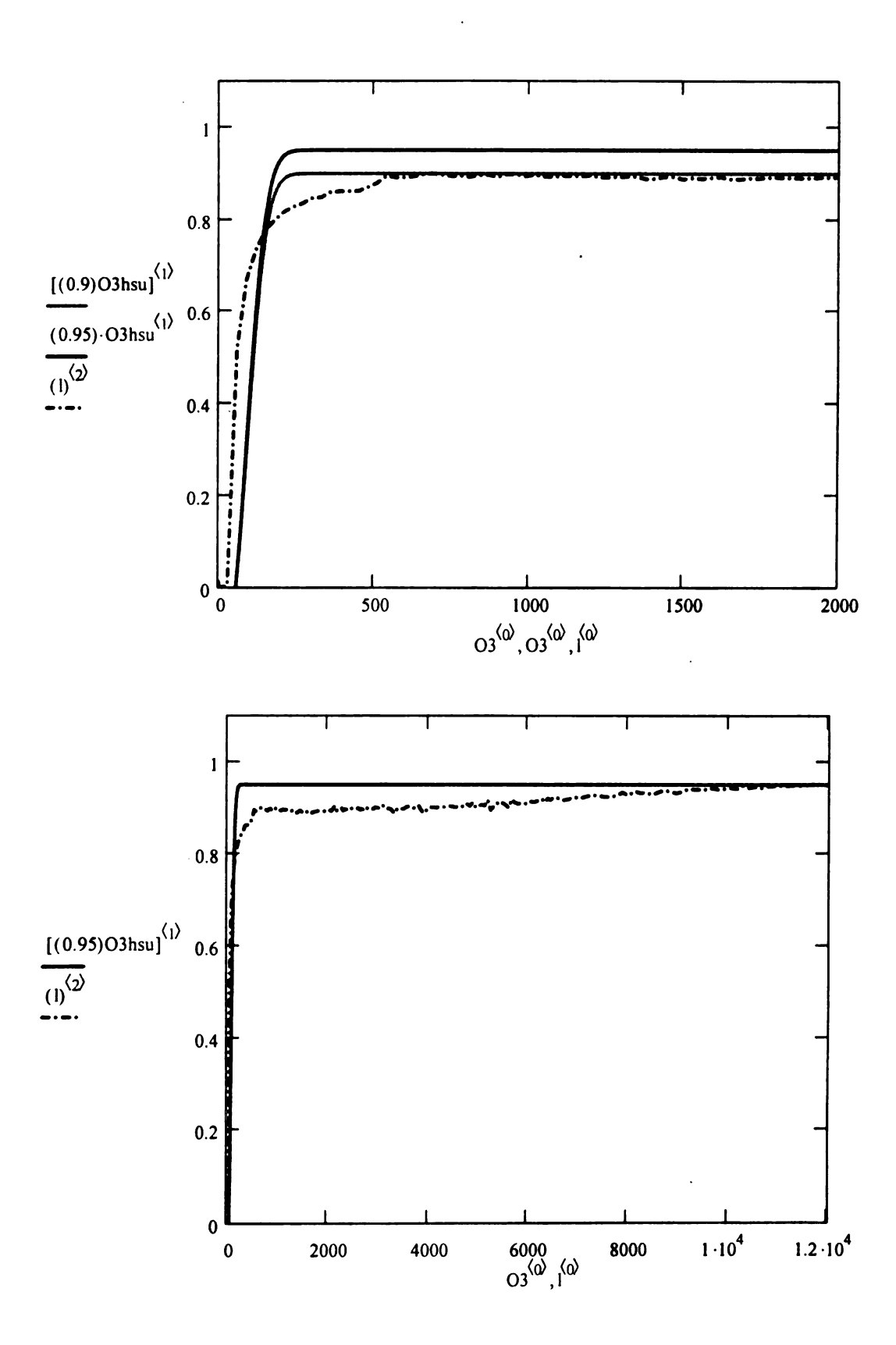
$$O3hsu_{m+1,\,1} := O32_{m,\,0} - \left[ \frac{v_{m,\,0}}{dz} \cdot \left( O32_{m+1,\,0} - O32_{m,\,0} \right) + \left( \rho b \cdot \frac{kom}{n \cdot sa} \right) \cdot \left( O32_{m,\,0} \right) \cdot OM_{m,\,1} \right] \cdot dt$$

$$O3_{0,0} := 0$$

$$O3_{m+1,0} := O3_{m,0} + dt$$

$$O3^{\langle 1 \rangle} := \left(1 - \frac{O3^{\langle 1 \rangle}}{55}\right)$$

$$O3hsu^{\langle 1 \rangle} := \left(1 - \frac{O3hsu^{\langle 1 \rangle}}{55}\right)$$



\*Modeling Note: The arrays in MathCad have a default setting where the first row and first column in the array is denoted as (0,0) and not (1,1). In this program, the rows and columns start at 0, the second column or the second row is therefore denoted by 1.

L := 15 Column length (cm)

pb := 1.1 Bulk density (g/cm<sup>3</sup>)

n := 0.42 total porosity X gas saturation (From HSU)

sa := 1 gas saturation

a.- 1

yos := 4.7 Stoiciometric coefficient for ozone gas ratio/organic matter

Kexp := 1.4·10<sup>-4</sup> Second order rate constant determined from experiments (1/s)(mg O3/kg soil)^-1

kom := 5.8·10<sup>-7</sup> second order organic matter rate constant for OM (calculated) (s^-1)((mg OC/kg soil)^-1)(L gas/kg soil)

kd := 0.0798 First order rate constant for ozone self-decomposition

Gas conductivity in Metea

Pin := 1525 Inlet pressure (cm H20)

Pout := 1494 Outlet pressure (cm H20)

Loops and Interations

m := 0..499 miterations := 500

C := 0..(L-1)

O3<sub>0,1</sub> := 55 initialize array for Ozone concentration in gas stream (mg ozone/L gas)

 $O3om_{0,0} := 55$ 

 $OM_{0,1} := 4000$  initialize arrat for Organic matter concentration in (mg OC/Kg soil)

 $OM_{0,0} := 0$  initialize row for OM time step

Pressure distribution through the column (Matrix Form)

Gas velocity calculation along flow path through the column (Matrix form)

$$P2_{m,0} := \left[ Pin^2 - \left( \frac{Pin^2 - Pout^2}{L} \cdot m \right) \right]^{0.5} \quad v_{m,0} := kd \cdot \frac{\left( Pin^2 - Pout^2 \right)}{2L} \cdot \left[ Pin^2 - \frac{\left( Pin^2 - Pout^2 \right)}{L} \cdot m \right]^{-0.5}$$

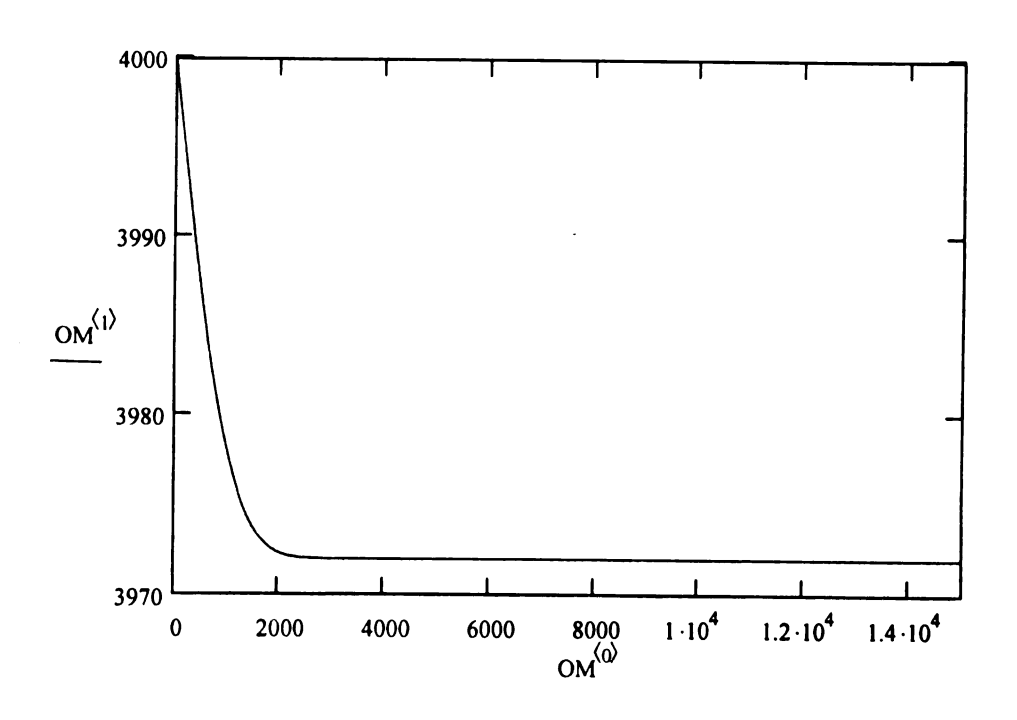
Assuming immobile OM available to react over 4 hour runtime

$$dt := \frac{15000}{\text{miterations}}$$

$$O3om_{m+1,0} := O3om_{m,0} \cdot \frac{P2_{m,0}}{Pin}$$

$$OM_{m+1,1} := OM_{m,1} - \left(\frac{kom}{yos} \cdot OM_{m,1} \cdot O3om_{m,0}\right) \cdot dt \qquad \text{Finite difference Equation Hsu 4-7}$$

$$OM_{m+1,0} := OM_{m,0} + dt$$



OMss := 3972

Steady state concentration of OM at time step ( $\Delta t = (15000/240)=62.5$ ) used in runga-kutta

$$O3_{0.0} := 55$$

Gas velocity calculation along flow path

$$v(dz) := kd \cdot \frac{\left(Pin^2 - Pout^2\right)}{2L} \cdot \left[Pin^2 - \frac{\left(Pin^2 - Pout^2\right)}{L} \cdot dz\right]^{-0.5}$$

Gas velocity defined as a function

$$DHsu(t,O3) := \left[ \frac{-v(L)}{L} \cdot O3 - \left( \frac{\rho b \cdot kom}{n \cdot sa} \cdot OMss \right) \cdot O3 \right]$$

Equation and model proposed by Hsu

ZHsu := rkfixed(O3,0,15000,240,DHsu)

$$AHsu^{\langle 1 \rangle} := ZHsu^{\langle 1 \rangle}$$

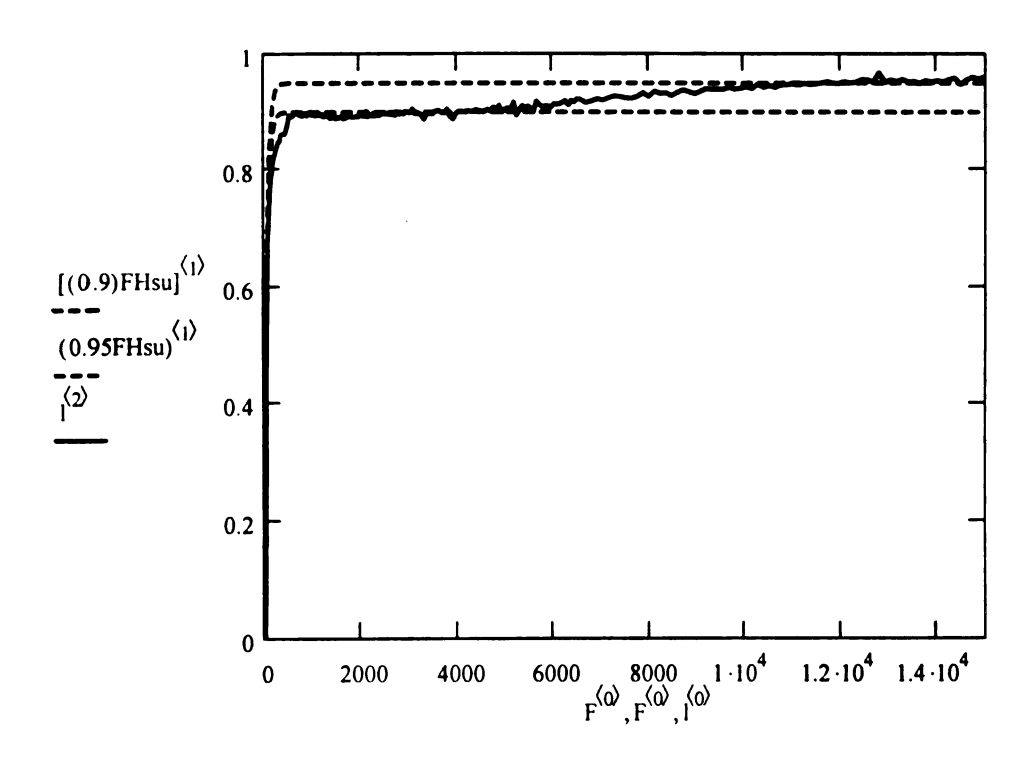
$$F^{\langle 0 \rangle} := ZHsu^{\langle 0 \rangle}$$

Experimental results in Day (1994), Hsu (1995), Cole (1996) and the present study observered the effluent ozone concentration from the column did not reach the influent concentration. Day (1994) and Cole (1996) describe this phenomenom was called "tailing" which reached levels between 90 - 98% of influent ozone concentration

$$\mathsf{FHsu}^{\langle 1 \rangle} := \left[ \left[ 1 - \left( \frac{\mathsf{AHsu}^{\langle 1 \rangle}}{\mathsf{O3}_0} \right) \right] \right]$$

## Non-contaminated, dry Metea at pH 6

## (O3/O3 inital) versus time Plot of Experimental data compared to Hsu and Lim Models Tailing factor = 0.95



Modeling Note: The arrays in MathCad have a default setting where the first row and first column in the array is denoted as (0,0) and not (1,1). In this program, the rows and columns start at 0, the second column or the second row is therefore denoted by 1.

L := 91 Column length (cm)

 $\rho b := 1.1$  Bulk density (g/cm<sup>3</sup>)

n := 0.42 total porosity (From HSU)

sa := 1 gas saturation

 $K := 4.10^{-3}$  first order rate constant for ozone reaction in Metea (1/s)(mg/kg)^-1

kd := 0.0798 Gas conductivity

 $kom := 5.7 \cdot 10^{-7}$  second order organic matter rate constant

initalO3 := 55 Inlet gas concentration (mg/L)

 $O3_{0,1} := 55$  initialize array for ozone concentration

OM := 0 Organic matter concentration (mg/kg)

 $OM_{0,1} := 0$  array for Organic Matter

Pin := 1664 Inlet pressure (cm H20)

Pout := 1033 Outlet pressure (cm H20)

Loops and Interations

C := 0..(L-1)

m := 0..239 miterations := 240

 $dt := \frac{15000}{\text{miterations}}$ 

Pressure distribution through the column in 1 cm increments

$$P2_{m,0} := \left[ Pin^2 - \left( \frac{Pin^2 - Pout^2}{L} \cdot m \right) \right]^{0.5}$$

Gas velocity calculation along flow path through the column in 1 cm increments

$$v_{m,0} := kd \cdot \frac{\left(Pin^2 - Pout^2\right)}{2L} \cdot \left[Pin^2 - \frac{\left(Pin^2 - Pout^2\right)}{L} \cdot m\right]^{-0.5}$$

$$yos := 4.7$$

O32<sub>0,0</sub> := 55

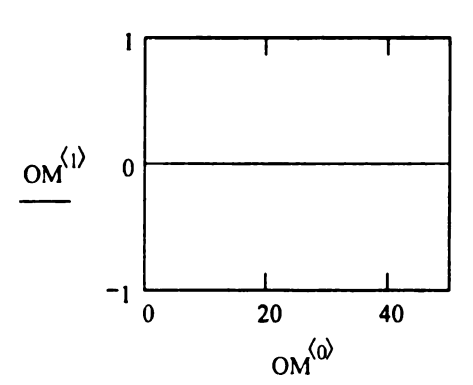
OM<sub>0,1</sub> := 0

O32<sub>m+1,0</sub> := O32<sub>m,0</sub> · 
$$\frac{P2_{m,0}}{Pin}$$

OM<sub>m+1,1</sub> := OM<sub>m,1</sub> -  $\left(\frac{kom}{vos} \cdot OM_{m,1} \cdot O32_{m,0}\right) \cdot dt$ 

$$OM_{0,0} := 0$$

$$OM_{m+1,0} := OM_{m,0} + 1$$



$$OM := 0$$

$$O3_{0,0} := 55$$

Gas velocity calculation along flow path through the column in 1 cm increments

$$v(z) := kd \cdot \frac{\left(Pin^2 - Pout^2\right)}{2L} \cdot \left[Pin^2 - \frac{\left(Pin^2 - Pout^2\right)}{L} \cdot z\right]^{-0.5}$$

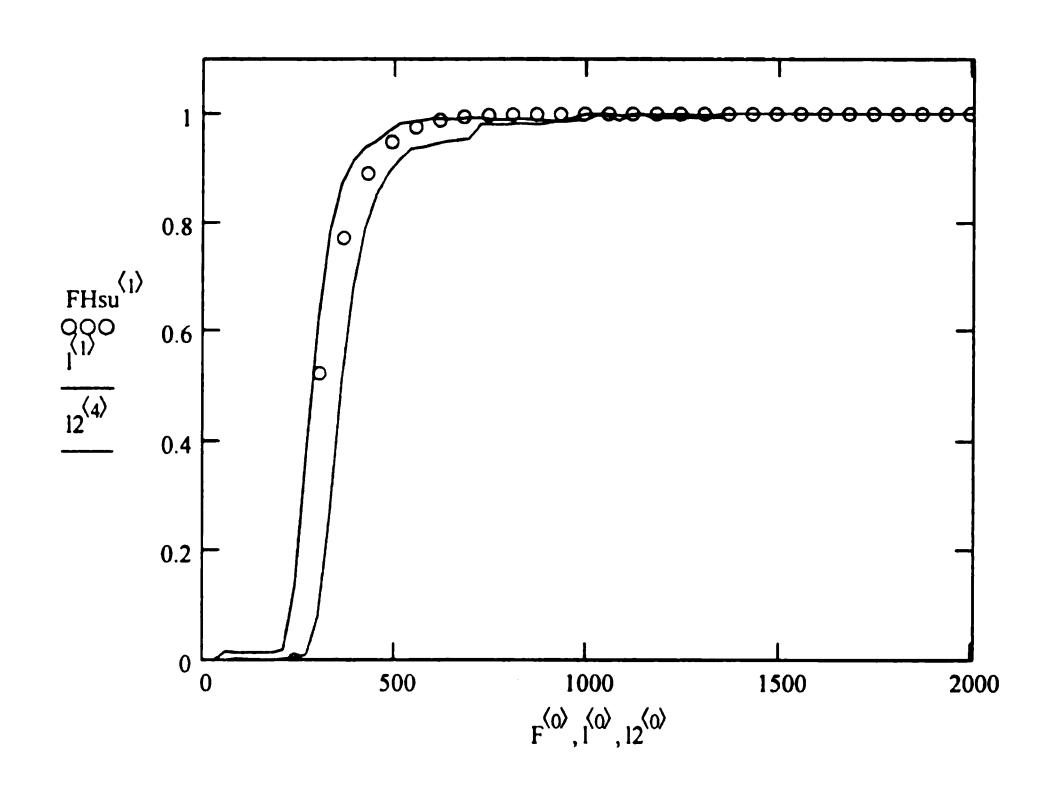
$$DHsu(t, O3) := \left[\frac{-v(L)}{L} \cdot O3 - \left(\frac{pb \cdot kom}{n \cdot sa} \cdot OM\right) \cdot O3 - K \cdot O3\right]$$

ZHsu := rkfixed(O3,0,15000,240,DHsu)

$$F^{\langle 0 \rangle} := ZHsu^{\langle 0 \rangle} + 4.60$$

$$AHsu^{\langle 1 \rangle} := ZHsu^{\langle 1 \rangle}$$

$$\mathsf{FHsu}^{\langle 1 \rangle} := \left[ \left[ 1 - \left( \frac{\mathsf{AHsu}^{\langle 1 \rangle}}{\mathsf{O3}_0} \right) \right] \right]$$



Modeling Note: The arrays in MathCad have a default setting where the first row and first column in the array is denoted as (0,0) and not (1,1). In this program, the rows and columns start at 0, the second column or the second row is therefore denoted by 1.

$$\begin{array}{lll} L:=91 & \text{Column length (cm)} \\ \rho b:=1.1 & \text{Bulk density (g/cm^3)} \\ n:=0.42 & \text{total porosity X gas saturation (From HSU)} \\ sa:=1 & \text{gas saturation} \\ K:=1.5\cdot 10^{-4} & \text{second order rate constant for ozone reaction in Metea (1/s)(mg/L)(mg/kg)^-1} \\ kd:=0.0798 & \text{Gas conductivity} \\ kom:=5.7\cdot 10^{-7} & \text{second order organic matter rate constant} \\ inital O3:=55 & \text{Inlet gas concentration (mg/L)} \\ O3_{0,1}:=55 & \text{initialize array for ozone concentration} \\ OM:=4000 & \text{Organic matter concentration (mg/kg)} \\ OM_{0,1}:=4000 & \text{initialize array for OM concentration} \\ Pin:=1664 & \text{Inlet pressure (cm H20)} \\ Pout:=1209 & \text{Outlet pressure (cm H20)} \\ \end{array}$$

Loops and Interations

$$\frac{\text{Pout}}{\text{Pin}} = 0.727$$

$$C := 0..(L - 1)$$
  
 $m := 0..239$  miterations := 240

$$dt := \frac{15000}{240}$$
 Experiment time in seconds divided by iterations (m)

Pressure distribution through the column in 1 cm increments

$$P2_{m,0} := \left[ Pin^2 - \left( \frac{Pin^2 - Pout^2}{L} \cdot m \right) \right]^{0.5}$$

Gas velocity calculation along flow path through the column in 1 cm increments

$$v_{m,0} := kd \cdot \frac{\left(Pin^2 - Pout^2\right)}{2L} \cdot \left[Pin^2 - \frac{\left(Pin^2 - Pout^2\right)}{L} \cdot m\right]^{-0.5}$$

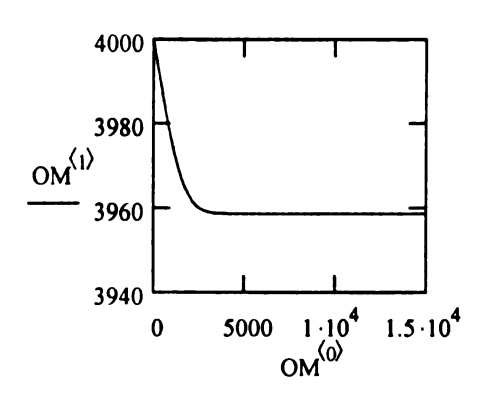
O32<sub>0,0</sub> := 55

O32<sub>m+1,0</sub> := O32<sub>m,0</sub> · 
$$\frac{P2_{m,0}}{Pin}$$

OM<sub>m+1,1</sub> := OM<sub>m,1</sub> -  $\left(\frac{kom}{yos} \cdot OM_{m,1} \cdot O32_{m,0}\right) \cdot dt$ 

OM<sub>0,0</sub> := 0

OM<sub>m+1,0</sub> := OM<sub>m,0</sub> + dt



Stoichiometric ratio

yos := 4.7

OM := 3960 OM concentration from finite difference

$$O3_0 := 55$$

Gas velocity calculation along flow path through the column in 1 cm increments

$$v(z) := kd \cdot \frac{\left(Pin^2 - Pout^2\right)}{2L} \cdot \left[Pin^2 - \frac{\left(Pin^2 - Pout^2\right)}{L} \cdot z\right]^{-0.5}$$

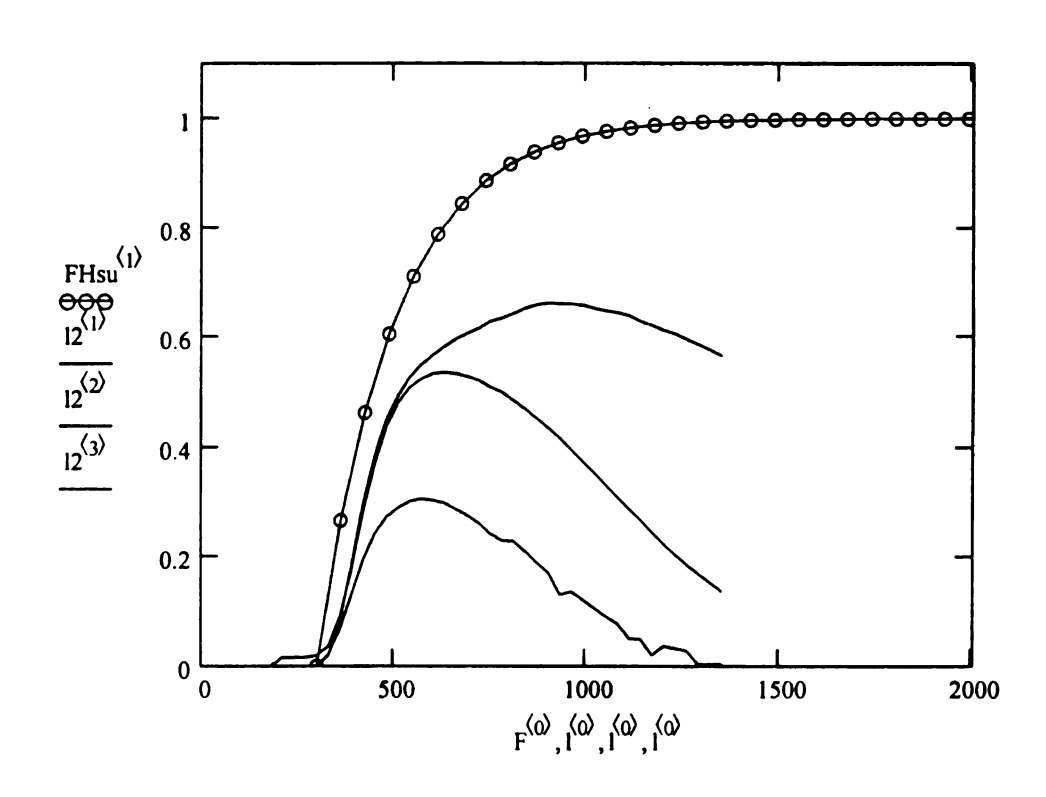
$$DHsu(t, O3) := \left[\frac{-v(10)}{10} \cdot O3 - \left(\frac{\rho b \cdot kom}{n \cdot sa} \cdot OM\right) \cdot O3\right]$$

$$ZHsu := rkfixed(O3, 0, 15000, 240, DHsu)$$

$$F^{\langle 0 \rangle} := ZHsu^{\langle 0 \rangle} + 5 \cdot 60$$

$$AHsu^{\langle 1 \rangle} := ZHsu^{\langle 1 \rangle}$$

$$\mathsf{FHsu}^{\langle 1 \rangle} := \left[ \left[ 1 - \left( \frac{\mathsf{AHsu}^{\langle 1 \rangle}}{\mathsf{O3}_0} \right) \right] \right]$$



## Sample Calculation of Kom

Ws 0.05 kg Vg 0.03679688 L O3 initial 55 mg/L

O3 step

om initial 4000 mg/kg

A 0.00327623 L/kg B 4.1583E-06

kom 5.7702E-07 Solver/Goal Seek value

beta 0.7359375 L/kg

ko' 0.00014 1/s\*mg/kg chi 4.77

S 0.6 XO3 start 0

		IN	OUT	X	Left	Right	solver < 0
Abs influent	Abs effluent	mg/L				_	
0	0						
0.7106	0	56.848	0	1		0.098162	
0.7162	0.5884	57.296	47.072	0.178442	0.196326	0.196324	1.56E-06
0.7444	0.6584	59.552	52.672	0.115529	0.122619	0.294487	-0.171867
0.7458	0.6609	59.664	52.872	0.113837	0.12071	0.392649	-0.271938
0.7354	0.6602	58.832	52.816	0.102257	0.107742	0.490811	-0.383069
0.7358	0.6681	58.864	53.448	0.092009	0.096404	0.588973	-0.492569
0.7365	0.6653	58.92	53.224	0.096673	0.101548	0.687135	-0.585587
0.7312	0.6614	58.496	52.912	0.09546	0.100207	0.785298	-0.685091
0.7421	0.6713	59.368	53.704	0.095405	0.100147	0.88346	-0.783313
0.7494	0.6784	59.952	54.272	0.094742	0.099416	0.981622	-0.882206
0.7544	0.6803	60.352	54.424	0.098224	0.103264	1.079784	-0.97652
0.7491	0.6576	59.928	52.608	0.122147	0.130121	1.177946	-1.047826
0.7354	0.6551	58.832	52.408	0.109192	0.115488	1.276109	-1.16062

Equations for solving k<sub>om</sub> from Hsu (1995) pgs. 55-57

$$S = \frac{-(\frac{d\rho_{O3}}{dt})_{vv}}{-(\frac{d\rho_{O3}}{dt})_{om}} = \frac{k_o \rho_{O3}}{(\frac{W_v}{V_v})k_{om}(om)(\rho_{O3})} = \frac{\beta(k_o)}{k_{om}(om)} = \frac{(\Delta W_{O3})_{vys}}{(\Delta W_{O3})_{om}}$$

where 
$$\beta = \frac{V_g}{W_s}$$

and  $(\Delta W_{O3})_{sys}$  and  $(\Delta W_{O3})_{om}$  are the masses of gaseous ozone consumed be system decomposition and soil organic matter, respectively.

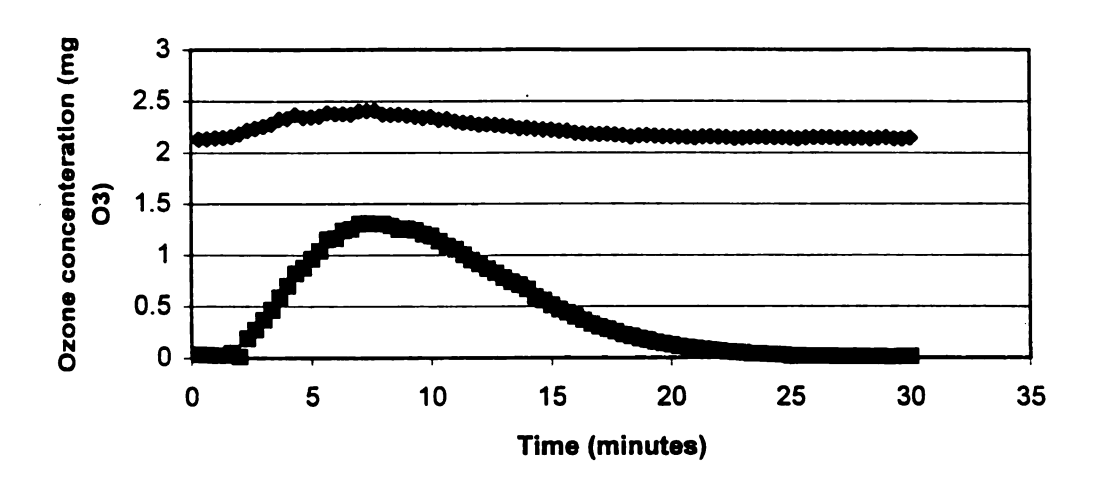
$$X_{O3} = \frac{\rho_{O3}^0 - \rho_{O3}}{\rho_{O3}^0}$$

$$\ln \left[ \frac{(A - BX_{O3})}{(1 - X_{O3})} \right] = (A - B)(t - t_0)$$

or, 
$$\rho_{O3} = \rho_{O3}^0 \left( 1 - \frac{Ae^{(A-B)t} - A}{Ae^{(A-B)t} - B} \right)$$
, when  $X_{O3} = 0$  at  $t_0 = 0$ 

where 
$$A = k_0' + \frac{k_{om}(om^0)}{\beta}$$
 and  $B = \frac{k_{om}(\rho_{O3}^0)}{\xi(1+S)}$ 

## **Ozone concentraiton Influent and Effluent**



Breakthrough curve for preliminary ozonation system set-up without the use of a gas wash bottle to provide a moisturized gas stream of ozone to the column. The experiment used the 15 cm column and Metea soil: • influent ozone concentration.

Figure D1. Example of the ozone breakthrough curve for soil in 15 cm column acting as an ozone destruct unit.

